YOLLA 4

T/L1 OFFSHORE BASS BASIN

WELL COMPLETION REPORT
INTERPRETIVE DATA

D.M. Brooks, K. Bierbrauer, J. Parvar
Origin Energy Resources Ltd
339 Coronation Drive
MILTON QLD 4064
Australia

MAY 2005

Distribution List:

Chief Geologist

Chief Geophysicist

Subsurface Manager BassGas

Contents

1. WELL INDEX SHEET

Permit Interests:	Origin Energy Resources Ltd (32.5%) - OPERATOR Origin Energy Northwest Pty Ltd (5%) AWE Petroleum Pty Ltd (30%) CalEnergy Gas (Australia) Ltd (20%) Wandoo Petroleum Pty Ltd (12.5%)
Rig on Location:	06/06/2004
Spud:	18/06/2004
Reached TD:	11/07/2004
Rig Released:	08/08/2004
Total Rig Days:	64
Rig Name:	ENSCO 102
Drilling Contractor:	ENSCO
Total Depth:	3235m MDRT (Drillers) 3054.2 mSS (Drillers)
Well Status:	Cased Gas Producer

Well Name:	Yolla 4
Basin:	Offshore Bass
Permit:	T/L1
Type:	Deviated Production Well
Water Depth:	80.8m (MSL to seabed)
Elevation:	43m (RT-sea level)
Latitude:	39° 50' 40.592"S
Longitude:	145° 49' 06.0569"E
Easting:	398 905.07metres
Northing:	5 588 821.47metres
(GDA 94; UTM Zone 55S, Central Meridian 147° East).	
Seismic Reference: (platform)	Yolla 3D Survey: Inline 480, X-line 1000
(2755 Sst)	Inline 475, X-line 951
Actual Well Cost:	A$ 24,603,034

FORMATION TOPS

FORMATION / *SEISMIC MARKER*	**TOPS (m)**				**REMARKS/SHOWS**
	m MDRT	m TVDSS	THICK (rel to TVD)	TWT (ms)	
Torquay Group	123.8	80.8	971.2	108	No Returns 123.8 – 900.0 mMDRT. Claystone, calcareous.
Upper Angahook Formation	1095	1052	188.0	942	Claystone, calcareous in part
Angahook Volcanics	1283	1240	134.0	1134	Volcanic Tuff interbedded with claystone and sandstone and minor siltstone
Lower Angahook (Oligocene)	1418	1374	288.2	1232	Interbedded sandstone, siltstone and claystone, grain size decreasing with depth
Demons Bluff Formation	1726	1662.2	142	1419	Siltstone with minor interbedded sandstone and occasional dolomite
Eastern View Coal Measures	1883	1804.2	1198	1517	Interbedded Sandstone, coal, siltstone and minor claystone
TEV4	*1912*	*1830.6*	*(17.4)*	*1534*	*Sandstone*
Fault	*2582.5*	*2441.4*	*NA*	*1915*	
2458 sand	*2603.7*	*2460.7*	*(14.5)*	*1933*	*Oil-bearing sandstone*
Top Igneous Intrusive	*2723.4*	*2569.7*	*(40.1)*	*1998*	*Gabbro*
2718 sand	*2864.8*	*2698.3*	*(6.1)*	*2064*	*Tight sandstone*
2755 sand	*2902.7*	*2733.3*	*(8.7)*	*2081*	*Gas-bearing sandstone*
2809 sand	*2962.6*	*2789.0*	*(20.8)*	*2108*	*Gas-bearing sandstone*
2844 sand	*3005.0*	*2828.8*	*(9.4)*	*2126*	*Gas-bearing sandstone*
2952 sand	*3118.2*	*2938.5*	*(11.7)*	*2183*	*Tight sandstone*
2973 sand	*3149.4*	*2969.3*	*(15.9)*	*2198*	*Gas-bearing sandstone*
Basal Volcanics	3182.6	3002.2	52.1+	2215	Volcanics: basalt and weathered basalt
TOTAL DEPTH	3235.0	3054.3			

FORMATION EVALUATION WHILE DRILLING

Hole Size (inches)	Interval (mMDRT)	MWD services	LWD services
16	220 - 900	DWD	none
12.25	905 – 2614	P4M-DIR-FE	DGR-EWR
8.5	2614 – 2892	P4M-DIR-FE	DGR-EWR
8.5	2892 – 2958	P4M-DIR-FE	DGR-EWR
8.5	2958 - 3235	P4M-DIR-FE	DGR-EWR

WIRELINE LOGS

Suite #	Run #	Interval (mMDRT)	Logs Acquired
1	1	2776 - 2542	PEX-HRLA-CMR-SP-GR-LEHQT
1	2	3235.5 - 2590	PEX-HRLA-CMR-SP-GR-LEHQT
1	3	3220 – 2590 (HNGS-DSI to 120)	FMI-DSI-HNGS-ECS-LEHQT
1	4	765 – 3225	VSI-GR-LEHQT (offset VSP survey)
1	5	3206 – 2594	MDT-GR-CMR-LEHQT
1	6	3159 - 2604	MSCT-GR-LEHQT
1	7	3185 - 2546	USIT-CBL-VDL-GR-CCL

CORES

CONVENTIONAL

Core #	Interval (mMDRT)	Cut (m)	Rec (m)	Formation
1	2892.05 – 2919.60	27	27.55 (100%)	EVCM 2755 sand
2	2958.07 – 2985.37	27	27.3 (100%)	EVCM 2809 sand

SIDEWALL

Suite#	Run#	Type	Interval (mMDRT)	Bullets	Mud	Empty	Low Rec	Recovered
1	6	Rotary (MSCT)	3159 – 2604	20	9	3		8

PRESSURE TESTING AND FLUID SAMPLING

Suite#	Run#	Type	Interval (mMDRT)	Total Tests	Valid Tests	Supercharged	Tight Tests	Retests	Lost Seal	Samples Collected
1	5	MDT	3206 – 2594	53	35	4	12		2	5

HOLE & CASING DETAILS

Hole Size	Interval (mMDRT)	Casing Size	Shoe Setting Depth (mMDRT)
		20"	220
16 "	124 - 900	$13\ ^{3}/_{8}$ "	885
12 ¼ "	900 - 2614	$9\ ^{5}/_{8}$ "	2586
8 ½ "	2614 - 3235 (TD)	$6\ ^{5}/_{8}$ "	3233

2. WELL SUMMARY

Yolla 4 was drilled as a deviated development well in the northern part of the Yolla Gas Field in the offshore Bass Basin, Tasmania within Production Licence T/L1. The well is located approximately 120 kilometres offshore from Tasmania and 200 kilometres south south-east of Melbourne, Victoria (Figure 1). The well was drilled using the ENSCO 102 jack up drilling rig, which was temporarily cantilevered over the top of the Yolla A permanent production platform. The well was directionally drilled in a southerly direction from the platform. Yolla 4 targeted the sandstone reservoirs of the Eastern View Coal Measures (EVCM) previously intersected and evaluated in Yolla 1 and Yolla 2. The well was designed to intersect the top Eastern View Coal Measures (EVCM) 1290m NNE of Yolla 2 and the top of the 2809 gas reservoir (intra-EVCM) 940m NNE of Yolla 2.

Yolla 4 spudded on the 18th June 2004. Primary objectives within the Paleocene, termed 2718, 2755, 2809 and 2973 sand units, were intersected close to prognosed depth. Surprisingly the 2718 sand was found to be water wet. All other objectives were production tested and flowed gas and condensate. An unpredicted oil zone was encountered higher in the EVCM, termed 2458 sand unit which flowed oil on test. The well reached total depth of 3235mRT (3054.25mTVDSS) on 11th July 2004. Following production testing, the rig was released to Yolla 3 on 8th August 2004.

On 30th September 2004, after the Yolla 3 operations were completed, the rig skidded back to the Yolla 4 well bore. This was to determine the source of a leakage down hole and undertake further testing of the 2809 sand unit to obtain uncontaminated samples. This retesting was necessary as the analysis of the original samples collected from Yolla 4 were spurious due to leakage of hydrocarbons from the 2973 sand mixing with the hydrocarbons produced from the shallower gas zones. After successfully completing these objectives the rig was then released on 16th October 2004 to the T/18P joint venture to drill Trefoil 1.

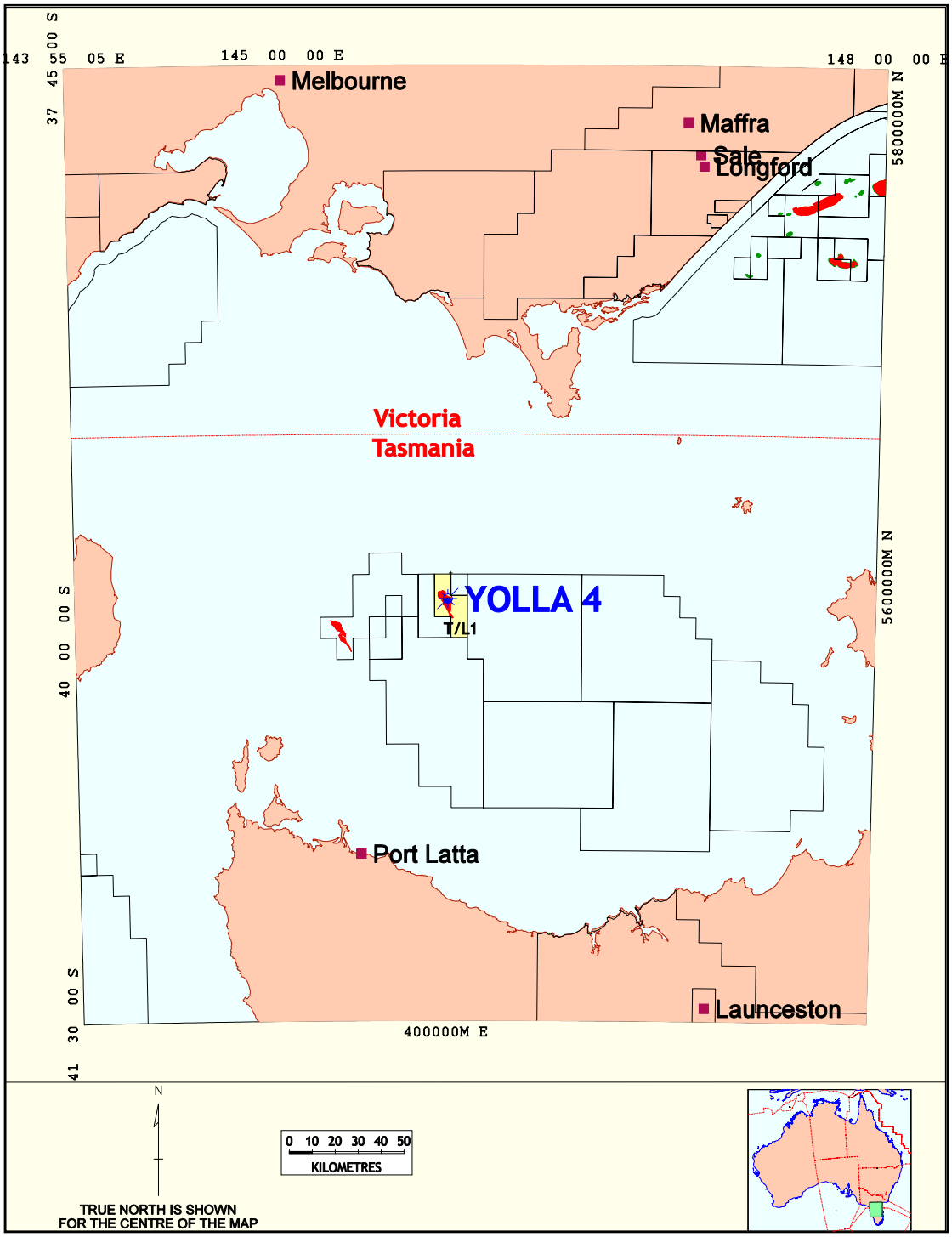

Figure 1: Location Map

3. WELL RESULTS

3.1 Hydrocarbons Encountered

In this section 3.1, all depths of shows described while drilling are referenced to driller's depths.

Mudlog gas readings commenced from 900mRT. Background gas readings in Yolla 4 remained fairly steady down to the base of the Miocene section of the upper Angahook Formation (total gas range 4 – 38 units). No significant gas peaks were recorded and no fluorescence was observed.

The first sandstone in the well was intersected at a depth of 1315mRT, within the Miocene age Angahook volcanics. At this depth a gas peak of 221 units, including up to C5, was recorded. Gas readings dropped to background levels (average 12 units total gas) below 1322mRT.

Throughout the remainder of the Angahook Formation and the underlying Demons Bluff Formation, background gas readings steadily increased from average 20 units to 60 units, with very minor gas peaks recorded within sandstone interbeds at 1396mRT (49 units), 1501mRT (57 units) and 1526mRT (48 units).

Immediately upon entering the Eastern View Coal Measures gas readings climbed sharply to a total gas peak of 173 units at 1908mRT. Trace fluorescence was noted between 1908mRT and 1914mRT. The fluorescence is described as very dull, pinpoint, dark yellow, no direct cut, no crush cut and no residue ring. The well is interpreted to have encountered the basal 3m of the oil column which was discovered in Yolla 1. The OWC for this accumulation is at –1831mTVDSS.

Gas readings reduced to high background levels averaging 79 units between 1912mRT to 1938mRT. Total gas remained at background levels averaging between 6 and 43 units from 1938mRT to 2602mRT, except for peaks at coal beds. The most significant peaks associated with coals are 158 units at 2318mRT, 125 units at 2375mRT, 109 units at 2406mRT, 184 units at 2481mRT, 354 units at 2595mRT.

At 2602mRT total gas readings rose to 364 units accompanied by significant increase in gas wetness ratio and direct 70% fluorescence in sandstone cuttings. The fluorescence is bright, even, light green, no direct cut, very slow bleeding crush cut, bright, light green patchy residue ring. This sandstone was subsequently tested with MDT samples and production tested. The sandstone interval 2603.7 to 2619.6mRT (-2460.7 to 2475.2mTVDSS) is interpreted to be oil-bearing with 2.5 metres of net pay. No OWC is interpreted from the pressure data however a water sample was obtained at 2614.5mRT. This oil-bearing sand is referred to as the 2458 sand (2458mTVDSS being the drillers depth at which the top of the sand was encountered in Yolla 4).

Below the small oil zone, gas readings remained at background levels from 5 to 61 units from 2614mRT to 2894mRT. Gas peaks associated with coals were encountered at 2657mRT (121 units) and 2663mRT (139 units). Fluorescence was noted at 3 intervals:

2614 to 2630mRT – 50% fluorescence in sandstone aggregates, bright yellow, moderately fast, even crush cut, bright green, bleeding direct cut and a thin pale green residue.

2652 to 2658mRT – trace fluorescence in sandstone cuttings, dull yellow, no direct cut, no crush cut, trace broken pale cream residue ring.

2860 to 2883mRT – trace fluorescence, dim yellow, trace to very slow direct and crush cut, dim cream broken film residue.

At 2894mRT the 2755 sand (gas zone) was intersected and total gas readings rose to 390 units, dropping to background levels at 2909mRT. Within core #1 taken in the 2755 sand, fluorescence between 2895mRT to 2907.8mRT is described as 5 to 90% dull to bright green, no to very slow direct cut, very slow to no crush cut, dull to bright cream broken film residue. Log analysis, MDT and production test results indicate a 7.6m net gas column was intersected with the GWC at 3009.0mRT (-2832.0mTVDSS).

Between the 2755 sand and the 2809 sand (2909 to 2958mRT), gas levels generally remained at background levels between 4 and 12 units, except for a peak of 30 units at 2946mRT within a tight sandstone.

The 2809 sand (gas zone) was cored (core #2 2958 to 2985.4mRT) and had average total gas readings of 446 units and fluorescence occurred intermittently between 2958 and 2981mRT. The fluorescence was trace to nil, dull to bright green, patchy, no direct cut, very slow to trace crush cut, dull white cream residue ring. Log analysis, MDT and production test results indicate a 20.8m net gas column was intersected with the GWC at 3266.2mRT (-2826.5mTVDSS).

Below the 2809 sand, from 2985.4 to 3130mRT total gas levels within the predominantly siltstone and claystone interval remained at 8 to 22 units. One small sandstone unit (termed the 2844 zone) contained a gas peak of 94 units between 3003 to 3006mRT.

The 2952 sand was intersected from 3118 to 3130mRT where gas peaked at 207 units. Background gas readings remained relatively high (30 to 77 units) from 3120mRT to the top of the 2973 gas zone at 3145mRT.

The 2973 sand (gas zone) exhibited high gas peaks up to 258 units between 3145 and 3164mRT. Log analysis, MDT and production test results indicate a 9.8 meter net gas column was intersected in this well with the GWC interpreted at 3170.3mRT (-2990.0mTVDSS).

From the base of the 2973 sand to total depth, total gas readings remained low averaging between 5 and 6 units.

3.2 Stratigraphy

A generalised stratigraphy of the Bass Basin is illustrated in Figure 2. Figure 3 contains a comparison between the pre-drill prognosis and actual stratigraphy encountered at Yolla 4. A further report by Dr Roger Morgan (Morgan Palaeo Associates) on the age and palaeo-environment of 15 cuttings samples is included in Appendix 6. This report also contains maturity data derived from the spore colour index method.

Lithological descriptions from ditch cuttings, sidewall core and conventional core (see Appendices 1, 2 and 3, Yolla 4 Well Completion Report Volume 1, Basic Data), together with the MWD and wireline log interpretation (Appendix 1, this volume), provide the basis for the stratigraphic breakdown in the Composite Well Log (Enclosure 1). All thicknesses quoted are referenced to TVDSS depths.

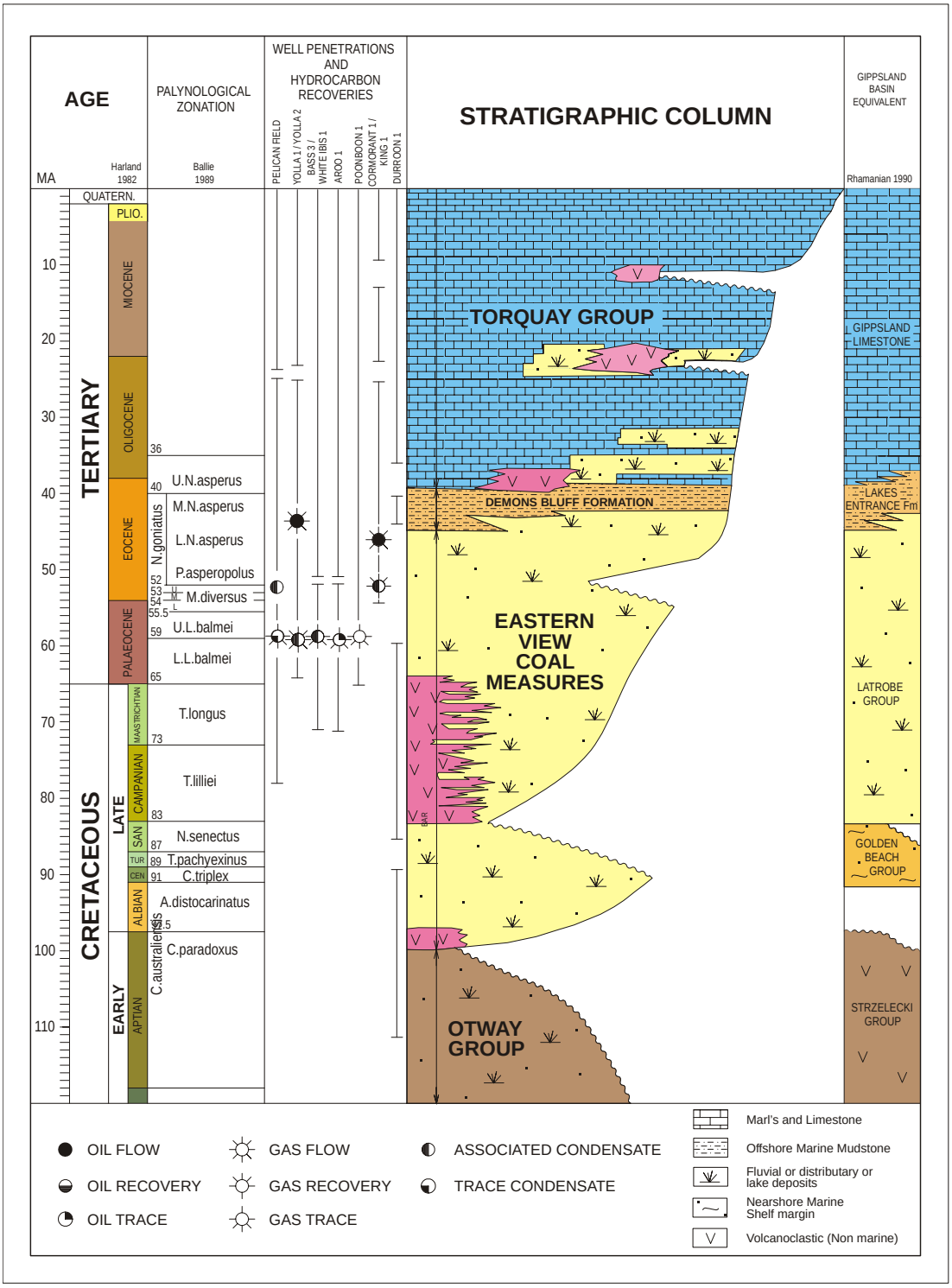

Figure 2: Generalised Stratigraphy of the Bass Basin

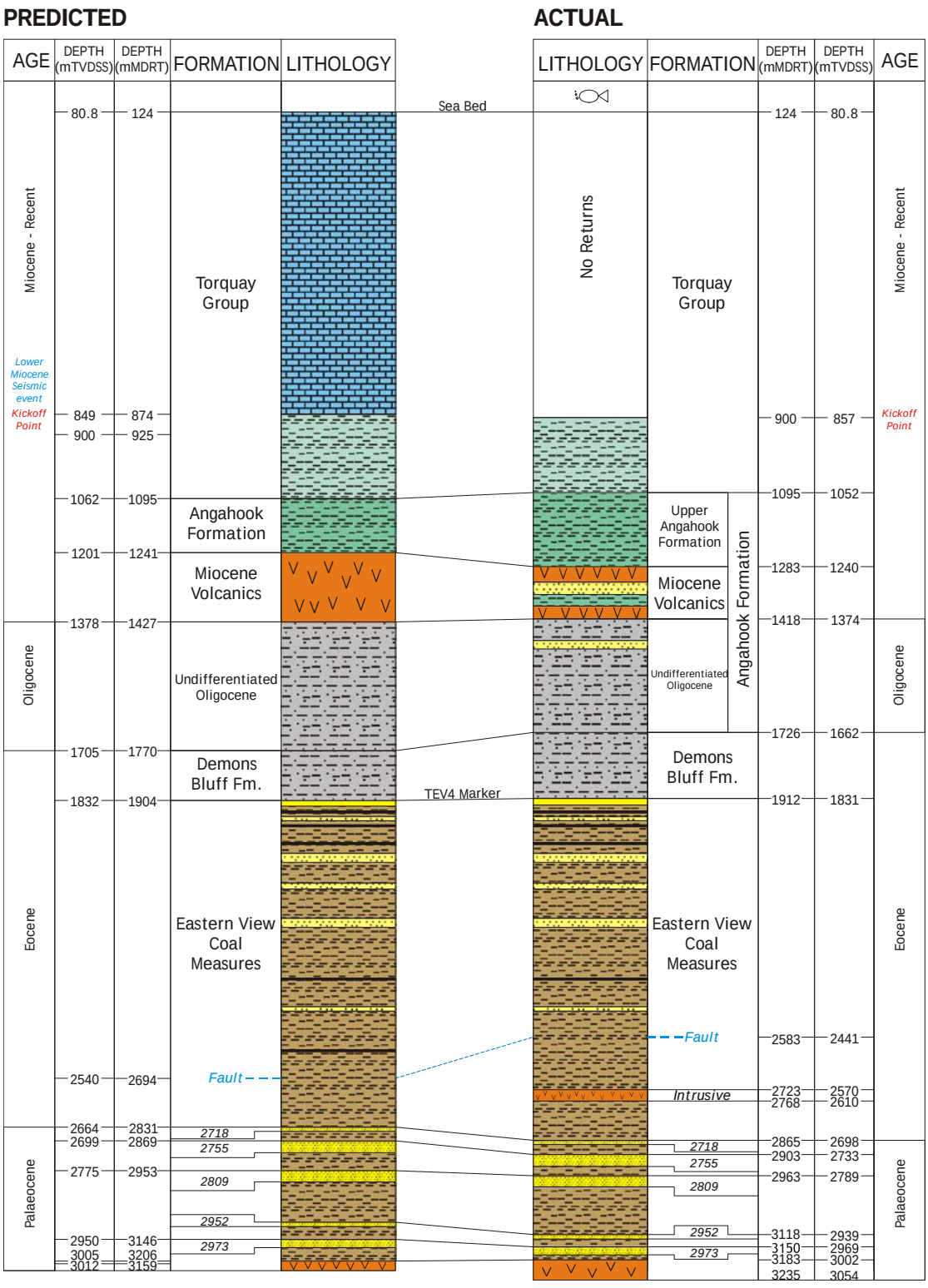

Figure 3: Predicted versus Actual Stratigraphy

Torquay Group
(123.8 to 1095.0mRT, 80.8 to 1052.0mTVDSS)

The Torquay Group in Yolla 4 is approximately 971.2 mTVD thick. The unit is interpreted to be deposited under shallow marine conditions and can be seismically divided into two upper units separated by a prominent seismic marker called the 'Lower Miocene Seismic event'. This event separates the Pliocene to Miocene mainly calcareous dominated lithology from the underlying Miocene age claystone. The third and lowermost unit of the group is the Angahook Formation, which itself can be divided into 3 sub-units.

Returns were established from 900mRT therefore lithology above this depth is assumed to be similar to the offset well Yolla 1. In Yolla 1 the top portion of the Torquay Group consists of a bioclastic limestone. This upper limestone section comprises white to mid-grey, coarse- to fine-grained unconsolidated bioclastic calcarenite to calcirudite composed of friable and loosely cemented skeletal debris consisting of pelecypods, bryozoans, foraminifera and gastropods. The fragment size decreases with depth with biocalcirudites grading to biocalcarenites and calcarenites and finally calcilutites. Quartz grains appear in the lower portion of the limestone interval. There is a general increase in the proportion of clay in silt towards the base of this interval.

The lower portion of the Torquay Group is described in Yolla 4 as olive grey to green grey and light to medium grey, off white, soft to very soft, dispersive to sub-blocky, up to 20% calcareous, with trace amounts of: silt, fossil fragments, forams, shell fragments, carbonaceous matter and disseminated pyrite.

Angahook Formation
(1095.0 to 1726.0mRT, 1052.0 to 1662.2mTVDSS)

Overall the thickness of the Miocene to Oligocene Angahook Formation in Yolla 4 is 610.2mTVD. This unit is distinctive from the overlying upper units of the Torquay Group due to reworking and presence of volcanics and sediments proximal to centres of Miocene volcanism (*Lennon et al, 1999*).

Upper Angahook Formation
(1095.0 to 1283.0mRT, 1052.0 to 1240.0mTVDSS)

In Yolla 4 the upper part of the Angahook Formation consists of claystone which is light olive grey to light to medium grey, off white, loose to very soft, sub-blocky to dispersive, is up to 7% calcareous and contains traces of silt, very fine sand, carbonaceous grains, siderite and lithic grains. The basal interval from 1244mRT – 1283mRT also contains a second claystone lithology which consists of off white to rare red brown, very soft to dispersive clays with a rare slight tuffaceous texture.

The log response through this interval is a fairly uniform GR and resistivity response with a slight decrease in GR from the top of the unit to the base suggesting a gradual fining upward trend in grainsize. The mudlog shows a minor but consistent increase in gas and wet gas from the top to the base.

Angahook Volcanics
(1283.0 to 1418.0mRT, 1240.0 to 1374.0mTVDSS)

The volcanic-rich interval within the Angahook Formation in Yolla 4 is described as interbedded volcanic tuff, claystone, sandstone and minor

siltstone. The top of the unit is distinctive on logs due to the gamma-ray (GR) response of the tuffs compared to the overlying claystone. The top of the unit is picked on a thin very high GR response (4 m drilled thickness in Yolla 4) which is immediately underlain by a thicker low GR (15 m drilled thickness in Yolla 4). Both of these features are correlatable to Yolla 1 and Yolla 3. The tuff is assumed to be sourced from the Miocene volcano which is evident on seismic and located just to the north of the Yolla Field.

The volcanic tuff is blue-grey in colour, soft, sub-blocky to amorphous, with tuffaceous texture in part with a predominantly silt to very fine sand size quartz and glassy ground mass, commonly the tuff is weathered to claystone. The claystone is light brown grey to light medium grey colour, very soft, dispersive containing 10% calcareous grains and trace of pyrite. The sandstone grains are clear to translucent, loose to rare soft small aggregates consisting of 40% very fine grains, 50% fine grain and 10% medium grain size which are moderately sorted, subrounded to occasionally rounded, sub-elongate to sub-spherical, weak siliceous cement and 3% tuff matrix and inferred 20% intergranular porosity. The siltstone which is only described in the base of the unit between 1370 – 1418mRT is medium to light grey, soft, sub-blocky and contains 10% calcareous grains and 10% clay, 20% very fine sand and 10% fine sand size grains, 3% glauconite and trace siderite.

The Angahook Volcanics unit lies within the spore-pollen zone upper P.tuberculatus (lower Miocene). Spores and pollens are subordinate to dinoflagellates indicating a marine depositional environment ranging from shelfal at the base to offshore higher up in the interval suggesting a gradational deepening of water depth upwards in the stratigraphy.

Undifferentiated Oligocene
(1418.0 to 1726.0mRT, 1374.0 to 1662.2mTVDSS)

The remaining basal interval of the Angahook Formation is a clastic dominated marine unit of interbedded sandstone, siltstone and claystone, within increasing percentage of siltstone and decreasing sand content down hole.

An apparent increase in sandiness from the GR response, compared to the overlying unit, characterises the top of this interval. There is a gradual decrease in grain size down hole. The overall GR and resistivity log responses (from the LWD tools) is fairly bland.

Siltstone is the dominant lithology in this interval and consists of light to medium grey colour, very soft to soft, sub-blocky, 10-15% calcareous grains, 5-10% clay, 50% silt, 20% very fine sand size grains and 0-10% fine sand grains, weak calcareous cement, up to 3% glauconite grains, 0 – 3% lithics and trace siderite. The sandstone is light grey, off-white to light brown, very soft to soft, sub-blocky fracture, with 5% calcareous grains, 5- 0% clay size grains, 10-30% silt, 40% very fine sand, 0-20% fine sand and 0-10% medium sand size grains, well to poorly sorted, sub-angular to angular, sub-spherical grains with a weak calcareous cement weakly argillaceous matrix in part and accessories are 0 3% glauconite, 0-5% lithics, trace pyrite and 3-5% intergranular porosity. The claystone interbeds are light grey to olive green coloured, very soft, dispersive, and is made up of 5-30% calcareous grains, 50-60% clay, 10-30% silt and 5 – 10% very fine sand grains and trace glauconite.

The one sample analysed for palynology within this sub-formation is assigned to the lower *P. tuberculatus* spore-pollen zone (Oligocene), or

could be as old as *N. asperus*. Spore and pollens are dominant and diverse compared to scarce low diversity dinoflagellates suggesting a very nearshore marine depositional environment.

Demons Bluff Formation
(1726.0 to 1883.0mRT, 1662.2 to 1804.2mTVDSS)

The Demons Bluff Formation lithology is dominated by siltstone within minor interbedded sandstone and claystone and trace dolomite. This formation forms a thick regional seal over the EVCM.

The GR logs at the top of the unit show a distinct baseline shift indicating a reduction in overall grainsize compared to the Angahook Formation. The LWD GR and resistivity log responses throughout the interval are very uniform.

The siltstone is medium grey to dark grey-brown, soft to firm, sub-blocky with 0 – 5% calcareous grains, 20-30% clay, 50-60% silt, 5-15% very fine sand, 0 – 10% fine sand size grains with trace mica and trace carbonaceous matter. The sandstone consists of medium to light brown grains and dark grey coloured clasts, firm, sub-blocky made up of 5% clay, 15% silt, 50% very fine sand and 30% fine sand, moderately sorted, sub-angular, sub-elongate, siliceous cement with moderate strength, 5% calcite and 5% visual intergranular porosity. The claystone interbeds are silty, light grey coloured, very soft, dispersive, 5% calcareous grains, 60% clay, 30% silt, 5% very fine sand. The minor dolomite is described as medium brown, firm to moderately hard, angular, sharp fragments.

Near to top of the Demons Bluff Formation, one cuttings sample was examined for spore-pollen age assignment. Very few diagnostic palynomorphs were recovered from the sample and an uncertain zonation of *N. asperus* is assigned. Marginal marine depositional conditions are interpreted due to the rare dinoflagellates compared to the dominant and diverse spores and pollen present.

Eastern View Coal Measures
(1883.0 to 3182.6mRT, 1804.2 to 3002.2mTVDSS)

The Eastern View Coal Measures (EVCM) is a very thick succession of non-marine fluvio-lacustrine deposits at the base to nearshore and marginal marine sediments at the top of the formation. Younger volcanic related intrusives are also present within this formation. The formation ranges in age from Eocene to Paleocene in Yolla 4.

The formation can be split into 3 broad lithological units. The top unit dated as Middle to Late Eocene, based on the presence of the middle to lower *N.asperus* spore pollen zone, is sandstone-rich and is interpreted to be deposited in a marginal marine to near-shore marine environment. The middle unit is a highly thinly interbedded coal, siltstone and minor sandstone and is Early Eocene as it includes the *P.asperopolus* (from Yolla 1 data) to middle *M.diversus* spore pollen zones. These sediments are interpreted to have been deposited in a nearshore marine to non-marine lacustrine/lagoonal settings. The basal interval is dominated by thick beds of siltstone and sandstone and was deposited in a dominantly fluvial setting with minor nearshore or marginal marine influence. The age of these sequences is Early Eocene to Paleocene, as they span the spore-pollen zones lower *M.diversus* to lower *L.balmei*.

The topmost unit of the EVCM occurs between 1883.0 to 2182mRT in Yolla 4. As soon as the top of the EVCM is penetrated the GR log shows increasing grainsize accompanied by increase in gas readings. These both increase over the next 30 m (relative to TVDSS thickness), though the lithology is still dominantly siltstone with increasing fine sandstone appearing. The TEV4 unit (informal name) heralds the topmost sandstone of the EVCM in Yolla 1. This interval is dominated by sandstone within interbedded siltstone, and minor thin coal beds appearing near the base of the unit. The sandstone is medium brown to light brown grey, light green to off-white, clear to translucent, loose to soft, sub-blocky, composed of 20-30% clay, 0-30% silt, 0 – 70% very fine sand grains, 0 – 30% fine sand and 0 – 40% medium sand grains, 0 – 40% coarse sand grains, 0 – 20% very coarse sand grain size, which are poorly to well sorted, sub-rounded, sub spherical to sub-elongate, weakly argillaceous and weak silica cement, occasionally strongly pyrite cemented, trace carbonaceous grains and trace to 20% intergranular visual porosity. The interbedded siltstone is medium brown to brownish grey to black-grey to black-brown to white-brown, very soft to soft – friable, sub-blocky to sub-fissile, with trace calcareous grains, consisting of 10-50% clay, 40 – 70% silt and trace 30% very fine sand grains, and traces of pyrite, mica and carbonaceous grains. The coals are described as black, firm to friable, brittle, blocky, vitreous to sub-vitreous, sub-conchoidal to hackly fracture.

The middle EVCM unit occurs between 2182 to 2723mRT. This portion of the EVCM is composed of thinly bedded siltstone, coals, sandstone and minor claystone. The siltstones intersected are sandy in part, off-white to light brown to speckled black and becoming medium to dark brown and dark grey to grey with depth, moderately hard to very soft, sub-fissile to blocky, composed of 0 – 40% clay, 40 – 100% silt, trace – 20% very fine sand grains, 0 – 10% fine sand grains with traces of argillaceous matrix and micro mica and up to 5% carbonaceous grains and up to 15% carbonaceous laminae. The coals are black to dark brown, friable to firm, brittle, sub-vitreous to vitreous, blocky, sub-conchoidal to hackly fracture with trace argillaceous matter and silt. The sandstones are described as off-white to clear to light brown, translucent, loose to soft and composed of 0 – 40% clay, 5-10% silt, 15-80% very fine sand, trace – 40% fine sand, 10 – 60% medium sand, 0-20% coarse sand grains, very poorly to well sorted, rounded to sub-angular, sub-spherical to sub-elongate, and trace to 30% weak argillaceous or kaolinite matrix weak, trace rarely weak calcareous cement, fossils and carbonaceous grains and 3-20% intergranular visual porosity.

A normal fault was intersected in the well at an interpreted depth of 2582.5mRT, based on wireline log correlation with the other Yolla Field wells. Approximately 40 to 50 metres of section appear to be missing due to crossing from the downthrown side of the fault to the up-thrown side of the fault. This fault was predicted pre-drill from seismic interpretation but came in approximately 100m shallower than predicted.

An oil-bearing sand was encountered from 2603.7 – 2619.7mRT. This sand is informally named the *2458 sand*. The lithology was determined by petrological analysis of two MSCT's taken within this sand (Appendix 7) and is described as thinly laminated, well sorted very fine grained quartz arenites. The quartz grains are angular to subrounded. One sample contains abundant siderite with probable very high grain density. The thin laminae include fine organic fragments /stringers and compacted mica flakes. The minor lithics present (1.7 – 3.0%) are all low-grade metasedimentary rock fragments. Clays are mostly authigenic kaolin with very minor illite. Mica is a common accessory. Quartz overgrowths are minor having been inhibited by the presence of siderite and authigenic kaolin. Reservoir quality is poor in the 2 MSCT's examined with less than 2% total visual porosity.

At the base of this middle section, from 2723.4 – 2767.7mRT, a thick igneous sill has intruded into the sediment pile. The intrusive is a dolerite/gabbro described in Yolla 4 as mottled white green, speckled black, soft to firm occasionally hard, medium to coarse crystal size, common quartz, biotite, plagioclase, black to green pyroxene, calcareous, commonly altered to clay with a chloritic ground mass.

Below the intrusive, the lowermost portion of the EVCM was intersected between 2767.7 – 3182.6mRT. This interval is dominated by thickly bedded siltstones and sandstones, minor claystone and rare coal. This section contains the primary targets of the well which are the gas-bearing reservoirs of the Yolla Field known as the *2755, 2809 and 2973 sands*. The *2755* and *2809 sands* were almost entirely cored in Yolla 4. Detailed descriptions of these cores can be found in Appendix 8.

Above each of the reservoir zones are thick siltstone units which are providing top seal over the gas pay. The siltstones are described as light to medium to dark grey to grey black, brownish grey, soft to hard, blocky to sub-fissile, composed of 10-30% clay, 50-90% silt, 0-40% very fine sand grains and 0 – 5% fine sand grains with traces of dolomite, micro mica and pyrite, occasionally very carbonaceous.

The first sand unit encountered in this interval is the *2718 sand*. This sand is 6.1m thick (relative to TVD) in Yolla 4 was present between 2864.8 to 2871.4mRT. The sand had previously been interpreted as gas-bearing in Yolla 1, but is clearly water saturated in Yolla 4 based on wireline log and MDT data. The interval is interpreted from the wireline logs to have 4.2 mMD of net sand with an average porosity of 17.7%. The sandstone is described as light greyish yellow, soft to firm, sub-blocky consisting of 10% clay, 10% silt, 50% very fine sand and 30% fine sand grains which are moderately sorted, sub-angular, sub-elongate to sub-spherical and weakly cemented with silica and weak argillaceous matrix (10 – 20% of total cuttings) 3% visual intergranular porosity.

The next major sand unit to be drilled was the *2755 sand* between 2902.7 – 2912.1mRT. This gas-bearing sand was fully cored and consisted of mainly sandstone with minor siltstone and coal. The sandstone colour varies from pale cream to light to medium brown with clear to translucent grains and is moderately hard to friable, composed of 20% silt, 40% very fine sand, 40% fine sand, moderately sorted, sub-angular, sub-spherical, moderately strong argillaceous cement, silty in part with 5 – 15% visual intergranular porosity. Two core plugs within this sand were selected for petrological analysis (Appendix 7). One sample, taken in a low permeability interval, is a very fine grained quartzarenite with little intergranular porosity mainly due to authigenic kaolin filling pore space along with minor quartz overgrowths and compacted siderite grains. The other sample, taken in a high permeability zone is a much coarser quartzarenite, being upper medium grain size and more quartzose. Most porosity reduction is due to quartz overgrowths with minor kaolin formation and physical compaction. Core analysis through the sand (not including the non-net intervals at the top and base of the core) had average measured porosity of 17.3% (range 2.0 – 23.1%) and average permeability of 853 mD (range 0.41 – 4616mD. Detailed core description (Appendix 8) of the 2755 sand interprets the overall facies as alluvial to lacustrine with sheetflood deposition dominant. The top half of the sand is thin bedded and deposited in a lacustrine fan-delta shoreline within a transgressive systems tract. The basal half of the sand is thick bedded and may have been deposited in an alluvial fan/fan delta within a lowstand systems tract. The overlying siltstone and coal was probably deposited within a coastal plain environment. The basal section of core is

siltstone and mudstone dominated and is interpreted as back barrier lagoon facies with coastal mire/vegetation mats to progradational lacustrine sheetflood fan delta facies.

The *2809* gas-charged sand is the third sand body encountered in this section and is present between 2962.6 – 2984.8mRT with a vertical thickness of 20.8m. Core #2 covered the entire gas column. The sands in this interval are described as light to medium brown and light brownish grey to medium grey, firm to moderately hard comprising occasional clay matrix (0 – 20%), trace 30% silt, 5-40% very fine sand, 10-70% fine sand grain size, 10-30% medium sand, trace – 30% coarse sand, 20% very coarse sand and trace granule size grains, which is mainly very poorly to moderately sorted, well sorted at the base, sub-angular and sub-spherical to sub-elongate grains with moderate to strong siliceous and weak to moderately strong argillaceous cement, 10 – 20% visual intergranular porosity, decreasing to 3% at the base of the sand. Two thin sections from core plugs which represented end members in the permeability measured within the 2809 sand were submitted for petrological analysis (Appendix 7). The low permeability sample is a well sorted fine grained sublitharenite containing thin siderite and heavy mineral laminae. Authigenic kaolin has almost completely filled available pore space. The high permeability sandstone is an upper coarse grain size quartzarenite that has undergone severe grain contact dissolution. Further porosity reduction is due to minor quartz overgrowths and patchy kaolin matrix. Framework grains are commonly rimmed by bitumen which has inhibited quartz overgrowth cementation leading to very high porosity and permeability. Core analysis results show an average measured porosity of 17.3% (range 0.5 – 23.1%) and average permeability of 337 mD (range 0.05 – 2121mD). The interpretive core description (Appendix 8) places most of the sand as deposited within a sheetflood dominated alluvial fan/fan delta facies. The basal 5m section of the core is slightly finer grained and is interpreted as deposited within a prograding lacustrine wave-influenced shoreline.

Below the *2809 sand*, 2 poorly developed coarsening upward sequences are present and these both culminate in 2 thin sand units at the top. They have been correlated with the *2844 sand unit* in Yolla 1. In Yolla 4 the *2844 sand* is gas-bearing and was intersected from 3005.0 – 3014.9mRT. The sand unit is mainly tight and is interpreted to contain of 1.3 metres of net-pay only.

The *2844 sand unit* consist of white, clear to translucent grains, loose to soft, 20% fine sand, 40% medium sand, 30% coarse sand and 10% very coarse sand, poorly sorted, angular, elongate, weak siliceous cement and 20% visual intergranular porosity.

A very thick siltstone with minor claystone is present between the *2844 sand unit* and the deepest sandstone units in the well. The unit is very argillaceous and silty with 30% very fine sand and 10% fine sand grains, well sorted, sub-rounded, sub-spherical, weak argillaceous cement with trace carbonaceous grains and trace visual intergranular porosity. The claystone is light grey, soft, dispersive, composed of 50% clay, 30% silt and 20% very fine sand.

The lowermost sandstone intervals in Yolla 4 are termed the *2952* and the *2973 sands.* The *2952 sand* is interpreted to be tight and water saturated and was intersected between 3118.3 to 3130.1mRT in Yolla 4 and is 11.7m thick (referenced to TVD). This sand is off-white to light brown, moderately hard, sub-blocky comprising 15% clay, 5% silt, 40% very fine sand, 40% fine sand and trace of medium sand size grains. The sand is well sorted and grains are sub-angular and sub-spherical with moderately hard argillaceous matrix with trace carbonaceous matter and 5% visual intergranular porosity.

The *2973 sand* is the deepest gas-bearing unit in Yolla 4. It is 15.7m thick (referenced to TVD) and occurs between 3149.4 – 3165.4mRT in the well. The sands of this interval are off-white to light brown, soft, sub-blocky composed of 10% clay, 20% very fine sand, 30% fine sand and 40% medium sand grains which are moderately sorted, sub-angular and sub-spherical with weak argillaceous cement and 10% visual intergranular porosity.

Below the gas-bearing zones in the well, the basal 17m of the EVCM consists of interbedded argillaceous very fine sandstone and siltstone. The sandstone is off-white to light brown, firm, sub-blocky comprising 30% clay, 60% very fine sand and 10% fine sand which is well sorted, sub-angular and sub-spherical grains with a moderately to strong argillaceous cement and up to 5% visual intergranular porosity.

Basal Volcanics
(3182.6 to 3235.0mRT, 3002.2 to 3054.3mTVDSS)

Between the base of the EVCM and total depth in Yolla 4 a basalt sequence was drilled. The basalt varied from relatively fresh to extremely altered, probably due to weathering. The age of the basalts is interpreted to be Late Cretaceous or Early Paleocene.

The weathered basalt is described as off-white to very light brown mottled, occasionally pale yellowish brown, firm, blocky, very fine groundmass, rare weathered feldspar and pyroxene, trace indistinct flow structure, commonly weathered to clay, trace black obsidian. The unaltered basalt is dark greenish black, reddish brown to purple grey, very common olivine to 70% occasionally weathered, minor pyroxene, occasional red/brown ground mass, common free calcite, rare indistinct flow structure.

Within the basalt are some minor interbedded sandstone and siltstone. The sandstone is light brown to light grey, firm, sub-blocky consisting of 30% clay, 60% very fine sand and 10% fine grained sand which is well sorted, sub-angular and sub spherical grains with a moderate strength argillaceous matrix and up to 25% kaolinite and 5% intergranular visual porosity. The siltstone is medium to dark grey, moderately hard, sub-fissile and composed of 30% clay, 40% silt, 30% very fine sand, trace fine sand grains and trace carbonaceous matter.

3.3 Reservoir Evaluation

3.3.1 Petrophysical Summary

A comprehensive petrophysical review was conducted to assess the reservoir quality and hydrocarbon saturation of all zones which displayed good hydrocarbon shows while drilling (Appendix 1). These zones were concentrated in the Eastern View Coal Measures (EVCM) but included one zone within the Angahook Formation. The study entailed an analysis of all available lithological data, core samples and MDT and production test data. Full diameter cores were acquired through the entire section of the 2755 and 2809 sandstone and have been analysed to determine RCA and SCAL properties which were then used to calibrate the log analysis. A summary of the log analysis is presented in Table 1. The results through the main gas reservoirs in the EVCM are summarized below:

The 2718 sand (2864.8 – 2871.4mRT) is good quality sandstone, but water bearing at Yolla-4. The interval is interpreted from the wireline logs to have 4.2 mMD of net sand with an average porosity of 17.7% and

permeability of 588 mD. There is no net pay. A minor sandstone at 2882mRT is gas bearing and was proved by MDT testing to be potentially productive. Log analysis indicates that this zone has a net pay thickness of 2.1 mMD, with an average porosity of 19.5% and permeability of 41 mD. The average water saturation is 28%.

The 2755 sand (2902.7 – 2912.1mRT) was cored throughout. The interval contains a shaly sandstone down to 2907mRT and is then clean at the base. MDT and log analysis indicates that the interval is gas saturated and productive. The 2755 zone is interpreted from the wireline logs to have 7.7 mMD of net sand with an average porosity of 17.4% and permeability of 741 mD. All the net sand also qualifies as net pay with an average water saturation of 16.8%.

The 2809 sand (2962.6 – 2984.8mRT) was also cored throughout. The interval is composed of very clean sandstone with good reservoir properties. This interval is interpreted from the wireline logs to have 21.5 mMD of net sand with an average porosity of 17.3% and permeability of 429 mD. There is 21.3 mMD of net pay, defined as net sand with water saturation less than 60%, with an average porosity of 17.4% and permeability of 432 mD.

The 2973 sand (3149.4 – 3165.4mRT) has two reservoir intervals divided by a shaly non-net interval. The clean sandstones at top and base are productive intervals. From the wireline logs, the 2973 is interpreted to have 13.0 mMD of net sand with an average porosity of 14.7% and permeability of 212 mD. There are 9.8 mMD of net pay, defined as net sand with water saturation less than 60%, with an average porosity of 16.4% and permeability of 281 mD.

Two further potential reservoirs were discovered whilst drilling this well:

An Angahook sandstone at 1315 – 1324mRT, which was only logged with LWD GR-RES. The mud gas and MWD resistivity responses suggest either this interval is a tight oil sand or contains residual oil saturation.

An oil bearing sandstone, termed the 2458 sand, was penetrated at the base of the 12 ¼" hole section and logged in the TD suite. Rotary sidewall cores, MDT pressures and samples and a full wireline log suite were acquired in this interval. The 2458 sand is interpreted from the wireline logs to have 6.3 mMD of net sand with an average porosity of 21.1% and permeability of 95 mD. There is 2.5 mMD of net pay, defined as net sand with water saturation less than 60%, with an average porosity of 21.4% and permeability of 167 mD.

GROSS INTERVAL				NET PAY				
Reservoir Zone	Top mRT	Base mRT	Thickness* mMD (mTVDSS)	Thickness* mMD (mTVDSS)	Net / Gross [%]	Phi [%]	K [m]D	Sw [%]
2458	2603.7	2619.6	15.9 (14.5)	2.5 (2.3)	15.9	21.7	166.9	47.6
2718	2864.8	2871.4	6.6 (6.1)	0 (0)	NA	NA	NA	NA
	2882.5	2887.1	4.6 (4.2)	2.1 (1.9)	45.7	19.5	41.2	44.7
2755	2902.7	2912.1	9.4 (8.7)	7.7 (7.1)	81.9	17.4	742	16.8
2809	2962.6	2984.8	22.2 (20.8)	21.3 (20.0)	95.9	17.4	433	20.9
2844	3005.0	3014.9	9.9 (9.4)	1.3 (1.2)	13.1	19.9	674	54.8
2952	3118.2	3130.1	11.9 (11.7)	1.5 (1.5)	12.6	16.5	1.37	42.0
2973	3149.4	3165.4	16.0 (15.9)	9.8 (9.8)	61.3	16.5	281	23.5
2718 - 2973 inclusive								
Total Gas Zone	**2882.5**	**3165.4**	**80.6**	**43.7**	**54.2**	**17.3**	**427**	**23.9**
All reservoirs			96.3	46.2	48.0	16.7	413	24.4

* note: thickness calculation ignores effects of structural dip which is in the order of 0 to 5 degrees (see dip meter interpretation in Appendix 10 for local dip variation and azimuth)

Cut-offs applied				
Reservoir Zone	**shale volume**	**Porosity**	**permeability**	**Water saturation**
2458 (oil zone)	< 40%	Not directly applied	> 1 mD (oil)	< 60%
2718 – 2973	< 40%	Not directly applied	> 0.1 mD (gas)	< 60%

Table 1: Net Pay Summary

3.3.2 Core Analysis Summary

Routine Core Analysis (RCA) and Special Core Analysis (SCAL) were performed by ACS Laboratories Pty Ltd. The RCA report is contained in Appendix 4 of the Basic Well Completion Report. The Special Core Analysis (SCAL) report is included in Appendix 9 of this volume.

Two 36m cores were acquired in Yolla 4 within the EVCM main gas bearing intervals. The top core covered the entire 2755 sand and the second core covered the 2809 sand. In addition to the conventional core, MSCT's were recovered from within the 2458 oil sand and the 2973 gas sand. A plot of the porosity versus permeability, displayed by zone, is presented in Figure 4. The summary of the average porosity and permeability values for each of the reservoir intervals is shown in Table 2 below.

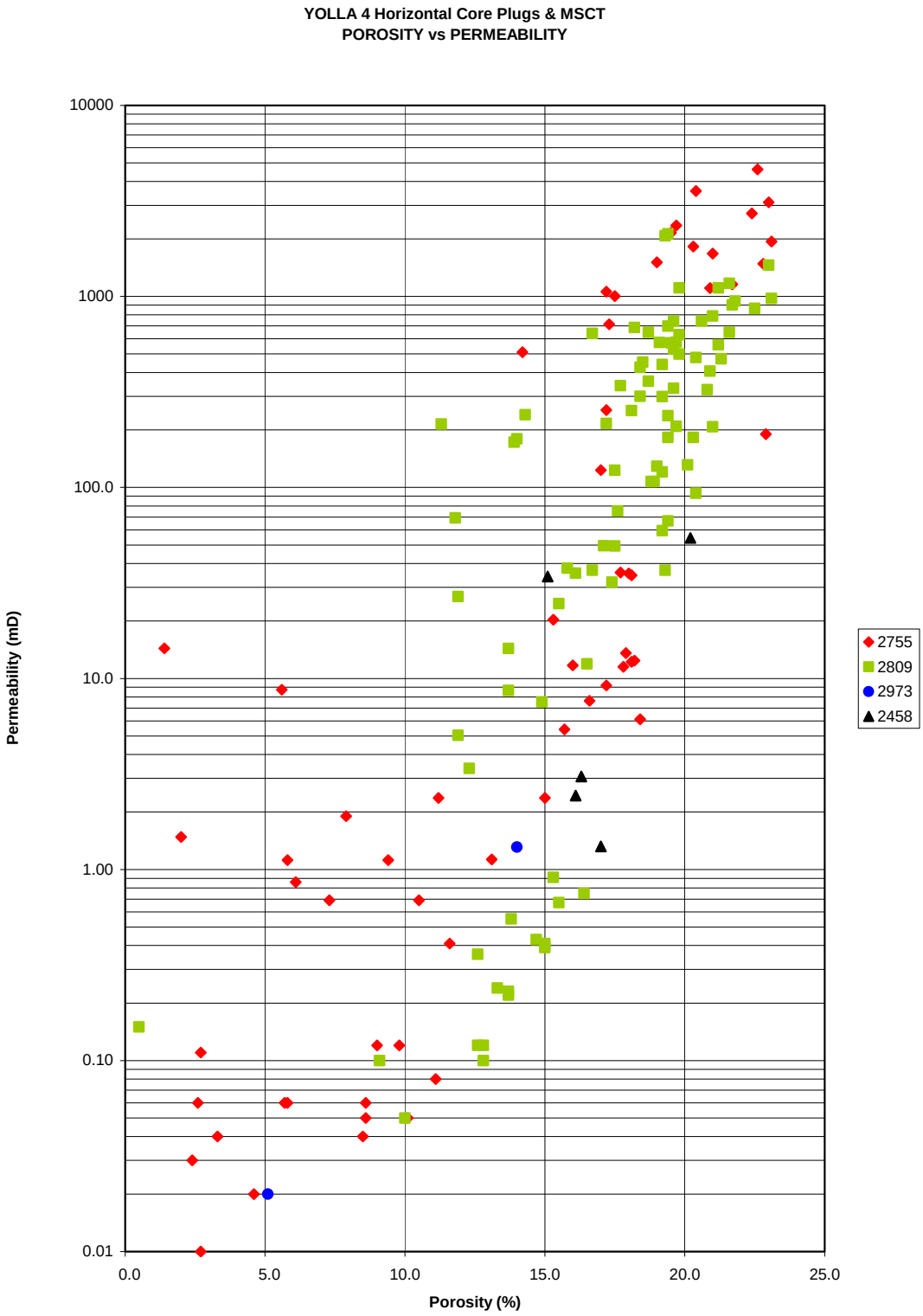

Figure 4: Measured Porosity versus Permeability

Zone Name	Average Porosity	Average Permeability
2458	15.7%	19.1 mD
2755	12.9% *	546.2 mD *
2809	17.3% *	336.8 mD *
2973	10.6% **	0.7mD **

* horizontal core plugs

** only 3 MSCT's recovered

Table 2: Average Porosity and Permeability Data

3.3.3 Facies Interpretation

A sedimentological study of Cores 1 and 2 from the Eastern View Coal Measures in Yolla 4 indicate that these intervals were deposited in a lacustrine shoreface and fan delta setting. Interpreted depositional environments include alluvial fan, shoal water type fan delta, interdistributary bay fill / low energy shoreline, wave influenced shoreface / fan delta, and offshore lacustrine. The alluvial fan facies indicate sediment dispersal by flashy, hyperconcentrated flows in the form of sheetfloods and weakly channelised flows. Abandonment facies comprising fine-grained, distal sheetflood deposits, coal, carbonaceous mudstone, and root traces represent lobe switching and transgression. The shoal water type fan delta indicates shallow water deposition from high density turbidity currents and suspension settling on a low gradient delta front. The wave influenced shoreface / fan delta and the interdistributary bay fill / low energy shoreface record sedimentation on the margins of the lake. No inferences about shoreline morphology; apart from higher energy, open to wave conditions, in Core 2, and possible restricted embayment in Core 1; can be made from the cores due to lack of spatial data. The offshore lacustrine sediments record anoxic bottom conditions indicating a stratified lake.

High resolution sequence stratigraphy has been used to subdivide the strata into fourth-order systems tracts and, longer period, third-order sequences. Falling stage and lowstand deposits of forced regressions are recorded by the sharp based, aggradational to progradational alluvial fan deposits. Transgressive phases overlie sharp surfaces across which there is a rapid deepening, with or without a transgressive lag (ravinement surface) and record normal regression (parasequences) stacked in an overall retrogradational style. Highstands are represented by stacked coarsening upward parasequences of shoreface and fan delta sediments.

The alluvial fan deposits represent progradation of coarse-grained sediments, from the footwall margin of the half graben, into the basin centre during tectonically quiescent periods, whereas variations in parasequences may result from climate induced sediment supply and lake level fluctuations. Reservoir quality is strongly influenced by facies with the highest permeability occurring in the alluvial fan facies. Other reservoirs occur in the shallow sub-aqueous fan delta and the wave influenced shoreface / fan delta, although the permeability in these facies is two to three orders of magnitude less than the alluvial fan facies. The core analysis and facies study report including core photographs and graphical core log representations are included in Appendix 6.

3.4 Hydrocarbon Source Evaluation

3.4.1 Maturation

Vitrinite Reflectance (Vr) studies were undertaken on a set of cuttings samples by Dr A. C. Cook of Keiraville Konsultants (Appendix 5). The results have been plotted against true vertical depth and are compared to the Vr results from Yolla 1 (Figure 5). The assumed source rocks for the Yolla Field oil and gas accumulations are the Paleocene to early Eocene coals within the EVCM (Boreham et al, 2003). All petroleum expulsion maturities quoted here are based on the coal maturity work as published by Boreham et al, 2003.

At the Yolla 4 well location the maturity for the main oil expulsion window between Vr 0.75 and 0.95% occurs between 2550 – 3050mTVDSS. The main gas window at Vr > 1.2% occurs below TD of the well, at an extrapolated depth of 3550mTVDSS. The igneous intrusion within the EVCM in Yolla 4 has caused an increase in maturity in the sediments immediately surrounding the intrusive, up to 4% Vr, based on cavings in samples below the intrusion. A.C. Cook estimates that the contact aureole around the intrusion is probably less than 75m in thickness as the heat-altered zone was not directly studied. The likely localised effect of the intrusion may have generated minor quantities of methane and may possibly have introduced some CO_2 of igneous origin to the gas charge.

The results from Yolla 4 show maturities slightly higher than the Yolla 1 Vr. The Yolla 1 results underestimate the maturity at any depth compared to Yolla 4 by 100 to 150m. This small difference in results can be mostly explained by the fact that different analysts undertook the work, with the Yolla 1 Vr being undertaken by Dr B. Watson of Amdel Laboratories (Amoco 1986). The Yolla 1 results include samples where the influence of cavings was not taken out of the final estimated Vr.

The Vr results do not appear to be suppressed at all and can be used with high confidence. This assumption is corroborated by comparison of Vr with vitrinite-inertinte reflectance and fluorescence (VIRF) in other Bass Basin wells (Boreham et al 2003).

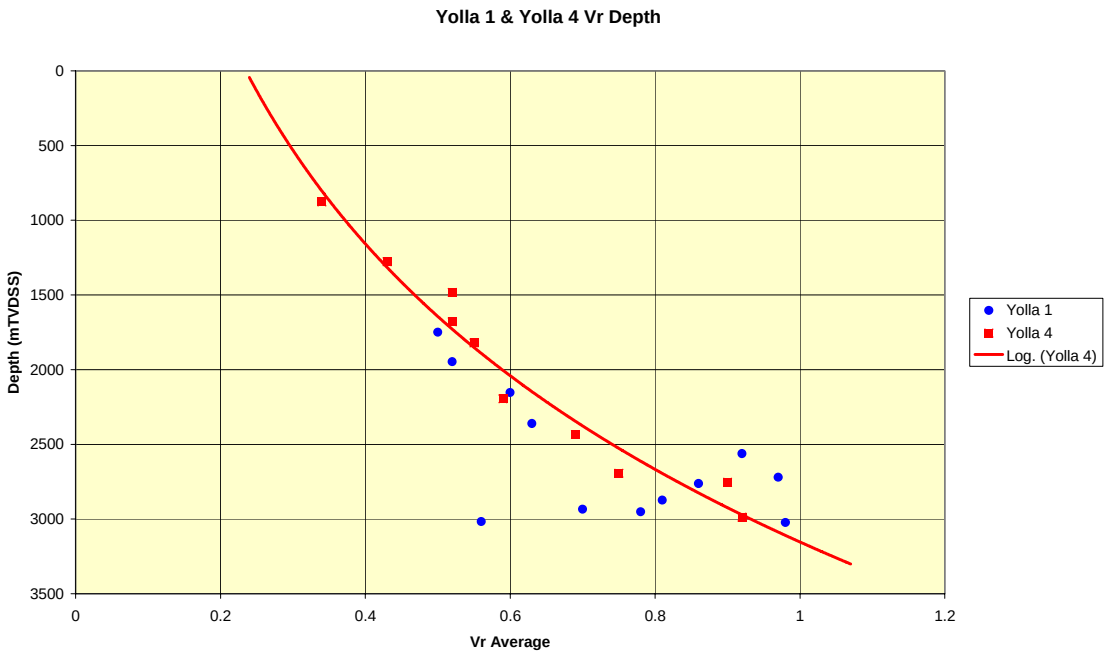

Figure 5: Vitrinite Reflectance profile with depth, Yolla 4 and Yolla 1

3.4.2 Source Rock and Hydrocarbon Evaluation

One oil sample and one sediment sample from Yolla 4 were analysed geochemically for biomarkers (see Appendix 4) to determine if the oil discovered in the 2458 sand could have been sourced from the coals within the EVCM.

Previous published studies (eg. Boreham et al 2003) concluded that the coals within the EVCM were the source of gases and liquids discovered in the Bass Basin to date. The oil recovered from Yolla 4 at 2609.5mRT is characterised as sourced from a mature source rock which contains a very high amount of terrestrial organic matter (most likely a coal) and was deposited under oxic conditions.

The sediment sample analysed was a core chip taken from a coal in Core #1. A core chip was preferred over cuttings for analyses to reduce the possibility of mud contamination and to have a clean coal sample which has not been diluted with other lithologies, such as a cutting sample would have. There was no need to analyse any more samples within the EVCM of Yolla 4, as Yolla 1 had an extensive geochemical programme undertaken.

As expected the coal sample has excellent potential to generate liquid hydrocarbons. TOC of the sediment sample is 68.52% and Rock-Eval pyrolysis results confirmed the oil-prone nature of the coal with high S2 of 170 mg/g and HI of 248. The high S1 value (12.00mg/g) could be attributed to the very close proximity to the 2755 gas reservoir which underlies the coal and is contained within the same core. The hydrocarbons extracted from the coal are interpreted to have been generated from highly terrestrial organic matter which was deposited in an oxic depositional environment.

The geochemical study concludes that there is a strong genetic relationship between the Yolla 4 oil and sediment extract and that the source rock of the oil is the same facies as the coal sample analysed. Similarities include

the almost complete lack of C_{27} diasteranes and steranes, the presence of diterpanes and the overall aromatic and branched/cyclic patterns.

The oil sample and one gas sample were submitted for CSIA (compound specific isotope analysis). The raw CSIA data can be found in Appendix 4. These were plotted against previous CSIA study results from other Yolla wells (Boreham et al 2003) to ascertain if the Yolla 4 oil shared the same source as oils, condensates and gases as the hydrocarbons seen in Yolla 1 and Yolla 2 (Figure 6).

The position and shape of the gas to oil CSIA profiles can be interpreted as a relatively smooth continuum in the n-C4 to n-C5 wet gas components to the C7 to C8 range of n-alkanes in the oil samples. This implies the gases and oils are genetically related and most likely generated from the same source (Boreham et al 2003).

The Yolla 4 oil CSIA profile strongly follows the profile from the top EVCM oil from Yolla 1 (and to a lesser extent the condensate from the 2809 sand in Yolla 1) indicating they have all probably been expelled from the same source rocks. The same can be said for the Yolla 4 gas sample which plots very closely to the Yolla 2 gases (Figure 6).

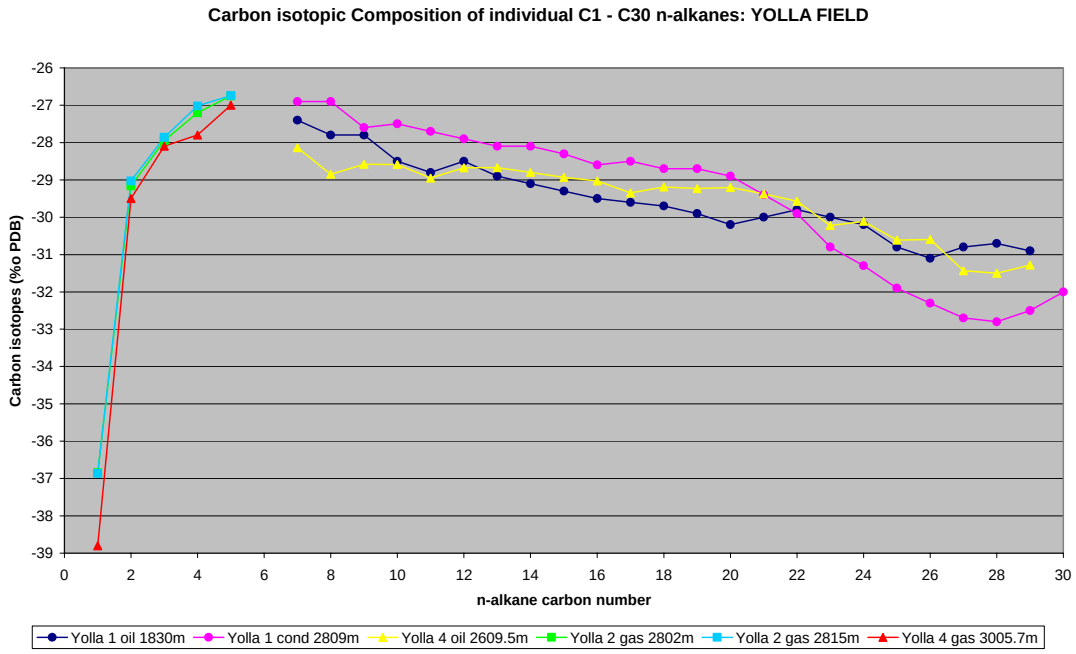

Figure 6: Carbon isotopic composition of individual C1 – C30 n-alkanes: Yolla Field

3.5 MDT Pressure Data Interpretation

The Yolla 4 MDT programme was conducted over the interval 2604.5 – 3174.7mRT. In total 53 pre-tests performed. 35 pre-tests were valid, 4 were supercharged, 12 were tight tests and 2 lost seal to formation. A summary of the pre-test data is included in Appendix 11 of the Yolla 4 WCR Basic Data. Appendix 2 this volume contains the interpretation and graphical representations of the MDT data.

A summary of the results is given below:

Yolla 4 – GWC Interpretation		
Sand	Fluid	GWC(mss)
2718	Water	-
2755	Gas	2834.0
2809	Gas	2828.2
2973 (Upper)	Gas	2990.2
2973 (Lower)	NA	-
2458	Oil	2470.0(est OWC)

Table 3: Post Yolla 4 Gas-Water Contact Interpretation

3.6 Production Testing Interpretation Results

A flow test program was carried out as a part of the Yolla 4 completion procedure using the drilling rig facilities and surface testing equipment (Appendix 3). Completion fluids, such as brine and diesel, had to be removed from the wellbores before they can be produced into the Yolla-A platform process facilities. All the completion intervals were opened to flow as part of the clean up operation in order to remove completion brine from all annular spaces and from the formation. This also provided a good opportunity to conduct a short flow test to clean up the well, estimate productivity, and obtain samples of produced fluids from each sand unit.

The table 4 summarises the results of the testing.

Yolla 4 Initial Clean-Up Flows - Estimates of Zone Productivity

Zone	Perfs Top m RT	Perfs Bot m RT	Flow Rate mmcfd/bopd	FWHP psia	FWHT deg C	Choke /64"	SIWHP psia	Mid Perfs m SS	FBHP psia@gauge	Gauge m SS	Gradient psi/m	FBHP psia@MPP	Pi (MDT) psia	k.h (est.) md.ft	D (est.)	Darcy Skin
2458	2604.0	2610.0	2700	1599	57	40	2311	-2464	2950	-2816.6	0.7	2703	3629			
2755	2902.5	2914.0	32.2	2787	61	52	3243	-2738	3740	-2816.6	0.331	3714	4148	25542	0.0001	52
2809	2962.5	2973.0	32.1	2860	77	52	3226	-2794	3829	-2816.6	0.352	3821	4161	18486	0.00005	45
2973	3149.0	3157.5	27.2	2823	60	44	3406	-2973	3731	-2823.2	0.31	3777	4388	4250	0.00003	22

Notes:

1 Flow rate from 2458 sand based on Gilberts correlation assuming 3 mmcfd flow past the plug above the 2973 Sand
2 Flowing bottomhole pressures, FWHP and FWHT were all rising during the tests indicating the well was still cleaning up and stabilising
3 k.h from core for 2755 and 2809 sands, from buildup for 2973
4 D coefficients from Woodside correlation (except 2973 sand - from test analysis)

Table 4: Yolla 4 Estimates of Zone Productivity from Initial Clean-up Flows

4. GEOPHYSICAL DISCUSSION

4.1 Seismic Data

Yolla 4 was located on the basis of the structure mapping derived from the reprocessing of the Yolla 3D seismic survey in 2000. The survey was reprocessed to improve resolution in the lower EVCM which suffered from severe multiple contamination and limited energy penetration below the coal seams which overlay the main reservoir sands. The final reprocessed data set improved attenuation of multiple energy and yielded better imaging of faults and dykes than the original data. Hence the main reservoir horizon reflectors, (coinciding with the 2718 and 2809 sands), while still weak, could be mapped with relative confidence. Detailed velocity analysis was conducted to yield depth maps. These provided the framework for constructing a detailed geological model prior to the field development decision. The Yolla 4 well path was designed on the basis of this model. A full account of the seismic reprocessing and final data quality can be found in the Yolla 3D 2000 Reprocessing and Interpretation Report, (Taylor, 2001).

4.2 Structure

The Yolla structure is a Paleocene-Eocene aged tilted fault block bounded by faults on two sides, one striking NW and the other approximately N-S. The faults intersect at approximately 120 degrees. An additional NW striking fault sets up a second culmination south of the main northern bounding fault, (Figure 7). Yolla 4 was drilled to drain reserves from the Paleocene gas bearing sands in this southern culmination. The top EVCM is also a hydrocarbon bearing closure formed by drape and some late fault movement over the deeper fault block, (Figure 8).

There was considerable volcanic activity in the area during the Miocene, during which time a volcano formed to the north, and a suite of dykes and sills developed that intersect the structure. The main sill in Yolla 4 while more than 40 metres thick, is relatively seismically transparent.

The well intersected the main reservoir sand (2755 Sand) at 2733m below MSL approximately 1000m north of Yolla 2.

4.3 VSP and Well Tie

A walk above VSP was conducted to provide an accurate seismic to well tie. In a walk above VSP the source is positioned vertically above the well bore, so that the recorded seismic ray paths are close to normal incidence. Schlumberger's VSI tool, (configured with four detectors) was used for the data acquisition. This yielded a high quality well-bore seismogram that was reliably tied to the seismic. A 28ms shift was required to tie the Yolla 3D repro 2000 dataset. Details of the acquisition and processing may be found in the Yolla 4 WCR, Basic Data Volume, Appendix 9.

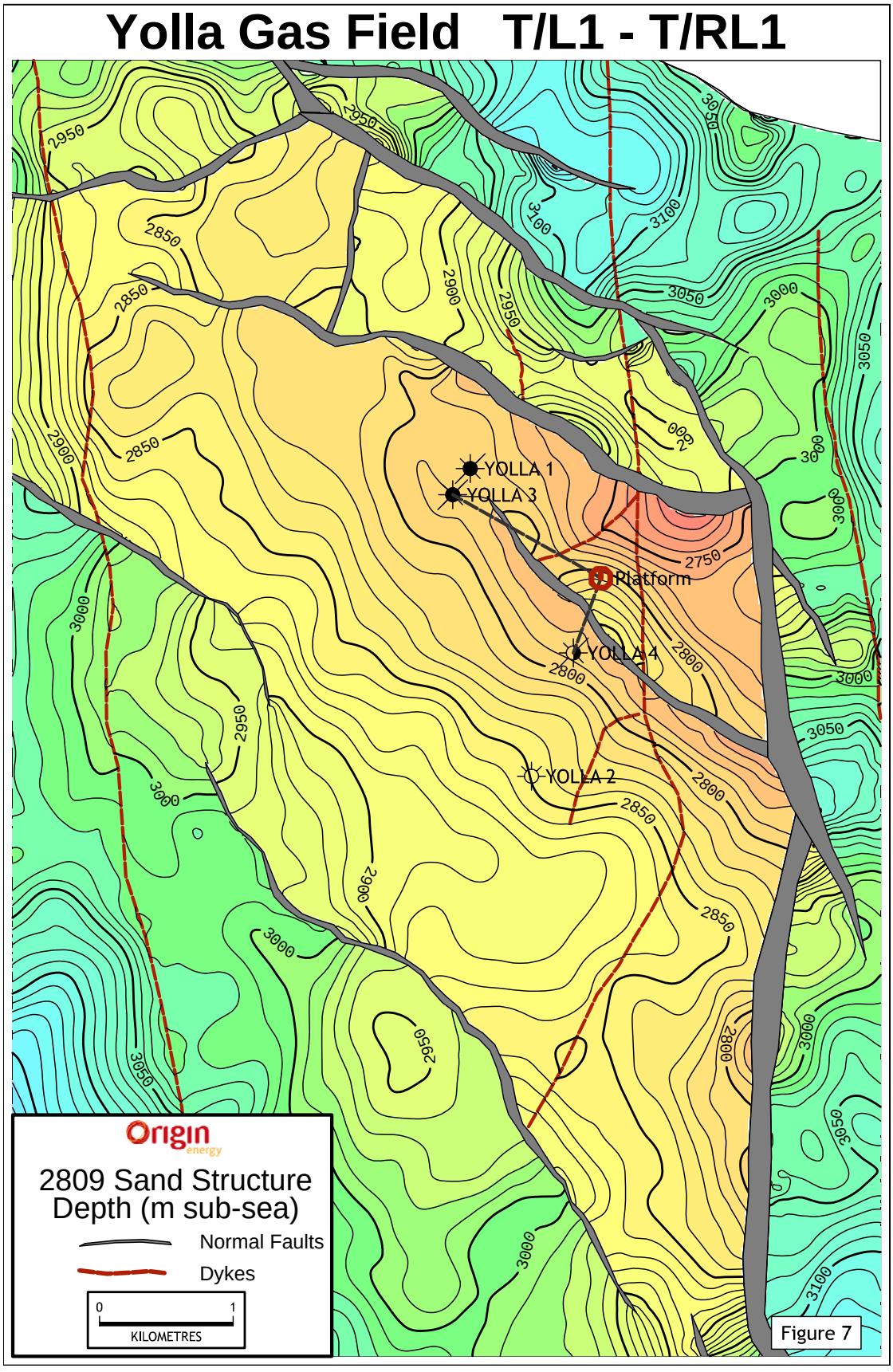

Figure 7: Top 2809 Sand - Depth Structure Map

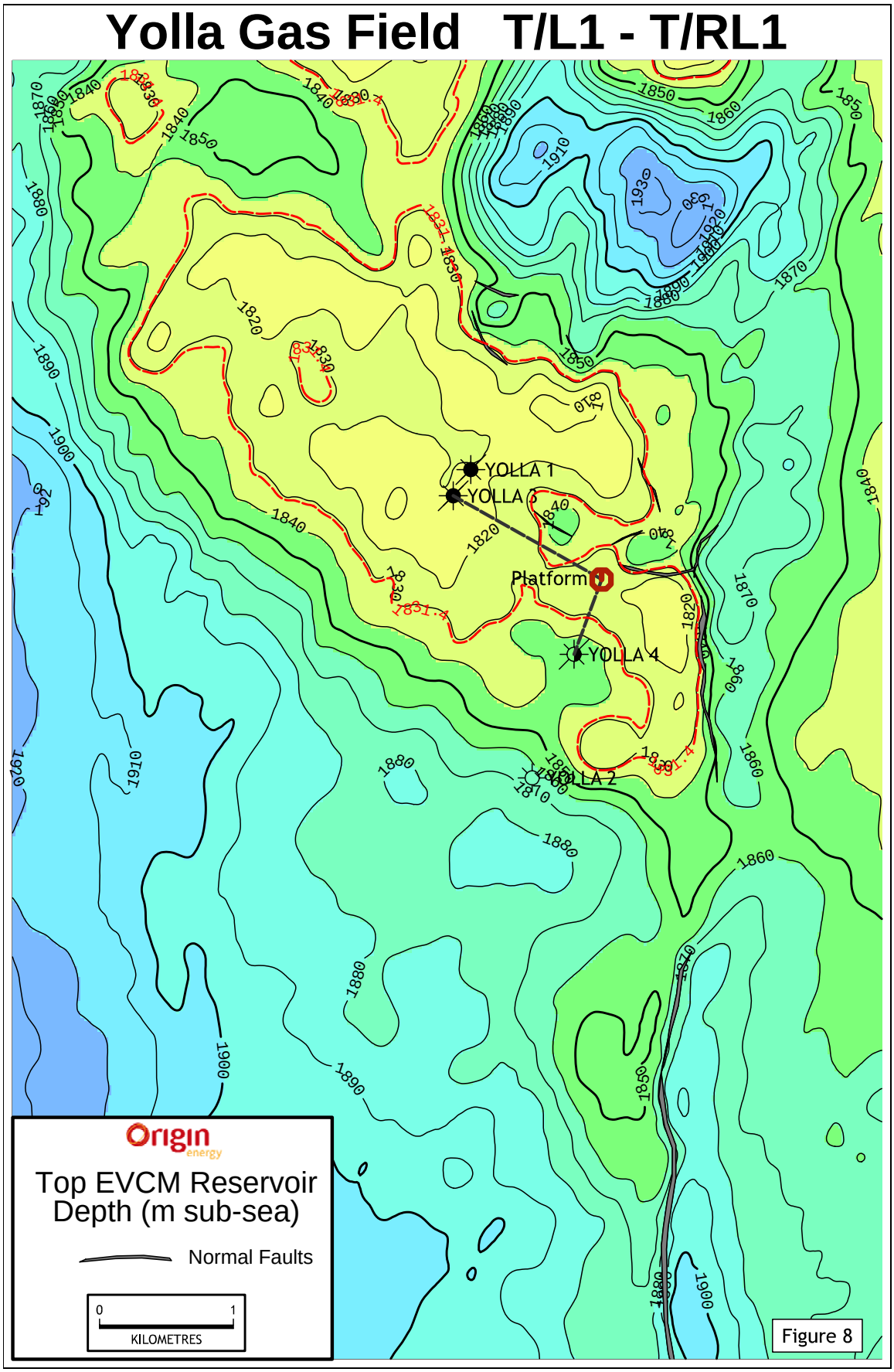

Figure 8: Top EVCM Reservoir - Depth Structure Map

4.4 Actual Versus Predicted Depths

Figure 3 shows the actual versus predicted formation tops. The VSP tie to the seismic indicates that the top EVCM event was correctly correlated, (as would be expected given the data quality at this level), however for the 2718 and 2809 sands, the pre-drill seismic picks were too high resulting in the actual depths being low to prognosis by 34m (2718 Sand) and 14m (2809 Sand) respectively. This difference is attributed to poor imaging of the seismic data in the shadow of the fault which bounds the Yolla 4 sub-culmination, Figure 9.

The position of the fault at 2436mSS was substantially higher than predicted from the seismic. This resulted from about 60m of lateral displacement between the position on the seismic and where the VSP tie shows the fault to be. The discrepancy may be related to imperfect lateral positioning after the seismic migration. The displacement is not considered enough to unduly affect the current maps, but suggests room for improvement in case of future seismic reprocessing. The inclusion of an anisotropy term in the migration may help reduce the discrepancy.

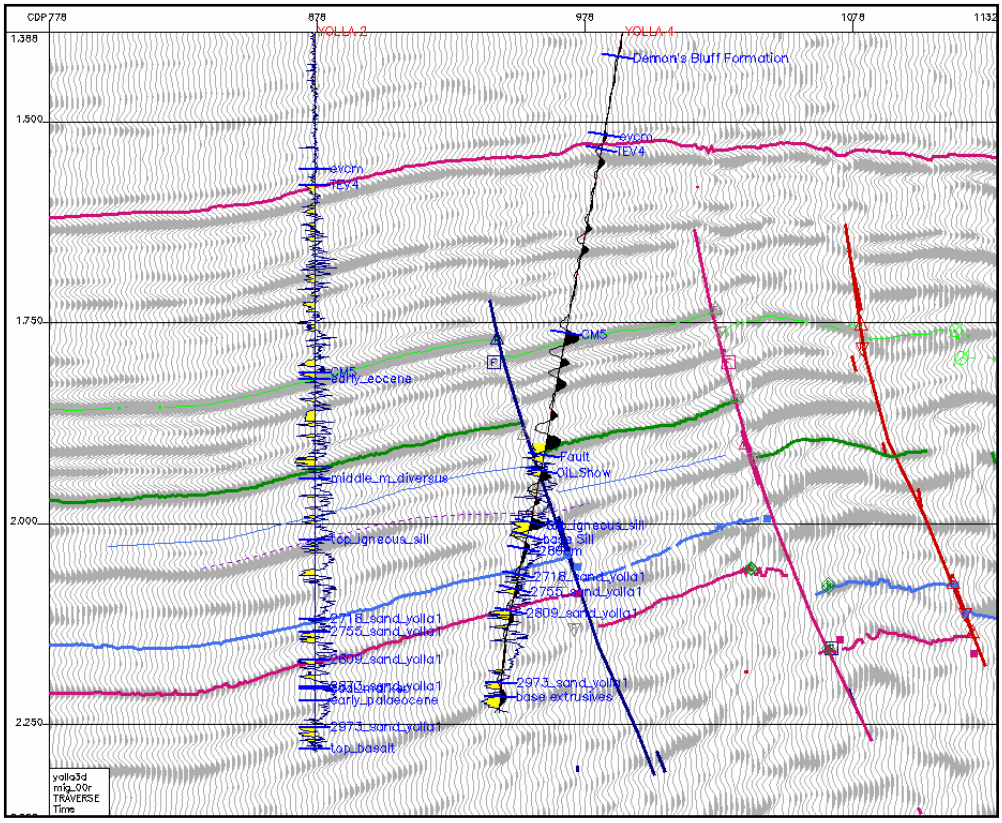

Figure 9: 3D Seismic Traverse from Yolla 2 to Yolla 3

5. GEOLOGICAL DISCUSSION

5.1 Exploration History

The Yolla Gas Field is a large northwest-southeast trending fault bounded structure which has been compartmentalised by major faults.

Two wells have been previously drilled in the Yolla Field. Yolla-1 was drilled in June 1985 by AMOCO Ltd and encountered gas in both the Intra-Eastern View Coal Measures (EVCM) between 2700m and 3000mRT, and also in the Upper-EVCM at approximately 1830mRT. Gas Pay was encountered in 5 separate zones within the Intra-EVCM, and these provide the main reserves for the BassGas development. DST 1 in Yolla-1 tested gas and liquids from the 2809 Sand of the Intra-EVCM at rates of up to 425 000 m^3/day and 92 kl/day respectively (15.1 mmscfd and 580 bcpd). Yolla-1 was suspended for possible future re-entry.

A 3D seismic survey was acquired over the Yolla Field in mid 1994 with the aim of enabling accurate depth mapping for the purpose of reserves estimation and appraisal/development planning. These data were subsequently reprocessed in early 2000. Updated depth maps were produced in December 2000 and January 2001 and form the basis for the latest field review and basis for the development plan issued in September 2002.

The Yolla-2 appraisal well was drilled in April and May 1998. The well was drilled 2.35km SSE of Yolla-1, and approximately 45m down-dip at the intra-EVCM reservoir level. The well demonstrated good correlation to the sands intersected in Yolla-1, although many were intersected below the gas-water contact due to the low structural location of the well. Pressure data allowed confident interpretation of GWC levels in the different Intra-EVCM units. Yolla-2 was plugged and abandoned.

5.2 Regional Geology

5.2.1 Structure

The Bass Basin is located offshore in south-eastern Australia between Victoria and Tasmania. It is one of a series of sedimentary basins that were formed in response to rifting during the Late Jurassic to Early Cretaceous between Australia and Antarctica (Williamson et al, 1987). The Bass Basin covers approximately 65,000 km2 and water depths range from 30 to 90 m.

The Bass Basin is a failed intra-cratonic rift basin with structural features which highlight three separate phases of evolution: 1) initial northeast-southwest extension during the early Cretaceous, 2) Late Cretaceous to Pliocene thermal subsidence and 3) Miocene compression. The rifting created a series of northwest-southeast oriented grabens offset by associated east-west wrench movement. The Pelican, Yolla and Cormorant Troughs comprise the major depocentres in the Bass Basin (Fig. 3). The Yolla Field is located on the flank of the Yolla and Cormorant Troughs. These depocentres are fault-bounded half-grabens that progressively developed via growth faulting during the active rifting and thermal subsidence phases of basin evolution. The dominant structural trend in the basin is northwest-southeast, highlighted by the orientation of the major faults and troughs.

5.2.2 Stratigraphy

The stratigraphic succession in the Bass Basin comprises sediments ranging in age from Early Cretaceous to Recent (Figure 2)

The Early Cretaceous Otway Group rests unconformably on pre-rift Palaeozoic black shales and quartzites and consists of clastic, volcaniclastic, fluvial and deltaic sediments ranging from coarse-grained sandstone to shale and coal. The Otway Group was deposited as a very thick sequence of sediments (*C.australiensis* to *C.paradoxus*) that have been intersected in the Bass Basin at only one locale, Durroon-1, in the extreme southeast.

Localised uplift and erosion then occurred on the basin margins as the initial rifting phase subsided (Middle Cretaceous). The Otway Drift phase then began along the southern margin of Australia, which was largely contemporaneous with the start of the Tasman Rifting event on the eastern edge of the southern margin. This recommenced rifting in the Bass Basin, which resulted in deposition of the prospective Early Cretaceous to Late Eocene Eastern View Coal Measures (EVCM) which comprise a thick succession of sandstone, siltstone, shale and coal, deposited primarily within fluvial, deltaic and lacustrine depositional environments. Seismic data suggests that the EVCM is over 4000m thick in the Troughs. The EVCM thins markedly towards the basin margins and exhibits both onlap onto basement and erosional truncation. In a broad sense, the EVCM can be divided into three sequences separated by erosional unconformities. The middle sequence was penetrated in Bass-1 and Yolla-1 and –2 and contains the major gas accumulations in the Yolla Field. This sequence is bounded at the base by the N. senectus unconformity and at the top by the upper M. diversus unconformity.

The Lower Eastern View Coal Measures (EVCM) depositional sequence was deposited from Cenomanian to Santonian times (*A.distocrinatus* to *N.senectus*). These units have only been intersected in Durroon-1 in the southeast of the Bass Basin and are equivalent to the Golden Beach Group in the Gippsland Basin.

An angular unconformity is identified over localised highs on the basin margins at the top of the *N.senectus* zone. The boundary is marked in places by significant extrusive volcanism, similar to that observed in the Gippsland Basin. This event signals the termination of Tasman rifting, which was followed by sea floor spreading in conjunction with the already active drift in the Otway region. During this time, thermal subsidence dominated throughout the basin and thick, ubiquitous deposition of the Late Cretaceous to Paleocene Lower EVCM occurred (*T.lillei* to Lower *M.diversus* / *P.asperopolus*).

The Late Cretaceous sediments are restricted mainly to the basin depocentres and axial reaches where accommodation space was sufficient for deposition and subsequent preservation. The section is missing on the basin margins due to sediment bypass. The Paleocene section is extensive throughout with the greatest thickness of sediments in the basin depocentres and significant thinning towards the basin flanks, as a result of both condensing of the section and basement onlap.

The Late Cretaceous/Paleocene Lower EVCM has been intersected in numerous wells in the basin, identifying it as a continuos sequence of late low stand sediments grading through a transgressive systems tract and finally capped by high stand sediments. Environments are gradational both laterally and temporally from alluvial through fluvio-deltaic and nearshore

to deeper restricted lacustrine. Primary sediment input to the basin was from the southeast with minor localised input also deposited transversely from the flanks of the troughs. Extensive coal measures dominate the sedimentary sequence in the southeast of the basin (Pelican Trough) with increasingly thicker homogeneous shale units occurring through the Yolla and Cormorant Troughs.

The top of the Lower EVCM is identified by localised uplift and inversion of the pre-existing sedimentary sequence, caused by mild regional compression. The effects of this uplift are variable with the degree of erosion extending from the Mid *M.diversus* through to the *P.asperopolus* in places.

The Eocene upper EVCM (Mid *M.diversus* / *P.asperopolus* to Mid *N.asperus*) was then deposited under a regime of slower subsidence, resulting in more widespread, highly variable facies development. Fluctuating conditions of alluvial, fluvio-deltaic and shallow marine processes resulted with more extensive deposition of coal measure sediments. A regional marine transgression then occurred, resulting in the basin-wide deposition of the Demons Bluff, the base of which is marked by a locally very thick transgressive sand.

Conformably overlying the EVCM is the Late Eocene Demon's Bluff Formation. Lithologically this unit consists of a basal sequence of fine-grained carbonaceous shale and siltstone deposited in an open marine environment. The unit has an average thickness over the basin of approximately 120 m, but thins toward the basin margins. The Demon's Bluff Formation provides a regional top seal to hydrocarbons reservoired in the top-most sandstone units of the EVCM as demonstrated in Yolla-1.

The Demon's Bluff Formation is overlain by the Late Eocene to Pliocene age Torquay Group which broadly consists of a basal sequence of marls and calcareous shales which grade upwards into a succession of bioclastic limestones. The Torquay Group signifies continual deposition under pervasive marine conditions. The Torquay Group is punctuated in places by episodes of minor uplift and/or erosion accompanied by varying effects of volcanism. Large-scale extrusives (volcanoes) are observable on the seismic data with extensive sill and dyke networks also resulting from these events (Yolla-1, Cormorant-1 and Aroo-1).

5.3 Contributions to Geological Concepts and Conclusions

Two new potential reservoirs were discovered whilst drilling this well.

- A sandstone within the Angahook Formation at 1315 – 1324mRT, which was only logged with LWD GR-RES. The mud gas response suggests either tight oil sands or residual oil saturation.

- An oil bearing sandstone in the Intra-EVCM at 2603mRT (called the 2458 sand) was penetrated at the base of the 12 ¼" hole section and logged in the TD suite. Rotary sidewall cores, MDT pressures and samples and a full wireline log suite were acquired in this interval. Geochemical analysis of the oil indicates this oil is very similar to the oil previously discovered at the top of the EVCM (within the TEV4 sand) and is probably from the same source rock. This discovery opens up a new oil play within the intra-EVCM which previously had been primarily targeted for gas.

The 2718 sand had previously been interpreted as gas-bearing from the limited data available from Yolla 1. The shows while drilling, MWD and wireline logs and MDT results in Yolla 4 all confirm the 2718 sand is water-wet.

All the 3 main reservoir zones within the intra-EVCM, namely the 2755, 2809 and 2973 sands, were encountered as predicted and are gas-bearing.

Prior to drilling the 2755 and 2809 sands were interpreted as sharing a common GWC, however the MDT data from Yolla 4 have proven that these sands have GWC's at different depths. The change in interpreted hydrocarbon-water contact depths from pre-drill to post-drill Yolla 4 are shown in table 5 below.

Depth units	TEV4 sand OWC		2458 sand OWC	2718 sand GWC		2755 sand GWC		2809 sand GWC		2973 sand GWC	
	Pre-drill	Post drill	Post drill*	Pre-drill	Post drill	Pre-drill	Post drill	Pre-drill	Post drill	Pre-drill	Post drill
mTVDSS	1831.5	1831.5		2727.0	Water	2834.0	2834.0	2834.0	2827.5	2997.0	2999.0
mMDRT			2609.5 to 2614.5		Water	2964.0	3010.5	2964.0	3003.7	3144.0	3170.3

*** not predicted pre-drill**

Table 5: Yolla 4 Hydrocarbon-Water contacts, pre- vs post-drill

The MDT data from Yolla 3 (a development well drilled immediately following Yolla 4) indicate that two separate gas columns exist within the 2973 zone (Upper and Lower sands). The Yolla 4 data appears to fit in with the upper sand.

6. REFERENCES

Amoco Australia Petroleum Company, 1986 – Yolla 1 Final Well Report, Volume 1 – Geology, Appendix 9, Part 2: Vitrinite reflectance Determinations and Organic Petrology

Boreham, C.J., Blevin, J.E., Radlinski, A.P. and Trigg, K.R., 2003 – *Coal as a source of oil and gas: A case study from the Bass Basin, Australia*. APPEA Journal 43 (1) 117-148

Lennon, R.G., Suttill, R.J., Guthrie, D.A. and Waldron, A.R., 1999 - *The renewed search for oil and gas in the Bass Basin: Results of Yolla 2 and White Ibis 1*. APPEA Journal 39 (1) 248 – 262.

Taylor, R., 2001 - *Yolla 3D 2000 Reprocessing and Interpretation Report*, Origin Energy Resources Ltd, unpublished report.

Williamson, P.E., Pigram, C.J., Colwell, J.B., Scherl, A.S., Lockwood, K.L. and Branson, J.C., 1987 – *Review of stratigraphy, structure and hydrocarbon potential of Bass Basin, Australia*. AAPG Bulletin V.71, No.3, 253-280

APPENDIX 1: PETROPHYSICS REPORT

TRL/1, BASS BASIN, TASMANIA

YOLLA - 4

PETROPHYSICAL INTERPRETATION

EASTERN VIEW COAL MEASURES

2590 – 3235 mRT

FINAL

Origin Energy Resources Limited
Second Floor, South Tower, John Oxley Centre
339 Coronation Drive
MILTON QLD 4064

Andy Hall, December 2004

EXECUTIVE SUMMARY

Yolla-4 was drilled as the 3rd well on the Yolla Field after the Yolla-1 exploration well in 1985 and the Yolla-2 appraisal well in 1999. The well was drilled as a gas producer from the Intra-Eastern View Coal Measures (EVCM) 2718, 2755, 2809 and 2973 Sandstones (named after their MD penetrations in Yolla-1), which were discovered by Yolla-1 and confirmed by Yolla-2.

Two further potential reservoirs were discovered whilst drilling this well. An Angahook sandstone at 1315 – 1324 mRT, which was only logged with LWD GR-RES. The mud gas response suggests either tight oil sands or residual oil saturation. An oil bearing sandstone in the Intra-EVCM at 2603 mRT (called the 2458 Sst) was penetrated at the base of the 12 ¼" hole section and logged in the TD suite. Rotary sidewall cores, MDT pressures and samples and a full wireline log suite were acquired in this interval.

Full diameter cores were acquired through the entire section of the 2755 and 2809 Sst and have been analysed with to determine RCA and SCAL properties.

The results of the petrophysical interpretation are presented in Table 1.

- The 2718 Sst (2864 – 2871 mRT) is good quality sandstone, but water bearing at Yolla-4. A minor sandstone at 2882 mRT is gas bearing and was proved by MDT testing to be potentially productive.

- The 2755 Sst (2903 – 2912 mRT) was cored throughout. The interval has a shaly sandstone down to 2907 mRT and is then clean at the base. MDT and log analysis indicates that the interval is gas saturated and productive.

- The 2809 Sst (2962 – 2985 mRT) was also cored throughout. The interval is a very clean sandstone with good reservoir properties.

- The 2973 Sst (3149 – 3165 mRT) has two reservoir intervals divided by a shaly non-net interval. The clean sandstones at top and base are productive intervals.

Composite plots of the well in the study interval at scales 1:200 and 1:500 are presented as Enclosures 1 &2 respectively.

Table 1: Net Sand and Net Pay Summary for Yolla-4

	Gross Interval			Net Sand				Net Pay				
Reservoir Zone	Top mRT	Base mRT	Thickness mMD	Thickness mMD	NTG Fraction	Porosity Fraction	Permeability[1] mD	Thickness mMD	NTG Fraction	Porosity Fraction	Permeability[1] mD	Sw Fraction
2458 Sst	2603.8	2619.5	15.7	6.2	0.395	0.184	42.3	2.5	0.159	0.217	116	0.476
2718 Sst	2864.8	2871.4	6.6	4.2	0.636	0.184	254	0	0.000	-	-	-
	2882.5	2887.1	4.6	2.1	0.457	0.195	13.6	2.1	0.457	0.195	13.6	0.447
2755 Sst	2902.7	2912.1	9.4	7.7	0.819	0.174	61.7	7.6	0.809	0.175	64.1	0.168
2809 Sst	2962.6	2984.8	22.2	21.5	0.968	0.173	150	21.3	0.959	0.174	156	0.209
2844 Sst	3005.0	3014.9	9.9	5.5	0.556	0.163	28.9	1.3	0.131	0.199	550	0.548
2952 Sst	3118.2	3130.1	11.9	2.0	0.168	0.150	0.86	1.5	0.126	0.165	0.97	0.420
2973 Sst	3149.4	3165.4	16.0	13.0	0.813	0.147	38.2	9.8	0.613	0.165	94.4	0.235
2718 Sst to 2973 Sst Inclusive												
Gas zone	**2882.5**	**3165.4**	**80.6**	**56.0**	**0.695**	**0.167**	**97.4**	**43.6**	**0.542**	**0.173**	**126**	**0.239**
All reservoirs			**96.3**	**62.2**	**0.646**	**0.169**	**91.9**	**46.1**	**0.480**	**0.167**	**125**	**0.244**

	Net Sand Parameters			*Net Pay (Net Sand + ...)*
Reservoir Zone	*Shale Volume*	*Porosity*	*Permeability*	*Water Saturation*
2458 Sst	*< 40%*	*Not directly applied*	*> 1 mD (oil zone)*	*< 60%*
2718 – 2973 Sst	*< 40%*	*Not directly applied*	*> 0.1 mD(water zone)*	*< 60%*

[1] Geometric average

TABLE OF CONTENTS

Figures

Enclosures

1.	Yolla-4 EVCM (2600 – 3200 mRT) Petrophysical summary plot	1 : 200
2.	Yolla-4 EVCM (2600 – 3200 mRT) Petrophysical summary plot	1 : 500

BOREHOLE DATA

Hole / Casing Diameters

Borehole			Casing OD		
Inches	**mm**	**Section TD (mDDRT)**	**Inches**	**mm**	**Casing Shoe (mDDRT)**
Casing driven into sea-bed			20	508	220
16	406	900	13 $^{3}/_{8}$	340	885
12 ¼	311	2614	9 $^{5}/_{8}$	244	2586
8 ½	216	3235	168 mm (6.625") liner run post logging to 3233 mRT		

Section TD for the 311 mm (12 ¼") hole was called within an oil bearing sandstone. To allow wireline logs to be acquired over this interval, the casing was set and cemented above the sandstone. Wireline logs, acquired to the 244 mm (9 $^{5}/_{8}$") casing shoe in the TD logging programme, provided good coverage of this potential reservoir interval.

Hole Deviation

The Yolla-4 well was drilled as a vertical hole to 1200 mRT and then deviated at an azimuth of 200^{o} and an inclination of approximately 24^{o} to the 2718 Sst. Final well inclination was 7^{o} at 3235 mRT.

The well was referenced on Kelly Bushing (KB), which was 43 metres above mean sea level. Water depth was 81 metres.

The hole plan and cross-section are given in Figure 1 and Figure 2.

Drilling Mud Properties

The following mud properties were read off the Schlumberger composite plot for Run 1 / 2 of the TD logging suite.

Rm		Rmf		Rmc	
(Ω.m)	(Deg C)	(Ω.m)	(Deg C)	(Ω.m)	(Deg C)
0.197	21.7	0.181	20.6	0.215	18.8

Borehole Temperatures

Bottom hole temperature (BHT) was measured in each of the logging runs. The temperature range was from 126^{o}C in Run 1 / 2 to 149.5^{o}C (corrected to logging TD) in Run 1 / 6. The Horner plot suggests a corrected BHT of 162.9^{o}C, equivalent to a temperature gradient of 49.1^{o}Ckm^{-1}, assuming a sea bed temperature of 10^{o}C (Figure 3).

The temperature from Run 1 / 2 PEX-CMR-HRLA-GR (126^{o}C at 3235.5 mRT) was used in the petrophysical analysis.

Figure 1: Plan View of the Yolla-4 Well Deviation

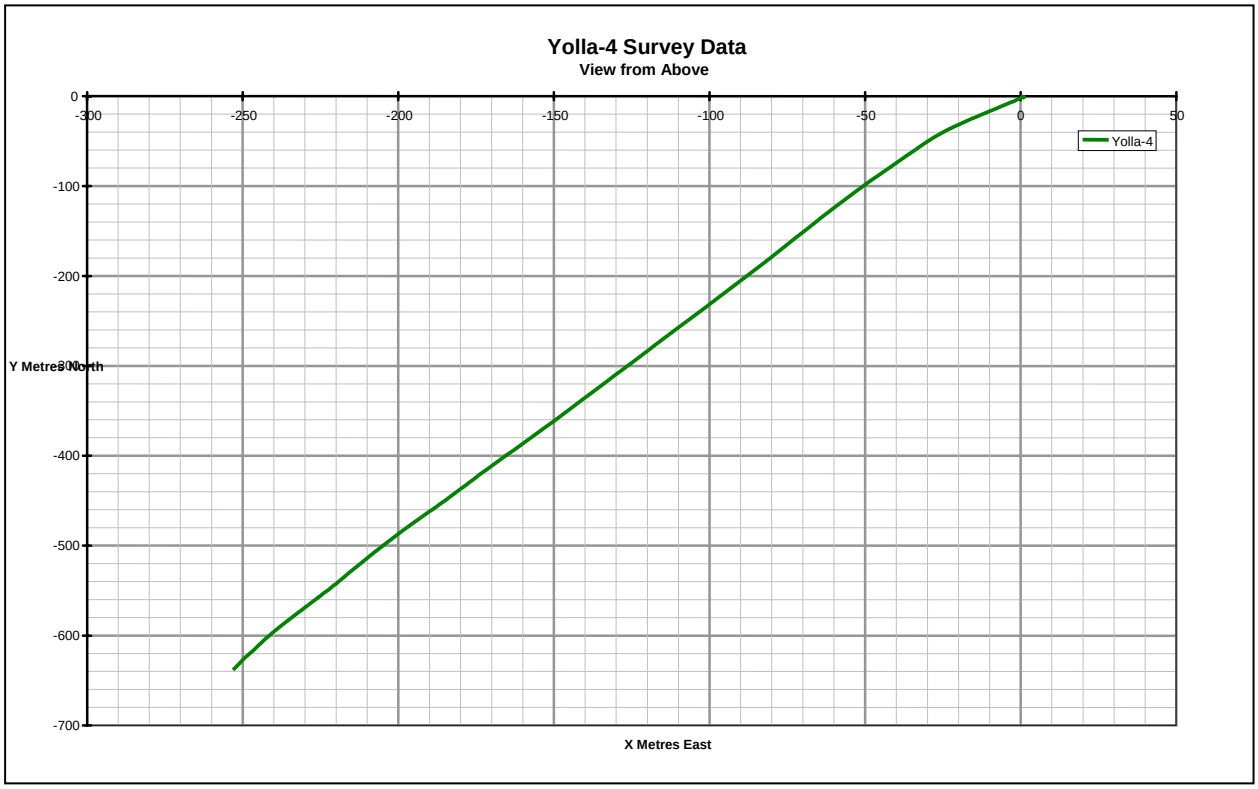

Figure 2: Cross-section View of the Yolla-4 Well

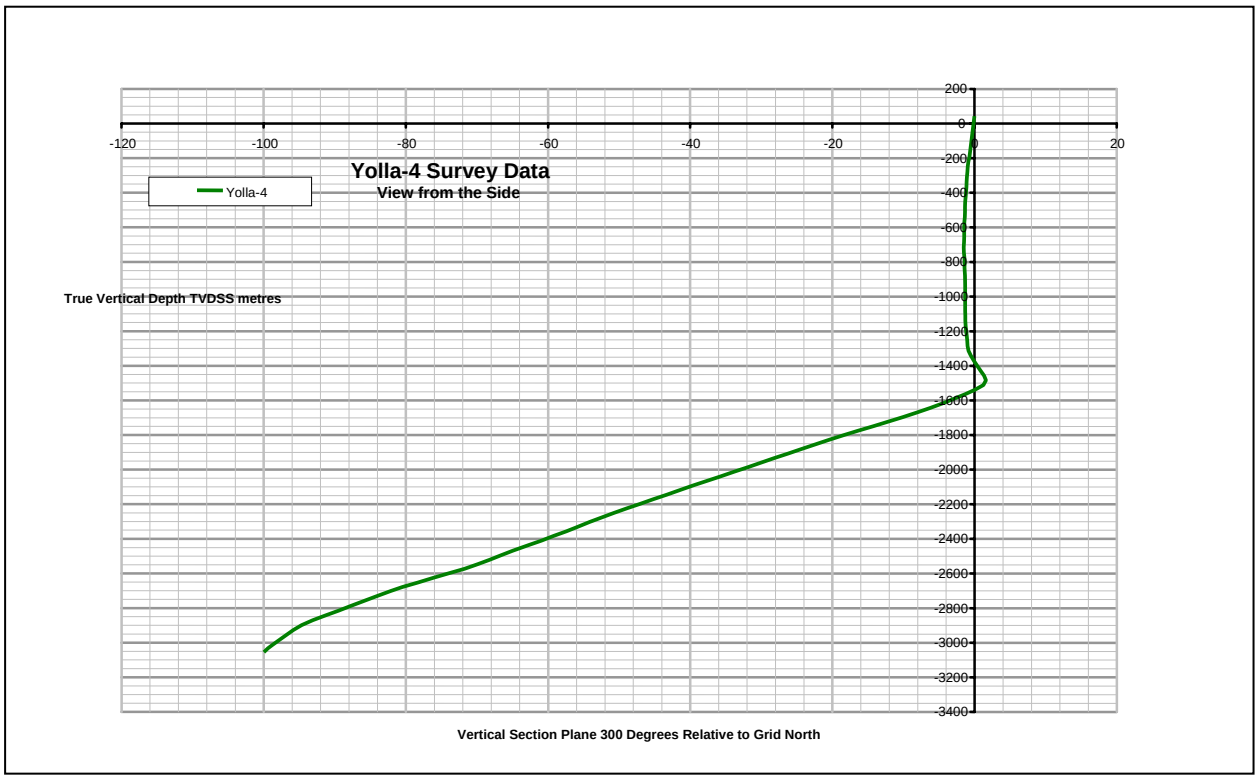

Figure 3: Horner temperature Plot for the TD Logging Suite at Yolla-4

HORNER TEMPERATURE PLOT

Yolla-4

RTE:	124	**m AGL**	**Corrected BHT:**		**deg C**
Surface temp:	10	**deg C**	**Temperature Gradient:**		**deg C / 100m**
LOG SUITE:	TD		**T.D.:**	3235.5	**mRT**
TD Reached:	11/07/2004 22:00		**Circulation Stopped:**		13/07/2004 18:00

LOG TYPE			BASE LOGS mRT	TIME ON BOTTOM	Tx (hrs)	T (hrs)	T/(Tx+T)	Max. TEMP Deg C	Eq. Max TEMP Deg C
Suite	Run								
1	2	PEX-HRLA-CMR	3235.5	14/07/2004 4:30	44.00	10.50	0.19	126.0	126.0
	3	HNGS-DSI-ECS-FMI	3208.0	14/07/2004 12:25	44.00	18.42	0.30	133.0	134.1
	4	VSP	2922.6	15/07/2004 18:00	44.00	48.00	0.52	136.0	150.6
	5	MDT-GR-CMR	3174.7	15/07/2004 4:00	44.00	34.00	0.44	146.0	148.8
	6	MSCT	3159.0	17/07/2004 4:00	44.00	82.00	0.65	146.0	149.5

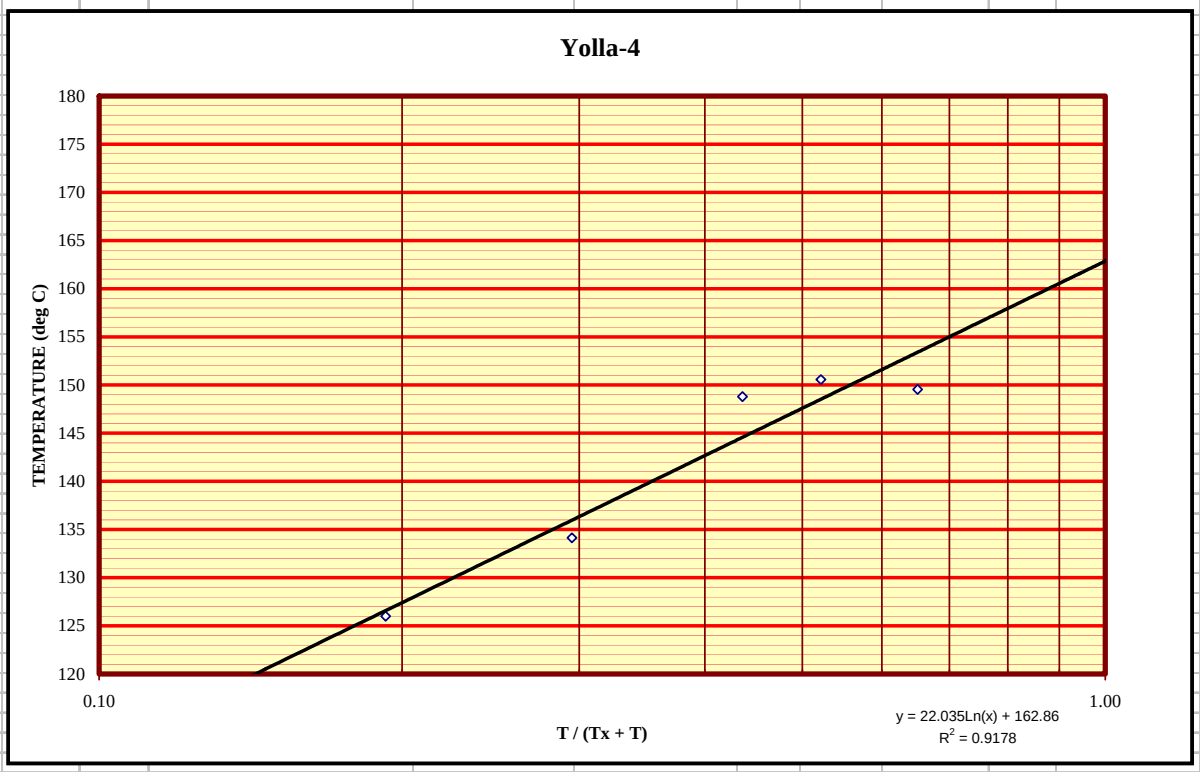

DATA AVAILABILITY

Logging While Drilling (LWD) Data

LWD GR and resistivity were acquired by Sperry Sun from the 340 mm (13 $^{3}/_{8}$") casing shoe at 885 mRT to final TD at 3235 mRT.

The 311 mm (12 ¼") section was drilled in one bit run. LWD logging comprised the dual gamma ray (DGR) and four-phase Electromagnetic Resistivity (EWR-P4) tool. This yielded the Smoothed Gamma ray log (SGRC) and the micro, shallow, medium and deep resistivity curves (SEXP, SESP, SEMP and SEDP respectively). At the end of the section, the potential reservoir section between 1310 – 1340 mRT was relogged with the gamma ray and SEXP / SEDP curves to obtain an invasion profile.

The 216 mm (8 ½") section was drilled in 3 bit runs, due to core being taken in the reservoirs. The section was logged throughout with the DGR – EWR-P4 tools. The cored sections were wiped with the tools when drilling recommenced after coring.

Wireline Log Data

Wireline data was acquired by Schlumberger over the section from the 244 mm (9 $^{5}/_{8}$") casing to TD (Table 2).

In the first wireline logging run (Run 1 / 1 : PEX-CMR–HRLA), the tools would not pass below 2776 mRT and so only the section between 2776 mRT and the casing shoe at 2590 mRT was logged. Schlumberger could not follow their normal depth correction procedure and the depths were tied to the LWD data and do not conform to the final depth datum for the well.

After reconfiguring the tool string, the PEX-CMR-HRLA was rerun (Run 1 / 2) over the interval between TD and the 244 mm (9 5/8") casing shoe. Upon reaching TD, the CMR failed to calibrate and would have had to be taken up hole for recalibration. If this had been done, the bottom hole temperature (BHT) would have exceeded the working limit for the PEX. Consequently, no CMR data was acquired in this run.

HNGS-DSI-ECS-FMI was acquired in Run 1 / 3 between TD and the 244 mm (9 5/8") casing shoe without any significant problems. Sonic and gamma ray logs were acquired through casing from the 244 mm (9 5/8") casing shoe to 116 mRT.

VSP data was acquired in Run 1 / 4 from 3225 mRT to 1205 mRT at 20 metre intervals. Between 1200 - 770 mRT, VSP data was acquired, but could not be used for time-depth processing as the formation first arrivals could not be distinguished from casing ringing.

Run 1 / 5 was planned to acquire MDT pressures and fluid samples from the reservoirs. Due to it's failure earlier in the logging programme, the CMR was also included in this run. CMR data was acquired without problems from 2576 – 3231 mRT. The MDT was used to acquire 52 pre-test pressure points and four 450 cc samples. One further sample was attempted, but the chamber failed to open. The samples were taken in a sandstone (at 3006 mRT) immediately beneath the 2809 Sst, the 2718 Sst water zone and in the 2458 Sst (2 samples).

Twenty-five MSCT plugs were planned to be acquired in Run 1 / 6. After failing with 3 cores in the 2973 Sst, the tool was pulled back to casing and recalibrated. Twenty further cores were cut, but only eight were accepted, six in the 2458 Sst and two in the 2973 Sst.

Core Data

Two 27 metre cores were acquired in Yolla-4.

Core #1 was taken in the 2755 Sst between 2892 - 2919.5 mDDRT with 100% recovery. Comparison of the core GR to wireline logs suggests that the core depths were 5.9 metres high of the wireline depth datum for the well.

- 259 probe permeability measurements were acquired
- 86 plugs were cut. 61 were used to measure horizontal permeability, 21 were used for vertical permeability. 4 were unusable.
- 21 overburden porosities and permeabilities were measured using an overburden pressure of 5000 psi.
- SCAL was calculated on 5 plugs with varying porosity and permeability

Core #2 was taken in the 2809 Sst between 2958 – 2985 mDDRT with 100% recovery. Comparison of the core GR to wireline logs suggests that the core depths were 4.2 metres high of the wireline depth datum for the well.

- 252 probe permeability measurements were acquired

- 117 plugs were cut. 91 were used to measure horizontal permeability, 26 were used for vertical permeability.

- 31 overburden porosities and permeabilities were measured using an overburden pressure of 5000 psi.

- SCAL was calculated on 5 plugs with varying porosity and permeability

Core plugs were planned to be sampled regularly every 0.30 metres to attempt to avoid biasing the data distribution. The core quality (fracturing etc) influenced the plugs taken. The spacing of the horizontal core plugs (Figure 4) illustrates that the data has been sampled in a relatively unbiased manner. Core #1 was shalier, and regular core plugs were harder to obtain. The lower, shaly section of core #1 was not sampled.

Overburden (OB) porosity and permeability were plotted from the two cores (Figure 5). This suggests that the compaction correction is very similar for both cores. The following equations were used to correct the ambient properties to down hole properties for cores #1 and #2. One apparently spurious point (ambient permeability = 2121 mD, OB permeability = 1369 mD) was removed from the core #2 distribution

$$\text{OB Porosity} = \text{Ambient Porosity} * 0.935$$

$$\text{OB Permeability} = \text{Ambient Permeability} * 0.833$$

Archie 'm' for Core #1 and #2 is calculated from the SCAL data to be 1.777 (average of 10 points) with no appreciable difference between the data from the two cores. The equivalent shaly sand 'm*' is 1.785.

The Cation Exchange Capacity (CEC) was calculated from the same 10 cores. In Core #1 (2755 Sst), the average CEC (uncrushed) is 0.10 meq/100g, which translates to a Clay Qv of 0.01 meq/cm^3. In Core #2 (2809 Sst), the average CEC (uncrushed) is 0.18 meq/100g, which translates to a Clay Qv of 0.02 meq/cm^3.

Ambient porosity and permeability were measured on 6 rotary sidewall core plugs from the 2458 Sst.

Petrology / Shows

Indications of lithology are available from the drill cuttings descriptions generated by the well site geologists on the rig. More detailed descriptions are also available from the petrology carried out on the cores by Julian Baker (Reference 1).

2458 Sst (2603.8 – 2619.6 mRT)

The Well Site Geologist (WSG) described the interval as sandstone and siltstones. The sandstones are predominantly medium sandstone with 20% fine sandstone and 20% clay. The sands are moderately sorted with sub-angular grains. There is a weak calcareous cement. The siltstones are 80% silt, 10% clay and 10% very fine sand with a trace of carbonaceous material and trace calcareous cement.

Shows during drilling consisted of heightened gas readings and 70% bright, light green fluorescence, with no direct cut and a very slow bright, light green bleeding crush cut with a patchy residue ring.

2718 Sst (2859.4 – 2872.4 mRT)

The WSG described the interval as 30% sandstone and 70% siltstone. The sandstones were 50% fine, 30% very fine with 10% silt and 10% clay, moderately sorted, sub-angular with a weak siliceous cement. The siltstone was 75% silt, 20% clay and 5% very fine sand and had a trace micro-mica and trace fine pyrite.

There was a trace of dim yellow fluorescence with a trace to very slow direct crush cut and a dim cream broken film residual ring from the sandstone.

2755 Sst (2895.3 – 2913.0 mRT)

The WSG described the sandstones as predominantly fine to very fine sandstone with some coarse intervals and weak argillaceous cement and good inter-granular porosity.

Petrologic analysis was conducted on samples from 2899.2 (S#21) and 2904.2 (S#40) mRT (core depths). S#21 is a well sorted, very fine grained sandstone that includes sporadic thin horizontal laminae, defined by concentrations of microcrystalline / finely crystalline siderite patches, heavy minerals and relatively fine grain size. S#40 is a moderately well sorted medium grained massive sandstone.

Good drilling gas shows were recorded. Fluorescence varied between 5 – 90%, increasing towards the base of the sandstone. The fluorescence was described as dull to moderately bright green, very slow to no direct cut, dull to bright cream broken film residue ring.

2809 Sst (2958.7 – 2984.9 mRT)

From the core chips, the WSG described the interval as a medium to coarse sandstone with a moderately strong siliceous cement and occasional carbonaceous grains.

Petrologic analysis was conducted on samples from 2963.9 (S#85) and 2981.4 (S#143) mRT (core depths). S#85 was a massive, clean, well compacted, moderately sorted coarse grained sandstone (quartz arenite) with common authigenic kaolin patches. S#143 is a well sorted, fine grained sandstone that includes sporadic, thin, slightly styolitic laminae that are defined by concentrations of micro-crystalline / finely crystalline siderite patches and fine organic fragments. Kaolinitic matrix is abundant throughout the sample.

Good drilling gas shows were recorded. Shows observed consisted of a trace to no fluorescence. Where present, the fluorescence was patchy, dull green with no direct cut and a very slow to trace crush cut. There was a dull white cream ring of residue.

2973 Sst (3145.0 – 3165.2 mRT)

The WSG described this interval as a 40% medium sandstone, 30 % fine sandstone, 20% very fine sandstone and 10% clay. The interval is moderately sorted, with sub-angular grains and a weak argillaceous cement.

There were good gas shows with no associated fluorescence between 3139 – 3151 mRT and between 3160 – 3164 mRT.

Table 2: Wireline Logging Runs Conducted in Yolla-4

Suite/Run	Tool String	Interval (mRT)	Max Recorded Temperature (deg C)
1/1	PEX – HRLA – CMR	2586 - 2776	111
1/2	PEX – HRLA – CMR	2590 – 3235.5	126
1/3	HNGS – DSI – ECS – FMI DSI - GR	2581 – 3235.5 116 - 2617	133
1/4	VSP	770 - 3525	136
1/5	MDT – GR - CMR	2604 – 3174.7	146
1/6	MSCT	2604 - 3159	146

Figure 4: Core Plug Spacing In Yolla-4 Cores #1 and #2

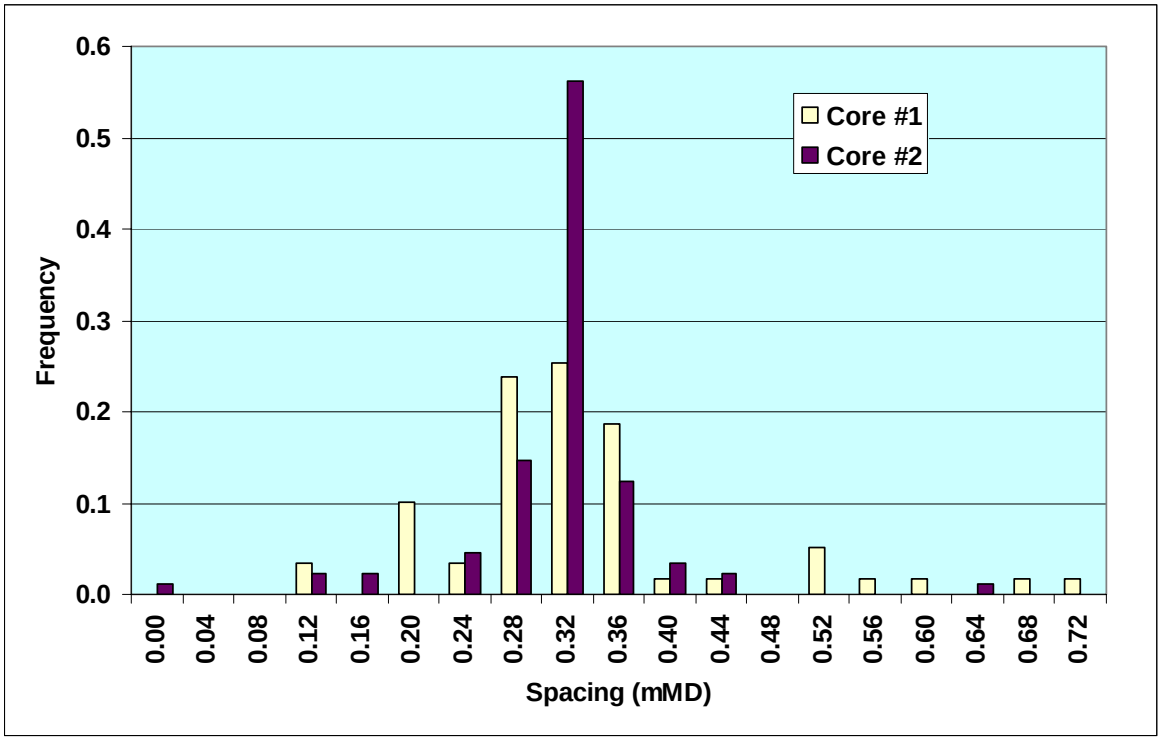

Figure 5: Overburden Porosity vs Ambient Porosity From Yolla-4 Cores #1 and #2

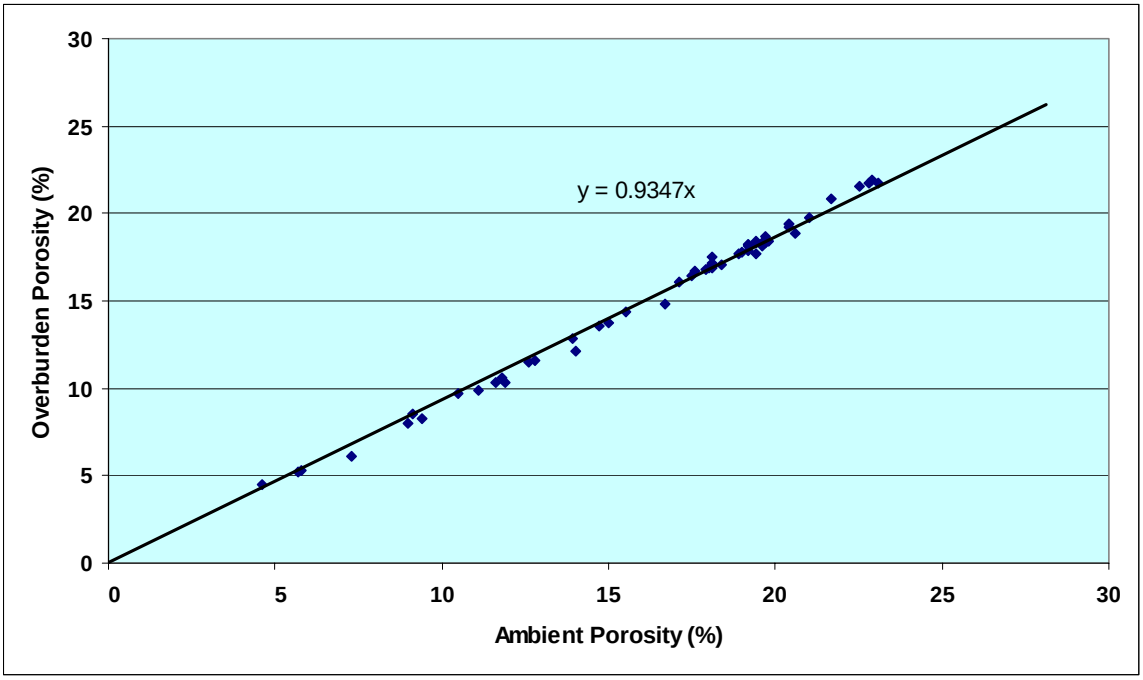

Figure 6: Overburden Permeability vs Ambient Permeability From Yolla-4 Cores #1 and #2

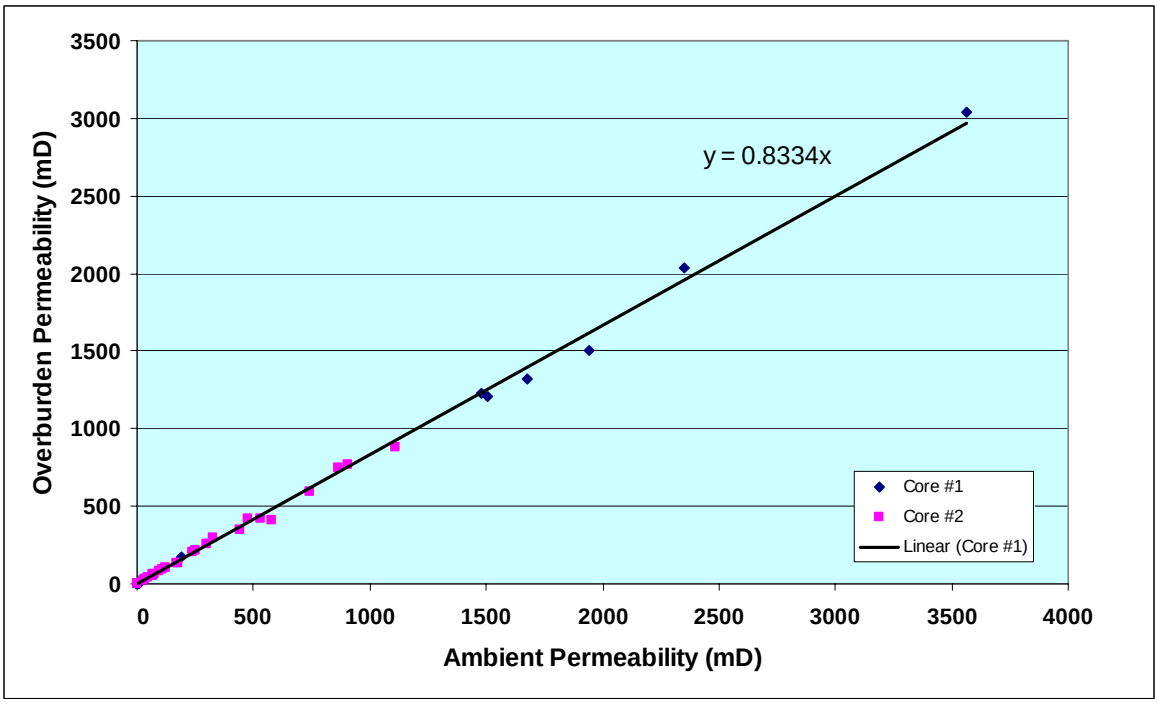

Note : one apparently spurious point from core #2 (Ambient permeability = 2121 mD, OB permeability = 1369 mD) was removed from the data set prior to calculating the trend line.

LOG ANALYSIS METHODOLOGY

The parameters for the different intervals in the well are given in Appendix A.

Shale Determination

Shale Volume

Shale volume (VSHGR) was determined from the CGR curve (spectral GR minus the effect of Uranium) and a linear interpolation between GR_{CLEAN} and GR_{SHALE}. GR_{CLEAN} and GR_{SHALE} were chosen as the mode of the HCGR distribution through the 2809 Sst (13 API) and the peak of the shale distribution (83 API) in the CGR distribution through the entire study interval (Figure 7).

Shale volume from neutron-density (VSHND) was also calculated. The agreement between VSHND and VSHGR was excellent in most areas.

The minimum of VSHGR and VSHND was taken to be the true shale volume.

Porosity

Porosity was determined from a combination of the CMR, density and neutron logs. An excellent agreement was obtained between the different tools for measuring porosity (sonic, CMR, density and neutron).

Density porosity was used in the determination of permeability (which was used to derive net sand thickness) and for the average net sand porosity.

Density

The density log was used with the core data in the 2755 and 2809 Sst to generate a core / wireline correlation.

The average grain density from core analysis in the 2809 Sst is 2.663 gcm^{-3}. Cross-plotting core porosity and the density log and using the core derived grain density as a fixed point at porosity = 0%, yields a value for the fluid density to honour average core porosity (Figure 8). The required fluid density for the 2809 Sst is 0.629 gcm^{-3}.

There is more variation in facies in the 2755 Sst. For the purposes of the core to log correlation, the core can be divided into three intervals (Figure 9). The fluid density is the density required to correlate the core porosity and density logs and not necessarily the actual pore fluid density.

Top (mRT)	Base (mRT)	Grain Density (gcm^{-3})	Fluid Density (gcm^{-3})
2900.0	2907.7	2.694	1.023
2907.7	2912.0	2.686	0.421
2912.0	2926.0	2.715	1.404

The ECS tool yields a matrix density curve (RHGE) that gives similar grain density averages across the cored interval to the core data. This was used as the matrix density throughout the interpreted interval.

The fluid density for the gas bearing 2809 Sst (0.605 gcm^{-3}) was also used in the 2973 Sst porosity determination.

Neutron Density

Neutron-density porosity was determined using the ECS matrix density curve and the parameters given in Appendix A. Prior to determining the porosity, the neutron log was converted to a sandstone matrix and shale corrected.

CMR

CMR porosity (TCMR) is the most accurately determined porosity in formations where the hydrogen index (HI) of the pore fluid can be assumed to be 1.0 (i.e. water or oil bearing formations). In gas bearing formations, the CMR under-reads the effective porosity by the ratio of the HI of the gas to that of water. The bound fluid volume is assumed to be water bearing, even in a gas zone, and is read correctly.

CO_2 in the formation has no hydrogen and will, therefore, not be read as porosity by CMR. The oxygen present will also increase the relaxation time of the hydrogen proton, making the pores appear smaller than they actually are.

Due to the factors above, the CMR was not directly used in the porosity analysis for this well.

Water Saturation

Formation Water Resistivity

Two MDT water samples were taken in Yolla-4 in the 2718 Sst and the 2458 Sst. Both of these are either mud filtrate or heavily contaminated with filtrate.

Three samples (all completion brine) were taken during the production test on the 2973 Sst. A further four samples were taken from the 2755 Sst production test and three from the 2809 Sst. These were all very fresh water and were attributed to water of condensation from the gas stream. Hence, none of the samples gathered in Yolla-4 are considered representative of the formation water.

Water resistivity was determined for the reservoirs either from Pickett Plots in Yolla-4 (basal section of the 2458 Sst (Figure 10) and the 2718 Sst (Figure 11)). Formation water resistivity for the other reservoirs was estimated from Yolla-2 as the sands are below the GWC there. Estimation of formation water resistivity for the 2755 Sst is more difficult as the reservoir is gas bearing at Yolla-2. The values used in the interpretation are given below.

Well Rw determined in	*Sandstone*	*Reservoir Conditions*		*Standard Conditions*	*Salinity*	*Quality*
		(ohm.m)	**(^{o}C)**	*(ohm.m at 25^{o}C)*		
Yolla-4	2458 Sst	0.17	102.3	0.453	12,340	Good (Figure 10)
Yolla-4	2718 Sst	0.24	112.1	0.689	7,870	Good (Figure 11)
Yolla-2	2755 Sst	As for the 2809 Sst				
Yolla-2	2809 Sst	0.17	106.5	0.468	11,910	Good
Yolla-2	2952 Sst	0.14	111.6	0.401	14,082	Reasonable
Yolla-2	2973 Sst	0.25	112.5	0.720	7,510	Good

Water Saturation Determination

Water saturation was calculated using the Archie and Waxman Smits equations. Since the CEC is very low (0.10 meq/100g and 0.18 meq/100g for cores #1 and #2 respectively), the equations yield a very similar answer.

Permeability

The overburden corrected porosity / permeability transform, from the Yolla-4 cores in the 2755 and 2809 Sst shows a fairly reliable trend of increasing permeability with porosity (Figure 12).

A log of permeability data was created using

$$P1 = 0.0193 * e^{(PHI\_D*100*0.5168)}$$

$$Permeability = P1 - P1*(VSH*0.064)$$

Permeability in the shales was set to the CMR permeability KTIM.

Net Sand and Net Pay Cut-offs

The ratio of RT_HRLA to RXO gives an indication of the potential for moving fluid through the formation. When this is cross-plotted against the permeability, an estimate of the potential minimum permeability for fluid to flow can be made. For the cored zones, there are indications of fluid movement at about 0.1 mD (Figure 13 and Figure 14). Hence, the net sand cut-off for permeability was set to be 0.1 mD in gas zones. This is probably too low to flow fluids. The net sand permeability in oil zones was, therefore, set to 1 mD. Net sand / net pay was calculated from the porosity derived permeability curve (POPE).

No direct porosity cut-off is applied to the net sand / net pay determination as net sand is defined by permeability. The porosity / permeability relationship used, with an OB permeability cut-off of 1mD, implies an OB porosity cut-off of approximately 8% in the main reservoir sandstones.

Net sand was assumed to have a shale volume of less than 40%.

Coal and volcanic filters, generated by manual inspection of the wireline logs, were applied to ensure that no none clastic intervals were included in the net sand interval.

Net pay was determined to be present where net sand is determined and water saturation is less than 60%.

Figure 7: Histogram of CGR from the 2809 Sst

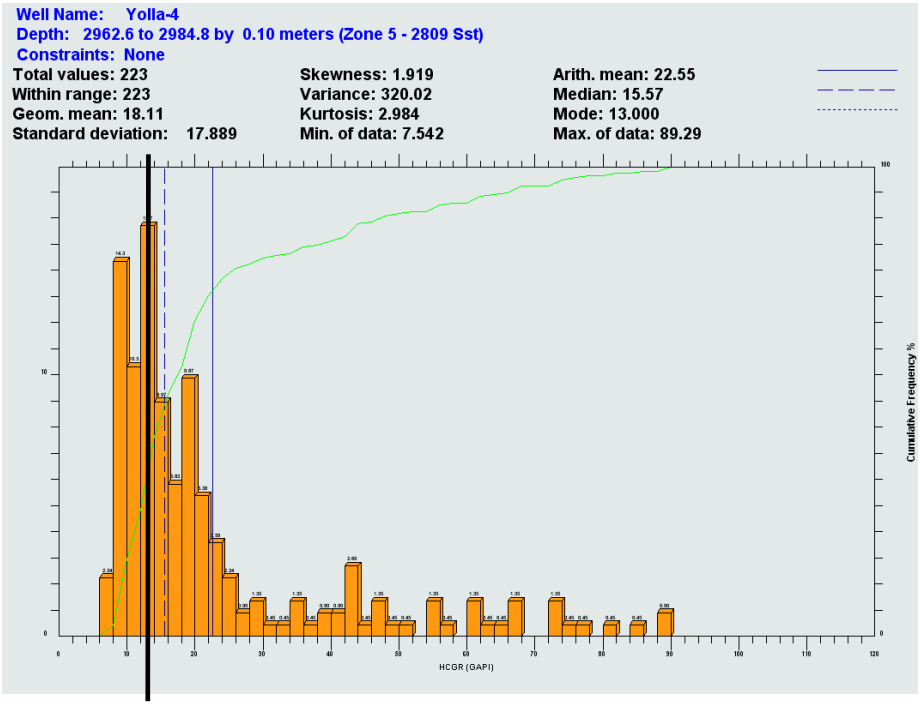

Sand line
13 API

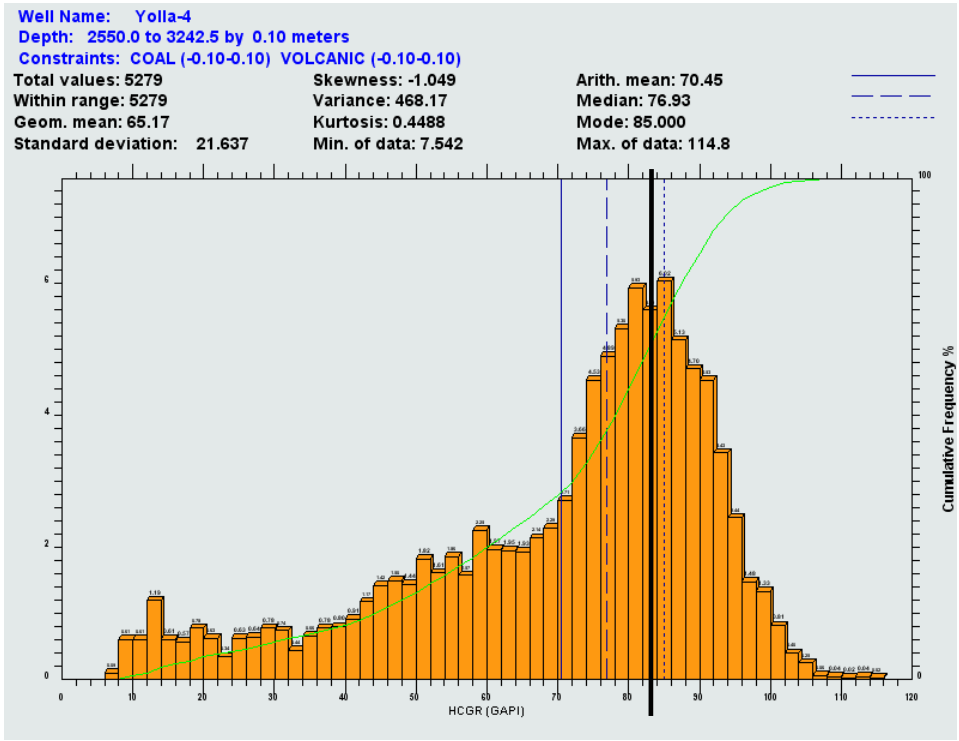

Shale line
83 API

Figure 8: Core Porosity / Density Log Correlation for the 2809 Sst

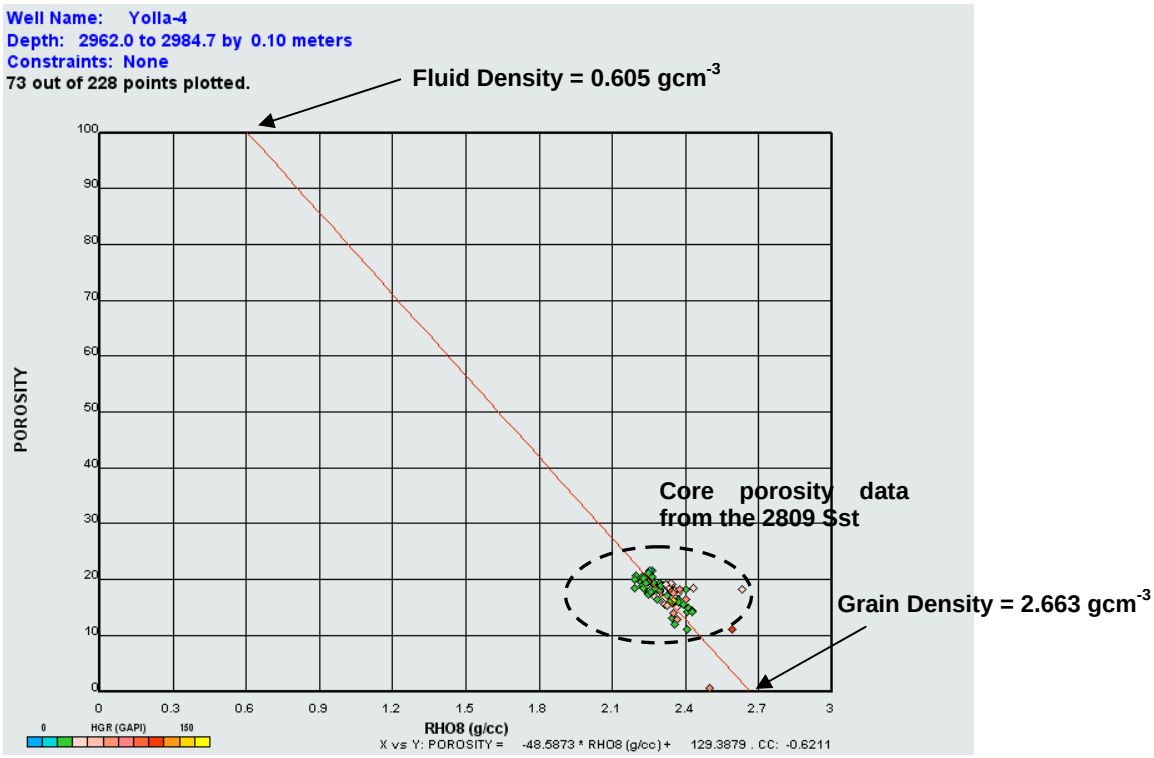

Figure 9: Core Porosity / Density Log Correlation for the 2755 Sst

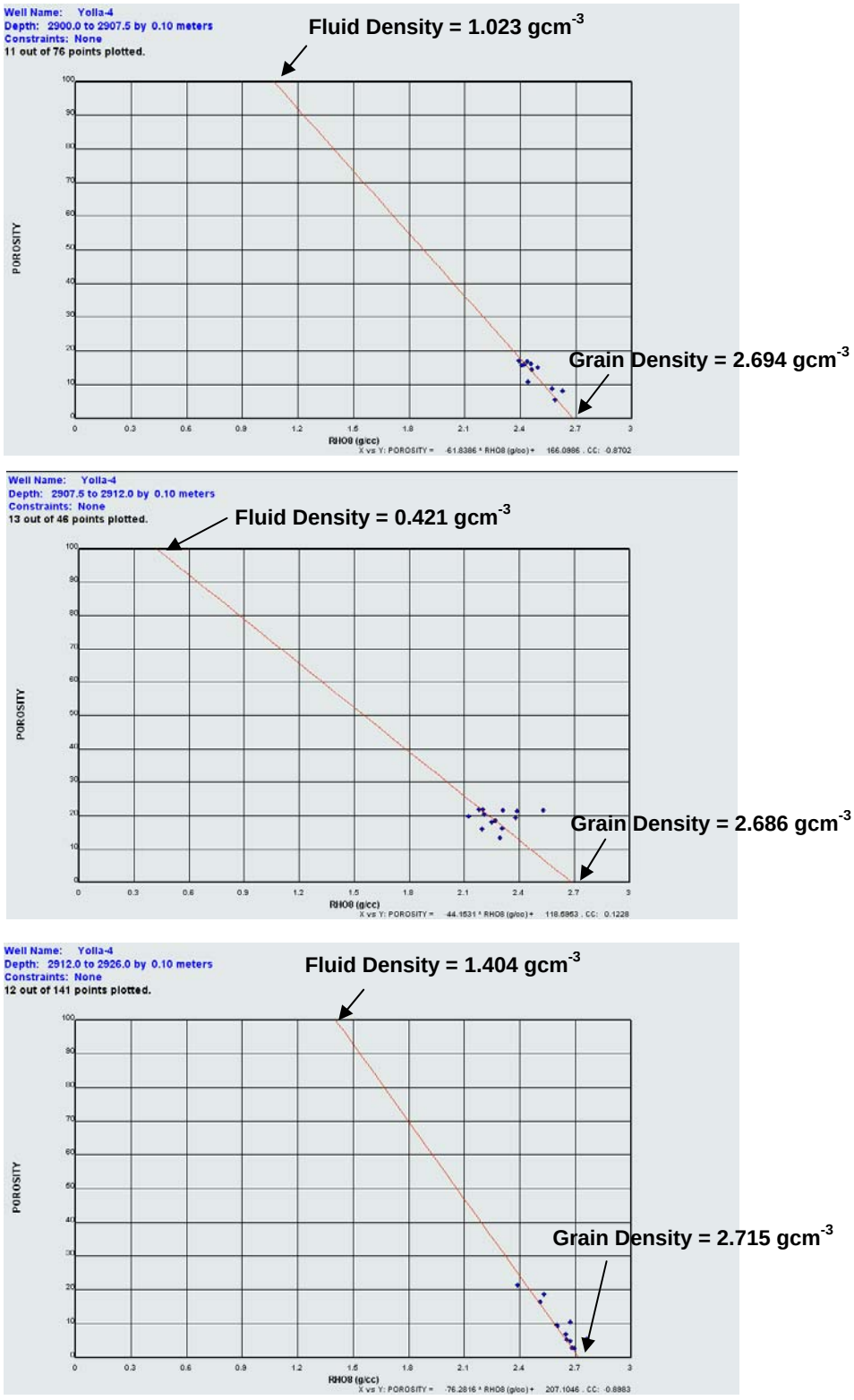

Figure 10: Pickett Plot for the 2458 Sst in Yolla-4

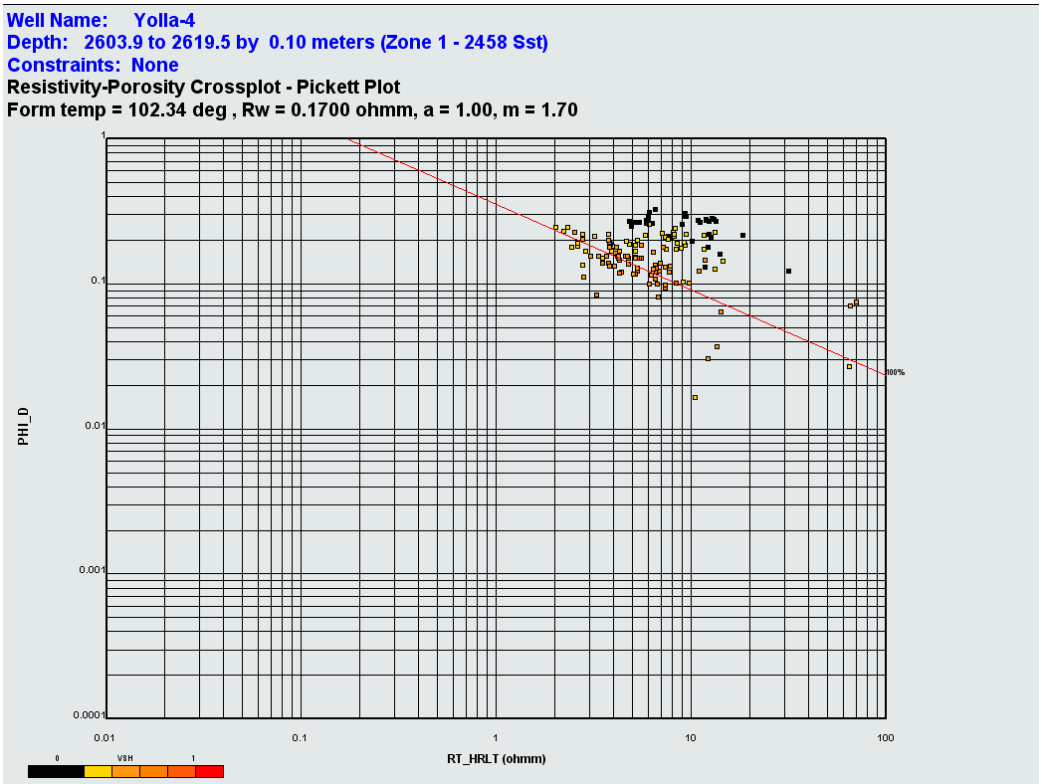

Figure 11: Pickett Plot for the 2718 Sst in Yolla-4

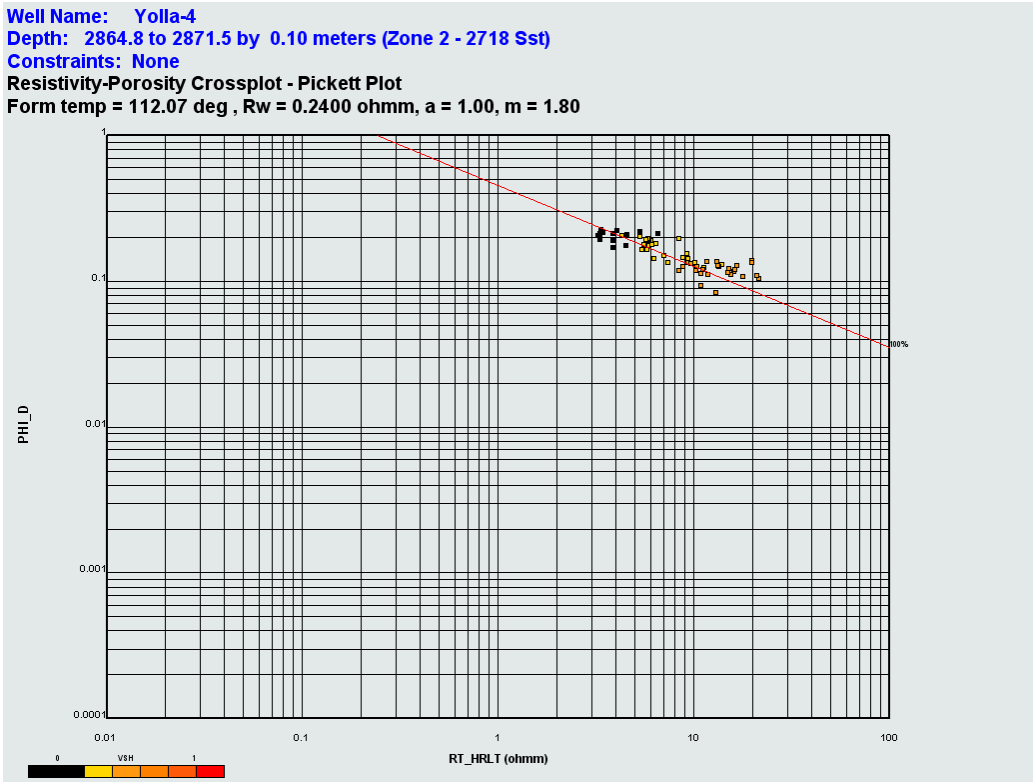

Figure 12: Overburden Corrected Porosity / Permeability Trend for Yolla-4 Cores #1 & #2

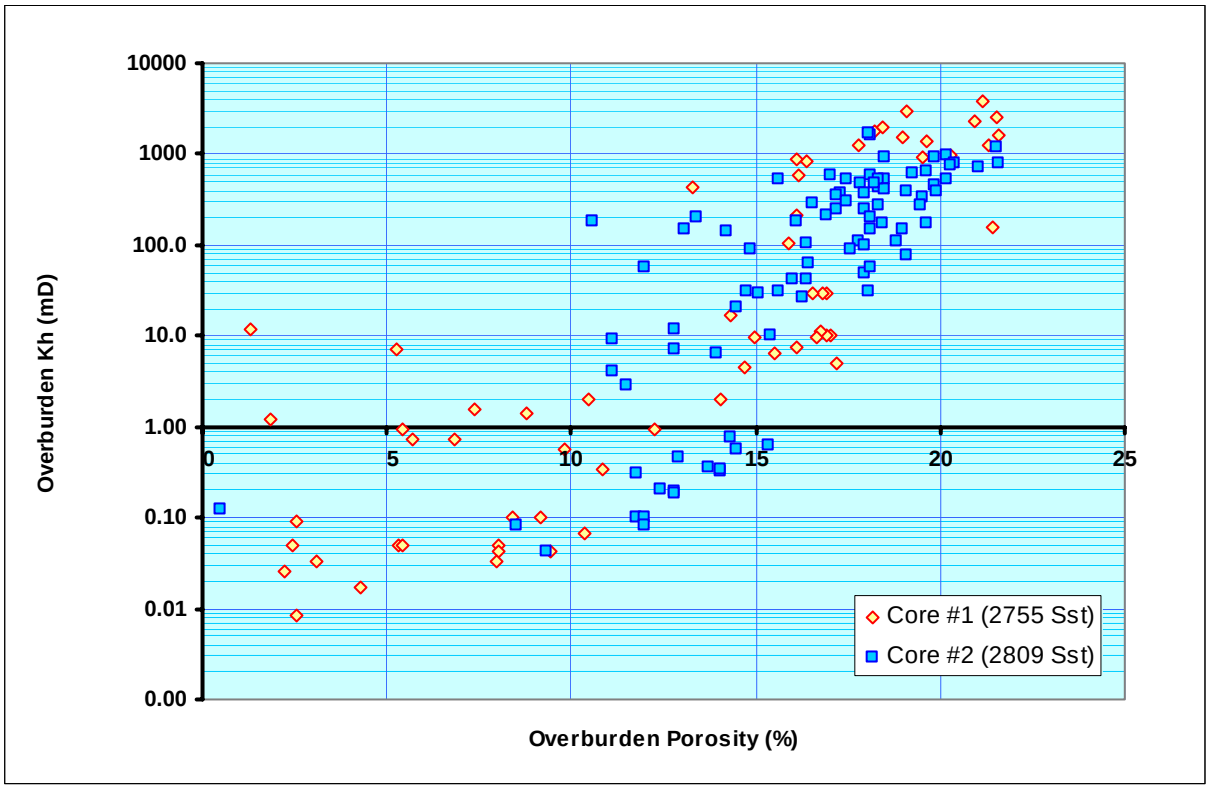

Figure 13: Ratio of Rt to Rxo Plotted against Permeability in the 2809 Sst

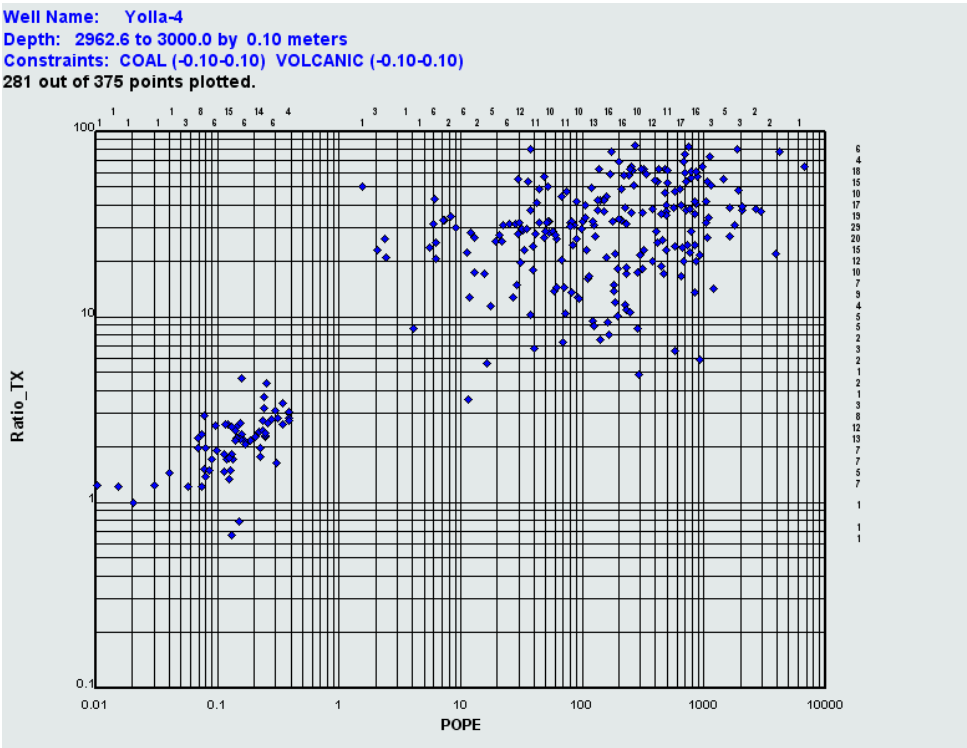

Figure 14: Ratio of Rt to Rxo Plotted against Permeability in the 2755 Sst

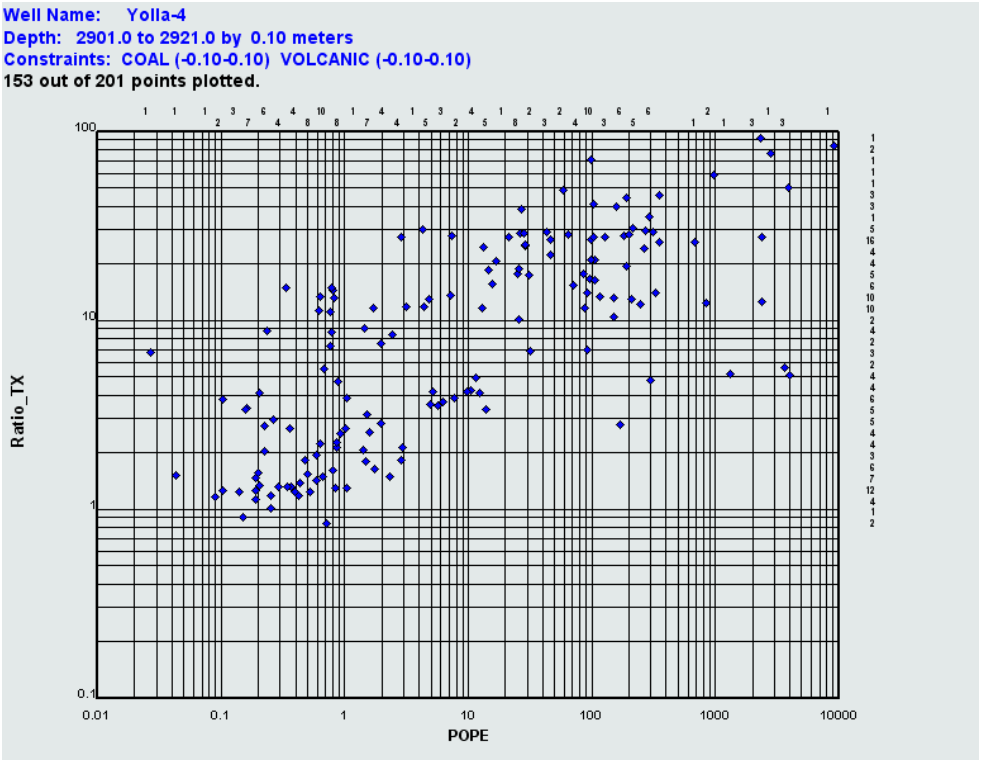

INTERPRETATION RESULTS

Angahook Sandstone (1315 – 1324 mRT)

A high gas response and increased resistivity was observed whilst drilling (Figure 15) across a sandstone at approximately 1320 mRT in the Angahook Formation. No porosity logs were acquired across the interval and the interval was not DST or wireline tested.

The ROP and gas profile suggest that the top of the sandstone is at 1315 mRT. This corresponds with a high GR peak on the LWD logs (which have been assumed to be on depth with the mud log). Although there is no mention of these in the lithology reports, the GR must, therefore, be reading radioactive minerals in the sandstone. The base of the ROP anomaly corresponds with the base of the sandstone on the gamma ray and the base of the high log resistivity. The base of the gas anomaly is approximately one metre higher.

Analysis of the mud log gas (Figure 15) suggests that the formation fluid is oil, but is either residual or in tight sandstones. The mud gas response in the cleaner sandstone (1320 – 1324 mRT) suggests a slightly higher, but still negligible, mobility.

This low mobility is supported by the LWD resistivity, which shows a slight invasion profile across the cleaner sandstone (1320 – 1324 mRT), but little invasion across the high GR sandstone (1315 – 1320 mRT). The MAD (measured after drilling) logs show a similar profile, suggesting that invasion has not significantly advanced during the drilling of the rest of the hole section.

From the somewhat limited data acquired, this interval is interpreted to be either a tight sandstone or a sandstone containing residual oil.

2458 Sst (2603 – 2619 mRT)

The 2458 Sst was drilled in the 311 mm (12 ¼") hole section at about the depth of the planned casing shoe. Hence, the casing was set further up the hole and this potential reservoir was logged in the TD suite.

Porosity and permeability were measured on 5 rotary sidewall core plugs (Figure 16). The maximum measured ambient permeability was 54 mD. The plug porosities (at standard conditions) vary between 15.1 – 20.2%, although the plug at 2609.5 mRT sampled two lithologies (17.9% and 7.6%). There is no clearly definable porosity / permeability trend in

this data set. The measured core porosity is poorly matched by the CMR or density derived porosity.

Samples 16 and 17 were examined under thin section (Reference 2). Sample 16 exhibited a 38% siderite cement. Siderite, which has a very high PEF signature, should be apparent on the PEF and density logs. Lack of a clear log signal suggests that the plug hit an isolated siderite rich streak.

MDT pre-test pressures were measured between 2604.4 mRT and 2654.5 mRT (Figure 17). The pressure gradient suggests a light oil column. Samples were taken at 2606.5 mRT, 2609.5 mRT (both oil) and 2614.5 mRT (water), suggesting an OWC between the deeper two points. The sample at 2606.5 mRT was analysed and found to be 37.4^{o} API oil with a Gas-Oil-Ratio (GOR) of 860 scf/bbl and a density of 0.666 gcm-3 (at reservoir conditions). The pour point of the fluid is approximately 40^{o}C.

There are several inconsistencies in the MSCT and MDT data sets when compared to the log interpretation presented here:

- The MDT recorded super-charged formation at 2612.0 – 2612.5 mRT where the CMR porosity and permeability would suggest good reservoir
- The MSCT porosities are less than the CMR and density porosity across most of the interval
- There is no clear trend between MSCT porosity and permeability

To determine net sand and net pay, the porosity determined using the CMR porosity (TCMR) and permeability (KTIM), which were assumed to be the best approximation to reservoir conditions. The water saturation was calculated from the Waxman Smits equation using a CEC of 0.14 mequiv/100g (the average of the values measured from core deeper in the EVCM).

Using the net sand criteria of shale volume < 40% and permeability > 1 mD, the interval is interpreted from the wireline logs to have 6.3 mMD of net sand with an average porosity of 21.1% and geometric average (ga) permeability of 42 mD.

There is 2.5 mMD of net pay, defined as net sand with water saturation less than 60%, with an average porosity of 21.4% and ga permeability of 116 mD.

2718 Sst (2865 – 2871 mRT)

The 2718 Sst (Figure 19) is water-bearing throughout and has been used as one of the calibration points for the water resistivity in the reservoirs. The formation water resistivity is determined to be 0.24Ω.m at 112°C (Figure 11) from the Pickett Plot.

Permeability was derived from the relationship generated from the relationship generated from the core data from the 2755 and 2809 Sst.

Three MDT pre-tests were taken in the reservoir and indicated mobilities up to 60 mD/cp.

Using the net sand criteria of shale volume < 40% and permeability > 1 mD, the interval is interpreted from the wireline logs to have 4.2 mMD of net sand with an average porosity of 17.7% and ga permeability of 254 mD. There is no net pay.

Five MDT pre-test pressures were also taken in two sandstones between 2882.5 – 2887.1 mRT and indicated that the top sandstone was predominantly tight, but that the lower sandstone (2885.8 – 2887.1 mRT) has mobilities up to 90 mD/cp. Log analysis indicates that the entire interval is gas bearing. The permeability for this interval was generated by scaling the CMR KTIM permeability to match the MDT mobility observations. Using the gas net sand and net pay criteria, the interval has a net pay thickness of 2.1 mMD, with an average porosity of 19.5% and ga permeability of 13.6 mD. The average water saturation is 28%.

2755 Sst (2902 – 2912 mRT)

The entire 2755 Sst was cored , with 100% recovery. RCA and SCAL have been carried out on the core and used to calibrate the porosity and permeability. The agreement between OB corrected core porosity / permeability and the log derived values is excellent (Figure 20).

Four MDT pre-test pressures were recorded in the reservoir. These were interpreted by Mark Mussared and indicated a gas gradient through the entire sandstone. They were also on the same pressure gradient as the 2755 Sst at Yolla-2, suggesting communication within the field. Using the water line pressure data from Yolla-2, the GWC in this reservoir is at approximately 2834 mTVDSS (Figure 21).

Using the net sand criteria of shale volume < 40% and permeability > 0.1 mD, the interval is interpreted from the wireline logs to have 7.7 mMD of net sand with an average porosity of 17.4% and ga permeability of 61.7 mD. Virtually all the net sand also qualifies as net pay with an average water saturation of 16.8%.

2809 Sst (2962 – 2985 mRT)

The entire 2809 Sst was cored with 100% recovery. RCA and SCAL have been carried out on the core and used to calibrate the porosity and permeability. The agreement between OB corrected core porosity / permeability and the log derived values is excellent (Figure 22).

Seven MDT pre-test pressures were recorded in the reservoir. These were interpreted by Mark Mussared and indicated a gas gradient through the entire sandstone. Using the water line pressure data from Yolla-2, the GWC in this reservoir is at approximately 2827.5 mTVDSS.

Using the net sand criteria of shale volume < 40% and permeability > 0.1 mD, the interval is interpreted from the wireline logs to have 21.5 mMD of net sand with an average porosity of 17.3% and ga permeability of 150 mD.

There is 21.3 mMD of net pay, defined as net sand with water saturation less than 60%, with an average porosity of 17.4% and ga permeability of 156 mD.

2844 Sst (3005 – 3015 mRT)

The 2844 Sst is a coarsening upward sequence with the uppermost 3 metres being a clean gas bearing sandstone (Figure 23). The resistivity profile suggests some invasion and, consequently some mobile gas.

Three MDT pre-test pressures were taken in this interval between 3005.7 – 3007.7 mRT. These varied between tight formation and a mobility of 348.1 mD/cp.

2952 Sst (3118 – 3130 mRT)

The 2952 Sst is a non-reservoir sequence in the field area and is characterised by high shale volume (Figure 25). A 1.5 mMD thick clean sandstone at the top of the interval is gas bearing. The resistivity profile suggests that little of the gas is moveable.

Two MDT pre-tests were taken in the clean sandstone and indicated a mobility of about 20 mD/cp.

2973 Sst (3149 – 3165 mRT)

The reservoir in the 2973 Sst is divided into two sections, between 3149 – 3157 mRT and between 3163 – 3165 mRT, separated by a shaly non-net sequence.

Two sidewall cores were taken in the shaly sequence (Reference 2). The deepest sample was a well sorted, fine grained sandstone containing scattered, compacted, sideritised clay grains. The sample at 3158 mRT was a bioturbated arenaceous mudstone in which a strongly sideritised detrital clay matrix supports very fine to medium sand grains.

Ten MDT pre-test pressures were recorded in this reservoir. Analysis of this data by Mark Mussared (Figure 24) and including the water gradient data from Yolla-2 suggests a gas-water-contact (GWC) at approximately 2991 mTVDSS. The mobility of the pre-tests varied from tight / super-charged in the shaly non-net sequence, to a peak mobility of 242 mD/cp at 3157.1 mRT.

Using the net sand criteria of shale volume < 40% and permeability > 0.1 mD, the interval is interpreted from the wireline logs to have 13.0 mMD of net sand with an average porosity of 14.7% and ga permeability of 38.2 mD.

There are 9.8 mMD of net pay, defined as net sand with water saturation less than 60%, with an average porosity of 16.4% and ga permeability of 94.4 mD.

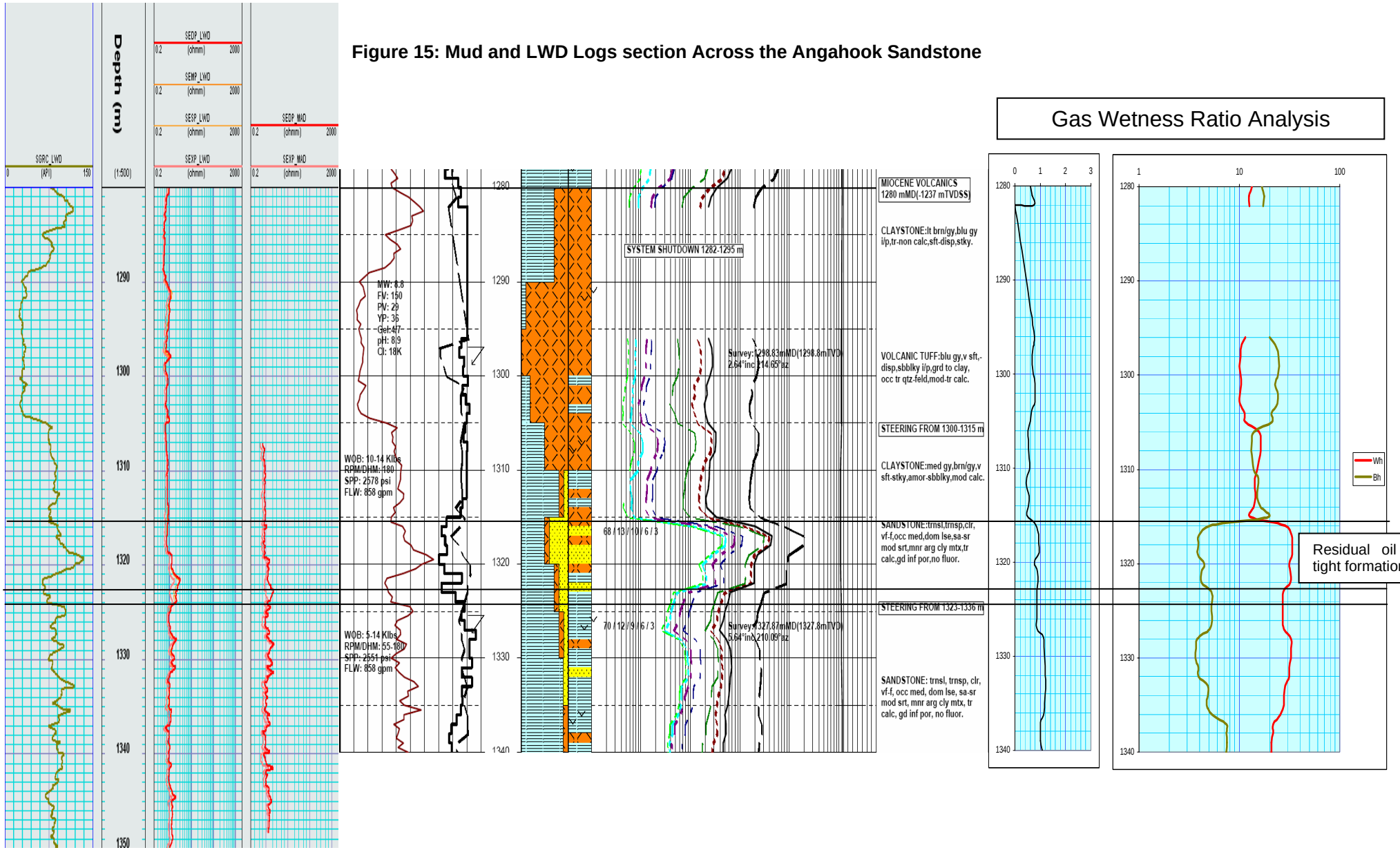

Figure 15: Mud and LWD Logs section Across the Angahook Sandstone

Figure 16: 2458 Sst MSCT Porosity / Permeability

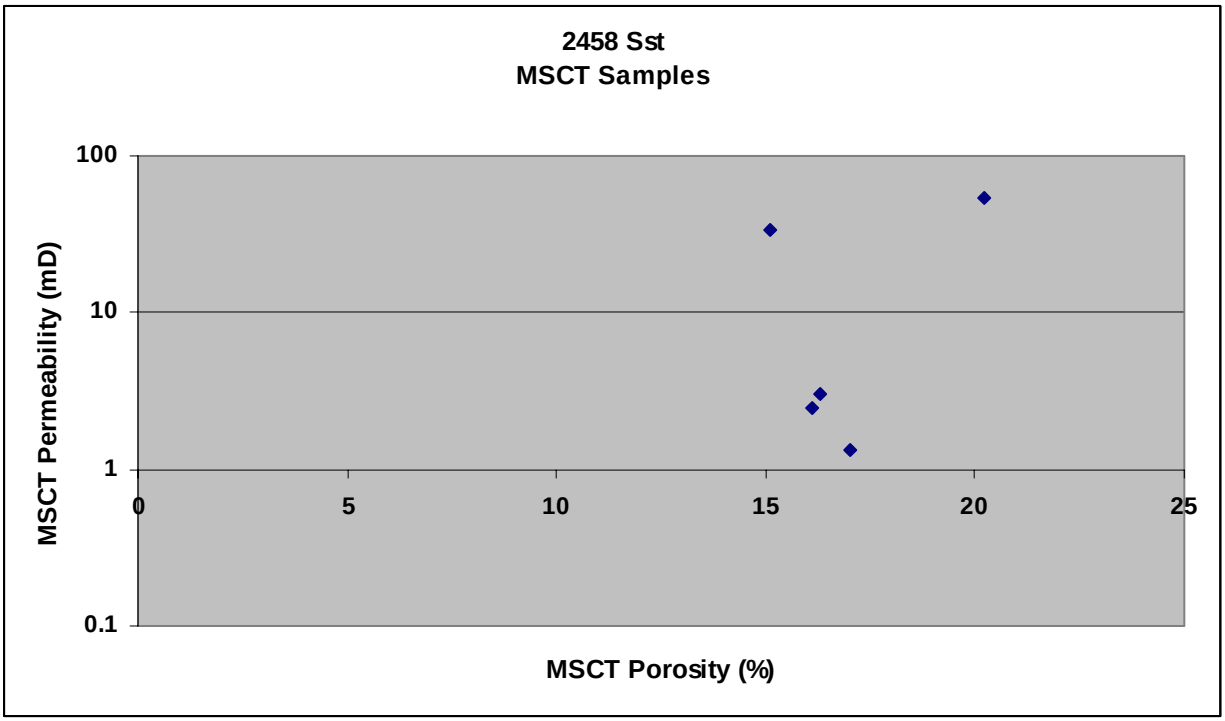

Figure 17: Pressure Profile through the 2458 Sst

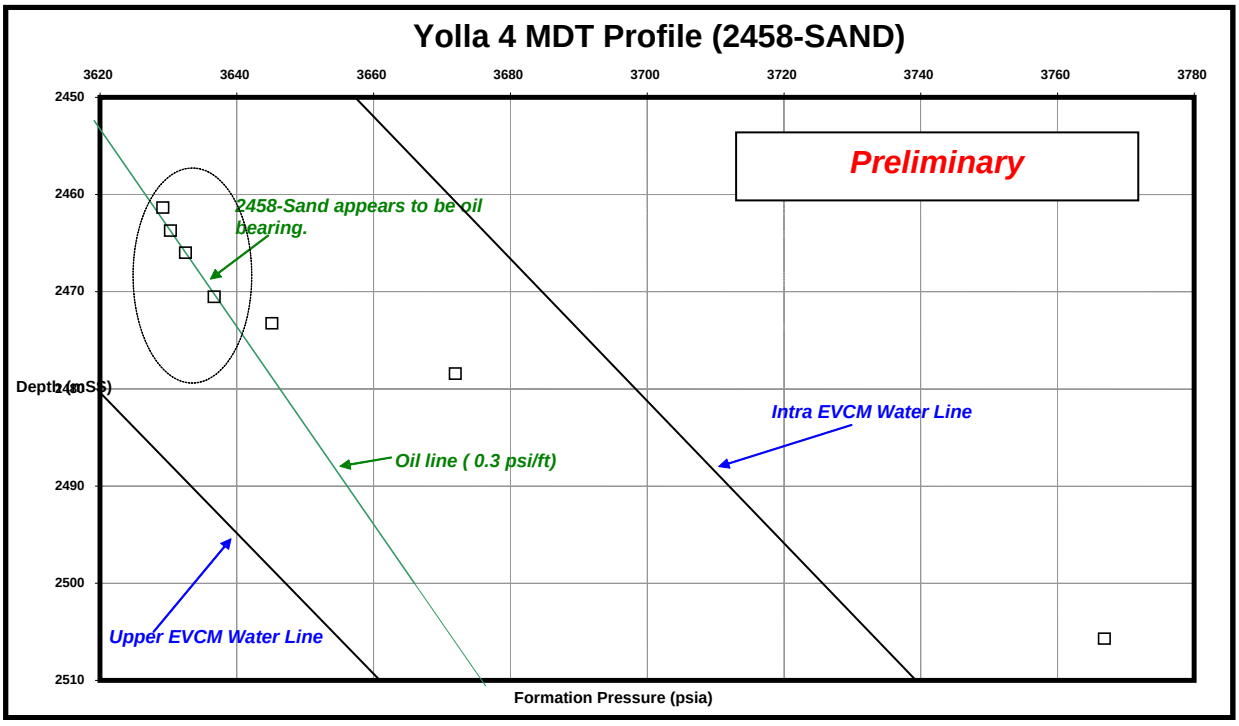

Figure 18: 2458 Sst Reservoir

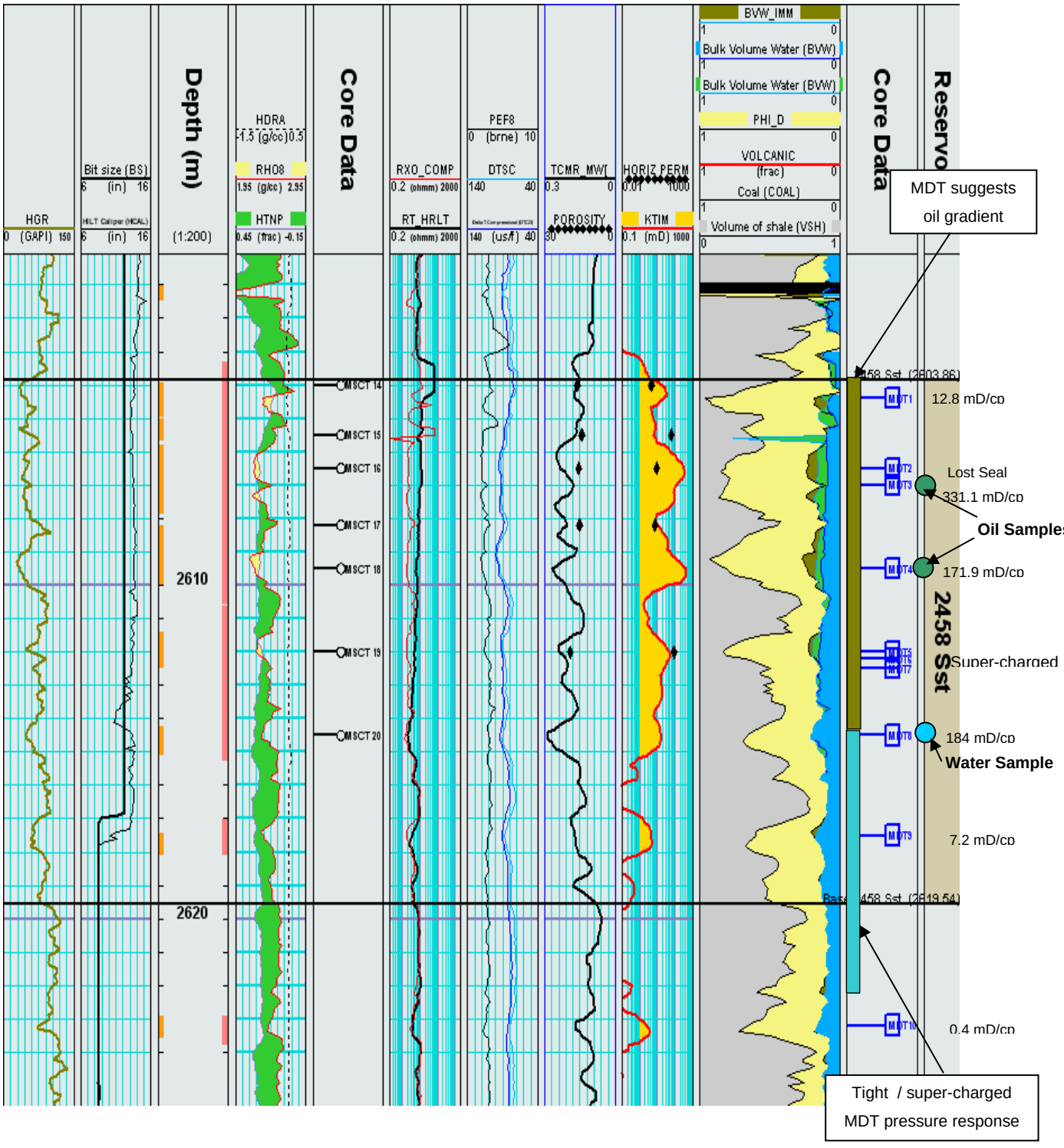

Figure 19: 2718 Sst Interval

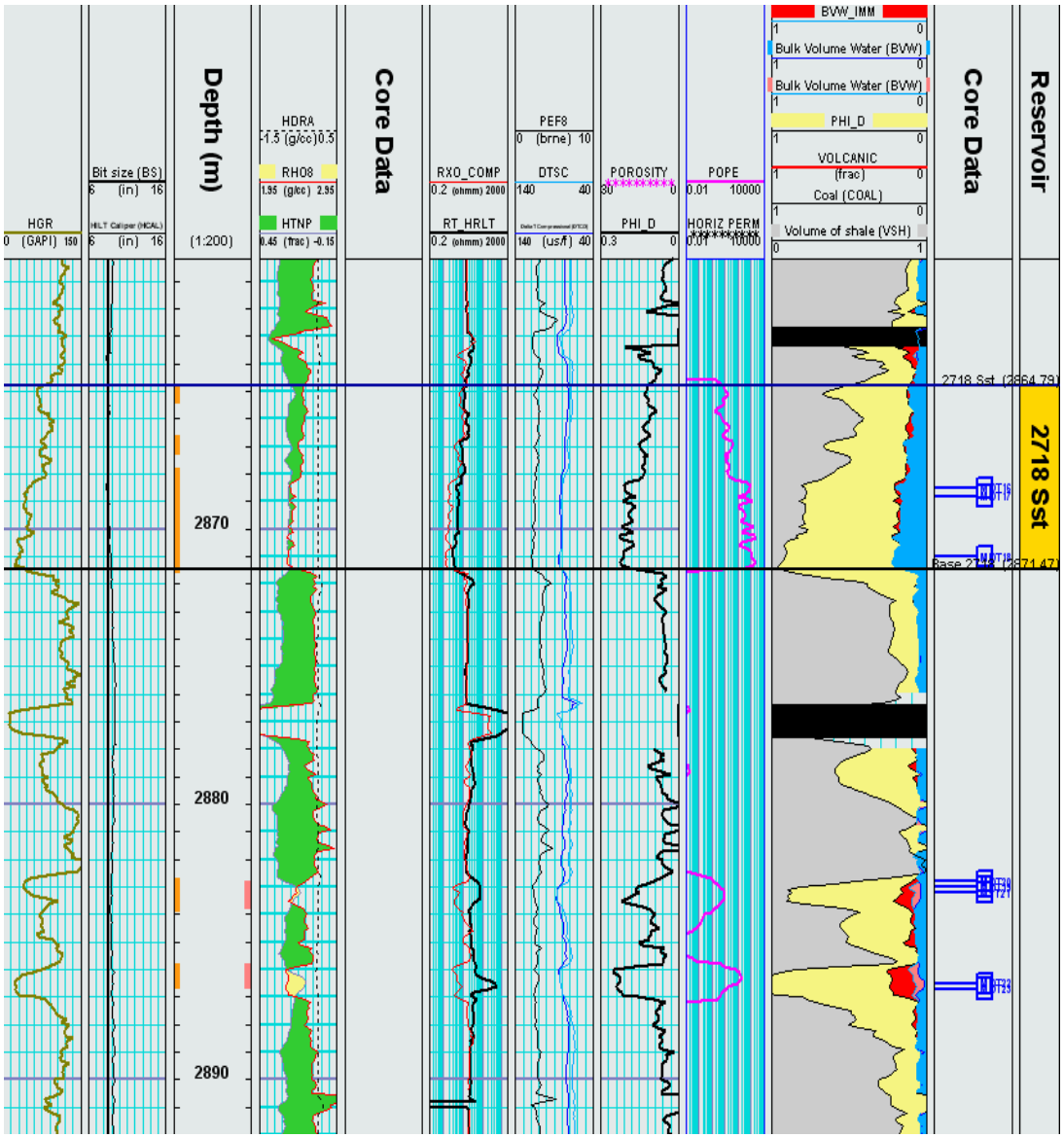

Figure 20: 2755 Sst Reservoir

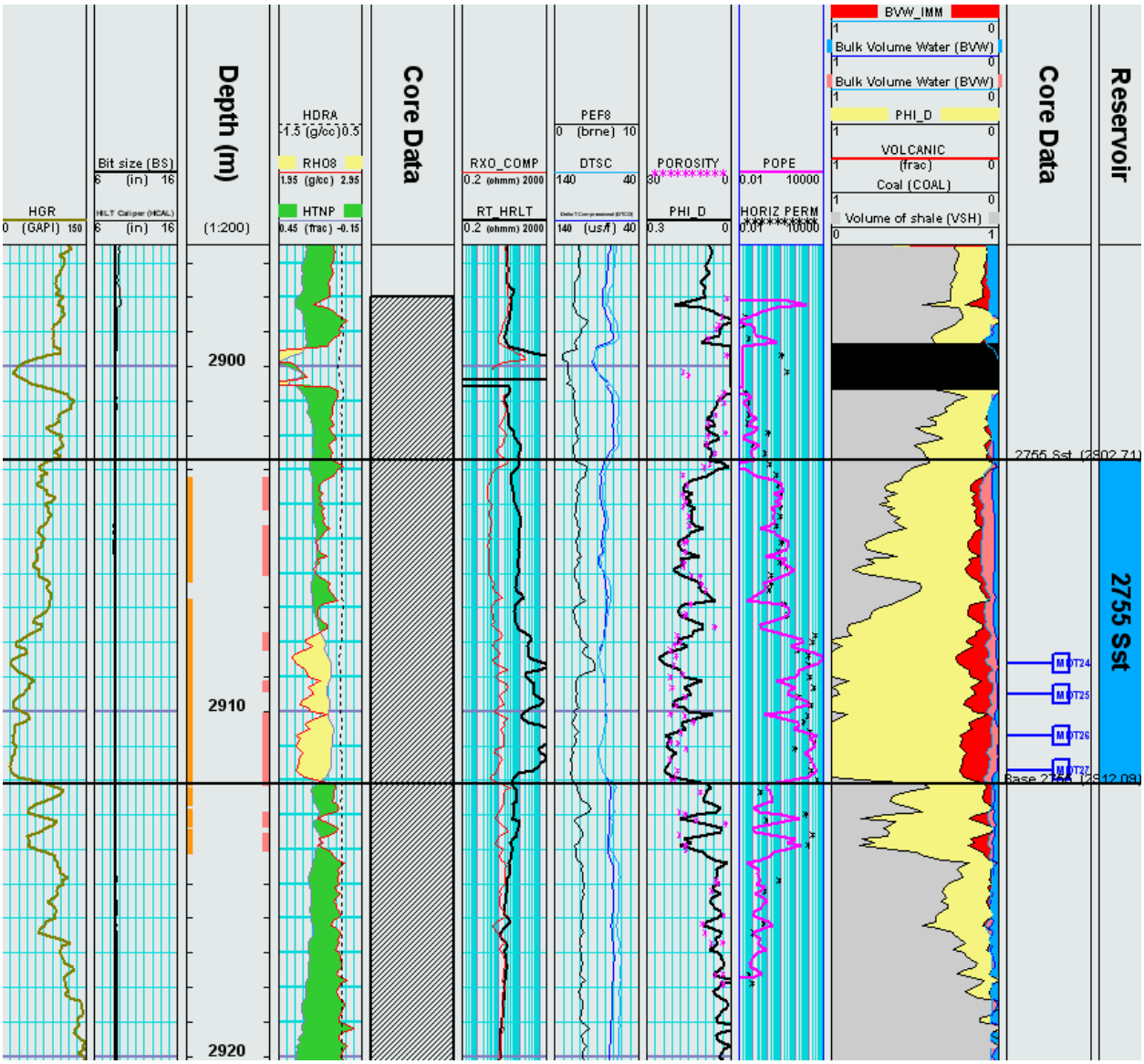

Figure 21: 2755 and 2809 Sst Reservoir MDT Pressure Data Analysis

(by Mark Mussared)

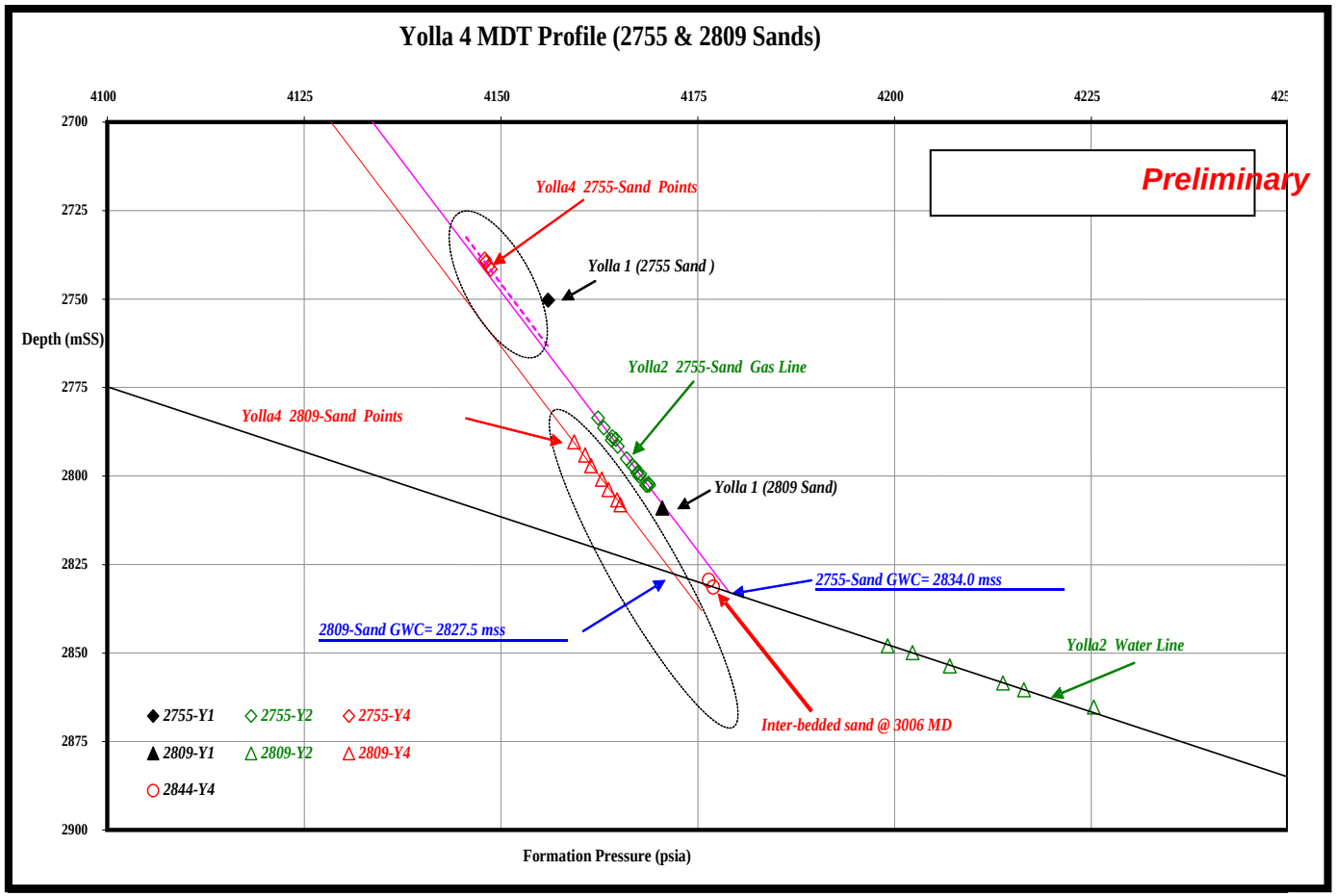

Figure 22: 2809 Sst Reservoir

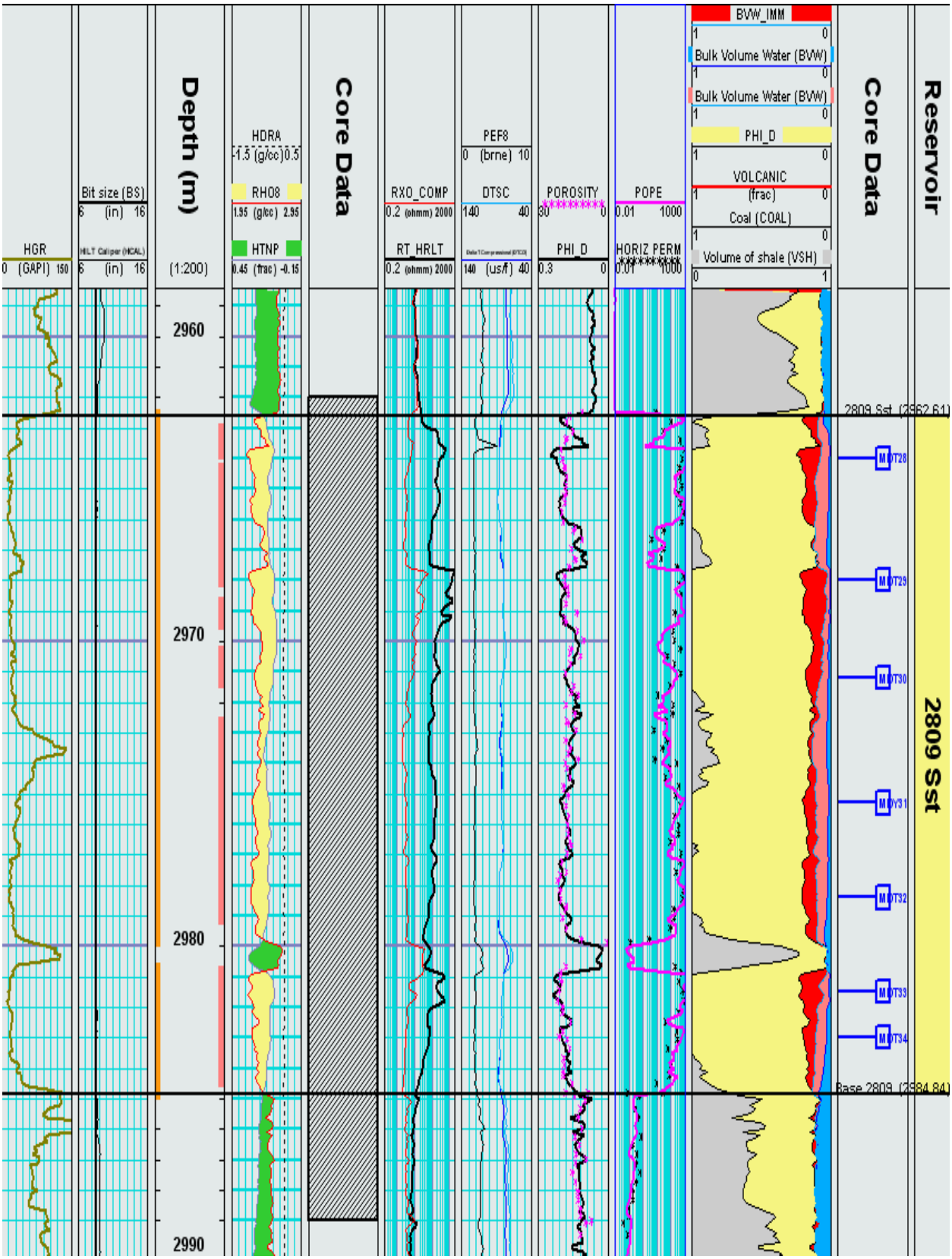

Figure 23: Log Section Across the 2844 Sst

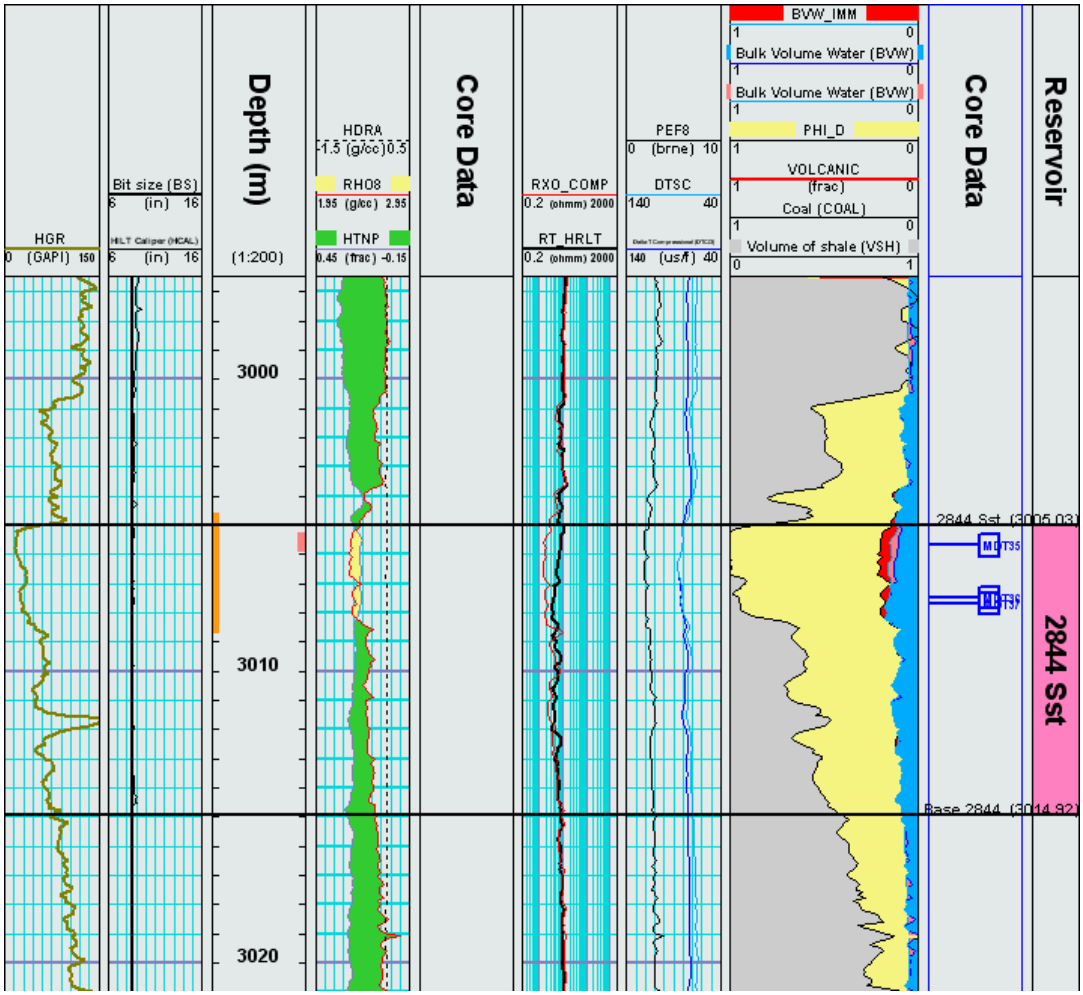

Figure 24: MDT Pressure Profile for the 2973 Sst in Yolla-4
(by Joe Parvar)

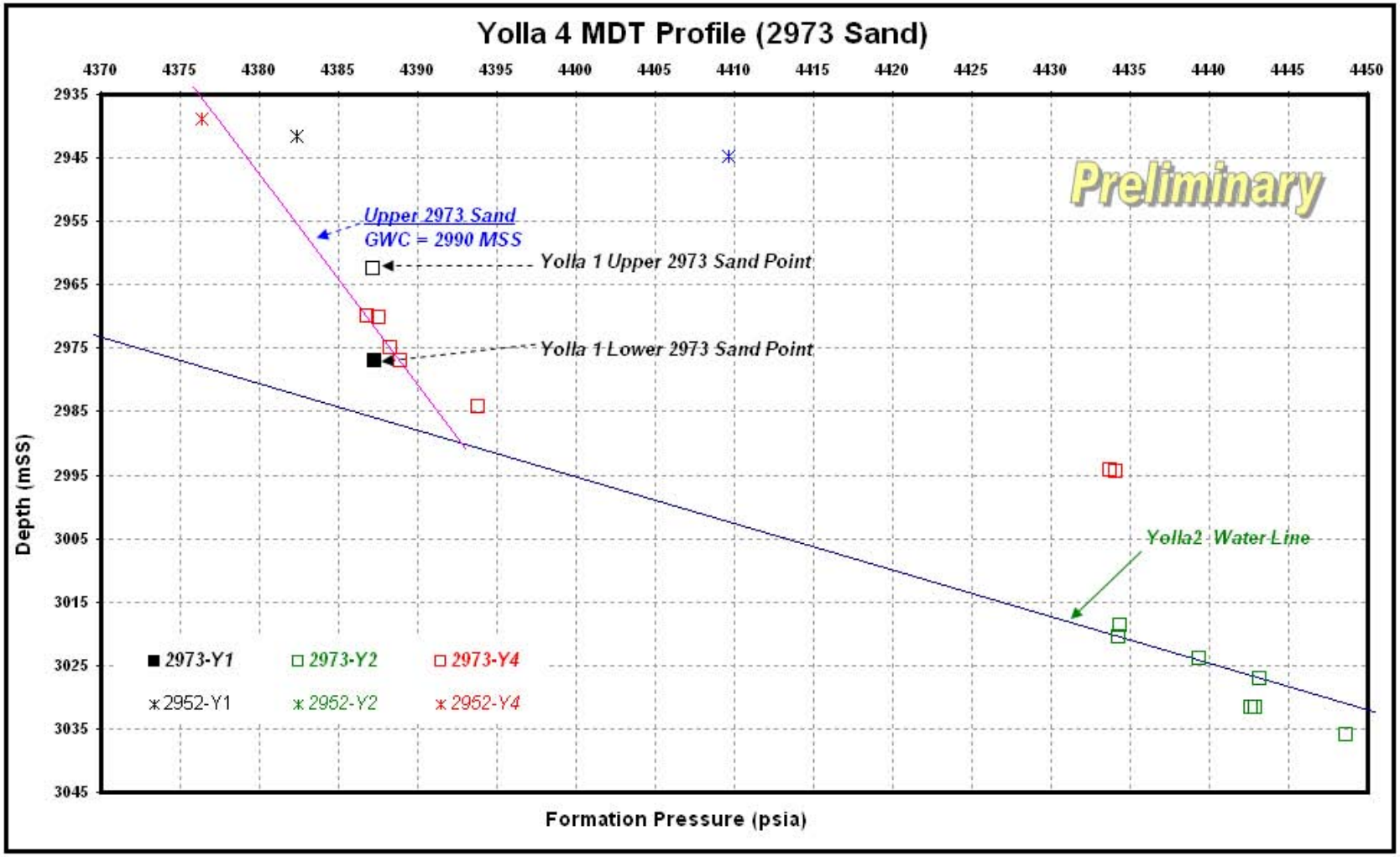

Figure 25: Log Section through the 2952 and 2973 Sst

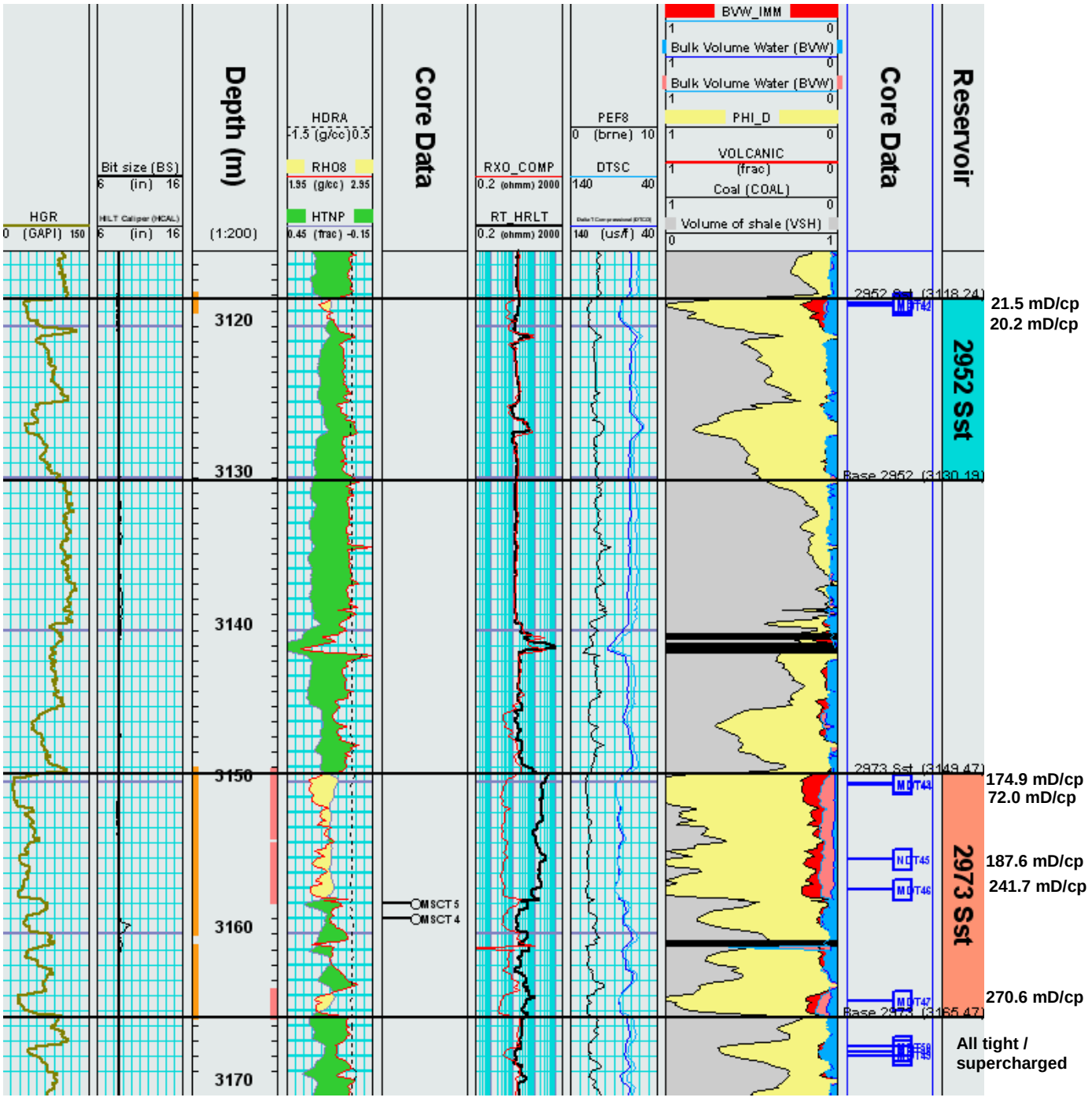

REFERENCES

1. Baker J.C. (2004) Petrology, Diagenesis and Reservoir Quality of Core Samples From Yolla-4
2. Baker J.C. (2004) Petrology, Diagenesis and Reservoir Quality of MSCT Samples From Yolla-4

Appendix A : Terrastation Macro for Processing Yolla-4

```
************************************************
CLEAR CHANNEL 70
SET CHANNEL NAME 70 VSH_GRL
*
CLEAR CHANNEL 57
SET CHANNEL NAME 57 VSHND
*
CLEAR CHANNEL 58
SET CHANNEL NAME 58 VSHRES
*
CLEAR CHANNEL 80
SET CHANNEL NAME 80 VSH
*
CLEAR CHANNEL 1375
SET CHANNEL NAME 1375 TEMPA
*
CLEAR CHANNEL 1376
SET CHANNEL NAME 1376 TEMPB
*
CLEAR CHANNEL 700
SET CHANNEL NAME 700 T
*
CLEAR CHANNEL 701
SET CHANNEL NAME 701 RW_T
*
CLEAR CHANNEL 702
SET CHANNEL NAME 702 RMF_T
*
CLEAR CHANNEL 328
SET CHANNEL NAME 328 SW_ARCH
*
CLEAR CHANNEL 340
SET CHANNEL NAME 340 SXO_ARCH
*
CLEAR CHANNEL 360
SET CHANNEL NAME 360 BVW
*
CLEAR CHANNEL 703
SET CHANNEL NAME 703 BVW_IMM
*
* Waxman Smits terms
*
CLEAR CHANNEL 674
SET CHANNEL NAME 674 QV
*
CLEAR CHANNEL 675
SET CHANNEL NAME 675 B
*
CLEAR CHANNEL 676
SET CHANNEL NAME 676 F_STAR
*
CLEAR CHANNEL 677
SET CHANNEL NAME 677 N_STAR
*
CLEAR CHANNEL 678
SET CHANNEL NAME 678 M_STAR
*
CLEAR CHANNEL 679
SET CHANNEL NAME 679 TERM1
*
CLEAR CHANNEL 680
SET CHANNEL NAME 680 SW_TP
*
CLEAR CHANNEL 681
SET CHANNEL NAME 681 NWS_T1
*
CLEAR CHANNEL 682
SET CHANNEL NAME 682 A_STAR
*
CLEAR CHANNEL 481
SET CHANNEL NAME 481 TEST
*
```

```
**********************************************
* Mud properties RM (C7), RMF (C9), RMC (C5), MW (C25)
* Temperatures RM (C8), RMF (C10), RMC (C6)
* From Yolla-4 HRLA-PEX-SP-GR print (1:500)
* MW
        C25= 9.35
* Rm
        C7 = 0.197
        C8 = 22
* Rmf
        C9 = 0.181
        C10 = 21
* Rmc
        C5 = 0.215
        C6 = 19
PRINT Mud Properties entered
*-------------------------------------------------------------------
* Temperature Log
*
* SET BHT (C13) and Depth (C20), Surface Temp (C14) and Depth (C34)
        C13 = 126
        C20 = 3235.5
        C14 = 8
        C34 = 124
BEGIN
        VT= C14 + (C13 - C14) * (VDEPTH - C34) / (C20 - C34)
ENDBEGIN
PRINT Temperature Log Created
**************************************************************************
* Matrix GR (C61), Density (C62), Sonic (C63), Neutron (C64)
        C61 = 13
        C62 = 2.67
        C63 = 51.5
        C64 = -0.06
*
* Shale GR (C65), Density (C66), Sonic (C67), Neutron (C68)
        C65 = 90
        C66 = 2.57
        C67 = 80
        C68 = 0.31
        C19 = 15
*
* Fluid GR (C69), Density (C70), Sonic (C71), Neutron (C72)
        C69 = 10
        C70 = 1.0
        C71 = 189
        C72 = 1.00
*
* Archie Parameters
* Set a (C16), m (C17), n (C18)
C16=1
C17=1.777
C18=1.8
**************************************************************************
SET DEPTH INTERVAL 2590 3240
BEGIN
        VVSH_GRL = (VHCGR-C61)/(C65 - C61)
        V1375 = (C62 - GFD) * (C72 - VHTNP) - (VRHO8 - GFD) * (C72 - C64)
        V1376 = (C62 - GFD)*(1 - C68)-(C62 - GFD)*(C72 - C64)
        VVSHND=V1375 / V1376
*
        if (VVSH_GRL<=VVSHND)
                VVSH = VVSH_GRL
        else
                VVSH=  VVSHND
        endif
        if (VVSH < 0)
                VVSH=0
        endif
        if (VVSH > 1)
                VVSH=1
        endif
*
        VPHI_D = (VRHGE_WAL - VRHO8) / (VRHGE_WAL - GFD)
```

```
            VNPSC = VHTNP_SS - VVSH * (0.41 - 0.06)
            VPHI_ND = @SQT((VPHI_D^2 + VNPSC^2) / 2)
            VDTSC = VDTCO - VVSH * 10
            VPHI_S = (VDTSC - 53) / (231 - 53)
*
* Water saturation
* Rw and Rmf correction
*
            VRW_T = GRW * (GTRW + 21.5) / (VT + 21.5)
            VRMF_T = C9 * (C10 + 21.5) / (VT + 21.5)
*
* Archie Water saturation
            VSW_ARCH = ((C16/VPHI_D^C17)*(VRW_T/VRT_HRLT))^(1/C18)
            VSXO_ARCH = ((C16/VPHI_D^C17)*(VRM_HRLT/VRXO_COMP))^(1/C18)
            if (VSW_ARCH > 1)
                        VSW_ARCH = 1
            endif
            if (VSXO_ARCH < VSW_ARCH)
                        VSXO_ARCH = VSW_ARCH
            endif
*
* Calculate BVW
            VBVW=VSW_ARCH*VPHI_D
            VBVW_IMM=VSXO_ARCH*VPHI_D
*
* Coal and volcanic correction of porosity
            if (VCOAL = 1)
                        VPHI_D=0
                        VPHI_ND=0
                        VPHI_S=0
            endif
            if (VVOLCANICS = 1)
                        VPHI_D=0
                        VPHI_ND=0
                        VPHI_S=0
            endif
*
* Waxman Smits water Saturation
* QV = CEC * RHOG * (1-PORO) / (100* PORO)
            VQV= GCEC * GGD * (1 - VPHI_D) / (100 * VPHI_D)
*
* B = (0.225 * T  - 1.28 + 0.0004059*T^2) / 1+Rw^1.23*(0.045T-0.27)
            VB=(0.225*VT-1.28+0.0004059*VT^2)/(1+VRW_T^1.23*(0.045*VT-0.27))
*
* F* = F (1+Rw*B*Qv)
            VF_STAR=(C16/VPHI_D^C17)*(1+VRW_T*VB*VQV)
*
* m* = m - LOG10(1+RwBQv)/LOG10(PORO)
            VM_STAR=C17-@LOG10(1+VRW_T*VB*VQV)/@LOG10(VPHI_D)
*
* a* = F* * PORO^m*
            VA_STAR = VF_STAR * VPHI_D ^ VM_STAR
*
            VTERM1=((VA_STAR*VRW_T)/(VRT_HRLT*VPHI_D^VM_STAR))
*
            VSW_TP=VSW_ARCH
            VNWS_T1=1+VRW_T*VB*VQV
            C47=0
:LOOP
            C47=C47+1
            if (C47>20)
                        OUTPUT NUMBER 10 3 VDEPTH
                        OUTPUT TEXT Did not converge
                        PRINT OUTPUT
                        GOTO ENDLOOP
            endif
            if (SW_TP = 1)
                        VN_STAR=C18
            else
                        VN_STAR=C18*((1+((VRW_T*VB*VQV)/VSW_TP))/(VNWS_T1))
            endif
            VSW_WS = ( VTERM1 * (1/(1+((VRW_T*VB*VQV)/VSW_TP))))^(1/VN_STAR)
            VTEST=@ABS(VSW_WS-VSW_TP)
*
```

```
        if (VTEST < 0.01)
                GOTO ENDLOOP
        else
                VSW_TP=VSW_WS
                GOTO LOOP
        endif
:ENDLOOP
*
ENDBEGIN
*
* Permeability
*
BEGIN
        VPOPE = (0.0193*@EXP((VPHI_D*100)*0.5168))
        VPOPE = VPOPE-((0.0193*@EXP((VPHI_D*100)*0.5168))*(VVSH*0.064))
ENDBEGIN
SET DEPTH INTERVAL 2590 2864.5
BEGIN
        VPOPE = VKTIM
ENDBEGIN
SET DEPTH INTERVAL 2871.5 2898
BEGIN
        VPOPE = VKTIM
ENDBEGIN
SET DEPTH INTERVAL 2882.5 2885.8
BEGIN
        VPOPE = VKTIM*10
ENDBEGIN
SET DEPTH INTERVAL 2885.8 2887.1
BEGIN
        VPOPE = VKTIM*200
ENDBEGIN
SET DEPTH INTERVAL 2917.8 2962.4
BEGIN
        VPOPE = VKTIM
ENDBEGIN
SET DEPTH INTERVAL 2984.9 3004.8
BEGIN
        VPOPE = VKTIM
ENDBEGIN
SET DEPTH INTERVAL 3008.6 3149
BEGIN
        VPOPE = VKTIM
ENDBEGIN
SET DEPTH INTERVAL 3165.3 3240
BEGIN
        VPOPE = VKTIM
ENDBEGIN
SET DEPTH INTERVAL 3165.3 3240
BEGIN
        VPOPE = VKTIM
ENDBEGIN
SET DEPTH INTERVAL 3165.3 3240
BEGIN
        VPOPE = VKTIM
ENDBEGIN
SET DEPTH INTERVAL 2901 2907.7
BEGIN
        VPOPE = 0.0923*VPOPE
ENDBEGIN
SET DEPTH INTERVAL 2901 2907.7
BEGIN
        VPOPE = 1.32*VPOPE
ENDBEGIN
STATUS HEADINGS
STATUS VSH_GRL
STATUS VSHND
STATUS VSH
STATUS PHI_D
STATUS PHI_ND
STATUS PHI_S
STATUS POPE
```

ENCLOSURE 1
Petrophysical summary plot
EVCM (2600 – 3200 mRT) (1:200)

Yolla-4

Permit: TRL/1, Bass Basin, Tasmania	RTE: 43.0 m	TD (logs): 3242.5 m
Latitude : 39 50' 40.5920' S	Bit Size: 8.5 in	BHT: 126.0 degC
Longtitude : 145 49' 06.0569' E	Rm: 0.197 ohmm at: 22.0 degC	Vertical Scale 1:200 m
Easting : 398905.07	Rmf: 0.181 ohmm at: 21.0 degC	Interpreter : Andy Hall
Northing : 5588821.47	Rmc: 0.215 ohmm at: 19.0 degC	
Datum : Rotary table (RT)	Plot created on: 10/Dec/04 at: 13: 7:40	

ENCLOSURE 2
Petrophysical summary plot
EVCM (2600 – 3200 mRT) (1:500)

Yolla-4

Permit:	TRL/1, Bass Basin, Tasmania	**RTE:**	43.0 m	**TD (logs):**	3242.5 m
Latitude :	39 50' 40.5920" S	**Bit Size:**	8.5 in	**BHT:**	126.0 degC
Longtitude :	145 49' 06.0569" E	**Rm:**	0.197 ohmm at: 22.0 degC	**Vertical Scale**	1:500 m
Easting :	398905.07	**Rmf:**	0.181 ohmm at: 21.0 degC	**Interpreter :**	Andy Hall
Northing :	5588821.47	**Rmc:**	0.215 ohmm at: 19.0 degC		
Datum :	Rotary table (RT)	**Plot created on:**	10/Dec/04 at: 12:11:52		

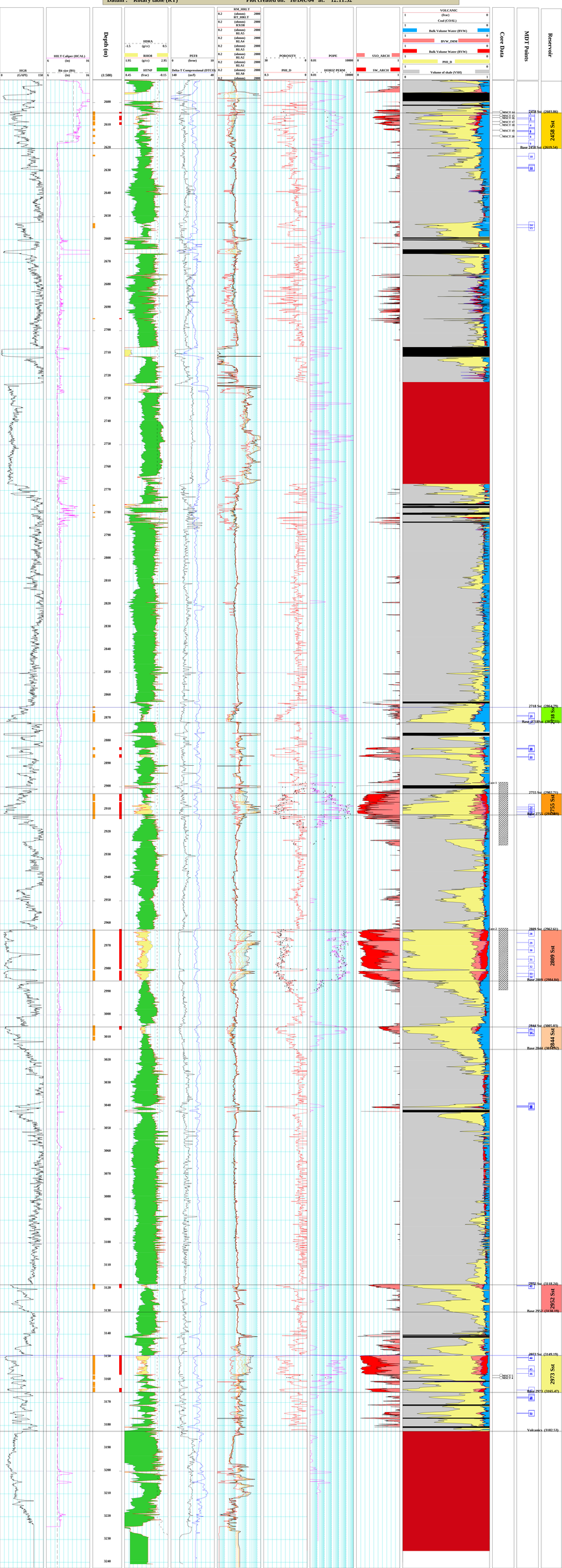

APPENDIX 2: MDT REPORT

YOLLA 4

MDT INTERPRETATION

JANUARY 2005

DATE OF SURVEY: 15/7/2004

A Schlumberger MDT tool with pump out module, resistivity tool, optical analyser, quartz and strain gauges was used to obtain pressure data and collects reservoir fluid samples from Yolla 4. The tool was also fitted with 6x450cc sample chambers.

The Yolla 4 MDT program was conducted over the interval 2604.5 to 3174.7 mRT on 15/07/2004 and 16/07/2004. A total of 53 pre-tests were attempted of which 35 tests were valid, 4 were supercharged, 12 were tight tests and two lost seal to formation.

A summary of the pre-test data is included in Appendix 11 of the Yolla 4 WCR Basic Data.

A total of 6 samples ware attempted, with all 6 samples successfully recovered. The descriptions of these samples are as follows.

3 x 450 CC Oil samples from 2458 Sand (2X2609.5 mRT & 2609.5 mRT)
1 x 450 CC Water sample from 2458 Sand (2614.5 mRT)
1 X 450 CC Water sample from 2718 Sand (2871 mRT)
1 X 450 CC Gas sample from 2844 Sand (3005.7 mRT)

The fluid composition and analysis of these samples are included in Appendix 19 of the Yolla 4 WCR Basic Data.

Meanwhile the pump out sub with optical fluid analyser (OFA) was used to identify the reservoir fluid at 3118.5 mRT (2952 Sand) and 3174.8 mRT as summarised below.

OFA at 3174.8 mRT …..(tight)
OFA at 3118.5 mRT (2952 Sand) Verified Gas trace water (21 minutes)

The interpretation of the MDT data is presented in figures 4 to 8 while figures 1 to 3 demonstrate the data validation process (quality check).

Figure1 shows the initial mud hydrostatic pressure recorded by the quartz gauge. The data indicates a slope of 0.483 psi/ft equivalent to a mud density of 9.3 ppg at the down hole condition.

Figure2 illustrates the difference between the initial and final mud hydrostatic pressures recorded by the quartz gauge. As shown in this plot this variance is very close to zero (+/- 0.5psi).

Figure3 shows the difference between reservoir pressure recorded by the quartz and strain gauges. As shown in this plot this variance is very close to zero (+/- 1psi).

Figure4 shows the pressure vs. depth plot of all the zones within the Intra-EVCM (excluding 2458). A water line with a gradient of 0.415 psi/ft, based on the Yolla 2 RFT data, was established for the Intra-EVCM

sands (with the exception of 2718 Sand which appears to be water saturated and has a separate water line).

Figure5 shows the MDT profile for the 2718 Sand. The MDT data indicates that this zone is water saturated at the Yolla 4 location. A MDT sample taken at 2871 mRT recovered formation water confirming this result. The single Yolla1 RFT point, from which a gas column has been inferred in the past, could have been supercharged (it was later confirmed by the Yolla3 MDT data).

The 2718 Sand has a separate water line which indicates that this zone is not connected to the hydrodynamic system of the main Intra-EVCM sands.

Figure6 Illustrates the pressure vs. depth profile for the 2755 and 2809 sands. The plot shows that these two sands have separate gas water contacts. A gas line with a gradient of 0.105 psi/ft (consistent with the measured gas density) fitted through the Yolla4 data points defines a GWC of 2834.0 mss. Also a gas line with a gradient of 0.109 psi/ft (based on the measured gas density) plotted through the Yolla4 2809 Sand MDT data gives a GWC of 2828.2 mss. The fluid samples taken from these sands during production test (and also Yolla 3 MDT sampling) indicate that the associated reservoir fluids have different gas densities consistent with the gradients used in this interpretation.

As shown in this plot the Yolla 2 MDT points do not lie on the Yolla-4 trend and are offset by approximately 1.1 psi (or 3.2 metres). This variance is thought to be due to imprecision in the Yolla-4 depth measurements (the Yolla 3 data backs up this theory).

The only two points from the Yolla-1 2755 and 2809 sands (from which gas columns have been defined in the past) are both offset by approximately 4 psi. This offset is likely to be a gauge error in the 1985 Yolla-1 measurements.

Figure7 Shows the MDT profile for the 2973 Sand. A gas line with a gradient of 0.097 psi/ft (consistent with the measured gas density) fitted through the Yolla-4 2973 Upper Sand data points defines a GWC of 2990.2 mss with the water line from Yolla-2.

A preliminary interpretation of the MDT data of the second development well (Yolla-3) indicates that there are two separate gas columns (Upper and Lower sands) within the 2973 zone. The Yolla-4 data appears to fit in with the upper sand.

The only point from Yolla-1 2973 Upper Sand (there is also one point related to the Lower Sand) is offset by approximately 3.0 psi which is likely due to a gauge error in the 1985 data.

Figure8 demonstrates the MDT profile for the 2458 Sand. The Yolla-4 MDT points lie on an oil line with a gradient of 0.29 psi/ft. This zone does not appear to be a part of the Intra-EVCM or UEVCM systems. Although no water line can be interpreted for this sand an MDT sample collected at 2614.5 mRT (2470.5mss) recovered water (even though mostly mud filtrate) with no oil, unlike the sample taken at 2609.m RT in this zone. Meanwhile the same MDT point (2614.5 mRT) lies on the 2458 Sand established oil line which indicates that the OWC should be very close to this level. On this basis an OWC of 2470.0 mss has been assumed for this zone.

At the time of this interpretation only preliminary results of Yolla-3 MDT were available. A complete analysis of the MDT data, incorporating all the Yolla wells, will be included in the Yolla-3 MDT report.

A summary of the results are shown in the following table.

Yolla-4 MDT Summary of Results			
Sands	**MDT Profile**	**Fluid**	**GWC (mss)**
2718	**Figure 5**	**Water**	**-**
2755	**Figure 6**	**Gas**	**2834.0**
2809	**Figure 6**	**Gas**	**2828.2**
2973 (Upper)	**Figure 7**	**Gas**	**2990.2**
2973 (Lower)	**NA**	**NA**	**-**
2458	**Figure 8**	**Oil**	**2470.0 (est OWC)**

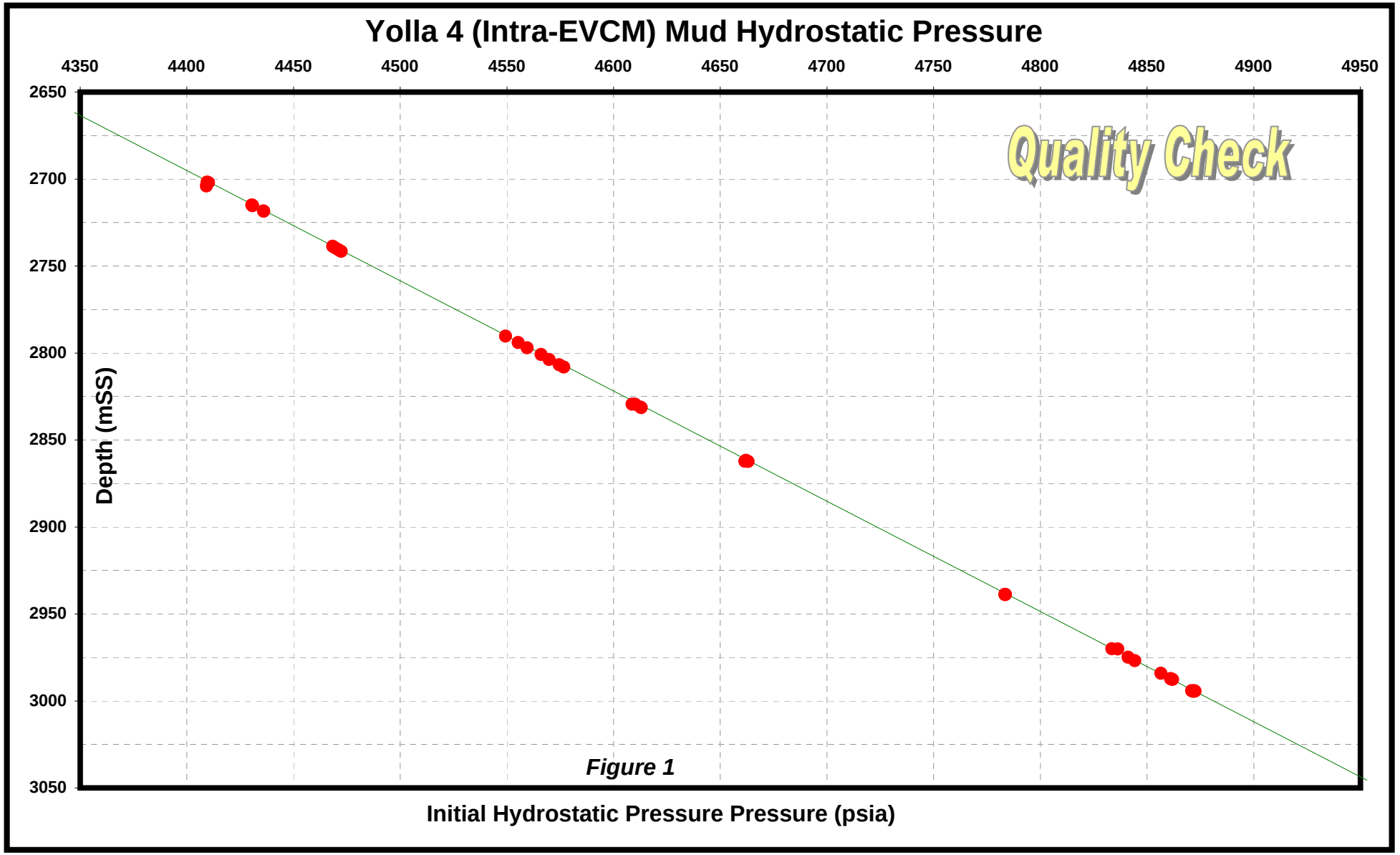
Yolla 4 (Intra-EVCM) Mud Hydrostatic Pressure
4350
4400
4450
4500
4550
4600
4650
4700
4750
4800
4850
4900
4950
2650
2700
2750
2800
2850
2900
2950
3000
3050
Depth (mSS)
Quality Check
Initial Hydrostatic Pressure Pressure (psia)

Figure 1

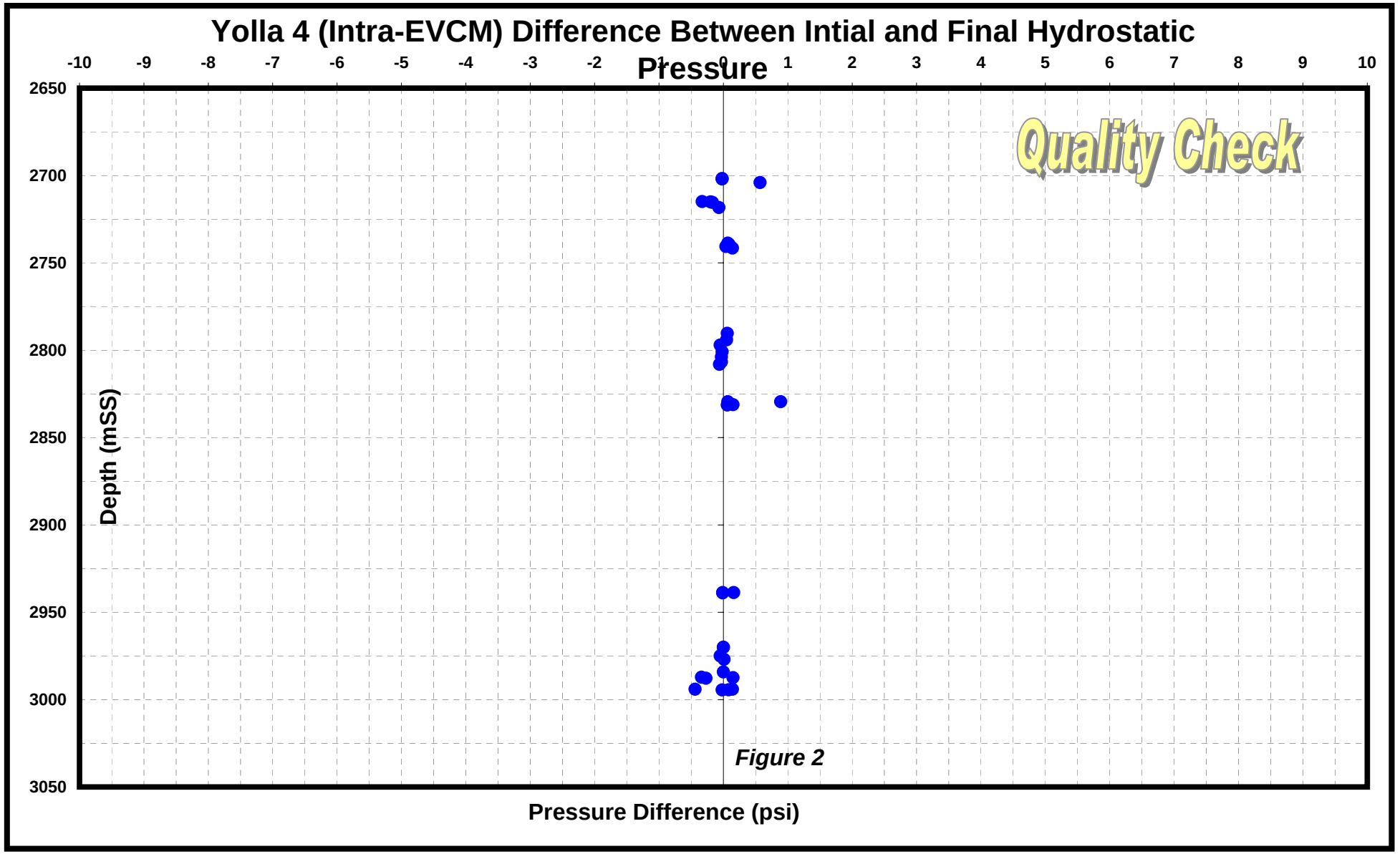
Yolla 4 (Intra-EVCM) Difference Between Intial and Final Hydrostatic Pressure
-10 -9 -8 -7 -6 -5 -4 -3 -2 -1 0 1 2 3 4 5 6 7 8 9 10
2650 2700 2750 2800 2850 2900 2950 3000 3050
Depth (mSS)
Quality Check
Pressure Difference (psi)

Figure 2

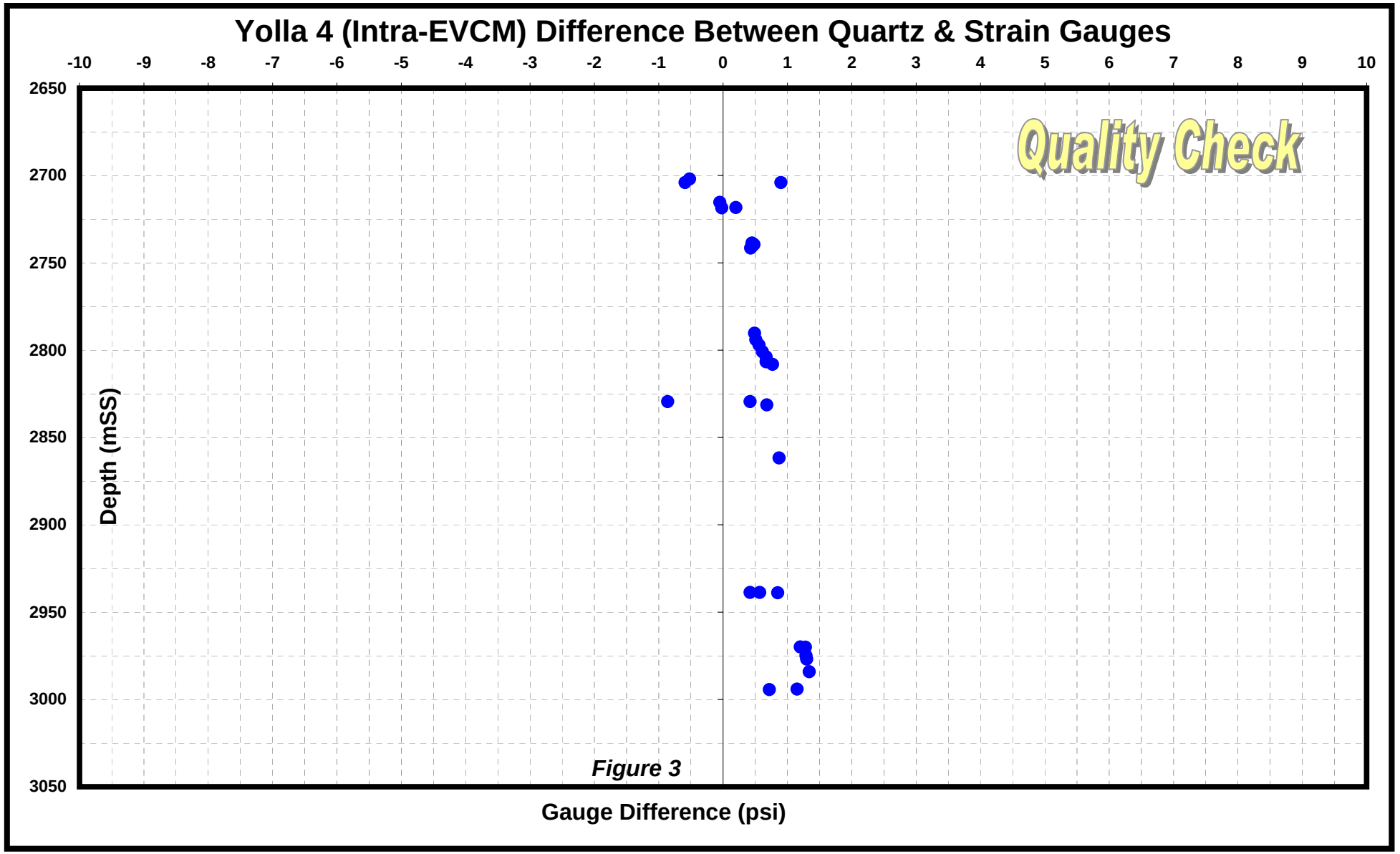
Yolla 4 (Intra-EVCM) Difference Between Quartz & Strain Gauges
-10
-9
-8
-7
-6
-5
-4
-3
-2
-1
0
1
2
3
4
5
6
7
8
9
10
2650
2700
2750
2800
2850
2900
2950
3000
3050
Depth (mSS)
Quality Check
Gauge Difference (psi)

Figure 3

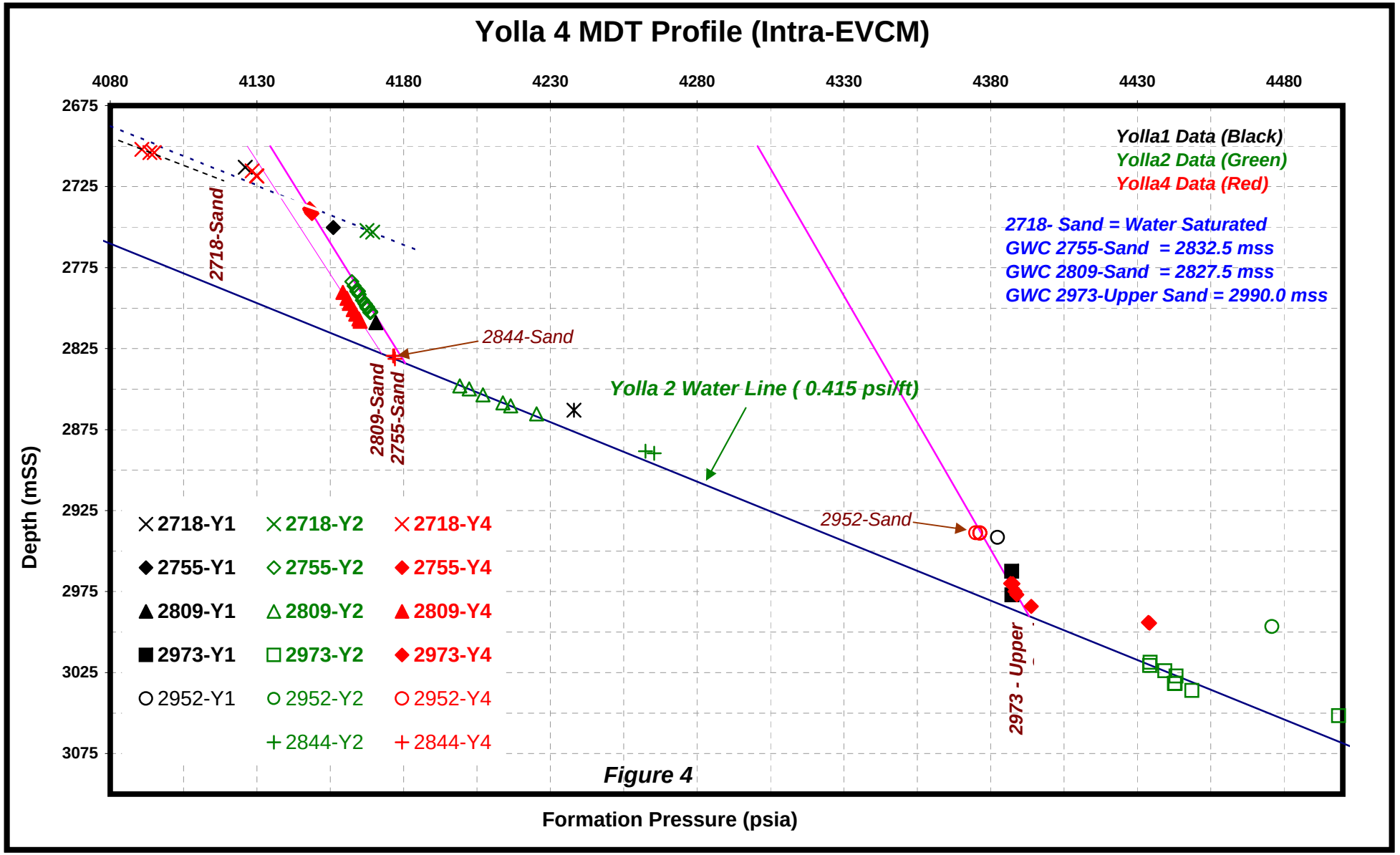
Yolla 4 MDT Profile (Intra-EVCM)
4080
4130
4180
4230
4280
4330
4380
4430
4480
2675
2725
2775
2825
2875
2925
2975
3025
3075
Depth (mSS)
Formation Pressure (psia)
Yolla1 Data (Black)
Yolla2 Data (Green)
Yolla4 Data (Red)
2718- Sand = Water Saturated
GWC 2755-Sand = 2832.5 mss
GWC 2809-Sand = 2827.5 mss
GWC 2973-Upper Sand = 2990.0 mss
2718-Sand
2844-Sand
2809-Sand
2755-Sand
Yolla 2 Water Line (0.415 psi/ft)
2952-Sand
2973 - Upper
2718-Y1
2718-Y2
2718-Y4
2755-Y1
2755-Y2
2755-Y4
2809-Y1
2809-Y2
2809-Y4
2973-Y1
2973-Y2
2973-Y4
2952-Y1
2952-Y2
2952-Y4
2844-Y2
2844-Y4

Figure 4

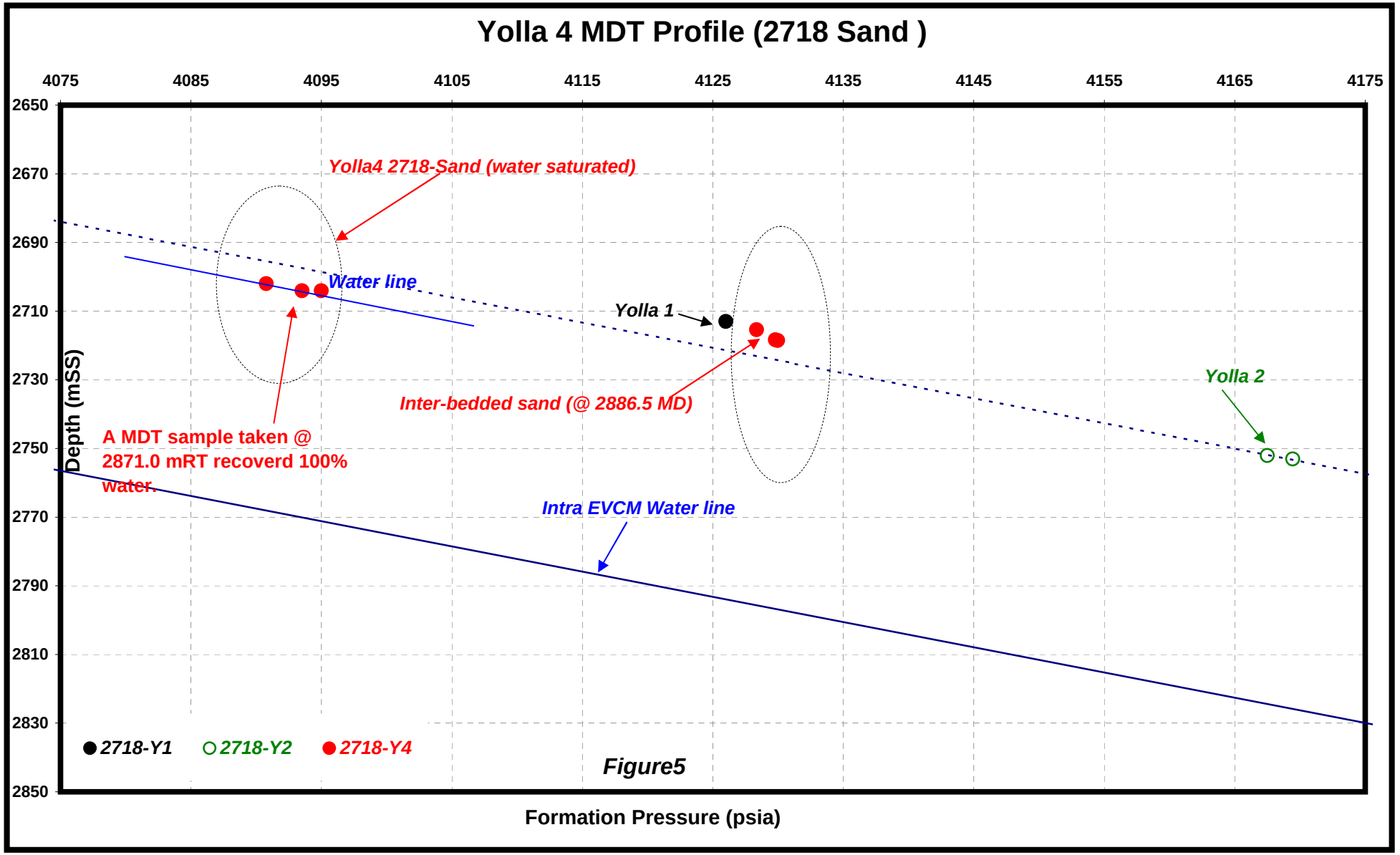
Yolla 4 MDT Profile (2718 Sand)
4075
4085
4095
4105
4115
4125
4135
4145
4155
4165
4175
2650
2670
2690
2710
2730
2750
2770
2790
2810
2830
2850
Depth (mSS)
Yolla4 2718-Sand (water saturated)
Water line
Yolla 1
Yolla 2
Inter-bedded sand (@ 2886.5 MD)
A MDT sample taken @ 2871.0 mRT recoverd 100% water.
Intra EVCM Water line
2718-Y1
2718-Y2
2718-Y4
Figure5
Formation Pressure (psia)

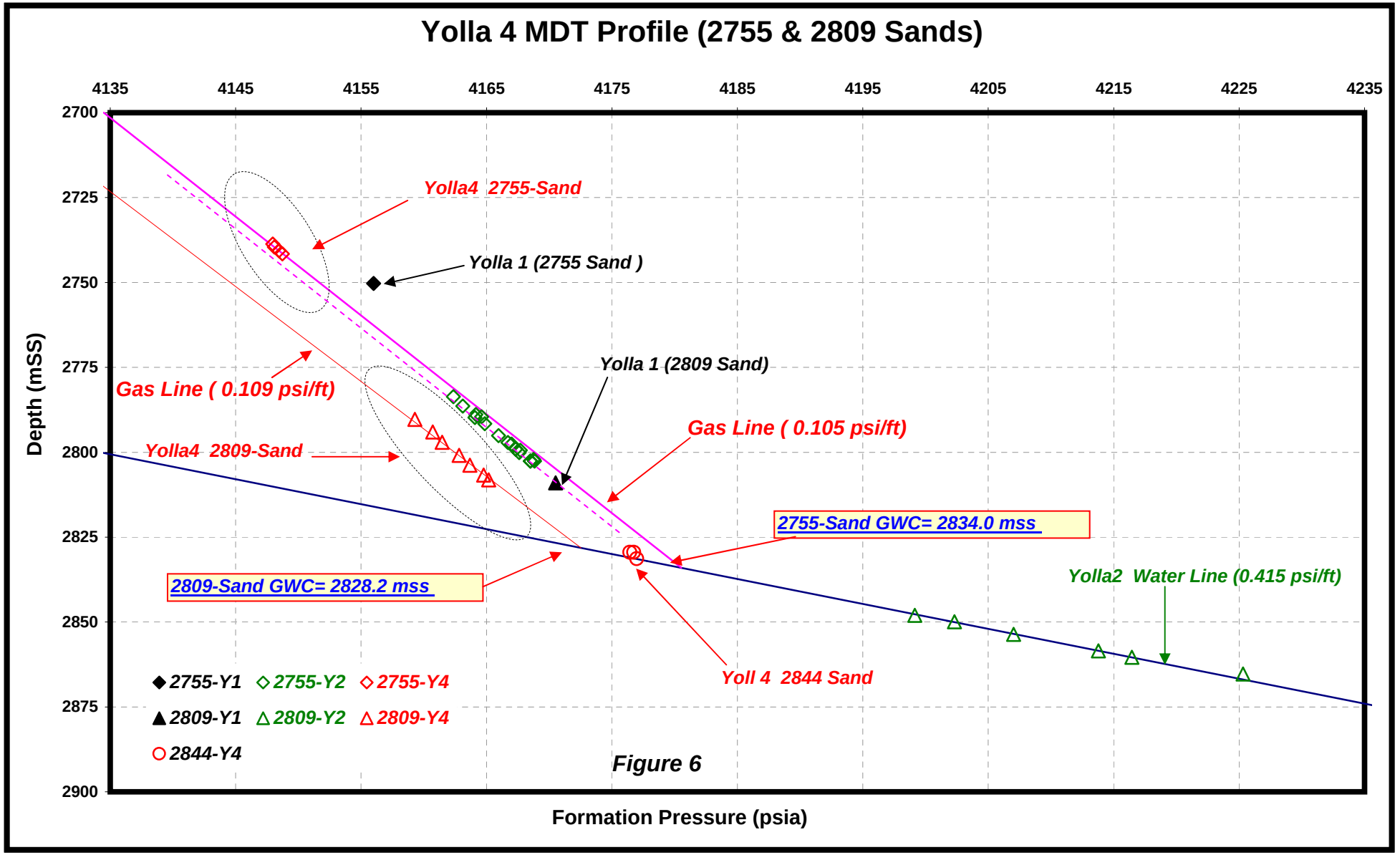
Yolla 4 MDT Profile (2755 & 2809 Sands)
4135
4145
4155
4165
4175
4185
4195
4205
4215
4225
4235
2700
2725
2750
2775
2800
2825
2850
2875
2900
Depth (mSS)
Yolla4 2755-Sand
Yolla 1 (2755 Sand)
Yolla 1 (2809 Sand)
Gas Line (0.109 psi/ft)
Gas Line (0.105 psi/ft)
Yolla4 2809-Sand
2755-Sand GWC= 2834.0 mss
2809-Sand GWC= 2828.2 mss
Yolla2 Water Line (0.415 psi/ft)
Yoll 4 2844 Sand
2755-Y1
2755-Y2
2755-Y4
2809-Y1
2809-Y2
2809-Y4
2844-Y4
Figure 6
Formation Pressure (psia)

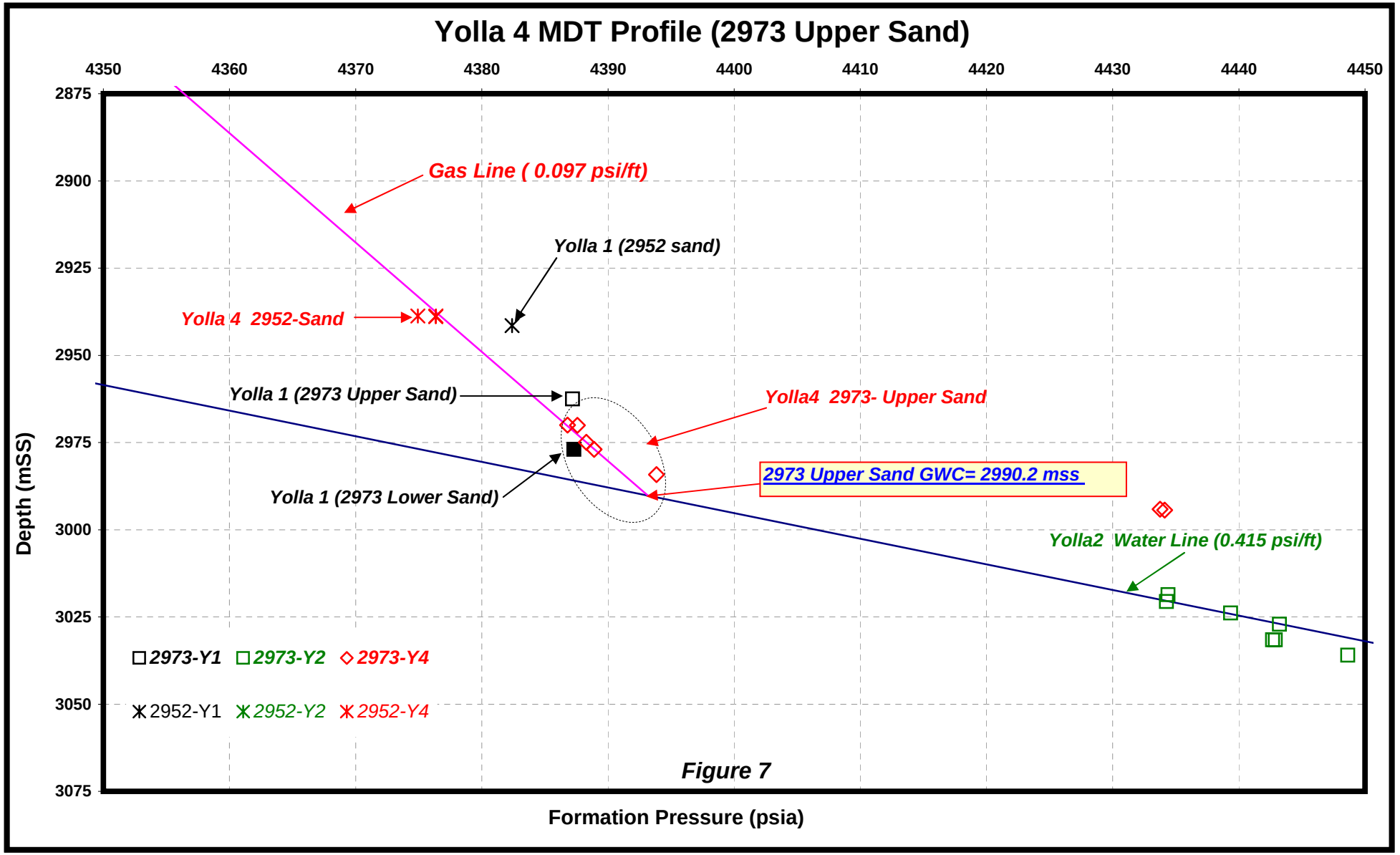
Yolla 4 MDT Profile (2973 Upper Sand)
4350
4360
4370
4380
4390
4400
4410
4420
4430
4440
4450
2875
2900
2925
2950
2975
3000
3025
3050
3075
Depth (mSS)
Gas Line (0.097 psi/ft)
Yolla 1 (2952 sand)
Yolla 4 2952-Sand
Yolla 1 (2973 Upper Sand)
Yolla4 2973- Upper Sand
Yolla 1 (2973 Lower Sand)
2973 Upper Sand GWC= 2990.2 mss
Yolla2 Water Line (0.415 psi/ft)
2973-Y1
2973-Y2
2973-Y4
2952-Y1
2952-Y2
2952-Y4
Figure 7
Formation Pressure (psia)

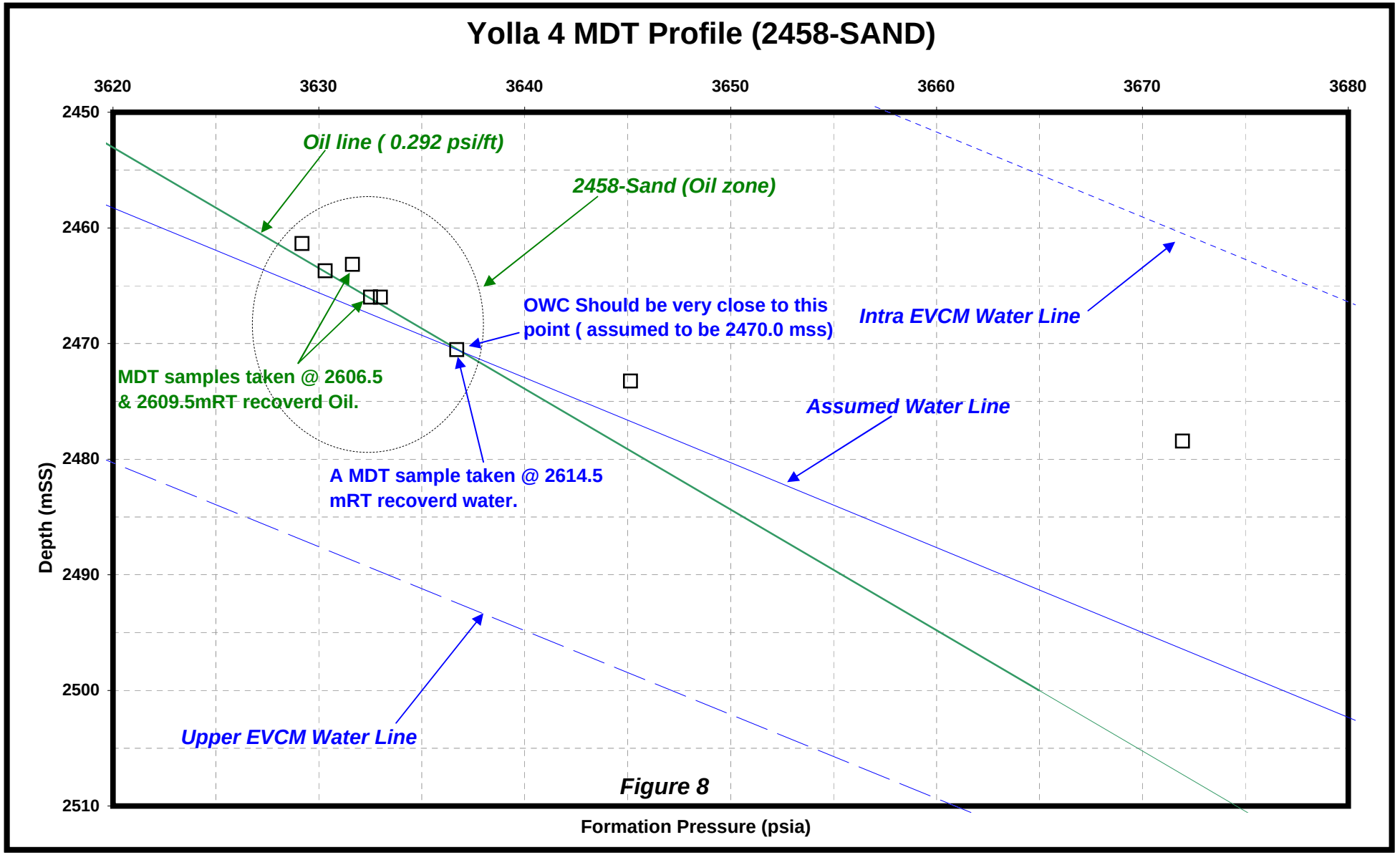
Yolla 4 MDT Profile (2458-SAND)
3620
3630
3640
3650
3660
3670
3680
2450
2460
2470
2480
2490
2500
2510
Depth (mSS)
Formation Pressure (psia)
Oil line (0.292 psi/ft)
2458-Sand (Oil zone)
OWC Should be very close to this point (assumed to be 2470.0 mss)
Intra EVCM Water Line
MDT samples taken @ 2606.5 & 2609.5mRT recoverd Oil.
Assumed Water Line
A MDT sample taken @ 2614.5 mRT recoverd water.
Upper EVCM Water Line

Figure 8

APPENDIX 3: PRODUCTION TESTING INTERPRETATION REPORTS

(A) Test Interpretation

Yolla 4 Initial Clean-Up Flow Tests – Interpretation Report

Introduction

As part of the completion procedure, the Yolla 4 well was flowed from each zone to clean up the well, estimate productivity, and obtain samples of produced fluids. Table 1 summarises the results of the testing by completion zone and the sections below describe the operational sequence, and the main test results and interpretations.

Surface production testing operations were carried out by Schlumberger (WCR Basic Data Appendix 16), surface sampling was carried out by Petrolab, the downhole gauges were provided by Halliburton (WCR Basic Data Appendix 16) and programme preparation and technical supervision of testing operations was provided by AWT .

Operational Summary

The comments below summarise the testing operations in the sequence they were carried out – further details are available in the Schlumberger test report, and the bottomhole and surface data plots are included in the figures and the Saphir report attached to this document.

1. **Commingled initial flow:** Following completion of the well, the surface equipment was set up and tested and the liquid meter calibrated to the surge tank. The sliding sleeves were opened over the 2809 and 2755 Sands with little pressure response and when the 2458 Sand SSD was opened the THP built up to 631 psia. On 28 July 2004 at 7:43 the well was opened up to the surge tank and beaned up to 24/64" choke. The well FTHP dropped to 18 psia over a 30 minute period and the well returned 9 bbls of the diesel cushion. The well was shut-in at the choke manifold, the SSD's over the 3 zones were closed, and a gradient survey was run. The low flow rates apparent from the well response are believed to be the result of plugging of the perforations by the completion brine fluid loss agent (sized salt) and inadequate drawdown being available to clear the perforations.
2. **Test of the 2973 Sand:** At 15:30 on 29 July, the 2973 sand was perforated with 6m of 2 1/8" Enerjet guns from 3149 – 3155m RT and the well immediately opened on 24/64" choke. The well unloaded the diesel cushion with gas to surface at 17:07 with a FTHP of 2554 psia. The well was shut-in, the spent guns pulled and a second 6m 2 1/8" Enerjet gun was run in. After opening the well at 22:53 on 20/64" choke, the second gun was fired from 3151.5 – 3157.5m RT at 00:07 on 30 July with a small response on the FTHP (2534 to 2583 psia). The well was shut-in and the guns pulled, and the Halliburton memory pressure gauges run in and set in the RN nipple in the tail pipe (approx gauge depth 2999m RT = -2832.2m SS). At 9:34 the well was opened on a series of increasing chokes up to 56/64". Metering through the test separator started at 13:03 with a steady flow rate of 27.2 mmcfd on 44/64" choke with FTHP 2823 psia and FTHT 60 deg C. The measured CGR was reasonably steady at 11 stb/mmscf with 3-4 bbls/mmscf of condensed water. The rates on the higher chokes were not metered, but the FTHP on 56/64" choke was stable at 2542 psia. The well was shut in at the choke manifold at 17:22 with THP building to 3398 psia in 8 minutes, and the gauges were retrieved.
3. **Commingled flows with 2973 Sand:** A series of flows of the 2809, 2755, and 2458 sands, each commingled in turn with the 2973 sand, were run over the period 19:30 on 30 July to 11:22 on 31 July 2004. (A plug was not run above the 2973 sand to let the higher zones clean up without risking debris falling on the plug.). During these flows, bottomhole pressure gauges were not run and surface flow rates were not metered. The 2809 Sand SSD was opened and the 2809/2973 Sands flowed for 53 minutes mainly on the final choke setting of 43/64" with an FTHP of about 3030 psia. The well was SI and the 2809 SSD was closed and the 2755 SSD was opened. The 2755/2973 Sands were flowed for 106 minutes mainly on the final choke setting of 44/64" with a rising FTHP of up to 3105 psia. The FTHP's were higher during the commingled flows of the 2809 and 2755 sands, than for the 2973 Sand alone, indicates that the upper zones were probably contributing to flow. The well was SI, the 2755 SSD closed and the 2458 SSD was opened. The 2458/2973 Sands were flowed for 77 minutes mainly on the final choke setting of 46/64" with a final FTHP of 2842 psia.
4. **Test of the 2755 Sand:** The 2458 SSD was closed and a plug was run in hole to attempt to set in the RN nipple to isolate the 2973 sand. Problems were encountered with the plug being left in the R nipple and needing to be fished. The plug was re-run and set in the RN nipple below the bottom packer. The plug was tested by bleeding off 1000 psi from the tubing and the test was accepted, though the wellhead

pressure was rising at about 2 psi/minute. Subsequent diagnostics (see Step 9 below) confirmed a leak past the plug. It should therefore be noted that the test results reported below are likely to be affected by a small proportion of the flow having come from the 2973 Sand. The 2755 SSD was opened and the WHP jumped up by 630 psi to 3144 psia. Production from the 2755 Sand was started at 16:32 on 1 August and the well was gradually beaned up to 40/64" choke. The well was SI at 17:40 to run in and hang off the pressure gauges in the bottommost sliding sleeve (below the bottom packer) with the sensing point at approximately 2992m RT (-2816.6m SS). The well was re-opened at 19:25 and gradually beaned up to 58/64" choke before beaning back to 52/64" choke. Production on 52/64" choke was metered via the test separator between 22:45 and 1:15 on 2 August 2004. The flow rate was steady at 32.2 mmcfd with a CGR of 20 stb/mmscf and 3-4 bbls/mmscf of condensed water, at an FTHP of 2787 psia and FTHT of 61 deg C.

5. **Test of the 2458 Sand:** The 2755 SSD was closed and the 2458 SSD was opened with SITHP then gradually falling from 3202 psia to 2984 psia. The 2458 sand was opened to production at 05:04 on 2 August 2004 and gradually beaned up to 40/64" choke. Oil arrived at surface in 67 minutes and the FTHP rose to stabilise at 1599 psia with FTHT of 59 deg C (the high FTHP is believed to be the result of the leaking plug above the 2973 Sand). The well was not flowed through the test separator to avoid potential problems with wax buildup. The well was shut-in at 09:11. The estimated leak rate past the 2973 plug was ~3 mmcfd based on the flow rate and drawdown using data from the flow in step 7 below. Using Gilbert's correlation, the estimated flow rate from the 2458 sand is about 2700 stb/d.
6. **Commingled flow of the 2458 and 2809 Sands:** A shifting tool was RIH to open the 2809 SSD for a commingled flow to clear out the oil from the tubing. At that time the SITHP was 2311 psia and gradually rising. The was well flowed on various chokes starting from 16/64" to 48/64" before finishing on 32/64" choke with an FTHP of 1689 psia. Review of the surface and FBHP data showed that the 2809 SSD was probably not open.
7. **Attempted test of the 2809 Sand:** The 2458 SSD was closed and the well opened at 13:00 on 2 August 2004. The FTHP pressure gradually fell from 2653 psia to 882 psia on 44/64" choke, with the well slugging oil and gas. Comparing the FTHP and FBHP indicated the well was flowing mostly gas at a rate of 6 – 8 mmcfd. The well was shut in at 15:11 and a slickline tool was RIH to check the 2809 sleeve and open the 2755 sleeve. On checking the 2809 sleeve there was a sudden jump in THP and the tool was blown up the hole and could not be pulled past 2940m RT. This result indicates that the gas produced earlier had probably come mainly via the leaking plug, rather than from the 2809 Sand. Fishing operations were conducted over the next 4 days resulting in eventual recovery of the fish.
8. **Test of the 2809 Sand:** The well was opened up at 20:41 on 6 August 2004 and gradually beaned up to 54/64" choke before settling back to 52/64" for the main 3 hour flow period through the test separator. The flow rate was stable at 32.1 mmcfd with a CGR of 24.5 stb/mmscf, and 3-4 bbls/mmscf of condensed water, with a final FTHP of 2860 psia and FTHT of 77 deg C. The well was shut in at 04:24 on 7 August 2004.
9. **Post test activities:** The 2809 SSD was closed, the tubing pressure was bled down and the well observed. The tubing pressure built up from 350 psia to 1244 psia in 21 minutes, confirming a leak. A number of diagnostics were run to identify the leak before setting another plug and moving the rig to Yolla 3. Further pressure data analysis and diagnostics, including a PLT log, showed that the plug in the RN nipple (above the 2973 Sand) was leaking. Anomalously high bottomhole SI pressures recorded after the 2755 and 2809 flow tests confirmed communication with the higher pressured 2973 sand. Therefore, the leak had probably been ongoing throughout the individual flow tests of the 2755, 2458 and 2809 sands.

Well Test Data Interpretation

Table 1 summarises the well test data including estimates of well productivity. It should be noted that the flow tests of the zones above the 2973 Sand were affected by the leak across the plug in the RN nipple – the 2973 sand is estimated to have contributed of the order of 1 – 8 mmcfd to the flow from the higher zones, depending on the drawdown. The flow rates and calculated skin factors in Table 1 are not corrected for the leak rate due to uncertainty regarding their magnitude (the correction would lower the zonal flow rates and increase the estimated skin). Conversely, the FBHP data showed that the zones were still cleaning up at the end of the drawdown phase (rising FBHP), indicating that the skin factors would fall with continued production.

It should also be noted that the condensate rates reported from the gas zone clean-up flows appear to be significantly too low. This was confirmed by MDT and production test sampling of the same zones in Yolla 3.

A thorough audit of the gas and condensate metering in Yolla 4 was carried out (Reference ?) and it was concluded that the surface metering was reasonably accurate. The lower than expected condensate rates are believed mainly the result of liquid carryover in the gas stream exiting the test separator (although the separator was operated within its stated capacity), and also due in part from the lower CGR 2973 Sand contributing to the later flows. It is recommended that the recombined reservoir gas compositions estimated from the Yolla 4 tests not be used.

The buildup for the 2973 Sand flow test was analysed and approximate estimates of permeability and skin factor were made (see the attached Saphir report). None of the other tests had usable buildup data due to a combination of short buildups, surface operations affecting the SIBHP and the impact of the 2973 plug leak.

Figures 1 - 6 show the bottomhole and surface pressure and temperature data for the entire test sequence and for the individual zone tests.

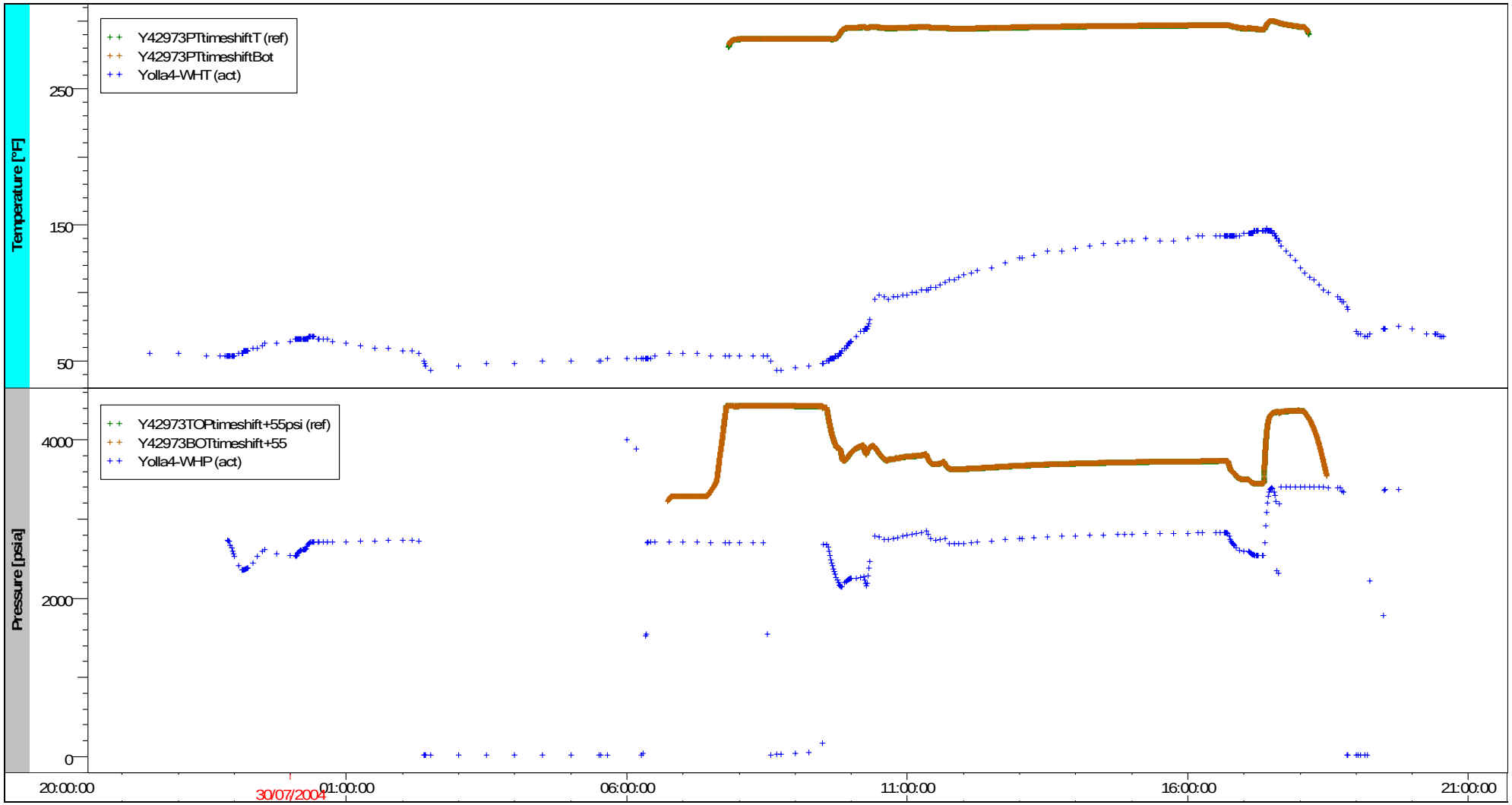

Relative temperature [°F], Pressure [psia] vs Time [ToD]

Figure 1 – 2973 Sand Initial Flow – Bottomhole and Surface Pressures & Temperatures

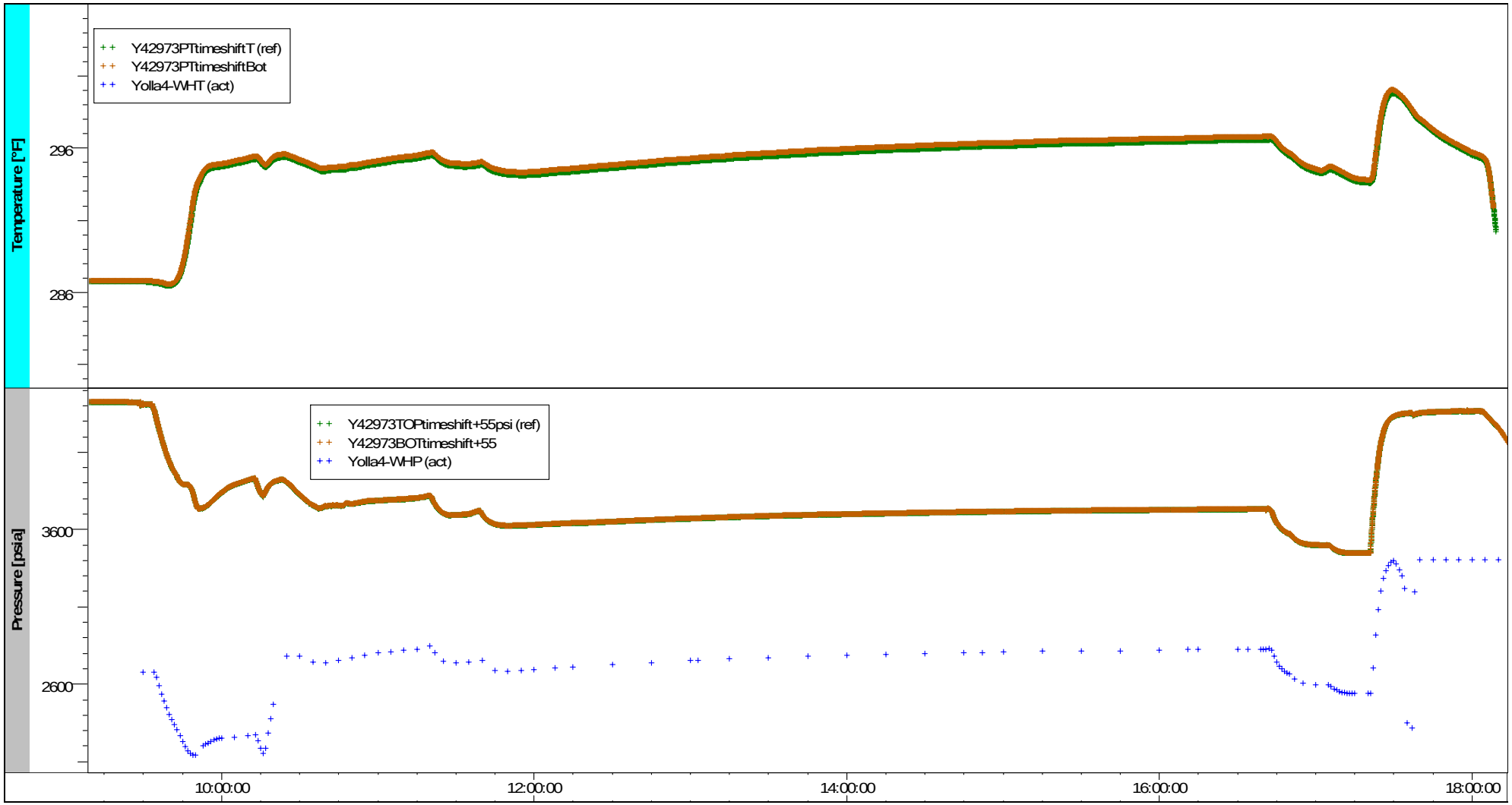

Figure 2 – 2973 Sand Initial Flow – Bottomhole and Surface Pressures & Temperatures (enlarged)

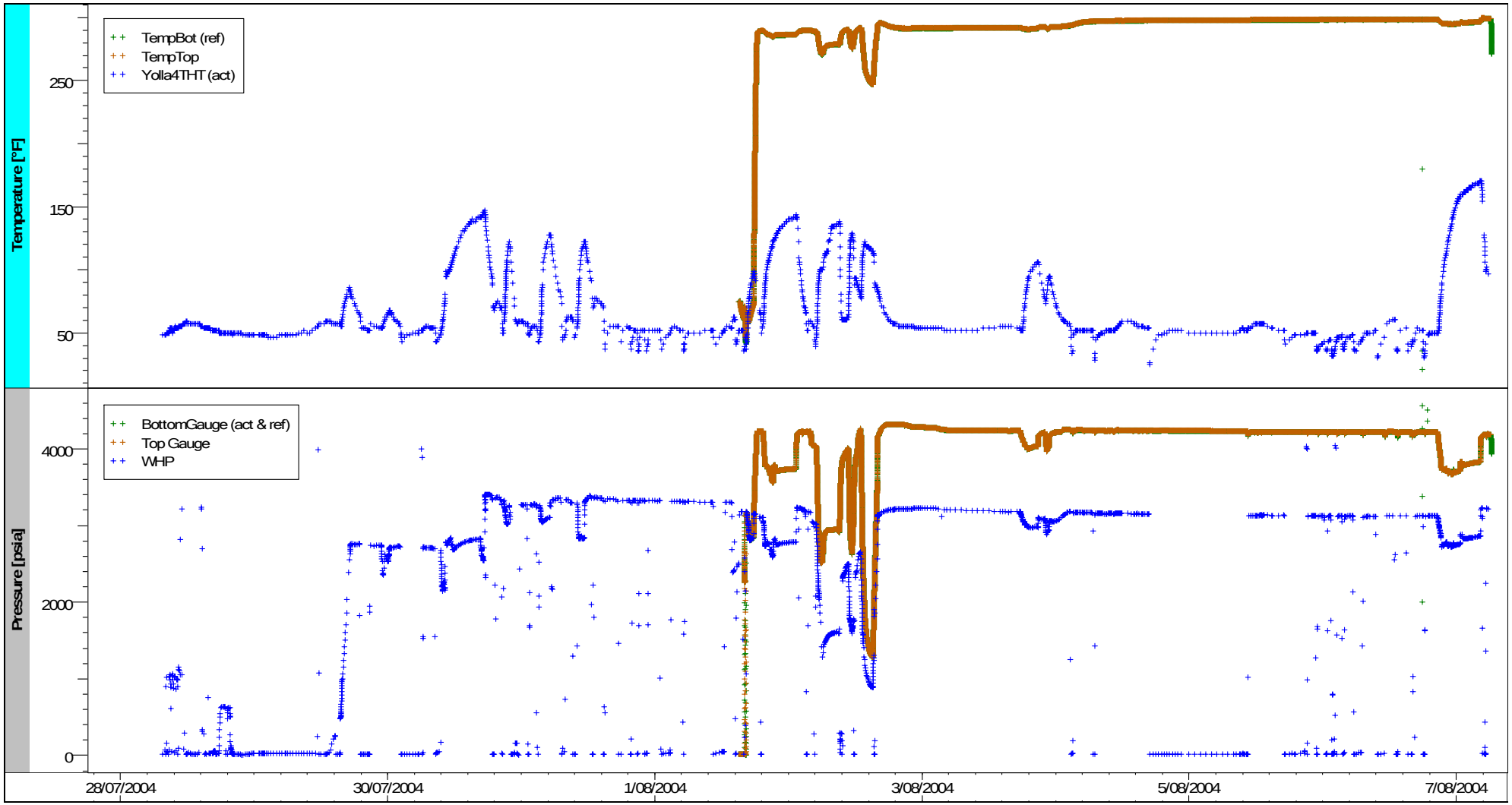

Relative temperature [°F], Pressure [psia] vs Time [ToD]

Figure 3 – Commingled and Upper Zone Flow Test Data - Overview

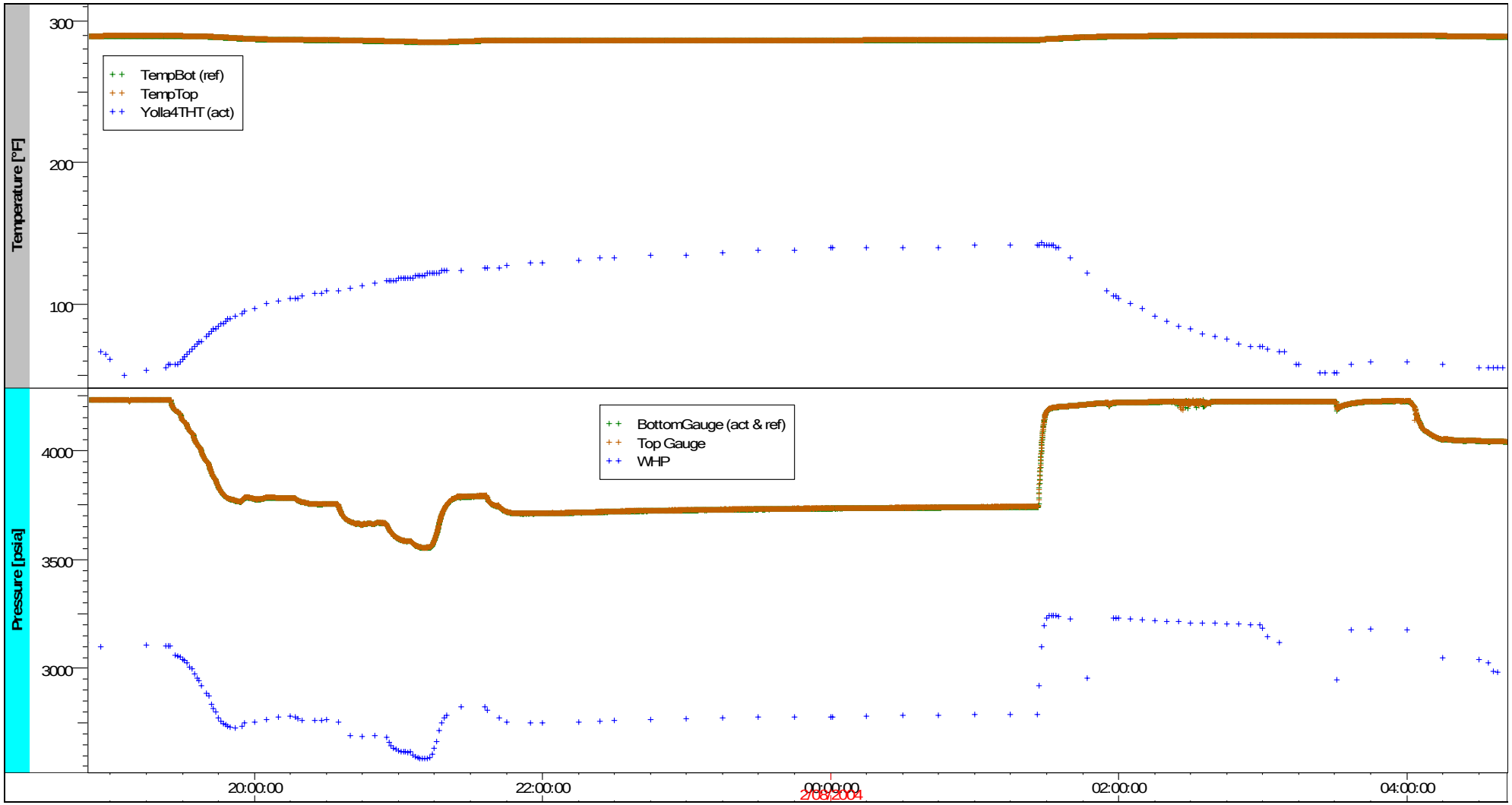

Relative temperature [°F], Pressure [psia] vs Time [ToD]

Figure 4 – 2755 Initial Flow Test – Bottomhole and Surface Data

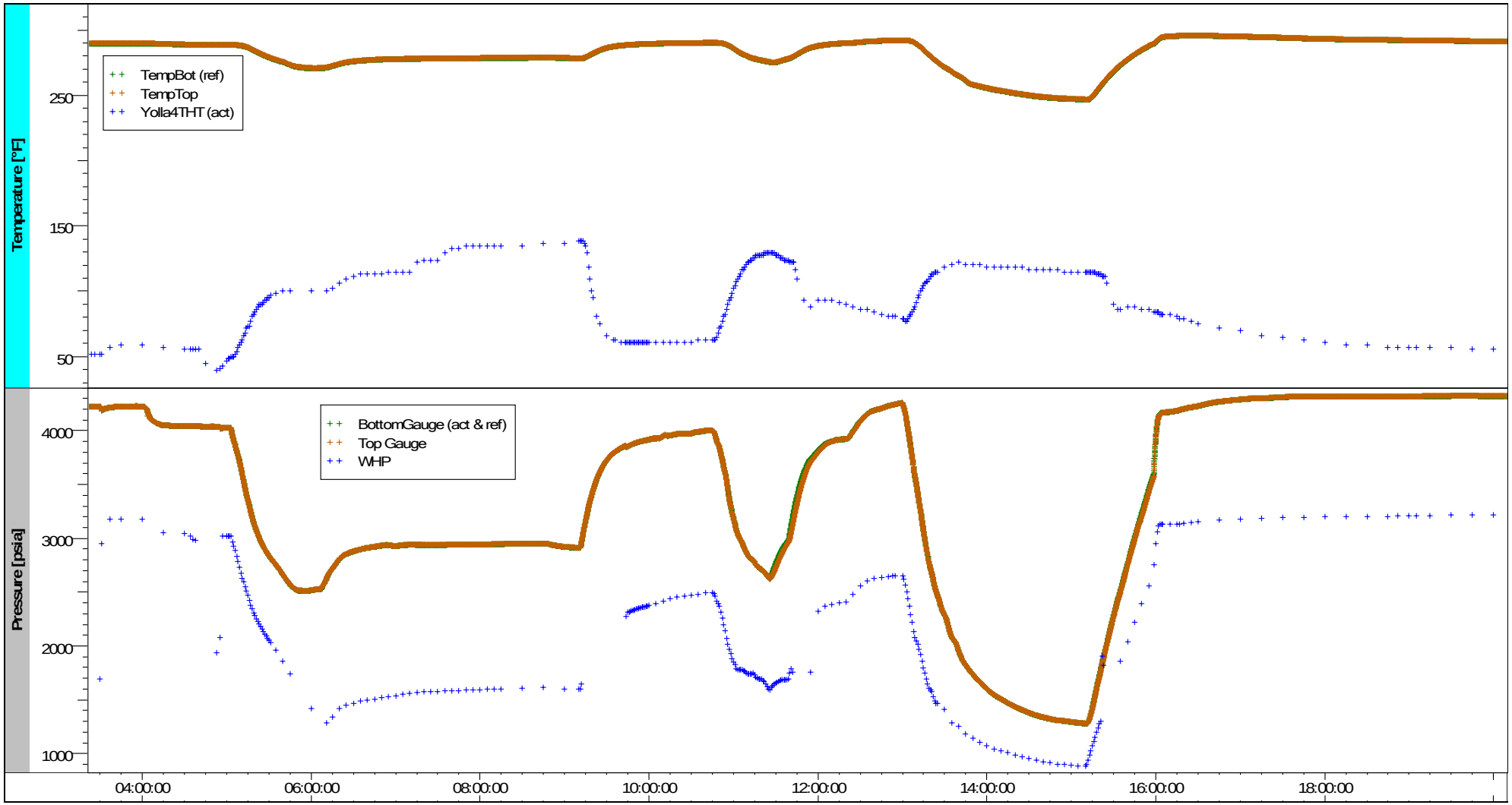

Figure 5 – 2458 Sand Initial Flow and attempt to commingle with the 2809 Sand

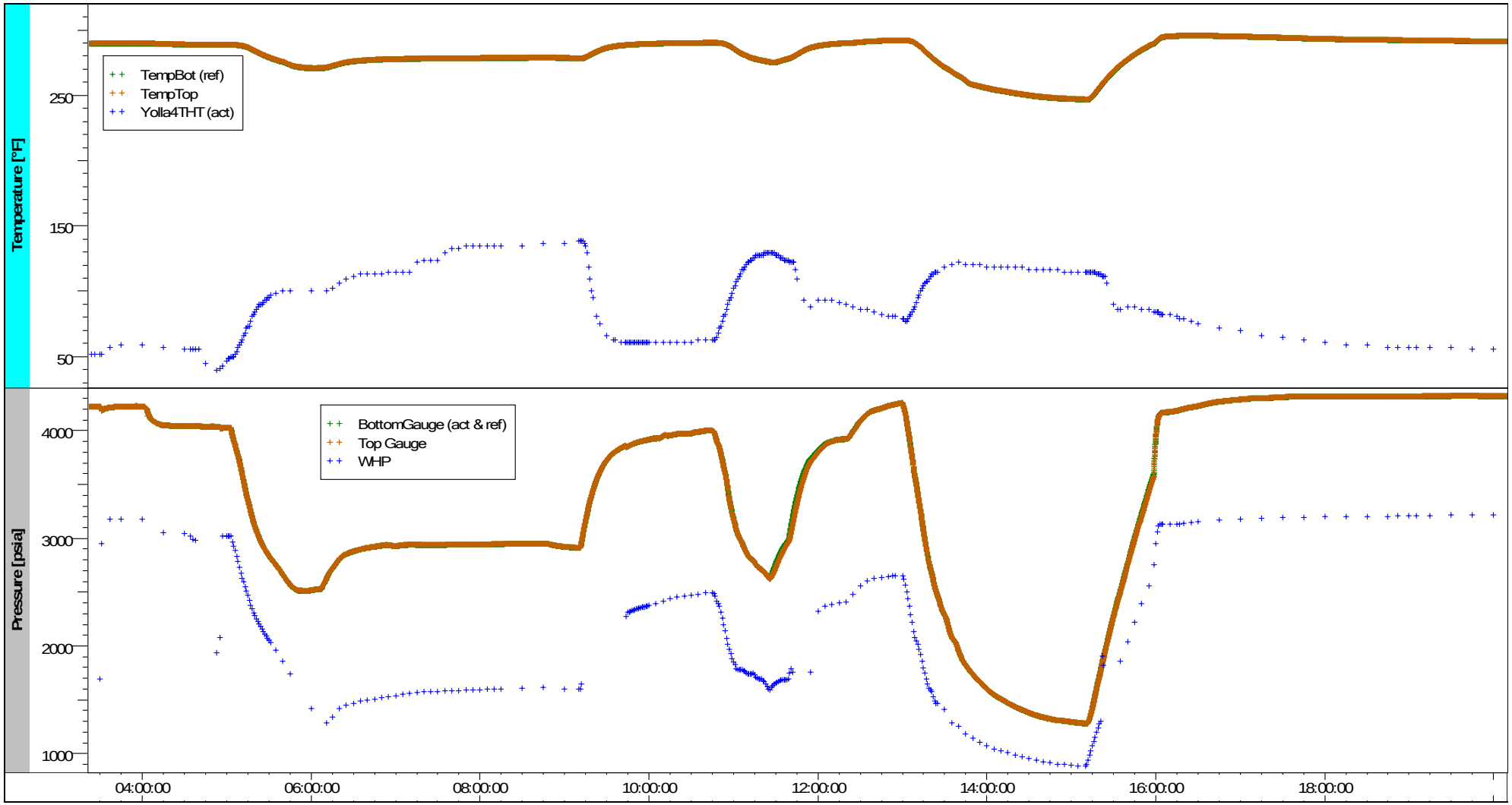

Figure 6 – 2809 Sand Initial Flow Test – Bottomhole and Surface Data

Yolla 4 Initial Clean-Up Flows - Estimates of Zone Productivity

Zone	Perfs Top	Perfs Bot	Flow Rate	CGR	FWHP	FWHT	Choke	SIWHP	Mid Perfs	FBHP	Gauge	Gradient	FBHP	Pi (MDT)	k.h (est.)	D (est.)	Darcy
	m RT	m RT	mmcfd/bopd	stb/mmscf	psia	deg C	/64"	psia	m SS	psia@gauge	m SS	psi/m	psia@MPP	psia	md.ft	/mcfd	Skin
2458	2604.0	2610.0	2700		1599	59	40	2311	-2464	2950	-2816.6	0.7	2703	3629			
2755	2902.5	2914.0	32.2	20	2787	61	52	3243	-2738	3740	-2816.6	0.331	3714	4148	25542	0.0001	52
2809	2962.5	2973.0	32.1	24.5	2860	77	52	3226	-2794	3829	-2816.6	0.352	3821	4161	18486	0.00005	45
2973	3149.0	3157.5	27.2	11	2823	60	44	3406	-2973	3731	-2823.2	0.31	3777	4388	4250	0.00003	22

Notes:

1 Measured CGR's appear tpo be too low (liquyid carryover?)
2 Flow rate estimate for 2458 sand based on Gilbert's correlation assuming 3 mmcfd flow past the plug above the 2973 Sand
3 Flowing bottomhole pressures, FWHP and FWHT were all rising during the tests indicating the zones were still cleaning up and stabilising
4 k.h from core for 2755 and 2809 sands, from buildup for 2973 sand
5 D coefficients from Woodside correlation (except 2973 sand - from test analysis)

Table 1 – Summary of Yolla 4 Initial Clean-up Flow Tests

Main Results	Analysis 1
Company AWE	Field Yolla
Well Yolla 4 - 2973 Sand	Test Name / # Initial Cleanup Flow

Test date / time	30 July 2004
Formation interval	
Perforated interval	3149 - 3155, 3151.5 - 3157.5m MDRT
Gauge type / #	Metrolog
Gauge depth	2999m RT(adj to 2973 Sand mid perfs -2973m SS, +55psi)
TEST TYPE	Standard
Porosity Phi (%)	18.7
Well Radius rw	0.3542 ft
Pay Zone h	27.4 ft
Water Salt (ppm)	26000
Form. compr.	4E-6 psi-1
Reservoir T	307 °F
Reservoir P	4393 psia
FLUID TYPE	Gas

Gas

Gas Gravity	0.8669
Pseudo-Critical P	705.702 psia
Pseudo-Critical T	393.758 °R

Sour gas composition

Hydrogen sulphide	0
Carbon dioxide	0.189
Nitrogen	0.002

Water

Salinity, ppm	26000
Temperature	307 °F
Pressure	4393 psia
Properties	@ Reservoir T&P

Gas

Z	0.990447
Mug	0.026507 cp
Bg	0.00488715 cf/scf
cg	1.80301E-4 psi-1
Rhog	0.217256 g/cc

Water

Rsw	28.0587 cf/bbl
Bw	1.07495 B/STB
cw	4.26058E-6 psi-1
Muw	0.198421 cp
Rhow	0.948873 g/cc
Total Compr. ct	1.54374E-4 psi-1
Connate Water (%)	17

Selected Model

Model Option	Standard Model
Well	Storage + Skin
Skin Type	Changing
Reservoir	Homogeneous
Boundary	Infinite

Results

TMatch	1010 [hr]**-1
PMatch	1.02E-7 [psi2/cp]**-1
C	0.05 bbl/psi
Skin0	22.8
Delta P Skin0	677.982 psi
Total Skin	24
Delta P Skin	714.992 psi
dS/dQ	3E-5 [Mscf/D]-1
Pi	4390.35 psia
k.h	4520 md.ft
k	165 md
Rinv	316 ft
Test. Vol.	2.86733E+5 Barrels

Measured gauge pressures were adjusted to the 2973 Sand mid perfs (-2973m SS) by adding 55psi (the gauges were at 2999m RT or -2823.2m SS). The pressure gauge data was also time shifted to align the bottomhole gauges with the surface gauges and operational summary. The two downhole gauges gave good quality data. Petrophysical data used was from A. Hall Email of 7 April 2005 and fluid properties were based on correlations using the Yolla-3 MDT sample compoition from the 2973 sand.

The post flow shut-in at the choke manifold was of very short duration and affected by a small leak after 15 minutes of shut-in. The buildup was mainly afterflow with only a very short radial flow period, so parameters can only be estimated roughly. Estimated permeability-thickness is 4520 md.ft and the skin was 23. The non-darcy D coefficient was difficult to estimate as the well was cleaning up throughout the flow and only one flow was measured (the rest were estimated from the choke size and FTHP). However, it appears to be small.

The estimated initial reservoir pressure at MPP (4390 psia) was consistent with the MDT data (4388 psia at -2973m SS) but there is uncertainty re the gauge to mid perforations correction. The maximum temperature recorded (just after shut-in) was 302 deg F but had probably not built up fully and reservoir temperature is likely to be a few degrees higher.

Date	ToD	FP #	Gas rate Mscf/D	Duration hr
29/07/2004	23:56:24	1	0	9.60944
30/07/2004	09:32:58	2	9000	0.3375
30/07/2004	09:53:13	3	11000	0.325556
30/07/2004	10:12:45	4	22000	1.13278
30/07/2004	11:20:43	5	27200	5.33667
30/07/2004	16:40:55	6	38000	0.402691
30/07/2004	17:05:05	7	40600	0.265555
30/07/2004	17:21:01	8	0	0.552414
30/07/2004	17:54:09	9	1	1.51212

QA / QC	Analysis 1
Company AWE	Field Yolla
Well Yolla 4 - 2973 Sand	Test Name / # Initial Cleanup Flow

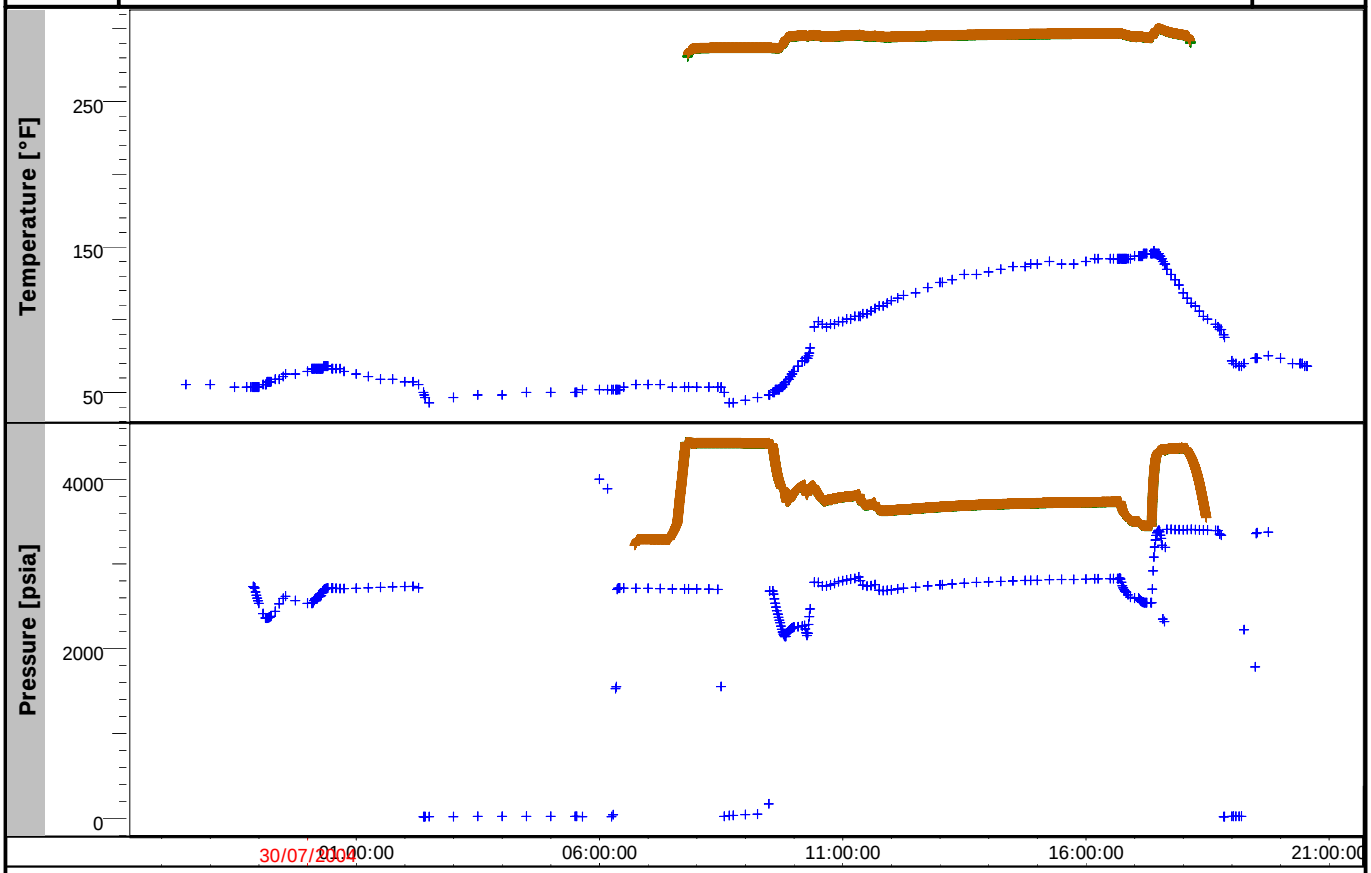

Relative temperature [°F], Pressure [psia] vs Time [ToD]

Temperature
++ Y42973PTtimeshiftT (ref)
++ Y42973PTtimeshiftBot
++ Yolla4-WHT (act)

Pressure
++ Y42973TOPtimeshift+55psi (ref)
++ Y42973BOTtimeshift+55
++ Yolla4-WHP (act)

Log-Log plot	Analysis 1
Company AWE	Field Yolla
Well Yolla 4 - 2973 Sand	Test Name / # Initial Cleanup Flow

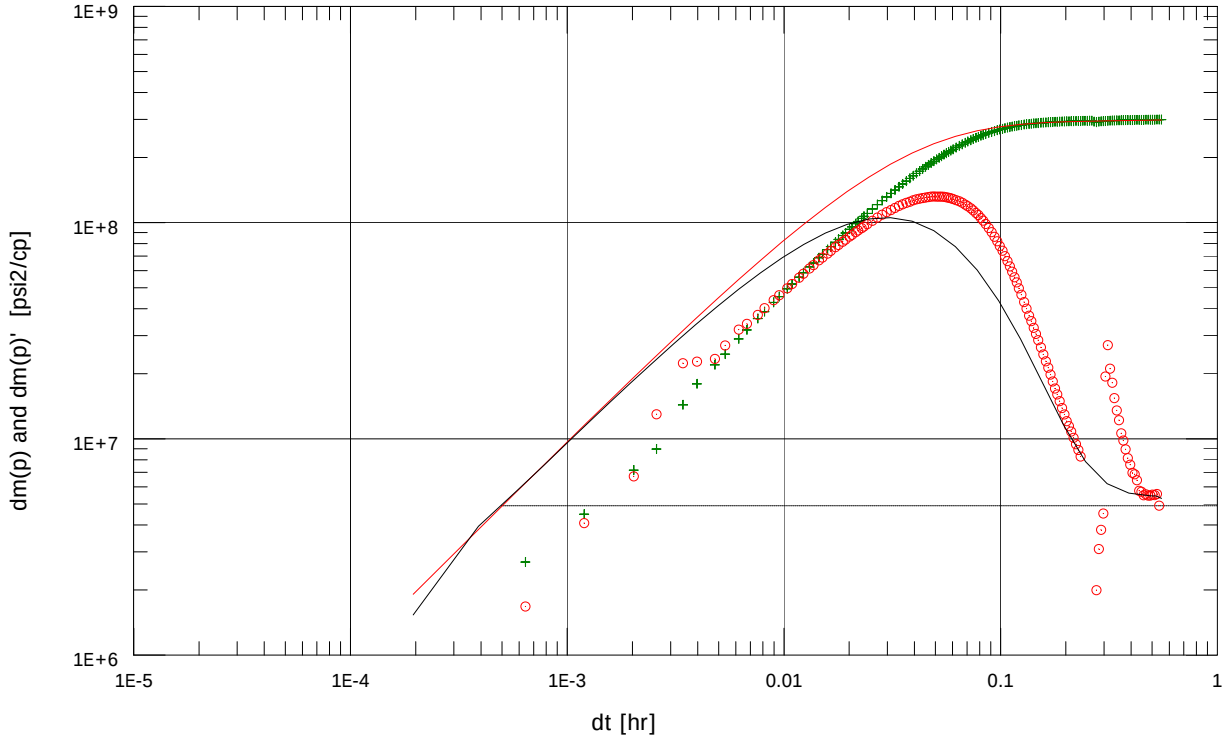

Y42973TOPtimeshift+55psi build-up #1

Rate	0 Mscf/D
Rate change	40600 Mscf/D
P@dt=0	3446.4 psia
Pi	4390.35 psia
Smoothing	0.1

Selected Model

Model Option	Standard Model
Well	Storage + Skin
Skin Type	Changing
Reservoir	Homogeneous
Boundary	Infinite

Results

TMatch	1010 [hr]**-1
PMatch	1.02E-7 [psi2/cp]**-1
C	0.05 bbl/psi
Skin0	22.8
Delta P Skin0	677.982 psi
Total Skin	24
Delta P Skin	714.992 psi
dS/dQ	3E-5 [Mscf/D]-1
Pi	4390.35 psia
k.h	4520 md.ft
k	165 md
Rinv	316 ft
Test. Vol.	2.86733E+5 Barrels

History plot	Analysis 1
Company AWE	Field Yolla
Well Yolla 4 - 2973 Sand	Test Name / # Initial Cleanup Flow

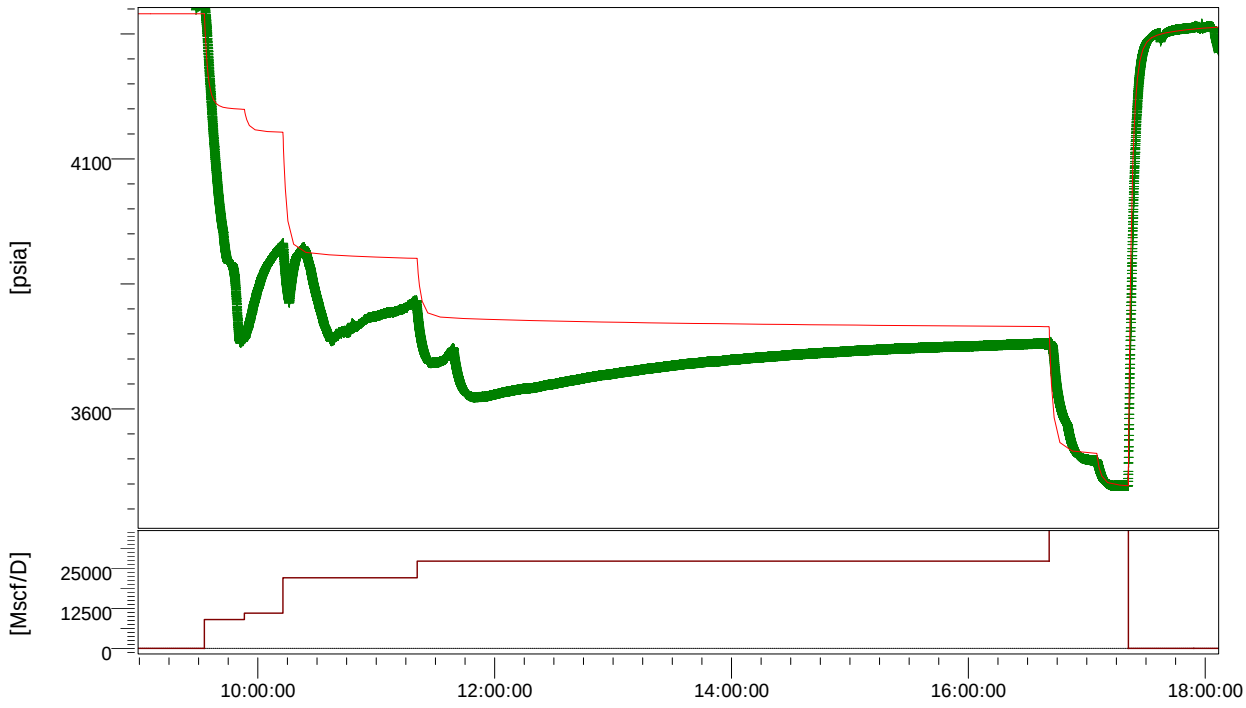

Pressure [psia], Gas Rate [Mscf/D] vs Time [ToD]

— Gas rate

Y42973TOPtimeshift+55psi build-up #1

Rate	0 Mscf/D
Rate change	40600 Mscf/D
P@dt=0	3446.4 psia
Pi	4390.35 psia
Smoothing	0.1

Selected Model

Model Option	Standard Model
Well	Storage + Skin
Skin Type	Changing
Reservoir	Homogeneous
Boundary	Infinite

Results

TMatch	1010 [hr]**-1
PMatch	1.02E-7 [psi2/cp]**-1
C	0.05 bbl/psi
Skin0	22.8
Delta P Skin0	677.982 psi
Total Skin	24
Delta P Skin	714.992 psi
dS/dQ	3E-5 [Mscf/D]-1
Pi	4390.35 psia
k.h	4520 md.ft
k	165 md
Rinv	316 ft
Test. Vol.	2.86733E+5 Barrels

Semi-Log plot	Analysis 1
Company AWE	Field Yolla
Well Yolla 4 - 2973 Sand	Test Name / # Initial Cleanup Flow

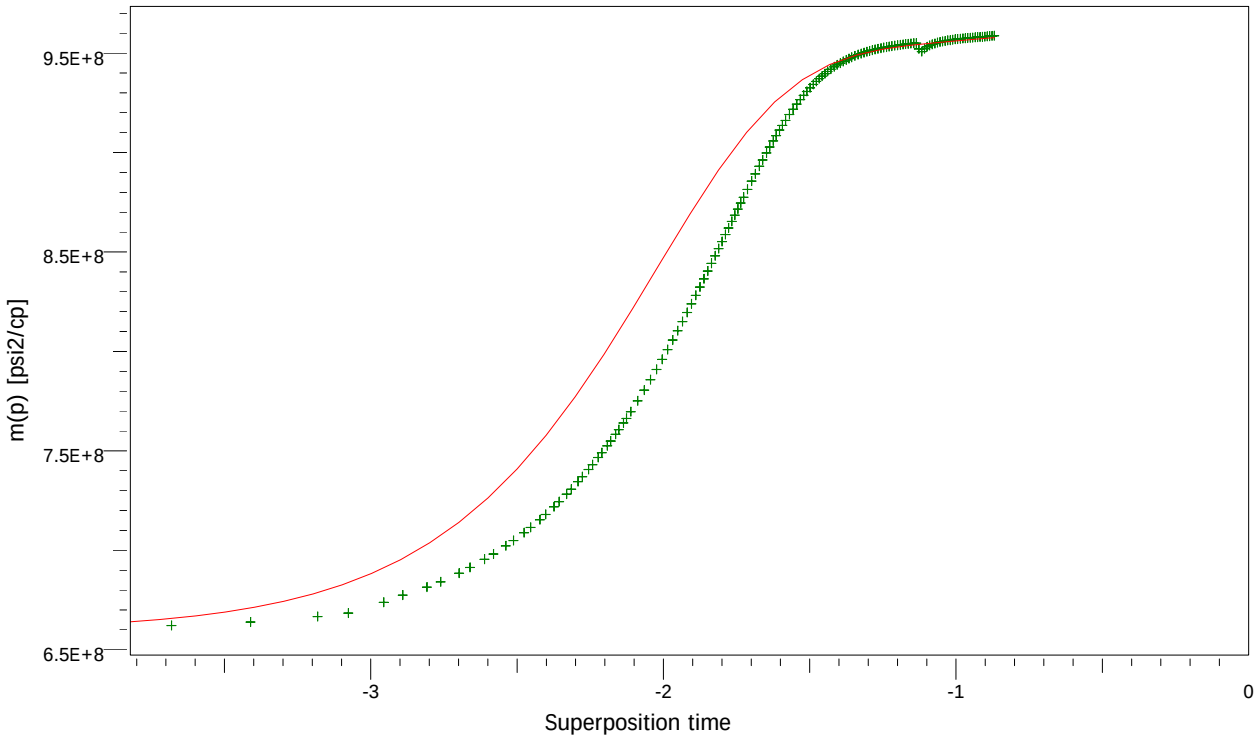

Y42973TOPtimeshift+55psi build-up #1

Rate	0 Mscf/D
Rate change	40600 Mscf/D
P@dt=0	3446.4 psia
Pi	4390.35 psia
Smoothing	0.1

Selected Model

Model Option	Standard Model
Well	Storage + Skin
Skin Type	Changing
Reservoir	Homogeneous
Boundary	Infinite

Results

TMatch	1010 [hr]**-1
PMatch	1.02E-7 [psi2/cp]**-1
C	0.05 bbl/psi
Skin0	22.8
Delta P Skin0	677.982 psi
Total Skin	24
Delta P Skin	714.992 psi
dS/dQ	3E-5 [Mscf/D]-1
Pi	4390.35 psia
k.h	4520 md.ft
k	165 md
Rinv	316 ft
Test. Vol.	2.86733E+5 Barrels

(B) Sand Production

CLAMPON
ULTRASONIC SAND DETECTION

WELL TESTING REPORT

YOLLA - 4

Performed by: Aquip Systems

Test Engineer: Simon Mason

Test Date: 30/07/04 – 06/08/04

Sand 2973 Separator Flow Period (30/07/04):
Flow was diverted through the separator at 12:08 until 16:34. Production rate was stable at @27.5 Mscfeet/day. (Approx 12m/sec). During this period the calculated sand production was negligible, indicating successful well clean up was achieved. (See fig 1.)
Total sand produced for the period = 2.44Kg

Sand 2755 Clean up Flow (01/08/04):
Flow direct to flare occurred from 16:31 through to 17:45. Production was stabilized at @20Mscfeet/day (Approx 8.5 m/sec). Well clean up was achieved with total sand production = 0.22Kg. (See fig 2.)

Sand 2755 Separator Flow (01/08/04 – 02/08/04):
The zone was opened to flare at 19:25 and, once stabilized diverted to the separator at 21:55. Maximum flow rate achieved was @39Mscfeet/day with testing being performed at @ 32Mscfeet/day (Approx 14.5 m/sec). Bottoms up can be seen clearly at 19:55. Total sand production for the period = 1.37Kg. (See fig 3.)

Sand 2458 Clean up Flow (02/08/04):
Separator flow could not proceed with the oil zone due to the fluid pour point and wax content. For this reason quantification of produced sand was achieved by using choke correlation data to calculate approximate flow velocity. Indicated sand production for this period was very low. Total mass of sand produced was approximately 0.28Kg. (See fig 4.)

Sand 2809 Clean up Flow (06/08/04):
Clean up flow commenced at 20:41. The maximum achieved flow rate was @35Mscfeet/day (Approx 16m/sec) with an increased level of water production in a slug regime, hence the increased sensor raw values. The data shows initial high levels of slugging with a declining trend. Sand production for this period totaled 3.14Kg. (See fig 5.)

Sand 2809 Separator Flow (07/08/04):
Following the clean up flow this zone was not shut in prior to diverting flow to the separator at 01:20. The decreasing trend in sensor raw value continued through the period with very little sand being produced. The well was shut in at 04:24.
Total sand mass detected was 0.16Kg

Tel: 08 9472 0122
Fax: 08 9472 5122
4/5 Brodie Hall Drive
Bentley WA 6102
simon@aquip.com.au

Fig 1. Separator Flow Period – Sand 2973:

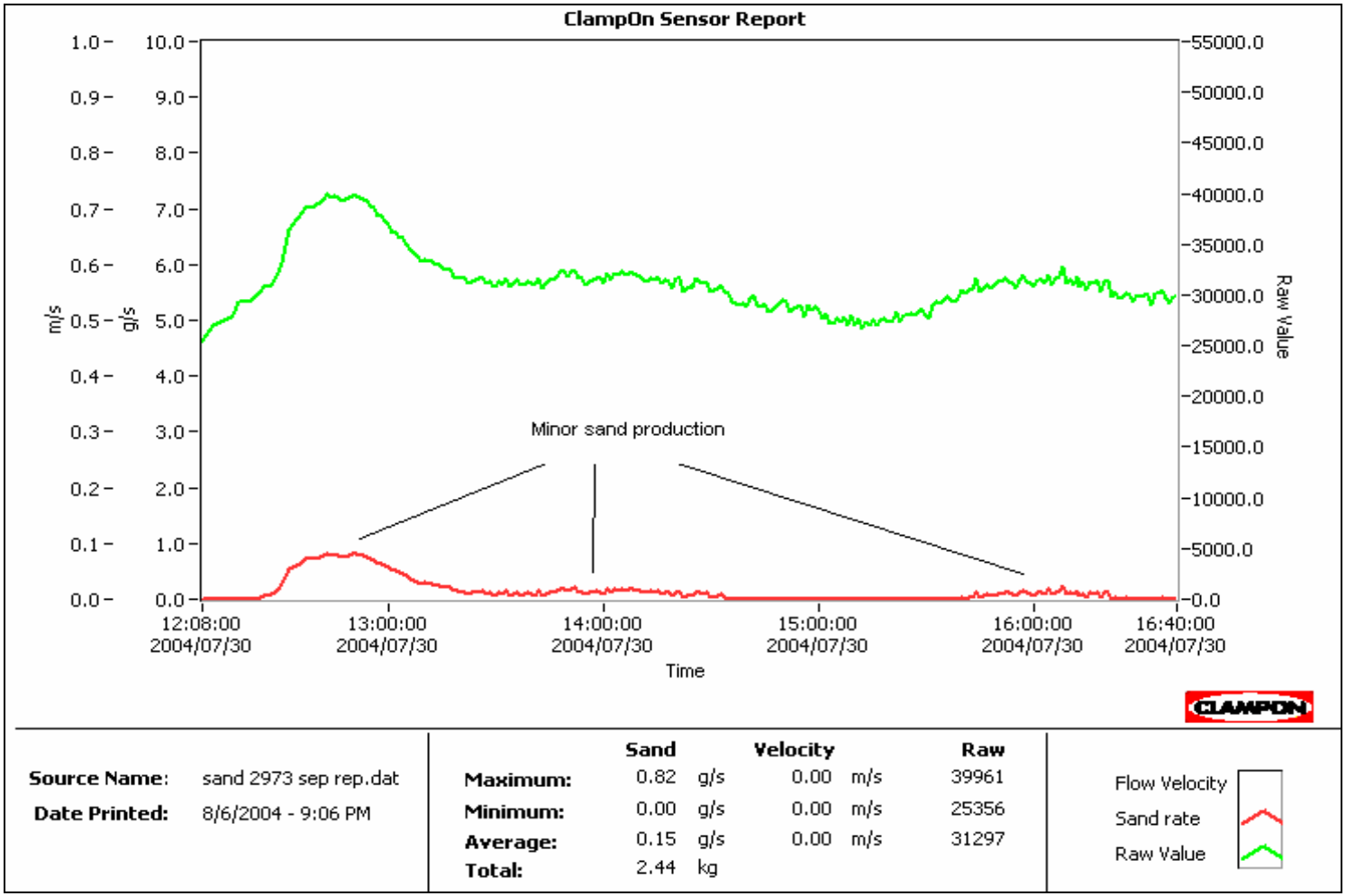

Fig 2. Sand 2755 Clean up Flow:

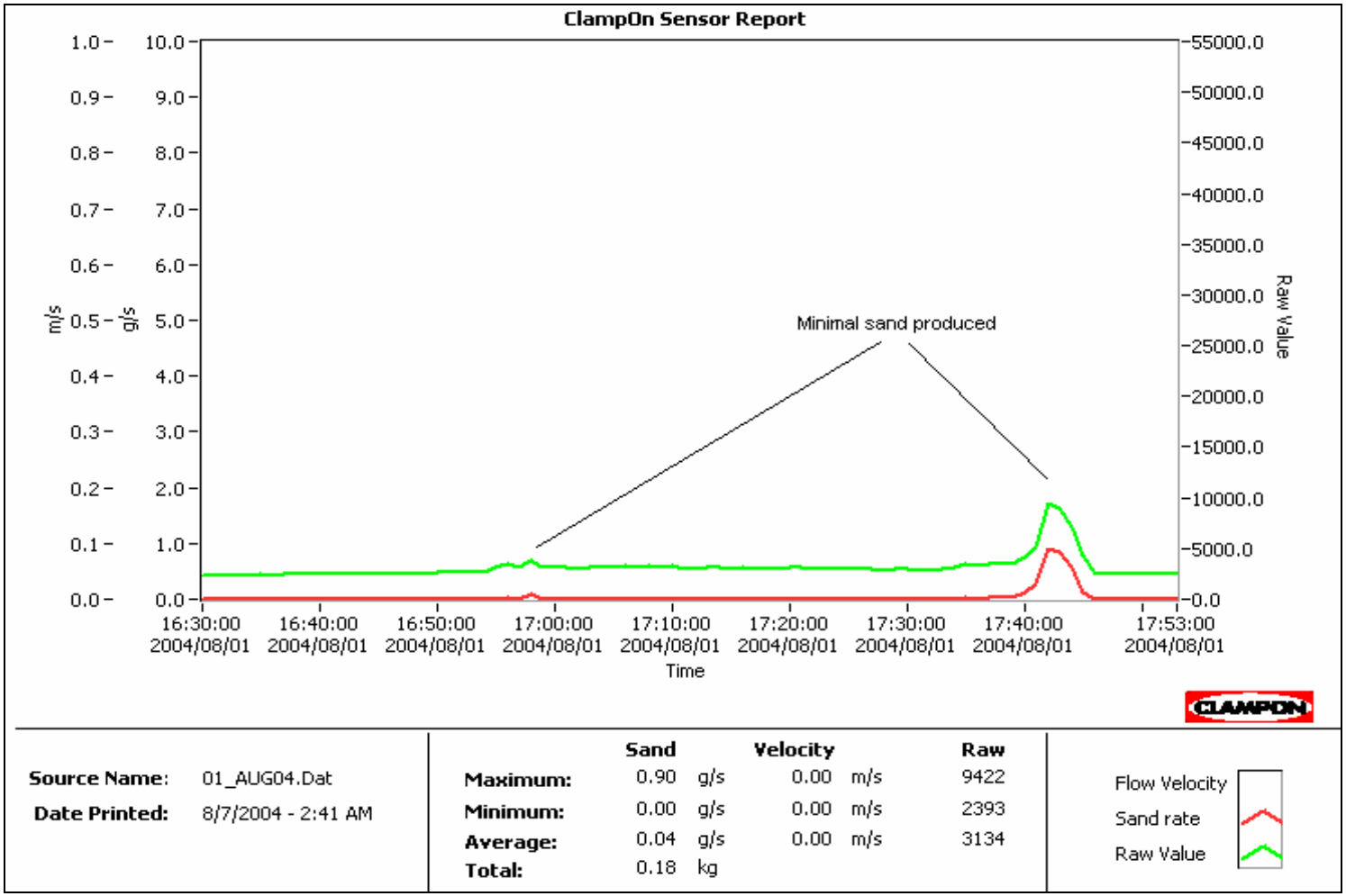

Fig 3. Sand 2755 Separator Flow:

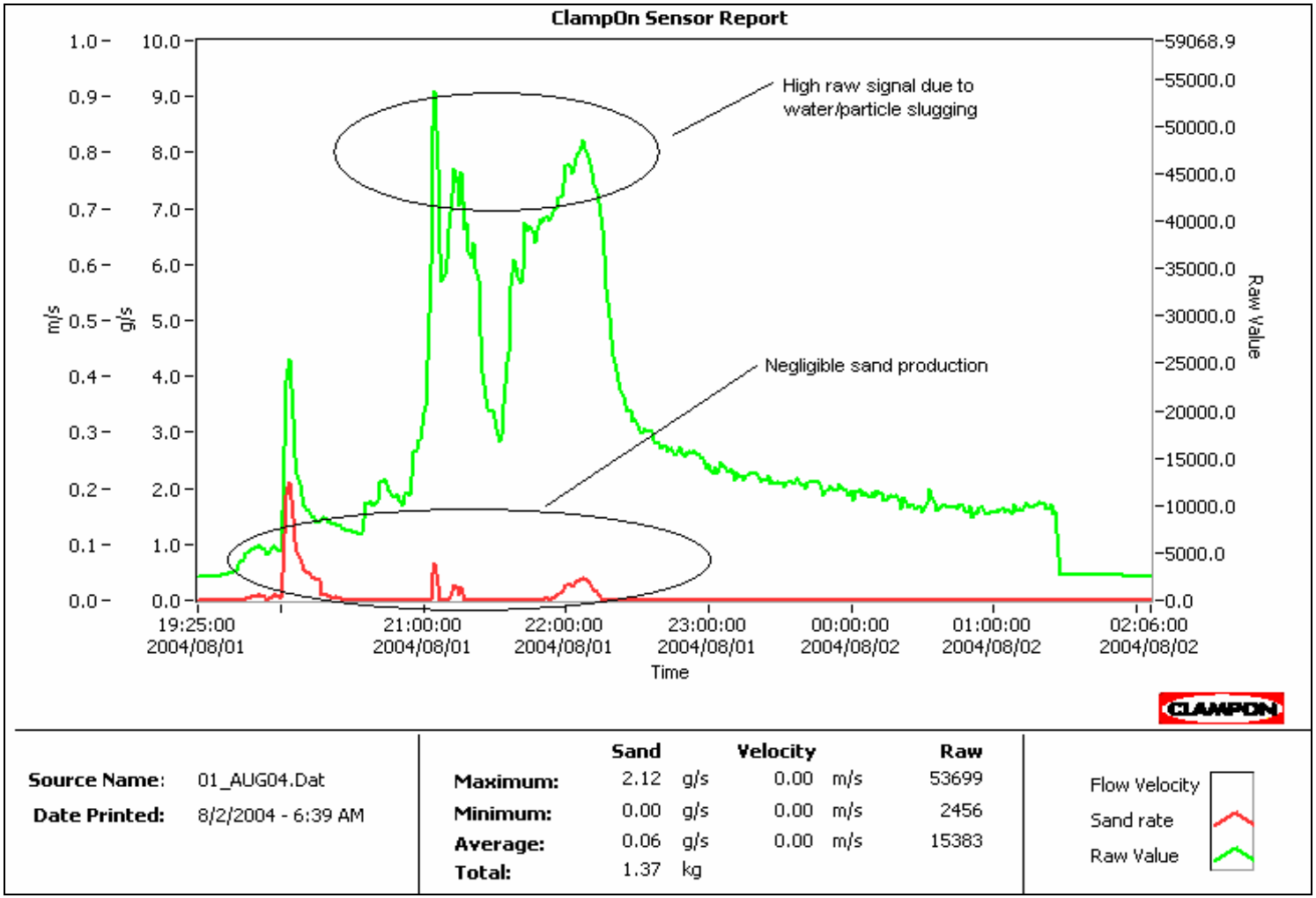

Fig 4 Sand 2458 (Oil zone):

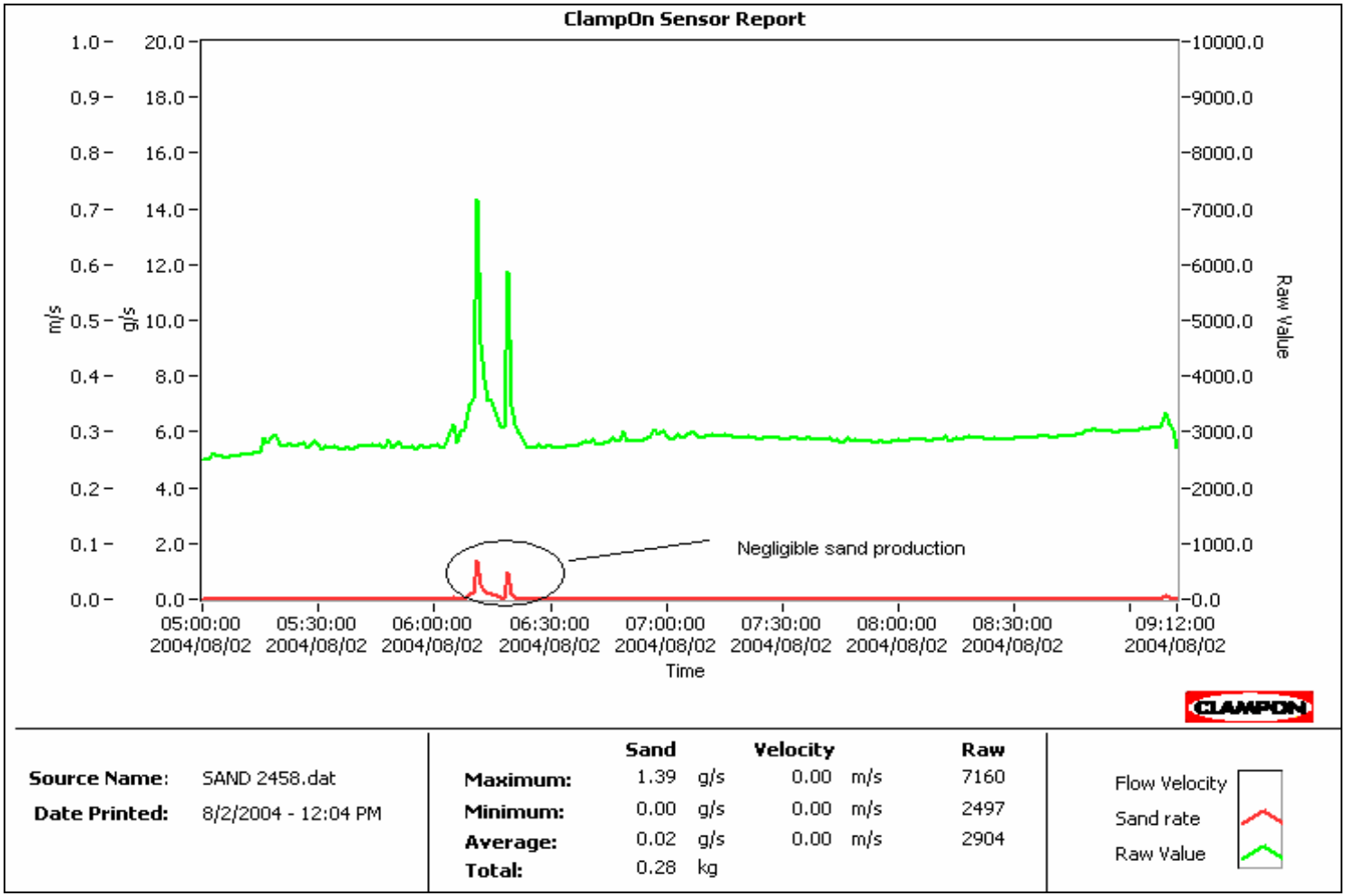

Fig 5 Sand 2809 Clean up Flow:

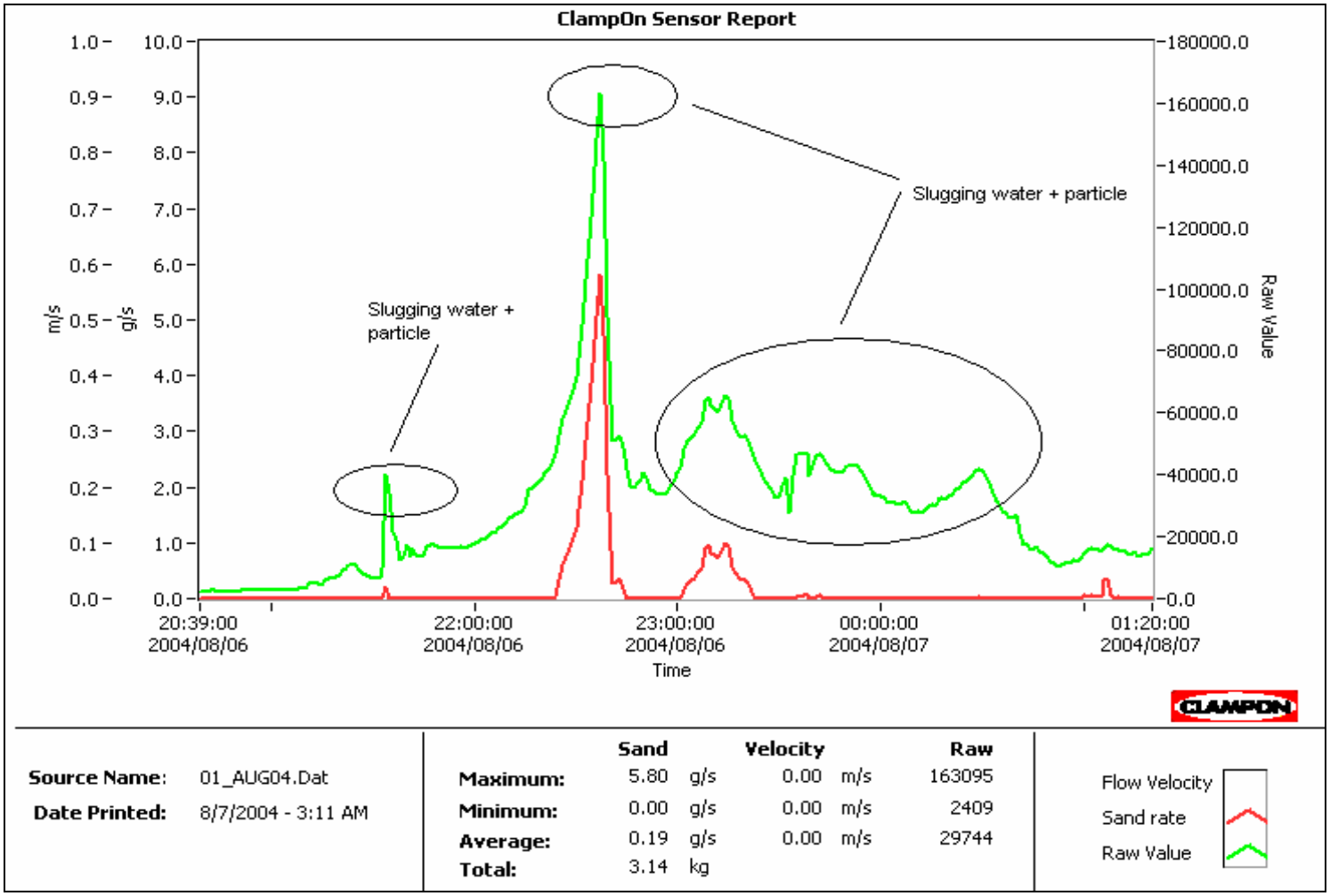

Fig 6 Sand 2809 Separator Flow Period:

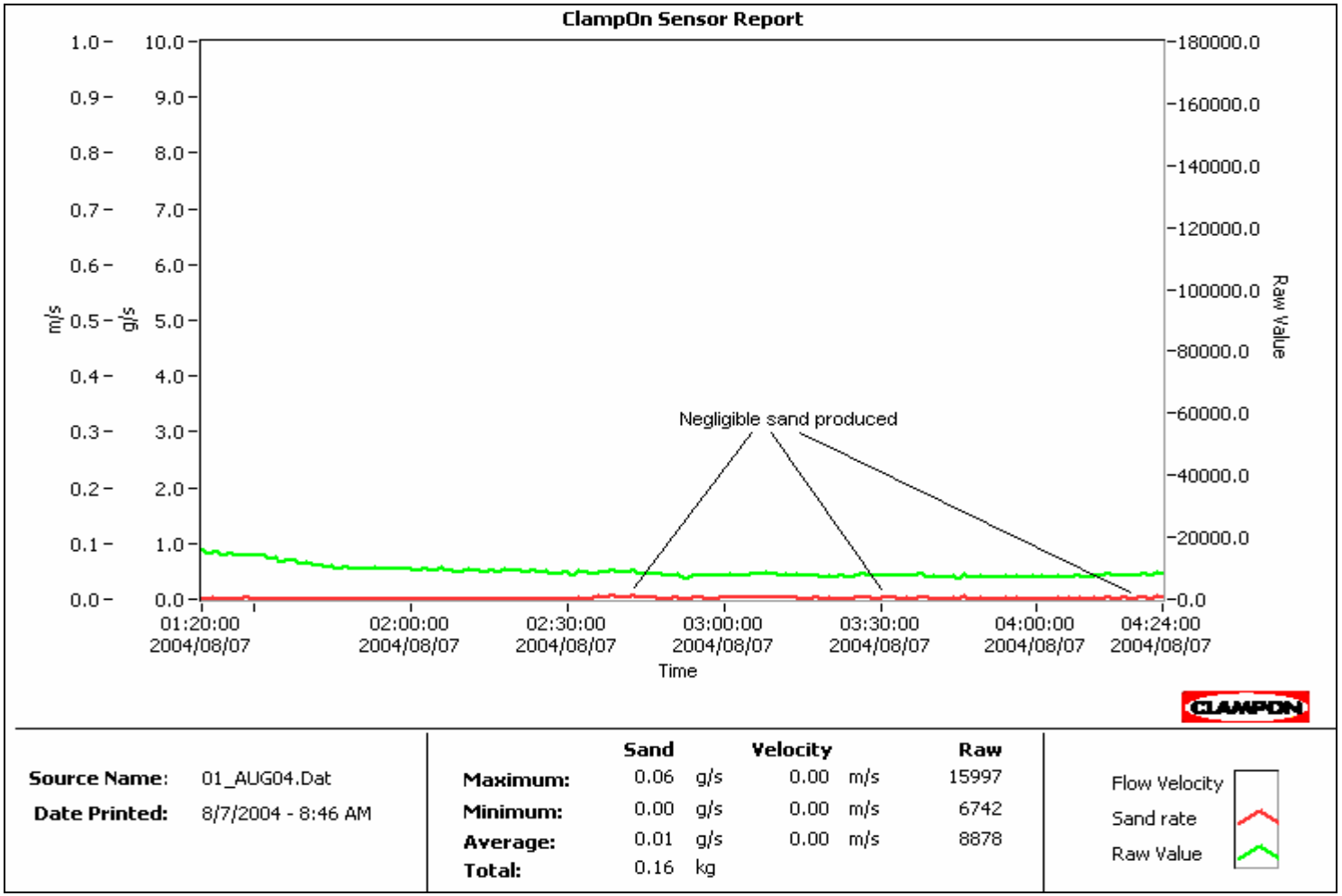

APPENDIX 4: GEOCHEMISTRY REPORT

HYDROCARBON CHARACTERISATION STUDY

YOLLA-4

PROFESSIONAL OPINION

Prepared by:
Christine West

Prepared for:
Origin Energy

December 2004

GEOTECH
GEOTECHNICAL SERVICES PTY LTD
41- 45 Furnace Road, Welshpool, Western Australia. 6106
Locked Bag 27, Cannington, Western Australia. 6987
Telephone: (08) 9458 8877 (24 Hours)
Facsimile: (08) 9458 8857

EXECUTIVE SUMMARY

Oil

The Yolla-4 oil sample from 2609.5m depth is characterised as mature and is believed to be sourced from highly terrestrial (most likely coaly) organic matter deposited under oxic conditions.

Sediment

TOC/Rock-Eval pyrolysis data characterise the sediment from 2894.0m as very mature and as having excellent potential to generate liquid hydrocarbons. The hydrocarbons extracted from this sediment are believed to be sourced from highly terrestrial organic matter deposited in an oxic depositional environment. The overall maturity assessment is marginal to moderate, with the branched/cyclic data suggesting moderate maturity, and the aromatic data suggesting marginal to moderate maturity.

Correlation

Overall, it is believed that a genetic relationship between the sediment extract and the oil exists, ie that the source rock of the facies analysed is the likely source of the oil.

HYDROCARBON CHARACTERISATION STUDY

YOLLA-4

TABLE OF CONTENTS

1 INTRODUCTION

One core sample (2894m) and one oil sample (2609.5m) from Yolla-4, drilled by Origin Energy, were submitted for geochemical analyses.

The purpose of this report is to characterise the hydrocarbons in terms of source, maturity and depositional environment, and to correlate the oil and sediment extract.

One hardcopy and one electronic copy of this report have been sent to Deidre Brooks at Origin Energy. Any queries related to it may be directed to Christine West or Dr Birgitta Hartung-Kagi at Geotechnical Services Pty Ltd.

All data and information are proprietary to Origin Energy and regarded as highly confidential by all Geotech personnel.

Geotechnical Services has endeavoured to use techniques and equipment to achieve results and information as accurately as it possibly can. However, such equipment and techniques are not necessarily perfect. Therefore, Geotechnical Services shall not be held responsible or liable for the results of any actions taken on the basis of the information contained in this document. Moreover, this report should not be the sole reference when considering issues that may have commercial implications.

2 ANALYTICAL PROCEDURES

2.1 OIL SAMPLE

An oil sample labelled 2609.5m ex MPSR-1695 was submitted for geochemical analyses, starting with whole oil GC-MS and followed by liquid chromatographic separation. The saturate and aromatic fractions obtained were submitted for GC-MS analysis. The saturate fraction was subsequently treated with ZSM5 sieves in order to remove the n-alkanes, and the branched/cyclic fraction remaining was analysed by GC-MS.

A sub-sample of the oil was also submitted for CSIA (compound specific isotope analysis). These data are included but not interpreted in this report.

2.2 SEDIMENT SAMPLE

A sediment from 2894m was submitted for source rock assessment, ie TOC and Rock-Eval pyrolysis. The sample was solvent extracted and the extracted sediment was submitted for pyrolysis-GC.

The extract obtained from the sediment was analysed by GC-MS and was then submitted for liquid chromatographic separation in order to separate the saturate, aromatic and NSO fractions. The saturate and aromatic fractions obtained were submitted for GC-MS analysis. The saturate fraction was subsequently treated with ZSM5 sieves in order to remove the n-alkanes, and the branched/cyclic fraction remaining was analysed by GC-MS.

2.3 GAS SAMPLE

A gas sample labelled 3005.7m ex MPSR-0066 was submitted for CSIA analysis. These data are given, but not interpreted, in this report.

3 RESULTS AND INTERPRETATION

3.1 OIL SAMPLE

Whole oil GC-MS analysis of the oil from 2609.5m shows that the sample contains a full suite of gasoline range hydrocarbons, suggesting that the oil is neither water washed nor biodegraded (Figure 1).

Figure 1: Chromatogram showing the gasoline range hydrocarbons in Yolla-4 2609.5m.

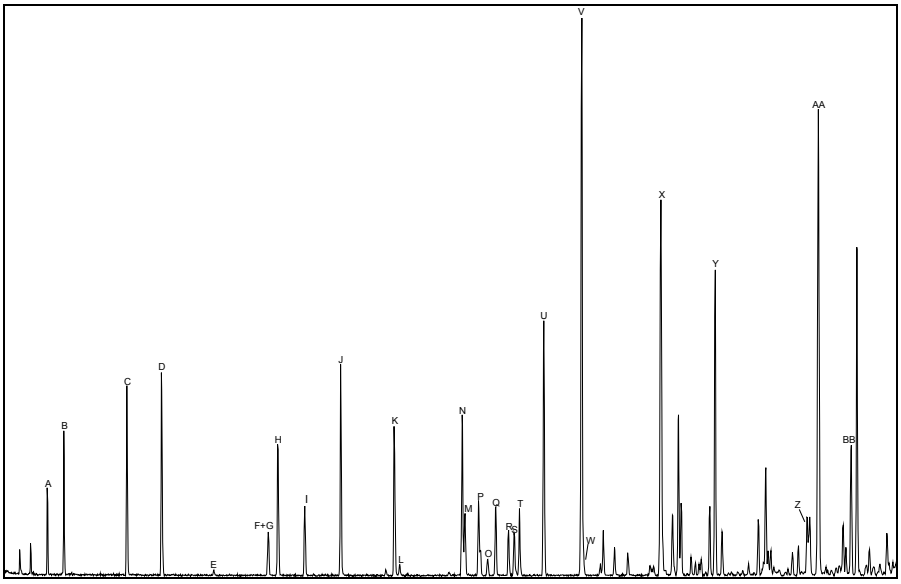

Liquid chromatography data indicate that the oil comprises approximately 78% saturates, 17% aromatics and 5% polars. The saturate chromatogram is characterised by a smooth n-alkane distribution in the C_{10} to C_{31} range, with a predominance at C_{22}/C_{23}, and a large abundance of high molecular weight n-alkanes (Figure 2). These features suggest that the oil is most likely mature and sourced from terrestrial organic matter. The pristane/phytane ratio of 7.67 and the pristane/n-C_{17} ratio of 1.09 are high and indicate an oxic depositional environment and a terrestrial source, respectively.

Figure 2: Chromatogram obtained by GC-MS analysis of the saturate fraction of the Yolla-4 oil.

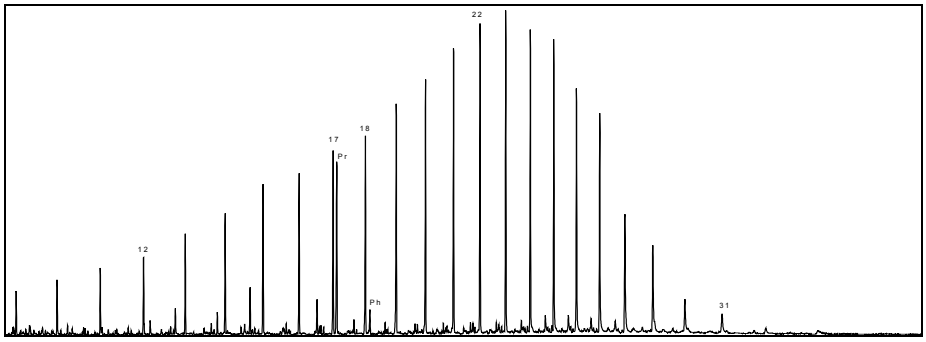

Branched/cyclic and aromatic GC-MS maturity parameters suggest that the oil is fully mature ($C_{29}S/C_{29}R$ sterane ratio of 0.84 and MPI value of 0.71). The oil is believed to be sourced from highly terrestrial organic matter, which is consistent with the interpretation of the saturate data. Features suggesting a terrestrial source include the lack/extremely low abundance of C_{27} diasteranes and steranes, and the presence of the diterpanes isopimarane, pimarane, phyllocladane, rimuane and 17-nortetracyclane (Figures 3 and 4). Generally samples with a highly terrestrial source signature also exhibit high HPI values. However, in the case of the Yolla-4 oil, the HPI of 0.41 is low, as the source (although terrestrial) does not contain high abundances of retene, cadalene and isohexylmethylnaphthalene.

Figure 3: Fragmentogram showing the sterane pattern in the Yolla-4 oil.

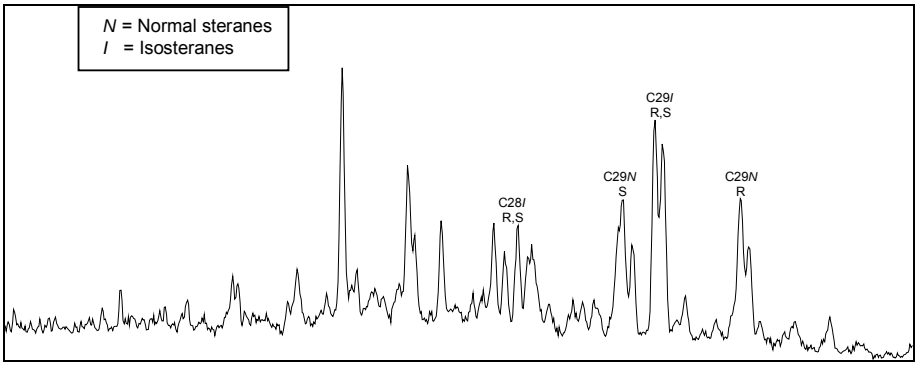

Figure 4: Fragmentogram showing the diterpane pattern in the Yolla-4 oil.

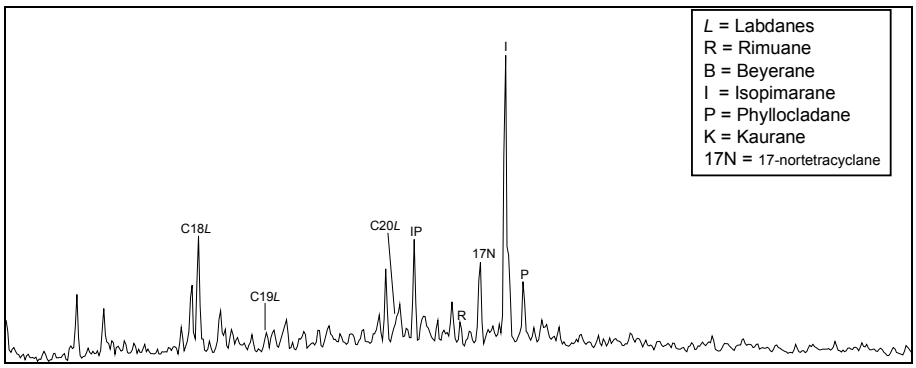

3.2 SEDIMENT SAMPLE

The core from 2894.0m yielded a TOC value of 68.52% which is typical of a coal. The Rock-Eval pyrolysis data indicate that the sediment is very mature (Tmax: 442^{o}C) and contains a high level of free hydrocarbons. (S1: 12.00mg/g). The S2 value of 170mg/g is also high, even for a coaly sample, and the HI of 248 suggests that the sediment is oil prone.

Pyrolysis-GC of the sediment generated a chromatogram characterised by a large amount of low molecular weight compounds as well as well-defined alkene+alkane pairs up to approximately C_{22} (Figure 5). A high abundance of peaks exist beyond this range (up to approximately C_{31}), but the alkene+alkane pairs are not well resolved. The C_{15}-C_{31} alkene+alkane abundance of 9.52% is considerably over the 5% threshold for oil generation, suggesting that this sample has excellent potential to generate oil.

Figure 5: Chromatogram obtained by pyrolysis-GC analysis of the sediment from 2894m.

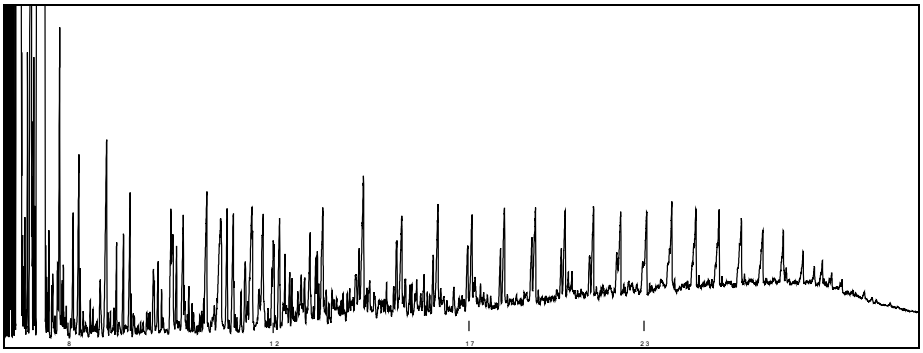

The sediment was solvent extracted and yielded a high amount of extract (13119ppm). GC-MS analysis of the extract indicates that it is dominated by aromatic compounds, particularly in the low molecular weight range (Figure 6). n-Alkanes up to approximately n-C_{30} are also clearly visible. These features are consistent with an extract from a coaly sediment.

Figure 6: Chromatogram obtained by GC-MS analysis of the 2894.0m extract.

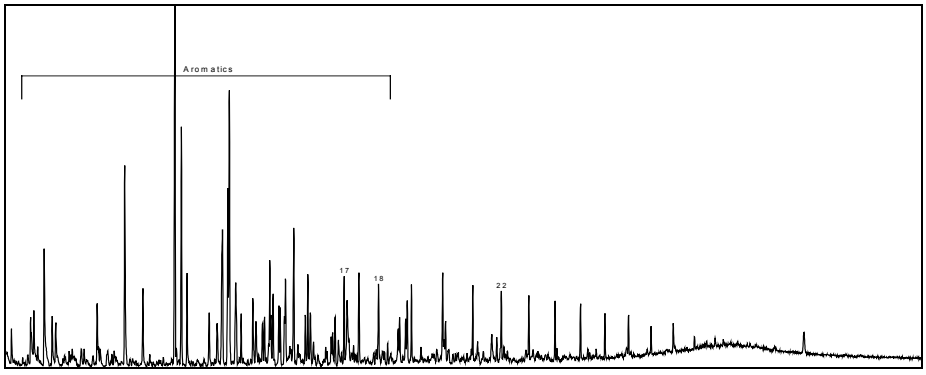

Liquid chromatography data of the extract indicate that it comprises approximately 17% saturates, 51% aromatics and 32% polars, data which are consistent with the whole extract GC-MS chromatogram. The saturate chromatogram comprises n-alkanes in the C_{10} to C_{31} range, with a predominance at C_{15} and a slightly bimodal profile (Figure 7). The pristane/phytane ratio of 7.79 is high, reflecting the organic matter was deposited under oxic conditions.

Figure 7: Chromatogram obtained by GC-MS analysis of the saturate fraction of the extract from 2894.0m.

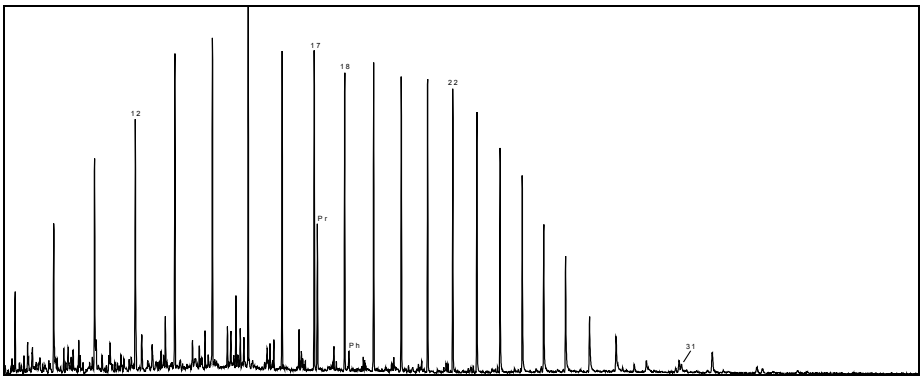

Branched/cyclic data (ie $C_{29}S/C_{29}R$ sterane ratio of 0.69) and aromatic maturity data (MPI of 0.44) suggest that the extract is marginally to moderately mature.

The extract is believed to be sourced from terrestrial (most likely coaly) organic matter, as suggested by the almost complete lack of C_{27} steranes, diasteranes and isosteranes, and the presence of the diterpanes isopimarane, pimarane, rimuane, kaurane and 17-nortetracyclane.

3.3 CORRELATION OF OIL AND SEDIMENT EXTRACT

There are strong similarities between the Yolla-4 oil and sediment extract, suggesting that a genetic relationship does exist between the two samples. Similarities include the almost complete lack of C_{27} diasteranes and steranes, the presence of diterpanes and the overall aromatic and branched/cyclic patterns. The branched/cyclic parameters for the two samples are also very similar, with the only exception being Parameter 12, a parameter calculated on the abundance of C_{30} hopane, C_{30} moretane, C_{29} steranes and C_{29} diasteranes.

4 CONCLUSION

Oil

The Yolla-4 oil sample from 2609.5m depth is characterised as mature and is believed to be sourced from highly terrestrial (most likely coaly) organic matter deposited under oxic conditions.

Sediment

TOC/Rock-Eval pyrolysis data characterise the sediment from 2894.0m as very mature and as having excellent potential to generate liquid hydrocarbons. The hydrocarbons extracted from this sediment are believed to be sourced from highly terrestrial organic matter deposited in an oxic depositional environment. The overall maturity assessment is marginal to moderate, with the branched/cyclic data suggesting moderate maturity, and the aromatic data suggesting marginal to moderate maturity.

Correlation

Overall, it is believed that a genetic relationship between the sediment extract and the oil exists, ie that the source rock of the facies analysed is the likely source of the oil.

5 REFERENCES

van Aarssen, B.G.K., Alexander, R. and Kagi, R.I. (2000) Reconstructing the geological history of Australian crude oils using aromatic hydrocarbons. *The APPEA Journal*, 283-292.

Alexander, R., Kagi, R.I., Rowland, S.J., Sheppard, P.N. and Chirila, T.V. (1985) The effects of thermal maturity on distributions of dimethylnaphthalenes and trimethylnaphthalenes in some Ancient sediments and petroleums. *Geochimica et Cosmochimica Acta* **49**, 385-395.

Huang, W.-Y. and Meinschein, W.G. (1979) Sterols as ecological indicators. *Geochimica et Cosmochimica Acta* **43**, 739-745.

Hunt, J.M. (1979) *Petroleum Geochemistry and Geology*. San Francisco: W.H. Freeman.

Peters, K.E. and Moldowan, J.M., 1993 –The Biomarker Guide - Interpreting molecular fossils in petroleum and ancient sediments. Prentice Hall, Englewood Cliffs, New Jersey 07632.

Radke, M. and Welte, D.H., 1983 – The methylphenanthrene index (MPI). A maturity parameter based on aromatic hydrocarbons. Advances in Org. Geochem., 1981. J. Wiley and Sons, New York, 504-512.

Thompson, K.F.M., 1983 – Classification and thermal history of petroleum based on light hydrocarbons. Geochim. Cosmochim. Acta. **47**, 303-316.

Tissot, B.P. and Welte, D.H., 1984 – Petroleum formation and Occurrence. Springer-Verlag, Berlin.

van Aarssen, B.G.K., Bastow, T.P., Alexander, R and Kagi, R.I., 1999 – Distributions of methylated naphthalenes in crude oils: indicators of maturity, biodegradation and mixing. Org. Geochem. **30**, 1213-1227.

Volkman, J.K., Alexander, R., Kagi, R.I., Rowland, S.J. and Sheppard, P.N., 1984 – Biodegradation of aromatic hydrocarbons in crude oils from the Barrow Sub-basin of Western Australia. Org. Geochem. **6**, 619-632.

APPENDIX A

DATA AND TABLES

DATA AND TABLES

YOLLA-4

TABLE OF CONTENTS

TABLE 1

ANALYSIS OF ORGANIC MATTER BY ROCK-EVAL PYROLYSIS

YOLLA-4

GEOTECH

Depth (m)		*Tmax*	*S1*	*S2*	*S3*	*S1+S2*	*S2/S3*	*PI*	*TOC*	*HI*	OI
2894.0	Core	442	12.00	170.20	21.60	182.20	7.88	0.07	68.52	248	32

A TMAX value is not reported if the S2 is <0.2mg/g

TMAX = Max. temperature S2 (^{o}C)

S1+S2 = Potential yield (mg/g rock)

OI = Oxygen Index

S1 = Volatile hydrocarbons (HC) (mg/g rock)

S3 = Organic carbon dioxide (mg/g rock)

TOC = Total organic carbon (wt % of rock)

nd = no data

S2 = HC generating potential (mg/g rock)

PI = Production index

HI = Hydrogen index

GEOTECHNICAL SERVICES PTY LTD

FIGURE 1

Sample : **YOLLA-4, 2894m, Core**
File ID : **344301P1**

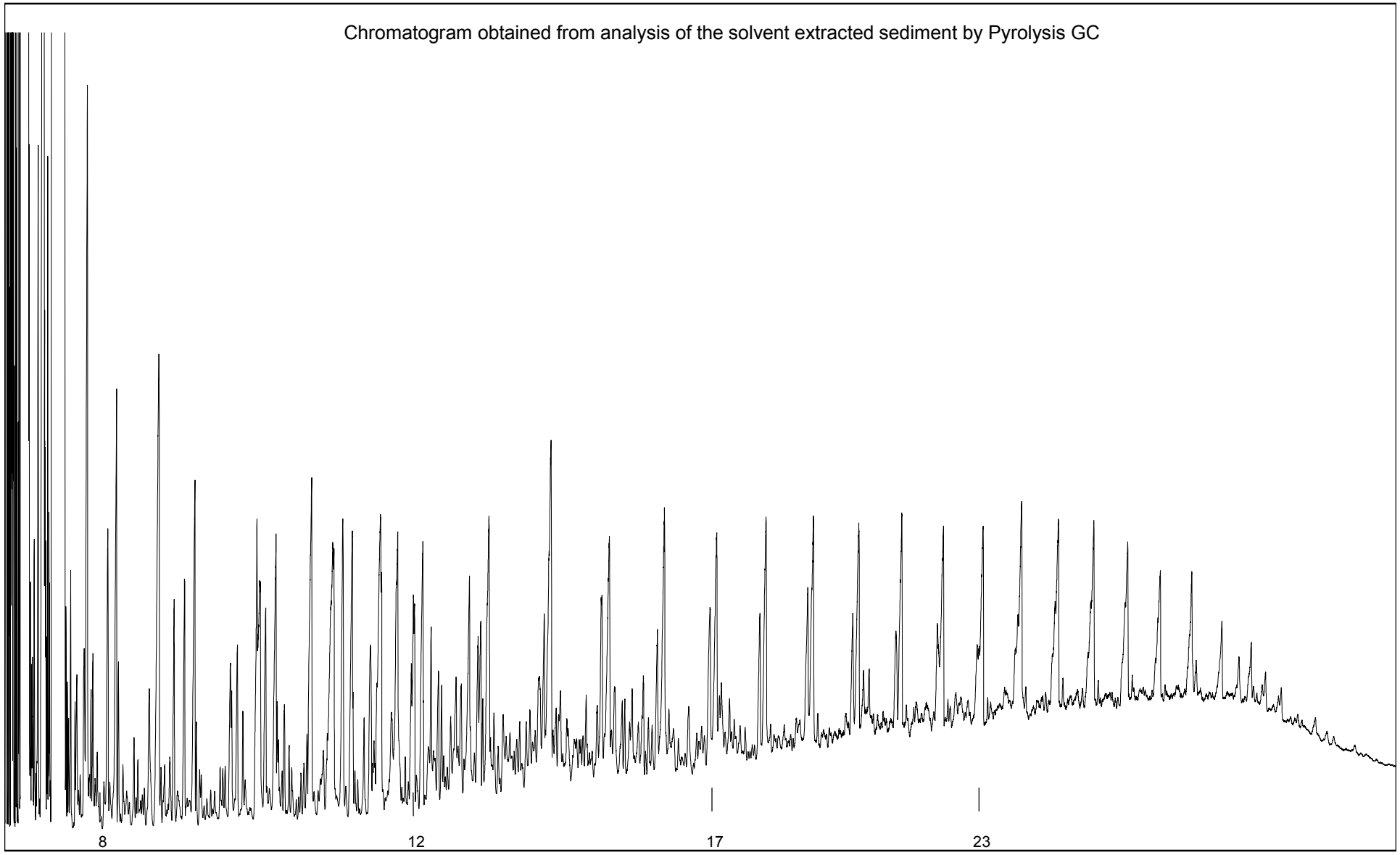

GEOTECHNICAL SERVICES PTY LTD

TABLE 2a

ALKENE AND ALKANE COMPONENT ANALYSIS FROM PYROLYSIS-GC

YOLLA-4, 2894m, Core Oct-04

Carbon No.	----Alkane + Alkene----			-------Alkane-------			-------Alkene-------			Alkane/Alkene
	A	B	C	A	B	C	A	B	C	
1	nd	nd	nd	nd	nd	nd	nd	nd	nd	nd
2	nd	nd	nd	nd	nd	nd	nd	nd	nd	nd
3	nd	nd	nd	nd	nd	nd	nd	nd	nd	nd
4	nd	nd	nd	nd	nd	nd	nd	nd	nd	nd
5	1.350	2.298	0.034	0.865	1.472	0.021	0.486	0.826	0.012	1.78
6	1.045	1.779	0.026	0.588	1.001	0.015	0.457	0.778	0.011	1.29
7	1.145	1.949	0.028	0.725	1.234	0.018	0.420	0.716	0.010	1.72
8	0.935	1.591	0.023	0.574	0.976	0.014	0.361	0.615	0.009	1.59
9	0.800	1.362	0.020	0.514	0.875	0.013	0.286	0.487	0.007	1.80
10	0.750	1.276	0.019	0.457	0.778	0.011	0.293	0.498	0.007	1.56
11	1.004	1.709	0.025	0.507	0.862	0.013	0.498	0.847	0.012	1.02
12	0.727	1.238	0.018	0.503	0.856	0.012	0.224	0.382	0.006	2.24
13	0.274	0.467	0.007	0.041	0.070	0.001	0.233	0.397	0.006	0.18
14	0.742	1.263	0.018	0.557	0.949	0.014	0.184	0.314	0.005	3.02
15	0.787	1.340	0.020	0.485	0.825	0.012	0.303	0.515	0.008	1.60
16	0.747	1.271	0.019	0.532	0.906	0.013	0.215	0.365	0.005	2.48
17	0.862	1.467	0.021	0.532	0.906	0.013	0.329	0.561	0.008	1.62
18	0.748	1.274	0.019	0.510	0.868	0.013	0.239	0.406	0.006	2.14
19	0.783	1.333	0.019	0.489	0.832	0.012	0.295	0.501	0.007	1.66
20	0.636	1.083	0.016	0.426	0.724	0.011	0.211	0.359	0.005	2.02
21	0.627	1.067	0.016	0.432	0.735	0.011	0.195	0.332	0.005	2.21
22	0.714	1.215	0.018	0.446	0.760	0.011	0.268	0.456	0.007	1.67
23	0.627	1.067	0.016	0.445	0.757	0.011	0.182	0.309	0.005	2.45
24	0.662	1.127	0.016	0.436	0.742	0.011	0.226	0.385	0.006	1.93
25	0.619	1.053	0.015	0.359	0.611	0.009	0.260	0.442	0.006	1.38
26	0.588	1.001	0.015	0.333	0.567	0.008	0.254	0.433	0.006	1.31
27	0.491	0.836	0.012	0.279	0.475	0.007	0.212	0.361	0.005	1.31
28	0.345	0.588	0.009	0.207	0.352	0.005	0.139	0.236	0.003	1.49
29	0.154	0.262	0.004	0.154	0.262	0.004	0.000	0.000	0.000	nd
30	0.131	0.223	0.003	0.131	0.223	0.003	0.000	0.000	0.000	nd
31	0.000	0.000	0.000	0.000	0.000	0.000	0.000	0.000	0.000	nd

nd = no data
A = % of resolved compounds in S2
B = mg/g Rock (Rock-Eval)
C = (mg/g Rock)/TOC

TABLE 2b

PARAMETER SUMMARY FOR PYROLYSIS GAS CHROMATOGRAPHY

YOLLA-4, 2894m, Core Oct-04

Parameter	Value A	Value B	Value C	Value D
C1-C4 abundance (all compounds)	30.86	52.52	0.77	
C5-C8 abundance (all compounds)	11.06	18.82	0.27	
C5-C8 abundance (alkanes + alkenes)	4.48	7.62	0.11	
C9-C14 abundance (all compounds)	25.32	43.10	0.63	
C9-C14 abundance (alkanes + alkenes)	4.30	7.32	0.11	
C15-C31 abundance (all compounds)	32.76	55.76	0.81	
C15-C31 abundance (alkanes + alkenes)	9.52	16.21	0.24	
C9-C31 abundance (all compounds)	58.08	98.86	1.44	
C9-C31 abundance (alkanes + alkenes)	13.82	23.52	0.34	
C5-C31 abundance (all compounds)	69.14	117.68	1.72	
C5-C31 abundance (alkanes + alkenes)	18.30	31.14	0.45	
C5-C31 alkane abundance	11.53	19.62	0.29	
C5-C31 alkene abundance	6.77	11.52	0.17	
C5-C8 alkane/alkene				1.60
C9-C14 alkane/alkene				1.50
C15-C31 alkane/alkene				1.86
C5-C31 alkane/alkene				1.70
(C1-C5)/C6+				0.50
R				2.75

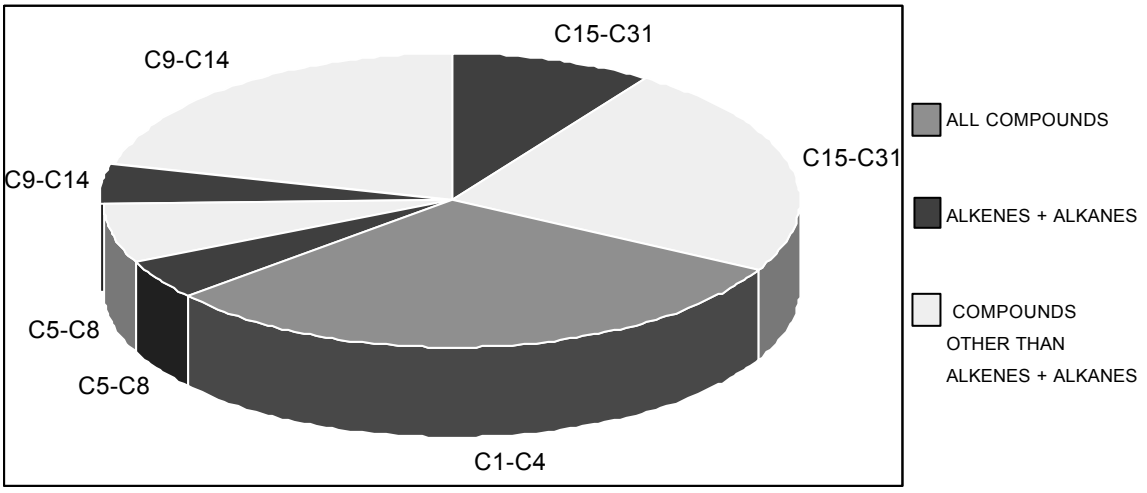

nd = no data
A = % of compounds in S2
B = mg/g Rock (Rock-Eval)
C = (mg/g Rock)/TOC
D = no units
R = m+p-xylene/n-octene

GEOTECH

GEOTECHNICAL SERVICES PTY LTD

TABLE 3

ANALYSIS OF CRUDE OIL BY GC-MS

YOLLA-4, 2609.5m ex MPSR-1695, Crude Oil

GEOTECH

Composition of C4 to C8 Fraction

Compound	*Rel.Wt%*	*Compound*	*Rel.Wt%*
isobutane (A)	1.5	1,1-dimethylcyclopentane (O)	0.5
n-butane (B)	2.5	2-methylhexane/2,3-dimethylpentane (P)	2.2
isopentane (C)	3.8	3-methylhexane (Q)	1.9
n-pentane (D)	4.5	1 cis-3-dimethylcyclopentane (R)	1.2
2,2-dimethylbutane (E)	0.2	1 trans-3-dimethylcyclopentane (S)	1.2
(cyclopentane		1 trans-2-dimethylcyclopentane (T)	1.7
2,3-dimethylbutane (F+G))	1.3	n-heptane (U)	6.3
2-methylpentane (H)	3.3	methylcyclohexane (V)	15.4
3-methylpentane (I)	1.7	1 cis-2-dimethylcyclopentane (W) +	0.2
n-hexane (J)	5.0	toluene (X)	8.9
methylcyclopentane (K)	3.8	n-octane (Y)	7.4
2,4-dimethylpentane (L)	0.3	ethylbenzene (Z)	1.5
benzene (M)	1.9	M+P-xylene (AA)	14.4
cyclohexane (N)	4.0	O-xylene (BB)	3.4

Calculated Data from the C4 to C8 Fraction

Paraffin Index I	1.0	I/M (Water washing)	0.9
Paraffin Index II	18.5	V/X (Water washing)	1.7
J/K (Maturity)	1.3	I/J (Biodegradation)	0.3
		V/U (Biodegradation)	2.4

- = Below detection limit or not determined
3/12/2004

Paraffin Index I = (P+Q)/(R+S+T)
Paraffin Index II = %U in N to V

FIGURE 2a

Sample : **YOLLA-4, 2609.5m ex MPSR-1695, Crude Oil**
File ID : **344302WB**

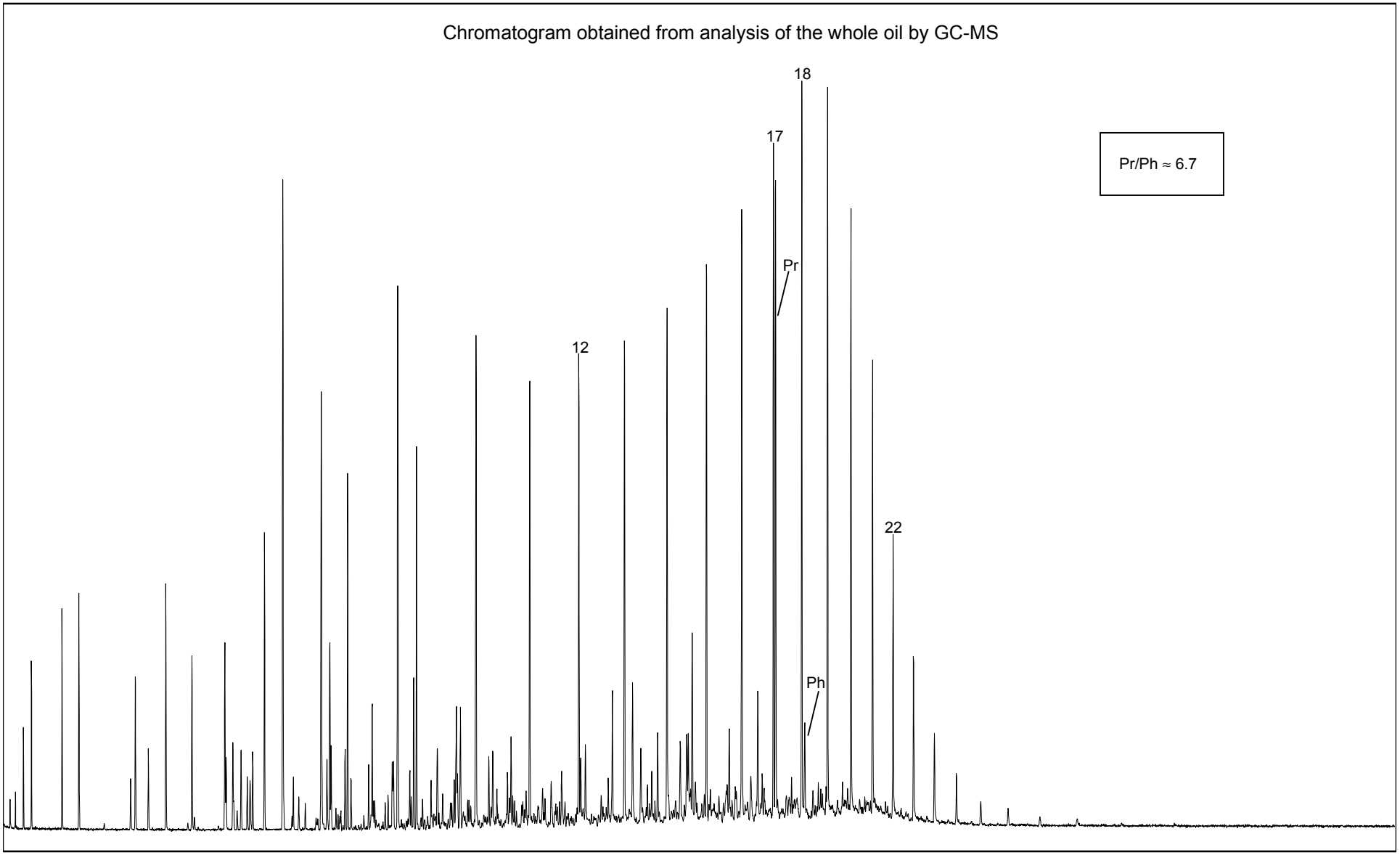

GEOTECHNICAL SERVICES PTY LTD

FIGURE 2b

Sample : **YOLLA-4, 2609.5m ex MPSR-1695, Crude Oil**
File ID : **344302WB**

GEOTECH

Partial chromatogram obtained from analysis of the whole oil by GC-MS

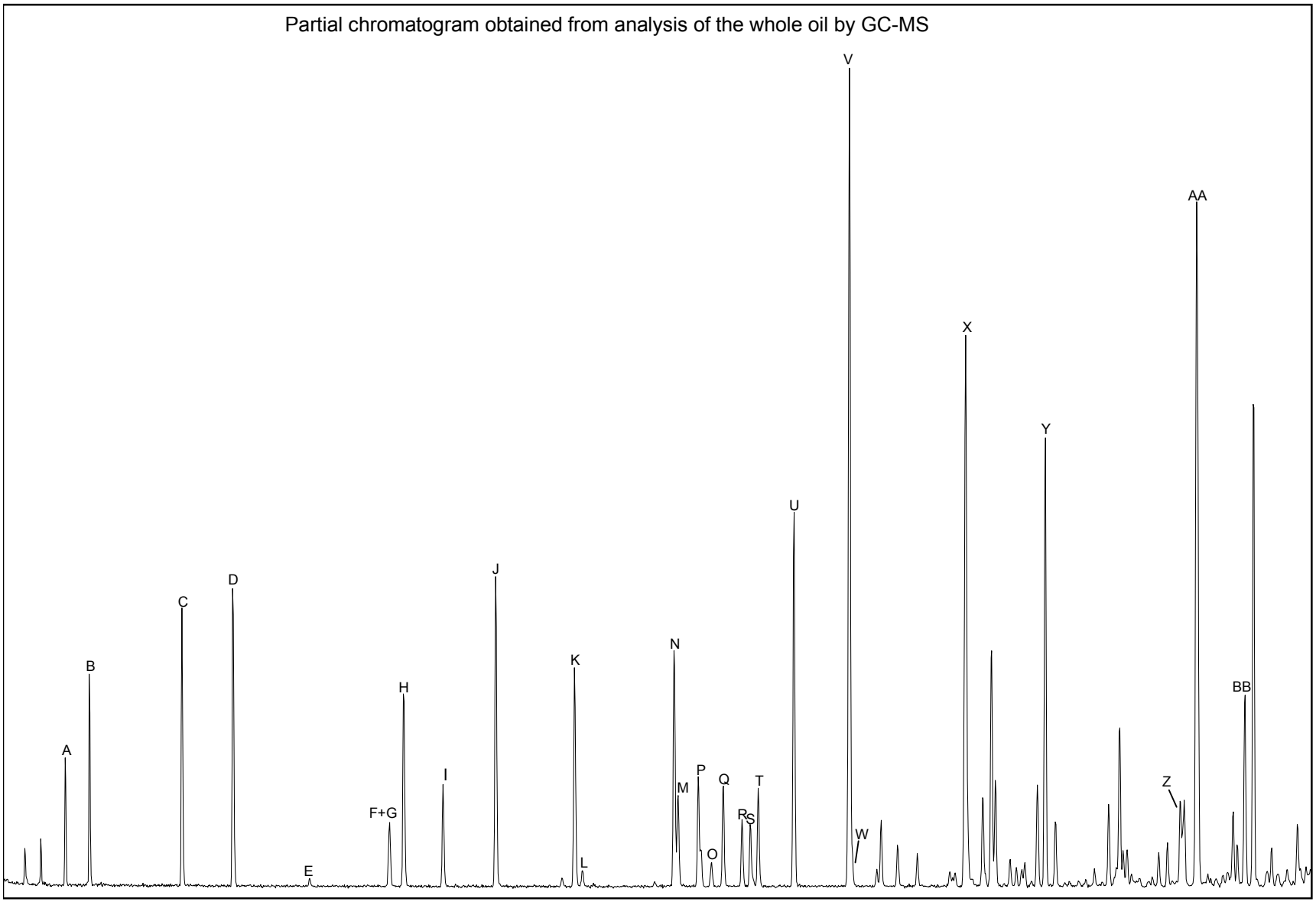

Key:
isobutane (A)
n-butane (B)
isopentane (C)
n-pentane (D)
2,2-dimethylbutane (E)
2,3-dimethylbutane + cyclopentane (F+G)
2-methylpentane (H)
3-methylpentane (I)
n-hexane (J)
methylcyclopentane (K)
2,4-dimethylpentane (L)
benzene (M)
cyclohexane (N)
1,1-dimethylcyclopentane (O)
2-methylhexane/
2,3-dimethylpentane (P)
3-methylhexane (Q)
1cis-3-dimethylcyclopentane (R)
1 trans-3-dimethylcyclopentane (S)
1 trans-2-dimethylcyclopentane (T)
n-heptane (U)
methylcyclohexane (V)
1,1,3-trimethylcyclopentane+ (W)
toluene (X)
n-octane (Y)
ethylbenzene (Z)
M+P-xylene (AA)
O-xylene (BB)

TABLE 4

SOLVENT EXTRACTION DATA

YOLLA-4

GEOTECH

DEPTH	Sample Type	Weight of Material Extd. (g)	Total Extract (mg)	Total Extract (ppm)
2894.0m	Core	5.1	67.3	13119

nd = no data

FIGURE 3

Sample : **YOLLA-4, 2894.0m, Core**
File ID : **342910X**

Chromatogram obtained from analysis of the whole extract by GC-MS

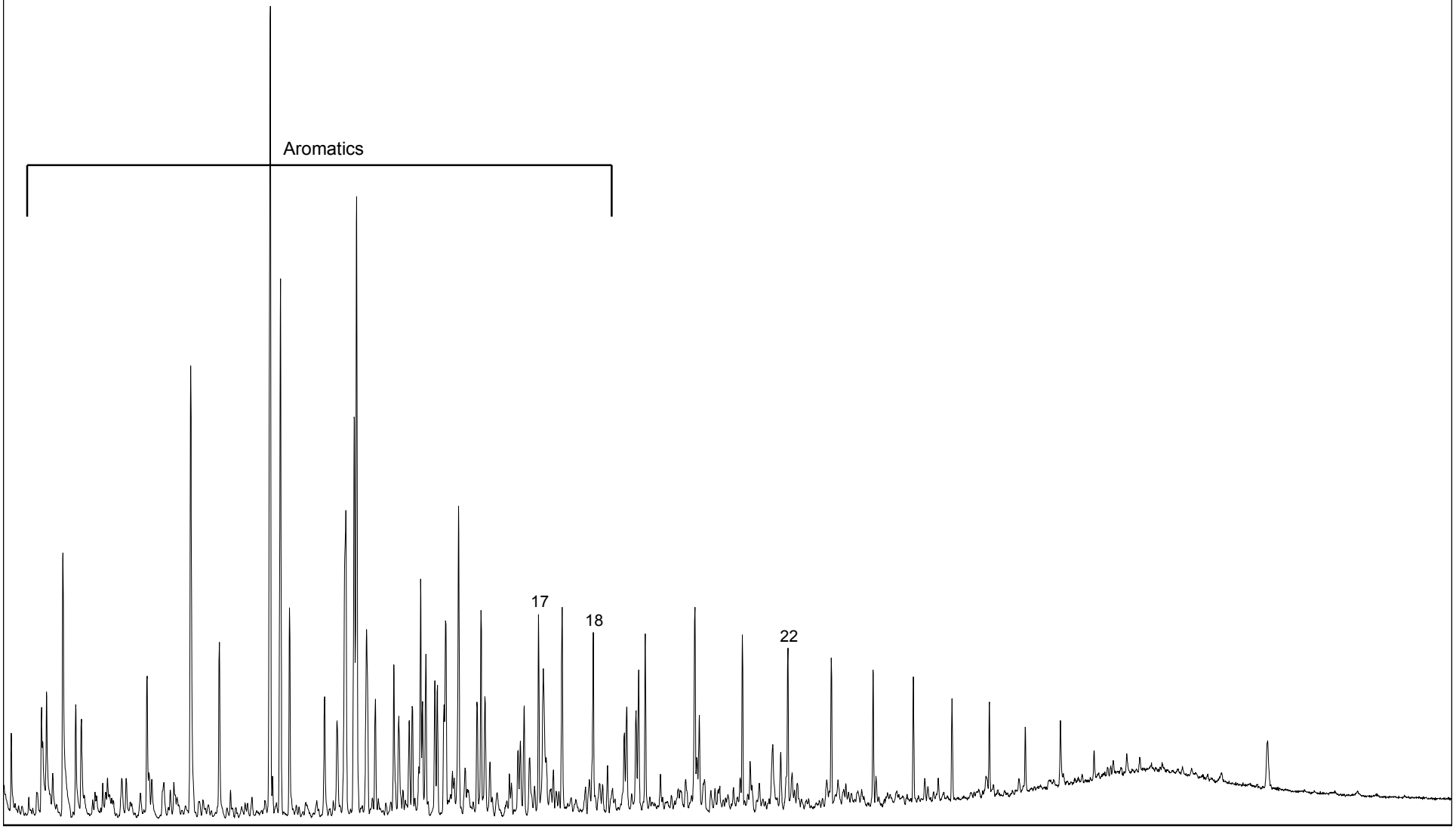

TABLE 5

LIQUID CHROMATOGRAPHY DATA

OIL

YOLLA-4

Yields (%) and Selected Ratios

		------Hydrocarbons------			------Non-hydrocarbons------			Sats	Asph.	HC
DEPTH	Sample Type	Sats	Aros	HC's	NSOs	Asph.	Non HC's	Aros	NSO	Non HC
2609.5m, ex MPSR-1695	Crude Oil	77.6	17.1	94.7	5.3	nd	5.3	4.5	nd	17.8

3/12/2004
nd = no data

TABLE 6

ANALYSIS OF SATURATED HYDROCARBONS BY GC-MS
OIL

YOLLA-4

A. Selected Ratios

DEPTH	Sample Type	Prist./Phyt.	Prist./n-C17	Phyt./n-C18	CPI(1)	CPI(2)	(C21+C22)/(C28+C29)
2609.5m, ex MPSR-1695	Crude Oil	7.67	1.09	0.13	1.11	1.08	2.01

YOLLA-4

B. n-Alkane Distributions

DEPTH	nC12	nC13	nC14	nC15	nC16	nC17	Pr	nC18	Ph	nC19	nC20	nC21	nC22	nC23	nC24	nC25	nC26	nC27	nC28	nC29	nC30	nC31
2609.5m, ex MPSR-1695	1.8	2.4	2.8	3.4	3.8	4.5	4.9	5.0	0.6	5.8	6.2	6.9	7.6	8.0	7.5	7.2	5.9	5.9	4.0	3.2	1.4	1.1

$$CPI(1) = \frac{(C23+C25+C27+C29)+(C25+C27+C29+C31)}{2x(C24+C26+C28+C30)}$$

$$CPI(2) = \frac{(C23+C25+C27)+(C25+C27+C29)}{2x(C24+C26+C28)}$$

3/12/2004
nd = no data

FIGURE 4

Sample : **YOLLA-4, 2609.5m, ex-MPSR-1695, Crude Oil**
File ID : 344302S

GEOTECH

Chromatogram obtained from the analysis of saturated hydrocarbons by GC-MS

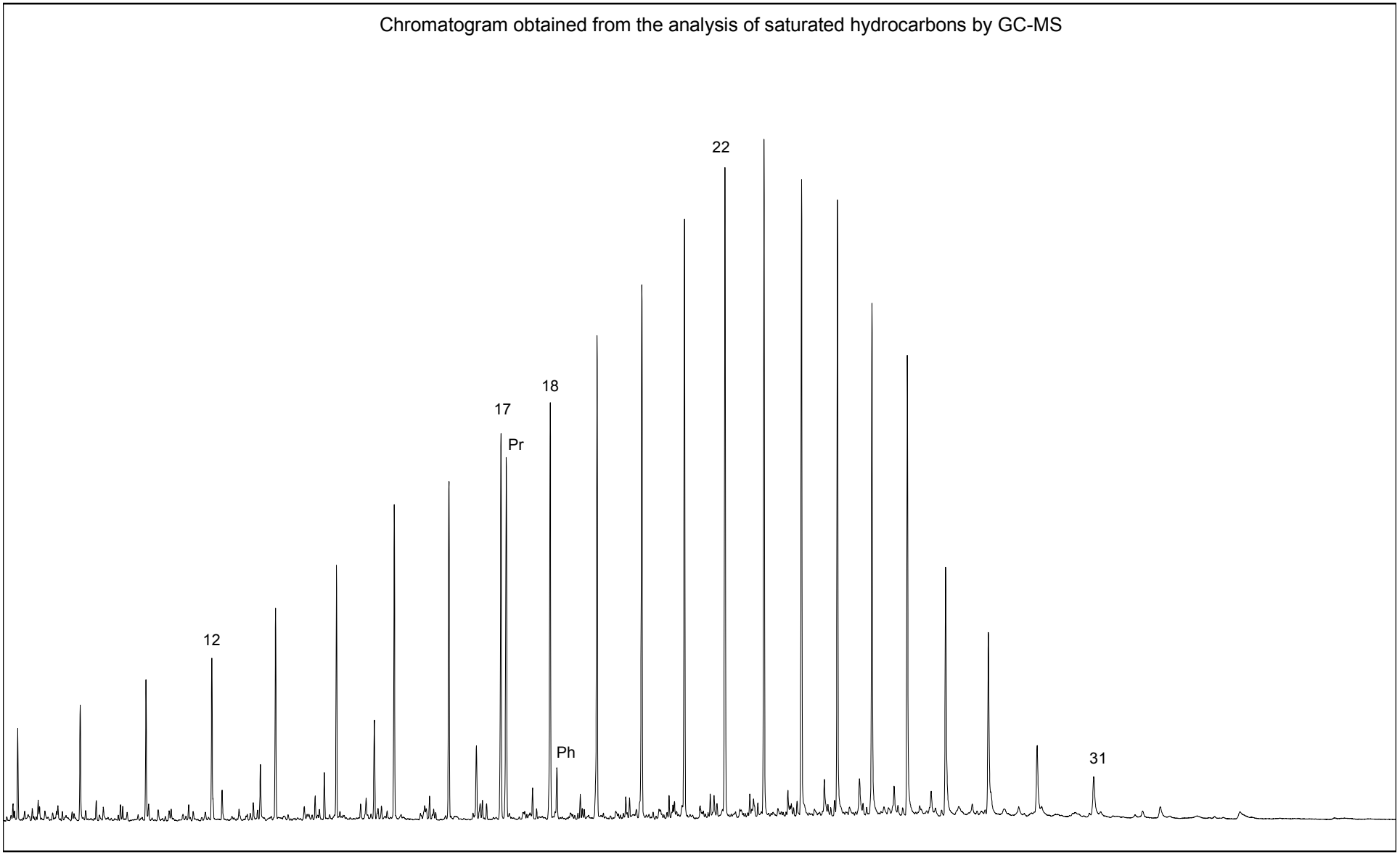

GEOTECHNICAL SERVICES PTY LTD

LIQUID CHROMATOGRAPHY DATA
EXTRACT

YOLLA-4

A. Yields (ppm)

DEPTH	Sample Type	-------Hydrocarbons------- Sats	Aros	HC's	------Non-hydrocarbons------ NSOs	Asph.	Non HC's	Loss on column
2894.0m	Core	1696	5244	6940	3275	nd	3275	2904

YOLLA-4

B. Yields (%) and Selected Ratios

DEPTH	Sample Type	------Hydrocarbons------ Sats	Aros	HC's	------Non-hydrocarbons------ NSOs	Asph.	Non HC's	Sats / Aros	Asph. / NSO	HC / Non HC
2894.0m	Core	16.6	51.3	68	32.1	nd	32	0.3	nd	2.1

3/12/2004
nd = no data

ANALYSIS OF SATURATED HYDROCARBONS BY GC-MS
EXTRACT

YOLLA-4

A. Selected Ratios

DEPTH	Sample Type	Prist./Phyt.	Prist./n-C17	Phyt./n-C18	CPI(1)	CPI(2)	(C21+C22)/(C28+C29)
2894.0m	Core	7.79	0.54	0.08	1.09	1.06	3.75

YOLLA-4

B. n-Alkane Distributions

DEPTH	nC12	nC13	nC14	nC15	nC16	nC17	Pr	nC18	Ph	nC19	nC20	nC21	nC22	nC23	nC24	nC25	nC26	nC27	nC28	nC29	nC30	nC31
2894.0m	5.9	6.9	6.9	7.5	6.6	6.7	3.6	6.0	0.5	6.3	6.2	6.1	5.8	5.5	4.8	4.3	3.5	3.1	1.8	1.3	0.5	0.4

$$CPI(1) = \frac{(C23+C25+C27+C29)+(C25+C27+C29+C31)}{2x(C24+C26+C28+C30)}$$

$$CPI(2) = \frac{(C23+C25+C27)+(C25+C27+C29)}{2x(C24+C26+C28)}$$

3/12/2004
nd = no data

FIGURE 5

Sample : **YOLLA-4, 2894.0m, Core**
File ID : 344301SB

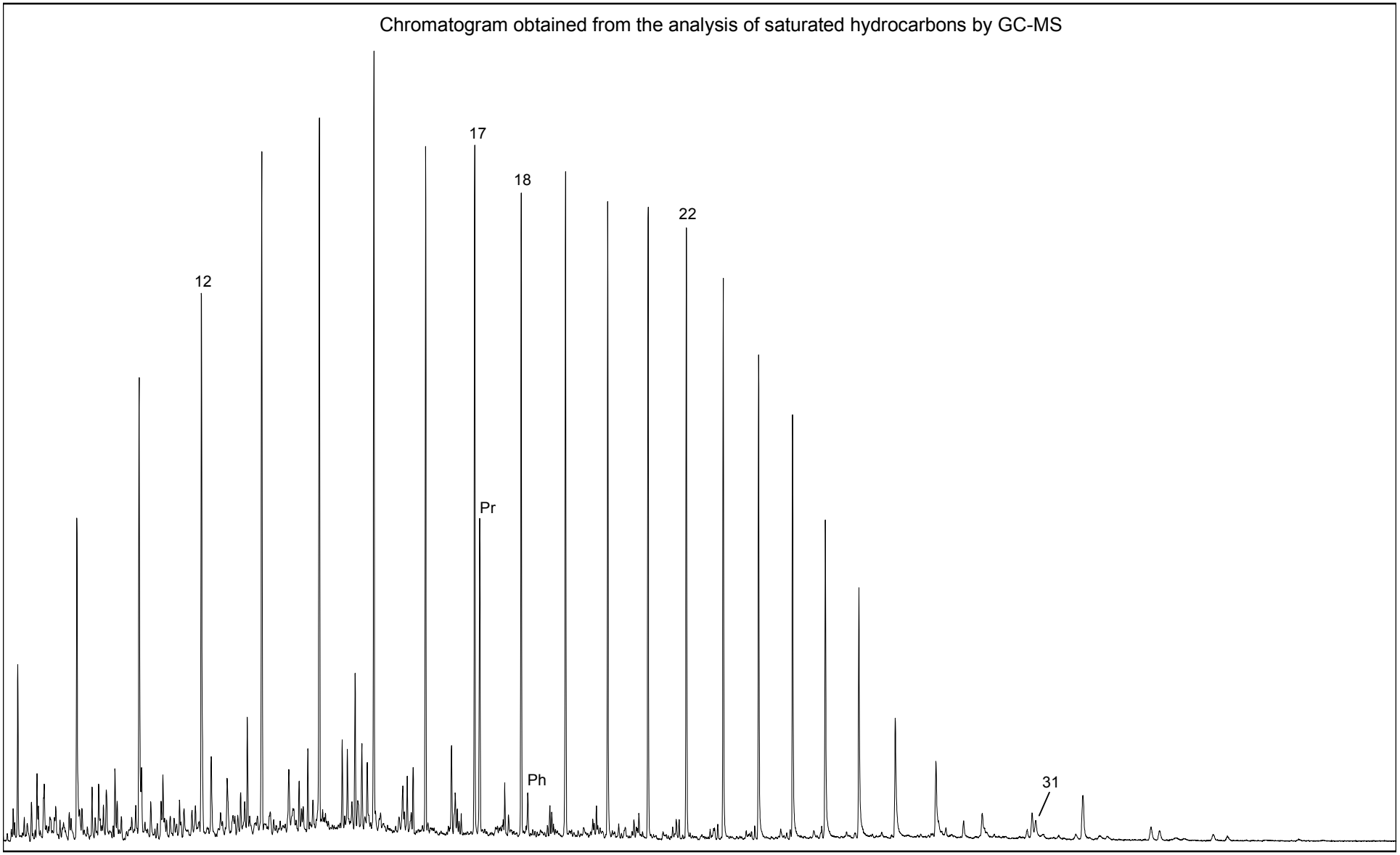

GEOTECHNICAL SERVICES PTY LTD

TABLE 9

ANALYSIS OF AROMATIC HYDROCARBONS BY GC-MS

YOLLA-4

DEPTH	TYPE	DNR-1	DNR-5	DNR-6	TNR-1	TNR-5	TNR-6	MPR-1	MPI-1	MPI-2	Rc(a)	Rc(b)
2894.0m	Core	6.74	nd	3.02	0.99	1.66	0.98	1.16	0.44	0.52	0.66	2.04
2609.5m	Oil	8.69	nd	3.87	0.97	0.82	0.50	1.77	0.71	0.75	0.82	1.88

response factors have not been applied to these ratios

YOLLA-4

DEPTH	TYPE	1,7-DMP/X (m/z 206)	RETENE/9-MP (m/z 219,192)	1MP/9MP	HPI
2894.0m	Core	1.28	0.18	1.22	0.72
2609.5m	Oil	0.66	0.25	0.97	0.41

HPI = Higher Plant Index (i.e (retene + cadalene + iHMN-IV)/1,3,6,7-TeMN))

FIGURE 6-1a

Sample: **YOLLA-4, 2894.0m, Core**

File ID: **344301AB**

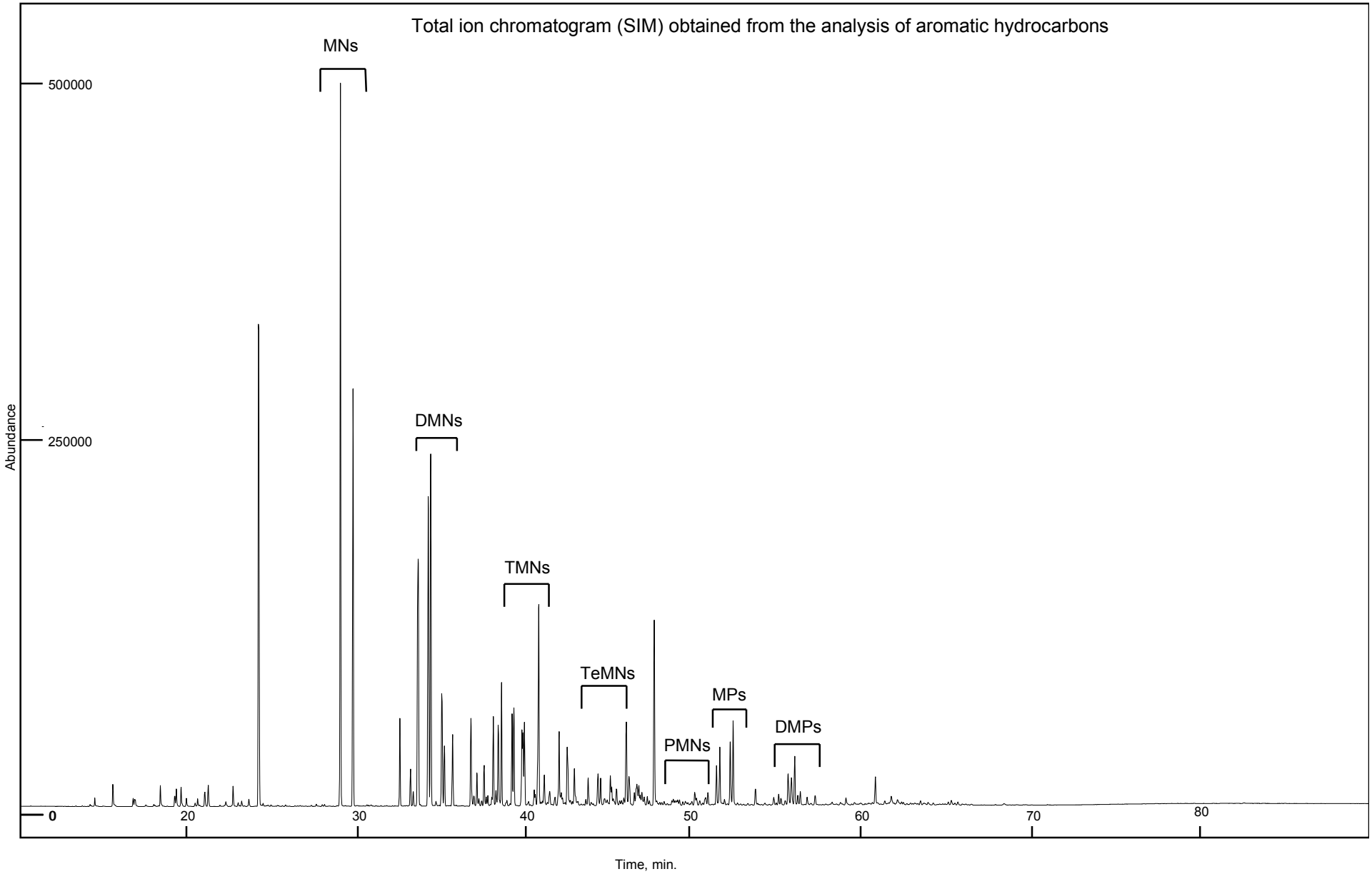

GEOTECHNICAL SERVICES PTY LTD

FIGURE 6-1b

Sample: **YOLLA-4, 2894.0m, Core**

File ID: **344301AB**

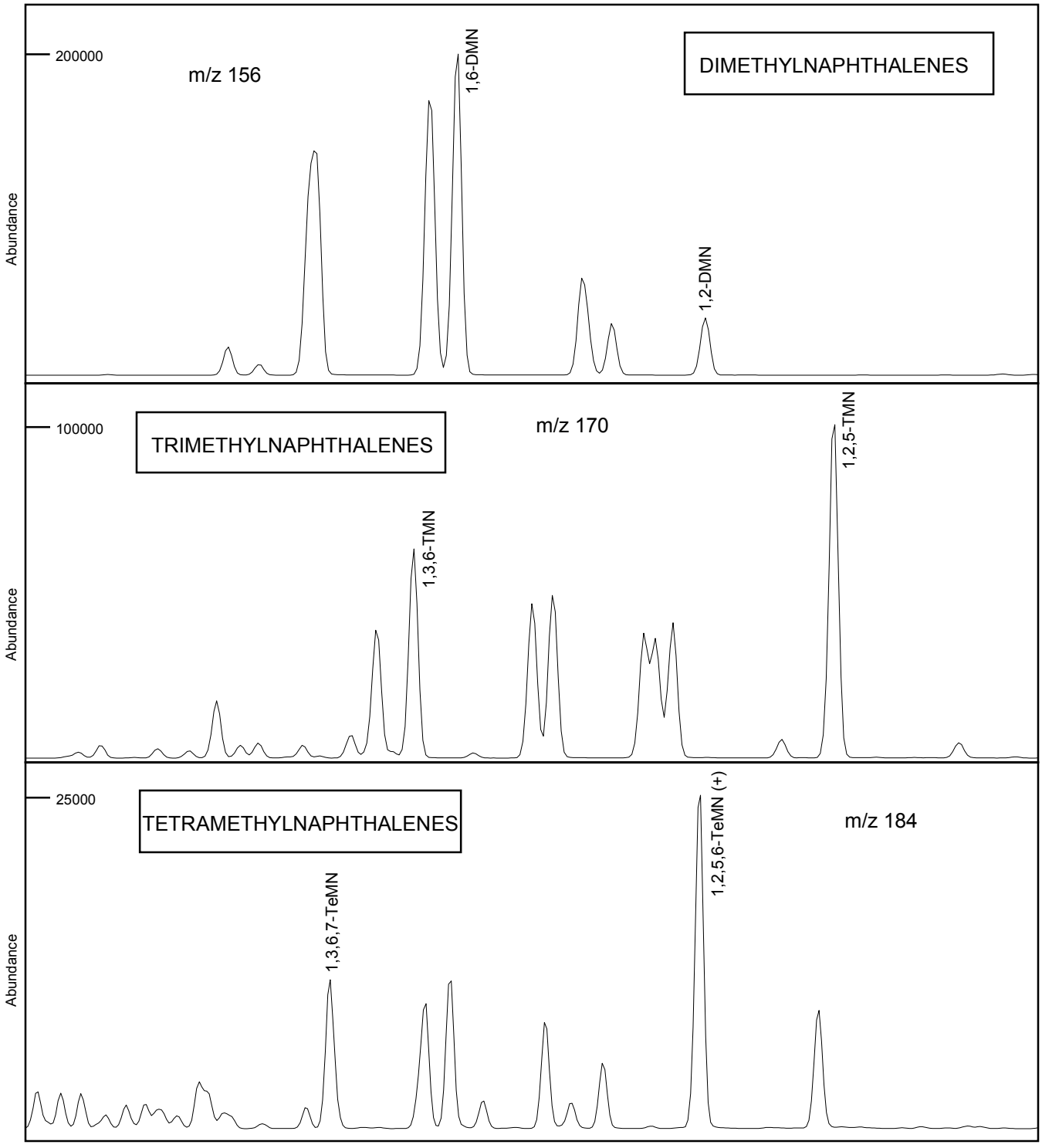

FIGURE 6-1c

Sample: **YOLLA-4, 2894.0m, Core**

File ID: **344301AB**

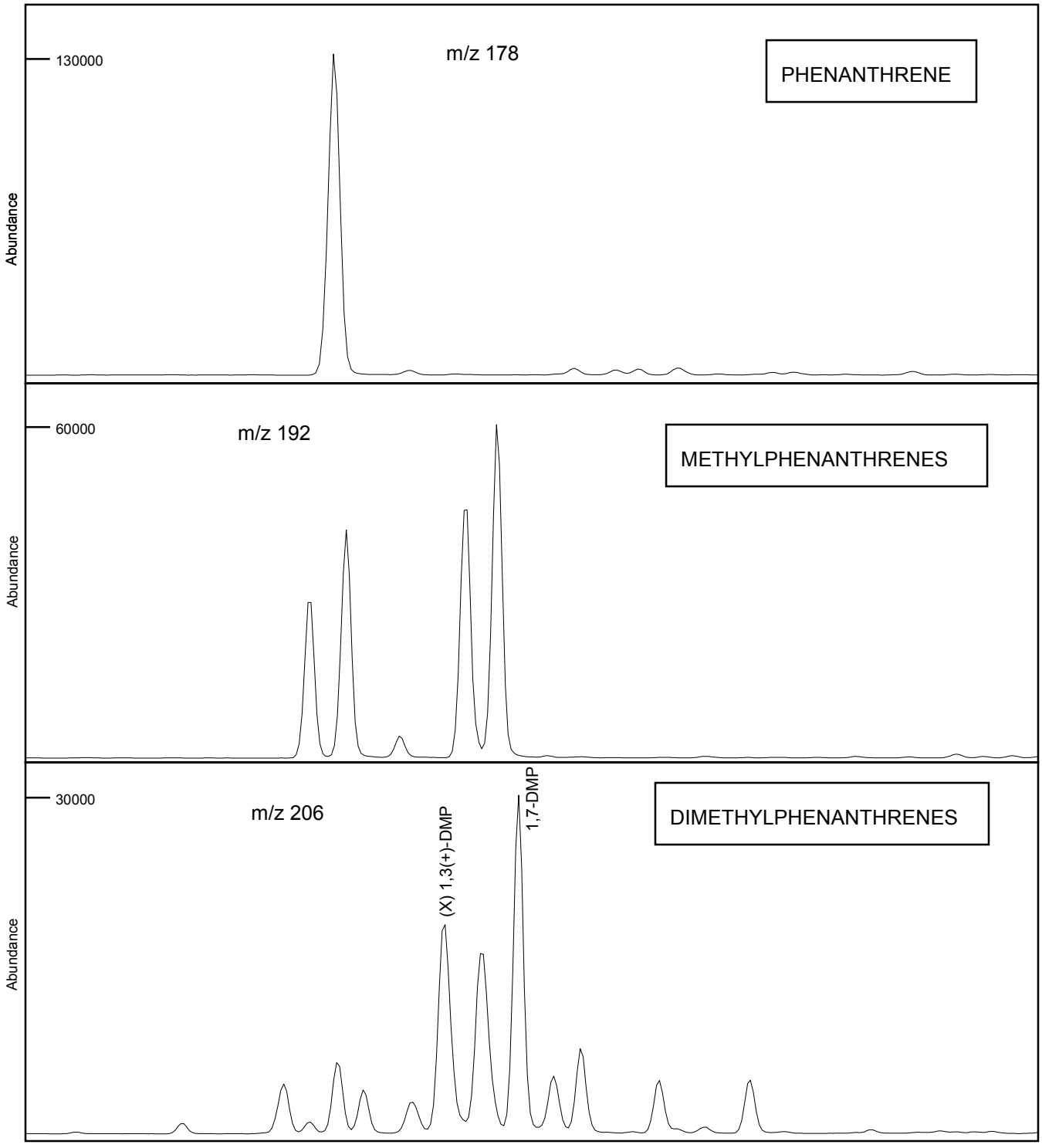

FIGURE 6-1d

Sample: **YOLLA-4, 2894.0m, Core**

File ID: **344301AB**

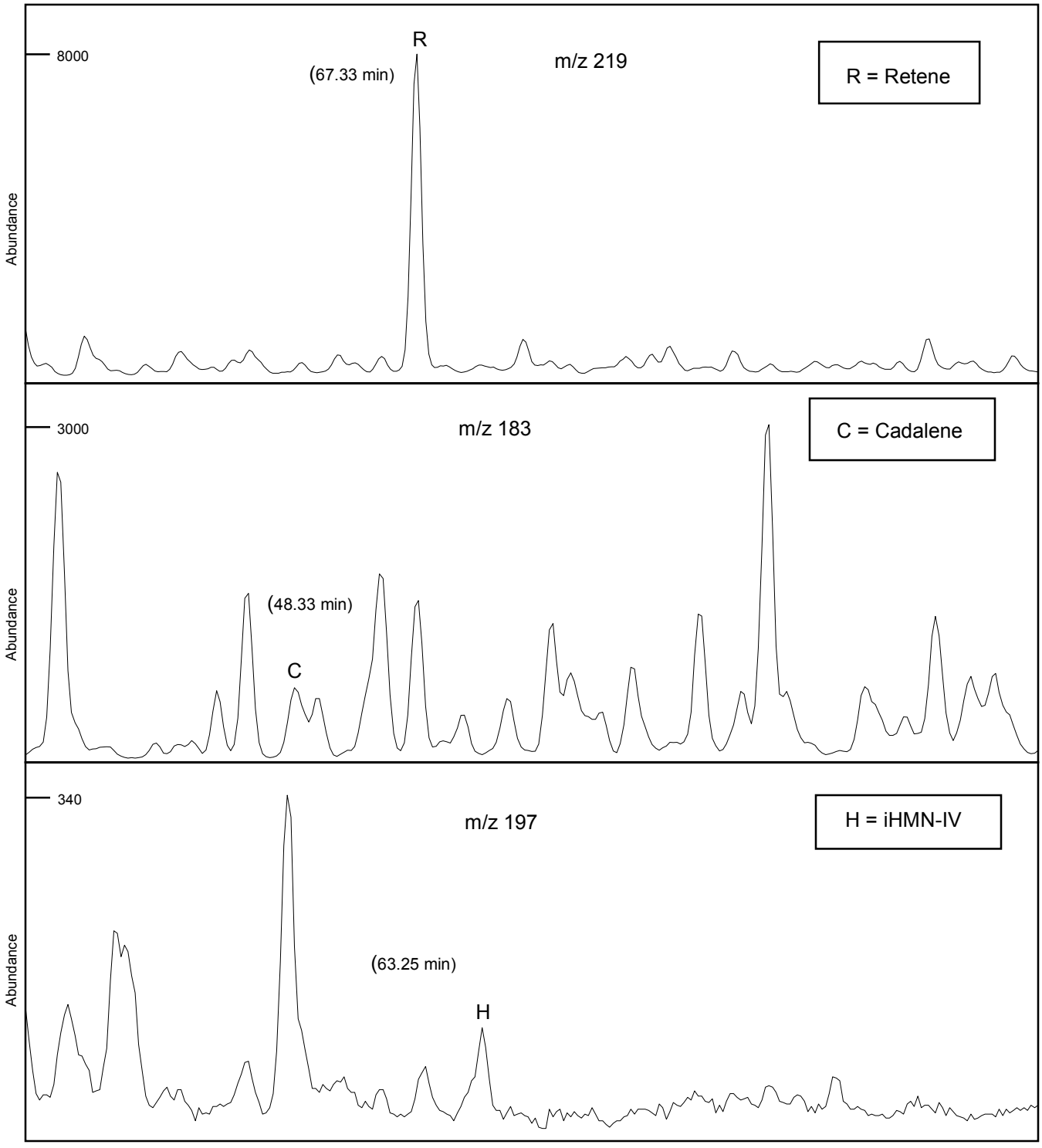

FIGURE 6-1e

Sample: **YOLLA-4, 2894.0m, Core**

File ID: **344301AB**

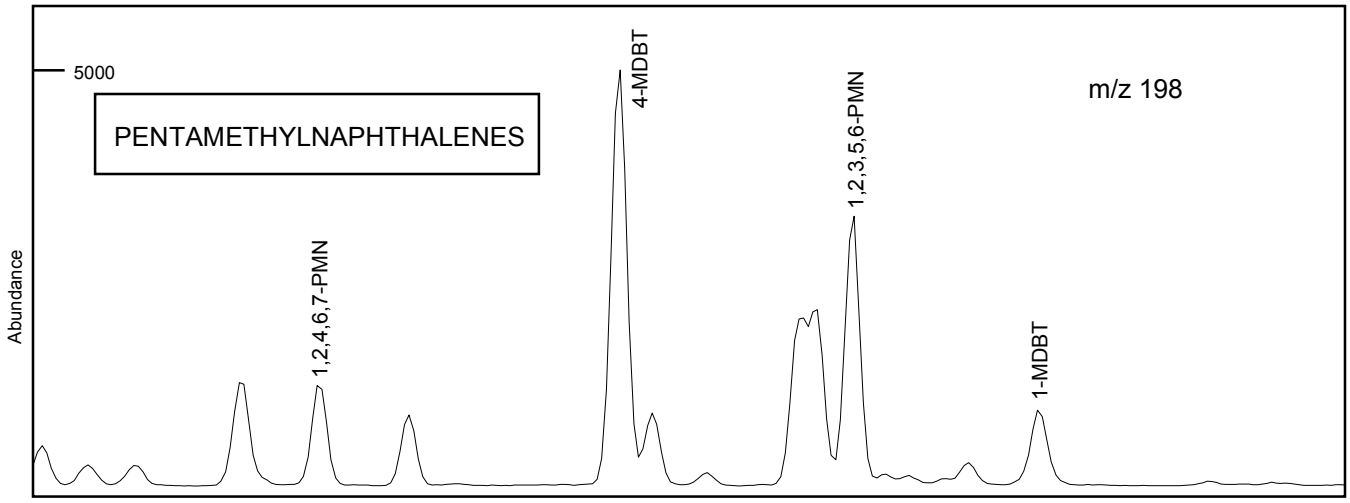

FIGURE 6-2a

Sample: **YOLLA-4, 2609.5m, ex MPSR-1695, Oil**

File ID: **344302AB**

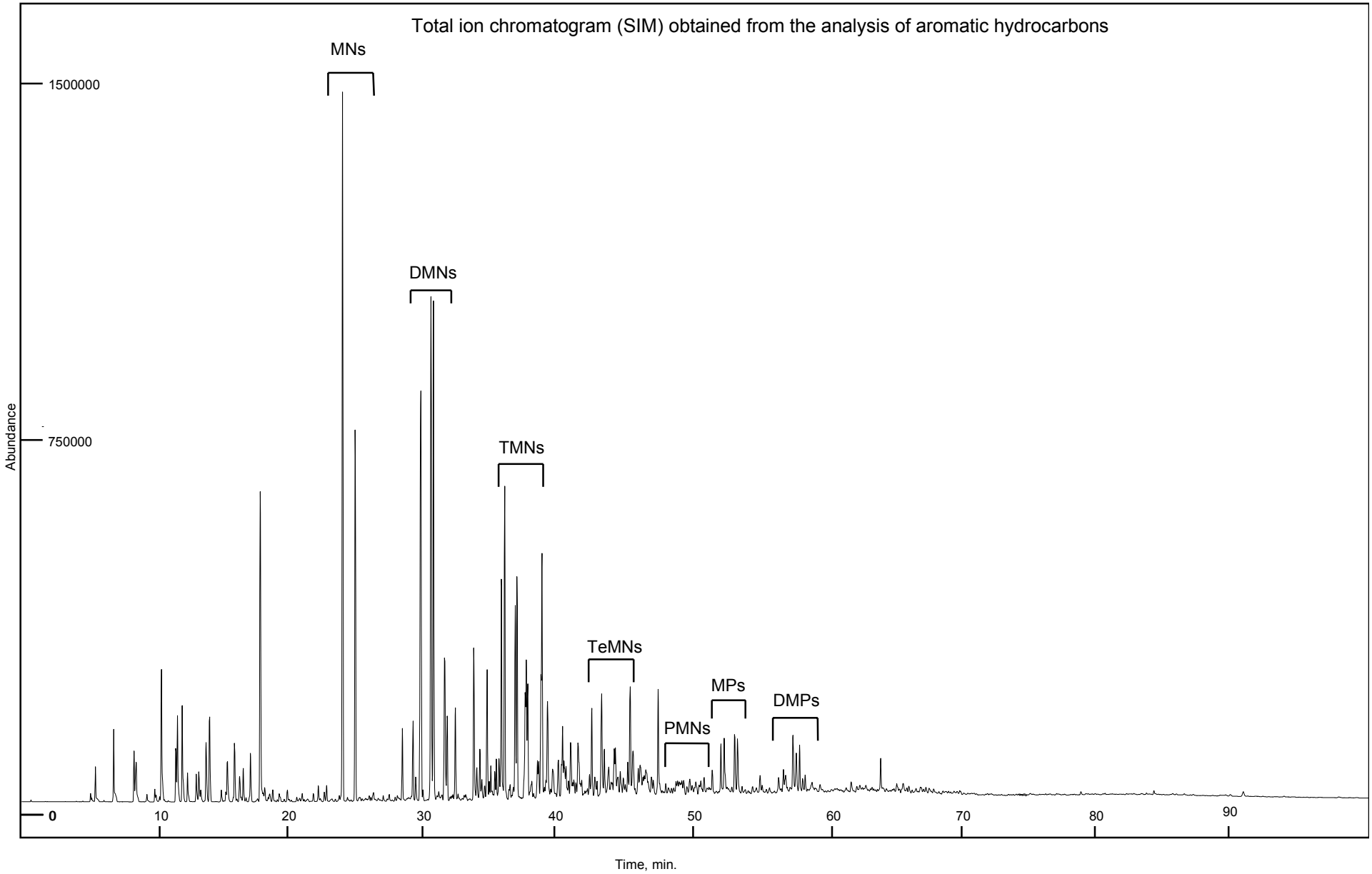

GEOTECHNICAL SERVICES PTY LTD

FIGURE 6-2b

Sample: **YOLLA-4, 2609.5m, ex MPSR-1695, Oil**

File ID: **344302AB**

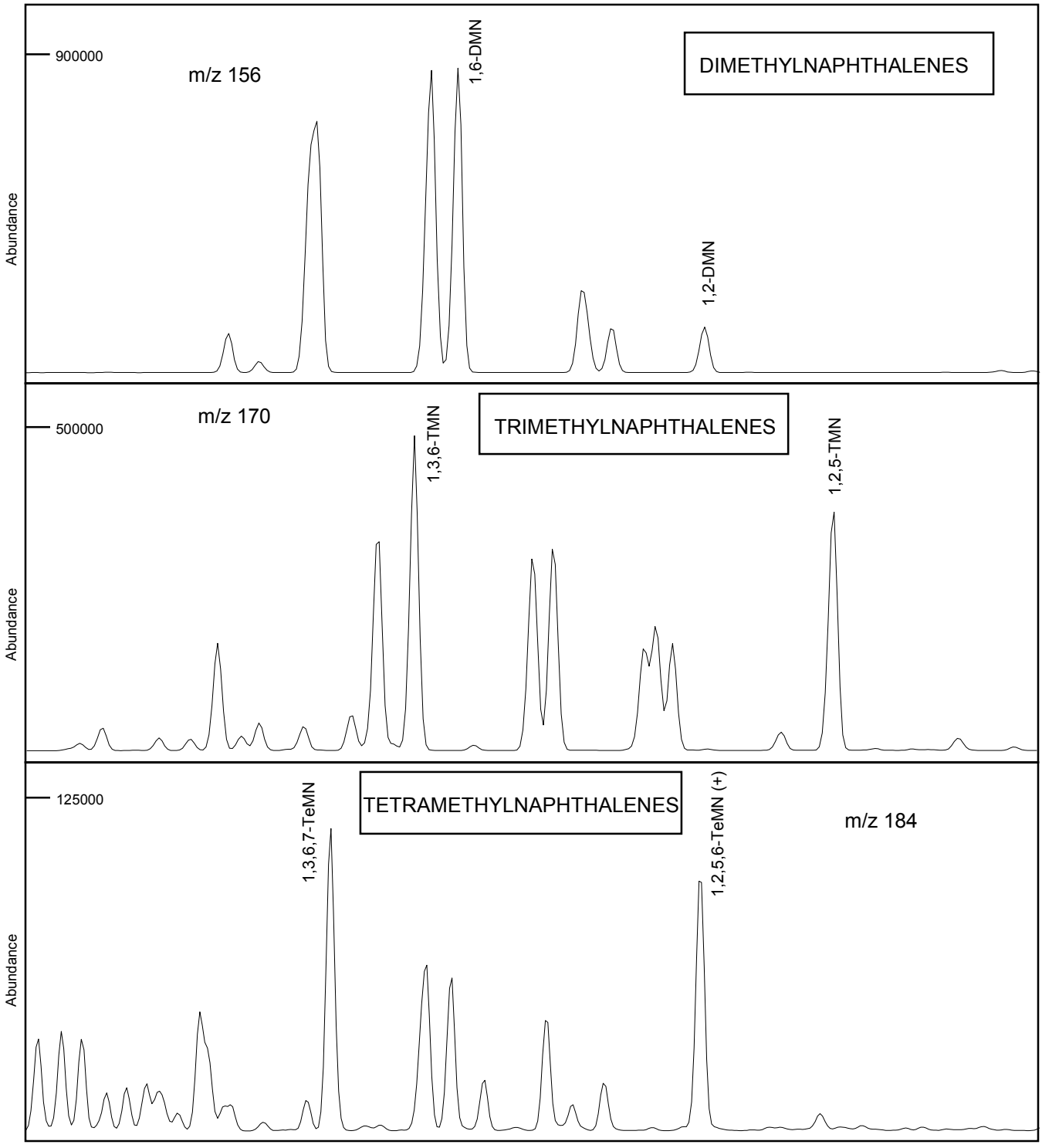

FIGURE 6-2c

Sample: **YOLLA-4, 2609.5m, ex MPSR-1695, Oil**

File ID: **344302AB**

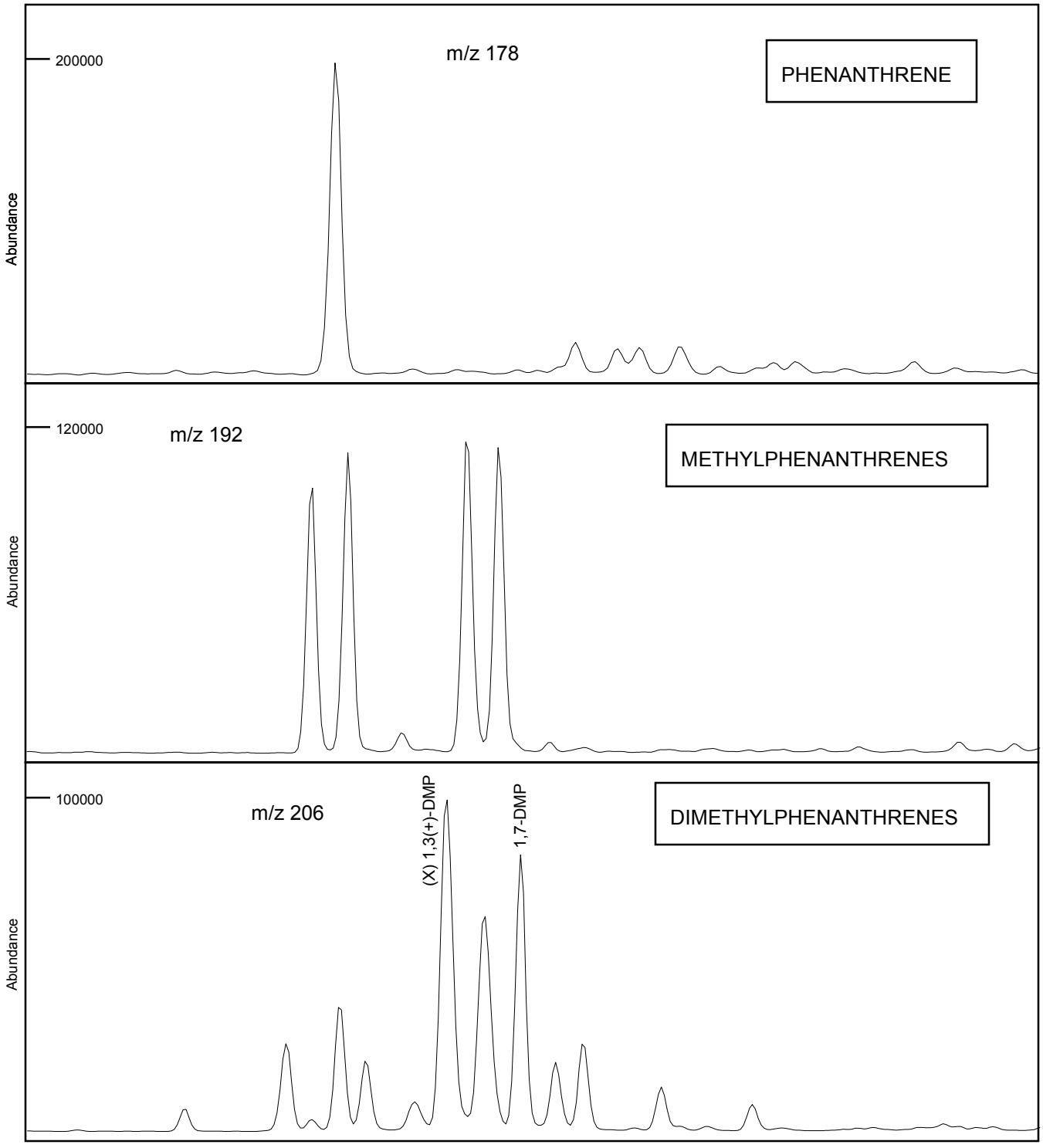

FIGURE 6-2d

Sample: **YOLLA-4, 2609.5m, ex MPSR-1695, Oil**

File ID: **344302AB**

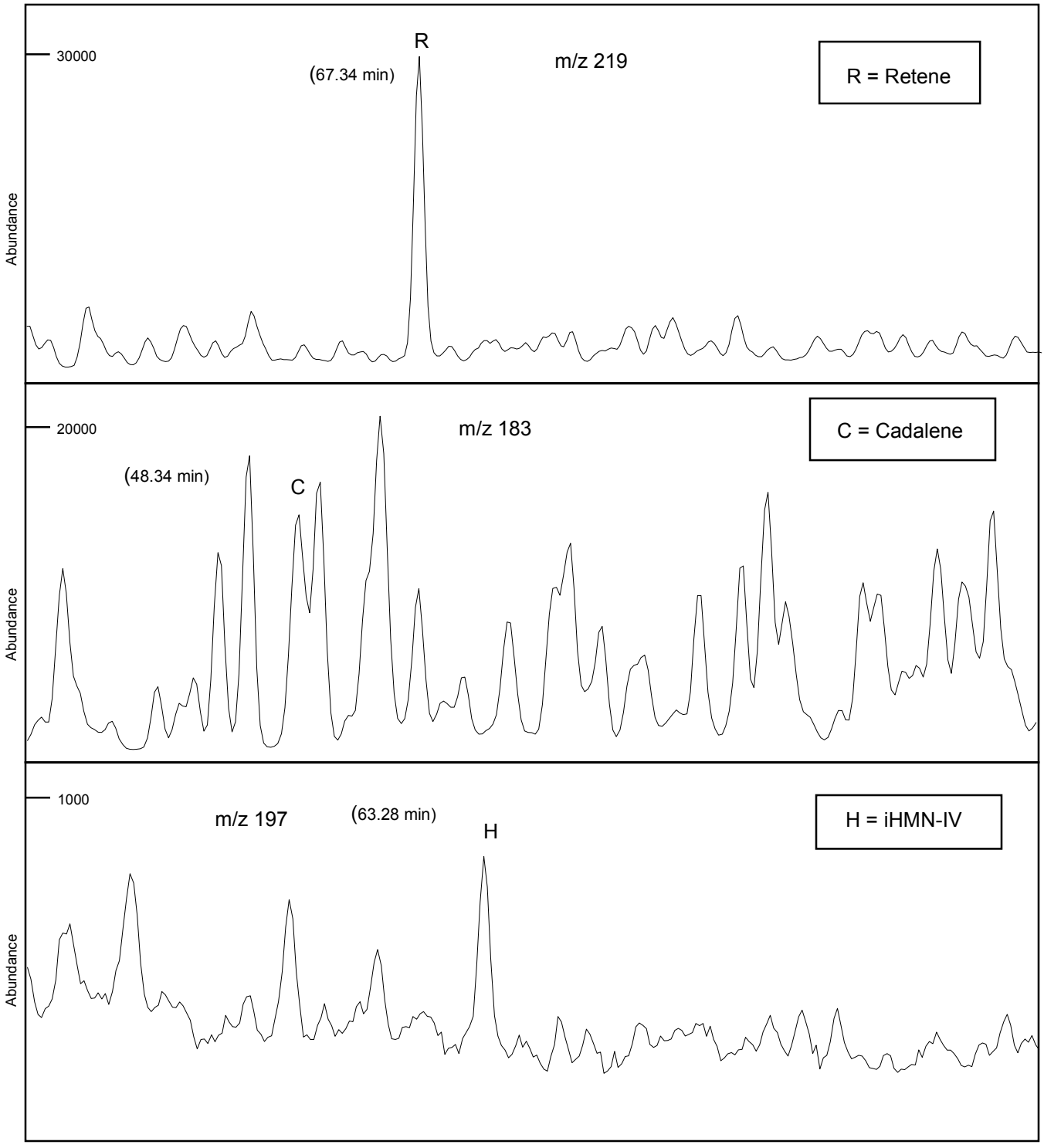

FIGURE 6-2e

Sample: **YOLLA-4, 2609.5m, ex MPSR-1695, Oil**

File ID: **344302AB**

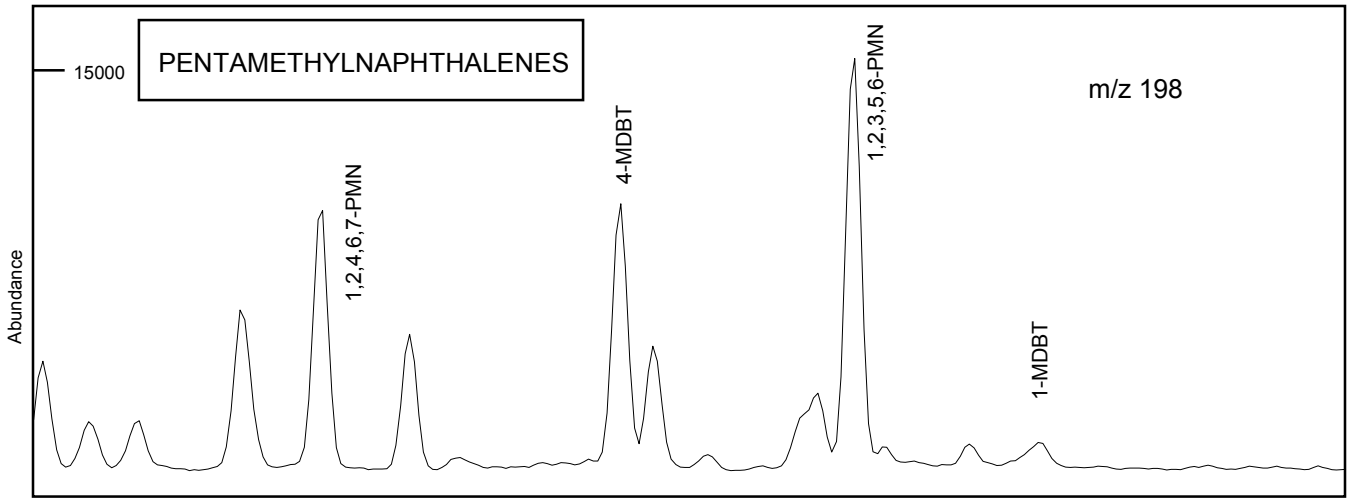

TABLE 10-1

ANALYSIS OF BRANCHED AND CYCLIC SATURATED HYDROCARBONS BY GC-MS

YOLLA-4, 2894.0m, Core

	Selected Parameters	*Ion(s)*	*Value*
1.	18α(H)-hopane/17α(H)-hopane (Ts/Tm)	191	0.40
2.	C30 hopane/C30 moretane	191	10.78
3.	C31 22S hopane/C31 22R hopane	191	1.40
4.	C32 22S hopane/C32 22R hopane	191	1.35
5.	C29 20S ααα sterane/C29 20R ααα sterane	217	0.69
6.	C29 ααα steranes (20S / 20S+20R)	217	0.41
7.	$\frac{\text{C29 } \alpha\beta\beta \text{ steranes}}{\text{C29 } \alpha\alpha\alpha \text{ steranes + C29 } \alpha\beta\beta \text{ steranes}}$	217	0.55
8.	C27/C29 diasteranes	259	nd
9.	C27/C29 steranes	217	nd
10.	18α(H)-oleanane/C30 hopane	191	nd
11.	$\frac{\text{C29 diasteranes}}{\text{C29 } \alpha\alpha\alpha \text{ steranes + C29 } \alpha\beta\beta \text{ steranes}}$	217	0.33
12.	$\frac{\text{C30 (hopane + moretane)}}{\text{C29 (steranes + diasteranes)}}$	191/217	21.61
13.	C15 drimane/C16 homodrimane	123	1.09
14.	Rearranged drimanes/normal drimanes	123	0.34

nd = no data

FIGURE 7-1a

Sample : **YOLLA-4, 2894.0m, Core**

File ID : 344301B

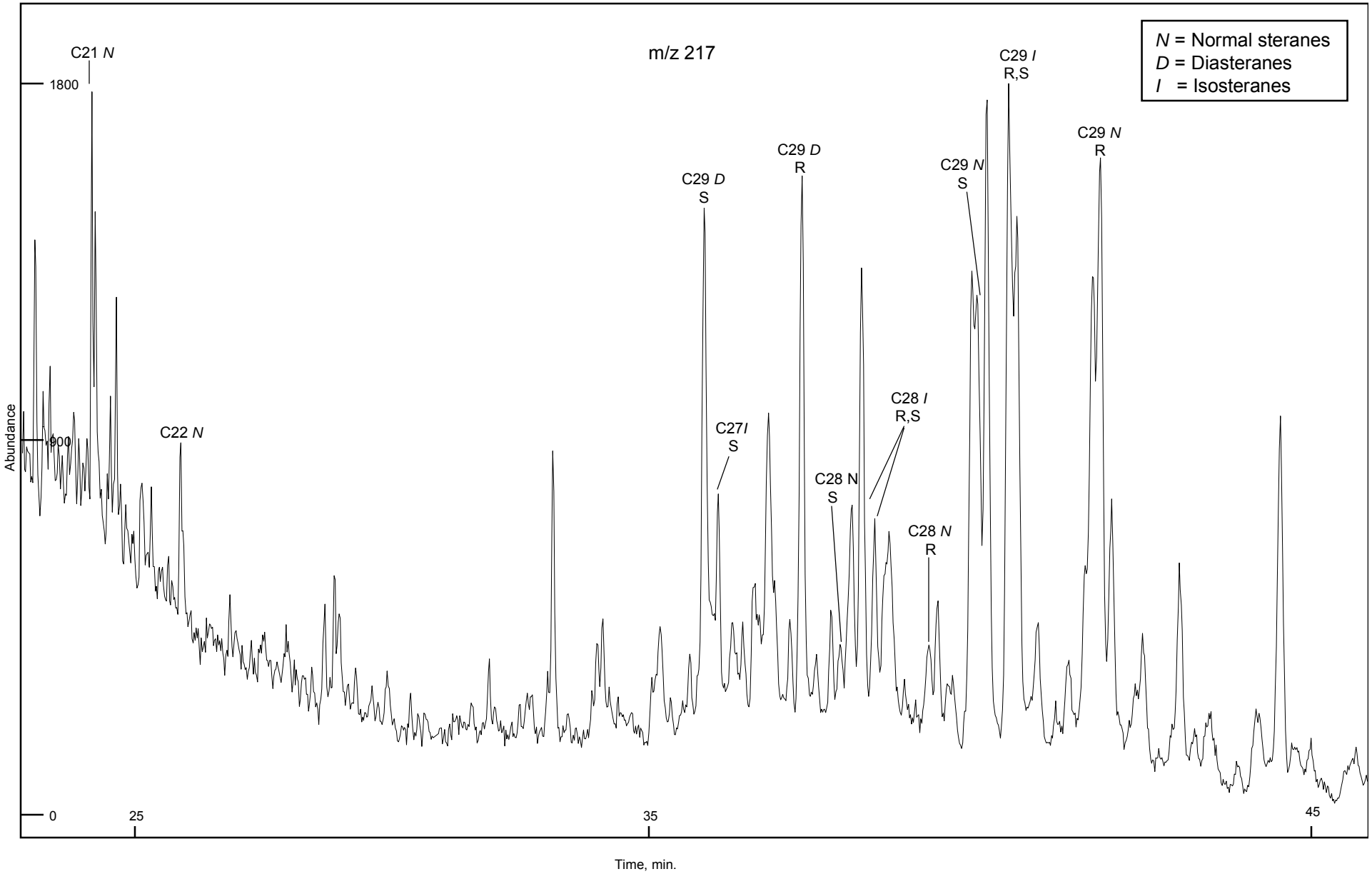

GEOTECHNICAL SERVICES PTY LTD

FIGURE 7-1b

Sample : **YOLLA-4, 2894.0m, Core**

File ID : 344301B

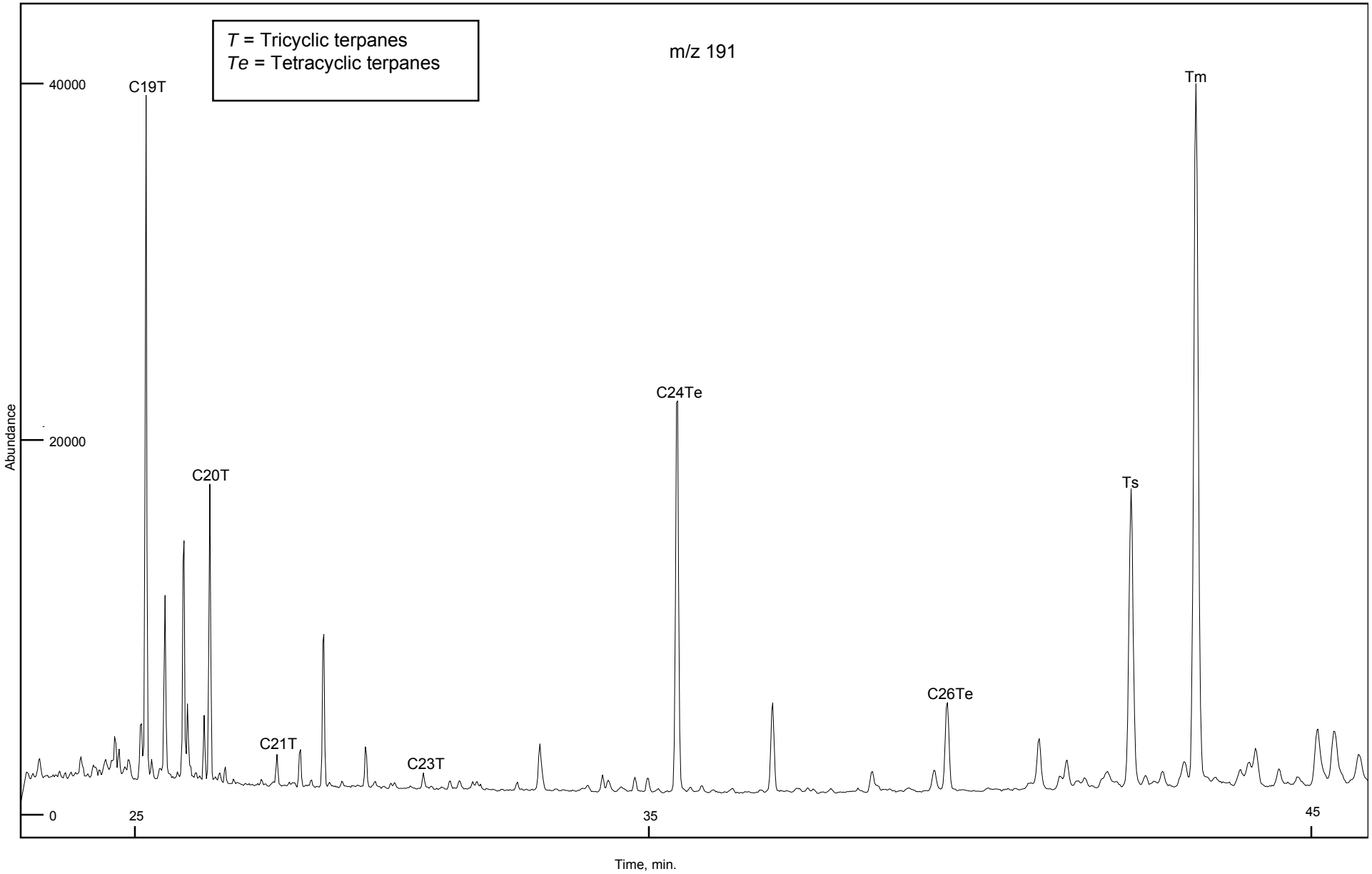

GEOTECHNICAL SERVICES PTY LTD

FIGURE 7-1c

Sample : **YOLLA-4, 2894.0m, Core**

File ID : 344301B

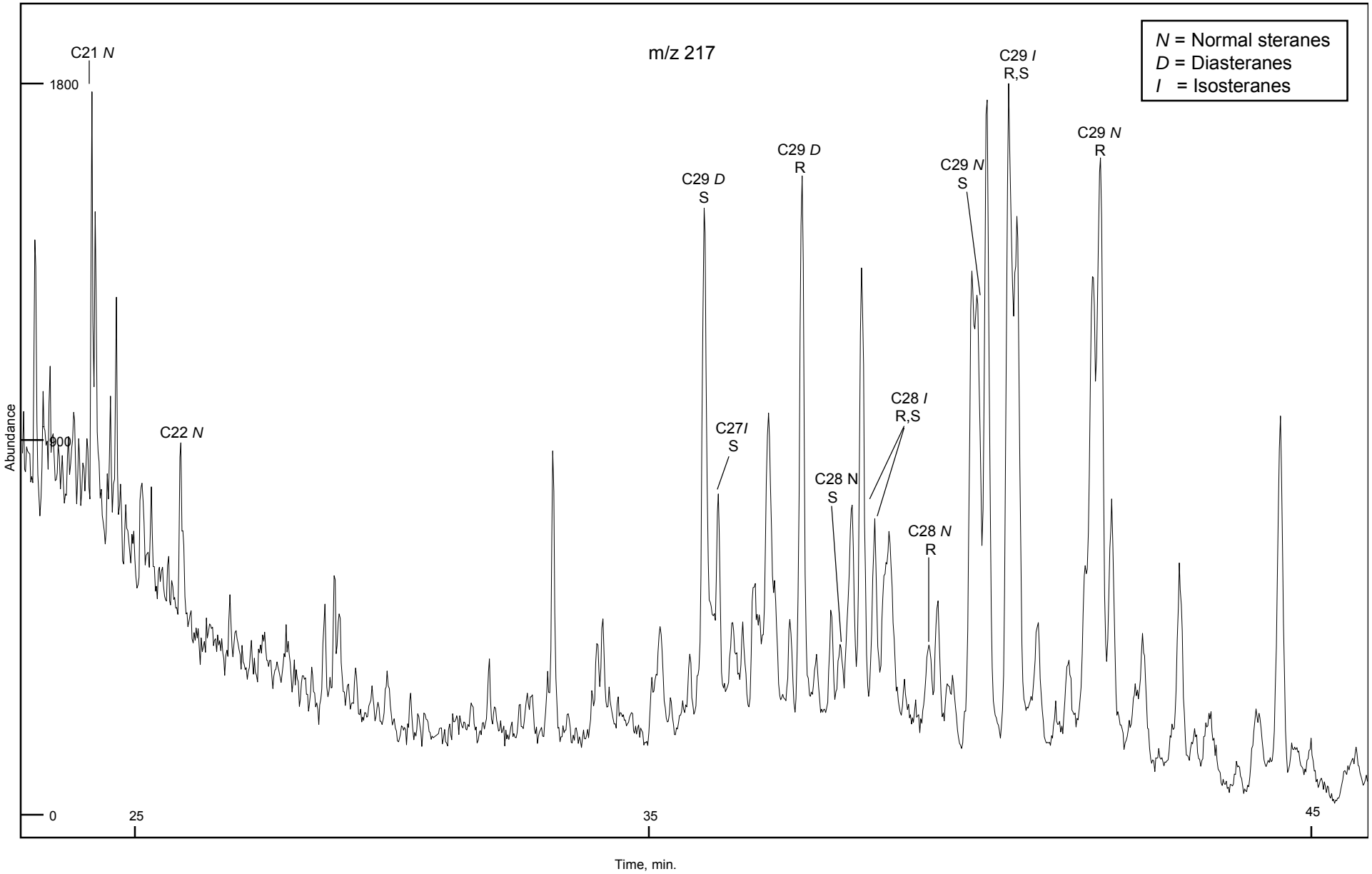

GEOTECHNICAL SERVICES PTY LTD

FIGURE 7-1d

Sample : **YOLLA-4, 2894.0m, Core**

File ID : 344301B

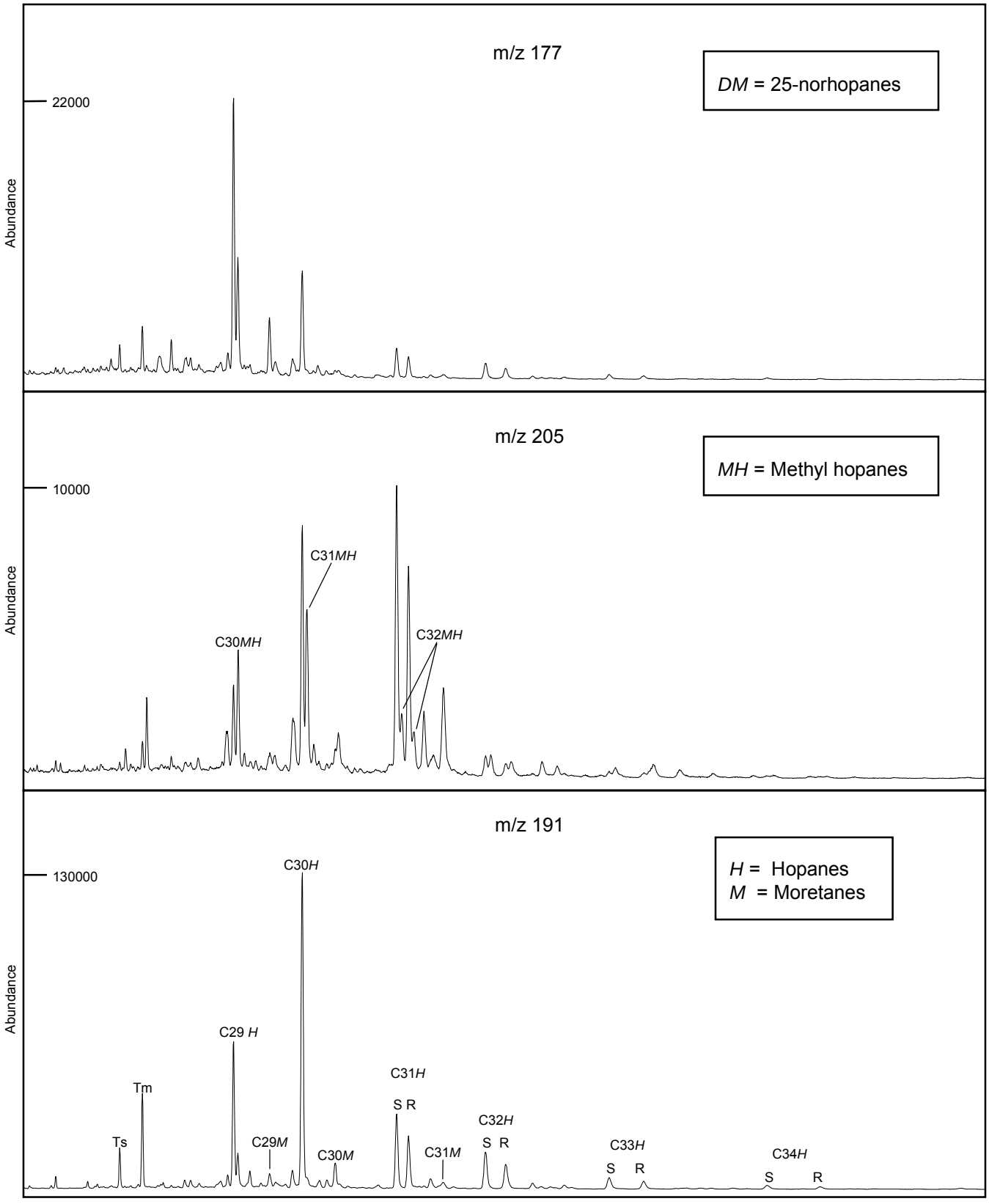

FIGURE 7-1e

Sample : **YOLLA-4, 2894.0m, Core**

File ID : 344301B

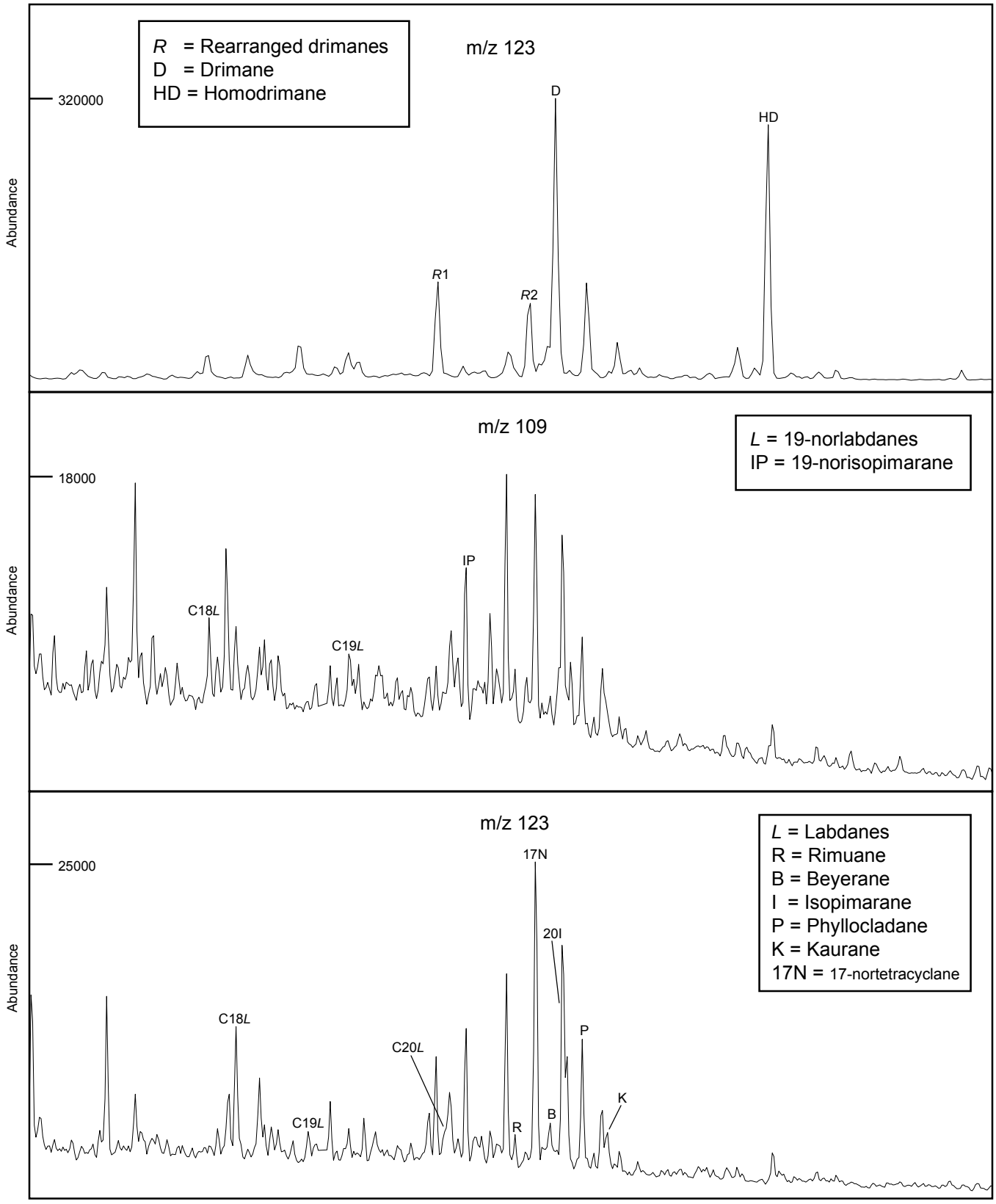

FIGURE 7-1f

Sample : **YOLLA-4, 2894.0m, Core**

File ID : 344301B

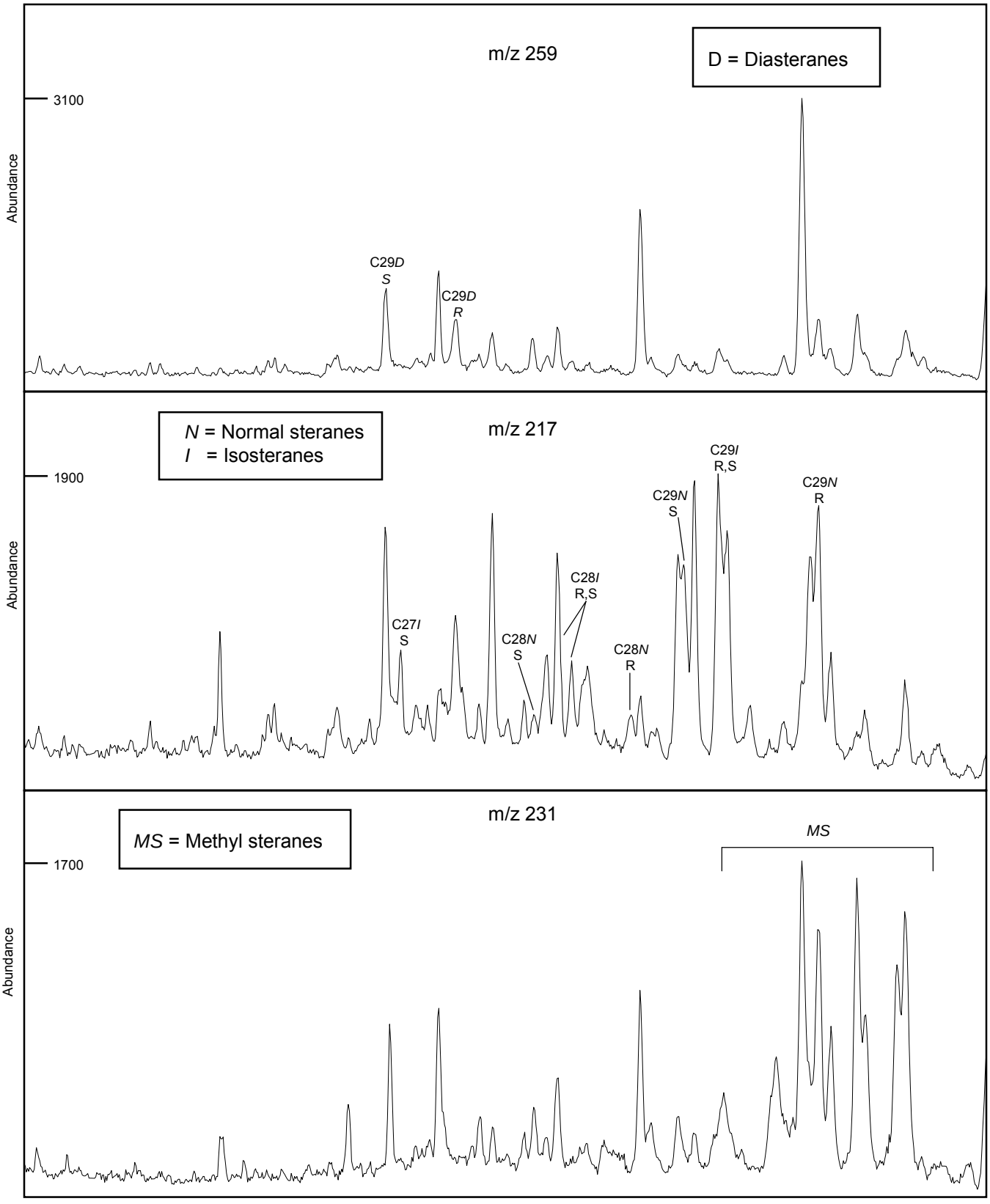

TABLE 10-2

ANALYSIS OF BRANCHED AND CYCLIC SATURATED HYDROCARBONS BY GC-MS

YOLLA-4, 2609.5m, ex MPSR-1695, Oil

GEOTECH

	Selected Parameters	*Ion(s)*	*Value*
1.	18α(H)-hopane/17α(H)-hopane (Ts/Tm)	191	0.37
2.	C30 hopane/C30 moretane	191	8.53
3.	C31 22S hopane/C31 22R hopane	191	1.36
4.	C32 22S hopane/C32 22R hopane	191	1.39
5.	C29 20S ααα sterane/C29 20R ααα sterane	217	0.84
6.	C29 ααα steranes (20S / 20S+20R)	217	0.46
7.	$\frac{\text{C29 } \alpha\beta\beta \text{ steranes}}{\text{C29 } \alpha\alpha\alpha \text{ steranes + C29 } \alpha\beta\beta \text{ steranes}}$	217	0.57
8.	C27/C29 diasteranes	259	nd
9.	C27/C29 steranes	217	nd
10.	18α(H)-oleanane/C30 hopane	191	nd
11.	$\frac{\text{C29 diasteranes}}{\text{C29 } \alpha\alpha\alpha \text{ steranes + C29 } \alpha\beta\beta \text{ steranes}}$	217	0.47
12.	$\frac{\text{C30 (hopane + moretane)}}{\text{C29 (steranes + diasteranes)}}$	191/217	7.50
13.	C15 drimane/C16 homodrimane	123	1.06
14.	Rearranged drimanes/normal drimanes	123	0.49

nd = no data

FIGURE 7-2a

Sample : **YOLLA-4, 2609.5m, ex MPSR-1695, Crude Oil**

File ID : 344302BB

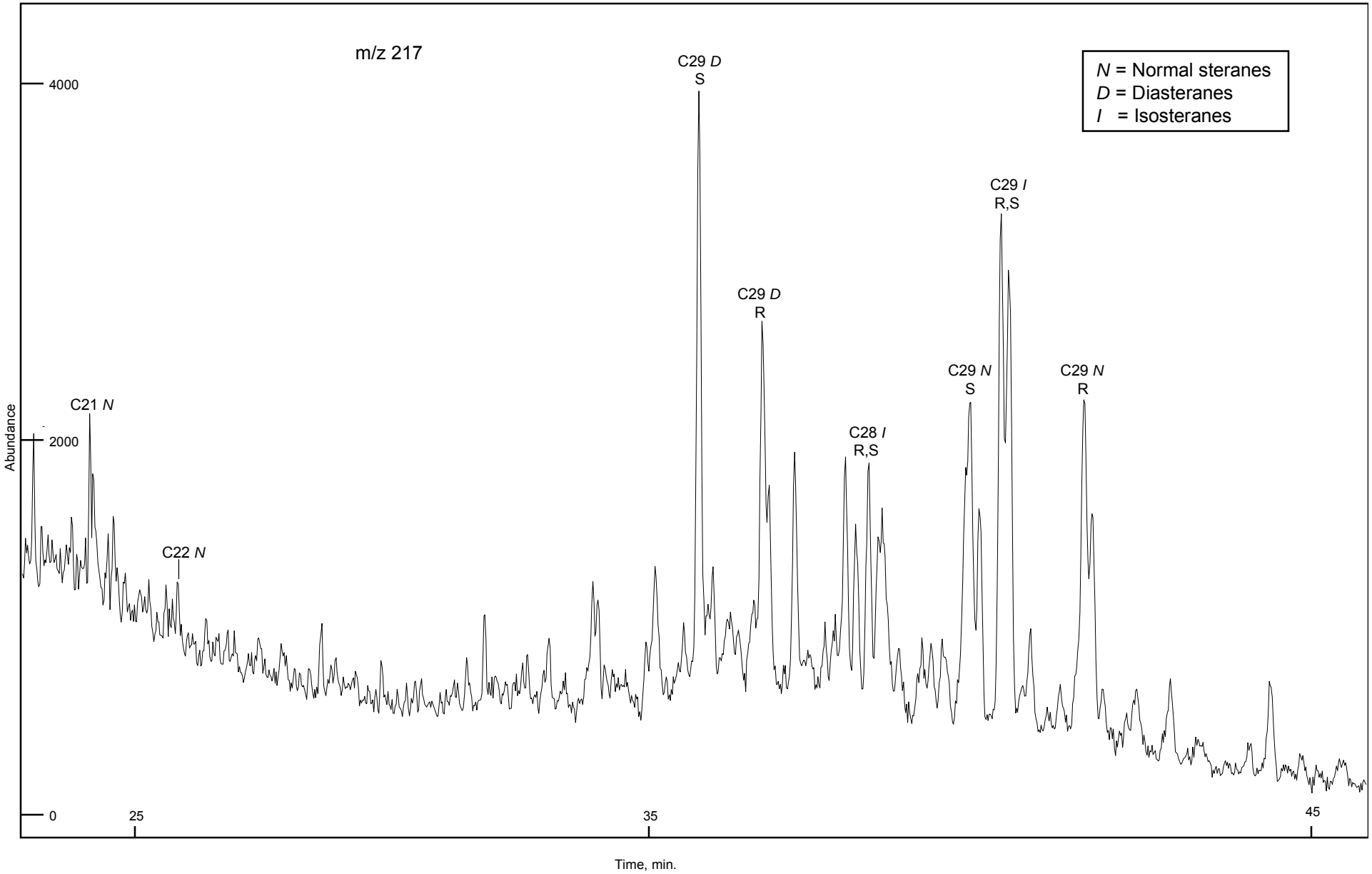

GEOTECHNICAL SERVICES PTY LTD

FIGURE 7-2b

Sample : **YOLLA-4, 2609.5m, ex MPSR-1695, Crude Oil**

File ID : 344302BB

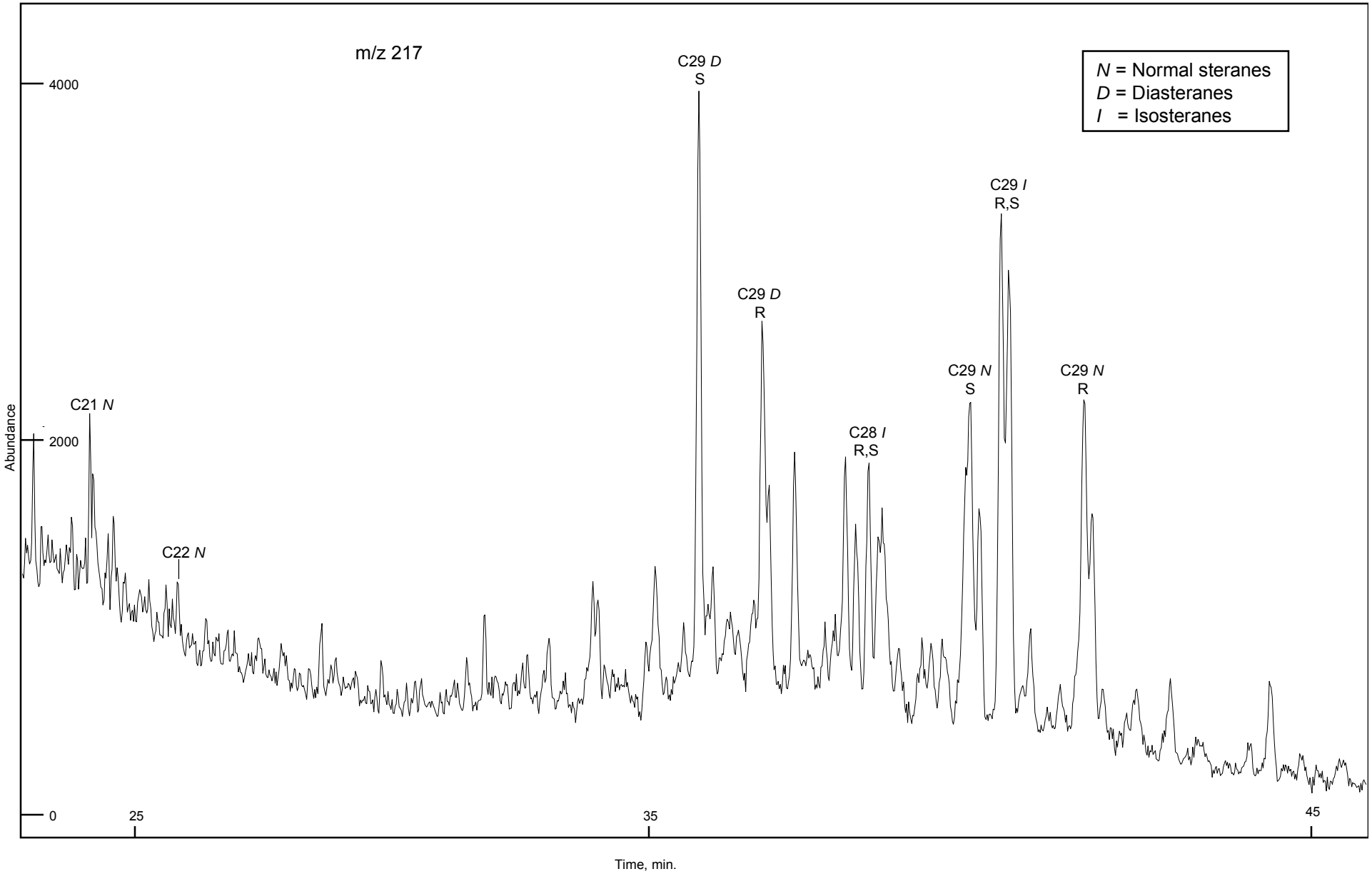

GEOTECHNICAL SERVICES PTY LTD

FIGURE 7-2c

Sample : **YOLLA-4, 2609.5m, ex MPSR-1695, Crude Oil**

File ID : 344302BB

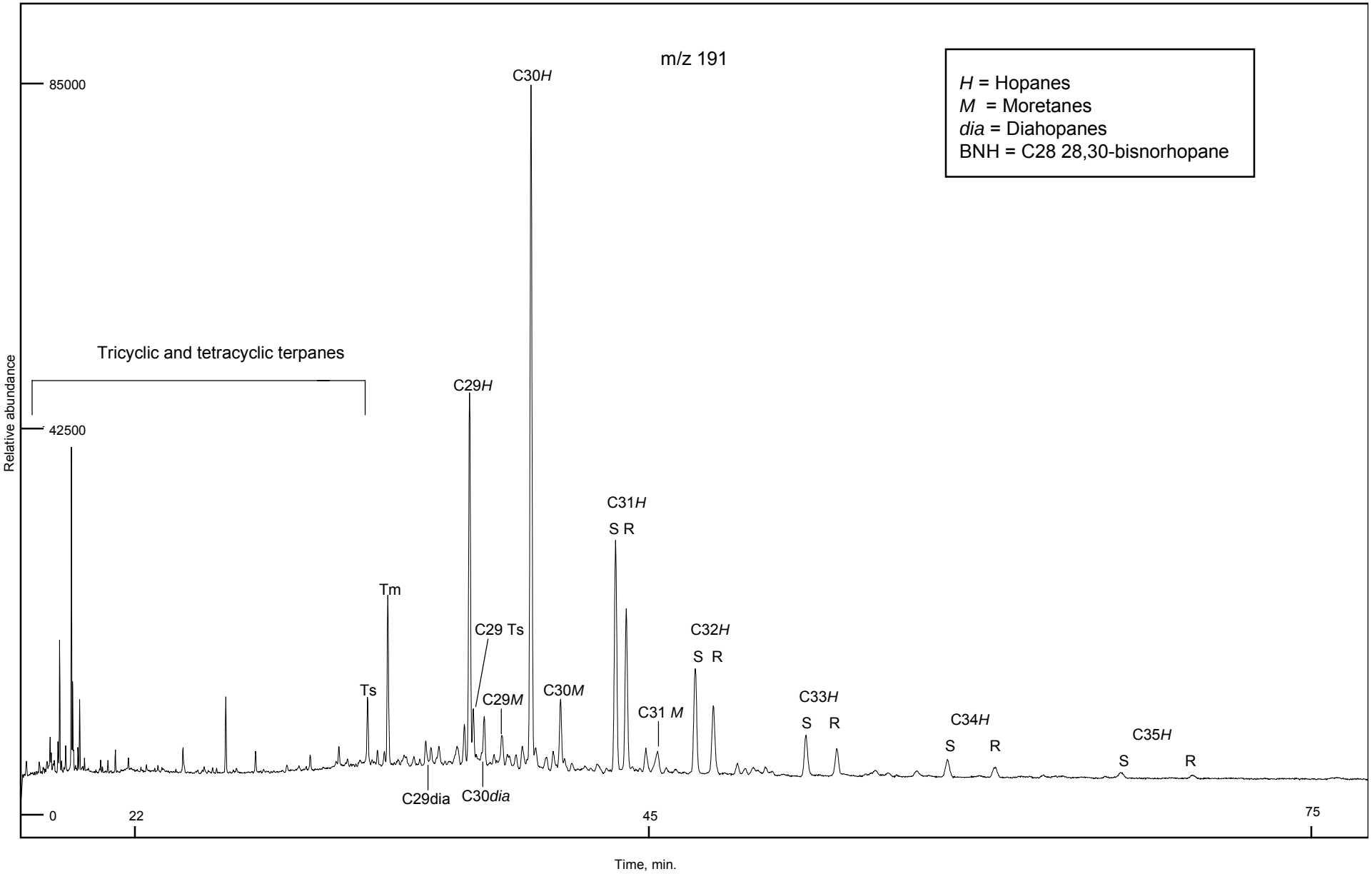

GEOTECHNICAL SERVICES PTY LTD

FIGURE 7-2d

Sample : **YOLLA-4, 2609.5m, ex MPSR-1695, Crude Oil**

File ID : 344302BB

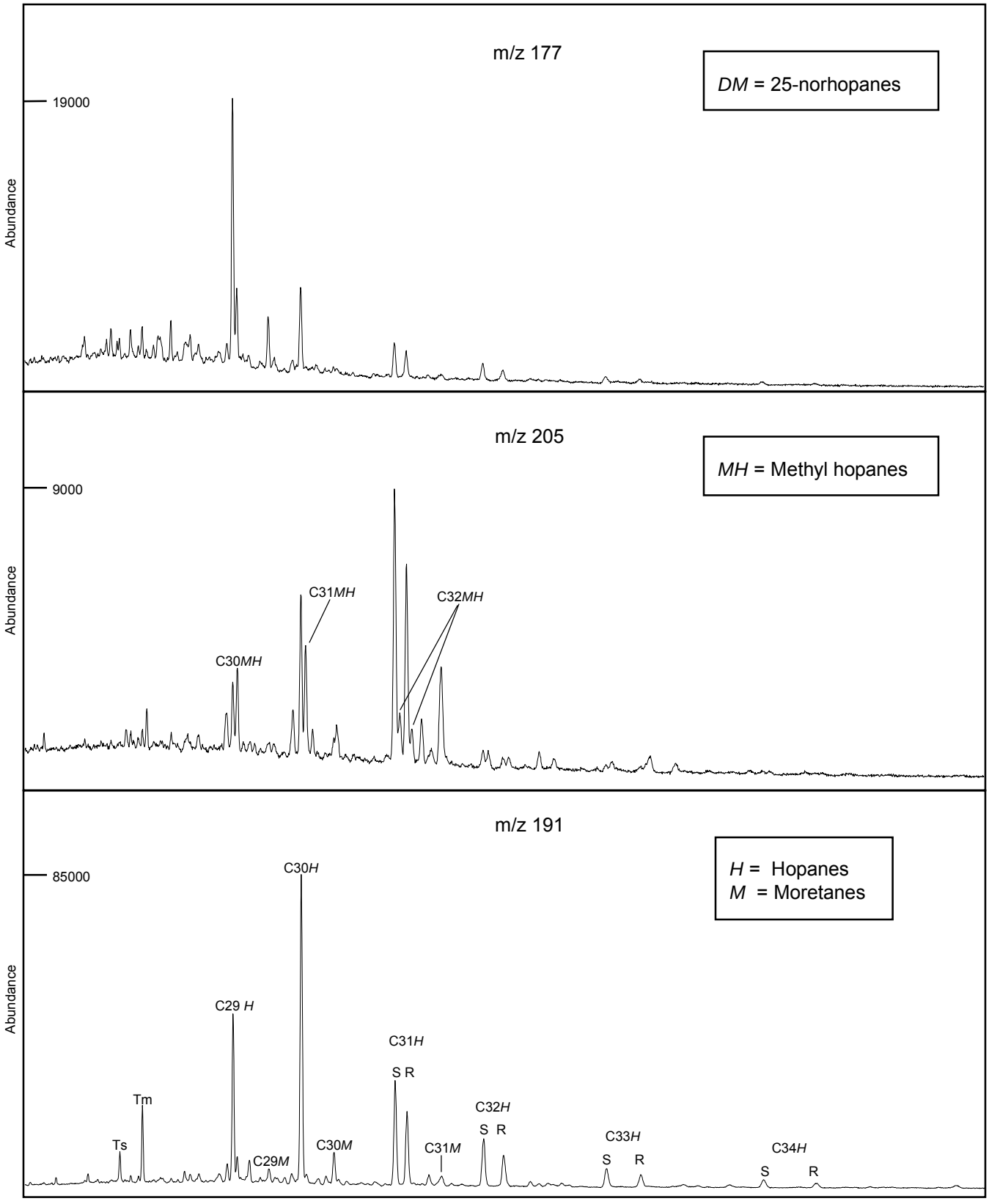

FIGURE 7-2e

Sample : **YOLLA-4, 2609.5m, ex MPSR-1695, Crude Oil**

File ID : 344302BB

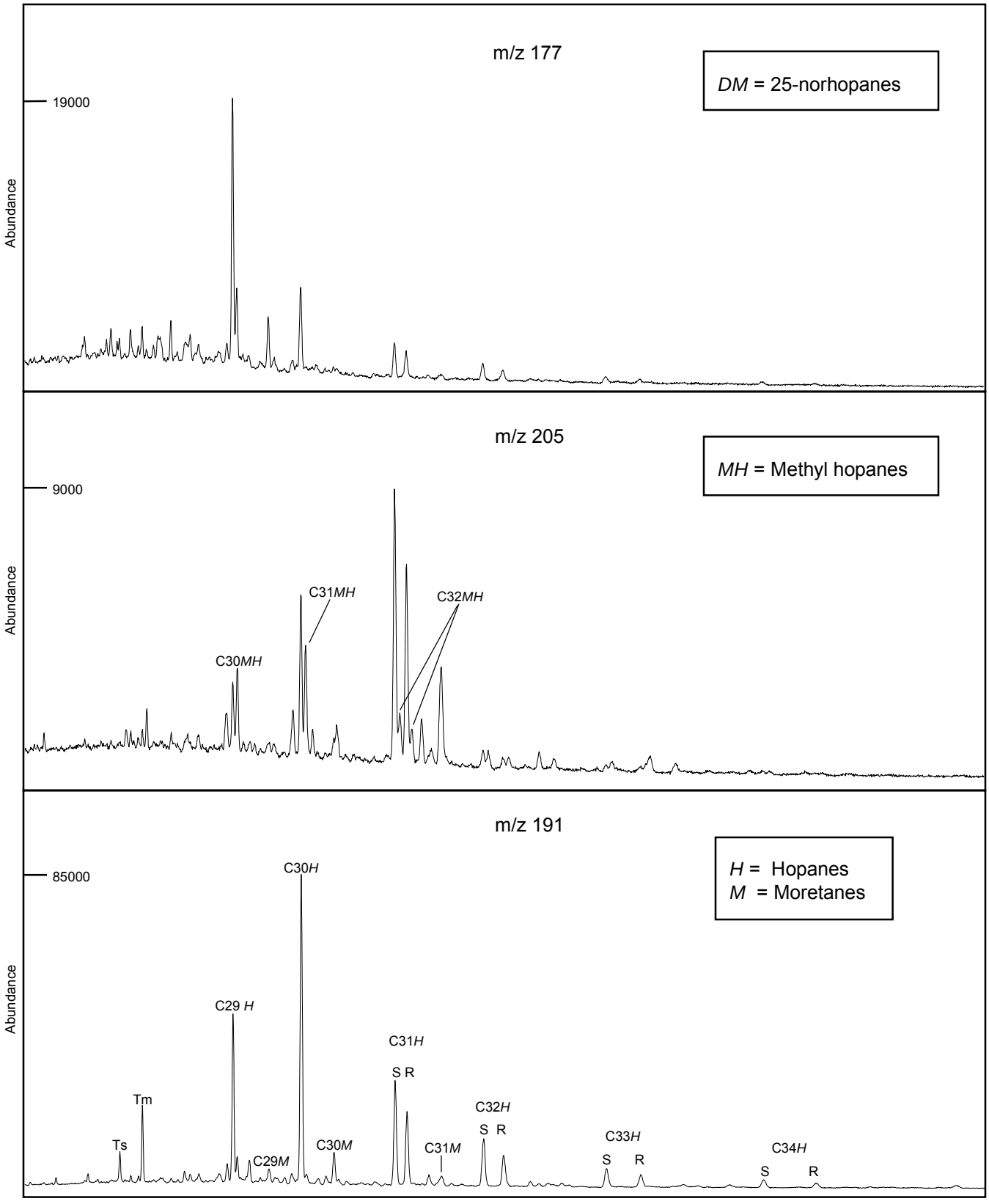

FIGURE 7-2f

Sample : **YOLLA-4, 2609.5m, ex MPSR-1695, Crude Oil**

File ID : 344302BB

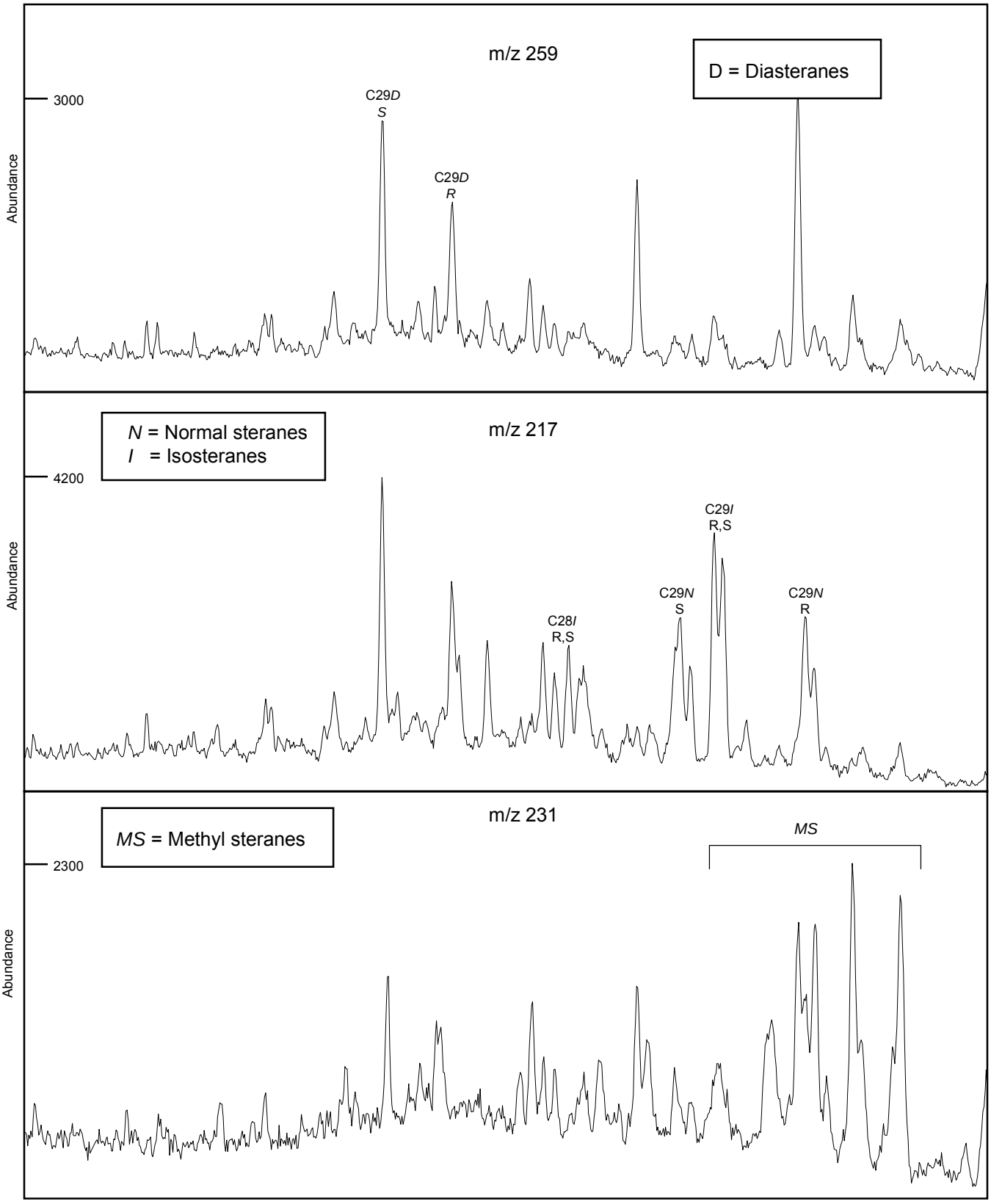

TABLE 11

COMPOUND SPECIFIC ISOTOPE ANALYSIS (GC-IRMS)

YOLLA-4, 3005.7m, Gas

Compound	$\delta^{13}C$	*SD*	*Misc. Information*
methane	-38.8	0.05	
ethane	-29.5	0.01	
propane	-28.1	0.10	
i-butane	-28.7	0.04	
n-butane	-27.8	0.12	
i-pentane	-27.5	0.01	
n-pentane	-27.0	0.13	
CO_2	-8.1	0.01	

* Misc. Information : indicates if the abundance of the compound is low and therefore the value calculated less reliable

Units: $^{o}/_{oo}$ PDB
(per mil International Standard Peedee Belemnite)

3/12/2004
nd = not detected

GEOTECH

COMPOUND SPECIFIC ISOTOPE ANALYSIS (GC-IRMS)

SAMPLE ID:YOLLA-4, 2609.5m, Crude Oil (344302)

Carbon No.	$\delta^{13}C$ (per mil)	SD	Misc. Information
7	-28.1	0.23	
8	-28.9	0.17	
9	-28.6	0.16	
10	-28.6	0.22	
11	-29.0	0.23	
12	-28.7	0.19	
13	-28.7	0.14	
14	-28.8	0.13	
15	-28.9	0.07	
16	-29.0	0.00	
17	-29.4	0.14	
18	-29.2	0.11	
19	-29.2	0.01	
20	-29.2	0.02	
21	-29.4	0.08	
22	-29.6	0.07	
23	-30.2	0.10	
24	-30.1	0.23	
25	-30.6	0.22	
26	-30.6	0.17	
27	-31.4	0.27	
28	-31.5	0.01	low
29	-31.3	0.16	low
30	nd	nd	
31	nd	nd	
32	nd	nd	
33	nd	nd	

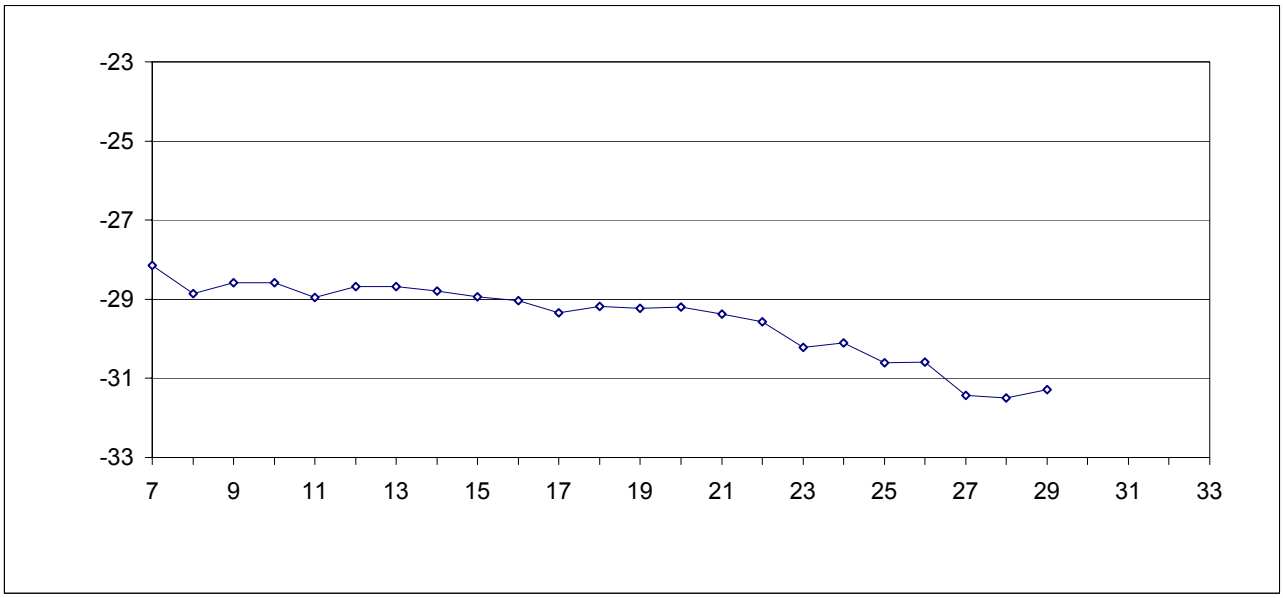

*Misc. Information: indicates if the abundance of the n-alkane is low and therefore the value calculated less reliable

APPENDIX B

THEORY AND METHODS

PETROLEUM GEOCHEMISTRY

1.0 INTRODUCTION

Petroleum geochemistry is primarily concerned with the application of organic chemistry to samples of geological interest in hydrocarbon exploration.

Analyses can be carried out on cuttings, sidewall cores, conventional cores, relatively unweathered outcrop samples and fluid hydrocarbons (oil, condensate, gas).

Source rock evaluation is best performed on sidewall cores, since cuttings are more susceptible to contamination from both cavings and organic additives in the mud system. In petroleum geochemical studies it is vitally important for the geochemist/geologist to be aware of the type of mud additives used and the stage at which they are used during the drilling program. Any anomalous results must be carefully considered in conjunction with mud system records.

Petroleum geochemistry in exploration is applied for three major purposes:

1. Identification of richness, maturity and type of kerogen in (a large number of) whole rock samples by screening analyses.

2. Semi-detailed characterisation of kerogen in sediments from selected source intervals, to determine maturity, source type and genetic potential.

3. Detailed characterisation of petroleum fluids (extracts, oils and condensates) by assessment of thermal maturity, source type and depositional environment to enable oil-to-oil and oil-to-source rock correlation studies.

2.0 THEORY & METHODS

Samples are analysed according to the scheme illustrated in Figure 1 which shows the order and type of analysis for both screening and detailed tests.

2.1 Screening Analyses of Whole Rock Samples

2.1.1 Headspace/Cuttings Gas Analysis

The headspace sample is usually provided in a sealed tin can which holds both cuttings and water to approximately three quarters capacity. This allows the volatile hydrocarbons to diffuse easily into an appreciable headspace.

The gas is taken into a syringe through a silicone seal on the lid of the container and analysed by packed column gas chromatography using the following conditions:

Instrument:	Shimadzu GC-8APF
Column:	6'x 1/8" Chromosorb 102
Injector/Detector Temperature:	120^{o}C
Column Temperature:	110^{o}C
Carrier Gas:	Nitrogen

Cuttings gas analysis is performed in the same manner but on samples which do not liberate volatile gases readily. These sediments are subjected to very vigorous agitation prior to sampling.

Values are given as volume of gas per million volumes of sediment (ppm) for each hydrocarbon (methane, ethane, propane, iso- and n-butane), as composite values including C_5-C_7, and as ratios.

FIGURE 1

FLOW DIAGRAM FOR PETROLEUM GEOCHEMICAL ANALYSES

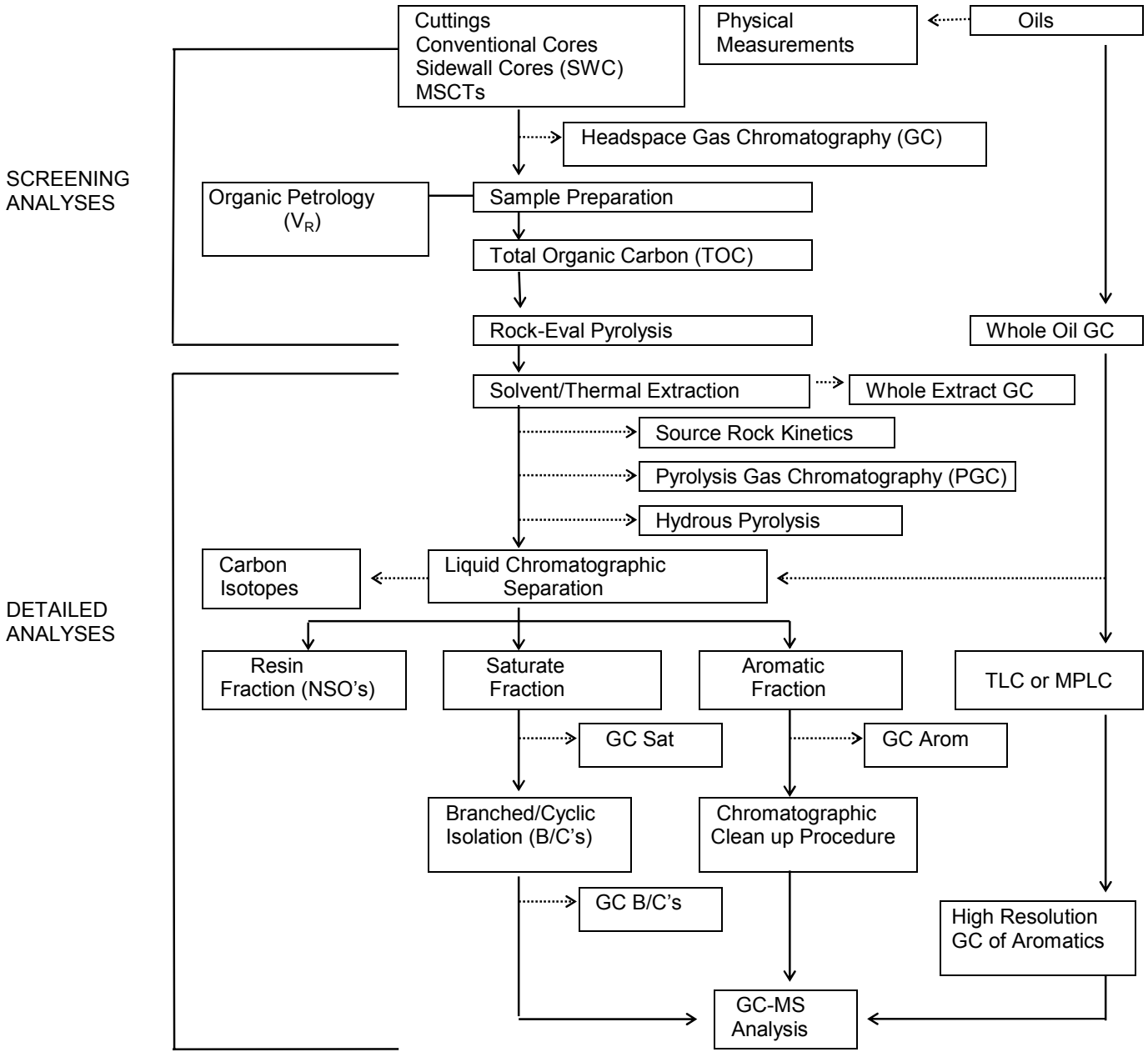

Headspace/cuttings gas analyses are used as a screening technique to identify zones of significant gas generation and out-of-place gas (Letran et al, 1974). The classification for gas content is listed below:

Total gas content (C_1;C_2-C_4; or C_5-C_7)	Description
10 -100ppm	very lean - lean
100-1,000	lean - moderate
1,000-10,000	moderate - rich
10,000-100,000	rich - very rich

The abundance of C_2-C_4 components (wet gas) is used to locate the zone of oil generation, since wet gas is commonly associated with petroleum (Fuex, 1977).

It is important to ensure that the gases analysed are not of a biogenic origin, so an anti-bacterial agent must be added to the cuttings when they are stored in water.

2.1.2 Sample Preparation

Depending on drilling mud content, cuttings samples may be water washed before they are air dried, picked free of contaminants and cavings, and then crushed to 0.1mm using a ring pulveriser.

Sidewall cores are freed of mud cake and other visible contaminants, sampled according to homogeneity, air dried and hand crushed to 0.1mm grain size.

Conventional core and outcrop samples are inspected for visible contaminants and crushed to 1/8" chips using a jaw crusher. After air drying, the chips are crushed with a ring pulveriser to small particle size (0.1mm).

Petroleum aqueous mixtures are separated into oil and water/mud fractions by decanting off the oil layer and producing a clean separation by gently centrifuging the oil. If separation by this method is not effective, the petroleum is solvent extracted.

2.1.3 Total Organic Carbon(TOC)

The TOC value is determined on crushed sediment. The minimum sample requirement is one gram, however, results may be obtained from as little as 0.2mg in very rich samples. Carbonate minerals are first removed by acid digest (HCl) and the remaining sample heated to 1700^{o}C (Leco Induction Furnace) in an atmosphere of pure oxygen. The CO_2 produced is measured with an infra-red detector, and values calculated according to standard calibration.

TOC is expressed as % of rock and is used as a screening procedure to classify source rock richness:

Classification	Clastics	Carbonates
Poor	0.00 - 0.50	0.00 - 0.25
Fair	0.50 - 1.00	0.25 - 0.50
Good	1.00 - 2.00	0.50 - 1.00
Very Good	2.00 - 4.00	1.00 - 2.00
Excellent	> 4.00	> 2.00

2.1.4 Rock-Eval Pyrolysis

Although a preliminary source rock classification is made using TOC data, a more accurate assessment of organic source type and maturity is possible by Rock-Eval pyrolysis. Two types of Rock-Eval analyses are offered: "one run" which involves pyrolysis of the crushed but otherwise untreated sediment and "two run" which involves pyrolysis of both the crushed, untreated sediment and the decarbonated sediment. The "two run" method provides more accurate S_3 values that the "one run" method. S_1 and S_2 values are of the same accuracy in both methods.

The method requires 0.4g of sample material, although reliable results can often be obtained from smaller amounts.

The crushed sediment is heated in an inert atmosphere of helium over a programmed temperature range.

Hydrocarbons present in the free or adsorbed state (S_1) are thermally distilled at 300^{o}C and measured by a flame ionisation detector (FID). Hydrocarbons are then cracked from the kerogen (S_2) during a temperature ramp from 300^{o} to 550^{o}C and also measured by FID. CO_2 released during the kerogen cracking process (S_3) is trapped and subsequently measured by a thermal conductivity detector.

The amount of free hydrocarbons in the sediment (S_1) represents milligrams of hydrocarbons distilled from one gram of rock and is a measure of both in situ and out-of-place petroleum.

Free hydrocarbon richness is described by the following:

S_1 (mg/g)	**Characterisation**
0.20 - 0.40	fair
0.40 - 0.80	good
0.80 - 1.60	very good
> 1.60	excellent

The total amount of hydrocarbons present in the free state and as kerogen is a measure of the potential yield (genetic potential) of the sample ($S_1 + S_2$) and is expressed as mg/g of rock.

Source rocks are classified accordingly:

$S_1 + S_2$ (mg/g)	**Source Rock Quality**
0.00 - 1.00	poor
1.00 - 2.00	marginal
2.00 - 6.00	moderate
6.00 - 10.00	good
10.00 - 20.00	very good
> 20.00	excellent

The Production Index (PI) represents the amount of petroleum generated relative to the total amount of hydrocarbons present ($S_1/S_1 + S_2$). It is a measure of the level of maturity of the sample. For oil prone sediments PI ranges from 0.1 at the onset of oil generation to 0.4 at peak oil generation. For gas prone sediments, PI shows only a small change with increasing maturity.

The temperature at which the maximum amount of S_2 hydrocarbons is generated is called T_{MAX}. This temperature increases with the increasing maturity of sediments.

FIGURE 2

SCHEMATIC PYROGRAM OF ROCK-EVAL PYROLYSIS

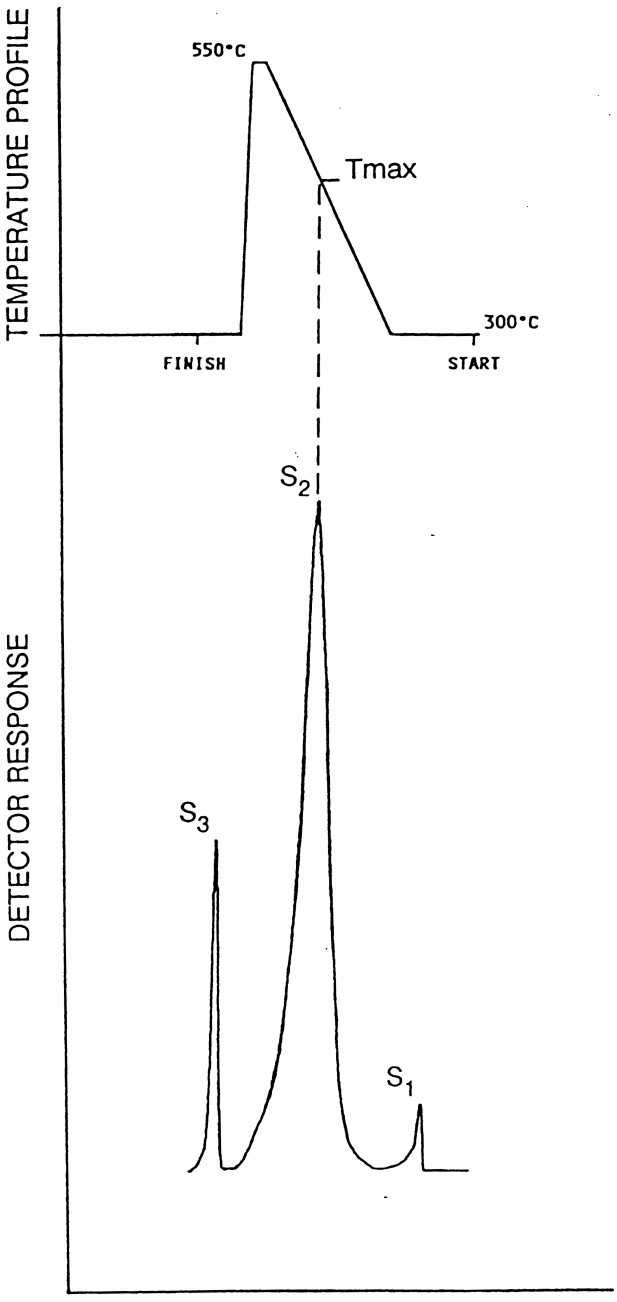

The variation of T_{MAX} is summarised as

< 430°C	immature
430/435° – 460°C	mature (oil window)
> 460°C	overmature

Hydrogen Index (HI = S_2 x 100/TOC) and Oxygen Index (OI = S_3 x 100/TOC), when plotted against one another, provide information about the type of kerogen and the maturity of the sample. Both parameters decrease in value with increasing maturity. Samples with high HI and low OI are dominantly oil prone and samples with low HI and high OI are gas prone.

2.2 Analysis of Kerogen

2.2.1 Organic Petrology - Vitrinite Reflectance

Vitrinite is a coal maceral which responds to increasing levels of thermal maturity. This response is measured microscopically by the percent of light reflected off the polished surface of a vitrinite particle immersed in oil.

Measurement of vitrinite reflectance can be carried out on uncrushed, washed and dried cuttings (10-50gms of sample material required), sidewall cores (2-10gms), conventional cores (2-10 gms) or outcrop samples (2-10gms).

The values given are for standard lower size limits. In special cases, however, useful data may be obtained from as little as 0.1gm.

For each sample a minimum of 25 fields is measured in order to establish a range and mean for reflectance values.

Maturity classifications according to vitrinite reflectance values are:

% V_R (approx)	**Maturity**
0.2 - 0.55	immature
0.55 - 1.2	mature
1.2 - 1.8	overmature
> 1.8	severely altered

Following vitrinite reflectance measurements, microscopic examination in fluorescence mode allows the description of liptinite macerals and an estimate of their abundances. The amount of dispersed organic matter is reported and its composition described.

Vitrinite reflectance results and maceral descriptions are best obtained from coals or rocks deposited in environments which received large influxes of terrestrially derived organic matter. Vitrinite reflectance cannot be measured in rocks older than Devonian age, since land plants had not evolved prior to this time.

2.2.2 Pyrolysis Gas Chromatography

Pyrolysis gas chromatography (PGC) is performed on solvent extracted source rocks or isolated kerogens. The sample is pyrolysed by an SGE pyrojector which is coupled directly to a Hewlett Packard 5890 gas chromatograph. The operating conditions are:

Pyrolysis temperature:	600^{o}C
Column:	25m x 0.22mm ID BP-1 (SGE)
Carrier gas:	helium
Oven conditions:	-20^{o} to 280^{o}C @ 4^{o}/min

Data are collected and recovered using DAPA scientific software.

Pyrolysis GC allows the examination of kerogen on the molecular level and thereby a better classification of source rocks with regard to source type and generative capacity than conventional bulk pyrolysis (ie. Rock-Eval). The analytical procedure is semi quantitative (with yield related to S_2 of Rock-Eval).

Samples are characterised according to the amounts of aliphatic, aromatic and phenolic components in the kerogen. The aliphatic carbon content of a kerogen is the critical factor in determining catagenic hydrocarbon yields in the earth's crust, while the gas/oil ratio is dictated by the distribution of the various structural elements in the kerogen (Larter, 1985). Using pyrogram fingerprint data, it is possible to distinguish substantial variations between kerogens, even those of the same bulk chemical type.

A major strength of pyrolysis methods is that, while quantitative yields of kerogens are maturity related, the qualitative pyrogram fingerprints obtained are relatively rank independent over much of the oil window (Espitatlie et al, 1977; Van Graas et al, 1980; Larter, 1985). At high maturities (>1.2% V_R) characteristics for all kerogen types tend to converge (Horstfield, 1984).

Data are presented by percentage and mg/g of individual substances as well as groups of compounds.

Significant parameters are:

$(C_1 – C_5)/C_6$ + abundance	gas/oil ratio
$C_9 – C_{31}$ (alkenes + alkanes)	oil yield
Type Index R:	aromaticity

(Larter & Douglas 1979, Larter and Senftle, 1985).

2.3 Detailed Analyses of Petroleum Fluids

2.3.1 Solvent Extraction of Sediment

The finely crushed sample (up to 100g) is extracted with dichloromethane (300mL) using sonic vibration. After Buchner flask filtration, the filtrate is re-vibrated with activated copper powder (1g) to remove elemental sulphur. The extractable organic matter (EOM) is afforded by further filtration and fractional distillation of the solvent.

Source rock richness based upon EOM is classified accordingly:

Yield	**ppm**
Poor	< 500
Fair/Good	500 - 2000
Very Good	2000 - 4000
Excellent	>4000

2.3.2 Liquid Chromatographic Separation

Sediment extracts, crude oil and condensate samples are separated into fractions corresponding to three structural types:

saturated hydrocarbons	(SAT)
aromatic hydrocarbons	(AROM)
resins plus ashphaltenes	(NSO)

This separation is achieved by liquid column chromatography using activated silicic acid adsorbent and eluting solvents of varying polarity. Saturated, aromatic and NSO concentrates are recovered by fractional distillation/evaporation of the solvent and quantitative transfer to a small vial.

The amount of hydrocarbons (SAT plus AROM) can be used to classify source rock richness and the amount of saturates to classify oil source potential, according to the following criteria:

Classification	**ppm HC**	**ppm SAT**
Poor	0 - 300	0 - 200
Fair	300 - 600	200 - 400
Good	600 - 1200	400 - 800
Very Good	1200 - 2400	800 - 1600
Excellent	>2400	>1600

The composition of the extracts can also provide information about their levels of maturity and/or source type (LeTran et. al., 1974; Philippi, 1974). Generally, marine extracts have relatively low concentrations of saturated and NSO compounds at low levels of maturity, but these concentrations increase with increasing maturation. Terrestrially derived organic matter often has a low level of saturates and large amount of aromatic and NSO compounds, irrespective of the level of maturity.

Specific ratios are measured from solvent extraction and liquid chromatography data which give an indication of source type and maturity. EOM (mg)/TOC(g) can be used as a maturation indicator when plotted against depth for a given sedimentary sequence. Generally an EOM/TOC value of >100 indicates high maturity. If such a sample has a SAT (mg)/TOC(g) ratio <20, it is likely that the organic matter is gas prone. A value for SAT (mg)/TOC (g) >40 suggests an oil prone source type.

2.3.3 Capillary Gas Chromatography (GC)

C_{12+} gas chromatography is most commonly carried out on saturate fractions, but in certain instances it is used to examine whole extracts/oils, aromatic or branched/cyclic fractions. It is also used as a tool to identify contamination. The analyses are performed under the following conditions:

Instruments:	Hewlett Packard 5890 Gas Chromatography
Injector:	SGE 0CI-3 on column
Column:	25m x 0.2mm ID BP-1
Injector Temp:	280°C
Detector Temp:	320°C
Column Temp:	45°C to 280°C at 4°/min
Carrier Gas:	Hydrogen

Data are collected using an IBM compatible PC and DAPA scientific software.

2.3.3.1 C_{12+} Saturate Gas Chromatography

Saturate GC results provide information pertaining to source type, maturity and depositional environment.

The n-alkane distribution from n-C_{12} to n-C_{31} is determined from the area under the peaks representing each of these n-alkanes. The profile can yield information about maturity and source type and is quantified in the C_{21} + C_{22}/C_{28} + C_{29} ratio and Carbon Preference Indices (CPI 1 and 2).

$$CPI\,(1) = \frac{(C_{23} + C_{25} + C_{27} + C_{29})\ wt\% + (C_{25} + C_{27} + C_{29} + C_{31})\ wt\%}{2\ x\ (C_{24} + C_{26} + C_{28} + C_{30})\ wt\%}$$

$$CPI\,(2) = \frac{(C_{23} + C_{25} + C_{27})\ wt\% + (C_{25} + C_{27} + C_{29})\ wt\%}{2\ x\ (C_{24} + C_{26} + C_{28})\ wt\%}$$

Carbon preference indices:

- are approximately 1 for marine samples, regardless of maturity
- decrease from 20--> 1 for terrestrial samples as maturity increases

The C_{21} + C_{22}/C_{28} + C_{29} ratio is generally >1.5 for aquatic source material and <1.2 for terrestrial organic matter, however, the values increase with maturity.

Pristane/phytane (Pr/Ph) ratios can indicate depositional environments:

.	<3.0	- relatively reducing depositional environments;
.	3.0-4.5	- mixed (reducing/oxidising) environments;
.	>4.5	- relatively oxidising depositional environments.

2.3.3.2 $C_1 – C_{31}$ Whole Oil Gas Chromatography

This analytical method is applied to oil and condensate samples. It provides a picture of the whole oil up to n-C_{31} and allows quantitation of components with more than 4 carbon atoms. Several parameters are measured which illustrate changes in the degree of biodegradation and water washing in the reservoir. Because these measurements are performed on very volatile components in the oil, care should be taken during sampling, transportation and storage of the fluid to minimise evaporation.

Whole oil analytical conditions are listed below:

Instrument:	Shimadzu GC-9A
Column:	25m x 0.2mm ID BP-1
Injector/Detector Temperature:	290^{o}C
Column Temperature:	-20^{o}C to 280^{o}C at 4^{o}/min
Carrier Gas:	hydrogen

2.3.4 Carbon Isotope Analysis

This measurement is normally carried out on one or more of the following mixtures: topped oil, saturate fraction, aromatic fraction, NSO fraction. The organic matter is combusted in oxygen to produce carbon dioxide which is purified and transferred to an isotope mass spectrometer. The carbon isotope ratio ($\delta C_{13}/\delta C_{12}$) is measured and compared to an international standard (the Peedee Belemnite Limestone - PDB).

Carbon isotope analysis is most commonly used to identify the source of methane according to the following criteria (Fuex 1977):

$\delta^{13}C$ $^{o}/_{oo}$ PDB	Source
-75 to -55	Biogenic methane
-58 to -40	Methane associated with oil
-40 to -25	Thermal methane

Source rock-crude oil correlations have been attempted by observing the change in $\delta^{13}C$ values of components of oils and rocks (Stahl 1977). Source rock extracts are usually isotopically heavier than the corresponding crude oil but are lighter than the asphaltenes of the oil and the kerogen of the rock (Hunt 1979). It has also been observed that marine organic carbon is generally isotopically heavier than contemporaneous terrestrial organic carbon (Tissot & Welte 1978). However, it should be noted that increasing maturity and biodegradation produce a shift toward heavier isotope values.

2.3.5 Gas Chromatography - Mass Spectrometry (GC/MS)

GC/MS analysis is normally performed on the branched and cyclic alkane fraction and/or the aromatic fraction of oils, condensates and sediment extracts. The specific fraction is first isolated and then injected into a gas chromatograph which is linked in series with a mass spectrometer. As compounds are eluted from the chromatography column they are bombarded with high energy electrons. This causes them to fragment into a number of ions each with a molecular weight less than that of the parent molecule. Individual compounds give a characteristic fragmentation pattern (mass spectrum), the major ions of which are presented in a series of mass fragmentograms [ie. plots of ion concentration against GC retention time].

GC/MS analysis can be carried out using one of the following modes of operation:

(i) Acquire mode - in which all ions (within a broad range) in each mass spectrum are memorised by the data system.

(ii) Selective Ion Monitoring (SIM) mode - in which only selected ions of interest are memorised by the data system.

2.3.5.1 GC/MS Analysis of Branched/Cyclic Alkanes

The group of compounds to be analysed is first isolated from the saturate fraction by refluxing the sample with activated 5Ä molecular sieves in cyclohexane for 24 hours. Branched/ cyclic alkanes, including alkylcyclohexanes, are recovered from the solvent by fractional distillation.

For condensates, and samples where information about alkylcyclochexanes is not required, the saturate fraction is passed through a small column packed with silicalite adsorbent. The branched/cyclic alkanes are recovered from the eluting solvent by fractional distillation.

Analysis is carried out in the SIM mode with a total of 33 ions being recorded over different time spans.

Operating conditions are:

Instrument:	5987HP GC mass spec data system
Column:	60m x 0.25mm ID cross linked methyl-silicone DB-1 (J&W) column of 0.25 micron film thickness connected directly to the ion source
Injector:	OCI-3(SGE)
Carrier gas:	hydrogen
Oven Conditions:	50^{o} to 274^{o}C at 8^{o} /min
	274^{o} to 280^{o}C at 1^{o} /min
EM Voltage:	2,000 - 2,300V
Electron Energy:	70eV
Source temperature:	250^{o}C

GC/MS mass fragmentograms are examined for particular 'biomarker' compounds which can be related to biological precursors. These allow the characterisation of petroleum with regard to thermal maturity, source, depositional environment and biodegradation.

The significance of selected parameters from branched/cyclic GC/MS analysis is outlined over the page.

1. 18α (H)-hopane/17α (H)-hopane (Ts/Tm)

Maturity indicator. The ratio of 18α (H) trisnorhopane to 17α (H) trisnorhopane increases exponentially with increasing maturity from approximately 0.2 at the onset to approximately 1.0 at the peak of oil generation, ie. Tm decreases with maturity. This parameter is not reliable in very immature samples.

2. C_{30} hopane/C_{30} moretane

Maturity indicator. The conversion of C_{30} 17β, 21β hopane to 17β, 21α moretane is maturity dependent. Values increase from approximately 2.5 at the onset of oil generation to approximately 10. Once the hopane/moretane ratio has reached 10, no further changes occur. A value of 10 is believed to represent a maturity stage just after the onset of oil generation and hopane/moretane ratios are therefore useful mainly as indicators of immaturity in a qualitative sense.

3&4. C_{31} and C_{32} 22S/22R hopanes

Maturity indicator. An equilibrium between the biological R- and the geological S-configuration occurs on mild thermal maturation. A ratio of S:R = 60:40, ie, a value of 1.5, characterises this equilibrium which occurs before the onset of oil generation. The C_{32} hopane pair is often more reliable for this purpose since co-elution sometimes affects the C_{31} ratio.

5. C_{29}20S ααα/C_{29}20Rααα steranes

Maturity indicator. Upon maturation, the biologically produced 20R sterioisomer is diminished relative to the 20S form and a stabilisation is reached at approximately 55% 20R and 45% 20S compounds. V_R equivalents are approximately 0.45% for a 20S/20R value of 0.2 and 0.8% for a 20S/20R value of 0.75. This parameter is most useful between maturity ranges equivalent to 0.4% to 1.0 V_R.

6. C_{29}20S αααα /C_{29}20R ααα+ C_{29}20S ααα steranes

Maturity indicator. This ratio is a different way of expressing the relative abundance of the biological 20R to the geological 20S normal sterane (see parameter 5). Expressed as a percentage, a value of about 25% indicates the onset of oil generation, and of about 50% the peak of oil generation.

7. C_{29} αββ /C_{29} ααα + C_{29} αββ steranes

Maturity indicator. The αα form is produced biologically. Its abundance diminishes upon maturation until a mixture of 65% ββ(iso) steranes and 35% αα (normal) steranes is reached, which is equivalent to approximately 0.9% V_R.

8&9. C_{27}/C_{29} diasteranes and steranes

Source indicator. It has been suggested that marine phytoplankton is characterised by a dominance of C_{27} steranes and diasteranes whereas a preponderance of C_{29} compounds indicates strong terrestrial contributions. Values smaller than 0.85 for C_{27}/C_{29} diasterane and sterane ratios are believed to be indicative for terrestrial organic matter, values between 0.85 and 1.43 for mixed organic material, and values greater than 1.43 for an input of predominantly marine organic matter.

It has been suggested, however, that marine sediments can also contain a predominance of C_{29} steranes, so the above rules have to be applied with caution. Any simplistic interpretation of C_{27}/C_{29} steranes and diasteranes can be dangerous and the interpretation of these data should be consistent with other geological evidence.

10. 18α (H) - oleanane/C_{30} hopane

Source indicator. Oleanane is a triterpenoid compound which has often been reported from deltaic sediments of Late Cretaceous to Tertiary age. It is thought to be derived from certain angiosperms which developed in the late Cretaceous. If the 18α (H) - oleanane/C_{30} hopane ratio is below 10, no significant proportions of oleanane are present. At higher values, it can be used as indicator for a reducing environment during deposition of land plant-derived organic matter.

11. C_{29} diasteranes/C_{29} ααα steranes + C_{29} αβ steranes

Source indicator. This parameter is used to characterise the oxidity of depositional environments. High values (up to 10) indicate oxic conditions, low values (down to 0.1) indicate reducing environments.

12. C_{30} (hopanes + moretanes)/C_{29} (steranes + diasteranes)

Source indicator. Triterpanes are believed to be of prokariotic (bacterial) origin, whereas steranes are derived from eukariotic organisms. This ratio reflects the preservation of primary organic matter derived from eukariots, relative to growth and preservation of bacteria in the sediment after deposition.

13. C_{15} drimane/C_{16} homodrimane

Drimanes and homodrimanes are ubiquitous compounds most likely derived from microbial activity in sediments. The C_{15} drimane/C_{16} homodrimane ratio is a useful parameter for correlation purposes in the low molecular weight region, especially for condensates which lack most conventional biomarkers. Drimanes are also useful to assess the degree of biodegradation as the removal of C_{15} to C_{16} bicyclics characterises an extensive level of biodegradation.

14. Rearranged/normal drimanes

Like parameter 13, this ratio can be used for correlation purposes in samples without conventional biomarkers, and to assess levels of biodegradation.

2.3.5.2 GC/MS Analysis of Aromatics

The aromatic fraction or the oil to be analysed is first subjected to thin layer chromatography (TLC) or medium pressure liquid chromatography (MPLC), depending upon the analytical requirements.

1. Di- and tri- nuclear aromatic compounds are isolated by TLC. To effect this separation, the sample is applied to an alumina coated glass plate (0.6mm thickness). The plate is developed with hexane and the required band located using short wavelength UV light. The fraction is recovered by extraction and fractional distillation.

   This aromatic fraction may be analysed by GC-FID, but GC/MS is recommended because of possible co-elution problems during GC.

   Samples are analysed by GC/MS in the acquire mode scanning from 50 to 450 atomic mass units (amu).

Analytical conditions are:

Instrument:	HP5970 MSD
Column:	60m x 0.25mm ID, 0.25 micron film thickness, 5% phenylmethyl silicone column DB-5 (J&W) connected directly to the ion source
Injector:	automatic on-column
Carrier Gas:	helium
Oven Conditions:	70°C for 1 min
	70°C --> 300°C at 3°/min
Data collection commences at 10 mins	
Mass spectrometry	
Em Voltage	1500 - 1800V
Electron Energy	70eV

Mass fragmentograms are presented for alkylbiphenyls, alkylnaphthalenes, alkylfluorenes and alkylphenanthrenes from a comprehensive data base. Aromatic compounds provide valuable information concerning thermal maturity since they can be applied outside the dynamic range

of saturate biomarker indicators and are particularly useful when conventional biomarkers are present in low amounts (Radke & Welte, 1983; Alexander et al, 1985). Maturity ratios are tabled below over the page.

Aromatic Maturity Indicators

Abbrev.	Definition	oil onset	Range Wet gas
DNR 1	(2,6DMN, + 2,7DMN)/1,5DMN	1.5	10
DNR 2	2,7DMN/1,8DMN	50	2500
DNR 5	1,6DMN/1,8DMN	50	>3000
DNR 6	(2,6DMN + 2,7DMN)/(1,4DMN + 2,3 DMN)	0.8	2
TNR 1	2,3,6TMN/(1,4,6TMN + 1,3,5TMN)	0.5	4
MPR 1	(2MP + 3MP)/1MP	1.5	3
MPI 1	1.5 x (2MP + 3MP)/(PH + 1MP + 9MP)	0.3	1
MPI 2	(3 x 2MP)/(PH + 1MP + 9MP)	0.3	2
Rc(a)	0.6(MPI-1) + 0.4 (for % Rm <1.35)		
Rc(b)	-0.6(MPI-1) + 2.3 (for % Rm ·1.35)		

(from Radke et al, 1982; Radke & Welte, 1983; Alexander et al, 1985)

Some aromatic marker compounds have specific natural product precursors and can be used as signatures for sediments of a particular source, depositional environment or geological age:

TNR 5	1,2,5TMN/1,3,6TMN	
TNR 6	1,2,7TMN/1,3,7TMN	(Strachen et al, 1988)
1,7/X	1,7DMP/(1,3 + 3,9 + 2,10 + 3,10 DMP)	
Retene/9MP		
1MP/9MP		(Alexander et al, 1988)

2. Mono- and triaromatic steranes are analysed by GC/MS under the same analytical conditions as used for di- and tri-nuclear aromatics. However, isolation of this fraction is performed by MPLC. To achieve this, the saturate plus aromatic mixture is injected onto a Merck Si60 column. The separation is monitored with a refractive index detector for saturates and a UV absorbance detector for aromatics.

   As aromatic steranes are generally present in low abundances, especially in oils, samples are analysed in the SIM mode and 16 ions are recorded.

   The conversion of monoaromatic steranes to triaromatic steranes and the dimethylation of triaromatic steranes in sediments are considered to be maturity dependent (Mackenzie et al, 1981; Mackenzie, 1984). The triaromatic sterane maturity indicator should, however, not be applied to crude oils because migration effects appear to selectively deplete the triaromatic steranes.

APPENDIX 5: VITRINITE REFLECTANCE REPORT

#2730 **YOLLA-4, BASS BASIN, p 1**

KK # / Ref #.	Depth (m)	$R_v$max Mean	$R_v$max Range	$R_v$max SD	$R_v$max N	Sample description including liptinite fluorescence maceral abundances, mineral fluorescence
T9933	920	0.34	0.24-0.45	0.065	9	Rare lamalginite and liptodetrinite greenish yellow to orange. (Claystone>argillaceous siltstone. Dom rare, I>V>L. All three maceral groups rare. Common foraminiferal tests. Mineral fluorescence moderate to weak orange. Iron oxides rare. Pyrite sparse, locally abundant.)
Ctgs	$\overline{R}_I$max	1.15	0.84-1.44	0.197	5	
						UPPER ANGAHOOK FORMATION - 1091.7m
						ANGAHOOK VOLCANICS - 1280.2
T9934	1320	0.43	0.32-0.55	0.060	18	Rare lamalginite and liptodetrinite greenish yellow to orange. (Claystone>argillaceous siltstone. Dom rare to sparse, V>I>L. Vitrinite rare to sparse, inertinite and liptinite rare. Rare coal particles of clarite composition, probably represent contaminants. Rare yellow fluorescing oil droplets in claystone Mineral fluorescence moderate to weak orange. Iron oxides rare. Pyrite common.)
Ctgs	$\overline{R}_I$max	0.98	0.96-1.00	0.020	2	
						OLIGOCENE ANGAHOOK FORMATION - 1414.71m
T9935	1530	0.52	0.45-0.59	0.070	2	Rare lamalginite and liptodetrinite yellow to orange. (Artificial composites>argillaceous siltstone>claystone>carbonate. Dom rare, L>I>V. All three maceral groups rare. Rare yellow fluorescing oil droplets in siltstone Mineral fluorescence weak orange. Iron oxides rare. Pyrite sparse.)
Ctgs	$\overline{R}_I$max	1.25	0.90-1.60	0.350	2	
						DEMONS BLUFF FORMATION - 1722.51m
T9936	1746	0.52	0.40-0.65	0.057	15	Rare lamalginite and liptodetrinite yellow to orange, rare sporinite. orange. (Artificial composites>argillaceous siltstone>claystone> carbonate. Dom rare, V>L>I. All three maceral groups rare. Rare dull orange fluorescing bitumen in siltstone Mineral fluorescence weak orange. Iron oxides rare. Pyrite abundant.)
Ctgs	$\overline{R}_I$max	1.40	1.00-1.80	0.400	2	
						EASTERN VIEW COAL MEASURES - 1879.4m
T9937	1902	0.55	0.48-0.68	0.050	25	Rare sporinite and liptodetrinite yellow to dull orange. (Artificial composites>argillaceous siltstone>claystone> carbonate. Dom sparse, V>I>L. Vitrinite sparse, inertinite and liptinite rare. Mineral fluorescence weak orange. Iron oxides rare. Pyrite abundant.)
Ctgs	$\overline{R}_I$max	1.31	1.12-1.46	0.122	4	
T9938	2313	0.59	0.47-0.68	0.048	25	Sparse sporinite and rare liptodetrinite yellow to dull orange, rare cutinite orange, rare resinite bright yellow. (Sandstone> argillaceous siltstone>coal. Coal abundant, V>>L>I, vitrite> vitrinertite(I)>duroclarite. Coal comprise about 4% of the sample and approximate maceral composition on mineral free basis: vitrinite 97%; liptinite 2%; inertinite 1%. Dom common, V>L>I. Vitrinite common, liptinite sparse, inertinite rare. Fungal sclerotinite is the only inertinite maceral in coal. Rare greenish yellow fluorescing oil droplets in siltstone. Mineral fluorescence weak orange to none. Iron oxides rare. Pyrite sparse.)
Ctgs	$\overline{R}_I$max	1.13	0.88-1.60	0.257	5	

#2730 **YOLLA-4, BASS BASIN, p 2**

KK # / Ref #	Depth (m)	$R_v$max Mean	$R_v$max Range	SD	N	Sample description including liptinite fluorescence maceral abundances, mineral fluorescence
						EASTERN VIEW COAL MEASURES - 1879.4m
T9939 Ctgs	2574	0.69	0.60-0.82	0.065	26	Sparse sporinite and rare liptodetrinite orange to dull orange, rare cutinite dull orange, rare resinite yellow. (Argillaceous siltstone> sandstone>coal. Coal common, V>>L>I, vitrite>clarite. Dom common, V>L>I. Vitrinite common, liptinite sparse, inertinite rare. Fungal sclerotinite is the only inertinite maceral in coal. Dom and coal cavings present, the coals show a mode at about 0.75%. The coal is Latrobe Valley facies. Mineral fluorescence orange to none. Iron oxides rare. Pyrite sparse.)
						OIL SAND "2458" - 2603.7 -2619.7m
						INTRUSIVE 2723.4 -2767.75m
T9940	2859	0.75	0.60-0.94	0.086	27	Fluorescing liptinite absent. (Argillaceous siltstone>carbonate>
Ctgs	Heat alt vit	1.71	-	-	1	coal. Coal rare, V, vitrite. Dom common, I>V. Inertinite common,
	$\overline{R}_{I}$max	1.73	1.32-2.24	0.234	20	vitrinite rare to sparse, liptinite absent. Rare heat altered coal with mean reflectance of 1.71%. The coal facies is indeterminate but the dom indicates Eastern View facies, inertinite being much more abundant compared with vitrinite in the dom of this sample. The heat altered coal grain is, however, Latrobe Valley facies. Mineral fluorescence patchy moderate orange. Iron oxides rare. Pyrite sparse.)
T9941	2925	0.90	0.70-1.11	0.090	15	Rare sporinite orange to dull orange, rare lamalginite orange.
Ctgs	Heat alt vit	1.78	1.51-2.06	0.191	9	(Siltstone>silty artificial composites>claystone>sandstone>coal.
	$\overline{R}_{I}$max	2.18	1.32-3.34	0.656	5	Coal rare, vitrite>clarite. Dom sparse, V>I>L. Vitrinite and inertinite sparse, liptinite rare. Rare to sparse heat altered coal with mean reflectance of 1.78%. The coal facies is either Upper Eastern View facies or transitional to Latrobe Valley facies. The heat altered coal is either Latrobe Valley facies or transitional to Upper EV facies. Mineral fluorescence patchy moderate orange. Abundant oil inclusions, yellow within artificial composites, rare yellow within quartz grains in sandstone. Iron oxides rare. Pyrite abundant.)
T9942	3168	0.92	0.80-1.11	0.132	35	. Rare sporinite dull orange, rare meta-exsudatinite dull orange, rare.
Ctgs	Heat alt vit	1.87	1.82-1.94	0.191	5	lamalginite dull orange. (Siltstone>artificial composites>claystone >
	$\overline{R}_{I}$max	1.44	-	-	2	coal>sandstone. Coal sparse, vitrite>clarite. Dom common, V>I>L.
	$R_{meta\text{-}exsudat}$	0.34	-	-	1	Vitrinite common, inertinite sparse, liptinite rare. Rare to sparse heat altered coal with mean reflectance of 1.87%. The coal facies is either Upper Eastern View facies or transitional to Latrobe Valley facies. The heat altered coal is either Latrobe Valley facies or transitional to Upper EV facies. Mineral fluorescence patchy moderate orange. Iron oxides rare. Pyrite sparse.)
						BASEMENT VOLCANCS – 3182.6m

The standard deviation of the vitrinite reflectance values show some evidence of cavings throughout the section and artificial composites are prominent in most of the samples. Towards the base, the artificial composites contain some very low rank coal particles. These may indicate either that recirculation of shallow returns has occurred or that a coal mud additive was used in the deeper part of the hole. From 2313 m the tails of the vitrinite reflectance distributions were cut to exclude most of the cavings. However, the means for the deeper samples are probably biased towards lower values by cavings. In the deepest three samples and additional complication occurs with the presence of heat altered coals and heat altered dispersed organic matter (dom).

#2730 **YOLLA-4, BASS BASIN, p 2**

The upper part of the section is immature and shows a relatively steady increase in maturation level to reach the top of the oil window at about 1750m. Mid-maturity for oil generation is reached at about 2500m. Below that depth a more complex pattern of maturation levels is found. The deepest three samples show vitrinite reflectance values indicating late to overmature for oil generation, although still within the window of oil preservation.

Additionally, the three deepest samples contain a population of heat-altered vitrinite. These heat-altered populations show a significant spread of reflectances, but can be interpreted as coming from essentially the same horizon. It is possible that heat alteration occurs throughout the interval below 2859m where the heat altered coal is first found, but this is considered unlikely. It is more probable that a heat-altered zone occurs shallower than 2859m and the two deeper samples contain materials caved from a shallower horizon. The optical properties and structures of the heat-altered coal also indicate some of the conditions of alteration. The heat altered coals show small incipient vesicles that indicate temperatures of above 200^{o}C, but the moderate reflectances indicate that the duration of the heating was not long in duration. The preferred interpretation is of a relatively small but proximal intrusion. No evidence was found of igneous rock fragments. The presence of a small occurrence of meta-exsudatinite at 3168m is consistent with some broader low temperature aureole from the igneous intrusion.

The upper samples are all from the Latrobe Valley facies of Cook and Smith (APPEA J, 1984, p208). The dom within the sample from 2859m suggests that the Lower Eastern View facies has been penetrated. However, the coals in this and the deeper samples are still either of Latrobe Valley facies or more probably represent vitrinite-rich examples of the Upper Eastern View facies. The progression in the vitrinite reflectance values means that the presence of coals with the characteristics of the shallower facies cannot be explained by cavings. It is possible that some degree of interbedding of the facies has occurred within the section at Yolla-4 or that the dom from 2859m is from the Upper Eastern View facies but is unusually rich in inertinite.

Oil drops are found in a number of the shallower samples and are present in a number of those from 2313m down. The sample from 2925m contains abundant oil drops within the artificial composites and rare oil drops also occur as inclusions within quartz grains. The oil in the artificial composites has come from the mud stream (but is not an additive) and that in the quartz is indigenous to the sample.

The main source materials are either coals themselves of coaly macerals present as dom. In type they are similar to the source sections that have generated prolific oil within the Gippsland Basin, although coals appear to be less abundant in the Yolla-4 samples compared with many other suites examined from the Bass Basin.

The main zone of gas generation lies below the deepest of the samples. The zone affected by heat alteration will have generated some additional gas, but the heat-affected zone is likely to be relatively thin.

ACC 22 August 2004

ADDITIONS MADE FOLLOWING THE SUPPLY OF STRATIGRAPHIC DATA.

The heat-altered coals are a result of the intrusions logged at 2723.4m to 2767.75m. As suspected, only one horizon (or set of horizons) has been affected by the contact alteration. With a thick intrusion such as that logged, reflectances near the intrusion are likely to be over 4%. The heat-altered zone has not been sampled directly and so it is clear that the contact aureole is less than about 75m in thickness. The samples from 2859 to 3168m indicate a coalification gradient within a section that is essentially unaffected by the intrusion. The lack of mineralization in the heat-altered coal suggests that the interval that has caved from the contact alteration aureole probably lies below the igneous intrusion. An estimate of the thickness of section between the contact and the horizon that has caved is 5 to 10m. Although some methane will have been generated by the contact alteration, the main effect is likely to have been the addition of carbon dioxide of igneous origin to the gas charge above the intruded section.

The oil inclusions within the artificial composites in the sample from 2925m can be presumed to represent oil that has entered the mud-stream from the interval reported as Oil Sand "2458".

The top of the Eastern View Coal Measures is reported at 1879m. The first entry of Eastern View organic facies is at 2859m. The persistence of Upper Eastern View facies coals down to the deepest sample could indicate a strong presence of cavings, but the rise in vitrinite reflectance within the coals suggests that this is not the case. Coals generally have a low abundance in the samples and it is possible that few coal seams have been directly sampled. The most likely coal lithologies to be present within cavings are those rich in vitrinite and this may have biased the interpretation of the organic facies present.

ACC 25 August 2004

HISTOGRAMS FOR YOLLA-4

Keiraville Konsultants Pty. Ltd.
7 Dallas Street,
Keiraville, NSW 2500
Australia.

Telephone: (02) 42 299843
International: +61-2-42 299843
Fax: +61-(0)2-42 299624
Email: acc@ozemail.com.au

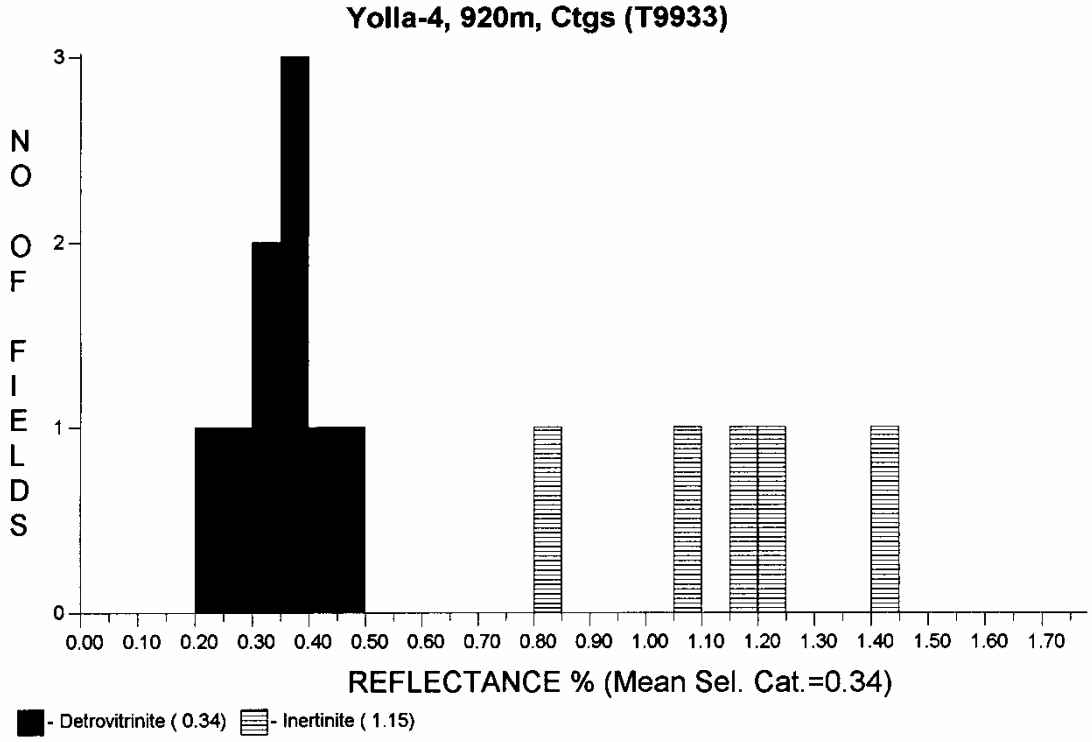

Category	No. of Readings	Mean	Standard Deviation
Detrovitrinite	9	0.34	0.065
Inertinite	5	1.15	0.197
Total:	14	0.63	0.408

Selected categories: Detrovitrinite,

No. of readings:	9
Mean of selected categories:	0.34
Standard deviation of selected categories:	0.065

Keiraville Konsultants Pty. Ltd.
7 Dallas Street,
Keiraville, NSW 2500
Australia.

Telephone: (02) 42 299843
International: +61-2-42 299843
Fax: +61-(0)2-42 299624
Email: acc@ozemail.com.au

YOLLA-4, Bass Basin, 1320m, Ctgs (T9934)

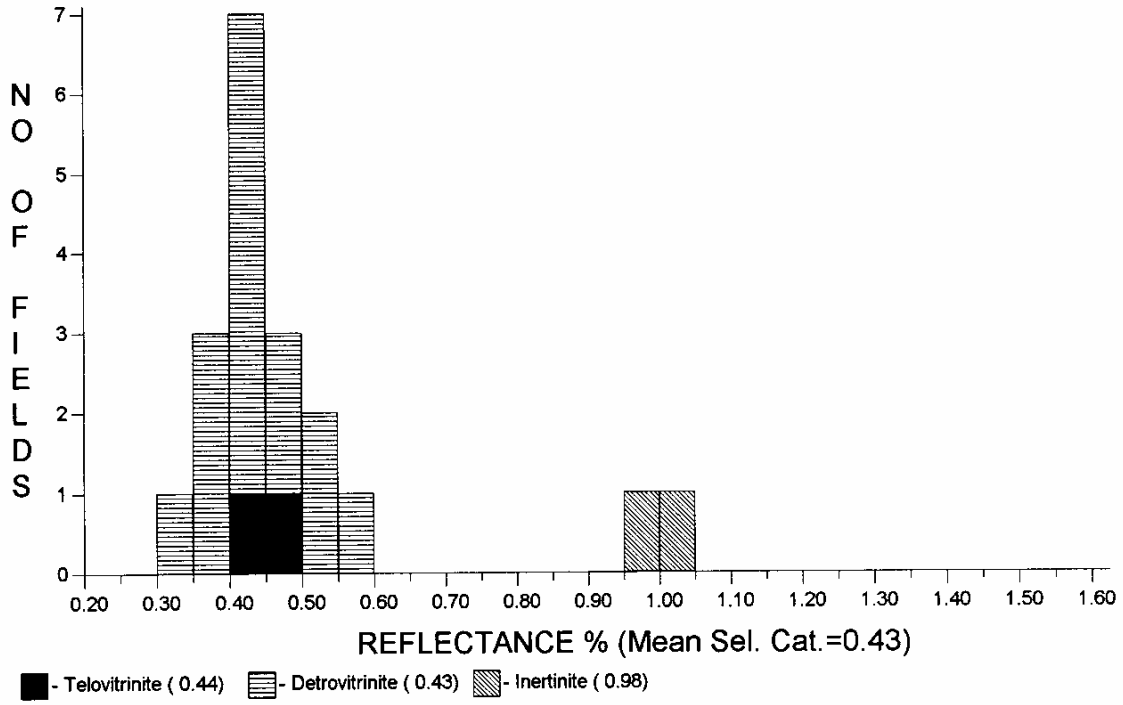

Category	No. of Readings	Mean	Standard Deviation
Telovitrinite	2	0.44	0.020
Detrovitrinite	15	0.43	0.063
Inertinite	2	0.98	0.020
Total:	19	0.49	0.179

Selected categories: Telovitrinite, Detrovitrinite,

No. of readings:	17
Mean of selected categories:	0.43
Standard deviation of selected categories:	0.060

Keiraville Konsultants Pty. Ltd.
7 Dallas Street,
Keiraville, NSW 2500
Australia.

Telephone: (02) 42 299843
International: +61-2-42 299843
Fax: +61-(0)2-42 299624
Email: acc@ozemail.com.au

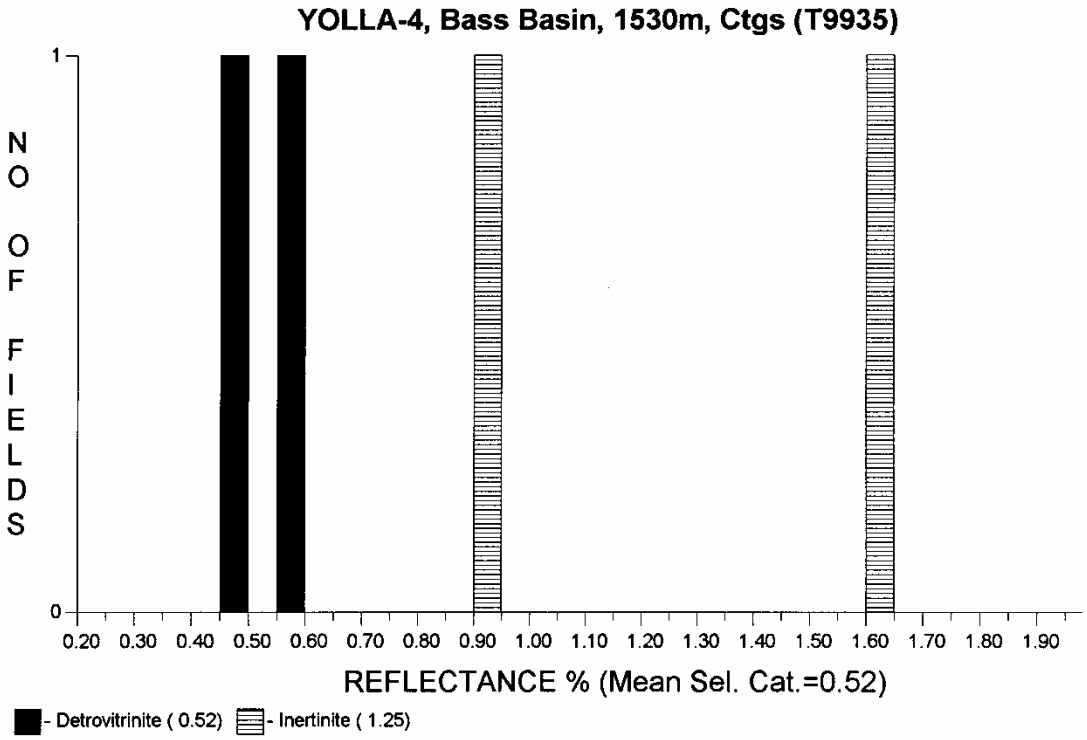

Category	No. of Readings	Mean	Standard Deviation
Detrovitrinite	2	0.52	0.070
Inertinite	2	1.25	0.350
Total:	4	0.89	0.444

Selected categories: Detrovitrinite,

No. of readings:	2
Mean of selected categories:	0.52
Standard deviation of selected categories:	0.070

Keiraville Konsultants Pty. Ltd.
7 Dallas Street,
Keiraville, NSW 2500
Australia.

Telephone: (02) 42 299843
International: +61-2-42 299843
Fax: +61-(0)2-42 299624
Email: acc@ozemail.com.au

YOLLA-4, Bass Basin, 1746m, Ctgs (T9936)

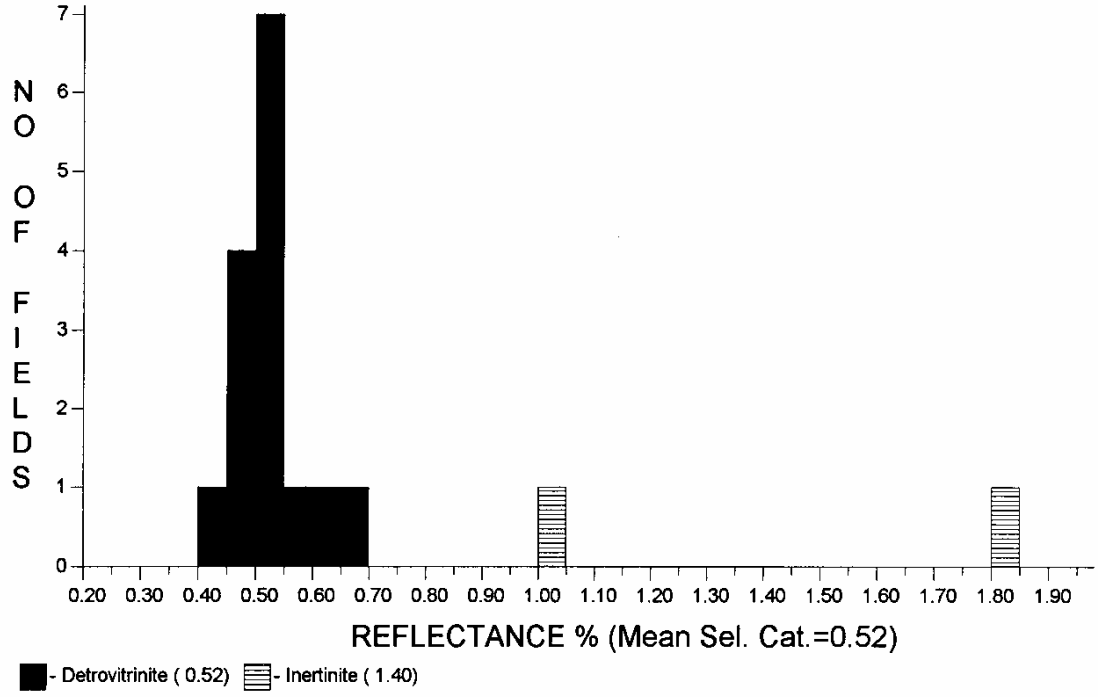

Category	No. of Readings	Mean	Standard Deviation
Detrovitrinite	15	0.52	0.057
Inertinite	2	1.40	0.400
Total:	17	0.62	0.320

Selected categories: Detrovitrinite,

No. of readings:	15
Mean of selected categories:	0.52
Standard deviation of selected categories:	0.057

Keiraville Konsultants Pty. Ltd.
7 Dallas Street,
Keiraville, NSW 2500
Australia.

Telephone: (02) 42 299843
International: +61-2-42 299843
Fax: +61-(0)2-42 299624
Email: acc@ozemail.com.au

YOLLA-4, Bass Basin, 1902m, Ctgs (T9937)

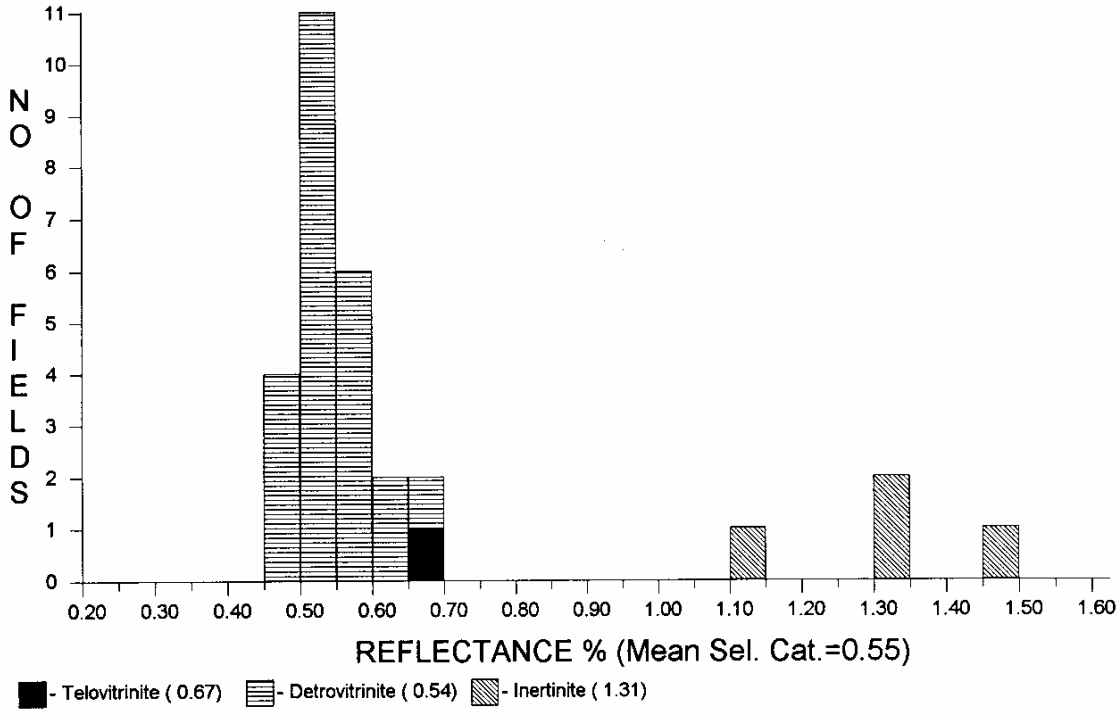

Category	No. of Readings	Mean	Standard Deviation
Telovitrinite	1	0.67	0.000
Detrovitrinite	24	0.54	0.044
Inertinite	4	1.31	0.122
Total:	29	0.65	0.271

Selected categories: Telovitrinite, Detrovitrinite,

No. of readings:	25
Mean of selected categories:	0.55
Standard deviation of selected categories:	0.050

Keiraville Konsultants Pty. Ltd.
7 Dallas Street,
Keiraville, NSW 2500
Australia.

Telephone: (02) 42 299843
International: +61-2-42 299843
Fax: +61-(0)2-42 299624
Email: acc@ozemail.com.au

YOLLA-4, Bass Basin, 2313m, Ctgs (T9938)

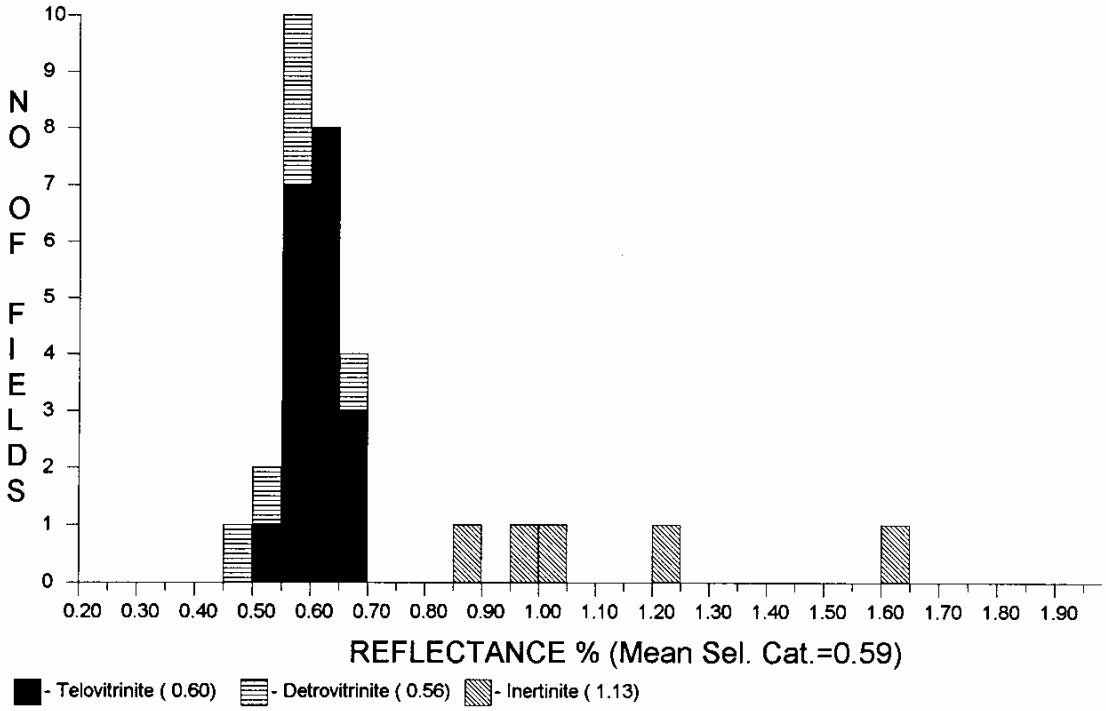

Category	No. of Readings	Mean	Standard Deviation
Telovitrinite	19	0.60	0.036
Detrovitrinite	6	0.56	0.062
Inertinite	5	1.13	0.257
Total:	30	0.68	0.231

Selected categories: Telovitrinite, Detrovitrinite,

No. of readings:	25
Mean of selected categories:	0.59
Standard deviation of selected categories:	0.048

Keiraville Konsultants Pty. Ltd.
7 Dallas Street,
Keiraville, NSW 2500
Australia.

Telephone: (02) 42 299843
International: +61-2-42 299843
Fax: +61-(0)2-42 299624
Email: acc@ozemail.com.au

Yolla-4, Bass Basin, 2574m, Ctgs (T9939)

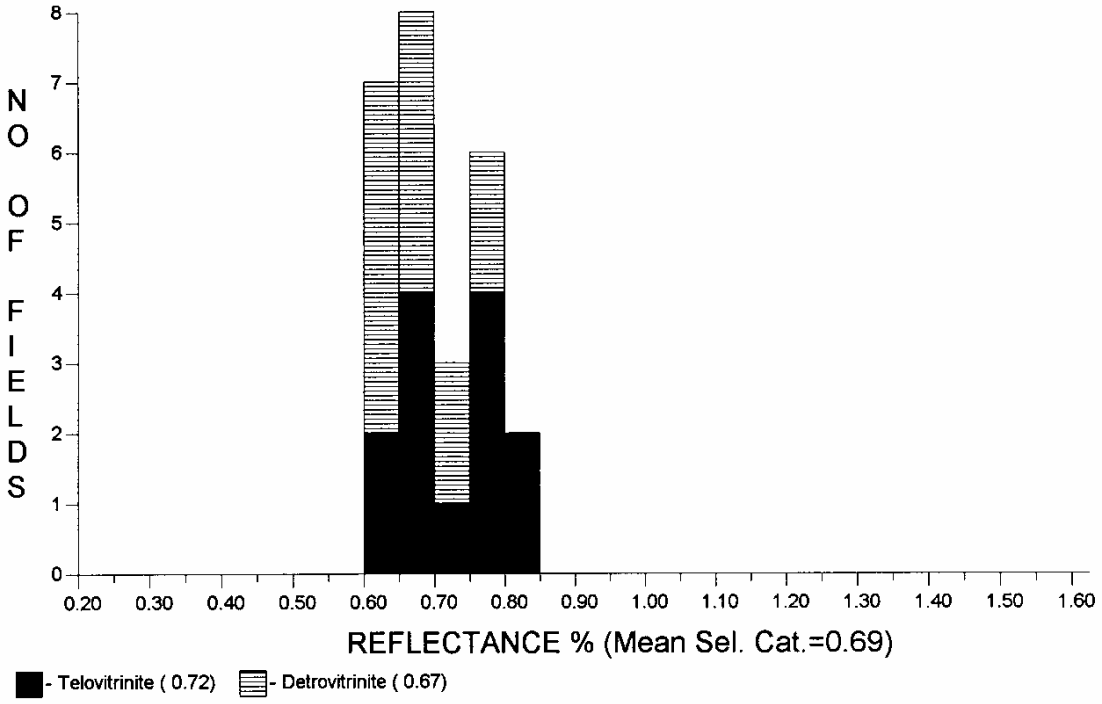

Category	No. of Readings	Mean	Standard Deviation
Telovitrinite	13	0.72	0.064
Detrovitrinite	13	0.67	0.058
Total:	26	0.69	0.065

Selected categories: Telovitrinite, Detrovitrinite.

No. of readings:	26
Mean of selected categories:	0.69
Standard deviation of selected categories:	0.065

Keiraville Konsultants Pty. Ltd.
7 Dallas Street,
Keiraville, NSW 2500
Australia.

Telephone: (02) 42 299843
International: +61-2-42 299843
Fax: +61-(0)2-42 299624
Email: acc@ozemail.com.au

YOLLA-4 Bass Basin, 2859m, Ctgs (T9940)

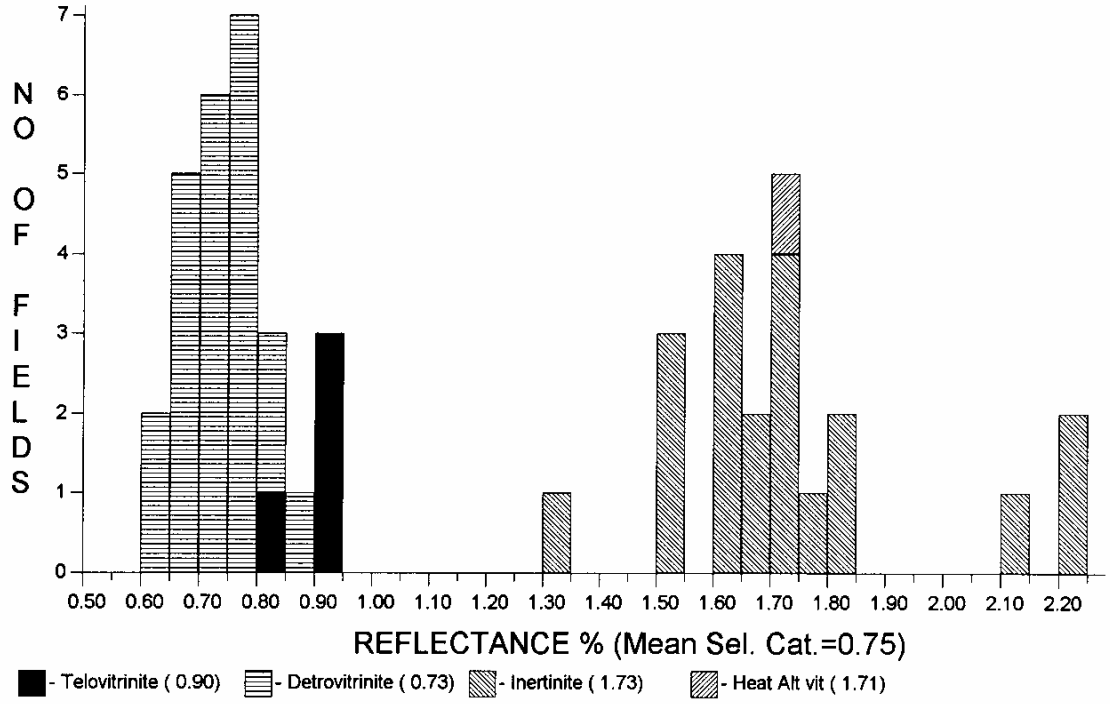

Category	No. of Readings	Mean	Standard Deviation
Telovitrinite	4	0.90	0.048
Detrovitrinite	23	0.73	0.062
Inertinite	20	1.73	0.234
Heat Alt vit	1	1.71	0.000
Total:	48	1.18	0.510

Selected categories: Telovitrinite, Detrovitrinite,

No. of readings:	27
Mean of selected categories:	0.75
Standard deviation of selected categories:	0.086

Keiraville Konsultants Pty. Ltd.
7 Dallas Street,
Keiraville, NSW 2500
Australia.

Telephone: (02) 42 299843
International: +61-2-42 299843
Fax: +61-(0)2-42 299624
Email: acc@ozemail.com.au

Yolla-4, Bass Basin, 2925m, Ctgs (T9941)

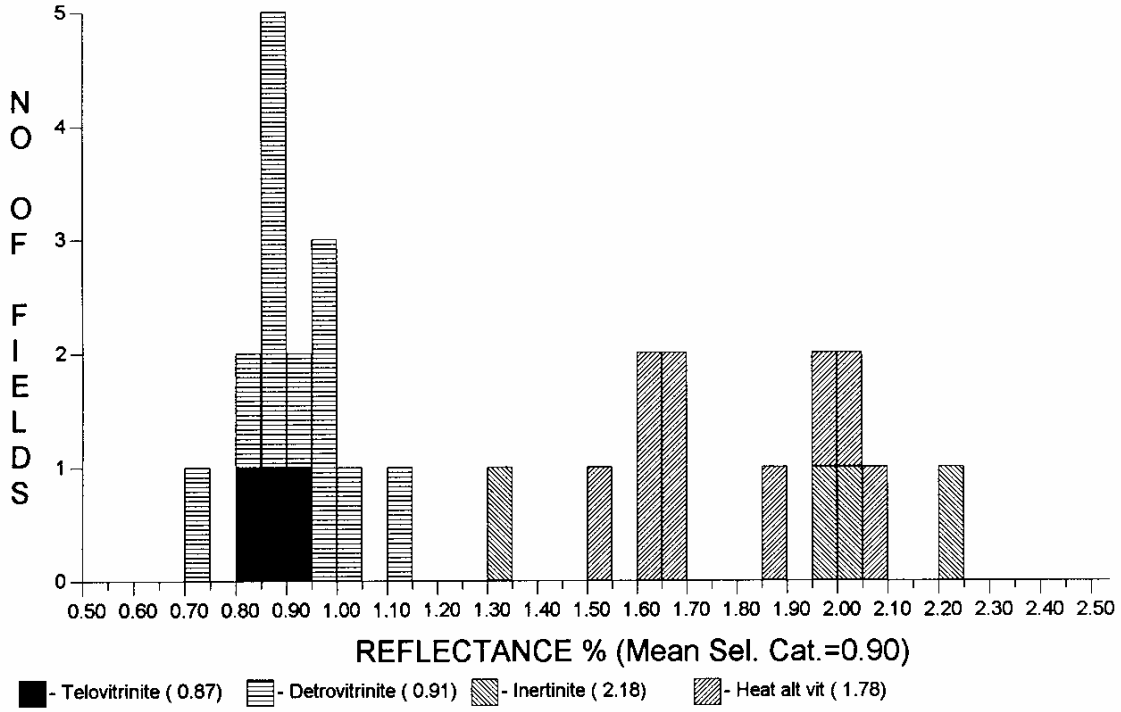

Category	No. of Readings	Mean	Standard Deviation
Telovitrinite	3	0.87	0.031
Detrovitrinite	12	0.91	0.097
Inertinite	5	2.18	0.656
Heat alt vit	9	1.78	0.191
Total:	29	1.39	0.607

Selected categories: Telovitrinite, Detrovitrinite,

No. of readings:	15
Mean of selected categories:	0.90
Standard deviation of selected categories:	0.090

Keiraville Konsultants Pty. Ltd.
7 Dallas Street,
Keiraville, NSW 2500
Australia.

Telephone: (02) 42 299843
International: +61-2-42 299843
Fax: +61-(0)2-42 299624
Email: acc@ozemail.com.au

Yolla-4, Bass Basin, 3168m, Ctgs (T9942)

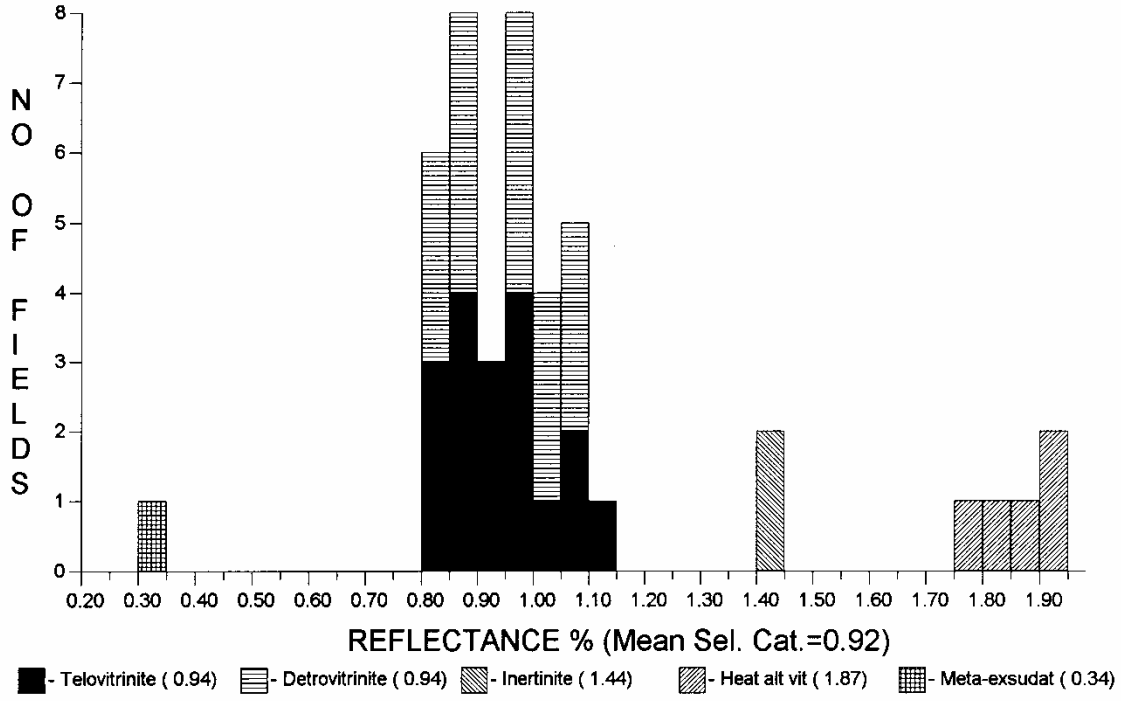

Category	No. of Readings	Mean	Standard Deviation
Telovitrinite	18	0.94	0.088
Detrovitrinite	17	0.94	0.091
Inertinite	2	1.44	0.000
Heat alt vit	5	1.87	0.057
Meta-exsudat	1	0.34	0.000
Total:	43	1.06	0.336

Selected categories: Telovitrinite, Detrovitrinite, Meta-exsudat.

No. of readings:	36
Mean of selected categories:	0.92
Standard deviation of selected categories:	0.132

MISCELLANEOUS SAMPLES - YOLLA -4

R	No Read	Pop Range	R	No Read	Pop Range	R	No Read	Pop Range	R	No Read	Pop Range	R	No Read	Pop Range	R	No Read	Pop Range	R	No Read	Pop Range	R	No Read	Pop Range	R	No Read	Pop Range
0.10			0.40	1		0.70			1.00			1.30			1.60			1.90			2.20			2.50		
0.11			0.41			0.71			1.01			1.31			1.61			1.91			2.21			2.51		
0.12			0.42			0.72			1.02			1.32			1.62			1.92			2.22			2.52		
0.13			0.43			0.73			1.03			1.33			1.63			1.93			2.23			2.53		
0.14			0.44		FGV	0.74			1.04			1.34			1.64			1.94			2.24			2.54		
0.15			0.45	1	↓	0.75			1.05			1.35			1.65			1.95			2.25			2.55		
0.16			0.46			0.76			1.06			1.36			1.66			1.96			2.26			2.56		
0.17			0.47			0.77			1.07			1.37			1.67			1.97			2.27			2.57		
0.18			0.48			0.78			1.08	1		1.38			1.68			1.98			2.28			2.58		
0.19			0.49			0.79			1.09			1.39			1.69			1.99			2.29			2.59		
0.20			0.50			0.80			1.10			1.40			1.70			2.00			2.30			2.60		
0.21			0.51			0.81			1.11			1.41			1.71			2.01			2.31			2.61		
0.22			0.52			0.82			1.12			1.42			1.72			2.02			2.32			2.62		
0.23			0.53			0.83			1.13			1.43		Inert	1.73			2.03			2.33			2.63		
0.24	1	↑	0.54			0.84	1	↑	1.14			1.44	1	↓	1.74			2.04			2.34			2.64		
0.25	1	FGV	0.55			0.85		Inert	1.15			1.45			1.75			2.05			2.35			2.65		
0.26			0.56			0.86			1.16	1		1.46			1.76			2.06			2.36			2.66		
0.27			0.57			0.87			1.17			1.47			1.77			2.07			2.37			2.67		
0.28			0.58			0.88			1.18			1.48			1.78			2.08			2.38			2.68		
0.29			0.59			0.89			1.19			1.49			1.79			2.09			2.39			2.69		
0.30			0.60			0.90			1.20			1.50			1.80			2.10			2.40			2.70		
0.31	1		0.61			0.91			1.21			1.51			1.81			2.11			2.41			2.71		
0.32			0.62			0.92			1.22			1.52			1.82			2.12			2.42			2.72		
0.33			0.63			0.93			1.23			1.53			1.83			2.13			2.43			2.73		
0.34	1		0.64			0.94			1.24	1		1.54			1.84			2.14			2.44			2.74		
0.35			0.65			0.95			1.25			1.55			1.85			2.15			2.45			2.75		
0.36	2		0.66			0.96			1.26			1.56			1.86			2.16			2.46			2.76		
0.37			0.67			0.97			1.27			1.57			1.87			2.17			2.47			2.77		
0.38			0.68			0.98			1.28			1.58			1.88			2.18			2.48			2.78		
0.39	1		0.69			0.99			1.29			1.59			1.89			2.19			2.49			2.79		

VITRINITE <0.1%		INERTINITE <0.1%						LIPTINITE <0.1%								OIL DROPS	BITUMEN
TV	DV	Sfus	Scler	Fus	Macr	ID	Micr	Spor	Cut	Sub	Res	Ld <0.1	Bituminite	Telalginite	Lamalginite <0.1	Oil cut	

Sample Number..T9933.....Well Name...Yolla-4 .....ORIGIN..... Depth...920m..... ..... SampleType....Ctgs...

Date. ..21/.08/ 2004.. Op..SPR..... FGV - First Generation Vitrinite, RV - Reworked Vitrinite, BTT - Bituminite, B - Bitumen, Inert - Inertinite, Cav - Cavings, DA - Drilling Mud Additives MICR D:\RWORK.ms6\misc04vr.doc

R	No Read	Pop Range	R	No Read	Pop Range	R	No Read	Pop Range	R	No Read	Pop Range	R	No Read	Pop Range	R	No Read	Pop Range	R	No Read	Pop Range	R	No Read	Pop Range	R	No Read	Pop Range
0.10			0.40	4		0.70			1.00	1	↓	1.30			1.60			1.90			2.20			2.50		
0.11			0.41			0.71			1.01			1.31			1.61			1.91			2.21			2.51		
0.12			0.42	1		0.72			1.02			1.32			1.62			1.92			2.22			2.52		
0.13			0.43			0.73			1.03			1.33			1.63			1.93			2.23			2.53		
0.14			0.44	2		0.74			1.04			1.34			1.64			1.94			2.24			2.54		
0.15			0.45			0.75			1.05			1.35			1.65			1.95			2.25			2.55		
0.16			0.46	3		0.76			1.06			1.36			1.66			1.96			2.26			2.56		
0.17			0.47			0.77			1.07			1.37			1.67			1.97			2.27			2.57		
0.18			0.48	1		0.78			1.08			1.38			1.68			1.98			2.28			2.58		
0.19			0.49			0.79			1.09			1.39			1.69			1.99			2.29			2.59		
0.20			0.50	1		0.80			1.10			1.40			1.70			2.00			2.30			2.60		
0.21			0.51			0.81			1.11			1.41			1.71			2.01			2.31			2.61		
0.22			0.52			0.82			1.12			1.42			1.72			2.02			2.32			2.62		
0.23			0.53	1		0.83			1.13			1.43			1.73			2.03			2.33			2.63		
0.24			0.54		FGV	0.84			1.14			1.44			1.74			2.04			2.34			2.64		
0.25			0.55	1	↓	0.85			1.15			1.45			1.75			2.05			2.35			2.65		
0.26			0.56			0.86			1.16			1.46			1.76			2.06			2.36			2.66		
0.27			0.57			0.87			1.17			1.47			1.77			2.07			2.37			2.67		
0.28			0.58			0.88			1.18			1.48			1.78			2.08			2.38			2.68		
0.29			0.59			0.89			1.19			1.49			1.79			2.09			2.39			2.69		
0.30			0.60			0.90			1.20			1.50			1.80			2.10			2.40			2.70		
0.31			0.61			0.91			1.21			1.51			1.81			2.11			2.41			2.71		
0.32	1	↑	0.62			0.92			1.22			1.52			1.82			2.12			2.42			2.72		
0.33		FGV	0.63			0.93			1.23			1.53			1.83			2.13			2.43			2.73		
0.34			0.64			0.94			1.24			1.54			1.84			2.14			2.44			2.74		
0.35	1		0.65			0.95			1.25			1.55			1.85			2.15			2.45			2.75		
0.36			0.66			0.96	1	↑	1.26			1.56			1.86			2.16			2.46			2.76		
0.37	1		0.67			0.97		Inert	1.27			1.57			1.87			2.17			2.47			2.77		
0.38	1		0.68			0.98			1.28			1.58			1.88			2.18			2.48			2.78		
0.39			0.69			0.99			1.29			1.59			1.89			2.19			2.49			2.79		

VITRINITE 0.1%		INERTINITE <0.1%						LIPTINITE <0.1%								OIL DROPS <0.1	BITUMEN
TV	DV	Sfus	Scler	Fus	Macr	ID	Micr	Spor	Cut	Sub	Res	Ld <0.1	Bituminite	Telalginite	Lamalginite <0.1	Oil cut	

Sample Number..T9934.....Well Name...Yolla-4 .....ORIGIN..... Depth...1320m..... ..... SampleType....Ctgs...
Date. ..21/.08/ 2004.. Op..SPR..... FGV - First Generation Vitrinite, RV - Reworked Vitrinite, BTT - Bituminite, B - Bitumen, Inert - Inertinite, Cav - Cavings, DA - Drilling Mud Additives MICR D:\RWORK.ms6\misc04vr.doc

R	No Read	Pop Range	R	No Read	Pop Range	R	No Read	Pop Range	R	No Read	Pop Range	R	No Read	Pop Range	R	No Read	Pop Range	R	No Read	Pop Range	R	No Read	Pop Range	R	No Read	Pop Range
0.10			0.40			0.70			1.00			1.30			1.60	1	↓	1.90			2.20			2.50		
0.11			0.41			0.71			1.01			1.31			1.61			1.91			2.21			2.51		
0.12			0.42			0.72			1.02			1.32			1.62			1.92			2.22			2.52		
0.13			0.43			0.73			1.03			1.33			1.63			1.93			2.23			2.53		
0.14			0.44			0.74			1.04			1.34			1.64			1.94			2.24			2.54		
0.15			0.45	1	↑	0.75			1.05			1.35			1.65			1.95			2.25			2.55		
0.16			0.46		FGV	0.76			1.06			1.36			1.66			1.96			2.26			2.56		
0.17			0.47			0.77			1.07			1.37			1.67			1.97			2.27			2.57		
0.18			0.48			0.78			1.08			1.38			1.68			1.98			2.28			2.58		
0.19			0.49			0.79			1.09			1.39			1.69			1.99			2.29			2.59		
0.20			0.50			0.80			1.10			1.40			1.70			2.00			2.30			2.60		
0.21			0.51			0.81			1.11			1.41			1.71			2.01			2.31			2.61		
0.22			0.52			0.82			1.12			1.42			1.72			2.02			2.32			2.62		
0.23			0.53			0.83			1.13			1.43			1.73			2.03			2.33			2.63		
0.24			0.54			0.84			1.14			1.44			1.74			2.04			2.34			2.64		
0.25			0.55			0.85			1.15			1.45			1.75			2.05			2.35			2.65		
0.26			0.56			0.86			1.16			1.46			1.76			2.06			2.36			2.66		
0.27			0.57			0.87			1.17			1.47			1.77			2.07			2.37			2.67		
0.28			0.58		FGV	0.88			1.18			1.48			1.78			2.08			2.38			2.68		
0.29			0.59	1	↓	0.89			1.19			1.49			1.79			2.09			2.39			2.69		
0.30			0.60			0.90	1	↑	1.20			1.50			1.80			2.10			2.40			2.70		
0.31			0.61			0.91		Inert	1.21			1.51			1.81			2.11			2.41			2.71		
0.32			0.62			0.92			1.22			1.52			1.82			2.12			2.42			2.72		
0.33			0.63			0.93			1.23			1.53			1.83			2.13			2.43			2.73		
0.34			0.64			0.94			1.24			1.54			1.84			2.14			2.44			2.74		
0.35			0.65			0.95			1.25			1.55			1.85			2.15			2.45			2.75		
0.36			0.66			0.96			1.26			1.56			1.86			2.16			2.46			2.76		
0.37			0.67			0.97			1.27			1.57			1.87			2.17			2.47			2.77		
0.38			0.68			0.98			1.28			1.58			1.88			2.18			2.48			2.78		
0.39			0.69			0.99			1.29			1.59		Inert	1.89			2.19			2.49			2.79		

VITRINITE <0.1%		INERTINITE <0.1%						LIPTINITE <0.1%								OIL DROPS	BITUMEN
TV	DV	Sfus	Scler	Fus	Macr	ID	Micr	Spor	Cut	Sub	Res	Ld <0.1	Bituminite	Telalginite	Lamalginite <0.1	Oil cut	

Sample Number..T9935.....Well Name...Yolla-4 .....ORIGIN..... Depth...1530m..... ..... SampleType....Ctgs...
Date. ..21/.08/ 2004.. Op..SPR..... FGV - First Generation Vitrinite, RV - Reworked Vitrinite, BTT - Bituminite, B - Bitumen, Inert - Inertinite, Cav - Cavings, DA - Drilling Mud Additives MICR D:\RWORK.ms6\misc04vr.doc

R	No Read	Pop Range	R	No Read	Pop Range	R	No Read	Pop Range	R	No Read	Pop Range	R	No Read	Pop Range	R	No Read	Pop Range	R	No Read	Pop Range	R	No Read	Pop Range	R	No Read	Pop Range
0.10			0.40	1	↑	0.70			1.00	1	↑	1.30			1.60			1.90			2.20			2.50		
0.11			0.41		FGV	0.71			1.01		Inert	1.31			1.61			1.91			2.21			2.51		
0.12			0.42			0.72			1.02			1.32			1.62			1.92			2.22			2.52		
0.13			0.43			0.73			1.03			1.33			1.63			1.93			2.23			2.53		
0.14			0.44			0.74			1.04			1.34			1.64			1.94			2.24			2.54		
0.15			0.45			0.75			1.05			1.35			1.65			1.95			2.25			2.55		
0.16			0.46	1		0.76			1.06			1.36			1.66			1.96			2.26			2.56		
0.17			0.47			0.77			1.07			1.37			1.67			1.97			2.27			2.57		
0.18			0.48	3		0.78			1.08			1.38			1.68			1.98			2.28			2.58		
0.19			0.49			0.79			1.09			1.39			1.69			1.99			2.29			2.59		
0.20			0.50	1		0.80			1.10			1.40			1.70			2.00			2.30			2.60		
0.21			0.51	1		0.81			1.11			1.41			1.71			2.01			2.31			2.61		
0.22			0.52	2		0.82			1.12			1.42			1.72			2.02			2.32			2.62		
0.23			0.53	2		0.83			1.13			1.43			1.73			2.03			2.33			2.63		
0.24			0.54	1		0.84			1.14			1.44			1.74			2.04			2.34			2.64		
0.25			0.55			0.85			1.15			1.45			1.75			2.05			2.35			2.65		
0.26			0.56	1		0.86			1.16			1.46			1.76			2.06			2.36			2.66		
0.27			0.57			0.87			1.17			1.47			1.77			2.07			2.37			2.67		
0.28			0.58			0.88			1.18			1.48			1.78			2.08			2.38			2.68		
0.29			0.59			0.89			1.19			1.49			1.79		Inert	2.09			2.39			2.69		
0.30			0.60	1		0.90			1.20			1.50			1.80	1	↓	2.10			2.40			2.70		
0.31			0.61			0.91			1.21			1.51			1.81			2.11			2.41			2.71		
0.32			0.62			0.92			1.22			1.52			1.82			2.12			2.42			2.72		
0.33			0.63			0.93			1.23			1.53			1.83			2.13			2.43			2.73		
0.34			0.64		FGV	0.94			1.24			1.54			1.84			2.14			2.44			2.74		
0.35			0.65	1	↓	0.95			1.25			1.55			1.85			2.15			2.45			2.75		
0.36			0.66			0.96			1.26			1.56			1.86			2.16			2.46			2.76		
0.37			0.67			0.97			1.27			1.57			1.87			2.17			2.47			2.77		
0.38			0.68			0.98			1.28			1.58			1.88			2.18			2.48			2.78		
0.39			0.69			0.99			1.29			1.59			1.89			2.19			2.49			2.79		

VITRINITE <0.1%		INERTINITE <0.1%						LIPTINITE <0.1%								OIL DROPS	BITUMEN
TV	DV	Sfus	Scler	Fus	Macr	ID	Micr	Spor <0.1	Cut	Sub	Res	Ld <0.1	Bituminite	Telalginite	Lamalginite <0.1	Oil cut	

Sample Number..T9936.....Well Name...Yolla-4 .....ORIGIN..... Depth...1746m..... ..... SampleType....Ctgs...

Date. ..21/.08/ 2004.. Op..SPR..... FGV - First Generation Vitrinite, RV - Reworked Vitrinite, BTT - Bituminite, B - Bitumen, Inert - Inertinite, Cav - Cavings, DA - Drilling Mud Additives MICR D:\RWORK.ms6\misc04vr.doc

R	No Read	Pop Range	R	No Read	Pop Range	R	No Read	Pop Range	R	No Read	Pop Range	R	No Read	Pop Range	R	No Read	Pop Range	R	No Read	Pop Range	R	No Read	Pop Range	R	No Read	Pop Range
0.10			0.40			0.70			1.00			1.30			1.60			1.90			2.20			2.50		
0.11			0.41			0.71			1.01			1.31			1.61			1.91			2.21			2.51		
0.12			0.42			0.72			1.02			1.32	1		1.62			1.92			2.22			2.52		
0.13			0.43			0.73			1.03			1.33			1.63			1.93			2.23			2.53		
0.14			0.44			0.74			1.04			1.34	1		1.64			1.94			2.24			2.54		
0.15			0.45			0.75			1.05			1.35			1.65			1.95			2.25			2.55		
0.16			0.46			0.76			1.06			1.36			1.66			1.96			2.26			2.56		
0.17			0.47			0.77			1.07			1.37			1.67			1.97			2.27			2.57		
0.18			0.48	2	↑	0.78			1.08			1.38			1.68			1.98			2.28			2.58		
0.19			0.49	2	FGV	0.79			1.09			1.39			1.69			1.99			2.29			2.59		
0.20			0.50	1		0.80			1.10			1.40			1.70			2.00			2.30			2.60		
0.21			0.51	2		0.81			1.11			1.41			1.71			2.01			2.31			2.61		
0.22			0.52	1		0.82			1.12	1	↑	1.42			1.72			2.02			2.32			2.62		
0.23			0.53	3		0.83			1.13		Inert	1.43			1.73			2.03			2.33			2.63		
0.24			0.54	4		0.84			1.14			1.44			1.74			2.04			2.34			2.64		
0.25			0.55	1		0.85			1.15			1.45		Inert	1.75			2.05			2.35			2.65		
0.26			0.56	4		0.86			1.16			1.46	1	↓	1.76			2.06			2.36			2.66		
0.27			0.57	1		0.87			1.17			1.47			1.77			2.07			2.37			2.67		
0.28			0.58			0.88			1.18			1.48			1.78			2.08			2.38			2.68		
0.29			0.59			0.89			1.19			1.49			1.79			2.09			2.39			2.69		
0.30			0.60	1		0.90			1.20			1.50			1.80			2.10			2.40			2.70		
0.31			0.61	1		0.91			1.21			1.51			1.81			2.11			2.41			2.71		
0.32			0.62			0.92			1.22			1.52			1.82			2.12			2.42			2.72		
0.33			0.63			0.93			1.23			1.53			1.83			2.13			2.43			2.73		
0.34			0.64			0.94			1.24			1.54			1.84			2.14			2.44			2.74		
0.35			0.65			0.95			1.25			1.55			1.85			2.15			2.45			2.75		
0.36			0.66			0.96			1.26			1.56			1.86			2.16			2.46			2.76		
0.37			0.67	1	FGV	0.97			1.27			1.57			1.87			2.17			2.47			2.77		
0.38			0.68	1	↓	0.98			1.28			1.58			1.88			2.18			2.48			2.78		
0.39			0.69			0.99			1.29			1.59			1.89			2.19			2.49			2.79		

VITRINITE 2.0%		INERTINITE <0.1%						LIPTINITE <0.1%								OIL DROPS	BITUMEN
TV	DV	Sfus	Scler	Fus	Macr	ID	Micr	Spor <0.1	Cut	Sub	Res	Ld <0.1	Bituminite	Telalginite	Lamalginite	Oil cut	

Sample Number..T9937.....Well Name...Yolla-4 .....ORIGIN..... Depth...1902m..... ..... SampleType....Ctgs...
Date. ..21/.08/ 2004.. Op..SPR..... FGV - First Generation Vitrinite, RV - Reworked Vitrinite, BTT - Bituminite, B - Bitumen, Inert - Inertinite, Cav - Cavings, DA - Drilling Mud Additives MICR D:\RWORK.ms6\misc04vr.doc

R	No Read	Pop Range	R	No Read	Pop Range	R	No Read	Pop Range	R	No Read	Pop Range	R	No Read	Pop Range	R	No Read	Pop Range	R	No Read	Pop Range	R	No Read	Pop Range	R	No Read	Pop Range
0.10			0.40			0.70			1.00			1.30			1.60	1	↓	1.90			2.20			2.50		
0.11			0.41			0.71			1.01			1.31			1.61			1.91			2.21			2.51		
0.12			0.42			0.72			1.02	1		1.32			1.62			1.92			2.22			2.52		
0.13			0.43			0.73			1.03			1.33			1.63			1.93			2.23			2.53		
0.14			0.44			0.74			1.04			1.34			1.64			1.94			2.24			2.54		
0.15			0.45			0.75			1.05			1.35			1.65			1.95			2.25			2.55		
0.16			0.46			0.76			1.06			1.36			1.66			1.96			2.26			2.56		
0.17			0.47	1	↑	0.77			1.07			1.37			1.67			1.97			2.27			2.57		
0.18			0.48		FGV	0.78			1.08			1.38			1.68			1.98			2.28			2.58		
0.19			0.49			0.79			1.09			1.39			1.69			1.99			2.29			2.59		
0.20			0.50			0.80			1.10			1.40			1.70			2.00			2.30			2.60		
0.21			0.51			0.81			1.11			1.41			1.71			2.01			2.31			2.61		
0.22			0.52			0.82			1.12			1.42			1.72			2.02			2.32			2.62		
0.23			0.53			0.83			1.13			1.43			1.73			2.03			2.33			2.63		
0.24			0.54	2		0.84			1.14			1.44			1.74			2.04			2.34			2.64		
0.25			0.55	3		0.85			1.15			1.45			1.75			2.05			2.35			2.65		
0.26			0.56	2		0.86			1.16			1.46			1.76			2.06			2.36			2.66		
0.27			0.57	2		0.87			1.17			1.47			1.77			2.07			2.37			2.67		
0.28			0.58	2		0.88	1	↑	1.18			1.48			1.78			2.08			2.38			2.68		
0.29			0.59	1		0.89		Inert	1.19			1.49			1.79			2.09			2.39			2.69		
0.30			0.60	2		0.90			1.20	1		1.50			1.80			2.10			2.40			2.70		
0.31			0.61	1		0.91			1.21			1.51			1.81			2.11			2.41			2.71		
0.32			0.62	3		0.92			1.22			1.52			1.82			2.12			2.42			2.72		
0.33			0.63	1		0.93			1.23			1.53			1.83			2.13			2.43			2.73		
0.34			0.64	1		0.94			1.24			1.54			1.84			2.14			2.44			2.74		
0.35			0.65			0.95			1.25			1.55			1.85			2.15			2.45			2.75		
0.36			0.66	3		0.96	1		1.26			1.56			1.86			2.16			2.46			2.76		
0.37			0.67		FGV	0.97			1.27			1.57			1.87			2.17			2.47			2.77		
0.38			0.68	1	↓	0.98			1.28			1.58			1.88			2.18			2.48			2.78		
0.39			0.69			0.99			1.29			1.59		Inert	1.89			2.19			2.49			2.79		

VITRINITE 4.5%		INERTINITE 0.2%						LIPTINITE 0.4%							OIL DROPS <0.1	BITUMEN
TV	DV	Sfus	Scler	Fus	Macr	ID	Micr	Spor 0.4	Cut <0.1	Sub	Res <0.1	Ld <0.1	Bituminite	Telalginite	Lamalginite	Oil cut

Sample Number..T9938.....Well Name...Yolla-4 .....ORIGIN..... Depth...2313m..... ..... SampleType....Ctgs...
Date. ..21/.08/ 2004.. Op..SPR..... FGV - First Generation Vitrinite, RV - Reworked Vitrinite, BTT - Bituminite, B - Bitumen, Inert - Inertinite, Cav - Cavings, DA - Drilling Mud Additives MICR D:\RWORK.ms6\misc04vr.doc

R	No Read	Pop Range	R	No Read	Pop Range	R	No Read	Pop Range	R	No Read	Pop Range	R	No Read	Pop Range	R	No Read	Pop Range	R	No Read	Pop Range	R	No Read	Pop Range	R	No Read	Pop Range
0.10			0.40			0.70	1		1.00			1.30			1.60			1.90			2.20			2.50		
0.11			0.41			0.71	1		1.01			1.31			1.61			1.91			2.21			2.51		
0.12			0.42			0.72			1.02			1.32			1.62			1.92			2.22			2.52		
0.13			0.43			0.73			1.03			1.33			1.63			1.93			2.23			2.53		
0.14			0.44			0.74	1		1.04			1.34			1.64			1.94			2.24			2.54		
0.15			0.45			0.75	3		1.05			1.35			1.65			1.95			2.25			2.55		
0.16			0.46			0.76			1.06			1.36			1.66			1.96			2.26			2.56		
0.17			0.47	1	↑	0.77	1		1.07			1.37			1.67			1.97			2.27			2.57		
0.18			0.48		Cav	0.78	1		1.08			1.38			1.68			1.98			2.28			2.58		
0.19			0.49			0.79	1		1.09			1.39			1.69			1.99			2.29			2.59		
0.20			0.50			0.80	1		1.10			1.40			1.70			2.00			2.30			2.60		
0.21			0.51			0.81		FGV	1.11			1.41			1.71			2.01			2.31			2.61		
0.22			0.52			0.82	1	↓	1.12			1.42			1.72			2.02			2.32			2.62		
0.23			0.53			0.83			1.13			1.43			1.73			2.03			2.33			2.63		
0.24			0.54	1		0.84			1.14			1.44			1.74			2.04			2.34			2.64		
0.25			0.55			0.85			1.15			1.45			1.75			2.05			2.35			2.65		
0.26			0.56			0.86			1.16			1.46			1.76			2.06			2.36			2.66		
0.27			0.57	1		0.87			1.17			1.47			1.77			2.07			2.37			2.67		
0.28			0.58	1	Cav	0.88			1.18			1.48			1.78			2.08			2.38			2.68		
0.29			0.59	1	↓	0.89			1.19			1.49			1.79			2.09			2.39			2.69		
0.30			0.60	1	↑	0.90			1.20			1.50			1.80			2.10			2.40			2.70		
0.31			0.61	2	FGV	0.91			1.21			1.51			1.81			2.11			2.41			2.71		
0.32			0.62	2		0.92			1.22			1.52			1.82			2.12			2.42			2.72		
0.33			0.63	1		0.93			1.23			1.53			1.83			2.13			2.43			2.73		
0.34			0.64	1		0.94			1.24			1.54			1.84			2.14			2.44			2.74		
0.35			0.65	1		0.95			1.25			1.55			1.85			2.15			2.45			2.75		
0.36			0.66	5		0.96			1.26			1.56			1.86			2.16			2.46			2.76		
0.37			0.67			0.97			1.27			1.57			1.87			2.17			2.47			2.77		
0.38			0.68	1		0.98			1.28			1.58			1.88			2.18			2.48			2.78		
0.39			0.69	1		0.99			1.29			1.59			1.89			2.19			2.49			2.79		

VITRINITE 1.0 %		INERTINITE <0.1%						LIPTINITE 0.3%								OIL DROPS	BITUMEN
TV	DV	Sfus	Scler	Fus	Macr	ID	Micr	Spor 0.3	Cut <0.1	Sub	Res <0.1	Ld <0.1	Bituminite	Telalginite	Lamalginite	Oil cut	

Sample Number..T9939.....Well Name...Yolla-4 .....ORIGIN..... Depth...2574m..... ..... SampleType....Ctgs...
Date. ..21/.08/ 2004.. Op..SPR..... FGV - First Generation Vitrinite, RV - Reworked Vitrinite, BTT - Bituminite, B - Bitumen, Inert - Inertinite, Cav - Cavings, DA - Drilling Mud Additives MICR D:\RWORK.ms6\misc04vr.doc

R	No Read	Pop Range	R	No Read	Pop Range	R	No Read	Pop Range	R	No Read	Pop Range	R	No Read	Pop Range	R	No Read	Pop Range	R	No Read	Pop Range	R	No Read	Pop Range	R	No Read	Pop Range
0.10			0.40			0.70	1		1.00			1.30			1.60	3		1.90			2.20			2.50		
0.11			0.41			0.71	3		1.01			1.31			1.61			1.91			2.21			2.51		
0.12			0.42			0.72	1		1.02			1.32	1	↑	1.62			1.92			2.22			2.52		
0.13			0.43			0.73			1.03			1.33		Inert	1.63			1.93			2.23		Inert	2.53		
0.14			0.44			0.74	1		1.04			1.34			1.64	1		1.94			2.24	2	↓	2.54		
0.15			0.45			0.75	1		1.05			1.35			1.65			1.95			2.25			2.55		
0.16			0.46			0.76	2		1.06			1.36			1.66	1		1.96			2.26			2.56		
0.17			0.47			0.77	1		1.07			1.37			1.67			1.97			2.27			2.57		
0.18			0.48			0.78	2		1.08			1.38			1.68	1		1.98			2.28			2.58		
0.19			0.49			0.79	1		1.09			1.39			1.69			1.99			2.29			2.59		
0.20			0.50			0.80	2		1.10			1.40			1.70	3		2.00			2.30			2.60		
0.21			0.51			0.81			1.11			1.41			1.71	1	HAV	2.01			2.31			2.61		
0.22			0.52			0.82	1		1.12			1.42			1.72			2.02			2.32			2.62		
0.23			0.53			0.83			1.13			1.43			1.73			2.03			2.33			2.63		
0.24			0.54			0.84			1.14			1.44			1.74	1		2.04			2.34			2.64		
0.25			0.55			0.85			1.15			1.45			1.75			2.05			2.35			2.65		
0.26			0.56			0.86	1		1.16			1.46			1.76	1		2.06			2.36			2.66		
0.27			0.57			0.87			1.17			1.47			1.77			2.07			2.37			2.67		
0.28			0.58			0.88			1.18			1.48			1.78			2.08			2.38			2.68		
0.29			0.59			0.89			1.19			1.49			1.79			2.09			2.39			2.69		
0.30			0.60	1	↑	0.90			1.20			1.50	2		1.80			2.10			2.40			2.70		
0.31			0.61	1	FGV	0.91			1.21			1.51			1.81			2.11			2.41			2.71		
0.32			0.62			0.92	1		1.22			1.52			1.82			2.12			2.42			2.72		
0.33			0.63			0.93	1	FGV	1.23			1.53			1.83			2.13			2.43			2.73		
0.34			0.64			0.94	1	↓	1.24			1.54	1		1.84	2		2.14	1		2.44			2.74		
0.35			0.65			0.95			1.25			1.55			1.85			2.15			2.45			2.75		
0.36			0.66			0.96			1.26			1.56			1.86			2.16			2.46			2.76		
0.37			0.67	3		0.97			1.27			1.57			1.87			2.17			2.47			2.77		
0.38			0.68	1		0.98			1.28			1.58			1.88			2.18			2.48			2.78		
0.39			0.69	1		0.99			1.29			1.59			1.89			2.19			2.49			2.79		

VITRINITE 0.1 %		INERTINITE 0.6%						LIPTINITE -%								OIL DROPS	BITUMEN
TV	DV	Sfus	Scler	Fus	Macr	ID	Micr	Spor	Cut	Sub	Res	Ld	Bituminite	Telalginite	Lamalginite	Oil cut	

Sample Number..T9940.....Well Name...Yolla-4 .....ORIGIN..... Depth...2859m..... ..... SampleType....Ctgs...

Date. ..21/.08/ 2004.. Op..SPR..... FGV - First Generation Vitrinite, RV - Reworked Vitrinite, HAV - heat altered vitrinite, B - Bitumen, Inert - Inertinite, Cav - Cavings, DA - Drilling Mud Additives MICR D:\RWORK.ms6\misc04vr.doc

R	No Read	Pop Range	R	No Read	Pop Range	R	No Read	Pop Range	R	No Read	Pop Range	R	No Read	Pop Range	R	No Read	Pop Range	R	No Read	Pop Range	R	No Read	Pop Range	R	No Read	Pop Range
0.10			0.40			0.70			1.00	1		1.30			1.60			1.90			2.20			2.50		
0.11			0.41			0.71	1	↑	1.01			1.31			1.61			1.91			2.21			2.51		
0.12			0.42			0.72		FGV	1.02			1.32	1	↑	1.62			1.92			2.22			2.52		
0.13			0.43			0.73			1.03			1.33		Inert	1.63	1		1.93			2.23			2.53		
0.14			0.44			0.74			1.04			1.34			1.64	1		1.94			2.24			2.54		
0.15			0.45			0.75			1.05			1.35			1.65	1		1.95			2.25			2.55		
0.16			0.46			0.76			1.06			1.36			1.66			1.96	1		2.26			2.56		
0.17			0.47			0.77			1.07			1.37			1.67			1.97			2.27			2.57		
0.18			0.48			0.78			1.08			1.38			1.68	1		1.98	1	Inert	2.28			2.58		
0.19			0.49			0.79			1.09			1.39			1.69			1.99			2.29			2.59		
0.20			0.50			0.80			1.10		FGV	1.40			1.70			2.00			2.30			2.60		
0.21			0.51			0.81			1.11	1	↓	1.41			1.71			2.01			2.31			2.61		
0.22			0.52			0.82			1.12			1.42			1.72			2.02	1	Inert	2.32			2.62		
0.23			0.53			0.83	1		1.13			1.43			1.73			2.03			2.33			2.63		
0.24			0.54			0.84	1		1.14			1.44			1.74			2.04	1		2.34			2.64		
0.25			0.55			0.85	4		1.15			1.45			1.75			2.05		HAV	2.35			2.65		
0.26			0.56			0.86			1.16			1.46			1.76			2.06	1	↓	2.36			2.66		
0.27			0.57			0.87			1.17			1.47			1.77			2.07			2.37			2.67		
0.28			0.58			0.88			1.18			1.48			1.78			2.08			2.38			2.68		
0.29			0.59			0.89	1		1.19			1.49			1.79			2.09			2.39			2.69		
0.30			0.60			0.90			1.20			1.50			1.80			2.10			2.40			2.70		
0.31			0.61			0.91	1		1.21			1.51	1	↑	1.81			2.11			2.41			2.71		
0.32			0.62			0.92			1.22			1.52		HAV	1.82			2.12			2.42			2.72		
0.33			0.63			0.93	1		1.23			1.53			1.83			2.13			2.43			2.73		
0.34			0.64			0.94			1.24			1.54			1.84			2.14			2.44	1		2.74		
0.35			0.65			0.95	1		1.25			1.55			1.85			2.15			2.45			2.75		
0.36			0.66			0.96	1		1.26			1.56			1.86	1		2.16			2.46			2.76		
0.37			0.67			0.97	1		1.27			1.57			1.87			2.17			2.47			2.77		
0.38			0.68			0.98			1.28			1.58			1.88			2.18			2.48					Inert
0.39			0.69			0.99			1.29			1.59			1.89			2.19			2.49			3.34	1	↓

VITRINITE 0.1 (+0.1HA) %		INERTINITE 0.1 %						LIPTINITE <0.1 %								OIL DROPS <0.1 (0.1 in art comp)	BITUMEN
TV	DV	Sfus	Scler	Fus	Macr	ID	Micr	Spor <0.1	Cut	Sub	Res	Ld	Bituminite	Telalginite	Lamalginite <0.1	Oil cut	

Sample Number..T9941.....Well Name...Yolla-4 .....ORIGIN..... Depth...2925m..... ..... SampleType....Ctgs...
Date. ..21/.08/ 2004.. Op..ACC..... FGV - First Generation Vitrinite, RV - Reworked Vitrinite, HAV- heat altered vitrinite, Inert - Inertinite, Cav - Cavings, DA - Drilling Mud Additives MICR D:\RWORK.ms6\misc04vr.doc

R	No Read	Pop Range	R	No Read	Pop Range	R	No Read	Pop Range	R	No Read	Pop Range	R	No Read	Pop Range	R	No Read	Pop Range	R	No Read	Pop Range	R	No Read	Pop Range	R	No Read	Pop Range
0.10			0.40			0.70			1.00	3		1.30			1.60			1.90			2.20			2.50		
0.11			0.41			0.71			1.01			1.31			1.61			1.91			2.21			2.51		
0.12			0.42			0.72			1.02			1.32			1.62			1.92	1		2.22			2.52		
0.13			0.43			0.73			1.03	1		1.33			1.63			1.93		HAV	2.23			2.53		
0.14			0.44			0.74			1.04			1.34			1.64			1.94	1	↓	2.24			2.54		
0.15			0.45			0.75			1.05	1		1.35			1.65			1.95			2.25			2.55		
0.16			0.46			0.76			1.06			1.36			1.66			1.96			2.26			2.56		
0.17			0.47			0.77			1.07	2		1.37			1.67			1.97			2.27			2.57		
0.18			0.48			0.78			1.08	1		1.38			1.68			1.98			2.28			2.58		
0.19			0.49			0.79			1.09	1		1.39			1.69			1.99			2.29			2.59		
0.20			0.50			0.80	1	↑	1.10		FGV	1.40			1.70			2.00			2.30			2.60		
0.21			0.51			0.81	1	FGV	1.11	1	↓	1.41			1.71			2.01			2.31			2.61		
0.22			0.52			0.82			1.12			1.42			1.72			2.02			2.32			2.62		
0.23			0.53			0.83	2		1.13			1.43			1.73			2.03			2.33			2.63		
0.24			0.54			0.84	2		1.14			1.44	2	Inert	1.74			2.04			2.34			2.64		
0.25			0.55			0.85			1.15			1.45			1.75			2.05			2.35			2.65		
0.26			0.56			0.86	6		1.16			1.46			1.76			2.06			2.36			2.66		
0.27			0.57			0.87	1		1.17			1.47			1.77			2.07			2.37			2.67		
0.28			0.58			0.88	1		1.18			1.48			1.78			2.08			2.38			2.68		
0.29			0.59			0.89			1.19			1.49			1.79	1	↑	2.09			2.39			2.69		
0.30			0.60			0.90	1		1.20			1.50			1.80		HAV	2.10			2.40			2.70		
0.31			0.61			0.91			1.21			1.51			1.81			2.11			2.41			2.71		
0.32			0.62			0.92			1.22			1.52			1.82	1		2.12			2.42			2.72		
0.33			0.63			0.93	2		1.23			1.53			1.83			2.13			2.43			2.73		
0.34			0.64			0.94			1.24			1.54			1.84			2.14			2.44			2.74		
0.35			0.65			0.95	1		1.25			1.55			1.85			2.15			2.45			2.75		
0.36			0.66			0.96	1		1.26			1.56			1.86	1		2.16			2.46			2.76		
0.37			0.67			0.97	1		1.27			1.57			1.87			2.17			2.47			2.77		
0.38			0.68			0.98	1		1.28			1.58			1.88			2.18			2.48			2.78		
0.39			0.69			0.99	4		1.29			1.59			1.89			2.19			2.49			2.79		

VITRINITE 0.6 (+0.2HA) %		INERTINITE 0.2 %						LIPTINITE <0.1 %								OIL DROPS	BITUMEN <0.1 Meta-exsudat
TV	DV	Sfus	Scler	Fus	Macr	ID	Micr	Spor <0.1	Cut	Sub	Res	Ld	Bituminite	Telalginite	Lamalginite <0.1	Oil cut	

Sample Number..T9942.....Well Name...Yolla-4 .....ORIGIN..... Depth...3168m..... ..... SampleType....Ctgs...
Date. ..21/.08/ 2004.. Op..ACC..... FGV - First Generation Vitrinite, HAV- heat altered vitrinite; ME - meta-exsudatinite, Inert - Inertinite, Cav - Cavings, DA - Drilling Mud Additives MICR D:\RWORK.ms6\misc04vr.doc

R	No Read	Pop Range	R	No Read	Pop Range	R	No Read	Pop Range	R	No Read	Pop Range	R	No Read	Pop Range	R	No Read	Pop Range	R	No Read	Pop Range	R	No Read	Pop Range	R	No Read	Pop Range
0.10			0.40			0.70			1.00			1.30			1.60			1.90			2.20			2.50		
0.11			0.41			0.71			1.01			1.31			1.61			1.91			2.21			2.51		
0.12			0.42			0.72			1.02			1.32			1.62			1.92			2.22			2.52		
0.13			0.43			0.73			1.03			1.33			1.63			1.93			2.23			2.53		
0.14			0.44			0.74			1.04			1.34			1.64			1.94			2.24			2.54		
0.15			0.45			0.75			1.05			1.35			1.65			1.95			2.25			2.55		
0.16			0.46			0.76			1.06			1.36			1.66			1.96			2.26			2.56		
0.17			0.47			0.77			1.07			1.37			1.67			1.97			2.27			2.57		
0.18			0.48			0.78			1.08			1.38			1.68			1.98			2.28			2.58		
0.19			0.49			0.79			1.09			1.39			1.69			1.99			2.29			2.59		
0.20			0.50			0.80			1.10			1.40			1.70			2.00			2.30			2.60		
0.21			0.51			0.81			1.11			1.41			1.71			2.01			2.31			2.61		
0.22			0.52			0.82			1.12			1.42			1.72			2.02			2.32			2.62		
0.23			0.53			0.83			1.13			1.43			1.73			2.03			2.33			2.63		
0.24			0.54			0.84			1.14			1.44			1.74			2.04			2.34			2.64		
0.25			0.55			0.85			1.15			1.45			1.75			2.05			2.35			2.65		
0.26			0.56			0.86			1.16			1.46			1.76			2.06			2.36			2.66		
0.27			0.57			0.87			1.17			1.47			1.77			2.07			2.37			2.67		
0.28			0.58			0.88			1.18			1.48			1.78			2.08			2.38			2.68		
0.29			0.59			0.89			1.19			1.49			1.79			2.09			2.39			2.69		
0.30			0.60			0.90			1.20			1.50			1.80			2.10			2.40			2.70		
0.31			0.61			0.91			1.21			1.51			1.81			2.11			2.41			2.71		
0.32			0.62			0.92			1.22			1.52			1.82			2.12			2.42			2.72		
0.33			0.63			0.93			1.23			1.53			1.83			2.13			2.43			2.73		
0.34			0.64			0.94			1.24			1.54			1.84			2.14			2.44			2.74		
0.35			0.65			0.95			1.25			1.55			1.85			2.15			2.45			2.75		
0.36			0.66			0.96			1.26			1.56			1.86			2.16			2.46			2.76		
0.37			0.67			0.97			1.27			1.57			1.87			2.17			2.47			2.77		
0.38			0.68			0.98			1.28			1.58			1.88			2.18			2.48			2.78		
0.39			0.69			0.99			1.29			1.59			1.89			2.19			2.49			2.79		

VITRINITE %		INERTINITE %						LIPTINITE %								OIL DROPS	BITUMEN
TV	DV	Sfus	Scler	Fus	Macr	ID	Micr	Spor	Cut	Sub	Res	Ld	Bituminite	Telalginite	Lamalginite	Oil cut	

Sample Number..T9943.....Well Name...Yolla-4 .....ORIGIN..... Depth...3168m..... ..... SampleType....Ctgs...
Date. ..21/.08/ 2004.. Op..ACC..... FGV - First Generation Vitrinite, RV - Reworked Vitrinite, BTT - Bituminite, B - Bitumen, Inert - Inertinite, Cav - Cavings, DA - Drilling Mud Additives MICR D:\RWORK.ms6\misc04vr.doc

APPENDIX 6: PALYNOLOGY REPORT

PALYNOLOGY OF

YOLLA-4

BASS BASIN, AUSTRALIA

by

ROGER MORGAN

Prepared for
ORIGIN ENERGY

October 2004

REF: BAS.YOLLA-4 REPORT

PALYNOLOGY OF

YOLLA-4

BASS BASIN, AUSTRALIA

CONTENTS **PAGE**

1 SUMMARY

1340 m (cutts) – 1405 m (cutts) : *P. tuberculatus* Zone, upper subzone : Miocene : offshore marine : immature

1530 m (cutts) : *P. tuberculatus* Zone, lower subzone – *N. asp*erus Zone : Oligocne-Eocene : very nearshore marine : immature

1746 m (cutts) : ?*N. asperus* Zone " ?Eocene : marginally marine : immature

1884 m (cutts) – 1902 m (cutts) : *N. asperus* Zone, middle-lower subzones : Middle-Late Eocene : marginally mature

2313 m (cutts) – 2370 m (cutts) : *M. diversus* Zone, upper subzone : Early Eocene : nearshore marine to non-marine : marginally mature

2574 m (cutts) – 2625 m (cutts) : *M. diversus* Zone, middle subzone : Early Eocene : nearshore marine : early mature

2859 m (cutts) – 2925 m (cutts) : *M. diversus* Zone, lower subzone : Early Eocene : nearshore marine : early mature

3168 m (cutts) : *L. balmei* Zone, lower subzone : Paleocene : marginally marine or non-marine : fully mature

2 INTRODUCTION

Fifteen cuttings samples have been studied from Yolla-4 to provide routine correlation.

The Tertiary zonation framework is shown in Figure 1, from Partirdge (1973) modified for the Bass Basin. The zonation was subsequently published as Partridge (1976) and privately circulated against the Haq time scale. Comparisons are made in the text with the earlier report for Yolla-1 by Morgan (1985).

Palaeoenvironmental assessments are based on specimen counts of 100 specimens, also providing a percentage content of all species. Criterea for the palaeo-environmental subdivisions are given on Table 1. Backup data (listing % content of major plant groups) is given as Table 2. In running text, rare = <1-3%, frequent = 4-10%, common = 11-30%, abundant = 31-50% and superabundant = 51-100%.

Maturity data was generated in the form of Spore Colour Index, and are plotted on Figure 2 Maturity Profile, Yolla-4. The oil and gas windows follow the general consensus of geochemical literature. The oil window corresponds to spore colours of light-mid brown (Staplin Spore Colour Inex of 2.7) to dark brown (3.6) equal to vitrinite reflectanus of 0.6% to 1.3%.

.

TABLE 1

SUMMARY OF PALYNOLOGICAL DATA : YOLLA-4

LOG DEPTH (m)	SAMPLE TYPE	MICROFOSSIL YIELD	PERCENTAGE				DIVERSITY *1		SPORE-POLLEN SUBZONE	DINOFLAGELLATE ZONE/ACME	ENVIRONMENT*2
			MICROPLANKTON			SPORE-POLLEN-	MICROPLANKTON	SPORE-POLLEN			
			DINOFLAG	SPINY AC.	FRESH ALGAE		-				
1340	CUTTS	LOW	68	5	2	25	MOD	MOD	P. TUBERCULATUS, UPPER		OFFSHORE MAINRE
1405	CUTTS	LOW	44	3	1	52	MOD	MOD	P. TUBERCULATUS, UPPER		SHELFAL MARINE
1530	CUTTS	LOW	6	0	1	93	LOW	MOD	P. TUBERC-N. ASPERUS		VERY NEARSHORE MARINE
1746	CUTTS	LOW	3	0	1	96	EX LOW	HIGH	?N. ASPERUS		MARGINAL MARINE
1884	CUTTS	LOW	2	0	8	90	EX LOW	HIGH	N. ASPERUS, MID-LOW		MARGINAL MARINE
1902	CUTTS	LOW	6	1	7	86	EX LOW	HIGH	N. ASPERUS, MID-LOW		VERY NEARSHORE MARINE
2313	CUTTS	LOW	0	0	34	66	NIL	HIGH	M. DIVERSUS, UPPER		NON-MARINE (LAKE)
2331	CUTTS	LOW	2	1	28	69	EX LOW	HIGH	M. DIVERSUS, UPPER		MARGINAL MARINE
2370	CUTTS	LOW	12	2	15	71	LOW	MOD	M. DIVERSUS, UPPER		NEARSHORE MARINE
2574	CUTTS	LOW	16	1	2	81	LOW	V. HIGH	M. DIVERSUS, MIDDLE	H. TASMANIENSE	NEARSHORE MARINE
2586	CUTTS	LOW	11	1	1	87	LOW	HIGH	M. DIVERSUS, MIDDLE	H. TASMANIENSE	NEARSHORE MARINE
2625	CUTTS	LOW	14	0	0	86	LOW	HIGH	M. DIVERSUS, MIDDLE	ADNATOSPHAERIDIUM	NEARSHORE MARINE
2859	CUTTS	LOW	23	0	0	77	EX LOW	HIGH	M. DIVERSUS, LOWER	MORKALLACYSTA	NEARSHORE MARINE
2925	CUTTS	LOW	13	0	2	85	LOW	HIGH	M. DIVERSUS, LOWER	APECTODINIUM	NEARSHORE MARINE
3168	CUTTS	LOW	<1	0	0	100	EX LOW	HIGH	L. BALMEI, LOWER		?NON-MARINE

*1 DIVERSITY	
V HIGH	30+ SPECIES
HIGH	20-29 SPECIES
MOD	10-19 SPECIES
LOW	5-9 SPECIES
EX LOW	1-4 SPECIES

*2 ENVIRONMENTS	DINOFLAGELLATE CONTENT%	DINOFLAGELLATE DIVERSITY	FRESHWATER ALGAE CONTENT %
OFFSHORE MARINE	67 to 100	VERY HIGH	LOW
SHELFAL MARINE	34 to 66	HIGH	"
NEARSHORE MARINE	11 to 33	MODERATE	"
VERY NEARSHORE MARINE	5 to 10	MODERATE-LOW	"
MARGINAL MARINE	<1 to 4	LOW-VERY LOW	"
BRACKISH	0, SPINY ACRITARCHS ONLY	EXTREMELY LOW	"
NON-MARINE (UNDIFF)	0, NO SPINY ACRITARCHS	NIL	LOW
NON-MARINE (LACUSTRINE)	0, NO SPINY ACRITARCHS	NIL	MODERATE 10%+

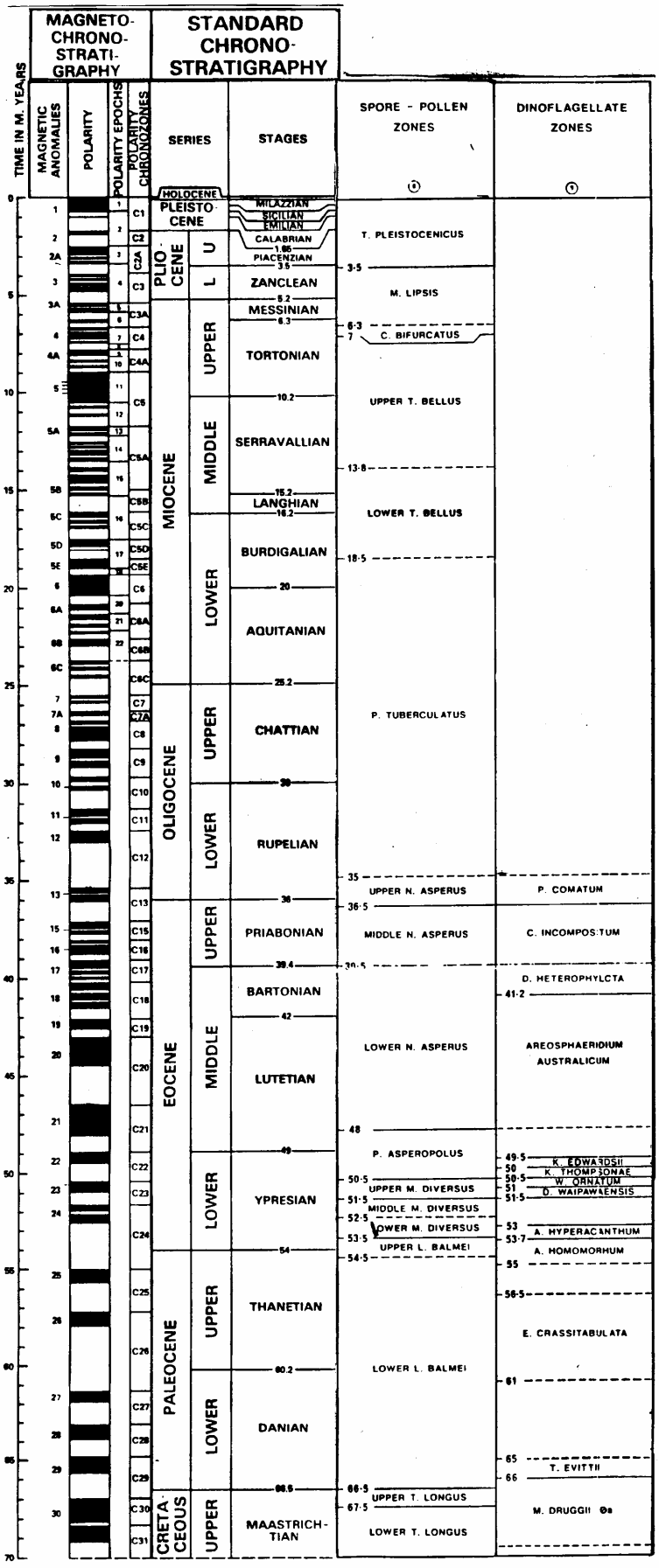

FIGURE 1 **TERTIARY ZONATION SCHEME (Partridge 1976 and pers. comm. using time scale of Haq et al)**

FIGURE 2 MATURITY PROFILE : YOLLA-4

3 PALYNOSTRATIGRAPHY

3.1 1340 m (cutts) – 1405 m (cutts) : *P. tuberculatus* Zone, upper subzone

Assignment of these lean assemblages is suggested at the top by the top of dominant *Nothofagidites* spp. amongst the spore-pollen and the absence of younger markers. It is suggested at the base by oldest *Acaciapollenites myriosporites* (although this could be caved). Spores and pollen are subordinant to the dinoflagellates but include common *Nothofagidites* spp. and *Haloragacidites harrisii*, frequent *Cyathidites minor, Falcisporites similis* and *Vitreisporites pallidus*. Rare elements include *A. myriosporites, Lygistepollenites florinii, Nothofagidites falcata* and *Nothofagidites flemingii.*

Dinoflagellates are dominant and include abundant *Spiniferites ramosus* and frequent *Hystrichokolpoma* spp. and *Operculodinium* spp. Rare elements include *Impletosphaeridium* sp. 1, *Lingulodinium machaerophorum, Systematophora placacantha* and *Thalassiphora delicata*, but none are zone diagnostic.

Offshore (1340 m) to shelfal (1405 m) marine environments are indicated by the dominant to subequal proportions of diverse marine dinoflagellates to terrestrial spores and pollen.

Yellow spore colours indicate immaturity for hydrocarbons.

3.2 1530 m (cutts) : *P. tuberculatus* Zone, lower subzone – *N. asperus* Zone

Assignment of this lean assemblage is suggested by youngest *Aglaoridia qualumis* and *Kuylisporites waterbolkii*, but the base is not crisply defined and the absence of *Cyatheacidites annulatus* and *Foveotriletes crater* suggests that it could be as old as the *N. asperus* Zone. Super-abundant are *Nothofagidites* spp. (mostly *N. emarcidus*) with frequent *C. minor, F. similis* and *H. harrisii*. Rare elements include *A. qualumis, R. waterbolkii, L. florinii, N. falcata* and *Proteacidites rectomargimus.*

Dinoflagellates are frequent but of low diversity with *S. ramosus* and *Operculodinium* spp. the most frequent. Rare elements include *Deflandrei phosphoritica.*

Very nearshore marine environments are indicated by the scarce low diversity dinoflagellates amongst the dominant and diverse spores and pollen.

Yellow spore colours indicate immaturity for hydrocarbons.

3.3 1746 m (cutts) :?*N. asperus* Zone

Assignment is uncertain as relatively few palynomorphs were seen amongst the dominant plant debris (mostly inertinite and amorphous organic matter (AOM)). Amongst the spores and pollen, abundant is *N. emarcidus* with common *C. minor* and *Phyllocladidites mawsonii* and frequent *Cyathidites australis, F. similis, H. harrisii* and *Nothofagidites deminutus*. Rare elements include *Malvacipollis subtilis, N. flemingii, P. rectomarginus* and *Verrucosisporites kopukuensis*.

Dinoflagellates are extremely rare and not age diagnostic.

Marginal marine environments are indicated by the rare low diversity dinoflagellates amongst the dominant and diverse spores and pollen.

Yellow spore colours indicate immaturity for hydrocarbons.

3.4 1884 m (cutts) – 1902 m (cutts) : *N. asperus* Zone, middle-lower subzones

Assignment is indicated at the top by youngest *Proteacidites pachypolus* and at the base by oldest dominant *Nothofagidites* spp. Common are *N. emarcidus* with frequent *C. australis, C. minor, F. similis, H. harrisii, Osmundacidites wellmanii* and *Vitreisporites pallidus.* Rare elements include *M. subtilis, N. flemingii, Periporopollenites vesicus, Proteacidites incurvatus, P. grandis, P. pachypolus* and *Stereisporites punctatus.*

Dinoflagellates are frequent but include rare *S. placacantha*, consistent with the spore-pollen assignment.

Very nearshore (1902 m) to marginal marine (1884 m) environments are indicated by the minor low diversity dinoflagellates amongst the dominant and highly diverse spores and pollen.

Light brown spore colours indicate marginal maturity for oil but immaturity for gas/condensate.

3.5 2313 m (cutts) – 2370 m (cutts) : *M. diversus* Zone, upper subzone

Assignment is indicated at the top by youngest *Myrtaceidites tenuis* and *Proteacidites ornatus* without younger markers, and at the base on oldest *M. tenuis*. *Proteacidites asperopolus* was not seen and suggests that the *P. asperopolus* Zone is unsampled. Common is *H. harrisii* with frequent *Proteacidites* spp. Rare elements include *Beaupreadites verrucosus, M. subtilis, M. tenuis, Polycolpites esobolteus, P. grandis, P. ornatus, Proteacidites leightonii, Proteacidites tuberculiformis* and *Triporopollenites ambiguus.*

Dinoflagellates are absent at 2313 m, rare at 2331 m and frequent at 2370 m, but not age diagnostic.

Environments are very nearshore to non-marine as indicated by the minor to absent dinoflagellates, and the dominant and diverse spores and pollen.

Light to mid brown spore colours indicate marginal maturity for oil.

3.6 2574 m (cutts) – 2625 m (cutts) : *M. diversus* Zone, middle subzone

Assignment is indicated at the top by youngest *Peninsulapollis gillii* and the absence of younger markers and at the base by oldest *P. ornatus* and *P. tuberculiformis*, supported at 2586 m by oldest *T. ambiguus*. Common are *H. harrisii* and *C. minor* with frequent *Araucariacites australis, Dilwynites granulatus, F. similis, N. emarcidus, Proteacidites* spp. and *V. pallidus*. Rare elements include *Intratriporopollenites notabilis, P. grandis, P. ornatus, P. tuberculiformis, P. incurvatus, T. ambiguus* and *P. gillii.*

Dinoflagellates include *Homotriblium tasmaniense* at 2574 m and 2586 m but this is usually associated with the *P. asperopolus* and upper *M. diversus* Zones and is seen in Yolla-1 at 2282-2417 m in the upper *M. diversus* Zone. At 2586 m and 2625 m, *Adnatosphaeridium* sp. occurs and was seen in Yolla-1 at 2417-2471 m in the upper *M. diversus* and middle *M. diversus* Zone. The dinoflagellates are thus approximately compatible but do suggest that some of this interval might belong to the upper rather than middle *M. diversus* Zone. On the other hand, the

dinoflagellates may be partly caved. At 2574 m and 2586 m, *S. ramosus* and *H. tasmaniense* are frequent with rare *Muratodinium fimbriatum* and *Apectodinium quinquelatum.* At 2625 m, *Adnatosphaeridium* sp. is frequent with rare *M. fimbriatum* and *Apectodinium homomorphum*.

Nearshore marine environments are indicated by the dominant and diverse spores and pollen and less numerous low diversity dinoflagellates.

Mid brown spore colours indicate early maturity for oil and early marginal maturity for gas/condensate. Some black spores at 2574 m suggest reworking or vulcanicity during deposition.

3.7 2859 m (cutts) – 2925 m (cutts) : *M. diversus* Zone, lower subzone

Assignment is indicated at the top by the absence of younger markers, and at the base by *P. grandis* without older markers. Common are *F. similis* and *C. minor* with frequent *A. australis, D. granulatus* and *V. pallidus*. Rare elements include *M. subtilis, N. flemingii, P. grandis, P. gillii* and a single *Polycolpites langstonii* at 2925 m.

Dinoflagellates include *Morkallacysta* sp., common at 2859 m and rare at 2925 m. This is consistent with Yolla-1 where *Morkallacysta* sp. was common at 2711-2731 m in the lower *M. diversus* Zone. At 2925 m, *Apectodinium* spp. are frequent, a feature seen in Yolla-1 at 2783 m. Rare elements include *Adnatosphaeridium* sp. (probably caved) and *M. fimbriatum. Apectodinium hyperacanthum* occurs in both samples.

Nearshore marine environments are indicated by the dominant and diverse spores and pollen and the less numerous low diversity dinoflagellates.

Mid brown spore colours indicate early maturity for oil and early marginal maturity for gas/condensate.

3.8 3168 m (cutts) : *L. balmei* Zone, lower subzone

Assignment is indicated by youngest *Gambierina rudata* and *Lygistepollenites balmei* without older markers. The lower subzone is indicated by the absence of the upper subzone markers seen in Yolla-1. Abundant is *F. similis* with common *D. granulatus* and frequent *C. minor, M. antarcticus, N. emarcidus, P. mawsonii, P. microsaccatus* and *V. pallidus*. Rare elements include *Cyathidites gigantis, G. rudata, L. balmei* and *Nothofagidites endurus.*

Dinoflagellates are extremely scarce and include only *Morkallacysta* sp. which may be caved.

Environments are marginally marine or freshwater, depending on the significance of *Morkallacysta* sp. which has been suggested to be a freshwater dinoflagellate. Totally dominant and diverse are the spores and pollen.

Dark brown spore colours indicate full maturity for oil and marginal maturity for gas/condensate.

4 REFERENCES

Morgan, R.P., (1985) Palynology of Amoco Yolla-1, Bass Basin, Australia *unpubl rept for Amoco Australia*

Partridge, A D (1973) Revision of the spore-pollen zonation in the Bass Basin, *Esso unpubl. palaeo. rept. 1973/4*

Partridge, A D (1976) The geological expression of eustacy in the Early Tertiary of the Gippsland Basin *Aust. Pet. Explor. Assoc., J,* 16:73-79

Well Name : YOLLA-4

Operator : ORIGIN

Interval : 1320m - 3188m — **Palynological Data Chart : BASIC DATA**

Scale : 1:10000 — **% Abundance histogram : Highest occurrence**

Chart date: 21 October 2004 — **Roger Morgan**

YOLLA-4

Morgan Palaeo Associates
Maitland, South Australia

Enclosure 1

Sampling
Cutting
Core
Sidewall core

Text Keys
*1 % within discipline (40mm=100%)
*2 In-Situ occurrences

Depth | Samples (Samples in Discipline(s) : Paly)

Dinoflagellate Cysts — % within discipline (40mm=100%); In-Situ occurrences

Apteodinium australiense
Compositosphaeridium sp.
Hystrichokolpoma rigaudiae
Hystrichokolpoma sp.
Hystrichosphaeridium tubiferum
Impletosphaeridium sp. 1
Linguludinium machaerophorum
Operculodinium spp.
Paralecaniella indentata
Spiniferites ramosus
Systematophora placacantha
Thalassiphora delicata
Cordosphaeridium inodes
Cordosphaeridium multispinosum
Dapsilidinium pastielsii
Hystrichokolpoma eisenackii
Impagidinium sp.
Nematosphaeropsis balcombiana
Areosphaeridium arcuatum
Deflandrea phosphorica
Spiniferites spp.
Morkatacysta spp.
Millioudodinium tenuitabulatum
Saeptodinium spp.
Homotryblium tasmaniense
Adnatosphaeridium spp.
Apectodinium quinquelatum
Cordosphaeridium fibrospinosum
Muratodinium fimbriatum
Apectodinium homomorphum
Glaphyrocysta sp.
Apectodinium hyperacanthum
Apectodinium homomorphum (short spines)
Micrhystridium spp.
Microforams -
Crassosphaera concinna
Botryococcus spp.
Reworking - Triassic
Acaciapolleniles myriosporites
Cyathidites australis
Cyathidites minor
Dilwynites tuberculatus
Falcisporites similis
Haloragacidites harrisii
Lygistepollenites florinii
Microcachryidites antarcticus
Nothofagidites emarcidus
Nothofagidites falcatus
Nothofagidites flemingii
Osmundacidites wellmanii
Phyllocladidites mawsonii
Tricolpites sp.
Nothofagidites asperus
Nothofagidites deminutus
Proteacidites spp.
Vitreisporites pallidus
Aglaoreidia qualumis
Araucariacites australis
Ceratosporites equalis
Dilwynites granulatus
Kuylisporites waterbolki
Periporopollenites vesicus
Proteacidites rectomarginis
Cycadopites follicularis
Dictyophyllidites spp.
Ericipites scabratus
Gleicheniidites spp.
Laevigatosporites ovatus
Malvacipollis subtilis
Podosporites microsaccatus
Triletes tuberculiformis
Verrucosisporites kopukuensis
Callialasporites dampieri
Corollina torosa
Ephedripites spp.
Proteacidites incurvatus
Proteacidites pachypolus
Retitrilites austroclavatidites
Stenesporites punctatus
Verrucosisporites spp.
Clavifera triplex
Proteacidites grandis
Proteacidites leightonii
Stereisporites antiquasporites
Cyathidites splendens
Myrtaceidites tenuis
Polycolporopollenites esobalteus
Proteacidites ornatus
Proteacidites sp.
Tricolporites "estoutus"
Cyathidites giganteus
Triporopollenites ambiguus
Intratriporopollenites notabilis
Proteacidites tuberculiformis
Beaupreaidites verrucosus
Tricolporites spp.
Callialasporites turbatus
Peninsulapollis gillii
Perinopollenites elatoides
Cupaneieidites orthoteichus
Proteacidites clinei ms
Leptolepidites verrucatus
Falcisporites grandis
Polycolpites langstonii
Lygistepollenites balmei
Nothofagidites erinduris
Fungate .

Depth | Samples (Samples in Discipline(s) : Paly) | In-Situ occurrences: Total count: Total Count | In-Situ occurrences: Category %: % Category

Depth	Samples	Total count	Category %
1340m	1340.00m CU	100	
1400m	1405.00m CU	100	
	1530.00m CU	100	
1600m			
	1746.00m CU	100	
1800m			
	1884.00m CU	100	
	1902.00m CU	100	
2000m			
2200m			
	2313.00m CU	100	
	2331.00m CU	100	
2400m	2370.00m CU	100	
	2574.00m CU	99	
2600m	2586.00m CU	100	
	2625.00m CU	100	
2800m	2859.00m CU	100	
	2925.00m CU	100	
3000m			
	3168.00m CU	100	

FU
MP
AC
AL
FT
ALBO
DC
SP

APPENDIX 7: PETROLOGY REPORT

RESERVOIR SOLUTIONS PTY LTD
LEVEL 2, 2 PARK RD, MILTON, 4064, QLD
PO BOX 2098, MILTON, 4064, QLD
ABN 27 088 995 073

PETROLOGY, DIAGENESIS AND RESERVOIR QUALITY OF MSCT SAMPLES FROM YOLLA-4

Julian C. Baker PhD

A report to:

Origin Energy Resources Ltd
339 Coronation Drive
Milton QLD 4064

15 October, 2004

CONTENTS

Page

C O N T E N T S cont.

EXECUTIVE SUMMARY

A petrological study was carried out on four msct samples from 2606.5-2608.2m and 3158.0-3159.0m in Yolla-4. Analytical techniques used were thin-section analysis, bulk-rock/fine-fraction X-ray diffraction analysis and scanning electron microscopy/energy dispersive spectroscopy.

Samples are thinly laminated, very fine grained quartzarenites (2606.5m, 2608.2m), a sideritic arenaceous mudrock (3158.0m) and a fine grained sublitharenite (3159.0m) in which grains are mainly quartz and also include metamorphic rock fragments, mica and organic fragments. Feldspar is absent.

Clay in the sandstones is mostly authigenic kaolin that forms scattered patches and patchy/dispersed pseudomatrix where compacted micaceous/illitic metamorphic rock fragments and mica have altered. Clay minerals detected by XRD are kaolinite, dickite, illite/mica and highly illitic mixed-layer illite/smectite.

Diagenetic effects in the sandstones besides authigenic kaolin formation include siderite replacement/cementation, quartz overgrowth cementation, grain contact dissolution, stylolite seam formation and ductile grain deformation. Detrital clay in arenaceous mudrock at 3158.0m is extensively replaced by siderite.

Visible porosity does not exceed 2% and is accounted for by widely scattered and erratically distributed primary intergranular pores and subordinate, commonly kaolin-clogged secondary labile grain dissolution pores. Severe porosity reduction in the sandstones results from the deleterious effects of diagenesis (siderite/quartz overgrowth cementation, authigenic kaolin formation, compaction).

Sandstones would have very low permeability.

Samples from 2606.5m and 3158.0m would have very high grain density (>3.0 g/cm^3) due to the presence of abundant siderite.

1. INTRODUCTION

A petrological study was carried out on four msct samples from 2606.5-2608.2m (#16, #17) and 3158.0-3159.0m (#10, #9) (log depths) in Yolla-4 in order to provide information on mineralogy, diagenetic effects and controls on reservoir quality. The study complements an earlier petrological study of core samples from Yolla-4 (2899.2-2981.4m) by Baker (2004).

2. ANALYTICAL PROGRAM

2.1 THIN-SECTION ANALYSIS

Thin-sections were cut in kerosene, impregnated with blue-dyed epoxy resin to aid porosity recognition, and stained with sodium cobaltinitrite to aid feldspar identification. Mineral composition and visible porosity were determined by a count of 400 points, and mean quartz grain size and sorting were estimated in thin-section with the aid of an eyepiece graticule. Photomicrographs were taken of each thin-section to illustrate texture, composition, clay distribution, diagenetic effects and porosity.

2.2 X-RAY DIFFRACTION ANALYSIS

Bulk-rock X-ray diffraction (XRD) analysis was carried out on each sample in order to quantify mineral abundance. The XRD analysis used a finely ground whole rock powder sample and the SIROQUANT processing technique was used to calculate mineral abundance.

XRD analysis was carried out on the fine fraction of each sample in order to precisely determine clay mineralogy. The fine fraction was separated from each sample by disaggregation and settling in distilled water and was air dried on glass discs to produce oriented specimens for XRD analysis. Samples were analysed in air dried condition and also following treatment with ethylene glycol.

2.3 SCANNING ELECTRON MICROSCOPY

Scanning electron microscopy (SEM) was carried out on two samples (#16, 2606.5m; #9, 3159.0m) in order to provide information on clay distribution, diagenetic effects and porosity characteristics. Analyses were done on freshly exposed surfaces that had been thoroughly washed in shellite to remove any volatile hydrocarbons. Energy dispersive spectroscopy (EDS) was used to determine the elemental composition of authigenic minerals.

3. TEXTURE

Lithology and texture are given in Table 1. The top two samples (#16, 2606.5m; #17, 2608.2m) are thinly laminated, well sorted, very fine grained sandstones with a mean grain size of 0.09mm and 0.12mm. Laminae in #16 are defined by concentrations of sideritised clay grains and fine organic fragments/stringers, whereas laminae in #17, which are stylolitic, are defined by concentrations of strongly compacted mica flakes and fine organic fragments.

The deepest sample (#9, 3159.0m) is a well compacted, well sorted, fine grained sandstone with a mean grain size of 0.16mm and in which there are scattered, compacted, medium to coarse sand-sized sideritised clay grains.

Sample #10 (3158.0m) is a bioturbated arenaceous mudrock in which strongly sideritised detrital clay matrix supports irregularly-distributed (due to burrowing), moderately-well sorted, very fine to medium sand-sized siliciclastic grains.

Ignoring quartz overgrowths and the effects of grain contact dissolution, most quartz grains are angular to subrounded.

4. THIN-SECTION COMPOSITION

Thin-section composition is given in Table 1, sandstone QFR composition is plotted in Figure 1, and annotated photomicrographs are presented in Appendix 2.

The arenaceous mudrock (#10, 3158.0m) consists mainly of detrital clay matrix that is extensively replaced by finely-crystalline siderite. Grains in the mudrock have the same composition as those in the sandstones (see below). The mudrock is not discussed further in this section.

4.1 FRAMEWORK GRAINS

The top two sandstones (#16, 2606.5m; #17, 2608.2m) are quartzarenites ($Q_{96}F_0R_4$ mean), whereas the deepest sandstone (#9, 3159.0m) is a sublitharenite ($Q_{88}F_0R_{12}$). Framework grains are mainly quartz and also include metamorphic rock fragments, mica and organic fragments.

Total detrital quartz content is variable (39.3-61.6%), reflecting wide differences in siderite content. Quartz is mainly monocrystalline. Polycrystalline quartz includes metaquartzite and recrystallised metamorphic quartz with aligned mica inclusions. Quartz grains are enveloped by well-developed quartz overgrowths where adjacent intergranular spaces are not filled by clay or siderite.

Total rock fragment content is 1.7-3.0% in the top two sandstones (#16, 2606.5m; #17, 2608.2m) and is 7.6% in the deepest sandstone (#9, 3159.0m). Lithic grains are almost entirely quartzose/micaceous/illitic, low-grade metasedimentary rock fragments (quartz/mica schist, mica/illite-bearing quartzite, metasandstone, metasiltstone, meta-argillite) and also include silicified volcanic rock fragments.

TABLE 1. THIN-SECTION ANALYSES

Sample #	16	17	10	9
Depth (mRT)	2606.5	2608.2	3158.0	3159.0
Lithology	sid sst	sst	sid mrk	sid sst
Quartz (monocrystalline)	38.6	61.3	22.0	53.4
Quartz (polycrystalline)	0.7	0.3	1.1	3.0
Quartz overgrowths	3.0	3.4	-	1.3
Chert	-	-	-	1.0
Feldspar	-	-	-	-
Volcanic rock fragments	-	-	-	0.3
Metamorphic rock fragments	1.7	3.0	0.7	7.6
Sedimentary rock fragments	-	-	-	-
Mica	2.3	7.3	0.3	1.7
Heavy minerals	1.0	-	-	-
Organic fragments	3.6	1.7	6.6	-
Siderite	38.1	2.0	50.4	15.3
Anatase/leucoxene	0.7	0.3	-	0.3
Authigenic kaolin	8.0	17.7	0.3	15.4
Authigenic illitic clay	0.3	1.3	-	0.7
Detrital clay	-	-	18.6	-
Primary porosity	1.7	1.4	-	-
Secondary porosity	0.3	0.3	-	-
Q (quartz + chert)	96.1	95.6	-	88.1
F (feldspar)	0.0	0.0	-	0.0
R (rock fragments)	3.9	4.4	-	11.9
Mean grain size (mm)	0.09	0.12	0.12	0.16
Grain size class	v fine	v fine	v fine	fine
Sorting class	well	well	m well	well

sid sst = sideritic sandstone sid mrk = sideritic arenaceous mudrock

FIGURE 1. QFR COMPOSITION

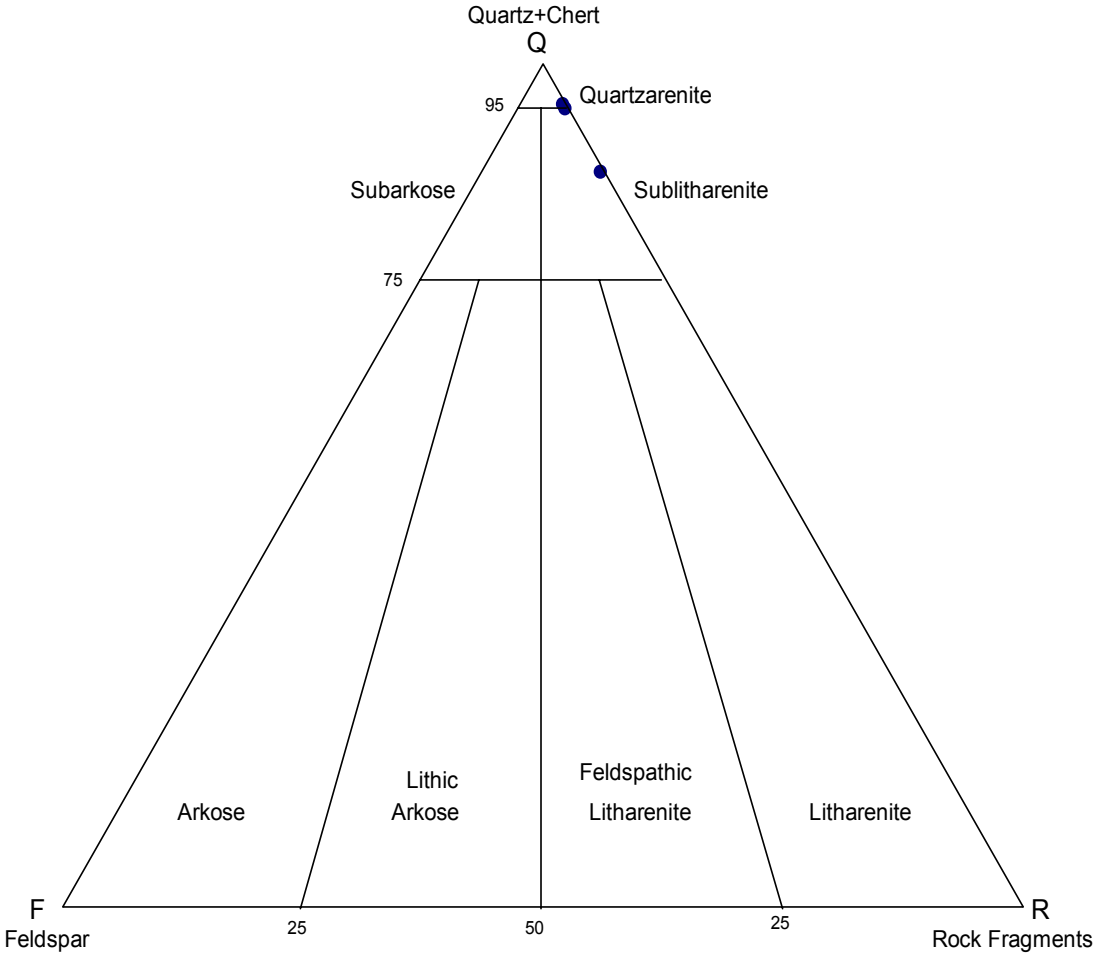

Other detrital grains include chert, mica (fresh and variably kaolinitised muscovite and subordinate biotite), sideritised clay grains (argillaceous intraclasts) and accessory heavy minerals (brown tourmaline, zircon, monazite, opaques). In #16 (2606.5m) and #17 (2608.2m), fine organic fragments/stringers are concentrated with sideritised clay grains and muscovite flakes along thin laminae. In #16, monazite grains are rimmed by radiogenically-immobilised bitumen. Feldspar is absent.

Detrital grain assemblages indicate a provenance that included low-grade metasedimentary rocks and granites.

4.2 Clays

Clay ranges from 8.3% to 19.0% and is mainly authigenic kaolin that forms scattered patches and patchy/dispersed pseudomatrix where compacted labile grains, particularly micaceous/illitic metamorphic rock fragments and mica, have altered. Clay also includes authigenic illitic clay that is associated with partly altered micaceous grains. Detrital clay is absent.

4.3 Cements

The top sample (#16, 2606.5m) contains 38.1% siderite, much of which is concentrated along thin laminae, where it forms grain-sized and oversized, microcrystalline/finely-crystalline patches that replace clay grains and altered biotite. Elsewhere in the sample, siderite is extensively developed between some laminae as a finely-crystalline, pore-filling cement. Siderite is also abundant (15.3%) in #9 (3159.0m), where it forms scattered, microcrystalline/finely-crystalline replacement patches and disseminated, fine rhombic crystals and microspherulites. In contrast to the other two sandstones, #17 (2608.2m) contains little (2.0%) siderite, most of which replaces clay grains along micaceous stylolitic laminae.

Quartz overgrowth content does not exceed 3.4% and would be much higher had quartz overgrowth cementation not been inhibited by the presence of abundant siderite and authigenic kaolin. Quartz overgrowths commonly completely fill intergranular spaces between juxtaposed quartz grains to form triple point grain junctions.

4.4 Visible Porosity

The top two sandstones (#16, 2606.5m; #17, 2608.2m) contain only minor (1.7-2.0%) visible porosity, and the deepest sandstone (#9, 3159.0m) contains negligible visible porosity, reflecting extensive pore filling by authigenic kaolin, siderite, quartz overgrowths and compacted ductile grains. Visible porosity is accounted for by widely scattered and erratically distributed primary intergranular pores and subordinate, commonly kaolin-clogged secondary labile grain dissolution pores.

5. X-RAY DIFFRACTION ANALYSES

Quantitative bulk-rock and fine-fraction XRD analyses were carried out on each sample. Quantitative XRD analyses are given in Table 2, fine-fraction clay mineralogy is given in Table 3, and annotated XRD traces are presented in Appendix 1.

Quantitative XRD analyses complement the thin-section analyses but cannot be compared directly. This is because thin-section kaolin and siderite include microporosity, and therefore total thin-section kaolin and siderite are elevated relative to other components. In addition, the thin-section rock fragment component includes quartz and illite/mica that are recorded as these phases by XRD.

Quantitative XRD analyses show that quartz content ranges from 31.0% to 68.3% and varies mainly according to siderite content (1.2-48.9%). The top sandstone (#16, 2606.5m) and arenaceous mudrock (#10, 3158.0m) are distinguished by their high siderite content. Total clay mineral content is 18.7-26.4%. Clay minerals are kaolinite (9.5-13.3%), illite/mica (6.9-12.0%), dickite (1.0-4.3%) and mixed-layer illite/smectite (<2.1%). Other detected minerals are anatase (0.1%) and contaminant barite (trace).

Fine-fraction XRD analyses (Table 3) show that kaolin (kaolinite + dickite) dominates over illite/mica and mixed-layer illite/smectite and that mixed-layer illite/smectite is a highly illitic variety, containing 80-85% illite interlayers at 2606.5-2608.2m and 90-95% illite interlayers at 3158.0-3159.0m. Smectitic clays are absent.

In the sandstones, detected kaolin has an authigenic origin, whereas most detected illite would occur as fine detrital mica, as a breakdown product of micaceous grains and as an original constituent of metamorphic rock fragments. Detected illitic mixed-layer illite/smectite would be a labile grain alteration product. Clay XRD analyses for the arenaceous mudrock (#10, 3158.0m) indicate that detrital clays are kaolinite and illite.

6. DIAGENESIS

Samples have been severely affected by diagenesis, with the main diagenetic effects being siderite cementation/replacement, authigenic kaolin formation and quartz overgrowth cementation. Textural relationships are consistent with the diagenetic paragenesis given by Baker (2004) for sandstones in Yolla-4 (2899.2-2981.4m).

Fine **siderite** is abundant (38.1%, 15.3%) in two sandstones (#16, 2606.5m; #9, 3159.0m), where it replaces clay grains and altered biotite and forms a pore-filling cement (Plates 1, 3, 6). Thin laminae in #16 (2606.5m) are defined by concentrations of siderite replacement (Plate 1). Fine siderite is also abundant (50.4%) in the arenaceous mudrock (#10, 3158.0m), where it extensively replaces detrital clay matrix (Plate 5). EDS analyses indicate that the siderite is enriched in magnesium and calcium.

Authigenic kaolin in the sandstones ranges from 8.0% to 17.7% and forms scattered patches and patchy/dispersed pseudomatrix where compacted labile grains, particularly micaceous/illitic metamorphic rock fragments and mica, have altered (Plate 1; Plate 2, Fig. 2; Plates 3, 4, 6, 7). Remnants of kaolin-precursor micaceous grains are locally included within authigenic kaolin patches, and mica grains are commonly partly altered to kaolin. With the arenaceous mudrock (#10, 3158.0m) lacking feldspar and containing little

TABLE 2. BULK-ROCK XRD ANALYSES

Sample #	16	17	10	9
Depth (mRT)	2606.5	2608.2	3158.0	3159.0
Quartz	36.5	68.3	31.0	63.8
Dickite	1.0	4.0	1.3	4.3
Kaolinite	12.8	13.3	9.5	12.9
Illite/mica	7.9	12.0	7.6	6.9
Illite/smectite	2.0	1.1	1.6	1.4
Siderite	39.7	1.2	48.9	10.6
Anatase	0.1	0.1	0.1	0.1
Barite	-	-	-	T

T = trace

TABLE 3. FINE-FRACTION CLAY MINERALOGY

Sample #	16	17	10	9
Depth (mRT)	2606.5	2608.2	3158.0	3159.0
Kaolin	A	A	A	A
Illite/mica	m	M	m	m
Illite/smectite	m	m	T	m
Smectite	-	-	-	-
Chlorite	-	-	-	-
I/S illite content (%)	80-85	80-85	90-95	90-95

A = abundant; M = major; m = minor; T = trace

I/S = mixed-layer illite/smectite

authigenic kaolin, it appears that no authigenic kaolin in the sandstones is a product of feldspar alteration. Accordingly, the absence of feldspar in the sandstones is not due to diagenesis. Consisting of loosely packed, stacked, 8-20µm pseudohexagonal plates (Plate 3), kaolin patches are typically highly microporous. XRD analyses indicate that the kaolin polytype is both kaolinite and dickite.

Quartz overgrowth content ranges up to 3.4% (Plates 1-3). Complete quartz overgrowth cementation has formed common triple point grain junctions between juxtaposed quartz grains (Plates 6, 7), but, between many quartz grains, quartz overgrowth cementation was inhibited by the presence of authigenic kaolin and siderite.

Other diagenetic effects include the compactional deformation of (sideritised/kaolinitised) micaceous/argillaceous grains (Plates 6, 7), grain welding by grain contact dissolution (pressure solution) (Plate 4), secondary porosity formation by labile grain dissolution, and anatase/leucoxene formation. Thin, low-amplitude stylolitic seams in #17 (2608.2m) are defined by concentrations of compactionally-deformed mica flakes and organic fragments (Plate 4).

7. RESERVOIR QUALITY

The top two sandstones **(#16, 2606.5m; #17, 2608.2m**) are very fine grained quartzarenites that contain little (<2.1%) macroporosity due to siderite (#16) and quartz overgrowth cementation, grain welding by grain contact dissolution, and authigenic kaolin formation. In addition, the sandstones are cut by several tight laminae along which well-compacted sideritised clay grains, organics and mica are concentrated. Laminae are stylolitic in #17. Macropores are isolated and erratically distributed and thus would have little or no interconnectivity on a thin-section scale, particularly in #16, which not only includes tight laminae, but also a 6mm-thick, strongly siderite-cemented zone in which all intergranular spaces are tightly filled by fine rhombic siderite crystals. Containing little macroporosity and being very fine grained, both samples would have very low permeability.

The deepest sample (**#9, 3159.0m**), which is significantly more lithic labile than the previous sandstones, is a fine grained sublitharenite that contains negligible macroporosity due to complete pore filling by kaolin, siderite, quartz overgrowths and compacted micaceous grains. Permeability would be very low.

All three sandstones therefore have poor reservoir quality due to the deleterious effects of diagenesis coupled with fine grain size.

The arenaceous mudrock (**#10, 3158.0m**) is totally microporous and thus would have negligible permeability.

Samples from 2606.5m and 3158.0m would have very high grain density (>3.0 g/cm^3) due to the presence of abundant siderite.

8. SUMMARY AND CONCLUSIONS

- Samples from 2606.5-2608.2m and 3158.0-3159.0m in Yolla-4 are thinly laminated, very fine grained quartzarenites (#16, #17), a sideritic arenaceous mudrock (#10) and a fine grained sublitharenite (#9) in which grains are mainly quartz and also include metamorphic rock fragments, mica and organic fragments. Feldspar is absent.

- Clay in the sandstones is mostly authigenic kaolin that forms scattered patches and patchy/dispersed pseudomatrix where compacted micaceous/illitic metamorphic rock fragments and mica have altered.

- XRD analyses indicate that clay minerals are kaolin (kaolinite, dickite), illite/mica and highly illitic mixed-layer illite/smectite.

- Diagenetic effects in the sandstones besides authigenic kaolin formation include siderite replacement/cementation (particularly in #16 and #9), quartz overgrowth cementation, grain contact dissolution, stylolite seam formation (#17) and ductile grain deformation (particularly in #9). Detrital clay in the arenaceous mudrock (#10) is extensively replaced by siderite.

- Visible porosity does not exceed 2% and is accounted for by widely scattered and erratically distributed primary intergranular pores and subordinate, commonly kaolin-clogged secondary labile grain dissolution pores. Severe porosity reduction in the sandstones results from the deleterious effects of diagenesis (siderite/quartz overgrowth cementation, authigenic kaolin formation, compaction).

- Sandstones would have very low permeability.

- Samples from 2606.5m and 3158.0m would have very high grain density (>3.0 g/cm^3) due to the presence of abundant siderite.

REFERENCES

Baker, J.C., 2004, Petrology, diagenesis and reservoir quality of core samples from Yolla-4. Report to Origin Energy Resources Ltd.

APPENDIX 1.

X-RAY DIFFRACTOGRAMS

Key to abbreviations:

A = anatase

Ba = contaminant barite

D = dickite

I = illite/mica

I/S = illitic mixed-layer illite/smectite

K = kaolinite

Q = quartz

S = siderite

#16 2606.5m
Bulk rock

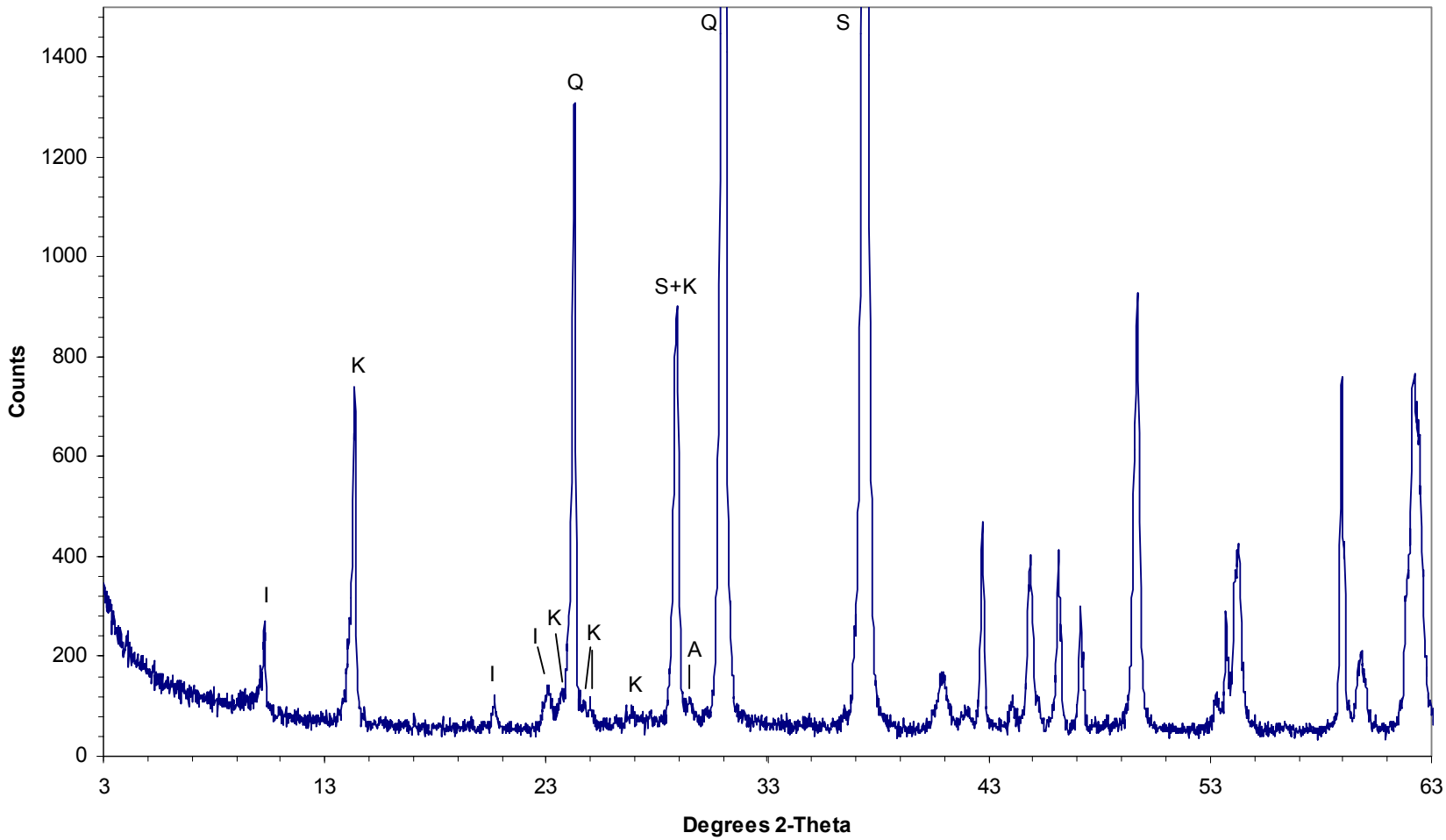

#16 2606.5m
Fine fraction

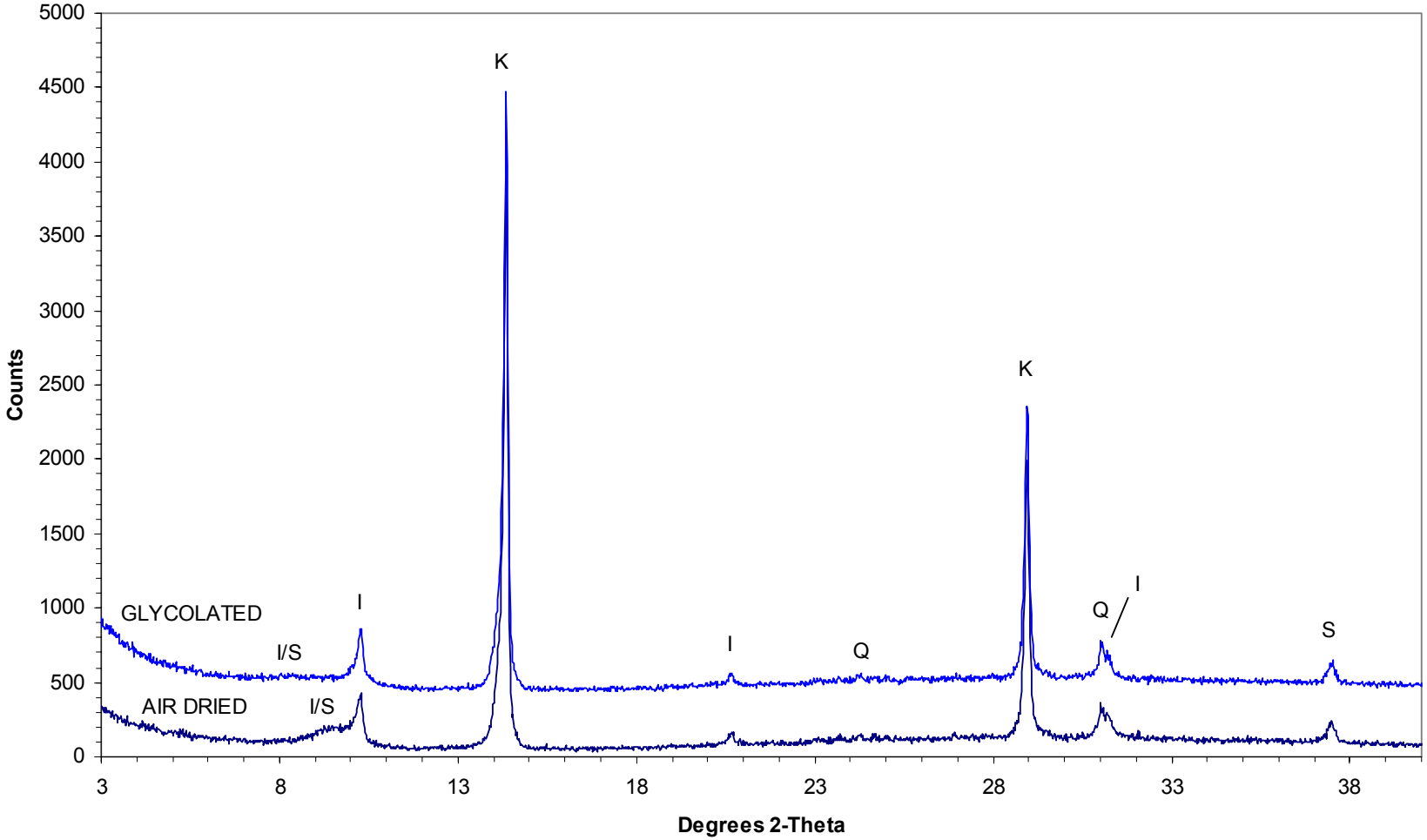

#17 2608.2m
Bulk rock

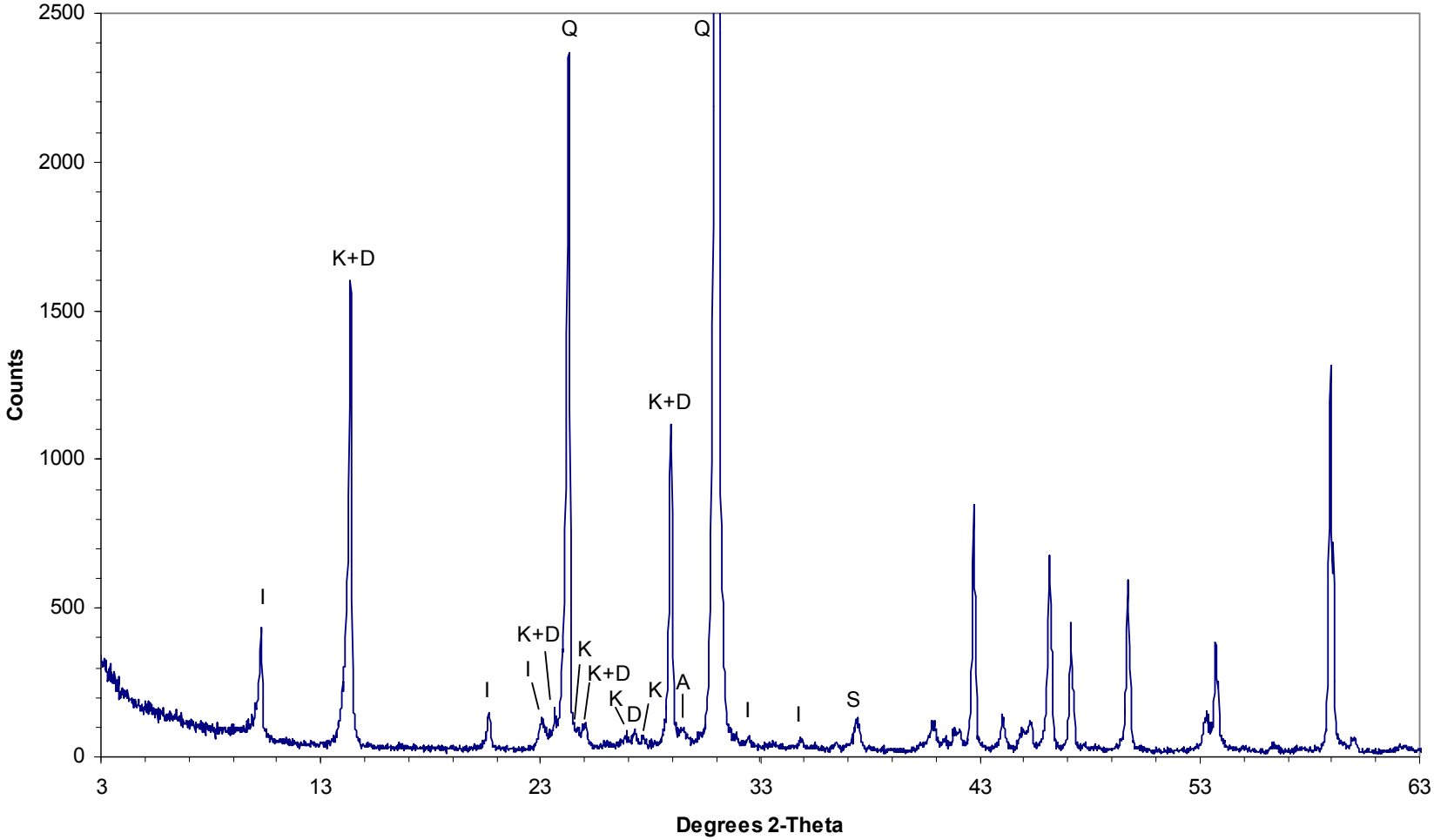

#17 2608.2m
Fine fraction

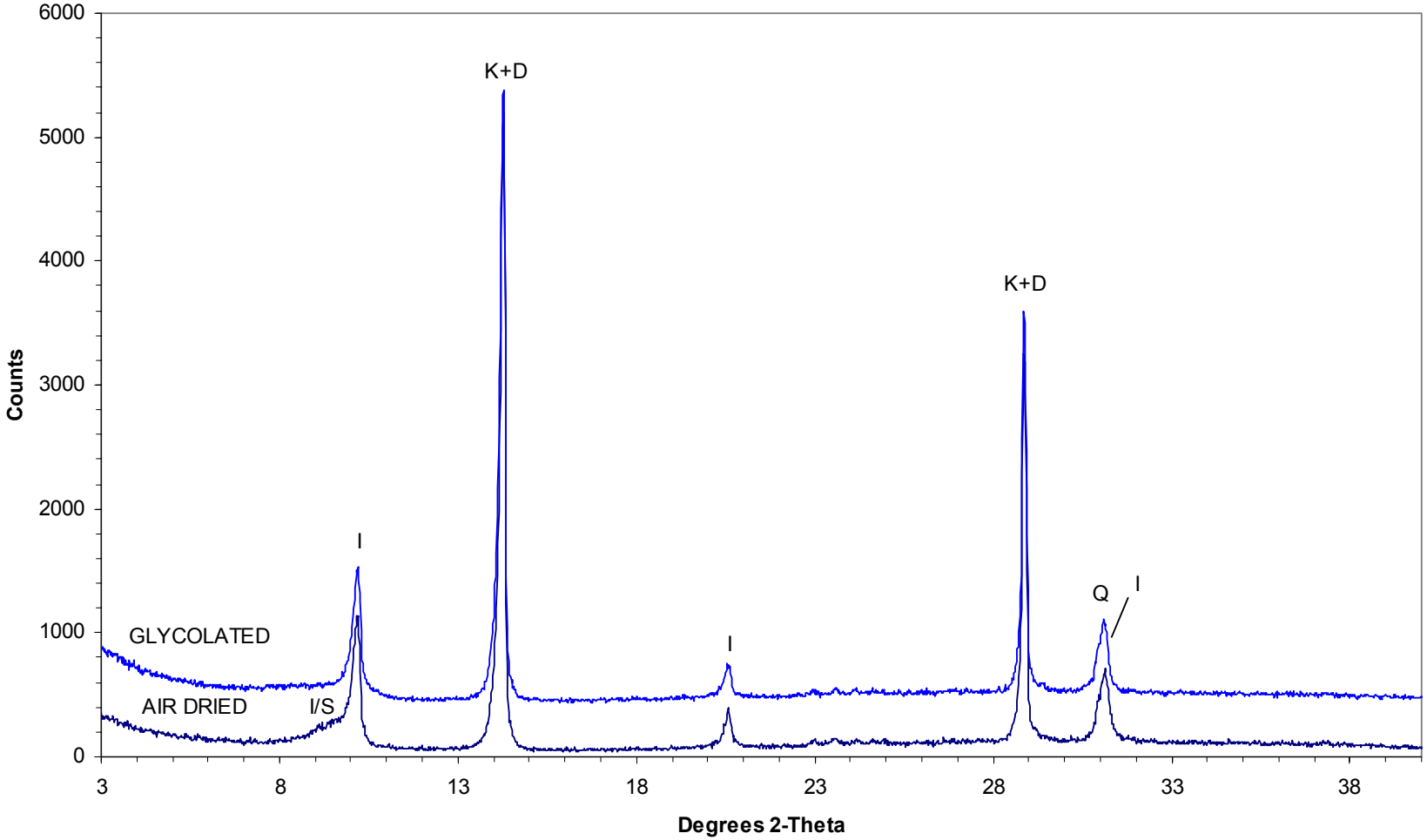

#10 3158.0m
Bulk rock

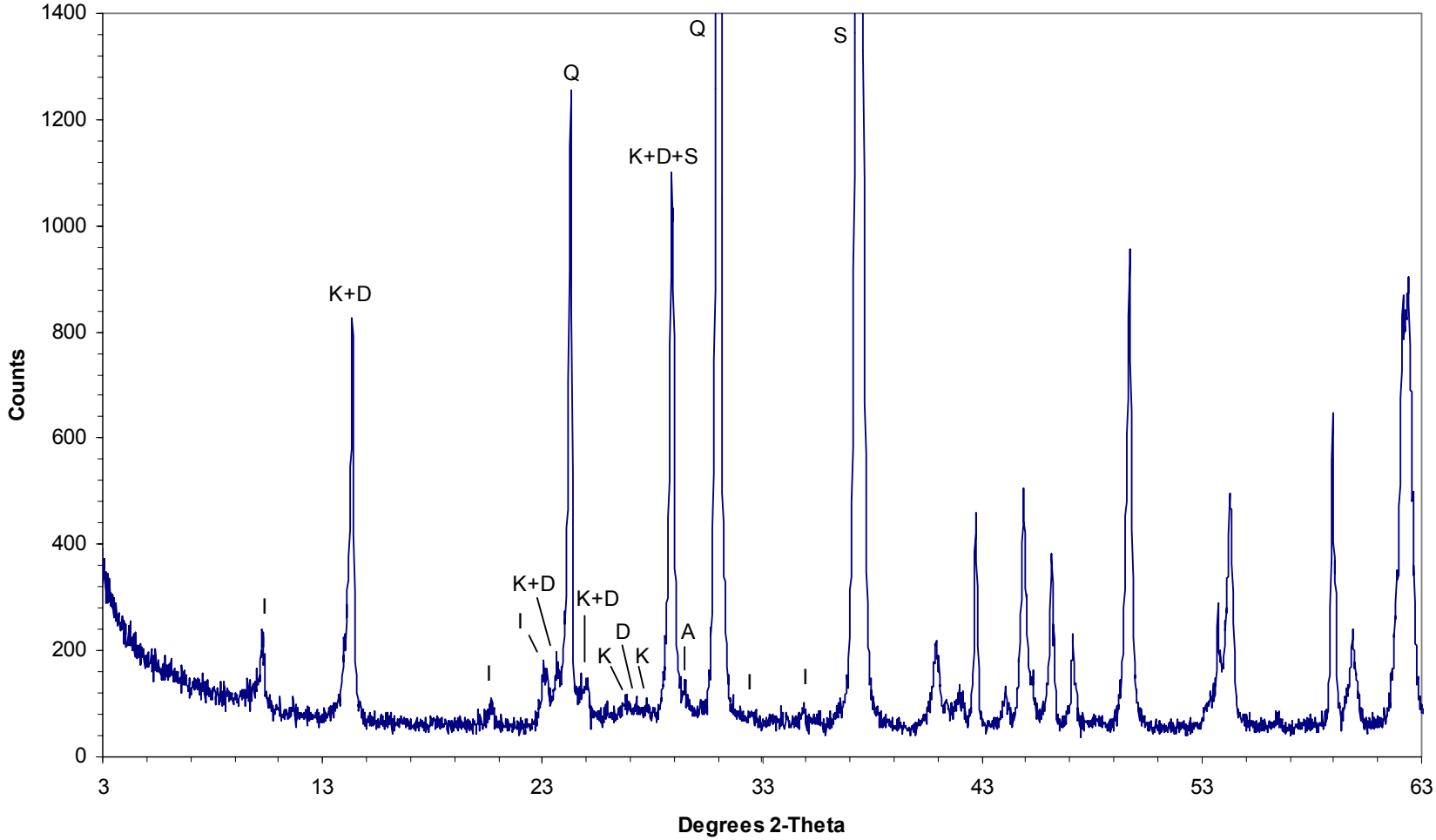

#10 3158.0m
Fine fraction

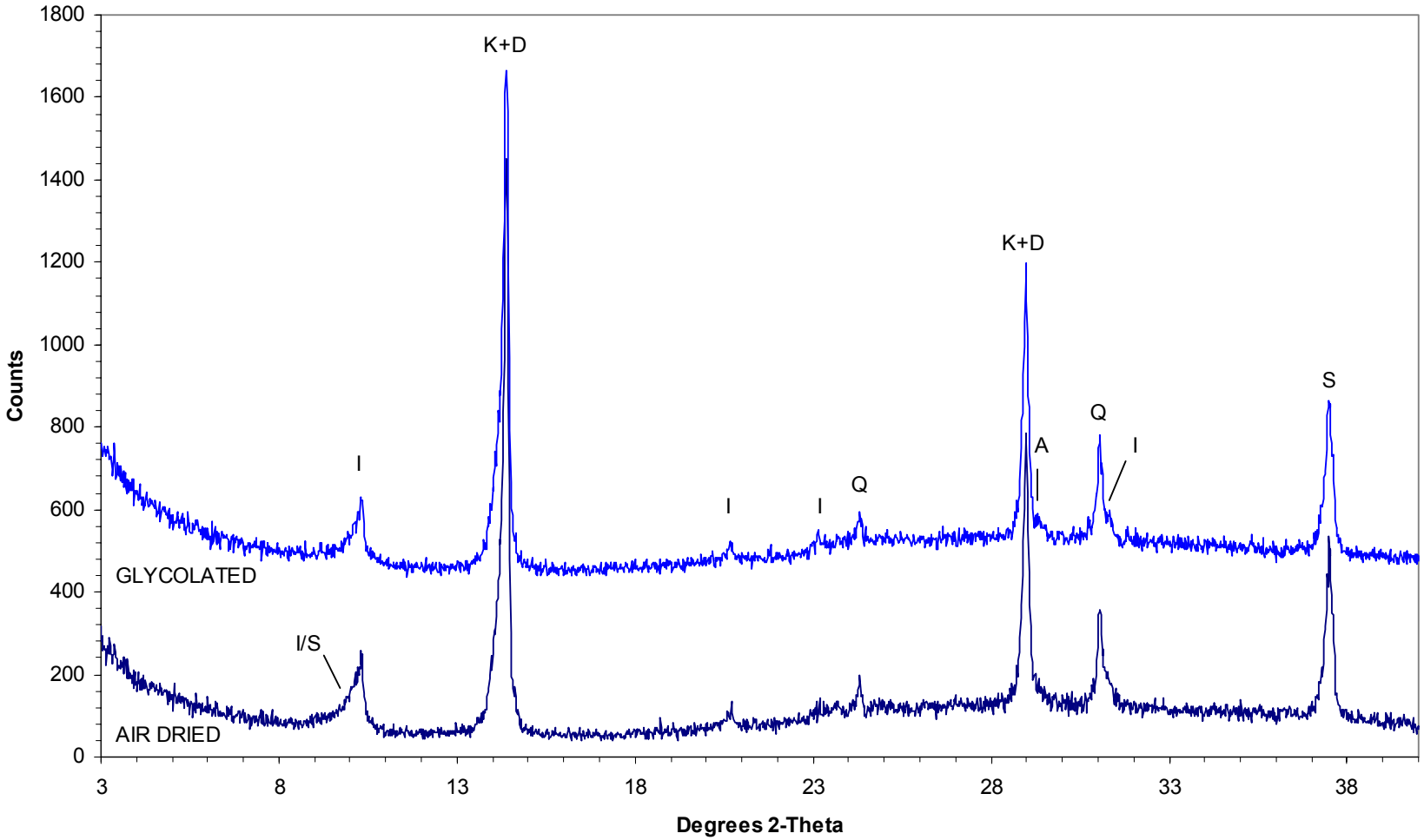

#9 3159.0m
Bulk rock

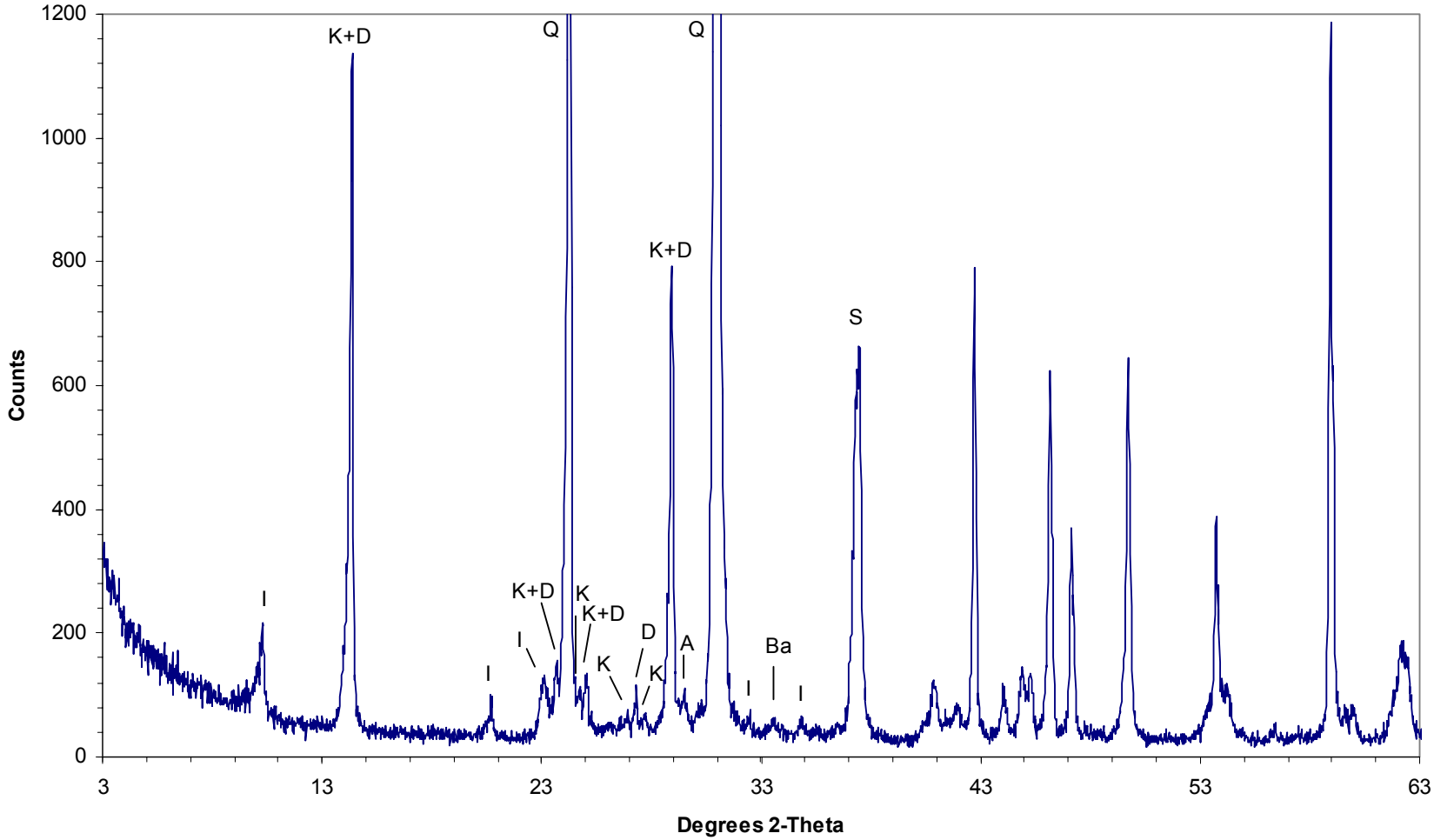

#9 3159.0m
Fine fraction

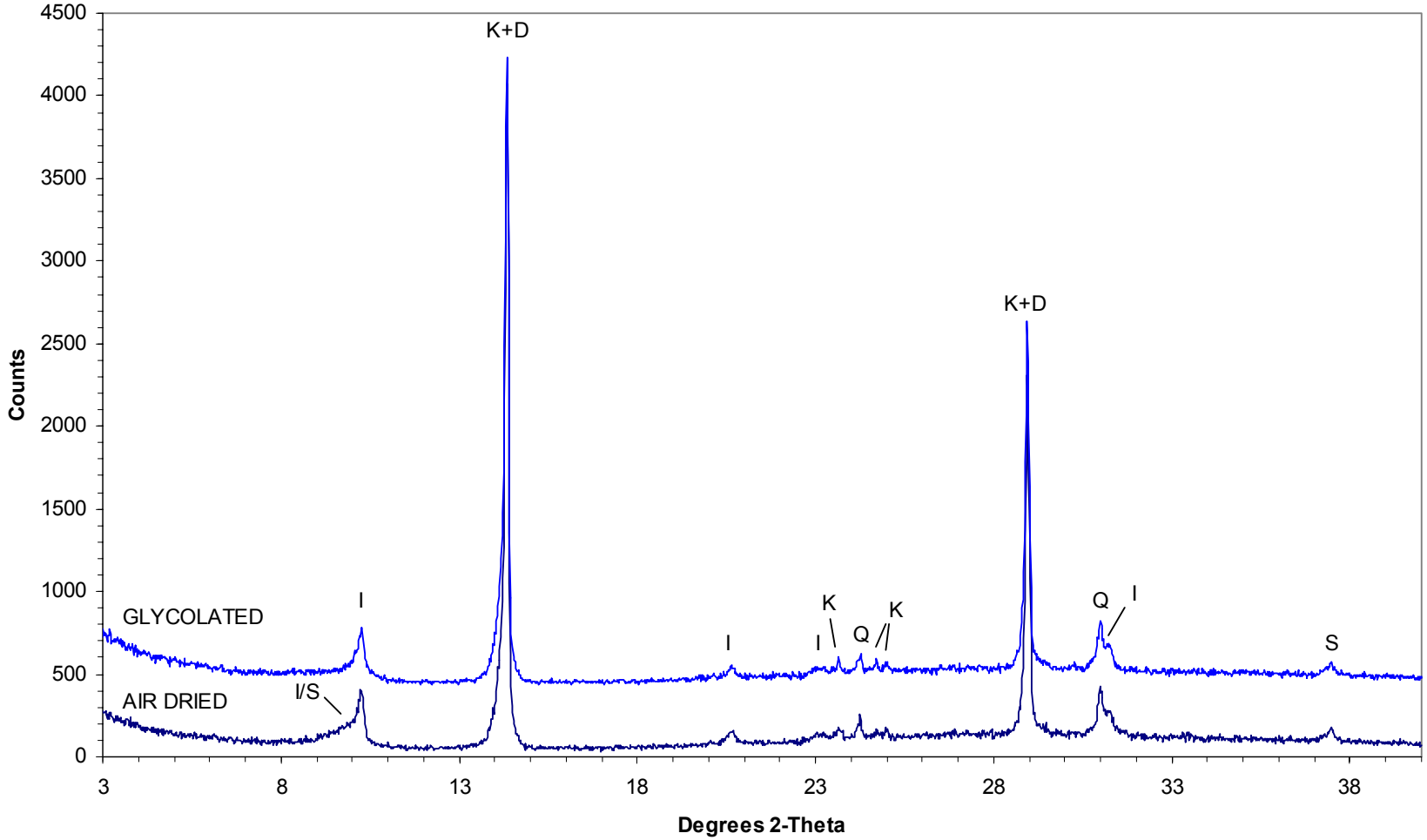

APPENDIX 2.

PHOTOMICROGRAPHS

Key to plates

Sample #	Depth (m)	Plate #
16	2606.5	1, 2*, 3*
17	2608.2	4
10	3158.0	5
9	3159.0	6, 7*

* SEM micrograph

PLATE 1: #16 2606.5m

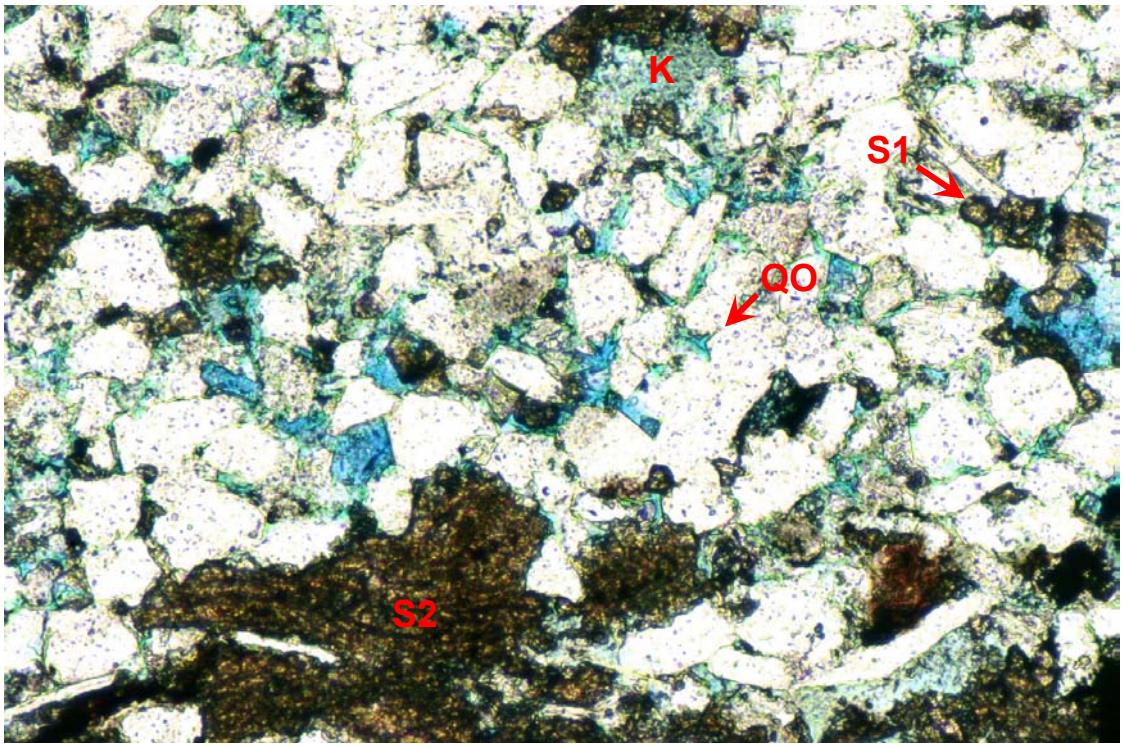

FIGURE 1 Plane polarised light
FIGURE 2 Crossed polarisers

0.2mm

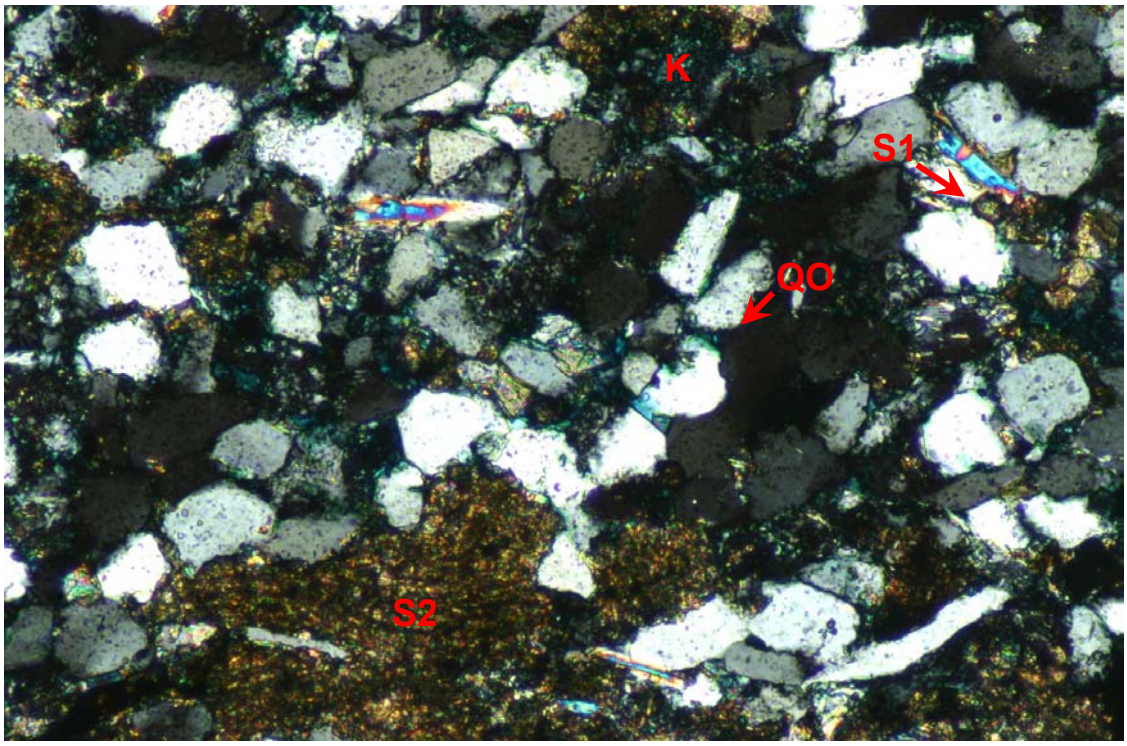

Severe porosity reduction in this very fine grained quartzarenite results mainly from siderite (S1) and quartz overgrowth (QO) cementation and authigenic kaolin (K) formation. Primary and secondary macropores (blue) are erratically distributed and thus would have little interconnectivity on a thin-section scale. Concentrations of sideritised clay grains (S2) and organics define tight, thin laminae throughout the sample. (Thin-section micrographs)

PLATE 2: #16 2606.5m (cont.)

FIGURE 1

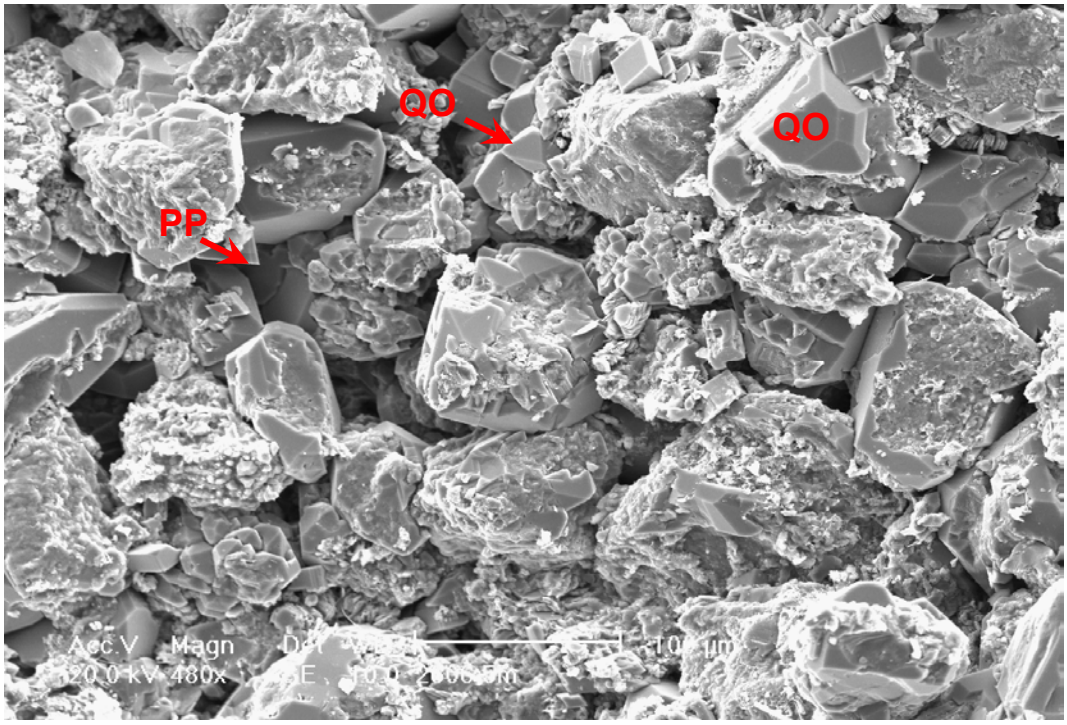

In localised areas, small primary intergranular pores (PP) are preserved where quartz overgrowths (QO) incompletely fill all available intergranular space, but, with most intergranular spaces being largely or completely filled by kaolin, quartz overgrowths and siderite (see below), permeability would be very low. (SEM micrograph)

FIGURE 2

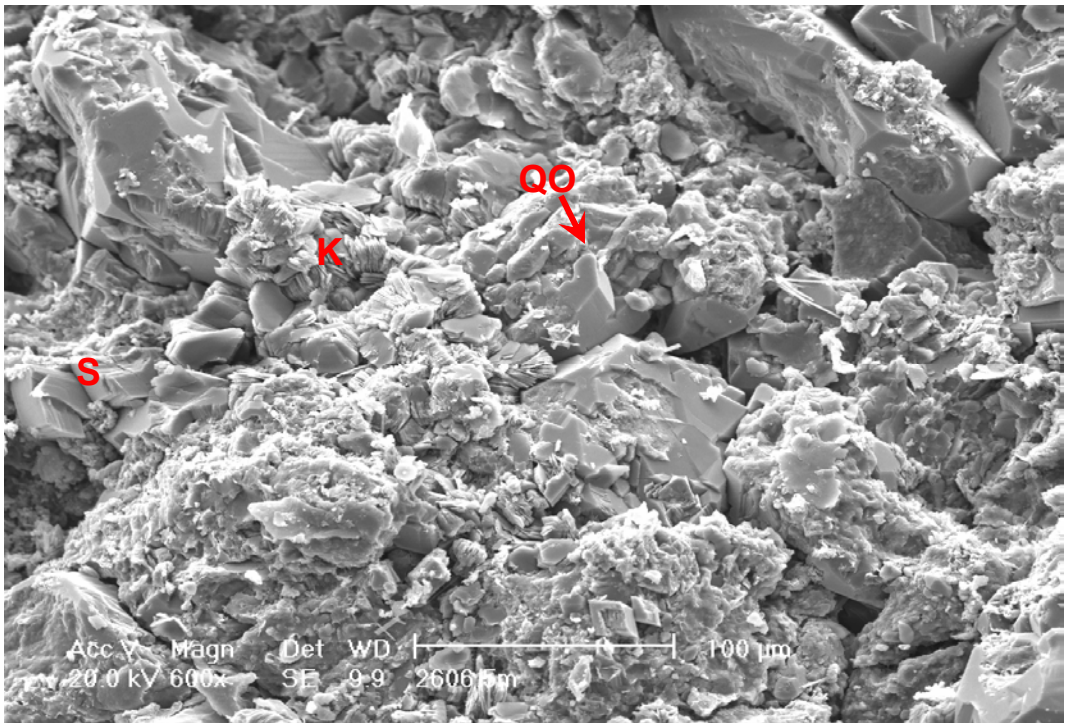

Throughout most of the sample, intergranular porosity has been almost completely eliminated by authigenic kaolin (K), quartz overgrowth (QO) and siderite (S) formation. Detail of pore-filling authigenic minerals is shown in Plate 3. (SEM micrograph)

PLATE 3: #16 2606.5m (cont.)

FIGURE 1

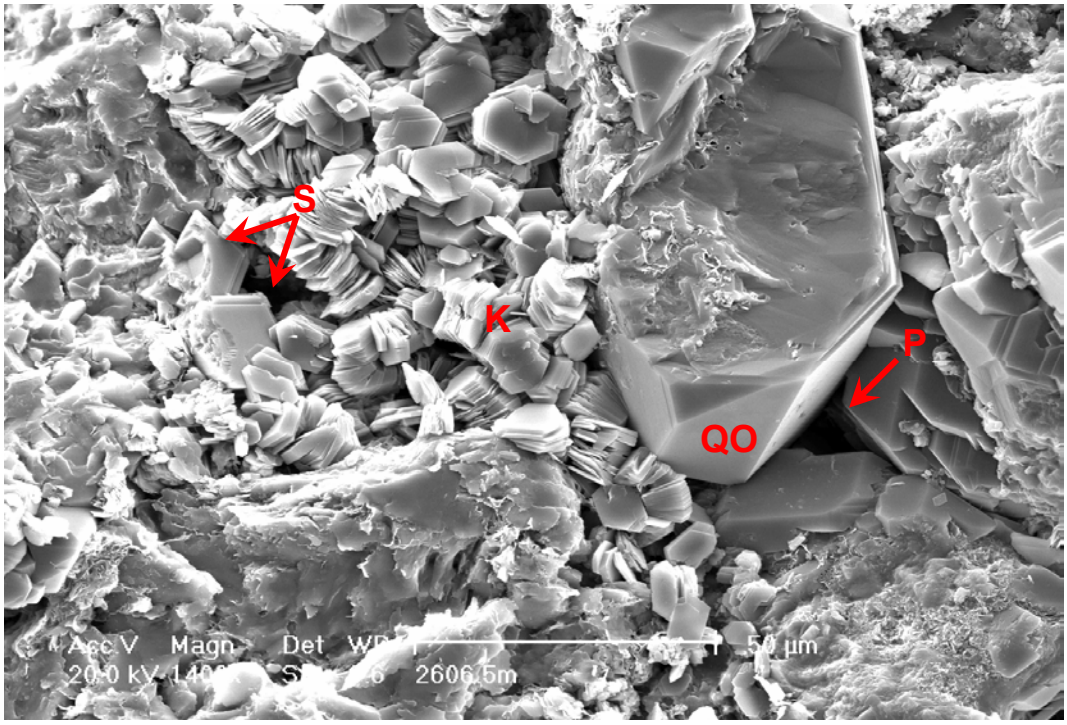

Intergranular spaces are almost completely filled by authigenic kaolin (K), quartz overgrowths (QO) and fine siderite rhombs (S). Being effectively sealed by kaolin and quartz overgrowths, a small intergranular pore (P) would not be conducive to permeability. (SEM micrograph)

FIGURE 2

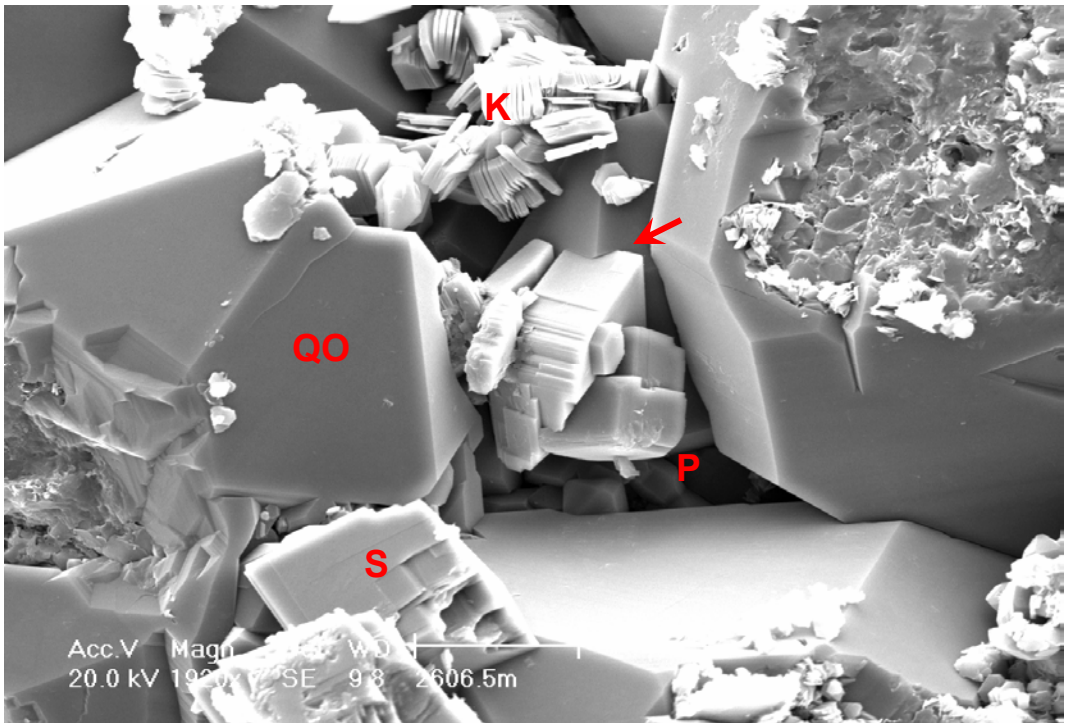

Detail of a typical intergranular pore (P) that is largely filled by quartz overgrowths (QO), siderite rhombs (S) and authigenic kaolin (K). Quartz overgrowths partly enclose (arrow) an earlier formed siderite rhomb. (SEM micrograph)

PLATE 4: #17 2608.2m

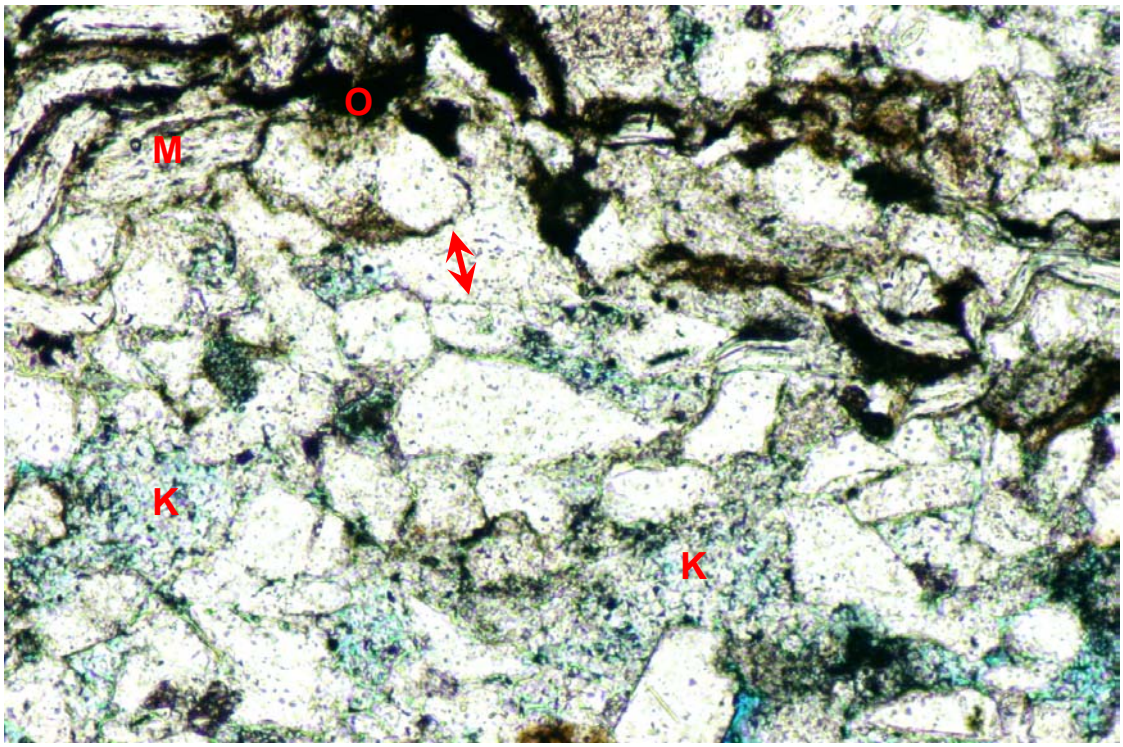

FIGURE 1 Plane polarised light
FIGURE 2 Crossed polarisers

0.2mm

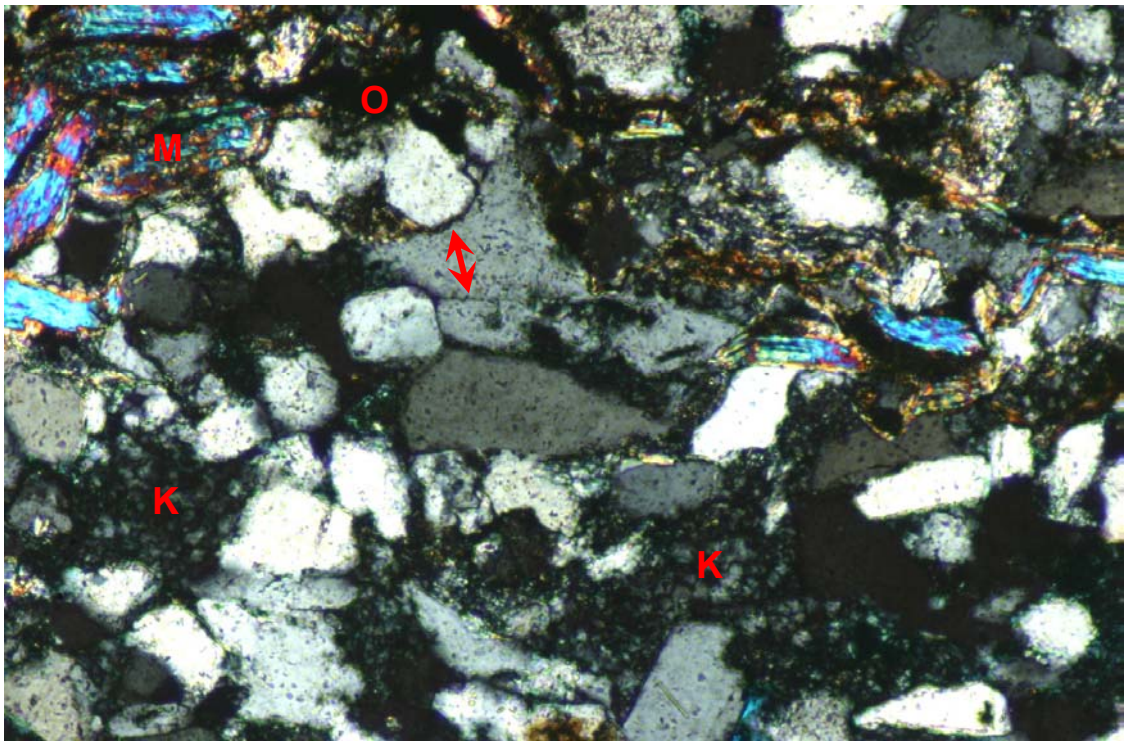

Little intergranular porosity is preserved in this very fine grained quartzarenite due to grain welding by grain contact dissolution (arrow) and extensive authigenic kaolin (K) formation. In addition, the sandstone is cut by sporadic, tight, stylolitic laminae along which well-compacted mica (M) and organics (O) are concentrated. Macropores (blue) are small and widely scattered and thus are not conducive to permeability. (Thin-section micrographs)

PLATE 5 #10 3158.0m

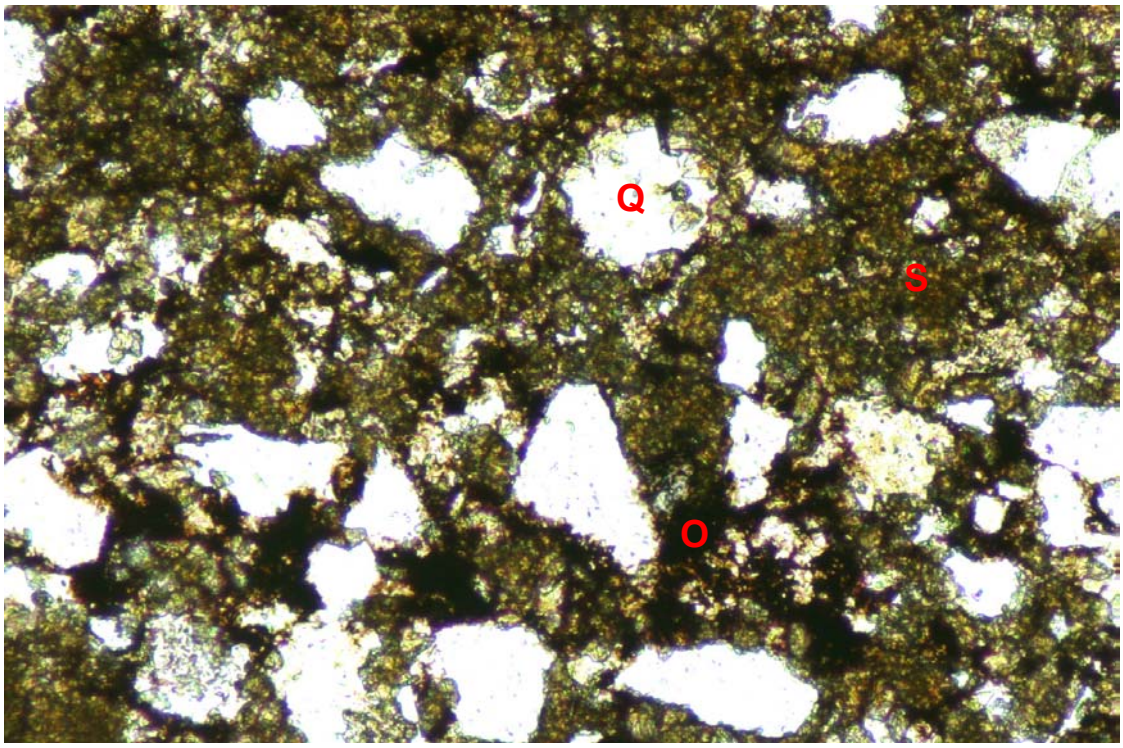

FIGURE 1 Plane polarised light
FIGURE 2 Crossed polarisers

0.2mm

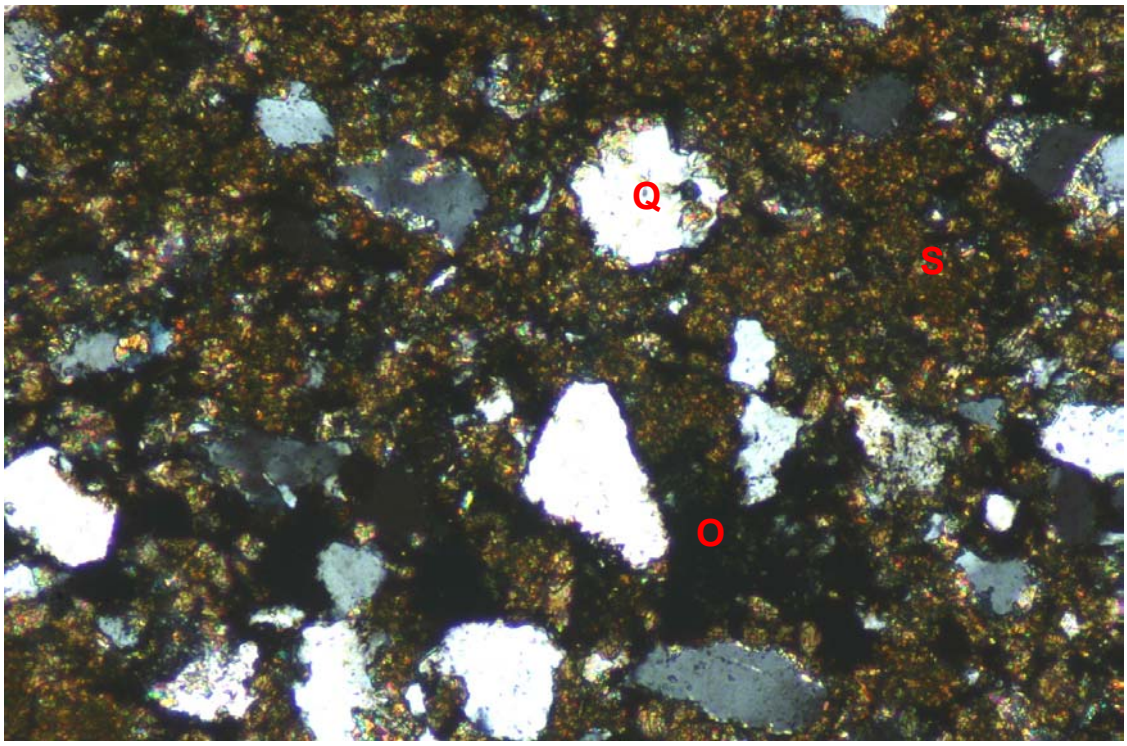

Arenaceous mudrock in which quartz grains (Q) and fine organic fragments (O) are supported by detrital clay matrix that is extensively replaced by finely-crystalline siderite (S). (Thin-section micrographs)

PLATE 6: #9 3159.0m

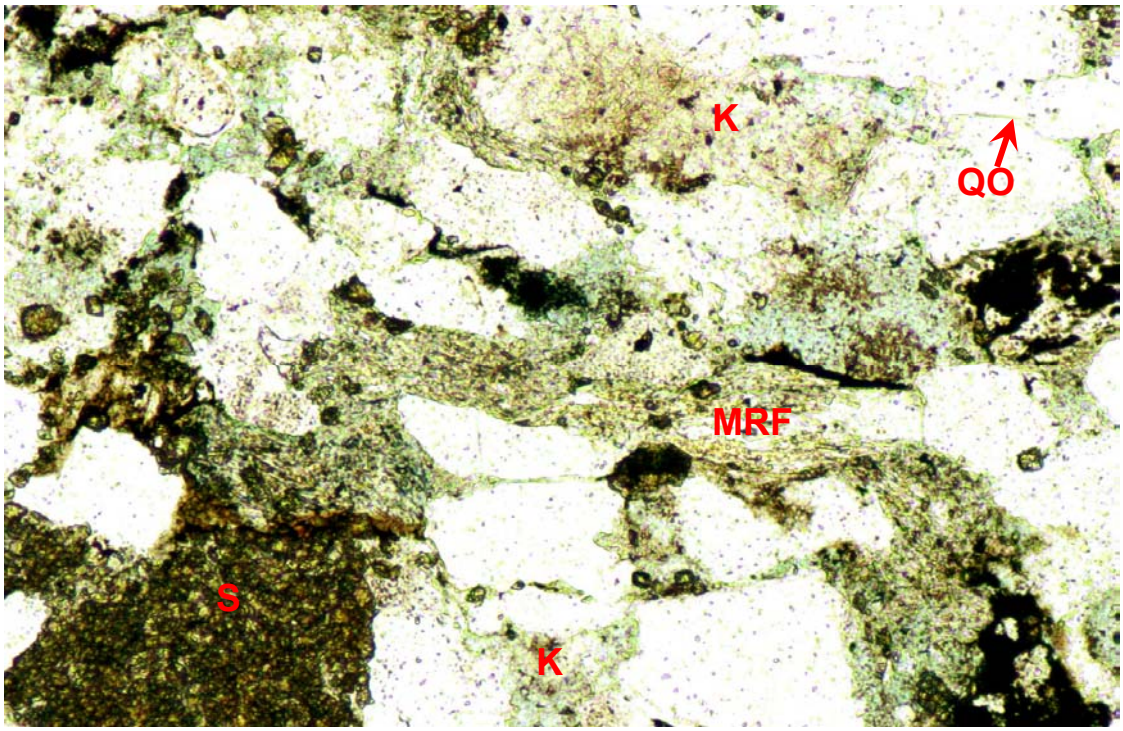

FIGURE 1 Plane polarised light
FIGURE 2 Crossed polarisers

0.2mm

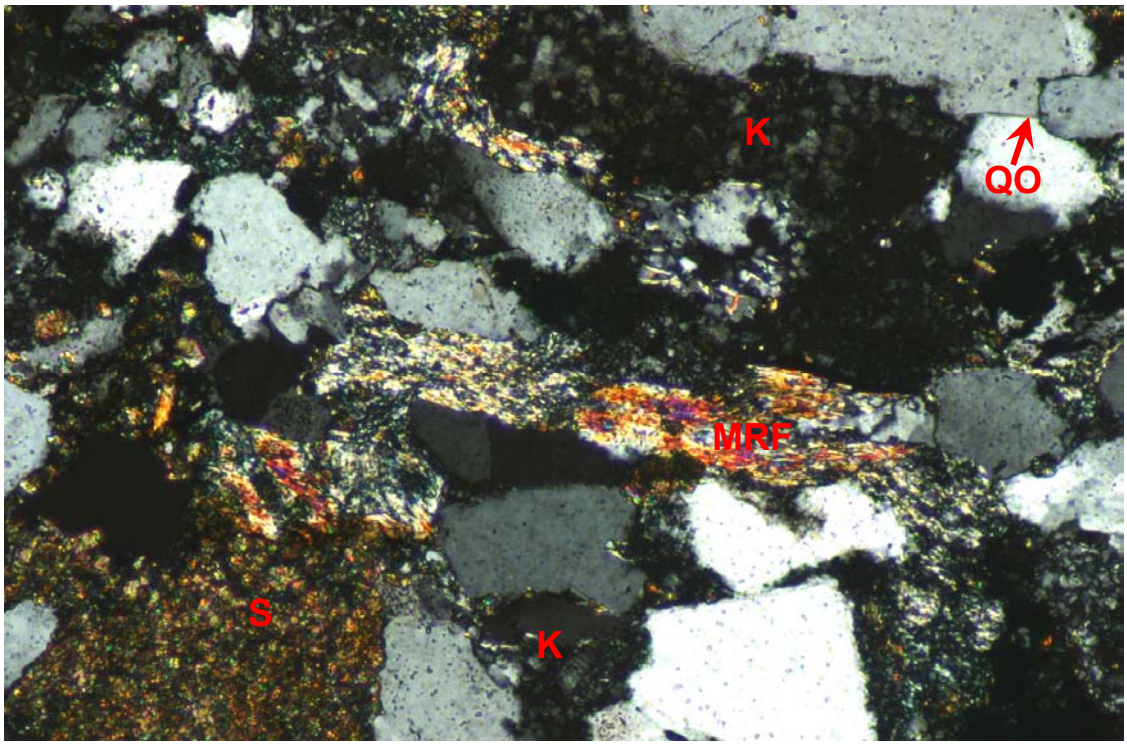

Containing common micaceous metamorphic rock fragments (MRF), this fine grained sublitharenite is significantly more lithic labile than the previous sandstones. Intergranular porosity is lacking due to micaceous grain compaction, localised quartz overgrowth (QO) cementation, grain contact dissolution and pore filling by authigenic kaolin (K) and sideritised clay (S). (Thin-section micrographs)

PLATE 7: #9 3159.0m (cont.)

FIGURE 1

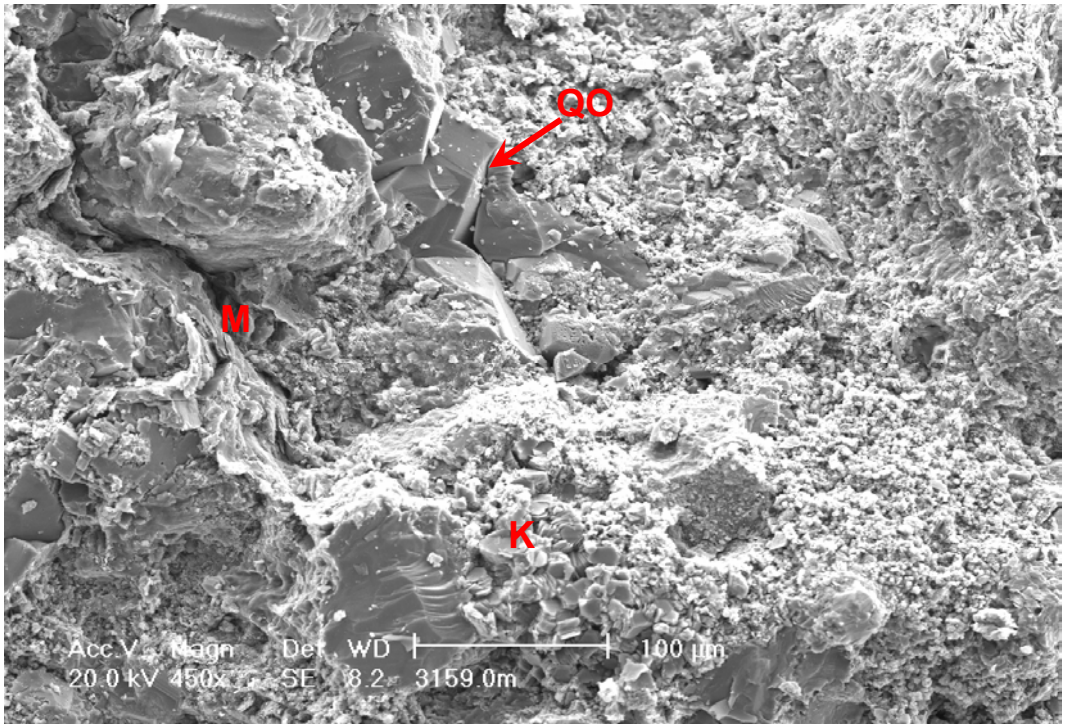

Representative area in which complete intergranular porosity occlusion results from authigenic kaolin (K) formation, micaceous grain (M) compaction and localised quartz overgrowth (QO) cementation. (SEM micrograph)

FIGURE 2

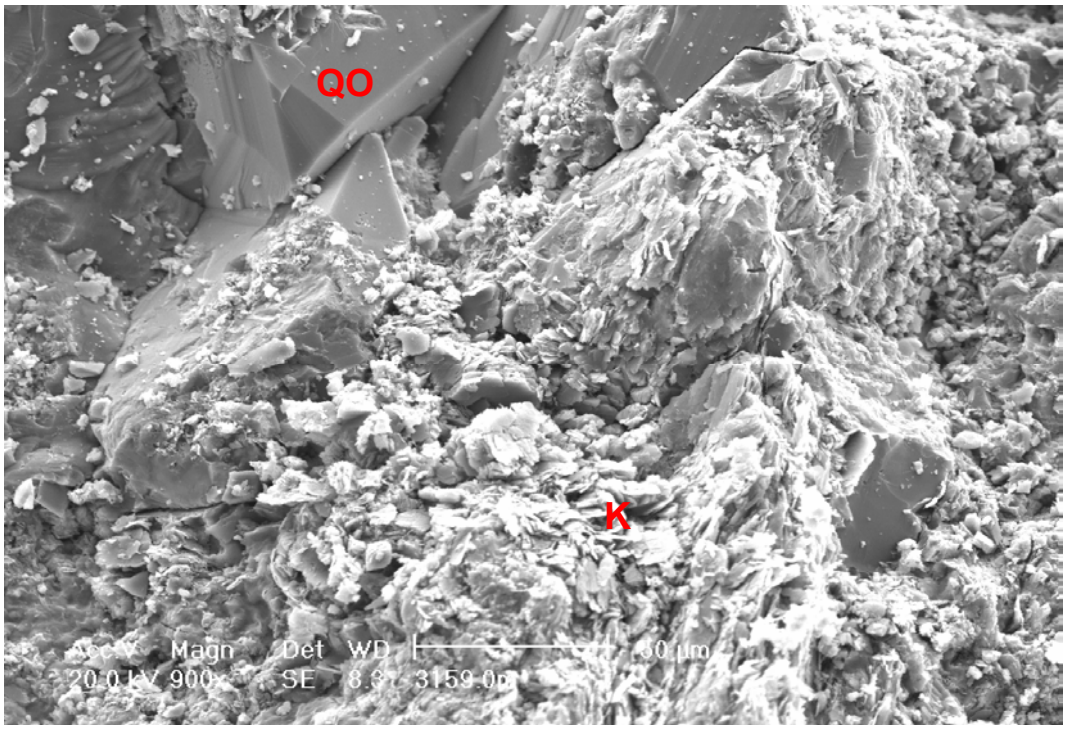

Intergranular spaces between quartz grains are tightly filled by quartz overgrowths (QO). Elsewhere, intergranular porosity has been obliterated by authigenic kaolin (K) formation and compaction. (SEM micrograph)

APPENDIX 8: CORE INTERPRETATION

Yolla 4

Core Description Report

T/L1
BASS BASIN

December 2004

EXECUTIVE SUMMARY

A sedimentological study of Cores 1 and 2 from the Eastern View Coal Measures in Yolla 4 indicate that these intervals were deposited in a lacustrine shoreface and fan delta setting. Interpreted depositional environments include alluvial fan, shoal water type fan delta, interdistributary bay fill / low energy shoreline, wave influenced shoreface / fan delta, and offshore lacustrine. The alluvial fan facies indicate sediment dispersal by flashy, hyperconcentrated flows in the form of sheetfloods and weakly channelised flows. Abandonment facies comprising fine-grained, distal sheetflood deposits, coal, carbonaceous mudstone, and root traces represent lobe switching and transgression. The shoal water type fan delta indicates shallow water deposition from high density turbidity currents and suspension settling on a low gradient delta front. The wave influenced shoreface / fan delta and the interdistributary bay fill / low energy shoreface record sedimentation on the margins of the lake. No inferences about shoreline morphology; apart from higher energy, open to wave conditions, in Core 2, and possible restricted embayment in Core 1; can be made from the cores due to lack of spatial data. The offshore lacustrine sediments record anoxic bottom conditions indicating a stratified lake.

High resolution sequence stratigraphy has been used to subdivide the strata into fourth-order systems tracts and, longer period, third-order sequences. Falling stage and lowstand deposits of forced regressions are recorded by the sharp based, aggradational to progradational alluvial fan deposits. Transgressive phases overlie sharp surfaces across which there is a rapid deepening, with or without a transgressive lag (ravinement surface) and record normal regression (parasequences) stacked in an overall retrogradational style. Highstands are represented by stacked coarsening upward parasequences of shoreface and fan delta sediments.

The alluvial fan deposits represent progradation of coarse-grained sediments, from the footwall margin of the half graben, into the basin centre during tectonically quiescent periods, whereas variations in parasequences may result from climate induced sediment supply and lake level fluctuations.

Reservoir quality is strongly influenced by facies with the highest permeability occurring in the alluvial fan facies. Other reservoirs occur in the shallow sub-aqueous fan delta and the wave influenced shoreface / fan delta, although the permeability in these facies is two to three orders of magnitude less than the alluvial fan facies.

TABLE OF CONTENTS

INTRODUCTION

Overview

Two cores totalling 54.9 m were described in detail from Yolla-4. A recovery of 100 % was achieved in both cores. All depths refer to drillers depth unless otherwise stated. The following intervals were cored (Table 1):

Table 1: Core intervals in Yolla-4. There is a 6 m depth shift between drillers depth and loggers depth.

Core	Depth Interval	Recovery
1	2892.05 – 2919.6 m	100 %
2	2958.07 – 2985.4 m	100 %

The cores were taken in the Eastern View Coal Measures in the 2755 Sand (Core 1) and the 2809 Sand (Core 2) and these intervals constitute the upper two reservoir intervals of the Yolla Field. This is the first core data for these reservoirs and allows detailed sedimentological and sequence stratigraphic interpretation of the depositional environments that can then be used to form facies models for the Yolla Field to assist in the reservoir modelling.

Objectives

The main objectives of the core description were the following:

1 Provide a detailed description of the cored intervals
2 Determine lithofacies and ichnofacies
3 Interpret depositional environment
4 Describe sedimentary sequences and key stratal surfaces present within the core
5 Describe the reservoir potential

Methodology

Cores were logged at 1:20 scale. Grainsize, colour, composition, physical sedimentary structures, macro palaeontology, ichnology (including Bioturbation index) were recorded. Bioturbation index (BI) records the intensity of bioturbation within a unit on a scale of 1 to 6. Where 1 indicates sparse bioturbation and disturbance of primary physical sedimentary structures and 6 indicates complete reworking of sediment and removal of all evidence of original sedimentary structures. Other ichnology characteristics including community succession resulting from environmental modification as the habitat becomes less suitable; and tiering in which bioturbation is vertically partitioned, resulting from vertical zoning of physical, chemical and biological parameters.

SEDIMENTOLOGY

The cored intervals can be subdivided into four fourth-order sequences on the basis of parasequence staking patterns. The sequences are characterised by facies assemblages that represent particular depositional environments. Nine sedimentary facies have been distinguished in the cored intervals. Not all facies are present in one cored interval. The facies, labelled A through I, range from gravel to mud, and some of the finer-grained facies also include thin coals. Most of these facies are compound units and their component lithofacies are listed in Table 2. A summary of the main features of the facies is in Table 3. Interpreted core photographs are included in Appendix 1.

Table 2. Component lithofacies of sedimentary facies from cored intervals in Yolla 4. Based on Miall, 1996; Martins-Neto, 1996; and Benvenuti, 2003

Lithofacies	Main descriptive characteristics (sediment texture and structure)
Gch	Massive, clast supported, moderately sorted, sub-angular to sub-rounded gravel with crude normal grading and stratification
Sl1	Planar parallel stratified / low angle laminated, medium- to coarse-grained sand
Sl2	Planar parallel stratified / low angle laminated, very fine- to medium-grained sand
Sr1	Ripple cross laminated, medium- to coarse-grained sand
Sr2	Ripple cross laminated, very fine- to medium-grained sand
Sg	Horizontally stratified, fine- to coarse-grained sands with normal grading
Sw	Wavy, undulatory fine- to medium grained sands with possible hummocky cross stratification
Slr	Planar parallel stratified / low angle laminated, very fine- to medium-grained sand, plant detritus and/or root traces
Sm1	Massive, very fine-grained sand with plant detritus
Sm2	Massive, medium- to coarse-grained sand with scattered gravel and/or mudstone rip up clasts
St	Small scale, trough cross stratified medium- to coarse-grained sand
Fm	Massive mudstone, siderite cemented bands
Fl	Laminated mudstone with linsen lamination and thin cross laminated silty sand or very fine-grained sand
Fmr	Massive mudstone with plant debris and/or root traces
C	Carbonaceous mudstone/coal

Table 2. Summary of the main features of the sedimentary facies in Yolla 4 Core 1 and 2.

Facies	Main features	Inferred depositional process	Depositional environment
A	Thick bedded *Fm*, lack of bioturbation	Suspension settling below storm wave base. Siderite and lack of bioturbation implies anoxic conditions.	Offshore lacustrine / restricted marine.
B	*Fl*, *Sg* often contains slumped intervals of sand and mud	Combination of suspension settling with sporadic low density turbidity currents. Slumped intervals due to gravity loading	Deeper water; below storm wave base sedimentation with "event" beds on prodelta.
C	Graded beds of *Sm2*, *Sg*, *Sr1*, *Fl*	Sub-aqueous hyperpycnal flow	Sub-aqueous portion (shoal water type delta front) of fan delta
D	Coarsening upward sequence of *Sw*, *Sr1*, *Sl2*, St, rare bioturbation	Combination of upper and lower flow regime, unidirectional and oscillatory currents	Middle to upper shoreface deposition on wave influenced shoreface / fan delta
E	Composite sequence of *Sr1*, *Sw*, *Sl2*,*Sm1*, *Fl*, *C*, rare bioturbation	Low energy deposition with periodic storm events in shallow sub-aqueous setting, grades into muddy marsh environment	Shallow interdistributary bay fill / low energy shoreline overlain by prograding muddy marsh.
F	Graded beds of *Sl1*, *Sr2*, *Sm2*, rare *St*	Sub-aerial low-concentration unconfined flow, *St* may indicate confined flow	Distal sub-aerial sand skirt facies.
G	Graded beds of *Gch*, *Sm2*, rare *Sr2*	Supercritical flow forming antidune bed forms. Gravel is transported as bedload and sand represents migration of antidunes.	Distal sub-aerial portion of alluvial fan – sheetflood couplets
H	Graded beds of *Sl2*, *Sr1*, *Sm2*, Sg, *Fl*	Sub-aqueous hyperpycnal flow	Sub-aqueous portion (nearshore – foreshore) of shoal water type delta front.
I	Beds of *Sl2*, *Slr*, *Sm1*, *Fmr*, *Fm*, *C*	Combination of sheetflood and suspension settling in shallow sub-aqueous to sub-aerial setting. Coal development reflects minimal clastic input.	Vegetated distal portion / abandoned fan lobe with intermittent sheetflood deposition

Facies A – Massive mudstone

This facies comprise massive, homogeneous mud (lithofacies *Fm*) and occurs only in Core 1. Siderite cemented bands up to several centimetres thick are common and bioturbation is absent. Carbonaceous material is also common.

Interpretation

This facies is interpreted to have been deposited an offshore lacustrine / restricted marine environment; as evident by the lack of traction current structures; with homogeneous and continued suspension fallout sedimentation in quiet waters (Basilici, 1997; Benvenuti, 2003). The presence of siderite cemented bands implies anoxic or reducing conditions. The formation of siderite is enhanced when interstitial pore waters are depleted with respect to free oxygen and dissolved sulphur. Thus the presence of siderite may be suggestive of rapid accumulation and decomposition of organic matter in an anoxic or oxygen limited environment (Beynon and Pemberton, 1992). It is not apparent if the overlying water column was oxygen depleted, however the lack of bioturbation and presence of siderite and carbonaceous fragments suggests that the interstitial waters were not well oxygenated (Beynon and Pemberton, 1992; Basilici, 1997).

Facies B – Laminated mudstone

The facies is composed of laminated mud (lithofacies *Fl*) with laminated silt and sandy silts (silty lithofacies *Sg*) that are typically millimetres thick and non-graded to normally graded. Siderite cemented bands up to several centimetres thick are common and bioturbation is absent. Carbonaceous material is also present. Synaeresis cracks are rare and this facies occurs in Core 1 only, overlying Facies A.

Interpretation

The deposits of this facies are interpreted to have accumulated in an offshore environment, but in a more proximal setting than Facies A. Anoxic conditions prevailed as indicated by the absence of bioturbation and the presence of siderite (Beynon and Pemberton, 1992; Basilici, 1997). The silty laminations represent transport by weak, transient traction currents. The deposition is attributed to the supply of suspended sediment by episodic floods, combined with flood generated, muddy, low-density turbidity currents, followed by normal suspension settling (Basilici, 1997; Benvenuti, 2003). This facies is overlain by the coarsening upward Facies C and is interpreted to represent prodelta deposits (Mastalerz, 1995).

Facies C – Sub-aqueous hyperpycnal flow

The beds of this facies are a few centimetres to a few decimetres thick and comprise massive sand (lithofacies *Sg*) overlain by ripple laminated sand (lithofacies *Sr1*). This facies consists of a series of stacked coarsening upward cycles with laminated mudstone (lithofacies *Fl*) at the base and beds of lithofacies *Sg* and *Sr1* increasing toward the top of the cycles. Scour surfaces are present at the base of some beds. Sharp based, massive to laminated sand (lithofacies *Sm2*) with mud rip up clasts, generally concentrated at the base, occurs at the top of some cycles. Lithofacies *Sg* is composed of very fine- to medium-grained sand with angular, irregularly shaped intraformational mud clasts present in some beds. Carbonaceous material is common on the foresets of ripple laminated sands and rare bioturbation comprising rare *Planolites* is present in heterolithic intervals (interbedded lithofacies *Sg* and *Fl*). Slumped intervals range from a few centimetres up to a few decimetres and are common in this facies.

Interpretation

These compound beds overlie Facies B and comprise a number of cycles that become progressively coarser grained toward the top, recording the progradation of the fan delta systems. The interbedded muds and sand indicates sub-aqueous emplacement as there is a lack of features indicative of sub-aerial exposure such as desiccation cracks; suggesting limited seasonal fluctuation in base level. The sedimentary features in the sands represent the final stage in the downslope fan delta evolution; each bed would thus have been formed by a high density turbidity current flowing down the gentle subaqueous slope of the distal fan delta margin (Martins-Neto, 1996).

During flood events, high concentration sandy sheetfloods flowed into the basin. These flows were diluted upon entering water and as they began to flow downslope, the grains in them were probably initially supported by the escaping pore fluid. As it accelerated, the density modified, liquefied sediment flow became turbulent, thus evolving into a sandy high density turbidity current. The turbulence was the main grain-support mechanism in the flows, as indicated by the normal grading within the beds. An additional grain-support mechanism would be hindered settling resulting from the high concentration of the water sediment mixture (Lowe, 1982).

There are three main stages for the deposition of sandy high density turbidity currents: 1) a traction sedimentation stage; 2) a traction carpet stage; and 3) a suspension sedimentation stage. In the first stage, a turbulent sandy high density turbidity current

deposits some of its load to form a sandy bed. Flow interactions with this bed can produce bedforms, including both plane beds and ripples; the latter is normally poorly developed due to flow unsteadiness. At this stage the current may also be locally erosive, producing scoured surfaces, amalgamated and lenticular deposits. In the second stage, increased unsteadiness can lead to the development of dispersive pressure in the basal layer of the flow. Turbulence is then suppressed and inverse grading develops in this layer, thus forming the basal traction carpet. In the third stage, turbulence fully develops; giving rise to normal graded or massive deposits, with traction structures normally lacking (Lowe, 1982).

The traction sedimentation stage is represented by the amalgamated intervals of the flat laminated and ripple laminated beds, as well as the scour and fill structures. The occurrence of these features toward the top of the cycles suggests that deposition in this stage was probably of limited duration due to increasing unsteadiness, and was located only in the proximal region of the fan delta slope. The traction sedimentation stage probably took place just after the liquefied stage of the flow. Alternatively, some of the ripple laminated beds could be the downslope, subaqueous product of waning flow phase of streamflood, produced from hyperpycnal flow. The products of the traction carpet are not present due to the absence of grains coarser than medium sand that possibly prevented the build up of dispersive pressure and simultaneously promoted the rapid development of turbulence, thus, probably leaving insufficient time for the formation of an organised traction carpet and leading also to the full development of the suspension sedimentation stage (Martins-Neto, 1996). The massive sand lithofacies *Sg* was probably deposited by a rapid dumping of the coarsest load directly from turbulent suspension, which rapidly reduced the current's density, mass and velocity (Benvenuti, 2003).

The high density turbidity currents occasionally travel farther into the basin, producing solitary, thin beds which are encased in mudstone. The finer grainsize of these beds suggests a more dilute character for the depositional flows. These beds thus would be the products of low density distal turbidity currents. Alternatively, the solitary beds within the mudstones may be the product of storm induced low density turbidity currents generated through the remobilisation of sediments on the fan delta slope during major storms (Martins-Neto, 1996).

The erosive nature of these currents is evident from the angular, irregularly shaped mud clasts in lithofacies *Sg* that imply sub-aqueous erosion of a plastic substrate, whereas the

angular, elongate mud clasts of lithofacies *Sm2* indicate desiccation and sub-aerial erosion indicating low concentration sheetflood deposition and possible transition to lacustrine / restricted marine conditions (Benvenuti, 2003). The increase in grainsize in lithofacies *Sm2* and the concurrent increase porosity and permeability, in conjunction with the sharp bed bases may represent possible seasonal fluctuations in relative base level.

The slumped beds consist of contorted laminated muds and silty sands to very fine-grained sands, and in rare beds, pebble conglomerate, formed when a sheet of sediment peeled off the slope and underwent gravitational deformation (Tamura and Masuda, 2003). The slumped mass was unconsolidated and underwent complex internal deformation as it moved downslope. Slumping was initiated either by hyperpycnal flows or by failure on the fan delta front induced by sediment loading. Slumping on the fan delta front may have been responsible for formation of some turbidity currents that developed by downslope acceleration, dilution and transformation of slumps (Stow et al, 1996).

Bioturbation is limited to simple structures of trophic generalists e.g. *Planolites* (Pemberton and Wightman, 1992). The inferred nature of the *Planolites* trace making organism (i.e. endostratal deposit feeding) suggests that although the sediments may have been organic rich, the interstitial environment was not completely devoid of oxygen. Thinly laminated zones devoid of biogenic structures imply that periodically, anoxic conditions may have been established. The monospecific nature of the bioturbation is interpreted to reflect an environment that includes low, possibly variable salinity and/or oxygen depleted conditions (Beynon and Pemberton, 1992).

Facies D – Coarsening upward sand sequence

This composite facies ranges from very fine-grained to fine-grained sand and encompasses lithofacies *Sl2* (planar parallel-stratified sand), *Sr1* (ripple laminated sand) *Sw* (wavy laminated sand) and *St* (cross stratified sand) that forms a coarsening upward succession. Beds are up to a few decimetres thick and have abrupt bases; however, erosional relief occurs at the base of the wavy laminated sand (lithofacies *Sw*). The ripple laminated beds contain unidirectional (current) and wave-modified current ripples. The wavy laminated sand contain low angle lamination that thicken off the crests and possibly represents hummocky cross stratification (HCS) and within this lithofacies, there are a number of vertical trends present: i) the heights of the possible HCS sets increase upward, ii) erosional contacts become more prominent upward, and iii) preferential truncation of

the hummocks results in the higher incidence of swales below the erosional surface. The amplitudes of the HCS sets are typically on the order of few centimetres only. The proportion of ripple laminated sands decrease upwards as the planar parallel-stratified sand (lithofacies *Sl2*) and cross stratified sand (lithofacies *St*) increase. Hydraulically light materials such as plant debris also decrease upwards.

The ichnofacies assemblage contains a very low diversity assemblage of isolated small *Skolithos* and *Planolites;* escape burrows (fugichnia) are also present. This assemblage is characterised by the diminutive size of the ichnofossils. *Skolithos* are less than 2 cm in length and 1-2 mm in diameter, while *Planolites* range from 0.5 to 2 mm in diameter.

Interpretation

The presence of possible HCS in this facies indicates storm generated currents (oscillatory and unidirectional) in a shoreface environment (George, 2000). Wave action is also indicated by the presence of wave modified ripples (Basilici, 1997). Multidirectional transport patterns are inferred from the cross laminated intervals (lithofacies *Sr1* and *St*) and may reflect the interaction of shore-normal waves, longshore and rip currents that are characteristic of a middle shoreface environment (Le Roux and Elgueta, 1997). The progressive increase in the height of the HCS, the more prominent erosion surfaces and the higher incidence of swales is interpreted to record the progradation of the shoreface (George, 2000). The storm wave produced structures (HCS etc.) are overlain by abundant lithofacies *Sr1, Sl2* and *St*, with a paucity of mud, suggesting a high-energy shoreface environment, probably on the middle to upper shoreface (Colquhoun, 1995). In this environment waves produce a net onshore sediment transport and low angle planar lamination commonly forms by bottom return flows (Le Roux and Elgueta, 1997).

The ichnofacies assemblage with the predominance of biogenic structures created by suspension-feeding organisms (*Skolithos*) is suggestive of agitated, nutrient rich and well-oxygenated bottom waters. Currents were of sufficient magnitude to suspend nutrients within the water column, but were moderate enough to allow organic detritus to settle from suspension, offering nutrient resources to deposit feeding organisms (*Planolites*). The characteristics of this assemblage; the predominance of vertical dwelling structures, the low diversity and low burrow density, is indicative of a *Skolithos* ichnofacies developed in a low salinity environment (Beynon and Pemberton, 1992).

Bioturbation, apart from escape structures (fugichnia), is generally absent from lithofacies *Sl2* and *Sw,* whereas the beds of lithofacies *Sr1* contain the low diversity *Skolithos*-dominated assemblages. This alternation of laminated and bioturbated, cross-laminated bedding is interpreted to reflect the dynamic interplay of between higher energy events and background, fair-weather sedimentation. Laminated zones represent energetic periods in which benthic boundary layer shear stress could not be tolerated by the benthic community, whereas the bioturbated, cross-laminated beds record periods during which current velocities were sufficiently reduced, permitting organisms to rework the substrate (Beynon and Pemberton, 1992).

Facies E – Interbedded sand and mud, rare coal

The deposits of this facies range from mud to silty sand and very fine-grained sand and include coal and carbonaceous mud. The beds of this facies are a few centimetres to decimetres thick and comprise interbedded ripple laminated sand (lithofacies *Sr1*) that is flaser bedded in places, parallel to flat laminated sand (lithofacies *Sl2*) and massive sand with common plant debris, and laminated mud. Organic rich mud and coal occur toward the top of this facies and there is a concurrent decrease in coarse clastics. Rare, thin beds of wavy laminated sands are also present. Bioturbation is sparse and limited to *Planolites* with rare, small *Thalassinoides* and fugichnia (escape burrows). Synaeresis cracks are associated with lithofacies *Sr1*, *Sw*, *Sl2* and *Fl* but do not occur within *Sm1* and the organic rich intervals toward the top of the facies.

The coal is dull brown, massive and has a greasy lustre and commonly grades into carbonaceous mudstone without associated root traces.

Interpretation

Facies E occurs at the base of Core 1 and the fine grainsize and the interlamination of sand and mud implies a low energy setting with periodic high energy (upper flow regime) deposition (lithofacies *Sl2* – planar stratified / low angle laminated, and *Sw* – wavy laminated; possible hummocky cross stratified sand). The association of low energy environments and organic rich facies implies an interdistributary bay fill with muddy and sandy flats (Holz, 2003; Phillips, 2003). The presence of lithofacies *Sw* and *Sl2* may record the effects of storms in a shallow bay environment. The presence of wave formed structures indicates that this bay was open and allowed direct access for storm waves (Phillips, 2003). The low density and monospecific bioturbation implies reduced salinity

levels (Pemberton and Wightman, 1992) suggesting a lacustrine or restricted marine environment. The presence of rare dinoflagellates in cuttings from 2925 m (Morgan, 2004) implies a restricted marine environment. The presence of synaeresis cracks; developed in clays in response to chemical variations in the water e.g. pH, salinity, etc. implies that the depositional environment was subject to periodic salinity variations (Beynon and Pemberton, 1992), although this is not indicative of a marine environment (Boggs, 1987).

Alternatively, the bay fill could result from crevasse splay deposition during flood stages (Reading and Collinson, 1996) in conjunction with the storm derived deposits.

The interdistributary bay fill strata grade upwards into the interlaminated lithofacies *Sm1* (massive sand containing plant debris) and *Fl*, and inturn are overlain by coal and carbonaceous mudstone, indicating anoxic conditions (Basilici, 1997). The common plant debris and the coal indicate a prograding coastal mire environment (Phillips, 2003). The dominance of clay, the lack of clastics and root traces implies a shallow lagoon or restricted embayment (Reading and Collinson, 1996). The coal is a boghead coal, comprising predominantly algal and fungal materials, contains little or no recognisable wood fragments, and is relatively low in ash and sulphur. Boghead coal is a sapropelic coal (allochthonous or redeposited coal composed of saprophytes – any organism that lives on decaying organic matter) formed by the degradation of peat swamp materials by algae (Moore, 1968). The coal accumulated in quiet lagoonal waters or restricted embayment (paralic environment), in areas away from the shallow, root crowded swampy shore (Bechtel et al, 2004) and lacks seat earth development at the base. The lack of clastic influx into the lagoon or embayment may argue against the crevasse splay depositional model for the interdistributary fill.

Facies F – Graded beds of stratified sand

The deposits of this facies are weakly graded coarse- to medium-grained sand ranging from a few decimetres to several metres in thickness. The basal surfaces of these beds are erosive and their lower parts comprise either massive sand (lithofacies *Sm2*) or planar parallel stratified / low angle laminated sand (lithofacies *Sl1*) with scattered pebbles and mud rip up clasts. The mudstone rip up clasts are elongate, angular to sub-angular and generally occur as lags. The upper parts consist of ripple laminated sand (lithofacies *Sr2*). Low amplitude cross stratified sand (lithofacies *St*) occurs at the base of some beds toward the base of this facies in Core 2. The beds within this facies tend to be stacked upon one

another such that the top of these cycles are commonly missing, having been replaced by the base of the overlying cycle.

Interpretation

Facies F is interpreted as characteristic of the distal sand skirt facies where the sandy sheetflood deposits accumulate under supercritical flow conditions, but in flows with reduced competency, related to the lesser slope (Blair and McPherson, 1994) (compare with Facies G). The low relief erosional surfaces and scale of the bedforms indicate deposition by unconfined flows. The weak normal grading and component bed lithofacies indicate traction deposition from a waning high energy current. The association of Facies F with Facies G implies sub-aerial deposition, and the origin of this facies is attributed to fully turbulent, low density sheetfloods (Benvenuti, 2003). Facies F is interpreted as a distal downfan equivalent of Facies G. The cross stratified sand represents sedimentation in broad, shallow, virtually unconfined channels that are eroded into the sheetflood deposits (Kelly and Olsen, 1993).

Sheetflood deposits are laterally continuous, and outcrop studies indicate a tabular geometry with only limited mud interbeds (Blair and McPherson, 1994; Benvenuti, 2003).

Facies G – Gravel and gravel sand beds

The beds of this facies are ungraded to normally graded gravel-sand couplets that range in thickness from decimetres to metres. The lower parts of these beds contain lithofacies *Gch*, typically only a few centimetres thick, however, there are beds up to 30 cm thick, composed of clast supported, moderately sorted, sub-angular to sub-rounded, pebble to granule sized clasts. The base of the gravel is sharp, commonly with a low relief erosion surface. The gravel lithofacies is sharply overlain by lithofacies *Sm2*, which is typically in the decimetre thickness range and comprises of medium to coarse-grained, planar parallel stratified / low angle laminated sand or massive with scattered pebbles and granules. Rare intervals of *Sr2* overlie the pebbly sands. Plant debris and wood fragments occur toward the top of lithofacies *Sm2* beds.

Interpretation

Facies G occurs only in Core 2 and is the coarsest sediment in the cores. The alternating gravel – sand couplet packages implies deposition by sheetflood processes (Blair and McPherson, 1994; Benvenuti, 2003). The clast size of the gravels and percentage of sand

relative to the gravel, suggests a distal setting. The bipartite gravel-sand beds are interpreted to have been deposited by density layered flows characterised by a highly concentrated lower part (gravel load), dominated by laminar shear and clast collisions, and a less concentrated, fully turbulent, and much faster flowing upper part (sand laden) (Benvenuti, 2003).

Alluvial fan (and fan delta) sheetflood facies differ from other deposits because of the distinctive hydraulic conditions (high Froude number, high flow attenuation rate, and high deposition rate) under which they are deposited. Flow conditions within sheetfloods are invariably supercritical due to the relatively high slope of the fan surface. Alternating phases of transportation and deposition of coarse gravel and sand + fine gravel in a sheetflood, which gives rise to the couplet packages, are caused by changing hydraulic conditions related to flow expansion and decreasing slope, in conjunction with intrinsic variations in depth and velocity typical of supercritical flow. Sheetflood deposition is the product of the migration and washout of submerged antidune bedforms (Blair and McPherson, 1994).

The deposition of the sand fraction was fully tractional and generally involved upper flow regime plane-bed configuration (lithofacies *Sm2*), but the presence of lithofacies *Sr2* (ripple laminated sand) indicates the subsequent development of low flow regime conditions. The bedform succession, together with the presence of hydraulically light material (plant and wood fragments) toward the top of beds implies a declining flow power and supports the notion of a waning flood (Benvenuti, 2003).

Outcrop studies of sheetflood dominated fan deltas have noted that this facies is tabular and have a sheet-like geometry (e.g. Mastalerz, 1995; Martins-Neto, 1996; Benvenuti, 2003)

Facies H – Graded sand beds

This facies comprises lithofacies *Sg, Sr1, Sm2* and *Fl*. Beds typically range in thickness from a few centimetres to a few decimetres that are stacked into thickening upward cycles. The thickening upward cycles comprise thin bedded lithofacies *Sg* overlain by *Sr1* (including flaser beds) with mud drapes (lithofacies *Fl*) that decrease upsection as the sand beds become thicker and amalgamate. The mud drapes preserve rippled surfaces showing unidirectional ripples. Lithofacies *Sg*, containing angular to sub-angular elongate mud rip

up clasts, which generally occur as lags, are present toward the top of the cycles. Bioturbation is extremely rare with possible *Planolites* present in one interval.

Interpretation

This facies is interpreted as fan delta dominated shoreface deposits that stratigraphically occur between Facies E and Facies C. The thickening upward cycles represent parasequences that record high-order, autocyclic processes of progradation and abandonment on individual fan lobes. The shoreline processes e.g. waves, were not a major sediment dispersal process as evident from the presence of unidirectional ripples (Cole and Stanley, 1995). The deposition primarily resulted from sub-aqueous high density turbidity currents forming traction deposits, followed by suspension fallout (see discussion in Facies C) (Martins-Neto, 1996). The lack of desiccation cracks implies continued sub-aqueous deposition. The lack of well developed foresets and the scale of the thickening upward cycles suggest a shallow water depth and a shoal-water type fan delta (Postma, 1990; Ilgar and Nemec, *in press*) as the shallow water depths inhibited the development of Gilbert-type foreset beds (Billi et al, 1991). The mud rip up clasts at the base of lithofacies *Sm2* indicates a genetic relationship to sub-aerial sheetflood processes.

Bioturbation, comprising a monospecific, extremely low density assemblage of *Planolites*, is limited to lithofacies *Fl*. The nature of the argillaceous sediments and horizontal, deposit feeding structures is suggestive of the *Cruziana* ichnofacies (Beynon and Pemberton, 1992). The absence of biogenic structures produced by suspension feeding organisms implies that continued sedimentation was unsuitable for these organisms, whereas deposit feeding communities were largely unaffected by continued sedimentation and only restricted by organic content and the distribution of the lithofacies (Beynon and Pemberton, 1992; Coates and MacEachern, 2000).

Facies I – Interbedded, massive to laminated sand and mud

These beds of this facies range from few centimetres to decimetres and consist of lithofacies *Sl2*, *Slr*, *Sm1*, *Fm, Fmr* and *C.* Individual beds are often graded and display horizontal laminations or are structureless, and are generally arranged in fining upward packages in Core 1 but show no overall trend in Core 2. The thickest intersection of this facies is in Core 1 and the base is delineated by a thick (approximately 50 cm) slumped interval that is overlain by a succession that is similar to Facies G; coarsening and thickening upward package of lithofacies *Sl2* and *Sm2*. The fining upward packages contain

root traces that include both deep vertical and shallow horizontal traces that increase in number toward the coal. Lithofacies *C* comprises shaley coal that is dull in colour with between 30 and 60% siliciclastic material that is mixed with the coal and carbonaceous mud with greater than 60% siliciclastic material. This lithofacies also contains pedogenic slickenslides. Bioturbation is rare and comprises *Planolites* and escape traces (fugichnia) only.

Interpretation

This facies represents complex series of environments that range from sub-aqueous shallow fan delta to sub-aerial alluvial fan. The slumped interval and the overlying coarsening upward package with structures that indicate high density turbidity current deposition (Lowe, 1982) is interpreted as a shallow sub-aqueous fan delta (Martins-Neto, 1996; Benvenuti, 2003). The lack of well defined shoreface deposits e.g. wave ripples, HCS etc. implies that it was a low energy shoreface that was dominated by input from the fan delta. The sub-aerial deposits are dominated by fine-grained sheetflood deposits that are overlain by lithofacies *Fm*, indicating rapid waning of the sheetflood events (Benvenuti, 2003).

The preservation of root traces and plant remains in this facies indicate colonisation of the distal sheetflood sediments (George, 2000) in which erosion was insignificant and sedimentation was rapid forming weakly developed, vertically stacked palaeosols that are separated by minimally weathered sediment. Waterlogged reduced conditions favour the accumulation and preservation of organic matter in an Ag (gleyed A) horizon. Fluctuations in the water table produce intersecting slickenslides in clayey sediments. The lack of development of a grey Bg horizon with redoximorphic features indicates an immature soil profile, inferred to be proximal to the sediment source as the degree of pedogenic development can infer distance from sediment source (Kraus, 1999).

The presence of shaley coal (autochthonous coal) and the deep vertical root traces indicate abandonment of the active lobe (George, 2000). In Core 1, the abandonment was a gradual process as evident from the underlying distal sheetflood deposits and the root traces that developed between sheetflood events, whereas in Core 2 abandonment was rapid. Periods of fan lobe abandonment / non-deposition are marked by root traces that overprint the previous facies e.g. in Core 1 root traces overprint Facies H (fan delta shoreface) and Facies I (distal sheetflood, fan lobe abandonment), whereas in Core 2, the root traces occur in Facies F (distal sand skirt). The origin of Facies I in Core 2 may be

attributed to ponds developed in local topographic depressions that were poorly drained, vegetated and subject to pedogenic processes (Benvenuti, 2003).

The presence of an extremely low density, monospecific assemblage of *Planolites*, within lithofacies *Fm*, implies that sedimentation was unsuitable for suspension feeding organism and that salinity was low, possibly freshwater (Beynon and Pemberton, 1992; Coates and MacEachern, 2000)

FACIES ASSOCIATIONS AND DEPOSITIONAL MODEL

The facies discussed in the Sedimentology section are arranged in a variety of facies associations that mostly display predictable vertical developments where the facies contacts are generally transitional. The significance of intervals where the contacts are sharp (either erosional or transgressive surfaces) with significant facies dislocations will be discussed in the Sequence Stratigraphy section.

Alluvial fan facies association

This facies assemblage is attributed to the sub-aerial sediment dispersal on alluvial fans. In Core 1 this comprises Facies F (distal sand skirt) and Facies I (abandoned lobe) whereas Core 2 represents a more proximal facies associations and comprises Facies F, G and I. The sheetflood couplets represent the most proximal sediments intersected in the cores and imply that the alluvial fan facies will thicken toward the fault escarpment (Benvenuti, 2003). The alluvial fan sediments in Core 1 overlie deposits of the shoal water type fan delta, whereas in Core 2 they overlie the wave influenced shoreface / fan delta.

Shoal water type fan delta facies association

The facies association of this depositional element consists of Facies H, C and B that occur in coarsening upward packages in Core 1 only. This stratigraphic occurrence indicates that progradation extended basinward as a result of the transformation of sub-aerial sheetfloods into sub-aqueous lobes of Facies H and C (Benvenuti, 2003). Periodic slumping of sediment on the delta front produced chaotic mixture of sediment. This facies association overlies the offshore deposits. The low density and diversity of bioturbation in this setting reflects continued sedimentation and reduced to low salinity (Bromley, 1996; Coates and MacEachern, 2000).

Interdistributary bay fill / low energy shoreface

This facies (Facies E) occurs at the base of Core 1 and is an incomplete sequence of coarsening, then fining upward sediments that record the infilling of an interdistributary bay and the development of a stagnant lagoonal environment (Phillips, 2003). The low diversity of bioturbation implies low or reduced salinities, which is common in this type of setting (Pemberton and Wightman, 1992; Beynon and Pemberton, 1992; Bromley, 1996).

Wave influenced shoreface / fan delta

This facies comprises the middle to upper shoreface of a wave influenced shoreface / fan delta. This facies occurs at the base of Core 2 and the lower shoreface deposits are not present in the core. The decrease in storm wave structures (HCS), the increase in fair-weather structures and increasing grainsize toward the top of the facies indicates progradation of the shoreline. The low diversity, low density and vertical orientation of the bioturbation are indicative of high levels of wave or current energy (Bromley, 1996).

Offshore lacustrine / restricted marine

This facies underlies the shoal water type fan delta and comprises massive mud with siderite cemented bands, plant debris and a lack of bioturbation that is indicative of anoxic conditions (Bromley, 1996). The lack of high diversity bioturbation in well oxygenated zones e.g. wave influenced shoreface / fan delta and shoal water type fan delta implies that salinity was low and only allowed the presence of trophic generalists (*Planolites, Skolithos* etc.) indicating a lacustrine environment is the most likely interpretation for this setting (Bromley, 1996).

SEQUENCE STRATIGRAPHY

The stratigraphic record can be subdivided into various scales or orders of cycles, resulting from cyclical variations in sediment supply and relative base level change, on the basis of the periodicities. These cycles occur at different time scales, forming a hierarchy of sequences at differing frequencies and, therefore, longer period sequences contain several shorter period, higher frequency sequences. In this nested periodicity, the longer period sequences influence the stratal patterns within the higher frequency sequences; this is a function of their position within the longer period sequence. The high resolution sequence stratigraphic approach to the analysis sedimentary successions focuses attention on key

stratal surfaces, facies dislocations and parasequence stacking patterns within the context of relative base level changes.

Stratal surfaces

Key stratal surfaces identified in the cores include sequence boundaries (SB), transgressive surfaces (TS), flooding surfaces (FS) and maximum flooding surfaces (MFS). The diagnostic features of these surfaces are described below.

Sequence boundaries (SB)

These surfaces are developed at the base of alluvial fan facies and are characterised by an increase in grainsize, increase in bed thickness and a change in parasequence set stacking patterns, and often by a thin lag of mud rip up clasts or quartz pebbles. From core it is difficult to determine the degree of erosional relief associated with these surfaces. In Core 1, the SB separates the alluvial fan facies association from the shoal water type fan delta, whereas in Core 2, the SB occurs between the alluvial fan and wave influenced shoreface / fan delta. The facies dislocations indicate a basinward shift in facies associated with a relative base level fall. There are different orders of SB present and are associated with the different orders (scales) of cycles. The SB associated with the high-order cycles possibly result from high frequency, possibly climatically driven relative base level falls, whereas the lower-order SB result from tectonic episodes (Plint et al, 1992).

Transgressive surface (TS)

These surfaces occur only in the fourth- and third-order sequences at the top of the alluvial fan facies association and are characterised by a change in parasequence set stacking patterns. TS result from an increase in the accommodation rate relative to sediment supply. In Core 1 the TS is marked by a rapid change in grainsize and bed thickness, and separates the alluvial fan facies association from the shoal water type fan delta. In Core 2 the TS occurs at the top of the core and is marked by a pebble to granule lag (ravinement surface), overlain by mud that possibly represents an offshore environment.

Flooding surfaces (FS) and maximum flooding surfaces (MFS)

Flooding surfaces are stratigraphic horizons across which prominent increases in water depths can be detected without evidence for significant erosion. These surfaces are best developed in Core 1 and are marked by abrupt contacts between facies e.g. lagoonal sediments overlain by offshore sediments, and alluvial fan sediments, including root traces, overlain by sub-aqueous fan delta deposits.

Maximum flooding surfaces record the maximum transgression and are commonly associated with mud dominated intervals predominantly deposited by suspension setting. As with SB there are differing orders of MFS, with only a high-order MFS present within the offshore sediments in Core 1.

Sequence stratigraphic model

The cored intervals are biased toward the reservoir intervals (alluvial fan, fan delta and shoreface) and these environments are developed in a predictable sequence stratigraphic framework.

Changes in relative base level, driven by allogenic processes (e.g. tectonics, climate change etc.) had a pronounced effect on the autocyclic, shoreface and fan delta depositional model. Relative base level falls within this setting caused forced regressions, in which alluvial fan sediments to be superimposed onto shoreface and fan delta environments. The lack of incised channel deposits implies a low gradient shoreface / fan delta that, when exposed, allowed the alluvial fan to prograde basinward. The alluvial fan sediments represent the lowstand systems tract (LST).

Subsequent rises in relative base level resulted in the flooding of the alluvial fan. In Core 2, the pebble lags at the top of the alluvial fan marks a transgressive ravinement surface, whereas in Core 1, the lower energy conditions did not permit reworking during the drowning of the fan and there is no ravinement surface. The increase in accommodation relative to sediment supply as evident from a change in stacking patterns across this surface implies a transgressive systems tract (TST) with episodic normal regressions. Only the basal portion of the TST, incorporating the shallow fan delta and lobe abandonment facies, is present in Core 1.

The transition from the TST to the highstand systems tract (HST) at the maximum flooding surface has not been intersected in core. The stacked progradational parasequences of the HST occur at the base of both cores and comprise shoreface and fan delta sediments that underlie the sequence boundaries.

Sequence development is generally controlled by the relationship between accommodation and sediment supply, which, in lacustrine settings, is controlled by climate and tectonics. If climate changes from drier to more humid conditions, there is an increase in both the lake water volume and the sediment yield, whereas a reverse climatic change will similarly reduce both. A rise in lake level thus tends to be accompanied by an increase in sediment supply, whereas a fall is accompanied by a supply decline. Furthermore, a lake responds to atmospheric changes in both precipitation and evaporation, whereas fluvial systems respond chiefly to the former. A climatically forced regression thus tends to be non-depositional, amounting to shoreface emergence, whereas a transgression may be countered by the coeval increase in sediment yield and stream discharge (delta growth), while being rapid and possibly non-depositional along a non-deltaic shoreline (Ilgar and Nemec, *in press*).

The lowering of the basin floor by tectonic subsidence, even if rapid, may have little effect on the lake water depth, because – unlike a marine basin – the subsidence is alone cannot change the basin's water volume. However, the subsidence in a lacustrine basin means lowering of the base level and has a direct effect on streams. Furthermore, the limited water volume and relatively small depth render lakes highly sensitive to changes in basin floor configuration. Asymmetrical subsidence can tilt the basin floor and make the water mass shift laterally, causing rapid regression (emergence) at one coast and coeval transgression at the other. Syndepositional faulting can form intrabasinal ridges and depressions, or can split the lake-hosting graben into narrower compartments and thus partition the water mass or displace it by draining (Ilgar and Nemec, *in press*). Tectonically induced cycles occur at a longer time scale than climatic cycles (typically 23 to 400 ka) and the periods of tectonic activity are represented by intervals of fine-grained sedimentation, whereas the coarse-grained sediments reflect tectonically quiescent periods when sediment dispersal processes have had time to adjust to the tectonic subsidence (Blair and Bilodeau, 1988).

With the limited cored intervals, it is unlikely that a definitive cause for the sequences present can be determined apart from some general points. The alluvial fans probably

represent tectonically quiescent periods in which coarse-grained sediment derived from the footwall prograded into the basin. The periods of tectonic activity are most likely represented by the thick intervals of mud (2780 – 2860 m KB and 3050 – 3110 m KB) that have not been cored. The parasequences present may indicate climatic variation controlling the sediment supply and lake level.

RESERVOIR QUALITY

Reservoir quality is strongly facies dependent with the alluvial fan facies association in the lowstand systems tract having the highest permeability, reflecting the higher depositional energy associated with sheetflood deposition. The shallow sub-aqueous fan delta (Facies H) in Core 1 has permeability values (1 – 20 mD) two orders of magnitude less than the alluvial fan facies association (40 – 2000 mD). The difference in permeability possibly results from the depositional process; upper flow regime traction currents on the alluvial fan and sub-aqueous high density turbidity current on the fan delta. The wave influenced shoreface / fan delta deposits provide a third reservoir interval, however, the permeability is low and varied, ranging from 0.1 to 5 mD, possibly reflecting the fine grainsize and degree of sorting. Graphic core logs for Cores 1 and 2 (Enclosures 1 and 2) show the porosity and permeability data from plugs and the probe permeameter for comparison with the sedimentological log.

REFERENCES

Basilici, G. 1997. Sedimentary facies in an extension and deep-lacustrine depositional system: the Pliocene Tiberino Basin, Central Italy. *Sedimentary Geology*, 109, 73-94.

Bechtal, A., Markic, M., Sachsenhofer, R.F., Jelen, B., Gratzer, R., Lücke, A. and Püttmann. W., 2004. Palaeoenvironment of the upper Oligocene Trbovlje coal seam (Slovenia). *International Journal of Coal Geology*, 57, 23-48.

Benvenuti, M., 2003. Facies analysis and tectonic significance of lacustrine fan-deltaic successions in the Pliocene-Pleistocene Mugello Basin, Central Italy. *Sedimentary Geology* 157, 197-234.

Beynon, B.M. and Pemberton, S.G., 1992. Ichnological signature of a brackish water deposit: an example from the Lower Cretaceous Grand Rapids Formation, Cold Lake Oil Sands area, Alberta. *In:* Pemberton, S.G., ed: *Applications of Ichnology to Petroleum Exploration: A Core Workshop.* Society for Sedimentary Geology, Tulsa, 199-221.

Billi, P., Magi, M. and Sagri, M., 1991. Pleistocene lacustrine fan delta deposits of the Valdarno Basin, Italy. *Journal of Sedimentary Petrology*, 61, No. 2, 280-290.

Blair, T.C. and Bilodeau, W.L., 1988. Development of tectonic cyclothems in rift, pull-apart, and foreland basins: Sedimentary response to episodic tectonism. *Geology*, 16, 517-520.

Blair, T.C. and McPherson J.G., 1994. Alluvial fans and their natural distinction from rivers based on morphology, hydraulic processes, sedimentary processes, and facies assemblages. *Journal of Sedimentary Research*, A64, 3, 450-489.

Boggs, S. Jr. 1987. Principles of Sedimentology and Stratigraphy. Macmillian Publishing Company, New York, 784p.

Bromley, R.G. 1996. Trace Fossils: Biology, taphonomy and applications. Chapman and Hall, London, 361p

Coates, L. and MacEachern, J.A., 2000. Differentiating river- and wave-dominated deltas from shorefaces: examples from the Cretaceous Western Interior Seaway, Alberta, Canada. http://www.cseg.ca/conferences/2000/443.pdf.

Cole, R.B. and Stanley, R.G. 1995. Middle Tertiary extension recorded by lacustrine fan-delta deposits, Plush Ranch Basin, Western Transverse Ranges, California. *Journal of Sedimentary Research*, B65, 455-468.

Colquhoun, G.P. 1995. Siliciclastic sedimentation on a storm- and tide-influenced shelf and shoreline: the Early Devonian Roxburgh Formation, NE Lachlan Fold Belt, southeastern Australia. *Sedimentary Geology*, 97, 69-98.

George, G.T., 2000. Characterisation and high resolution and sequence stratigraphy of storm-dominated braid delta and shoreface sequences from the Basal Grit Group (Namurian) of the South Wales Variscan peripheral foreland basin. *Marine and Petroleum Geology*, 17, 445-475.

Holz, M. 2003. Sequence stratigraphy of a lagoonal estuarine system – an example from the lower Permian Rio Bonito Formation, Paraná Basin, Brazil. *Sedimentary Geology*, 162, 305-331.

Ilgar, A. and Nemec, W. *in press*. Early Miocene lacustrine deposits and sequence stratigraphy of the Ermenek Basin, Central Taurides, Turkey. *Sedimentary Geology*.

Kelly, S.B., and Olsen, H.O., 1993. Terminal fans – a review with reference to Devonian examples. *Sedimentary Geology*, 85, 339-374.

Kraus, M.J., 1999. Paleosols in clastic sedimentary rocks: their geologic applications. *Earth Science Reviews*, 47, 41-70.

Le Roux, J.P. and Elgueta, S. 1997. Paralic parasequences associated with Eocene sea-level oscillations in an active margin setting: Trihueco Formation of the Arauco Basin, Chile. *Sedimentary Geology*, 110, 257-276.

Lowe, D.R., 1982. Sediment gravity flows: II Depositional models with special reference to the deposits of high density turbidity currents. *Journal of Sedimentary Petrology*, 52, 279-297.

Martins-Neto, M.A., 1996. Lacustrine fan-deltaic sedimentation in a Proterozoic rift basin: the Sopa-Brumadinhp Tectonosequence, southeastern Brazil. *Sedimentary Geology*, 106, 65-96.

Mastalerz, K., 1995. Deposits of high-density turbidity currents on fan-delta slopes: an example from the upper Visean Szczawno Formation, Intrasudetic Basin, Poland. *Sedimentary Geology,* 98, 121-146.

Miall, A.D., 1996. *The Geology of Fluvial Deposits; Sedimentary Facies, Basin Analysis and Petroleum Geology*. Springer-Verlag, New York. 582p.

Moore, J.R., 1968. Cannel coals, bogheads and oil shales. *In:* Murchison, D., and Westoll, T.S. eds. *Coal and Coal Bearing Strata.* Oliver & Boyd, Edinburgh, 19-29.

Morgan, R., 2004. Palynology of Yolla 4 Bass Basin, Australia. Unpublished report for Origin Energy.

Pemberton, S.G. and Wightman, D.M., 1992. Ichnological characteristics of brackish water deposits. *In:* Pemberton, S.G. ed. *Applications of Ichnology to Petroleum Exploration: A Core Workshop*. Society for Sedimentary Geology, Tulsa, pp141-167.

Phillips, R.L., 2003. Depositional environments and processes in Upper Cretaceous nonmarine and marine sediments, Ocean Point dinosaur locality, North Slope, Alaska. *Cretaceous Research*, 24, 499-523.

Plint, A.G., Eyles, N., Eyles, C.H. and Walker, R.G. 1992. Control of Sea Level Change. *In* Walker, R.G. and James, N.P. eds, *Facies Models: Response to Sea Level Change.* Geological Association of Canada, 15-26.

Postma, G. 1990. Depositional architecture and facies of river and fan deltas: a synthesis. *In:* Colella, A. and Prior, D.B., eds. *Coarse Grained Deltas*. Special Publication No. 10, International Association of Sedimentologists, Blackwell Scientific Publications, Oxford, 13-27.

Reading, H.R. and Collinson, J.D., 1996 Clastic coasts. *In:* Reading, H.G., ed. *Sedimentary Environments: Processes, Facies and Stratigraphy*. Blackwell Science, Oxford, 154-231.

Stow, D.A.V., Reading, H.G. and Collinson, J.D., 1996. Deep Seas. *In:* Reading, H.G., ed. *Sedimentary Environments: Processes, Facies and Stratigraphy*. Blackwell Science, Oxford, 395-453.

Tamura, T. and Masuda, F., 2003. Shallow-marine fan delta slope deposits with large-scale cross-stratification: the Plio-Pleistocene Zaimokuzwa formation in the Ishikari Hills, northern Japan. *Sedimentary Geology*, 158, 195-207.

APPENDIX 1

YOLLA 4 INTERPRETED CORE PHOTOGRAPHS

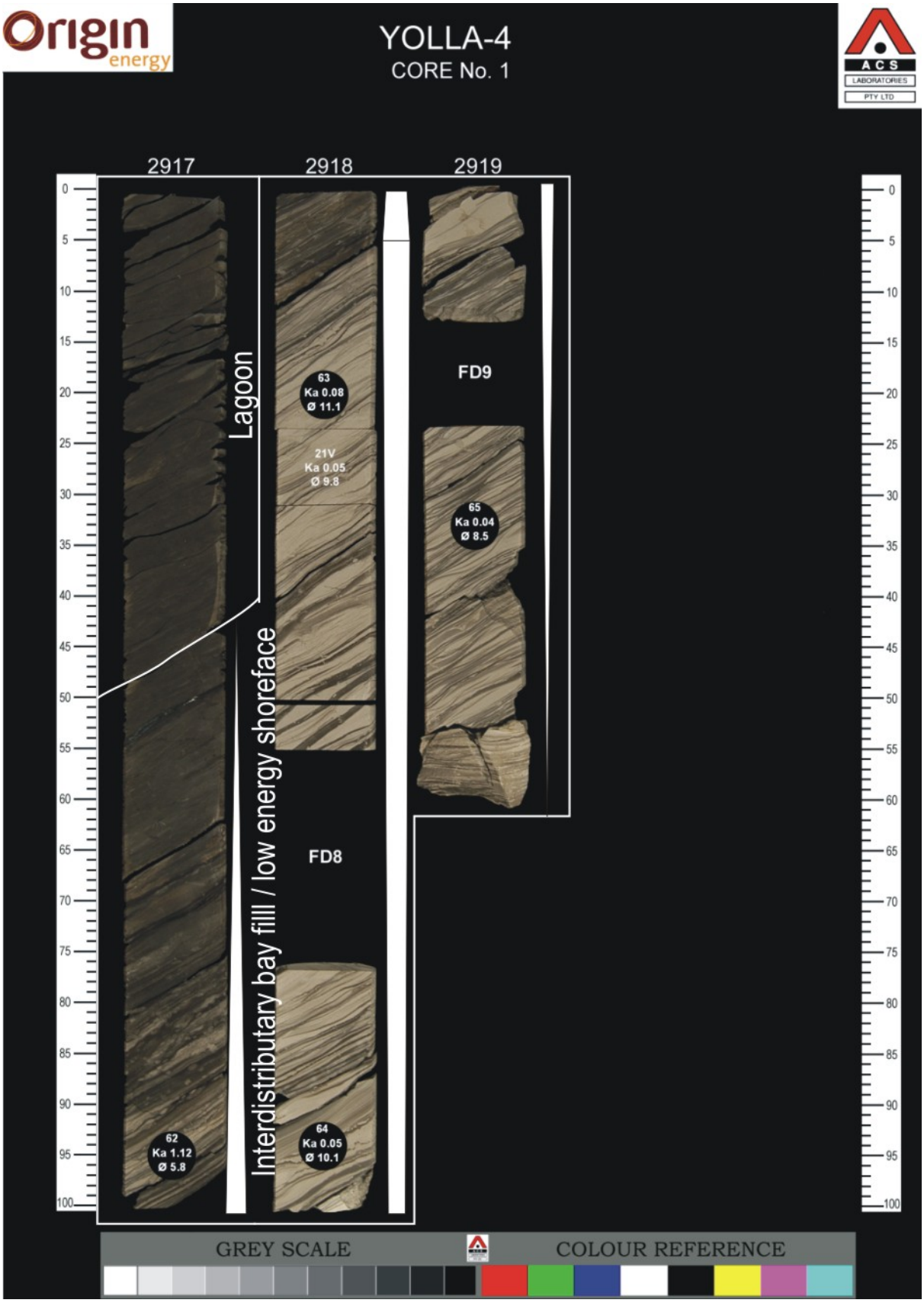
YOLLA-4
CORE No. 1
2917
2918
2919
Lagoon
Interdistributary bay fill / low energy shoreface
FD9
FD8
63
Ka 0.08
Ø 11.1
21V
Ka 0.05
Ø 9.8
65
Ka 0.04
Ø 8.5
62
Ka 1.12
Ø 5.8
64
Ka 0.05
Ø 10.1
GREY SCALE
COLOUR REFERENCE

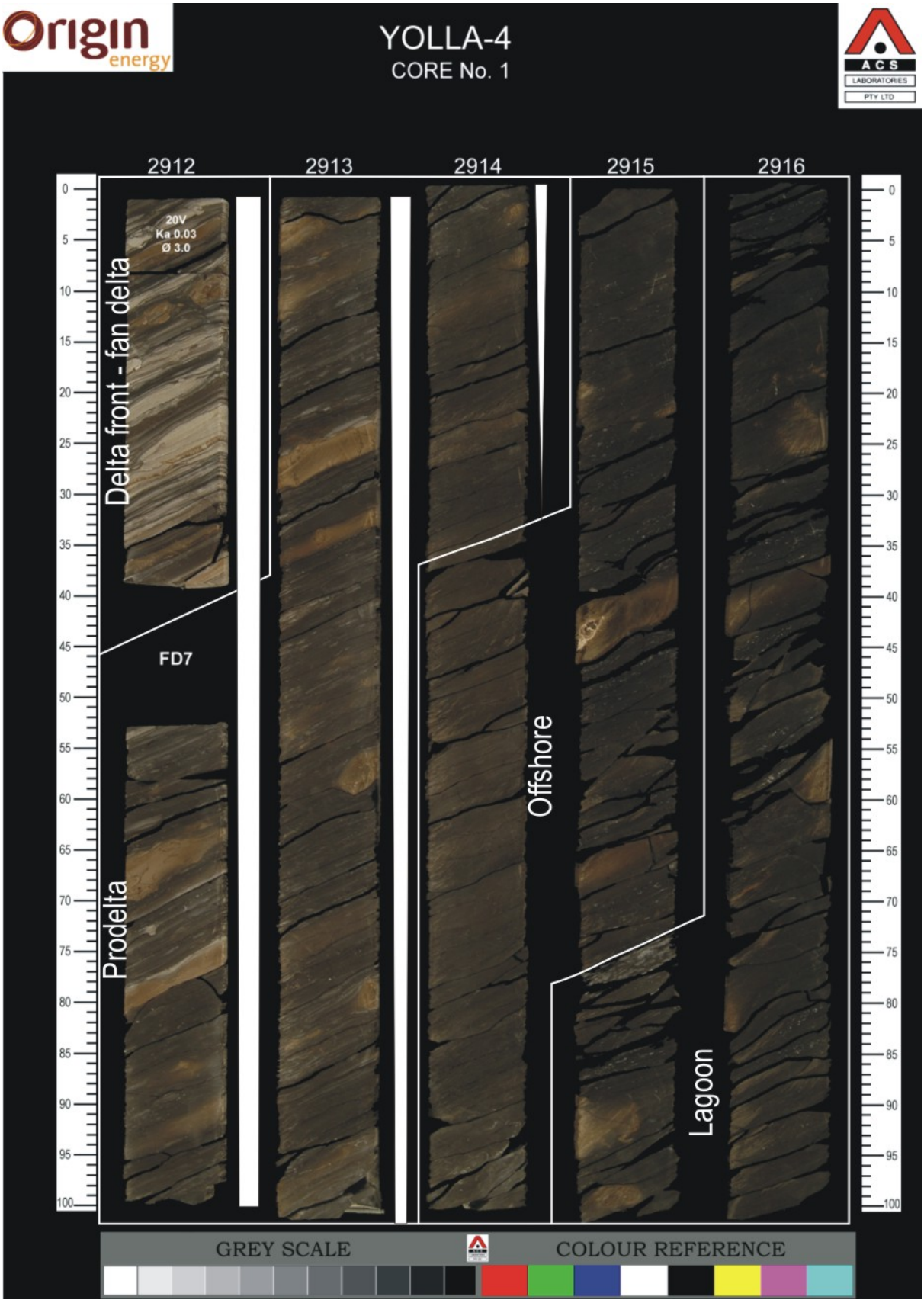
YOLLA-4
CORE No. 1
2912
2913
2914
2915
2916
20V
Ka 0.03
Ø 3.0
Delta front - fan delta
FD7
Prodelta
Offshore
Lagoon
GREY SCALE
COLOUR REFERENCE

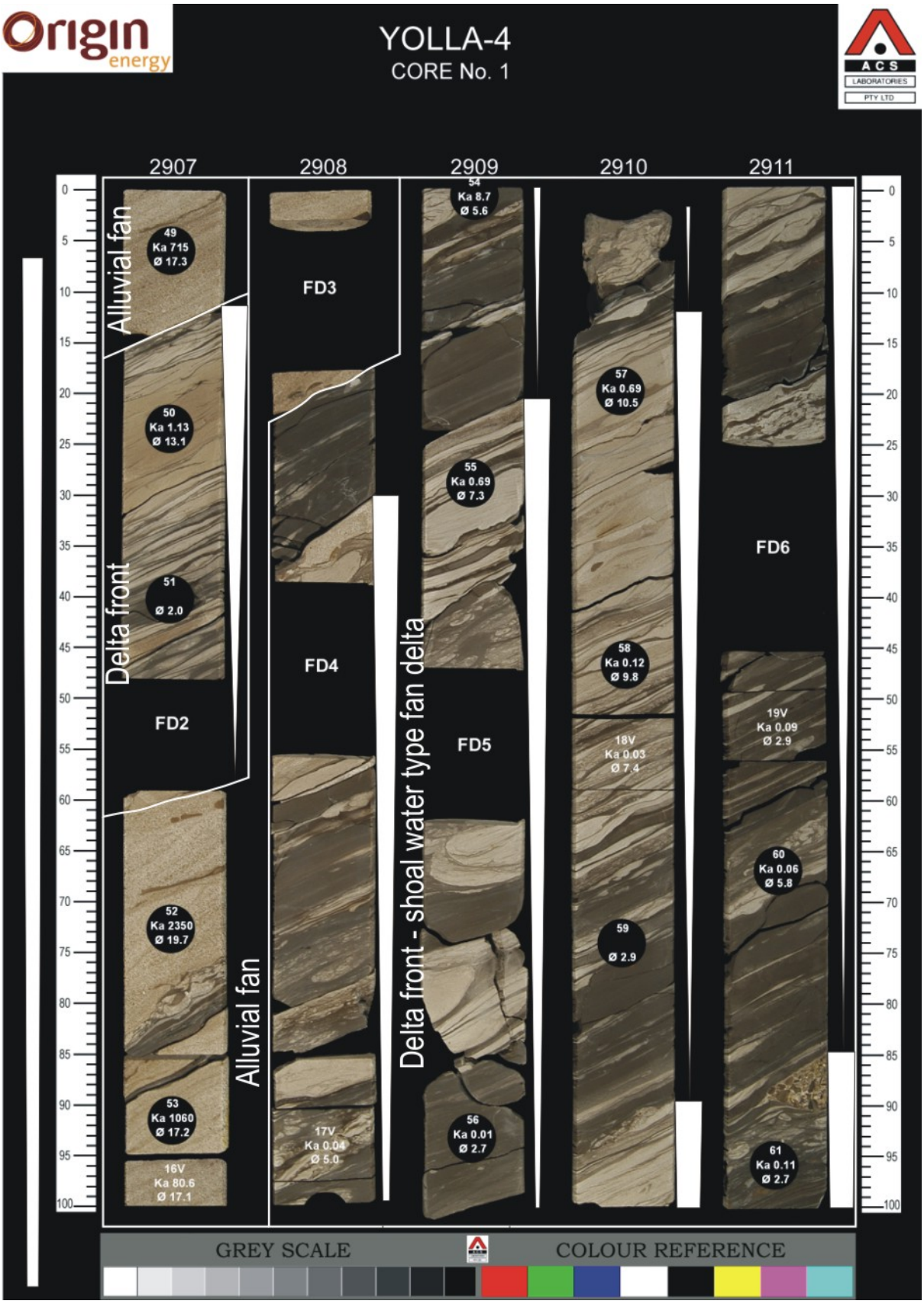
YOLLA-4
CORE No. 1
2907
2908
2909
2910
2911
Alluvial fan
Delta front
Alluvial fan
Delta front - shoal water type fan delta
FD2
FD3
FD4
FD5
FD6
49 Ka 715 Ø 17.3
50 Ka 1.13 Ø 13.1
51 Ø 2.0
52 Ka 2350 Ø 19.7
53 Ka 1060 Ø 17.2
16V Ka 80.6 Ø 17.1
17V Ka 0.04 Ø 5.0
54 Ka 8.7 Ø 5.6
55 Ka 0.69 Ø 7.3
56 Ka 0.01 Ø 2.7
57 Ka 0.69 Ø 10.5
58 Ka 0.12 Ø 9.8
18V Ka 0.03 Ø 7.4
59 Ø 2.9
19V Ka 0.09 Ø 2.9
60 Ka 0.06 Ø 5.8
61 Ka 0.11 Ø 2.7
GREY SCALE
COLOUR REFERENCE

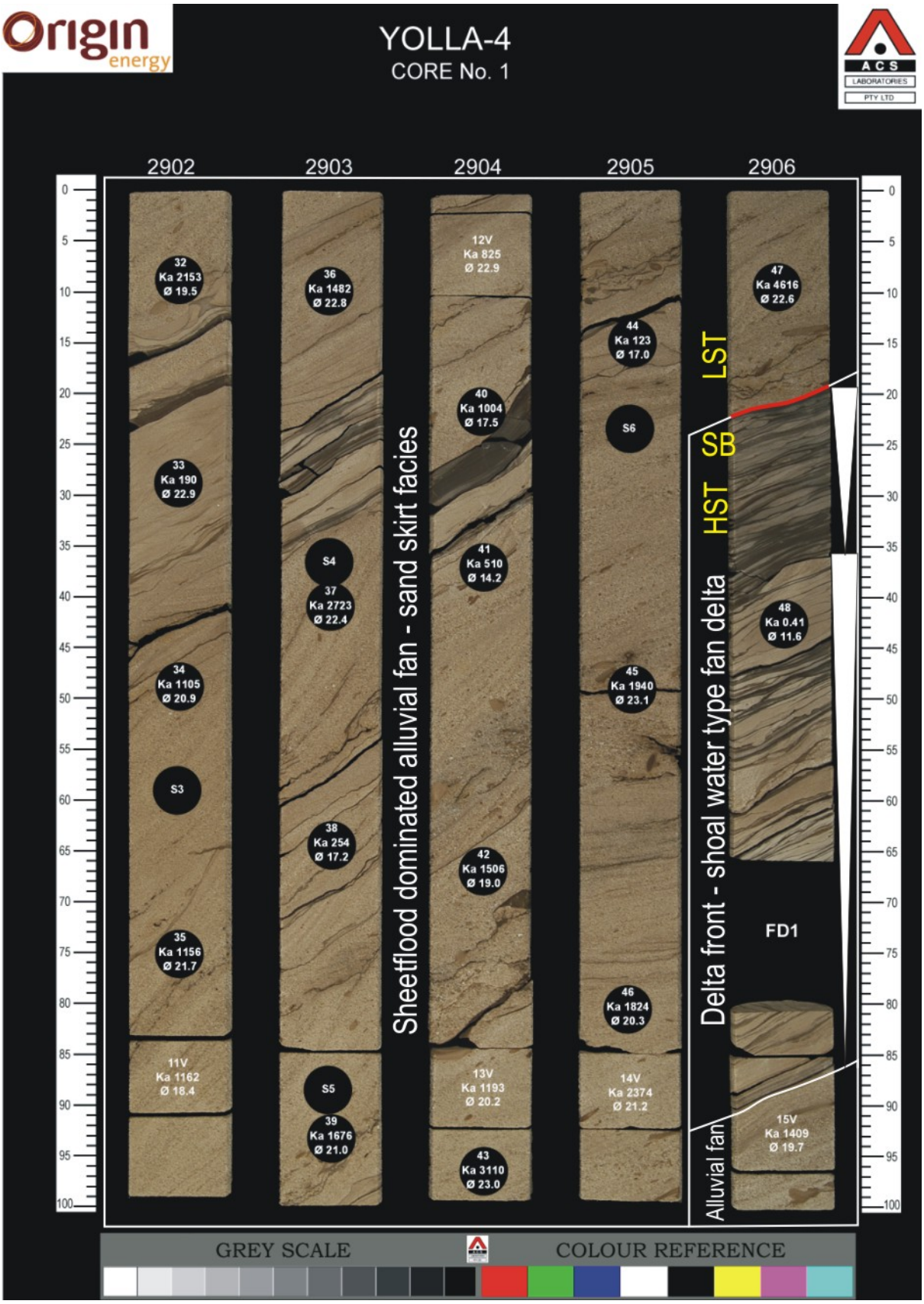
YOLLA-4
CORE No. 1
2902
2903
2904
2905
2906
32 Ka 2153 Ø 19.5
33 Ka 190 Ø 22.9
34 Ka 1105 Ø 20.9
S3
35 Ka 1156 Ø 21.7
11V Ka 1162 Ø 18.4
36 Ka 1482 Ø 22.8
S4
37 Ka 2723 Ø 22.4
38 Ka 254 Ø 17.2
S5
39 Ka 1676 Ø 21.0
12V Ka 825 Ø 22.9
40 Ka 1004 Ø 17.5
41 Ka 510 Ø 14.2
42 Ka 1506 Ø 19.0
13V Ka 1193 Ø 20.2
43 Ka 3110 Ø 23.0
44 Ka 123 Ø 17.0
S6
45 Ka 1940 Ø 23.1
46 Ka 1824 Ø 20.3
14V Ka 2374 Ø 21.2
47 Ka 4616 Ø 22.6
48 Ka 0.41 Ø 11.6
FD1
15V Ka 1409 Ø 19.7
Sheetflood dominated alluvial fan - sand skirt facies
LST
SB
HST
Delta front - shoal water type fan delta
Alluvial fan
GREY SCALE
COLOUR REFERENCE


YOLLA-4
CORE No. 1
2897
2898
2899
2900
2901
Slump
Shallow sub-aqueous shoal water type fan delta
Alluvial fan
TST
TS
LST
5V Ka 0.04 Ø 10.0
6V Ka 1.62 Ø 17.3
7V Ka 3.55 Ø 16.6
8V Ka 0.27 Ø 11.6
9V Ka 2.09 Ø 17.0
10V Ka 1340 Ø 21.4
15 Ka 6.1 Ø 18.4
16 Ka 7.7 Ø 16.6
17 Ka 12.4 Ø 18.2
18 Ka 12.2 Ø 18.1
19 Ka 11.7 Ø 16.0
20 Ka 5.4 Ø 15.7
21 Ka 13.6 Ø 17.9
22 Ka 9.2 Ø 17.2
23 Ka 11.5 Ø 17.8
24 Ka 35.5 Ø 18.0
25 Ka 2.37 Ø 15.0
26 Ka 2.37 Ø 11.2
27 Ka 1.12 Ø 9.4
28 Ka 20.3 Ø 15.3
29 Ka 35.9 Ø 17.7
30 Ka <0.01 Ø 6.0
31 Ka 3564 Ø 20.4
S1
S2
GREY SCALE
COLOUR REFERENCE

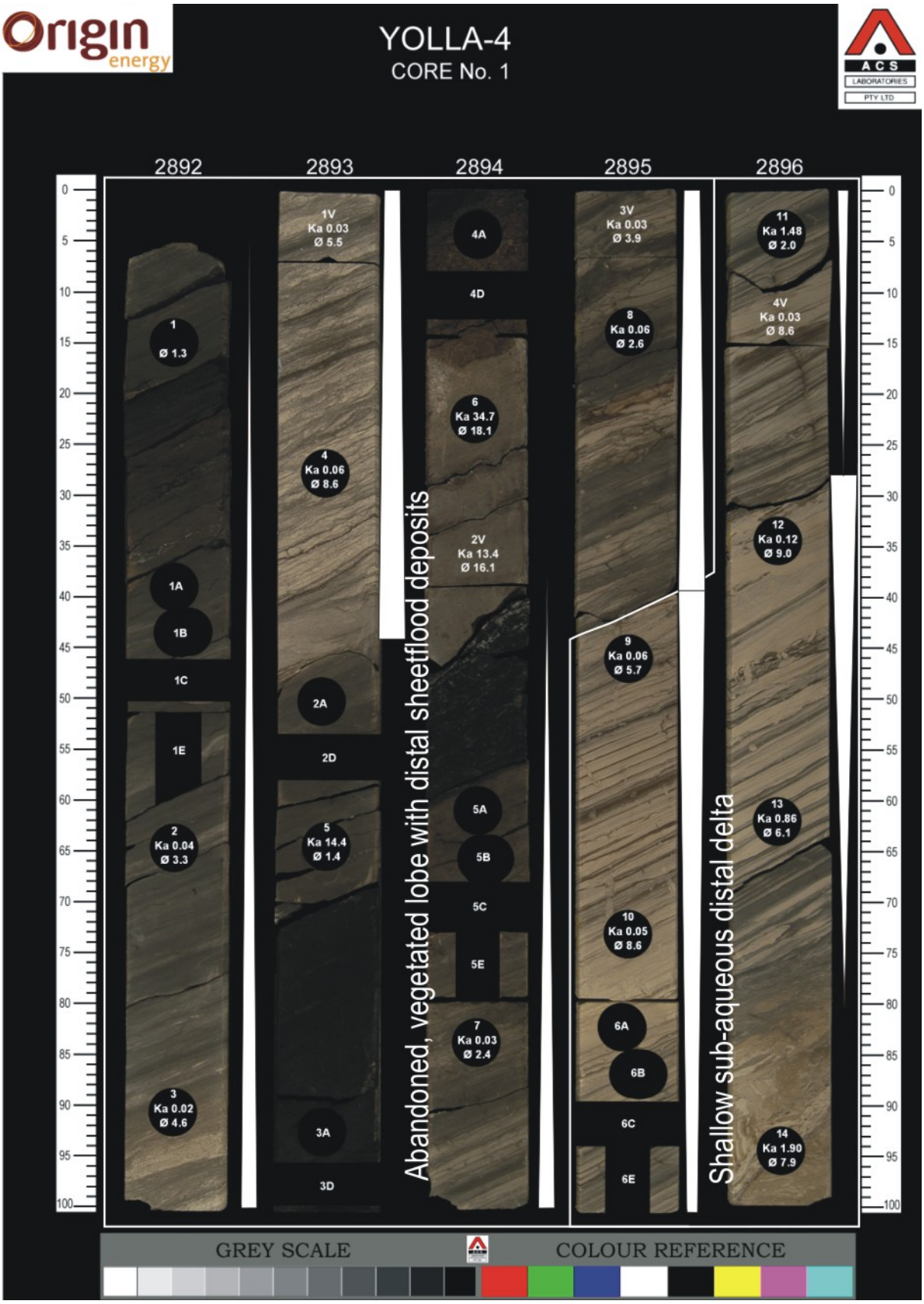
YOLLA-4
CORE No. 1
2892
2893
2894
2895
2896
1
Ø 1.3
1A
1B
1C
1E
2
Ka 0.04
Ø 3.3
3
Ka 0.02
Ø 4.6
1V
Ka 0.03
Ø 5.5
4
Ka 0.06
Ø 8.6
2A
2D
5
Ka 14.4
Ø 1.4
3A
3D
4A
4D
6
Ka 34.7
Ø 18.1
2V
Ka 13.4
Ø 16.1
5A
5B
5C
5E
7
Ka 0.03
Ø 2.4
3V
Ka 0.03
Ø 3.9
8
Ka 0.06
Ø 2.6
9
Ka 0.06
Ø 5.7
10
Ka 0.05
Ø 8.6
6A
6B
6C
6E
11
Ka 1.48
Ø 2.0
4V
Ka 0.03
Ø 8.6
12
Ka 0.12
Ø 9.0
13
Ka 0.86
Ø 6.1
14
Ka 1.90
Ø 7.9
Abandoned, vegetated lobe with distal sheetflood deposits
Shallow sub-aqueous distal delta
GREY SCALE
COLOUR REFERENCE

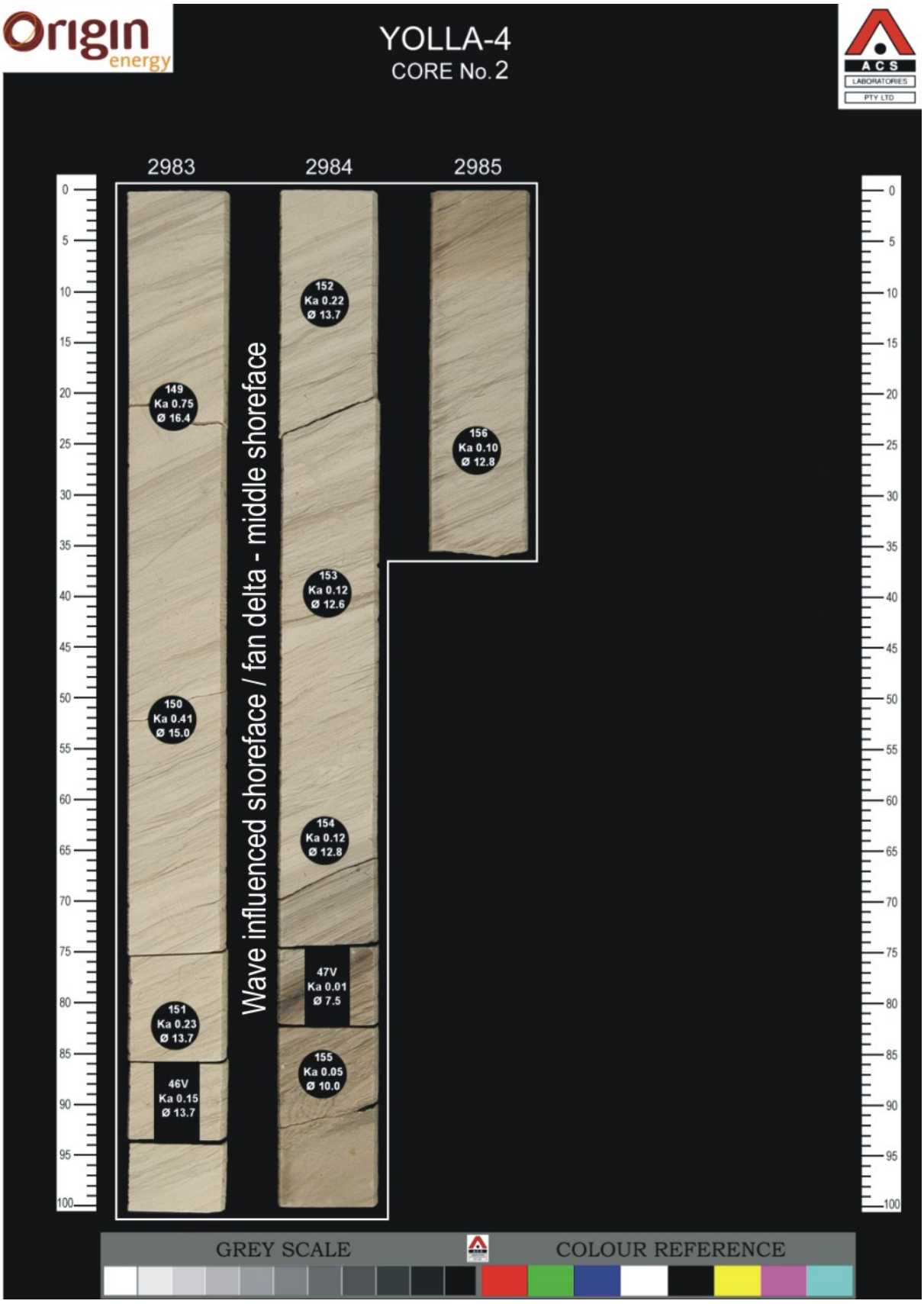
YOLLA-4
CORE No. 2
2983
2984
2985
Wave influenced shoreface / fan delta - middle shoreface
149 Ka 0.75 Ø 16.4
150 Ka 0.41 Ø 15.0
151 Ka 0.23 Ø 13.7
46V Ka 0.15 Ø 13.7
152 Ka 0.22 Ø 13.7
153 Ka 0.12 Ø 12.6
154 Ka 0.12 Ø 12.8
47V Ka 0.01 Ø 7.5
155 Ka 0.05 Ø 10.0
156 Ka 0.10 Ø 12.8
GREY SCALE
COLOUR REFERENCE

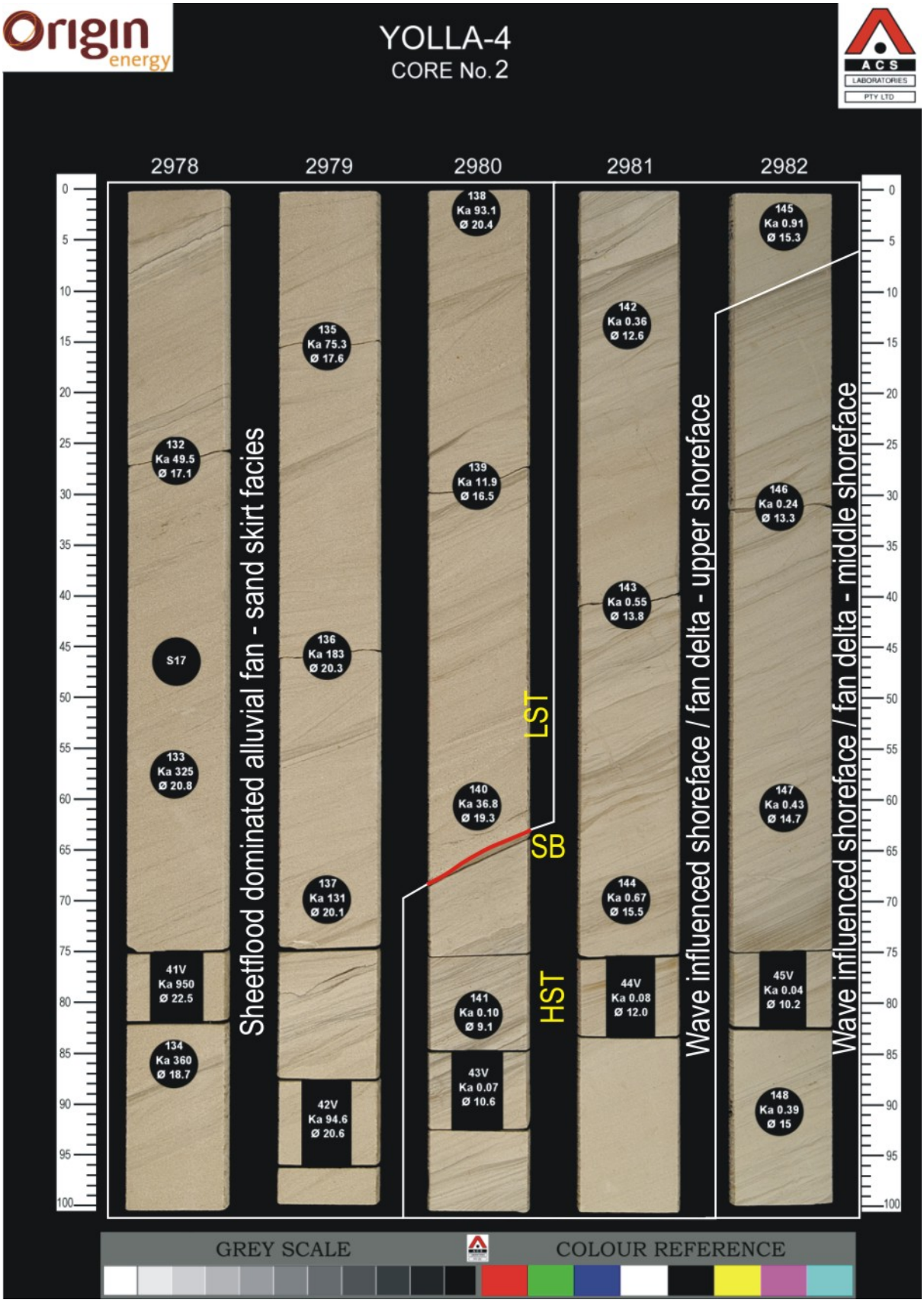
YOLLA-4
CORE No. 2
2978
2979
2980
2981
2982
Sheetflood dominated alluvial fan - sand skirt facies
Wave influenced shoreface / fan delta - upper shoreface
Wave influenced shoreface / fan delta - middle shoreface
LST
SB
HST
132 Ka 49.5 Ø 17.1
S17
133 Ka 325 Ø 20.8
41V Ka 950 Ø 22.5
134 Ka 360 Ø 18.7
135 Ka 75.3 Ø 17.6
136 Ka 183 Ø 20.3
137 Ka 131 Ø 20.1
42V Ka 94.6 Ø 20.6
138 Ka 93.1 Ø 20.4
139 Ka 11.9 Ø 16.5
140 Ka 36.8 Ø 19.3
141 Ka 0.10 Ø 9.1
43V Ka 0.07 Ø 10.6
142 Ka 0.36 Ø 12.6
143 Ka 0.55 Ø 13.8
144 Ka 0.67 Ø 15.5
44V Ka 0.08 Ø 12.0
145 Ka 0.91 Ø 15.3
146 Ka 0.24 Ø 13.3
147 Ka 0.43 Ø 14.7
45V Ka 0.04 Ø 10.2
148 Ka 0.39 Ø 15
GREY SCALE
COLOUR REFERENCE

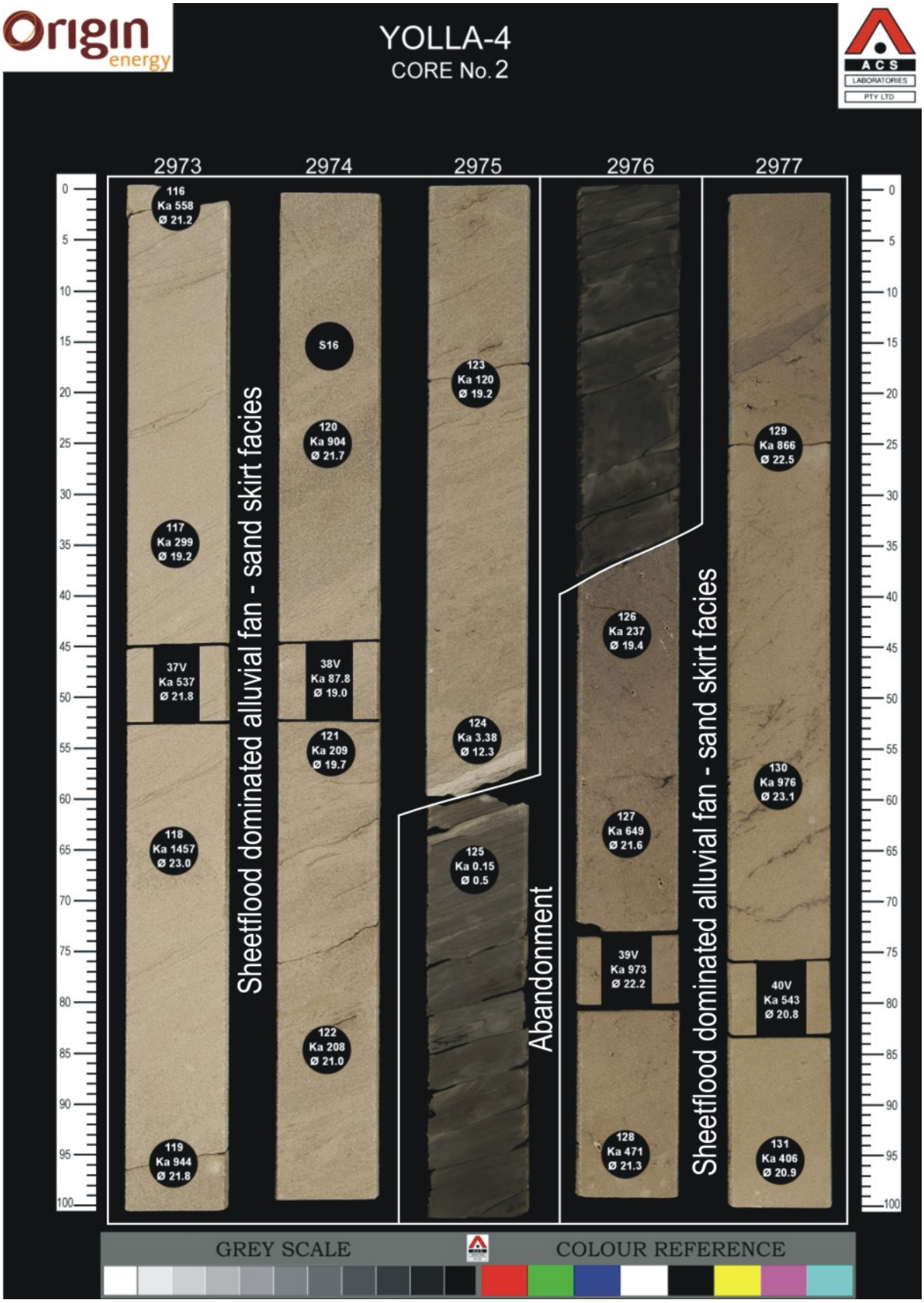
YOLLA-4
CORE No. 2
2973
2974
2975
2976
2977
116 Ka 558 Ø 21.2
117 Ka 299 Ø 19.2
37V Ka 537 Ø 21.8
118 Ka 1457 Ø 23.0
119 Ka 944 Ø 21.8
S16
120 Ka 904 Ø 21.7
38V Ka 87.8 Ø 19.0
121 Ka 209 Ø 19.7
122 Ka 208 Ø 21.0
123 Ka 120 Ø 19.2
124 Ka 3.38 Ø 12.3
125 Ka 0.15 Ø 0.5
126 Ka 237 Ø 19.4
127 Ka 649 Ø 21.6
39V Ka 973 Ø 22.2
128 Ka 471 Ø 21.3
129 Ka 866 Ø 22.5
130 Ka 976 Ø 23.1
40V Ka 543 Ø 20.8
131 Ka 406 Ø 20.9
Sheetflood dominated alluvial fan - sand skirt facies
Abandonment
Sheetflood dominated alluvial fan - sand skirt facies
GREY SCALE
COLOUR REFERENCE


YOLLA-4
CORE No. 2
2968
2969
2970
2971
2972
Sheetflood couplets
Sheetflood dominated alluvial fan - distal sand skirt facies
Sheetflood couplets
Sheetflood dominated alluvial fan - sand skirt facies
99 Ka 173 Ø 13.9
100 Ka 59.5 Ø 19.2
32V Ka 16.6 Ø 18.4
101 Ka 7.5 Ø 14.9
102 Ka 66.9 Ø 19.4
103 Ka 32 Ø 17.4
33V Ka 36.6 Ø 18.2
104 Ka 8.7 Ø 13.7
105 Ka 330 Ø 19.6
106 Ka 107 Ø 18.8
107 Ka 49.4 Ø 17.5
108 Ka 479 Ø 20.4
34V Ka 354 Ø 20.2
109 Ka 300 Ø 18.4
S14
110 Ka 570 Ø 19.5
111 Ka 253 Ø 18.1
35V Ka 499 Ø 18.5
112 Ka 454 Ø 18.5
113 Ka 426 Ø 18.4
114 Ka 123 Ø 17.5
36V Ka 39.6 Ø 16.7
115 Ka 649 Ø 18.7
S15
GREY SCALE
COLOUR REFERENCE

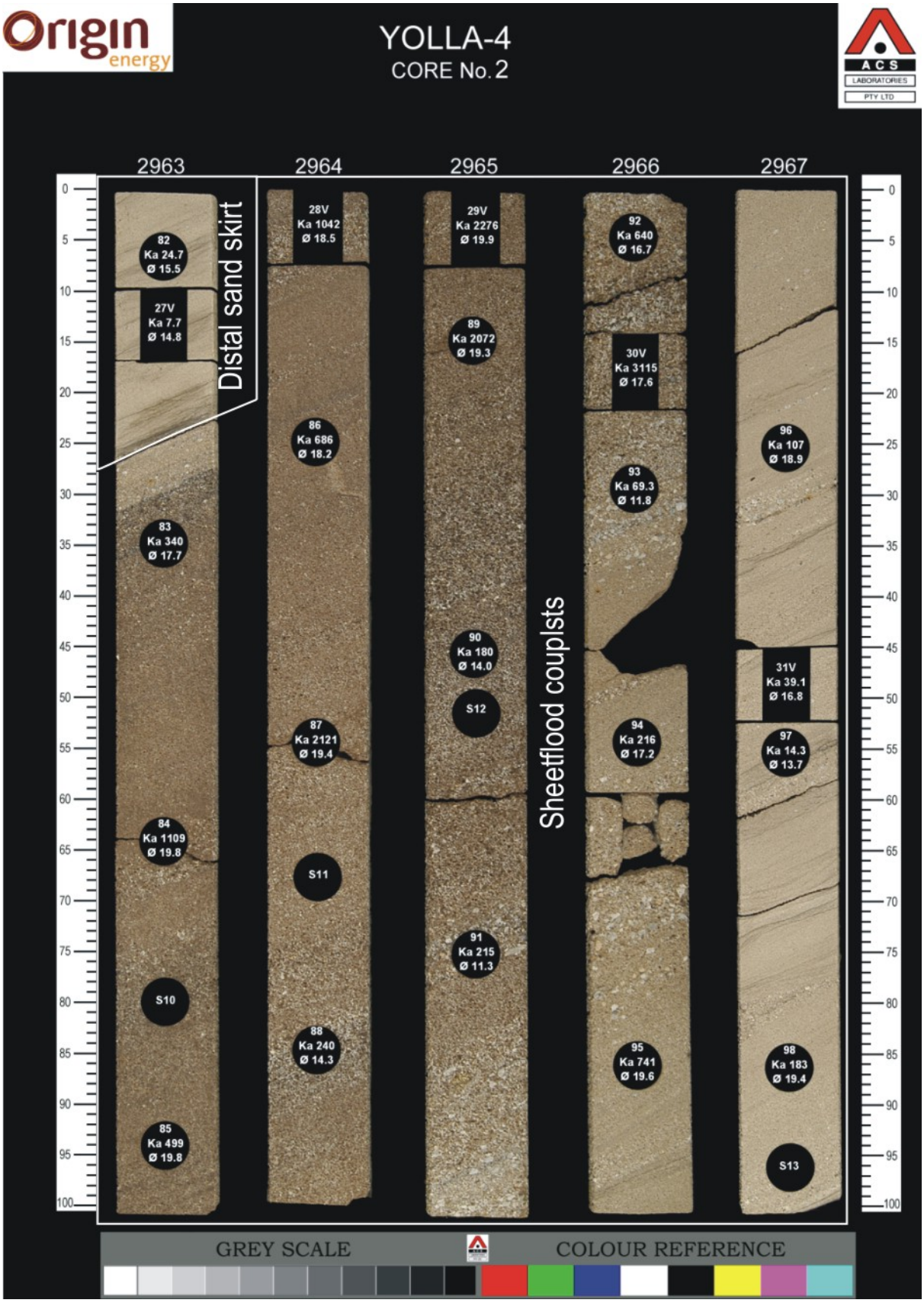
YOLLA-4
CORE No. 2
2963
2964
2965
2966
2967
Distal sand skirt
Sheetflood couplsts
82 Ka 24.7 Ø 15.5
27V Ka 7.7 Ø 14.8
83 Ka 340 Ø 17.7
84 Ka 1109 Ø 19.8
S10
85 Ka 499 Ø 19.8
28V Ka 1042 Ø 18.5
86 Ka 686 Ø 18.2
87 Ka 2121 Ø 19.4
S11
88 Ka 240 Ø 14.3
29V Ka 2276 Ø 19.9
89 Ka 2072 Ø 19.3
90 Ka 180 Ø 14.0
S12
91 Ka 215 Ø 11.3
92 Ka 640 Ø 16.7
30V Ka 3115 Ø 17.6
93 Ka 69.3 Ø 11.8
94 Ka 216 Ø 17.2
95 Ka 741 Ø 19.6
96 Ka 107 Ø 18.9
31V Ka 39.1 Ø 16.8
97 Ka 14.3 Ø 13.7
98 Ka 183 Ø 19.4
S13
GREY SCALE
COLOUR REFERENCE

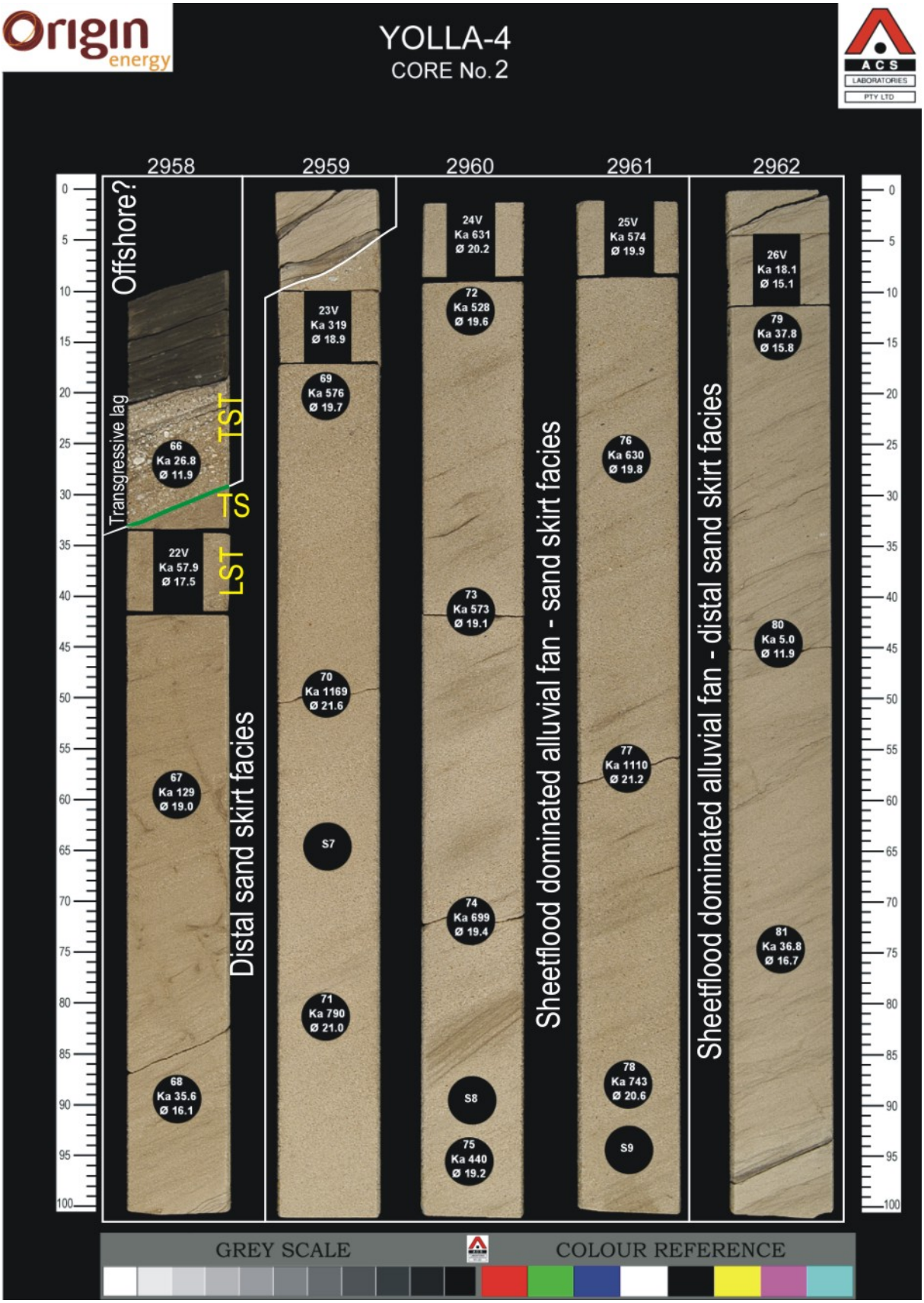
YOLLA-4
CORE No. 2
2958
2959
2960
2961
2962
Offshore?
Transgressive lag
TST
TS
LST
Distal sand skirt facies
Sheetflood dominated alluvial fan - sand skirt facies
Sheetflood dominated alluvial fan - distal sand skirt facies
66 Ka 26.8 Ø 11.9
22V Ka 57.9 Ø 17.5
67 Ka 129 Ø 19.0
68 Ka 35.6 Ø 16.1
23V Ka 319 Ø 18.9
69 Ka 576 Ø 19.7
70 Ka 1169 Ø 21.6
S7
71 Ka 790 Ø 21.0
24V Ka 631 Ø 20.2
72 Ka 528 Ø 19.6
73 Ka 573 Ø 19.1
74 Ka 699 Ø 19.4
S8
75 Ka 440 Ø 19.2
25V Ka 574 Ø 19.9
76 Ka 630 Ø 19.8
77 Ka 1110 Ø 21.2
78 Ka 743 Ø 20.6
S9
26V Ka 18.1 Ø 15.1
79 Ka 37.8 Ø 15.8
80 Ka 5.0 Ø 11.9
81 Ka 36.8 Ø 16.7
GREY SCALE
COLOUR REFERENCE

ENCLOSURE 1

YOLLA 4 CORE 1 – EVCM

YOLLA 4

CORE 1 - EVCM

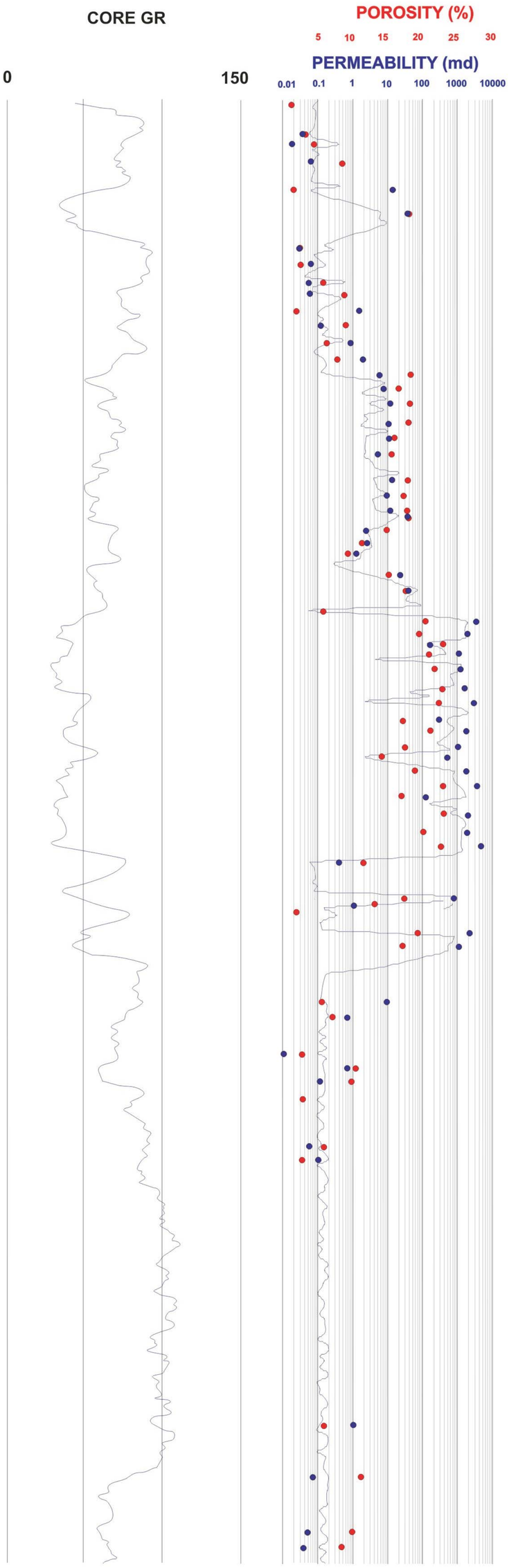

PLUG DATA

- Porosity
- Permeability

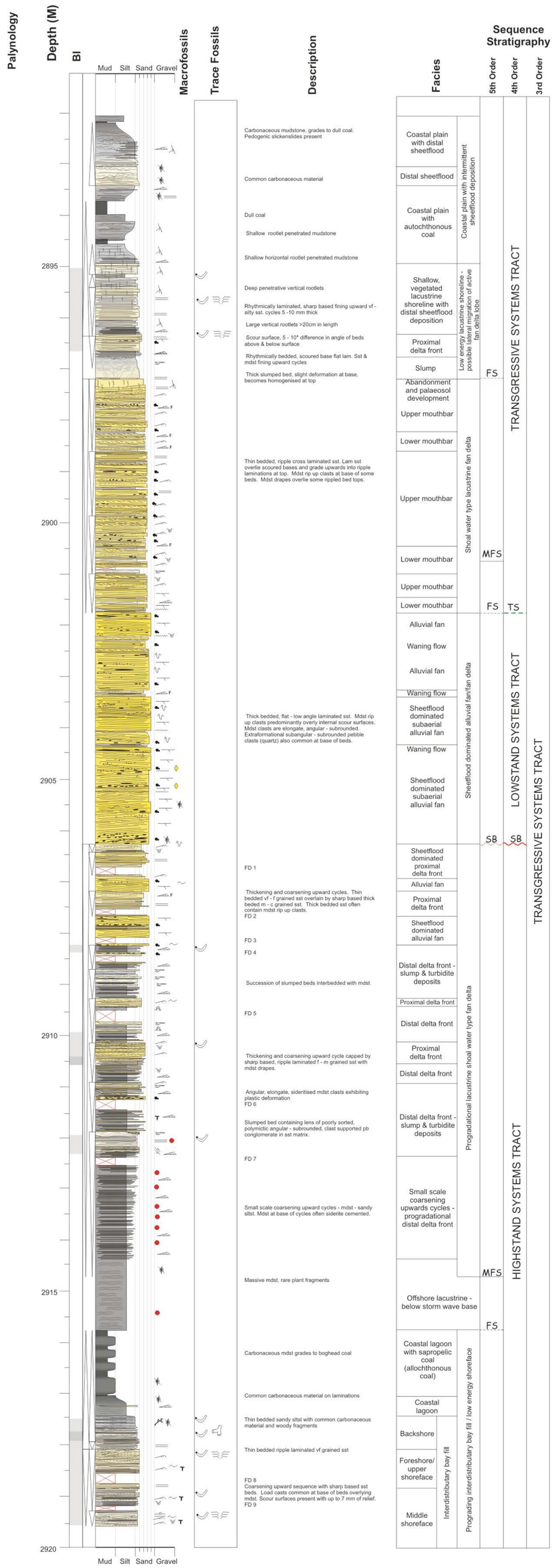

Siliciclastic

- Siltstone - mudstone/anoxic mudstone
- Sandstone
- Conglomerate
- Tuff

Origin energy

delivering the goods

PHYSICAL SEDIMENTARY STRUCTURES

- Trough cross-bedding
- Planar cross-bedding
- Flat lamination
- Plane bedding
- Low-angle lamination
- Current Ripple Cross-lamination
- Wave Ripple Cross-lamination
- Flaser bedding
- Lenticular lamination
- Wavy lamination
- Hummocky cross-stratification
- Bioturbation
- Plant debris
- Wood
- Rip-up clasts
- Extraformational pebbles
- Soft sediment deformation
- Convoluted bedding
- Synaeresis cracks
- Stylolites
- Coaly trace
- Root trace
- Carbonaceous laminae
- Fault
- Erosional base
- Slumped sediment
- Fining upwards
- Coarsening upwards
- Calcite cementation
- Glauconite
- Pyrite
- Siderite/Fe-concretion
- Silica cementation
- Calcite-healed fracture
- Silica-healed fracture
- Fracture/fault with slickensides

ICHNOLOGY

- *Ophiomorpha*
- *Skolithos*
- *Diplocraterion*
- *Macaronichnus*
- *Thalassinoides*
- *Planolites*
- *Palaeophycus*
- *Rhizocorallium*
- *Teichichnus*
- *Phycosiphon*
- *Taedium*
- *Cylindrichnus*
- *Zoophycus*
- *Rosselia*
- *Conichnus*
- *Chondrites*
- *Undifferentiated*
- *Asterosoma*
- *Helminthopsis*
- *Schaubcylindrichnus*
- *Terebellina*
- *Glossifungites surface*
- *Escape burrow*

Bioturbation Index

0 1 2 3 4 5 6

MACROFOSSILS

- *Brachiopods*
- *Molluscs*
- *Bryozoans*
- *Crinoids*
- *Forams*
- *Algae*
- *Stromatolites/stromatoporoids*
- *Unidentified shell fragments*
- *Ammonite*
- *Gastropods*

ENCLOSURE 2

YOLLA 4 CORE 2 - EVCM

YOLLA 4

CORE 2 - EVCM

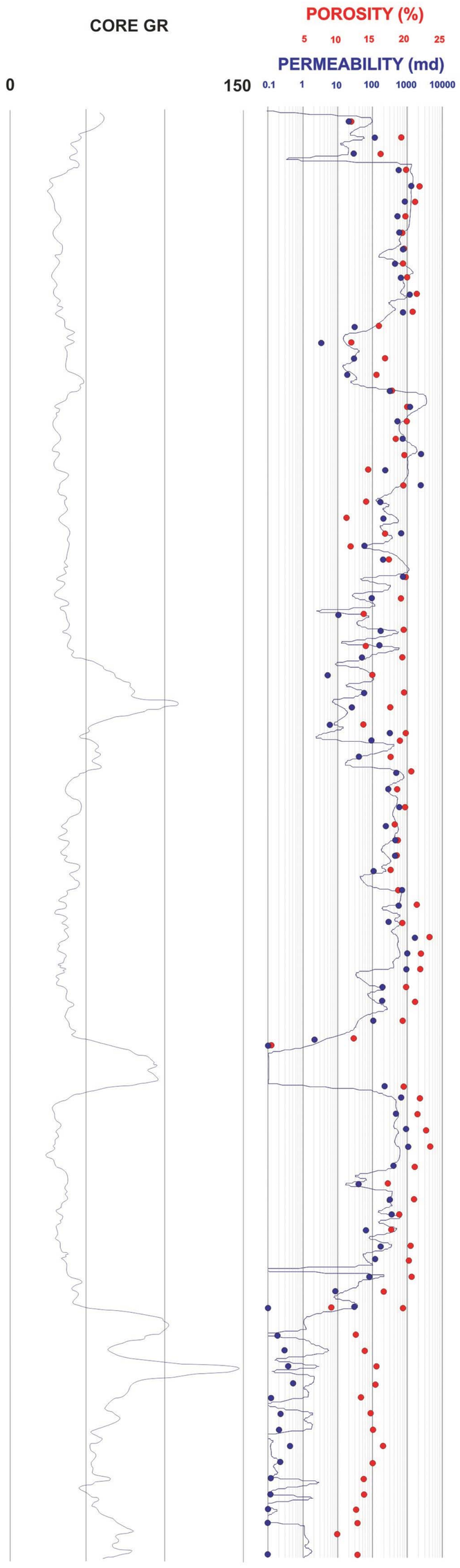

PLUG DATA
- Porosity
- Permeability

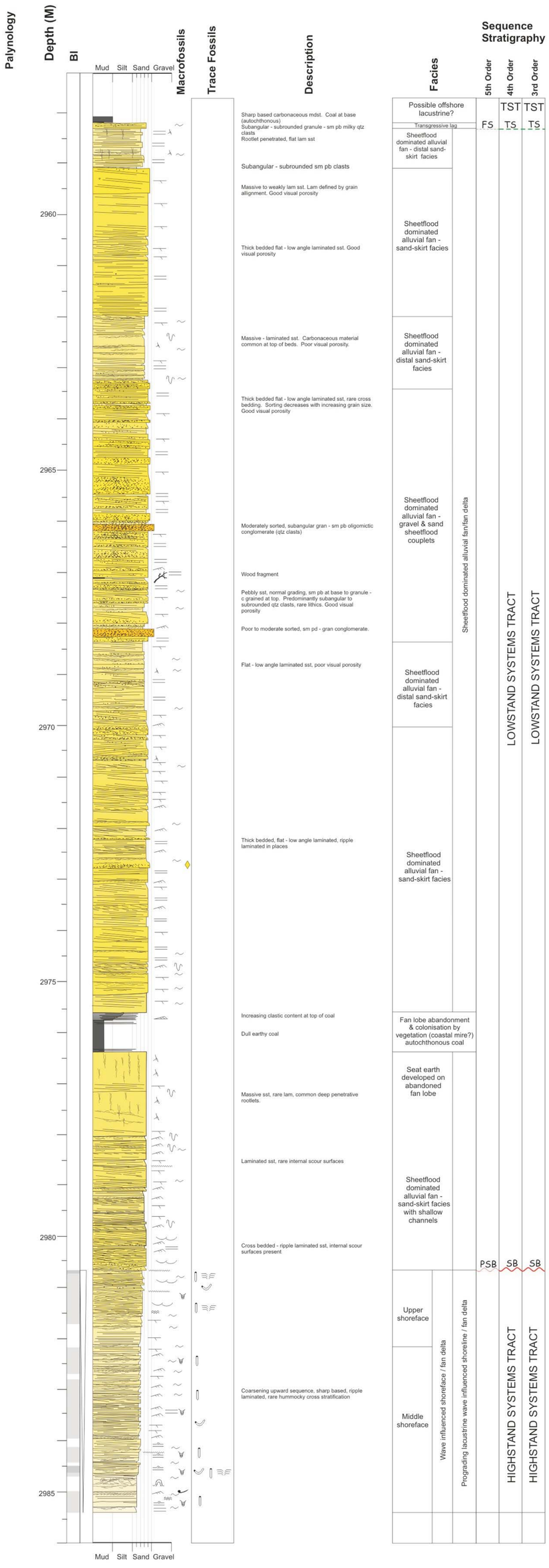

Siliciclastic
- Siltstone - mudstone/anoxic mudstone
- Sandstone
- Conglomerate
- Tuff

Origin energy

delivering the goods

PHYSICAL SEDIMENTARY STRUCTURES

- Trough cross-bedding
- Planar cross-bedding
- Flat lamination
- Plane bedding
- Low-angle lamination
- Current Ripple Cross-lamination
- Wave Ripple Cross-lamination
- Flaser bedding
- Lenticular lamination
- Wavy lamination
- Hummocky cross-stratification
- Bioturbation
- Plant debris
- Wood
- Rip-up clasts
- Extraformational pebbles
- Soft sediment deformation
- Convoluted bedding
- Synaeresis cracks
- Stylolites
- Coaly trace
- Root trace
- Carbonaceous laminae
- Fault
- Erosional base
- Slumped sediment
- Fining upwards
- Coarsening upwards
- Calcite cementation
- Glauconite
- Pyrite
- Siderite/Fe-concretion
- Silica cementation
- Calcite-healed fracture
- Silica-healed fracture
- Fracture/fault with slickensides

ICHNOLOGY

- *Ophiomorpha*
- *Skolithos*
- *Diplocraterion*
- *Macaronichnus*
- *Thalassinoides*
- *Planolites*
- *Palaeophycus*
- *Rhizocorallium*
- *Teichichnus*
- *Phycosiphon*
- *Taedium*
- *Cylindrichnus*
- *Zoophycus*
- *Rosselia*
- *Conichnus*
- *Chondrites*
- *Undifferentiated*
- *Asterosoma*
- *Helminthopsis*
- *Schaubcylindrichnus*
- *Terebellina*
- *Glossifungites surface*
- *Escape burrow*

Bioturbation Index

0 1 2 3 4 5 6

MACROFOSSILS

- *Brachiopods*
- *Molluscs*
- *Bryozoans*
- *Crinoids*
- *Forams*
- *Algae*
- *Stromatolites/stromatoporoids*
- *Unidentified shell fragments*
- *Ammonite*
- *Gastropods*

APPENDIX 9: SPECIAL CORE ANALYSIS

SPECIAL CORE ANALYSIS FINAL REPORT

of

YOLLA-4

for

ORIGIN ENERGY RESOURCES LIMITED

by

ACS LABORATORIES PTY LTD

31 January, 2005

Origin Energy Resources Limited
Level 6
1 King William Street
ADELAIDE SA 5000

Attention: Joe Parver

Origin Energy Resources Limited
1st Floor, John Oxley Centre
339 Coronation Drive
MILTON QLD 4064

Attention: Andy Hall

FINAL REPORT: 0475-08

CLIENT REFERENCE: O4641

MATERIAL: Core Plugs

LOCALITY: Yolla-4

WORK REQUIRED: Special Core Analysis

Please direct technical enquiries regarding this work to the signatories below under whose supervision the work was carried out.

KEVIN H FLYNN
General Manager

CONTENTS

CHAPTERS PAGE

APPENDICES

CHAPTER 1

INTRODUCTION

1. INTRODUCTION

This final report presents the results from a special core analysis study of the Yolla-4 core. The samples utilized were 1½ inch diameter core plugs originally drilled for a routine core analysis study (performed by ACS Laboratories) on the same well.

Following discussions between Origin Energy Resources Limited and ACS Laboratories representatives, the test program was refined to that presented in summary format in Chapter 2 of this report. The subsequent chapters encompass descriptions of procedures and test results. The Appendices include ancillary information pertinent to the study.

CHAPTER 2

SUMMARY OF TEST PROGRAM

FLOW CHART

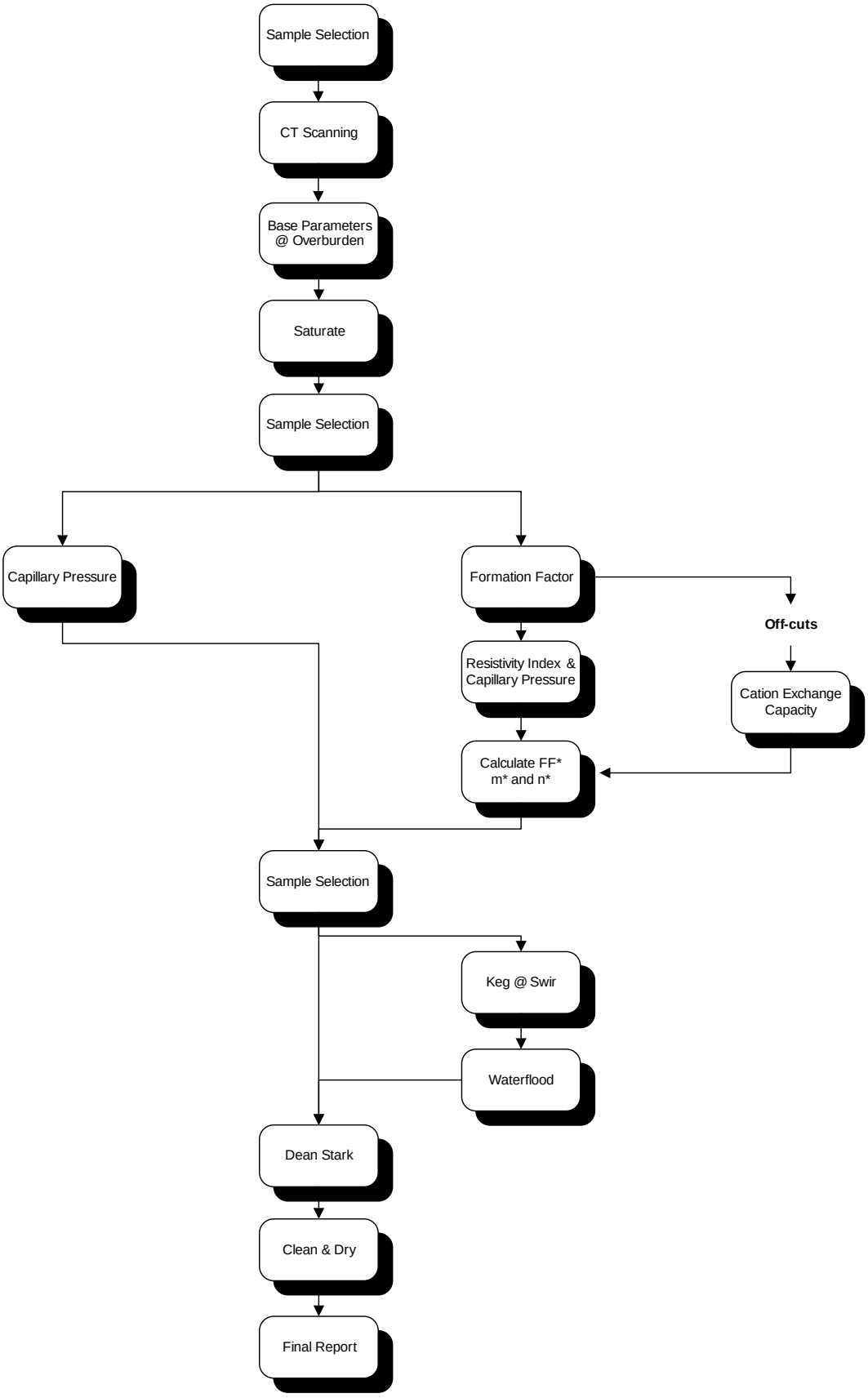
Sample Selection
CT Scanning
Base Parameters @ Overburden
Saturate
Sample Selection
Capillary Pressure
Formation Factor
Off-cuts
Resistivity Index & Capillary Pressure
Cation Exchange Capacity
Calculate FF* m* and n*
Sample Selection
Keg @ Swir
Waterflood
Dean Stark
Clean & Dry
Final Report

TEST SCHEDULE

Client: Origin Energy Resources Limited

F = Failed
C = Cancelled

Sample	Depth	Test Sequence										
		CT Scan	*Base Parameters @ Overburden*	*Saturate*	*Formation Factor*	*Air-Brine Capillary Pressure*	*Resistivity Index*	*Keg @ Swir*	*Waterflood*	*Dean Stark*	*Clean & Dry*	*Cation Exchange Capacity*
19	2898.45	X	X	X	X	X	X				X	X
29	2901.32	X	X	X		X					X	
34	2902.49	X	X	X	C	X	C	C	C		X	C
37	2903.41	X	X	X	X	X	X	X	X	X	X	X
39	2903.92	X		X	X	X	X	X	X	X	X	X
43	2904.98	X	X	X	X	X	X				X	X
44	2905.17	X	X	X	C	X	C	C	C		X	C
47	2906.08	X	X	X	X	X	X				X	X
70	2959.50	X	X	X		X					X	
71	2959.81	X	X	X	X	X	X				X	X
75	2960.95	X		X		X					X	
78	2961.87	X		X		X		X	X	X	X	
82	2963.06	X	X	X	X	X	X	X	X	X	X	X
85	2963.93	X	X	X	X	X	X				X	X
98	2967.87	X	X	X		X					X	
115	2972.75	X	X	X		X					X	
117	2973.35	X		X		X		X	X	X	X	
120	2974.25	X		X	X	X	X				X	X
121	2974.57	X	X	X		X					X	
132	2978.26	X		X		X					X	
135	2979.15	X		X	X	X	X	X	X	X	X	X
	Total	21	14	21	10	21	10	6	6	6	21	10

CHAPTER 3

SAMPLE PREPARATION AND BASE PARAMETER DETERMINATIONS

3.1 Test and Calculation Procedures

3. SAMPLE PREPARATION AND BASE PARAMETER DETERMINATIONS

3.1 Test and Calculation Procedures

3.1.1 CT Scanning

CT Scanning was undertaken in order that internal inhomogeneities and/or drilling fluid invasion zones may be noted. Typical inhomogeneities may be clasts, bedding sedimentary structures, cementation, fractures and any other discontinuities that may not be readily visible to the naked eye.

The principle of CT Scanning and its applications is presented by Hove et al, 1987 and Wellington and Vinegar, 1987.

CT Scanners generate cross-sectional image slices through the sample by revolving an X-ray tube around the sample and obtaining projections at many different angles (Appendix I). From these image slices, a cross-sectional image was reconstructed by a back projection algorithm in the scanner's computer.

Prior to analysis, an arbitrary orientation line was inscribed onto the sample using a marker to facilitate subsequent re-orientation. The sample was placed vertically within the scanner, with the orientation arrow left to right, and a longitudinal section image obtained. The sample was then rotated through exactly 90^o to the initial orientation, and another section image recorded. These two images are labelled '0' and '90' on the prints.

All images were reported in a separate report sent on 31 August 2004.

3.1.2 Base Parameters

All ambient base parameters were performed during the routine core analysis study.

Porosity

Porosity was determined in two stages. Initially each sample was placed in a sealed matrix cup. Helium held at 100 psi reference pressure was then introduced to the cup. From the resultant pressure drop the unknown grain volume was determined using Boyle's Law.

$$P_1 V_1 = P_2 V_2$$
$$\Rightarrow P_1 Vr = P_2 (Vr + Vc + Vl - Vg)$$

where

P_1	=	*initial pressure (psig)*
Vr	=	*reference cell volume (cm^3)*
Vc	=	*matrix cup volume (cm^3)*
Vl	=	*line volume (cm^3)*
Vg	=	*grain volume (cm^3)*
P_2	=	*final pressure (psig)*

$$\text{and} \quad \rho = \frac{Wt}{Vg}$$

where ρ = grain density (g/cm^3)
Wt = weight of sample (g)
Vg = grain volume (cm^3)

The samples were then placed into individual thick walled rubber sleeves and the assembly loaded into a hydrostatic cell. With an ambient pressure (400 psi) applied to the sample, helium held at 100 psi reference pressure was released into the samples pore volume. The resultant pressure drop was used to determine pore volume at ambient. The confining pressure was then increased to the overburden pressure of 5000 psi and the resultant change in internal pore pressure was monitored and used to determine pore volume at overburden conditions.

$$Vb = Vp + Vg$$

$$\text{Ambient Porosity \%} = \frac{Vp}{Vb} x\,100$$

$$\text{Overburden Porosity \%} = \frac{Vp - \Delta Vp}{Vb - \Delta Vp} x\,100$$

where Vp = ambient pore volume (cm^3)
Vb = ambient bulk volume (cm^3)
Vg = grain volume (cm^3)
ΔVp = change in pore volume (cm^3)

Permeability to Air

The samples were placed into a hydrostatic cell (Appendix II) with an ambient confining pressure of 400 psi applied. The confining pressure was used to prevent bypassing of air around the sample when the measurement was made. In order to determine permeability a known air pressure was applied to the upstream face of each sample, creating a flow of air through the core plug. Air permeability for each core sample was calculated using Darcy's Law through knowledge of the upstream pressure, flow rate, viscosity of air and sample dimensions.

$$Ka = \frac{2000.BP.\mu.q.L}{(P_1^2 - P_2^2).A}$$

where	*Ka*	=	*air permeability (milliDarcy's)*
	BP	=	*barometric pressure (atmospheres)*
	μ	=	*gas viscosity (cP)*
	q	=	*flow rate (cm^3/s)*
	L	=	*sample length (cm)*
	P_1	=	*upstream pressure (atmospheres)*
	P_2	=	*downstream pressure (atmospheres)*
	A	=	*sample cross sectional area (cm^2)*

The confining pressure was then increased to the overburden pressure of 5000 psi and the above procedure repeated to give permeability at overburden conditions.

3.1.3 Sample Saturation

The selected samples were initially vacuum saturated with 26000 ppm NaCl equivalent brine (Appendix I) followed by pressure saturation at 2000 psi for a minimum of 12 hours. To determine complete saturation, the saturations were determined by mass balance and compared with that of porosimetry. In all cases the samples were deemed suitable to proceed with the test program.

CHAPTER 3

SAMPLE PREPARATION AND BASE PARAMETER DETERMINATIONS

3.2 Test Results

BASE PARAMETERS

Client Origin Energy Resources Limited
Well Yolla-4

Overburden Pressure 5000 psi

Sample Number	Depth (metres)	Ambient Porosity (percent)	Overburden Porosity (percent)	Grain Density (g/cm^3)	Ambient Permeability (milliDarcy's)	Overburden Permeability (milliDarcy's)
19	2898.45	16.0	14.9	2.67	11.7	8.8
29	2901.32	17.7	16.9	2.66	35.9	31.7
34	2902.49	20.9	19.9	2.73	1105	875
37	2903.41	22.4	21.1	2.69	2723	2326
39	2903.92	21.0	19.8	2.70	1676	1325
43	2904.98	23.0	22.0	2.65	3110	2386
44	2905.17	17.0	16.1	2.69	123	100
47	2906.08	22.6	21.5	2.66	4616	3800
70	2959.50	21.6	20.6	2.64	1169	938
71	2959.81	21.0	20.0	2.65	790	658
75	2960.95	19.2	17.9	2.65	440	350
78	2961.87	20.6	18.9	2.64	743	593
82	2963.06	15.5	14.5	2.66	24.7	19.7
85	2963.93	19.8	17.8	2.63	499	357
98	2967.87	19.4	18.4	2.65	183	149
115	2972.75	18.7	17.5	2.65	649	534
117	2973.35	19.2	18.1	2.65	299	258
120	2974.25	21.7	20.8	2.64	904	763
121	2974.57	19.7	18.6	2.65	209	177
132	2978.26	17.1	16.1	2.66	49.5	41.8
135	2979.15	17.6	16.7	2.64	75.3	65.9

POROSITY vs PERMEABILITY

Client Origin Energy Resources Limited
Well Yolla-4

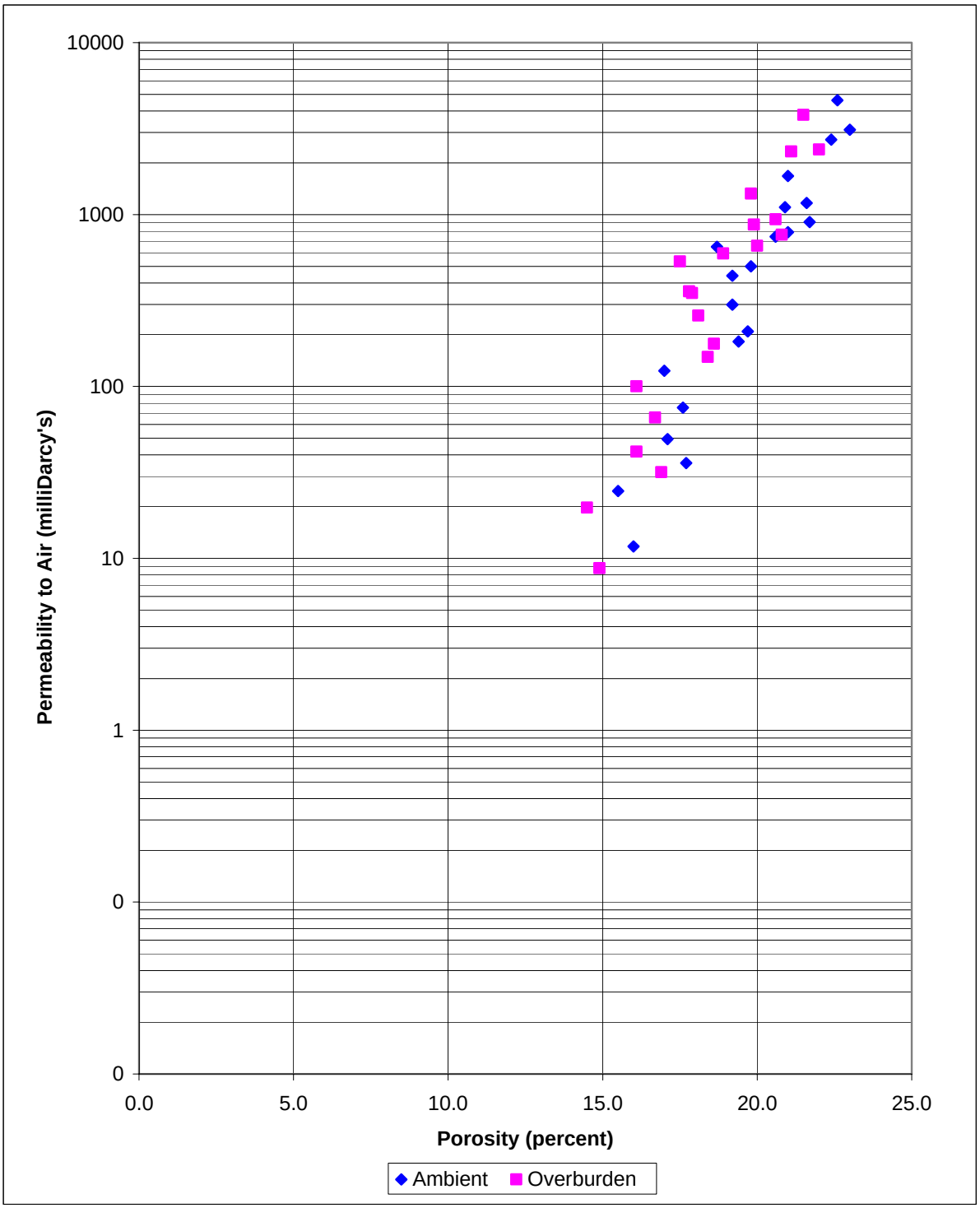

CHAPTER 4

ELECTRICAL PROPERTIES AND CAPILLARY PRESSURE

4.1 Test and Calculation Procedures

4. ELECTRICAL PROPERTIES AND CAPILLARY PRESSURE

4.1 Test and Calculation Procedures

4.1.1 Formation Resistivity Factor

On completion of base parameter and pressure saturation with 26000 ppm brine, the ten selected samples continued on for formation resistivity factor analyses.

Each fully brine saturated sample was sandwiched between a pair of stainless steel core holder platens. These platens also act as the current carrying and potential electrodes. A thin silver leaf was also placed between the plug endfaces and electrodes, to ensure electrical contact. A strongly hydrophilic membrane was placed at the bottom end of the sample. This assembly was placed into a snugly fitting rubber overburden sleeve and then loaded into a Hydrostatic type core holder. A confining pressure was gradually applied as an effective overburden pressure (see Appendix II for schematic).

Synthetic brine (Appendix I) was slowly flowed through each sample at a rate of 0.5cm^3/min. During this process sample resistivity was monitored on a digi-bridge capable of measuring sample resistance to 0.001 (ohms) accuracy. In each case the current frequency was selected to yield minimum phase angles, thus ensuring maximum electrical contact (between each sample and the current carrying and potential electrodes). Values of sample resistance (Rc) and effluent brine resistivity (Rw) were recorded daily. Each sample was deemed to be at ionic equilibrium when three consecutive daily readings were recorded within 1%.

From these stable data, the following results were recorded:

$$Ro = \frac{A \,.\, Rc}{100 L}$$

where Ro = *sample resistivity (ohm.m)*
Rc = *sample resistance (ohms)*
L = *electrode gap (sample length - cm)*
A = *cross sectional area (cm^2)*
100 = *units conversion*

Formation resistivity factor was calculated using the following equations:

$$FF = \frac{a}{\Phi^m}$$

and

$$FF = \frac{Ro}{Rw}$$

where Rw = *brine resistivity (ohm.m)*
a = *intercept (assumed = 1)*
m = *cementation exponent*

and Φ = *porosity (fraction)*

The brine resistivity (Rw) was accurately determined by a NATA certified fluids laboratory.

4.1.2 Formation Resistivity Index and Capillary Pressure

Upon completion of the preceding formation resistivity factor analyses, the ten selected samples continued immediately for formation resistivity index analyses in conjunction with drainage capillary pressure curves. The top endface port was connected to a supply of humidified air and the bottom port connected to a graduated receiving tube (Appendix II). The samples were desaturated by gradually increasing the displacing fluid pressure to the samples. The actual pressures utilised were inversely proportional to the individual sample permeability data. A small amount of oil was placed into the collection tubes to prevent any potential brine loss by evaporation. Sample resistances were measured at successive decreasing brine saturations, which were calculated from the following equation:

$$\textit{Water Saturation (\%)} = \frac{\textit{Pore Volume @ OB}\left(cm^3\right) - \textit{Brine Expelled}\left(cm^3\right)}{\textit{Pore Volume @ OB}\left(cm^3\right)} \textit{ x 100}$$

Capillary pressure curves plot water saturation (x-axis) against applied displacing fluid pressure. A hyperbolic curve is used to define this relationship. The ratio of the sample resistance (Rc) values to the previously determined FF values (at 100% saturation) were used to calculate the formation resistivity indices.

$$Rt = \frac{A \,.\, Rc}{100L}$$

where Rt = *resistivity of partially brine saturated sample (ohm.m)*
Rc = *sample resistance (ohms)*

and $$RI = \frac{Rt}{Rw \,.\, FF}$$

where RI = *resistivity index*
Rw = *resistivity of brine (ohm.m)*

(modified from standard Archie equation to include Rw).

These RI values (for each sample) were plotted against brine saturation (Sw) on graphs with logarithmic axes and the gradient of the best-fit line through the co-ordinate (1.0, 1.0) was calculated. Each gradient is quoted as the saturation exponent (n) for that sample, in accordance with Archie's formula.

$$RI = \frac{1}{Sw^n}$$

4.1.3 Capillary Pressure

Eleven samples were selected for air-brine capillary pressure. Each fully brine saturated sample was sandwiched between a pair of stainless steel core holder platens with a strongly hydrophilic membrane at the bottom end of the sample. This assembly was placed into a snugly fitting rubber overburden sleeve and loaded into a hydrostatic type core holder and an overburden pressure of 5000 psi applied.

The top endface port was connected to a supply of humidified air and the bottom port connected to a graduated receiving tube (Appendix II). The samples were desaturated by gradually increasing the displacing fluid pressure to the samples. The actual pressures utilised were inversely proportional to the individual sample permeability data. A small amount of oil was placed into the collection tubes to prevent any potential brine loss by evaporation. Sample resistances were measured at successive decreasing brine saturations, which were calculated from the following equation:

$$Water\ Saturation(\%) = \frac{Pore\ Volume\ @\ OB\ (cm^3) - Brine\ Expelled\ (cm^3)}{Pore\ Volume\ @\ OB\ (cm^3)}\ x\ 100$$

Capillary pressure curves plot water saturation (x-axis) against applied displacing fluid pressure. A hyperbolic curve is used to define this relationship.

4.1.4 Cation Exchange Capacity

Cation exchange capacity was determined on approximately 5 grams of sample (off-cuts) using the wet chemistry method. The samples were first washed with an ammonium chloride solution to exchange ions with the available clay cations. An exchange reagent was then washed through the sample and the resultant solution titrated. Where a smaller sample is used the limit of detection becomes greater and a minimum value is reported.

Values of exchangeable cations (theoretical minimum of zero) present in the samples are reported as milliequivalents per 100 grams of dry sample (meq/100 g). Values of Q_v have been calculated using the following equation:

$$Q_v = \frac{CEC\ (1 - \Phi)\rho}{100\ \Phi}$$

where ρ = *grain density (g/cm^3)*
Φ = *porosity (fraction)*
Q_v = *volume concentration of clay exchange cations (meq/cm^3 pore space)*
CEC = *cation exchange capacity (meq/100 g dry sample)*

Based on these CEC/Qv data, values of shaly sand equivalent formation factor (FF*), cementation factor (m*) and saturation exponent (n*) were calculated using the following equations:

$$FF^* = FF\,.\,(1 + B.Qv.Rw)$$

$$m^* = \frac{\log FF^*}{-\log \Phi}$$

$$n^* = \frac{\log\left[\dfrac{1 + Rw.B.Qv}{1 + Rw.B.Qv / Sw}\right] - \log FRI}{\log Sw}$$

where[1]

$$B = \frac{-1.28 + 0.225.T - 0.0004059.T^2}{1 + Rw^{1.23}\,.\,(0.045.T. - 0.27)}$$

FF = *formation resistivity factor*
*FF** = *shaly sand equivalent formation resistivity factor*
*m** = *shaly sand equivalent cementation factor*
Φ = *porosity (fraction)*
*n** = *shaly sand equivalent saturation exponent*
Rw = *brine resistivity (ohm.m @ 25°C)*
T = *temperature of 25°C*
B = *equivalent conductance of clay exchange cations*
Qv = *volume concentration of clay exchange cations*
Sw = *final saturation (fraction)*
FRI = *resistivity index @ saturation Sw*

[1] Juhasz, I., 1981, Normalized Q, - the key to shaly sand evaluation using the Waxman-Smits equation in the absence of core data, paper Z, in 22nd Annual Logging Symposium Transactions: Society of Professional Well Log Analysts, 36p.

CHAPTER 4

ELECTRICAL PROPERTIES AND CAPILLARY PRESSURE

4.2 Test Results

4.2.1 Formation Factor

FORMATION RESISTIVITY FACTOR

Client	Origin Energy Resources Limited	**Saturant**	26000 ppm
Well	Yolla-4	**Rw of Saturant**	0.241 at 25ºC
		Overburden	5000 psi
		Average m	1.78

Sample Number	Depth (metres)	Permeability to Air (milliDarcy's)	Porosity (percent)	Formation Factor FF	Cementation Exponent m
19	2898.45	8.8	14.9	30.3	1.79
37	2903.41	2326	21.1	14.7	1.73
39	2903.92	1325	19.8	19.0	1.82
43	2904.98	2386	22.0	15.1	1.79
47	2906.08	3800	21.5	14.0	1.72
71	2959.81	658	20.0	17.2	1.77
82	2963.06	19.7	14.5	33.2	1.81
85	2963.93	357	17.8	21.6	1.78
120	2974.25	763	20.8	16.6	1.79
135	2979.15	65.9	16.7	23.9	1.77

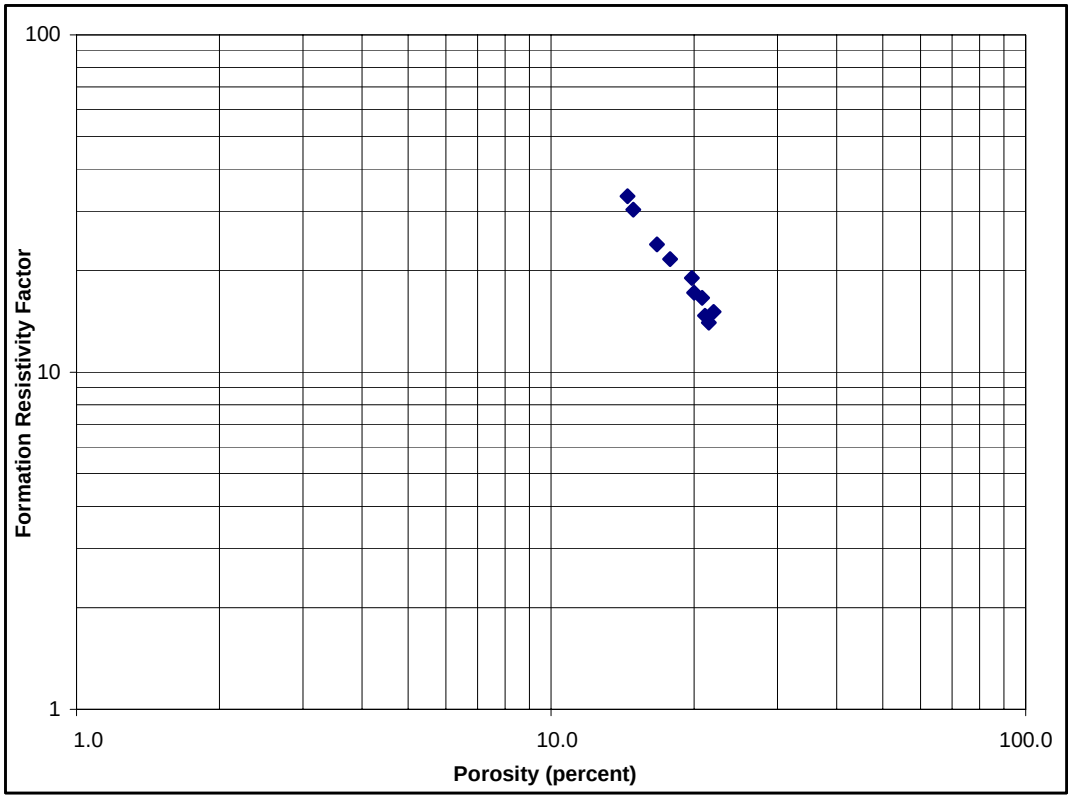

CHAPTER 4

ELECTRICAL PROPERTIES AND CAPILLARY PRESSURE

4.2 Test Results

4.2.2 Resistivity Index

RESISTIVITY INDEX

Client Origin Energy Resources Limited
Well Yolla-4

Rw of Saturant 0.241 at 25ºC
Method Air/Brine Porous Plate @ Overburden

Sample Number	Depth (metres)	Permeability to Air (milliDarcy's)	Porosity (percent)	Formation Factor FF	Brine Saturation (fraction)	Resistivity Index RI	Saturation Exponent n
19	2898.45	8.8	14.9	30.3	1.000	1.00	
					0.874	1.40	
					0.553	3.65	
					0.352	9.42	
					0.266	18.5	
					0.220	27.2	2.18

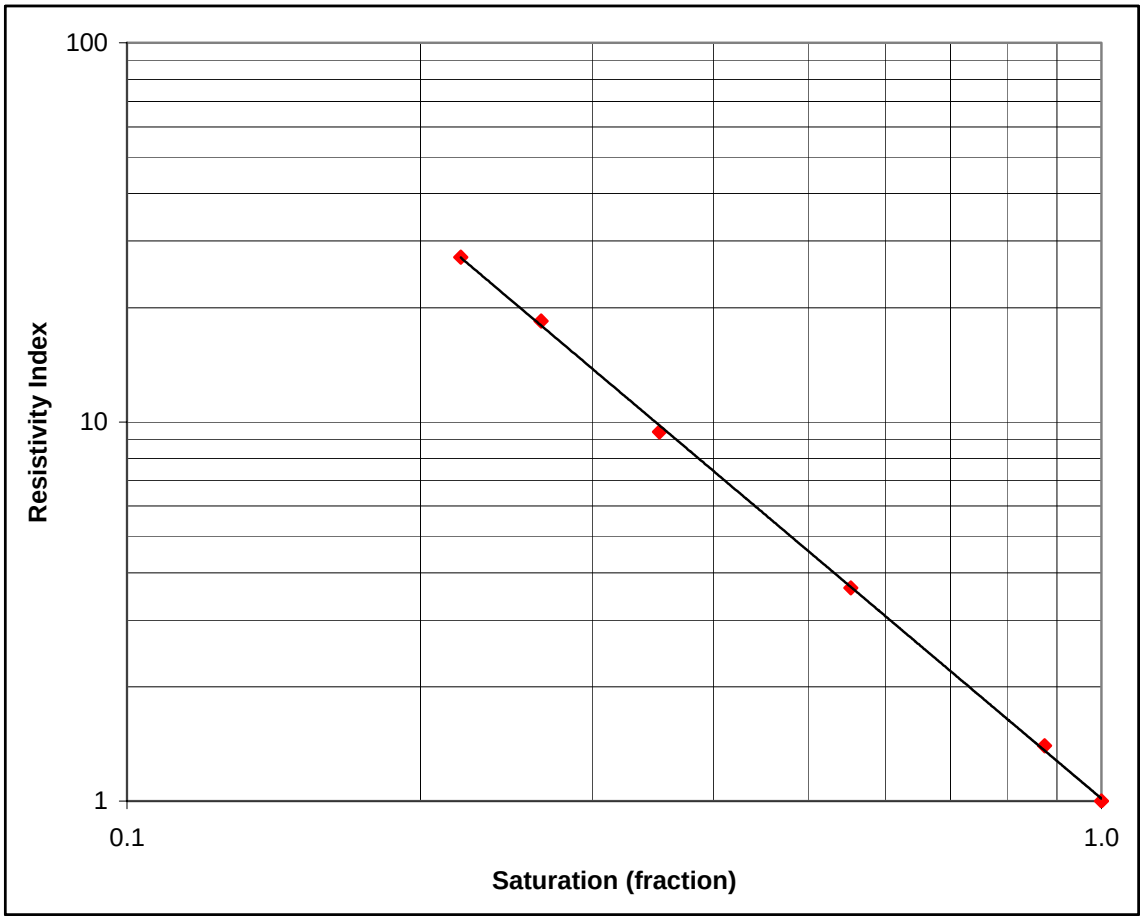

RESISTIVITY INDEX

Client Origin Energy Resources Limited
Well Yolla-4

Rw of Saturant 0.241 at 25ºC
Method Air/Brine Porous Plate @ Overburden

Sample Number	Depth (metres)	Permeability to Air (milliDarcy's)	Porosity (percent)	Formation Factor FF	Brine Saturation (fraction)	Resistivity Index RI	Saturation Exponent n
37	2903.41	2326	21.1	14.7	1.000	1.00	
					0.893	1.24	
					0.695	1.93	
					0.308	9.18	
					0.234	13.1	
					0.152	31.6	
					0.102	62.6	
					0.069	97.0	1.78

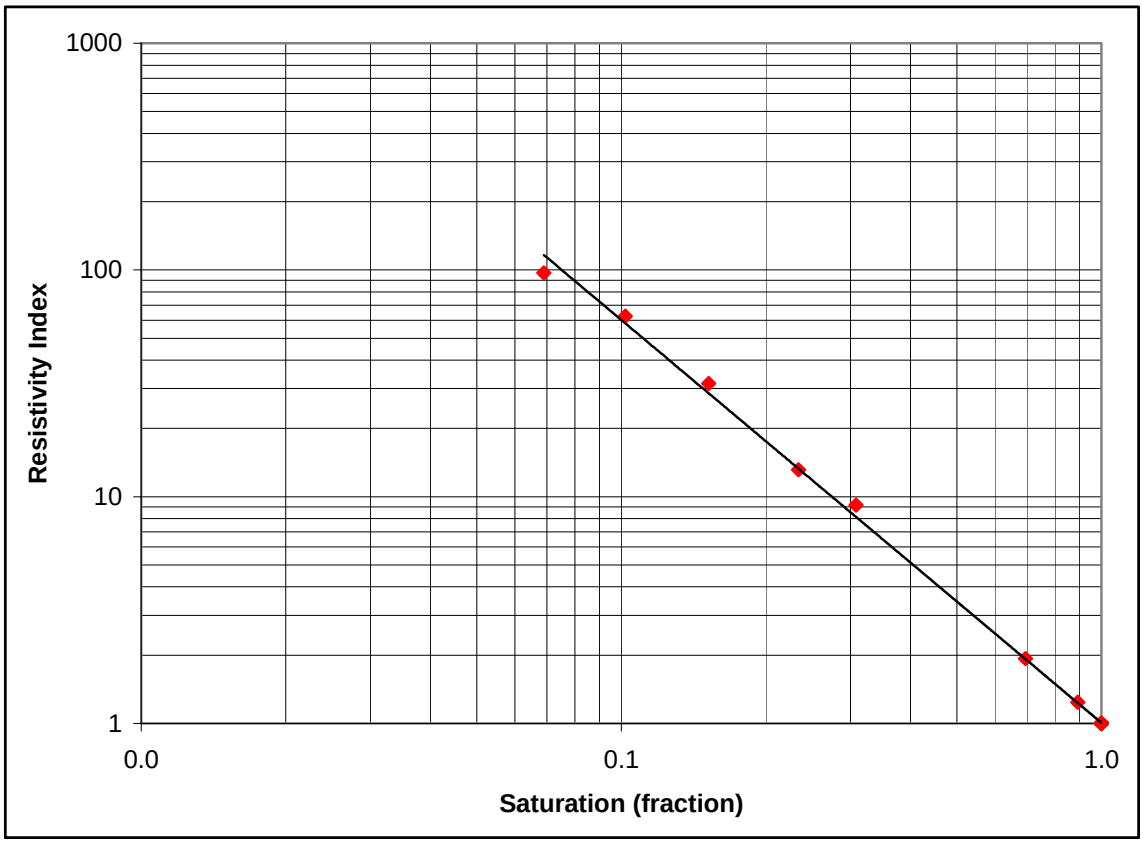

RESISTIVITY INDEX

Client Origin Energy Resources Limited
Well Yolla-4

Rw of Saturant 0.241 at 25ºC
Method Air/Brine Porous Plate @ Overburden

Sample Number	Depth (metres)	Permeability to Air (milliDarcy's)	Porosity (percent)	Formation Factor FF	Brine Saturation (fraction)	Resistivity Index RI	Saturation Exponent n
39	2903.92	1325	19.8	19.0	1.000	1.00	
					0.851	1.14	
					0.566	2.63	
					0.282	9.03	
					0.229	12.2	
					0.159	21.1	
					0.142	22.9	
					0.120	28.3	1.64

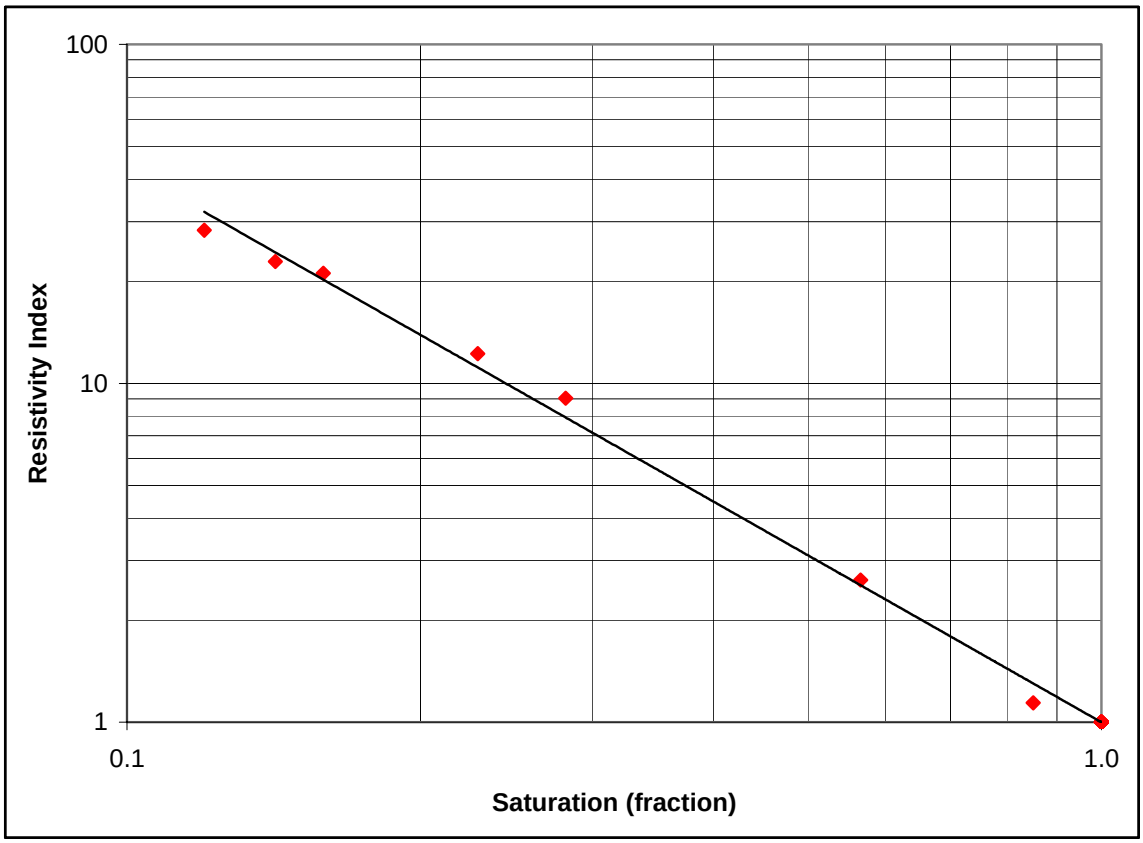

RESISTIVITY INDEX

Client Origin Energy Resources Limited
Well Yolla-4

Rw of Saturant 0.241 at 25ºC
Method Air/Brine Porous Plate @ Overburden

Sample Number	Depth (metres)	Permeability to Air (milliDarcy's)	Porosity (percent)	Formation Factor FF	Brine Saturation (fraction)	Resistivity Index RI	Saturation Exponent n
43	2904.98	2386	22.0	15.1	1.000	1.00	
					0.827	1.22	
					0.780	1.36	
					0.442	3.30	
					0.308	6.85	
					0.214	11.8	
					0.131	24.6	
					0.096	40.9	1.58

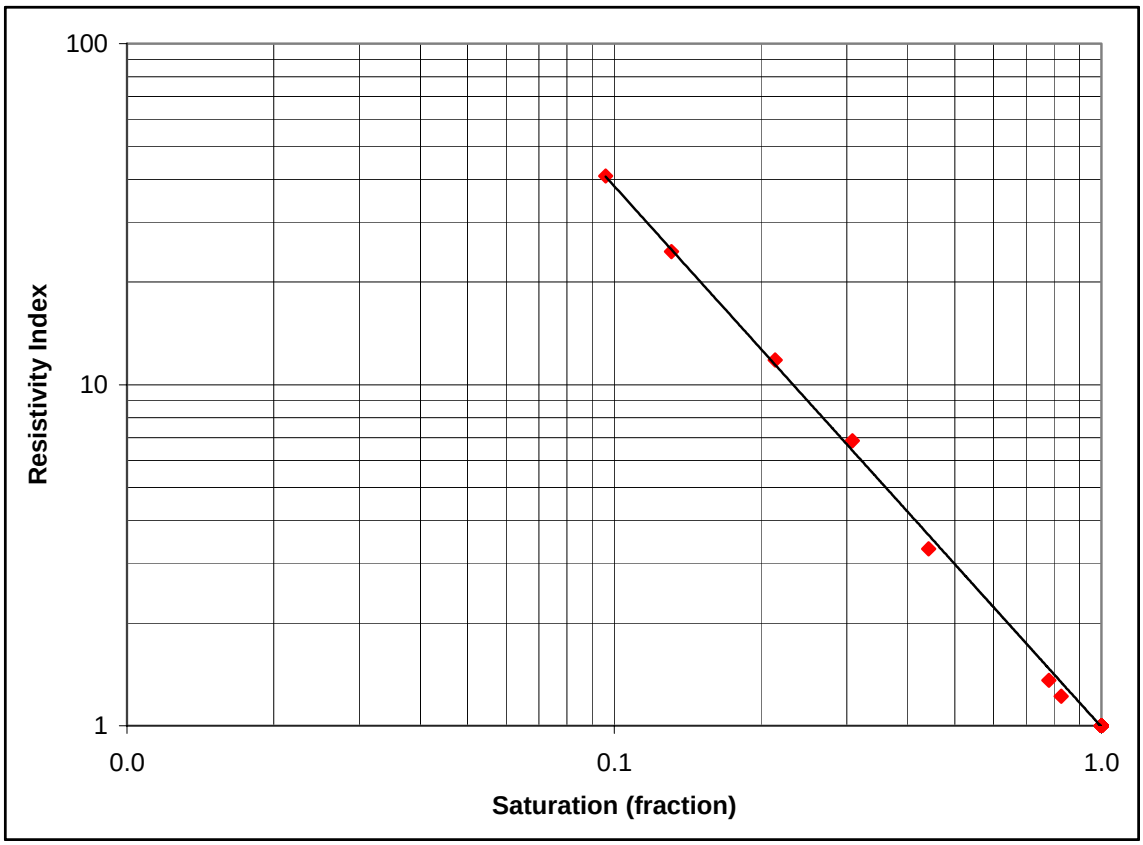

RESISTIVITY INDEX

Client Origin Energy Resources Limited
Well Yolla-4

Rw of Saturant 0.241 at 25ºC
Method Air/Brine Porous Plate @ Overburden

Sample Number	Depth (metres)	Permeability to Air (milliDarcy's)	Porosity (percent)	Formation Factor FF	Brine Saturation (fraction)	Resistivity Index RI	Saturation Exponent n
47	2906.08	3800	21.5	14.0	1.000	1.00	
					0.742	1.61	
					0.314	5.95	
					0.245	10.1	
					0.193	15.4	
					0.136	22.0	
					0.080	50.8	
					0.060	72.5	1.56

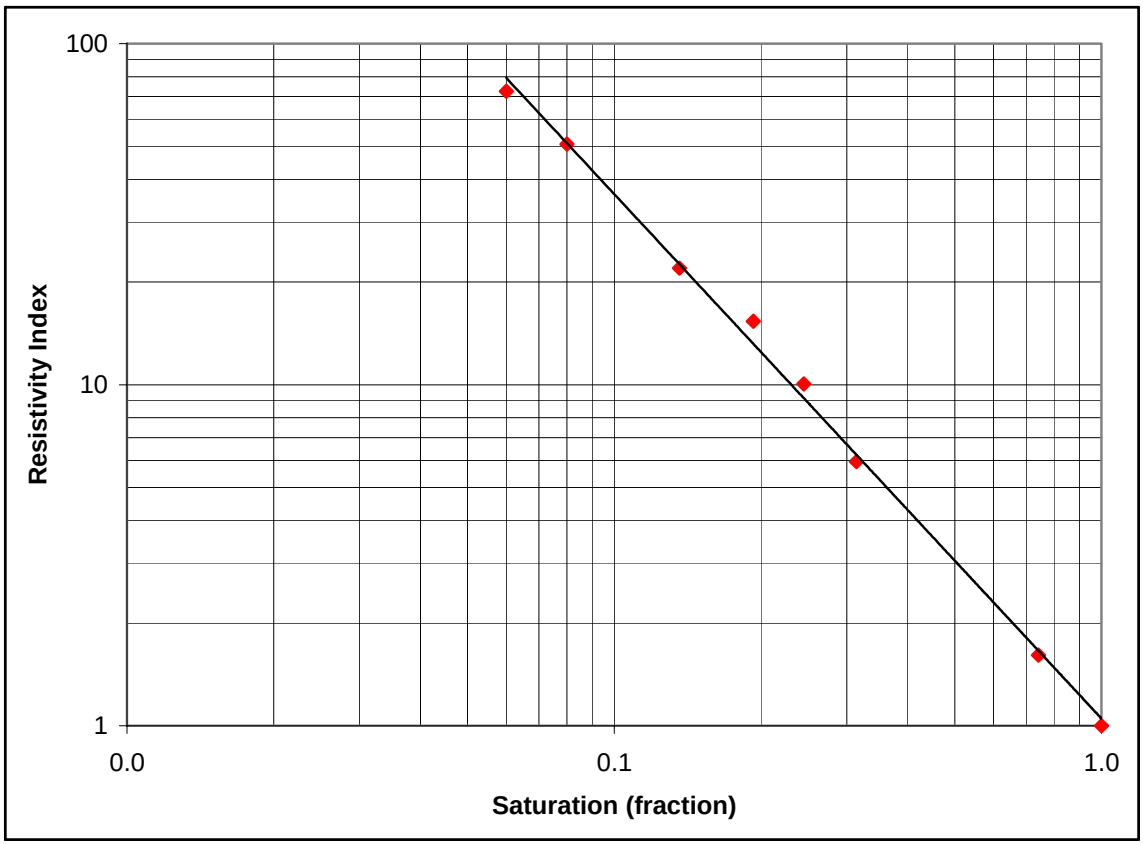

RESISTIVITY INDEX

Client Origin Energy Resources Limited
Well Yolla-4

Rw of Saturant 0.241 at 25ºC
Method Air/Brine Porous Plate @ Overburden

Sample Number	Depth (metres)	Permeability to Air (milliDarcy's)	Porosity (percent)	Formation Factor FF	Brine Saturation (fraction)	Resistivity Index RI	Saturation Exponent n
71	2959.81	658	20.0	17.2	1.000	1.00	
					0.879	1.28	
					0.533	3.12	
					0.412	5.70	
					0.351	8.27	
					0.213	18.6	
					0.144	30.9	
					0.087	52.1	1.76

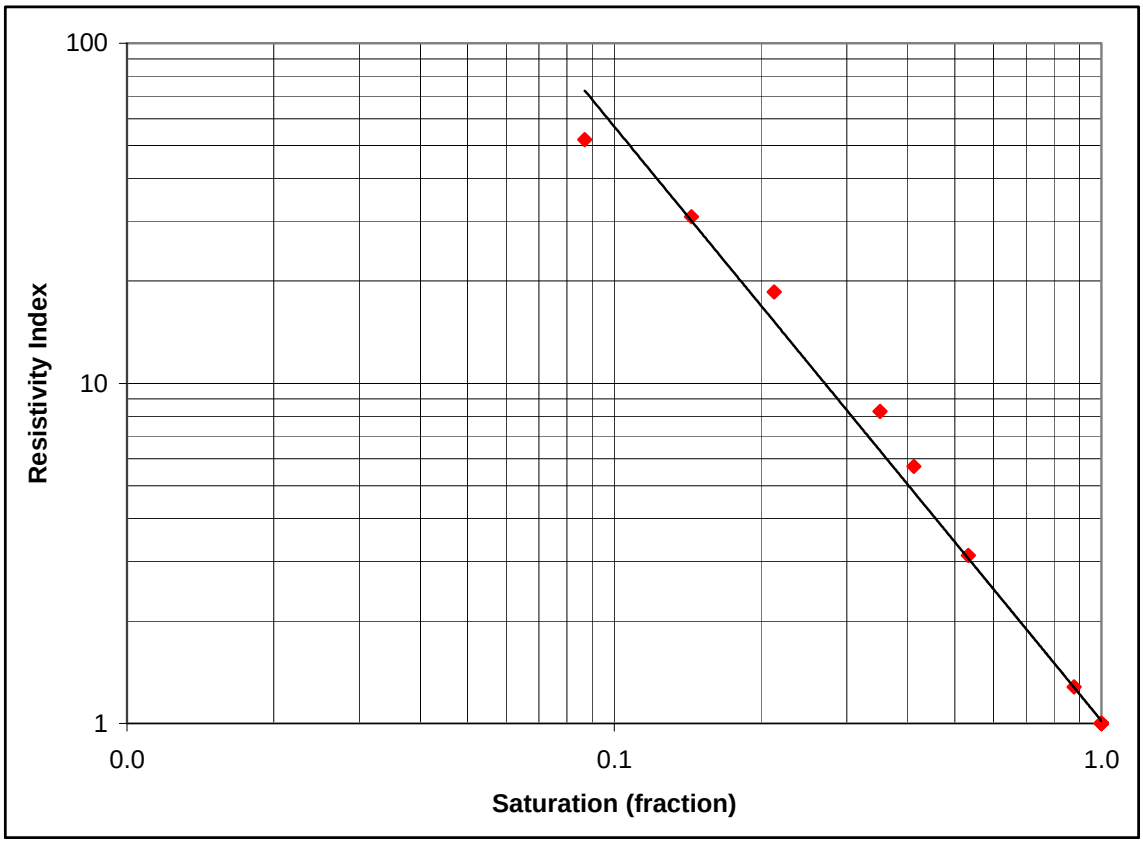

RESISTIVITY INDEX

Client Origin Energy Resources Limited
Well Yolla-4

Rw of Saturant 0.241 at 25ºC
Method Air/Brine Porous Plate @ Overburden

Sample Number	Depth (metres)	Permeability to Air (milliDarcy's)	Porosity (percent)	Formation Factor FF	Brine Saturation (fraction)	Resistivity Index RI	Saturation Exponent n
82	2963.06	19.7	14.5	33.2	1.000	1.00	
					0.959	1.06	
					0.829	1.43	
					0.504	3.13	
					0.344	6.36	
					0.255	9.16	
					0.208	13.1	1.66

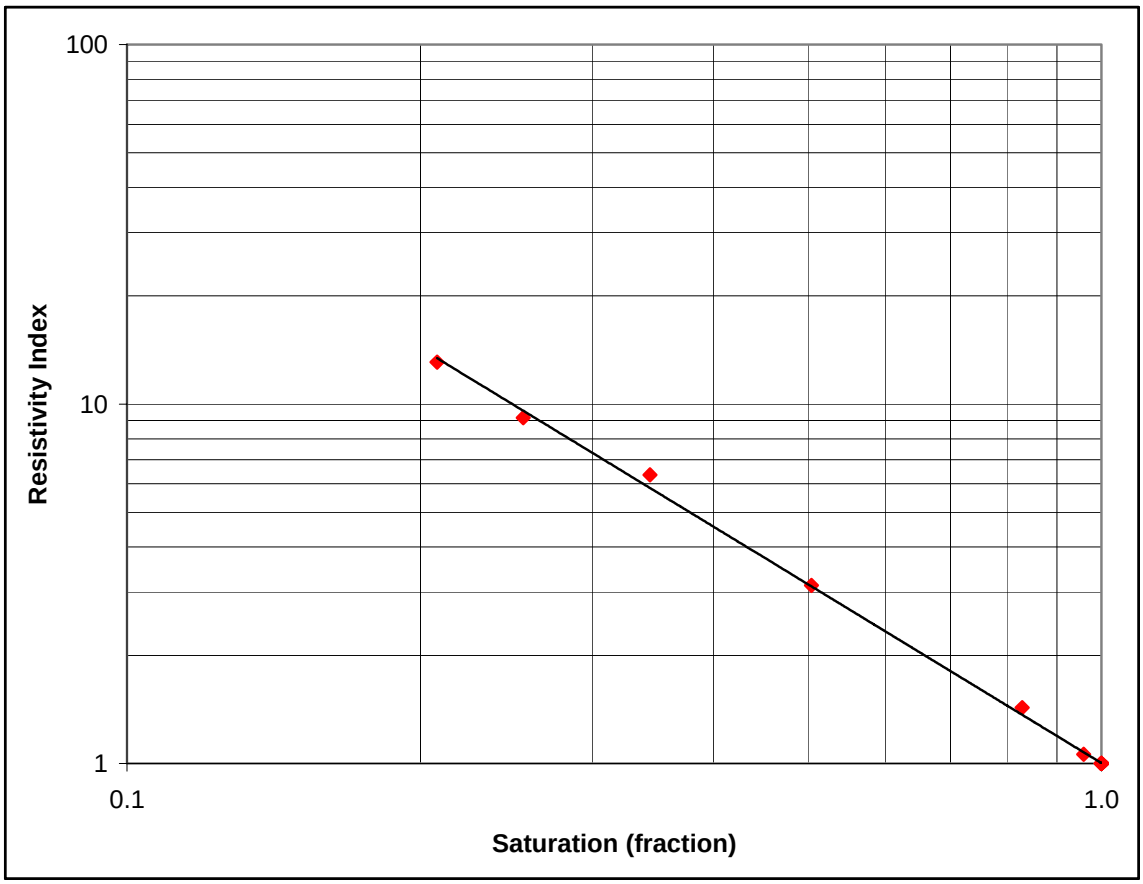

RESISTIVITY INDEX

Client Origin Energy Resources Limited
Well Yolla-4

Rw of Saturant 0.241 at 25ºC
Method Air/Brine Porous Plate @ Overburden

Sample Number	Depth (metres)	Permeability to Air (milliDarcy's)	Porosity (percent)	Formation Factor FF	Brine Saturation (fraction)	Resistivity Index RI	Saturation Exponent n
85	2963.93	357	17.8	21.6	1.000	1.00	
					0.804	1.44	
					0.501	3.15	
					0.388	5.65	
					0.295	8.05	
					0.212	16.6	
					0.158	25.6	
					0.124	40.4	1.77

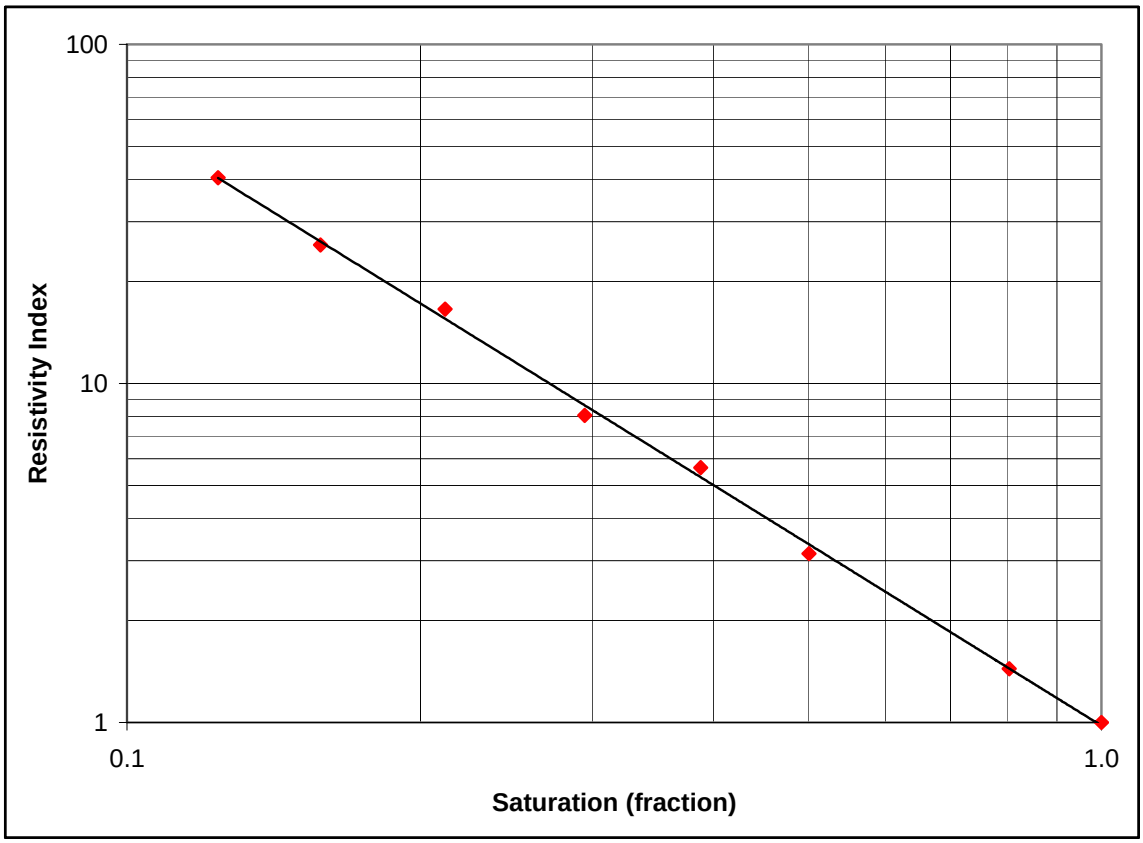

RESISTIVITY INDEX

Client Origin Energy Resources Limited
Well Yolla-4

Rw of Saturant 0.241 at 25ºC
Method Air/Brine Porous Plate @ Overburden

Sample Number	Depth (metres)	Permeability to Air (milliDarcy's)	Porosity (percent)	Formation Factor FF	Brine Saturation (fraction)	Resistivity Index RI	Saturation Exponent n
120	2974.25	763	20.8	16.6	1.000	1.00	
					0.925	1.30	
					0.586	2.66	
					0.354	7.15	
					0.288	11.1	
					0.188	22.6	
					0.126	42.4	
					0.089	72.3	1.82

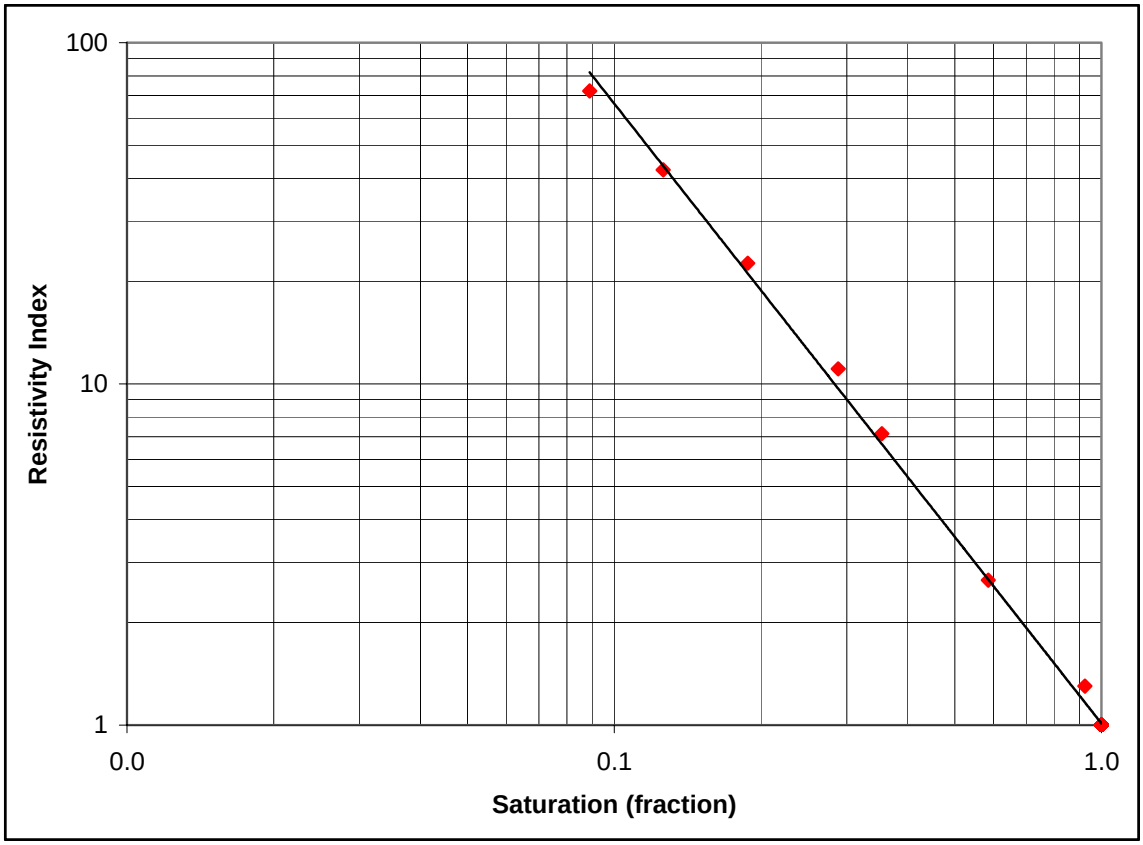

RESISTIVITY INDEX

Client Origin Energy Resources Limited
Well Yolla-4

Rw of Saturant 0.241 at 25ºC
Method Air/Brine Porous Plate @ Overburden

Sample Number	Depth (metres)	Permeability to Air (milliDarcy's)	Porosity (percent)	Formation Factor FF	Brine Saturation (fraction)	Resistivity Index RI	Saturation Exponent n
135	2979.15	65.9	16.7	23.9	1.000	1.00	
					0.964	1.13	
					0.913	1.29	
					0.548	2.82	
					0.353	6.16	
					0.240	12.0	
					0.189	17.1	
					0.163	23.7	1.73

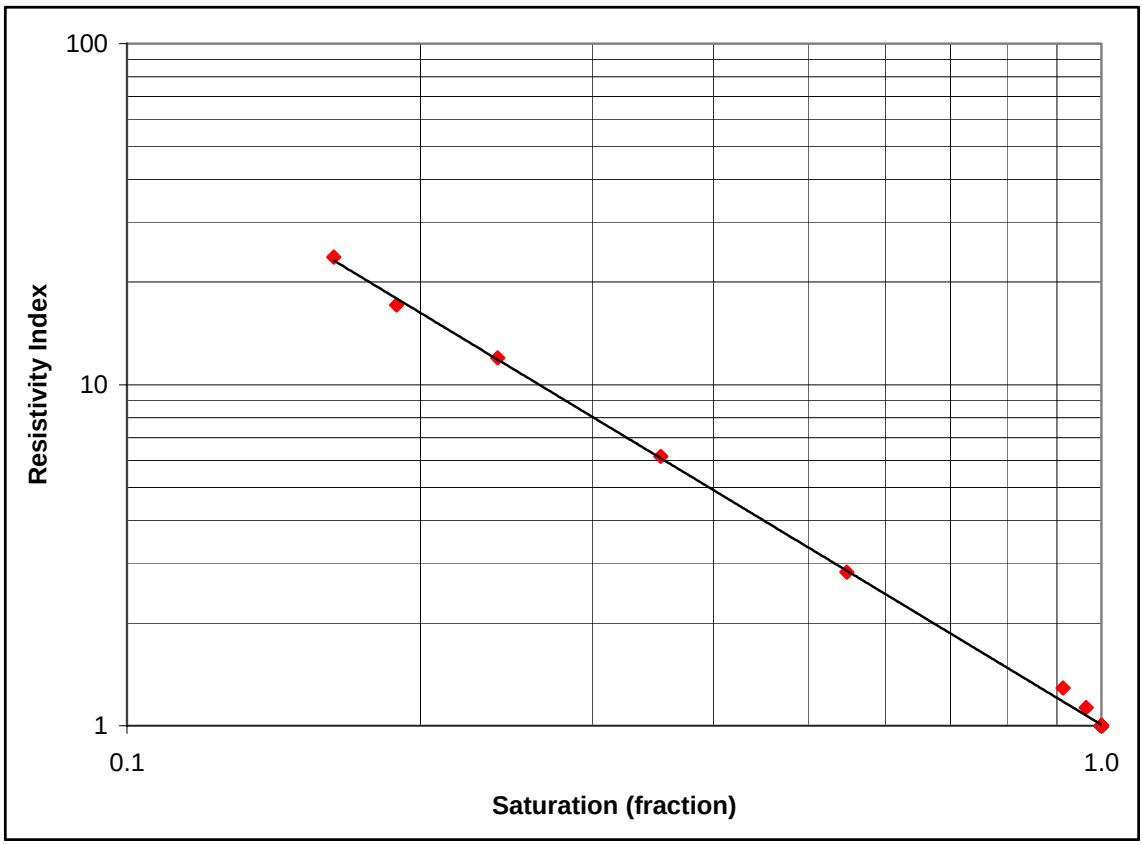

RESISTIVITY INDEX

Client Origin Energy Resources Limited
Well Yolla-4

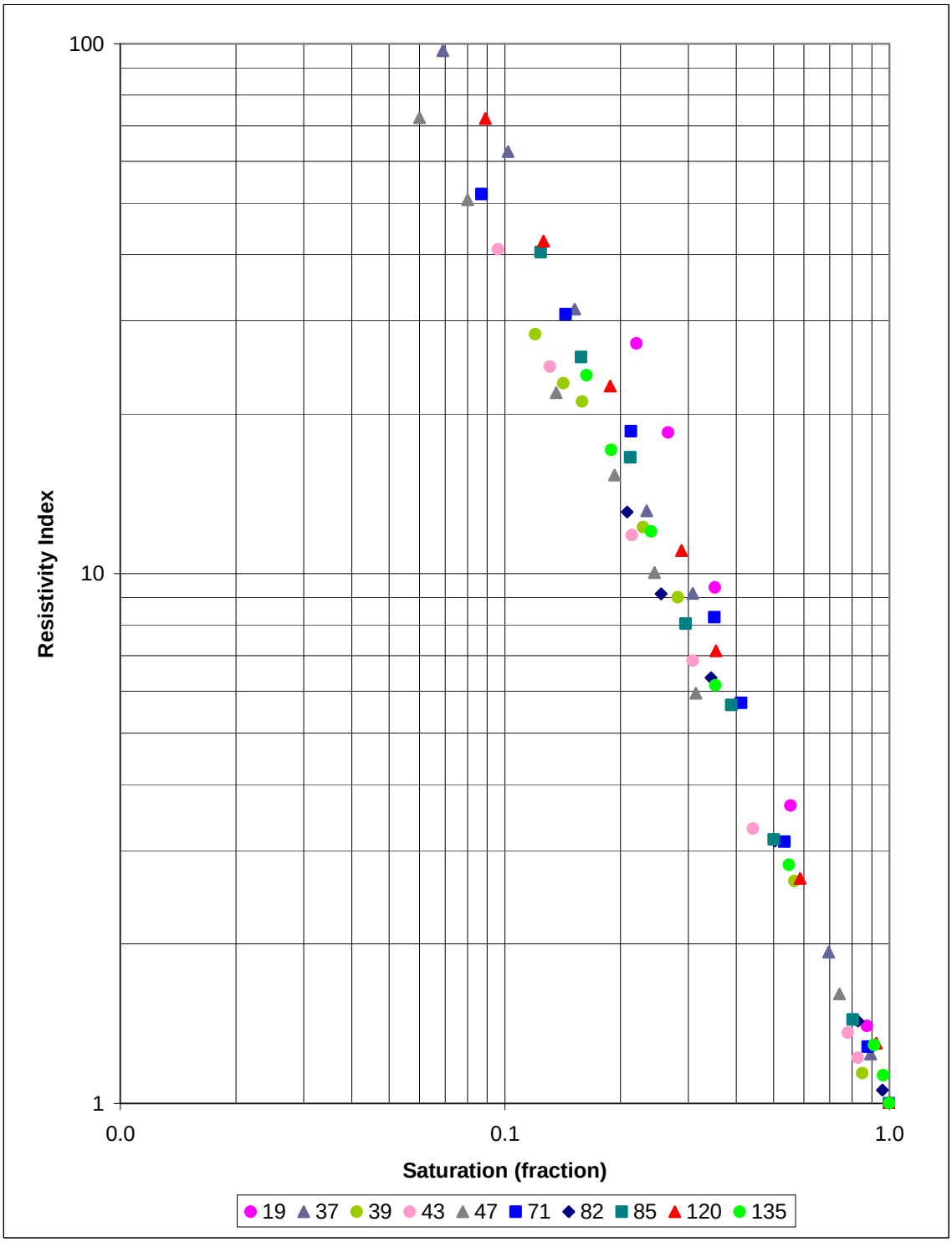

CHAPTER 4

ELECTRICAL PROPERTIES AND CAPILLARY PRESSURE

4.2 Test Results

4.2.3 Capillary Pressure

CAPILLARY PRESSURE
Overburden

Client	Origin Energy Resources Limited	**Air Permeability**	8.8 milliDarcy's
Well	Yolla-4	**Porosity**	14.9 percent
Sample	19		
Depth	2898.45 metres		
Test Method	Air/Brine Porous Plate @ Overburden		
Overburden	5000 psi		

Capillary Pressure (psi)	Brine Saturation (percent)
2.0	100.0
4.0	87.4
8.0	55.3
16	35.2
25	26.6
40	22.0

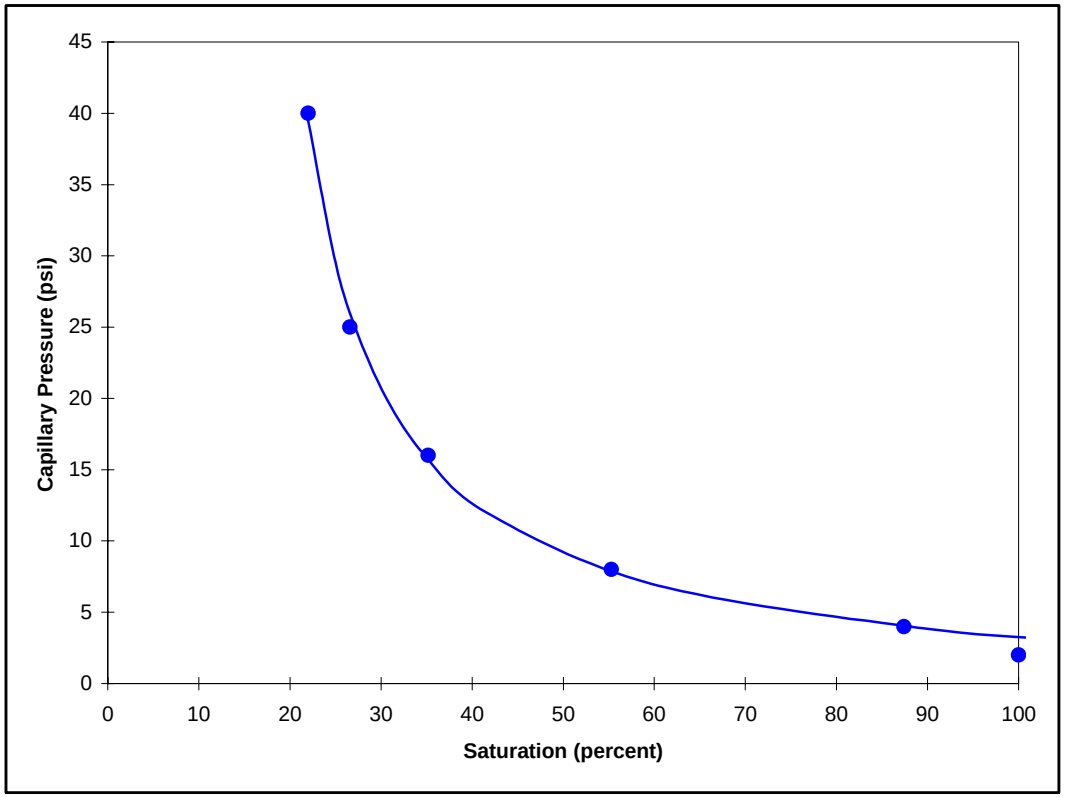

CAPILLARY PRESSURE
Overburden

Client	Origin Energy Resources Limited	**Air Permeability**	31.7 milliDarcy's
Well	Yolla-4	**Porosity**	16.9 percent
Sample	29		
Depth	2901.32 metres		
Test Method	Air/Brine Porous Plate @ Overburden		
Overburden	5000 psi		

Capillary Pressure (psi)	Brine Saturation (percent)
2.0	100.0
4.0	87.9
8.0	43.5
16	25.9
25	19.8
40	16.3

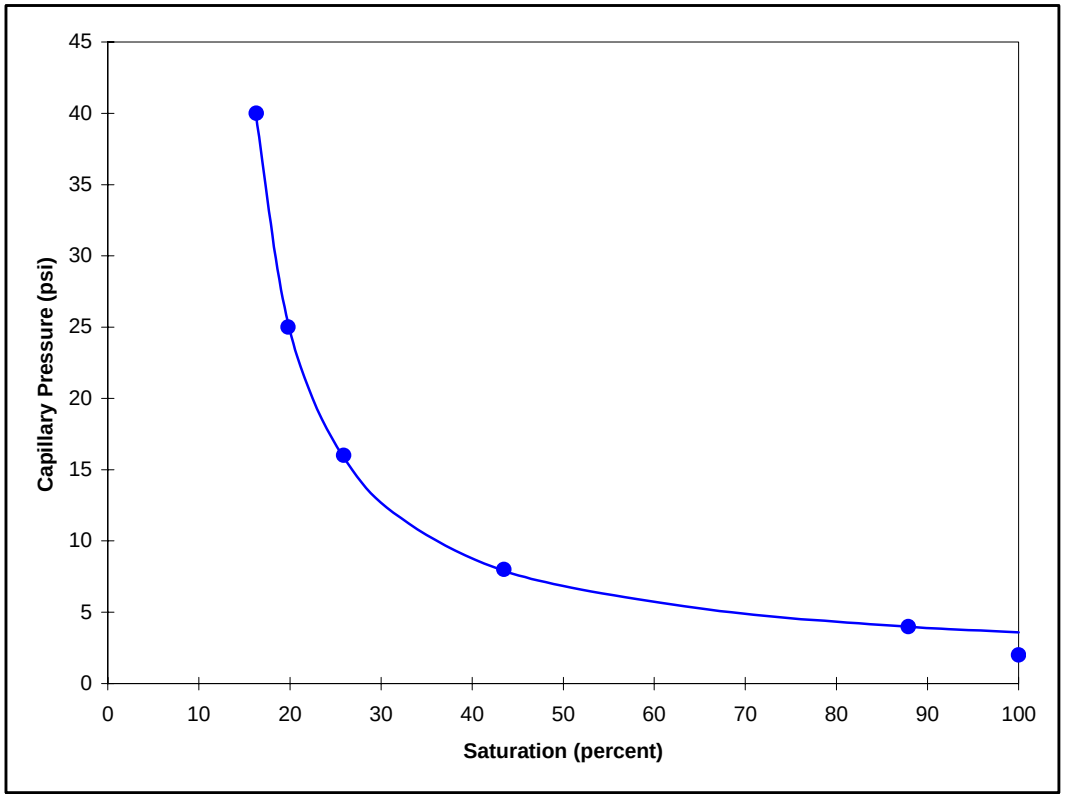

CAPILLARY PRESSURE
Overburden

Client	Origin Energy Resources Limited	**Air Permeability**	875 milliDarcy's
Well	Yolla-4	**Porosity**	19.9 percent
Sample	34		
Depth	2902.49 metres		
Test Method	Air/Brine Porous Plate @ Overburden		
Overburden	5000 psi		

Capillary Pressure (psi)	Brine Saturation (percent)
0.25	94.8
0.50	82.3
1.0	55.9
2.0	37.3
4.0	27.3
8.0	17.8
16	10.9
40	7.4

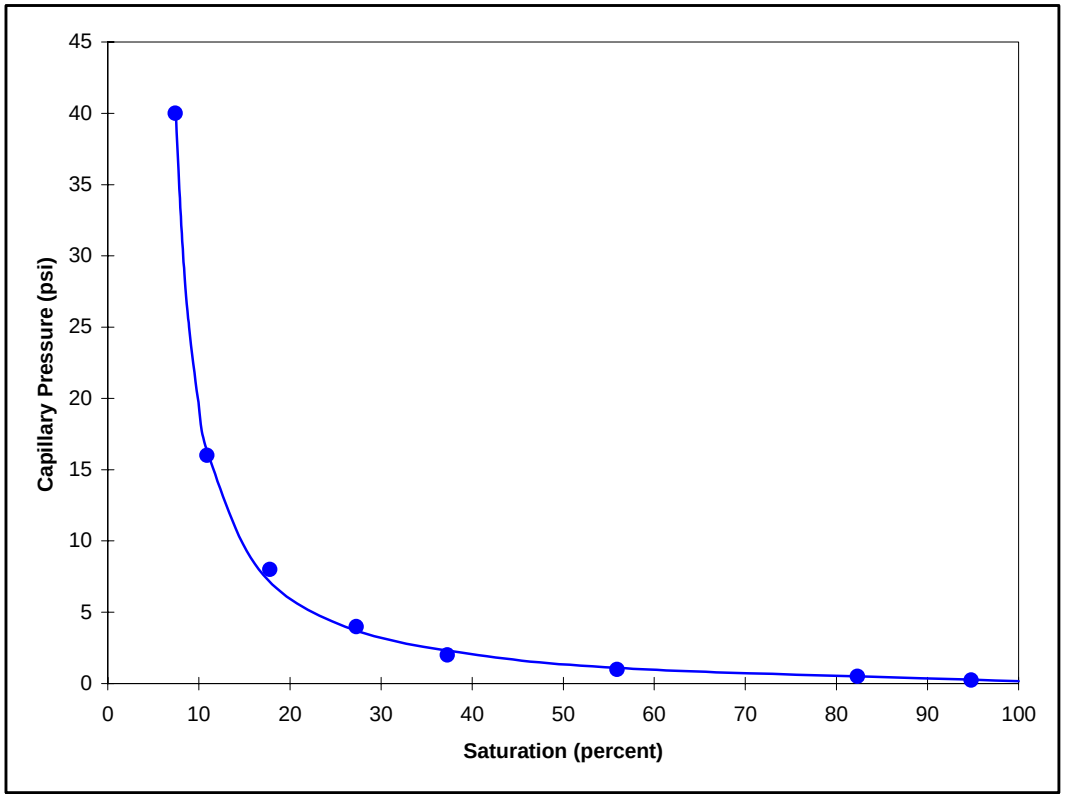

CAPILLARY PRESSURE
Overburden

Client	Origin Energy Resources Limited	**Air Permeability**	2326 milliDarcy's
Well	Yolla-4	**Porosity**	21.1 percent
Sample	37		
Depth	2903.41 metres		
Test Method	Air/Brine Porous Plate @ Overburden		
Overburden	5000 psi		

Capillary Pressure (psi)	Brine Saturation (percent)
0.25	89.3
0.50	69.5
1.0	30.8
2.0	23.4
4.0	15.2
8.0	10.2
40	6.9

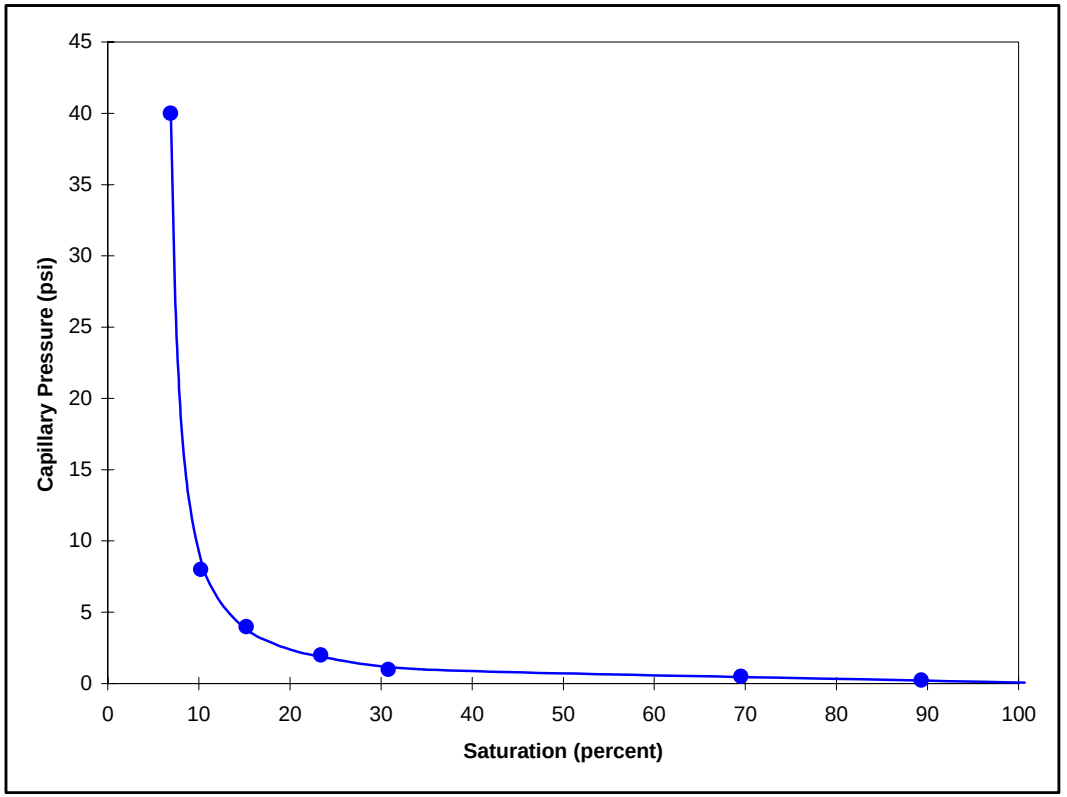

CAPILLARY PRESSURE
Overburden

Client	Origin Energy Resources Limited	**Air Permeability**	1325 milliDarcy's
Well	Yolla-4	**Porosity**	19.8 percent
Sample	39		
Depth	2903.92 metres		
Test Method	Air/Brine Porous Plate @ Overburden		
Overburden	5000 psi		

Capillary Pressure (psi)	Brine Saturation (percent)
0.50	85.1
1.0	56.6
2.0	28.2
4.0	22.9
8.0	15.9
16	14.2
40	12.0

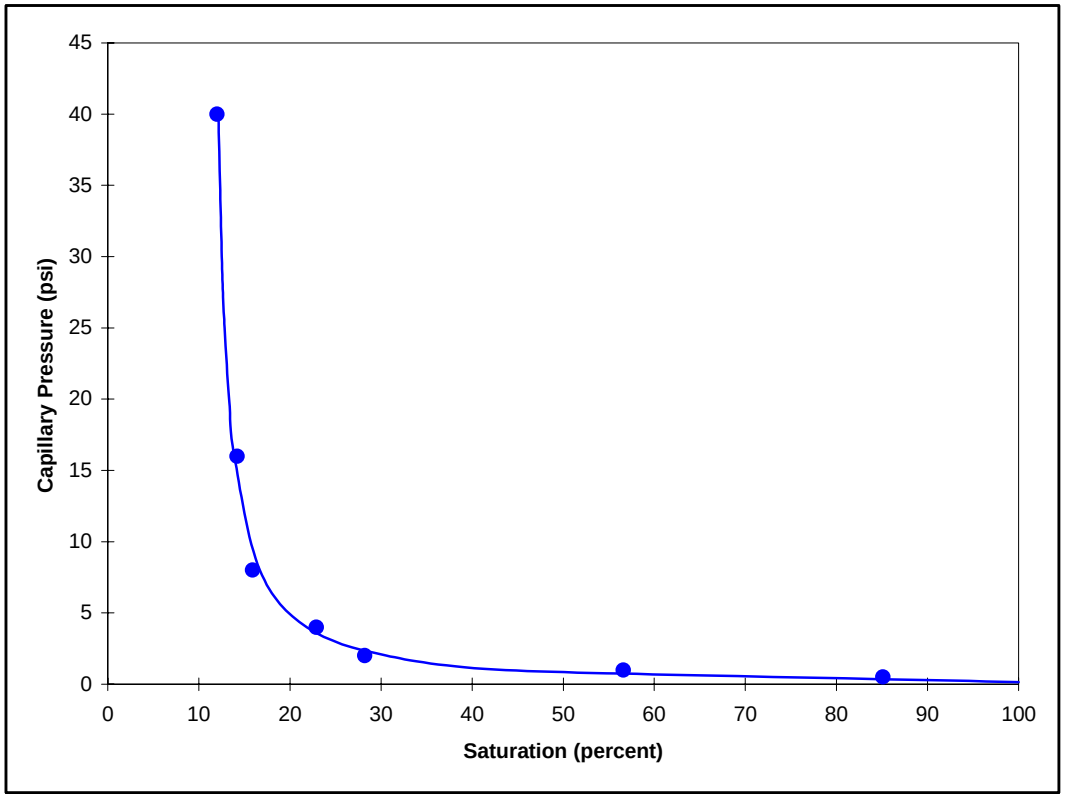

CAPILLARY PRESSURE
Overburden

Client	Origin Energy Resources Limited	**Air Permeability**	2386 milliDarcy's
Well	Yolla-4	**Porosity**	22.0 percent
Sample	43		
Depth	2904.98 metres		
Test Method	Air/Brine Porous Plate @ Overburden		
Overburden	5000 psi		

Capillary Pressure (psi)	Brine Saturation (percent)
0.25	82.7
0.50	78.0
1.0	44.2
2.0	30.8
4.0	21.4
16	13.1
40	9.6

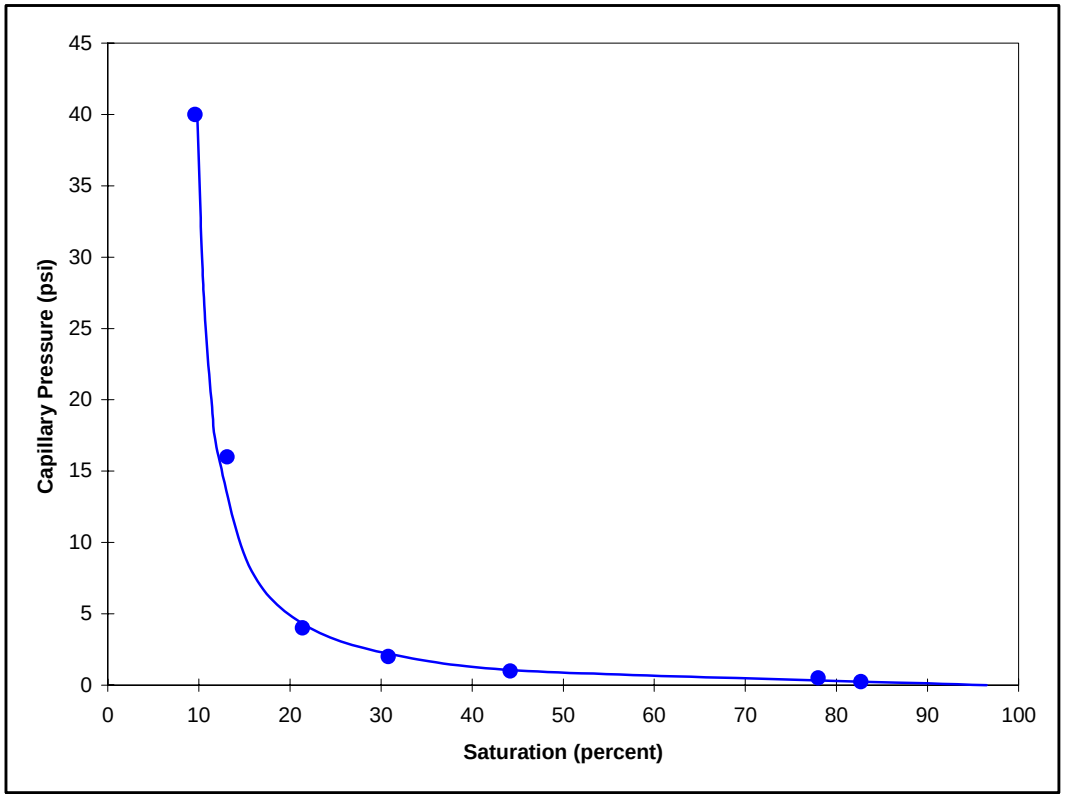

CAPILLARY PRESSURE
Overburden

Client	Origin Energy Resources Limited	**Air Permeability**	100 milliDarcy's
Well	Yolla-4	**Porosity**	16.1 percent
Sample	44		
Depth	2905.17 metres		
Test Method	Air/Brine Porous Plate @ Overburden		
Overburden	5000 psi		

Capillary Pressure (psi)	Brine Saturation (percent)
0.50	100.0
1.0	92.5
2.0	79.7
4.0	52.0
8.0	34.9
16	22.1
40	12.5

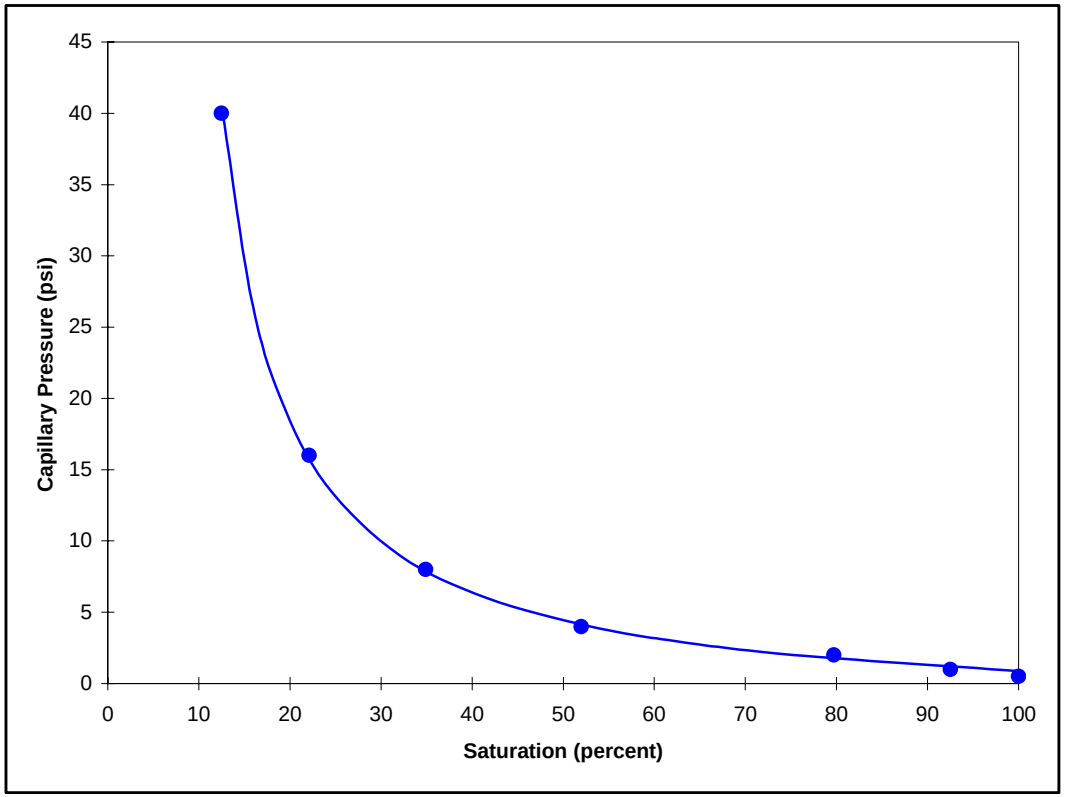

CAPILLARY PRESSURE
Overburden

Client	Origin Energy Resources Limited	**Air Permeability**	3800 milliDarcy's
Well	Yolla-4	**Porosity**	21.5 percent
Sample	47		
Depth	2906.08 metres		
Test Method	Air/Brine Porous Plate @ Overburden		
Overburden	5000 psi		

Capillary Pressure (psi)	Brine Saturation (percent)
0.25	74.2
0.50	31.4
1.0	24.5
2.0	19.3
4.0	13.6
16	8.0
40	6.0

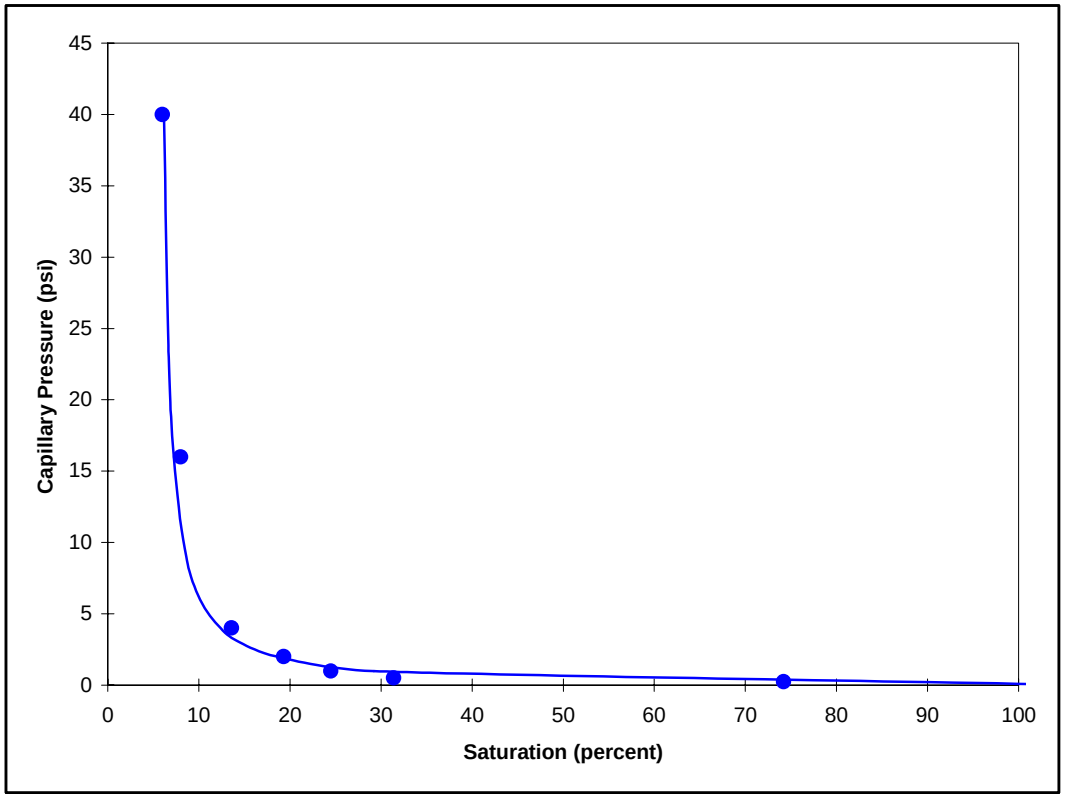

CAPILLARY PRESSURE
Overburden

Client	Origin Energy Resources Limited	**Air Permeability**	938 milliDarcy's
Well	Yolla-4	**Porosity**	20.6 percent
Sample	70		
Depth	2959.50 metres		
Test Method	Air/Brine Porous Plate @ Overburden		
Overburden	5000 psi		

Capillary Pressure (psi)	Brine Saturation (percent)
0.50	90.0
1.0	59.9
2.0	44.8
4.0	33.1
8.0	22.2
16	14.7
40	11.4

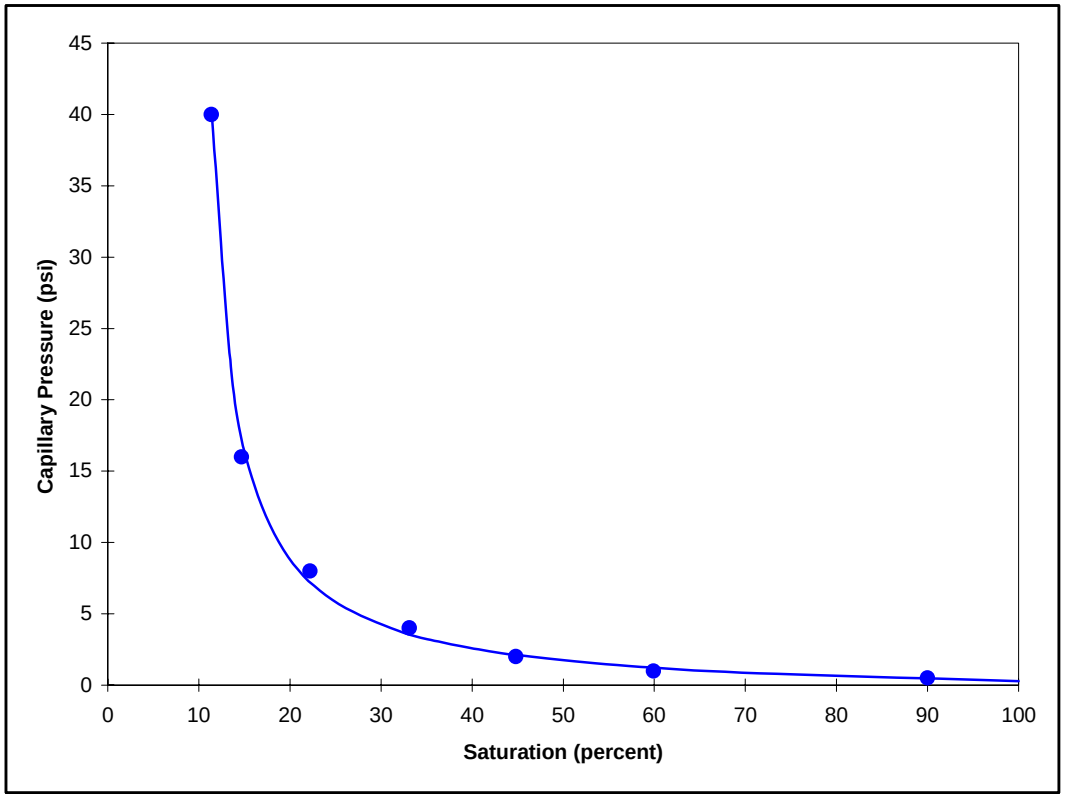

CAPILLARY PRESSURE
Overburden

Client	Origin Energy Resources Limited	**Air Permeability**	658 milliDarcy's
Well	Yolla-4	**Porosity**	20.0 percent
Sample	71		
Depth	2959.81 metres		
Test Method	Air/Brine Porous Plate @ Overburden		
Overburden	5000 psi		

Capillary Pressure (psi)	Brine Saturation (percent)
0.50	87.9
1.0	53.3
2.0	41.2
4.0	35.1
8.0	21.3
16	14.4
40	8.7

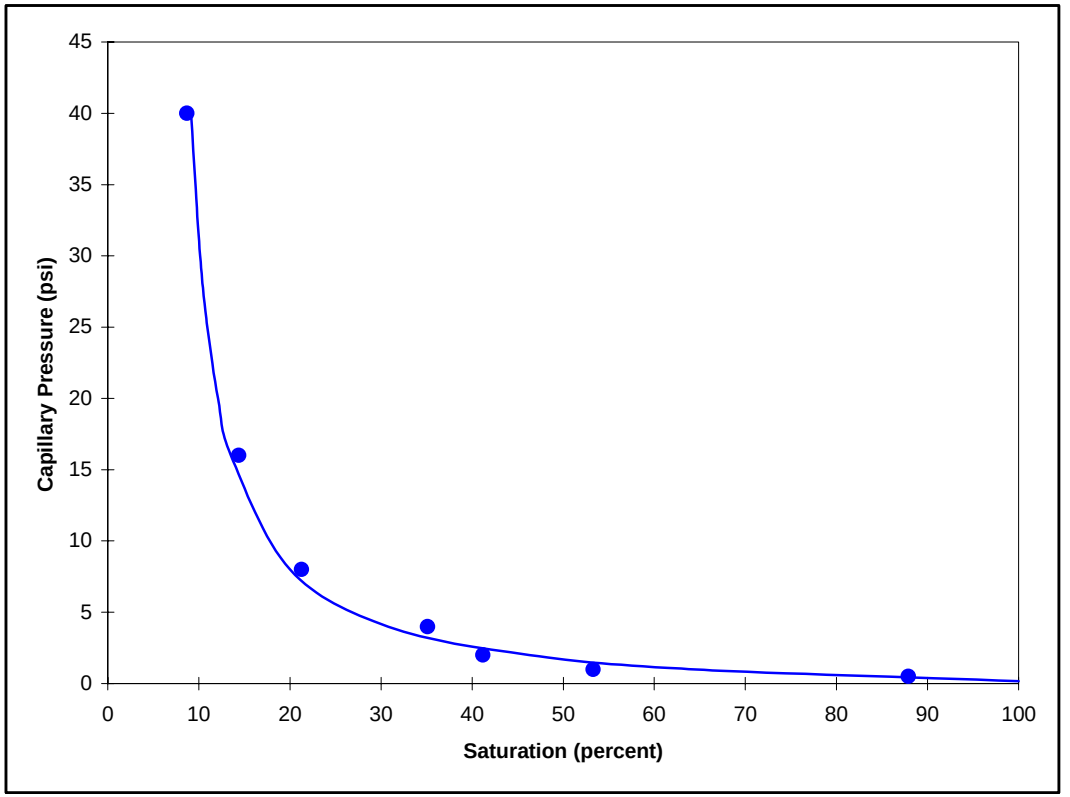

CAPILLARY PRESSURE
Overburden

Client	Origin Energy Resources Limited	**Air Permeability**	350 milliDarcy's
Well	Yolla-4	**Porosity**	17.9 percent
Sample	75		
Depth	2960.95 metres		
Test Method	Air/Brine Porous Plate @ Overburden		
Overburden	5000 psi		

Capillary Pressure (psi)	Brine Saturation (percent)
0.25	96.1
0.50	89.3
1.0	65.1
2.0	51.5
4.0	35.1
8.0	21.5
40	9.8

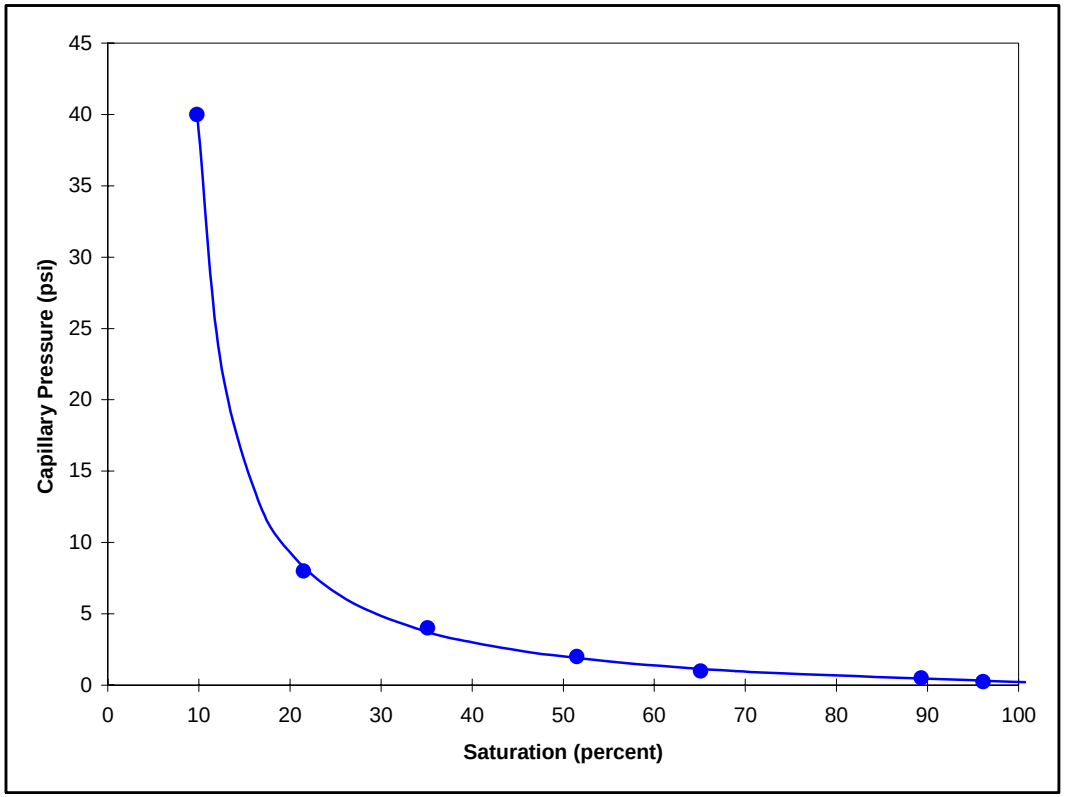

CAPILLARY PRESSURE
Overburden

Client	Origin Energy Resources Limited	**Air Permeability**	593 milliDarcy's
Well	Yolla-4	**Porosity**	18.9 percent
Sample	78		
Depth	2961.87 metres		
Test Method	Air/Brine Porous Plate @ Overburden		
Overburden	5000 psi		

Capillary Pressure (psi)	Brine Saturation (percent)
0.25	93.1
0.50	77.8
1.0	52.9
2.0	42.3
4.0	33.5
8.0	22.9
40	11.8

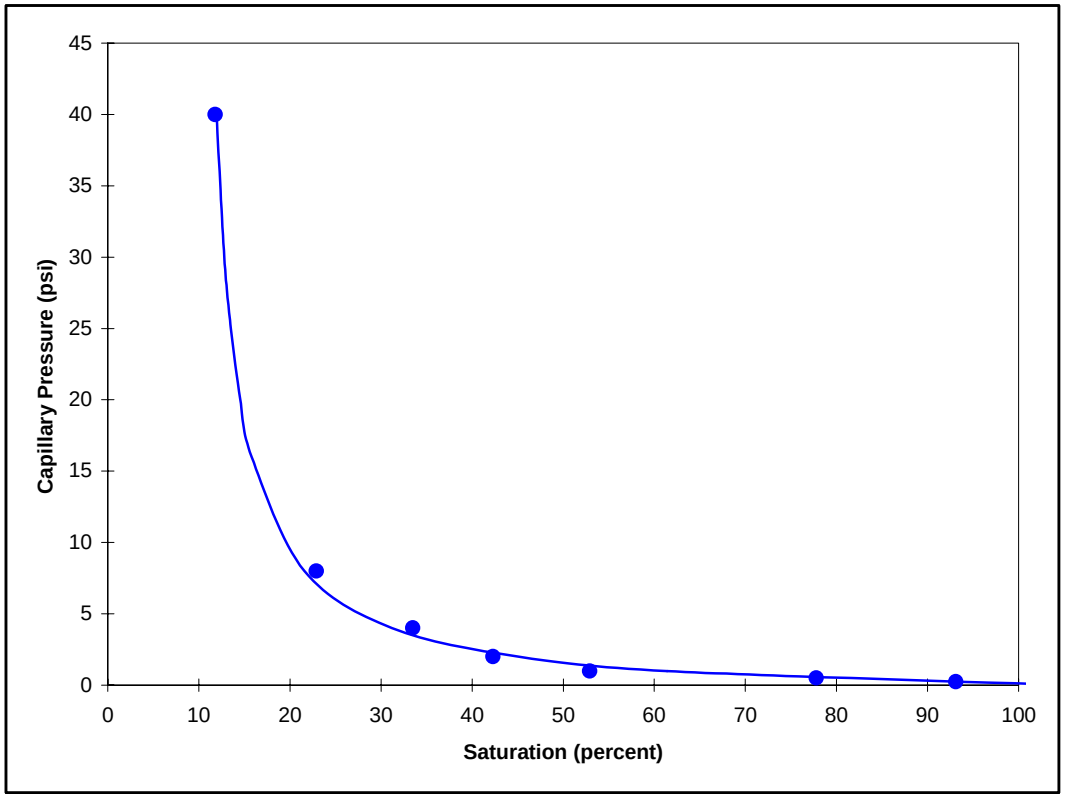

CAPILLARY PRESSURE
Overburden

Client	Origin Energy Resources Limited	**Air Permeability**	19.7 milliDarcy's
Well	Yolla-4	**Porosity**	14.5 percent
Sample	82		
Depth	2963.06 metres		
Test Method	Air/Brine Porous Plate @ Overburden		
Overburden	5000 psi		

Capillary Pressure (psi)	Brine Saturation (percent)
2.0	95.9
4.0	82.9
8.0	50.4
16	34.4
25	25.5
40	20.8

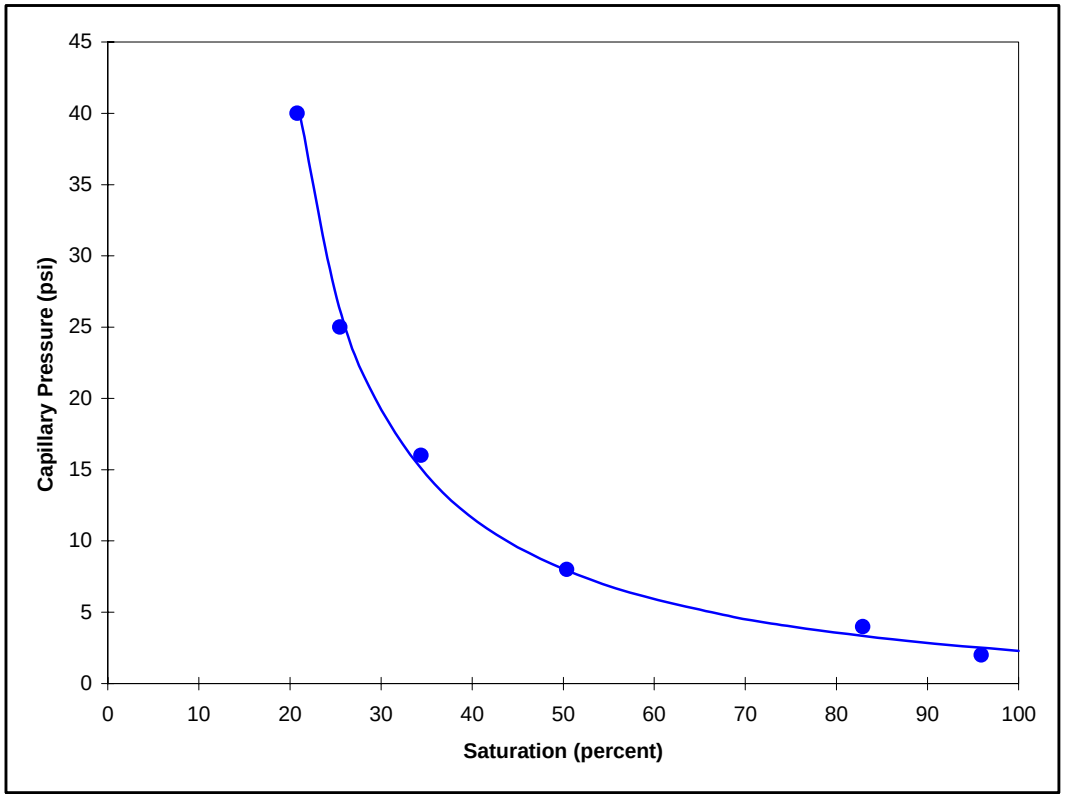

CAPILLARY PRESSURE
Overburden

Client	Origin Energy Resources Limited	**Air Permeability**	357 milliDarcy's
Well	Yolla-4	**Porosity**	17.8 percent
Sample	85		
Depth	2963.93 metres		
Test Method	Air/Brine Porous Plate @ Overburden		
Overburden	5000 psi		

Capillary Pressure (psi)	Brine Saturation (percent)
0.50	80.4
1.0	50.1
2.0	38.8
4.0	29.5
8.0	21.2
16	15.8
40	12.4

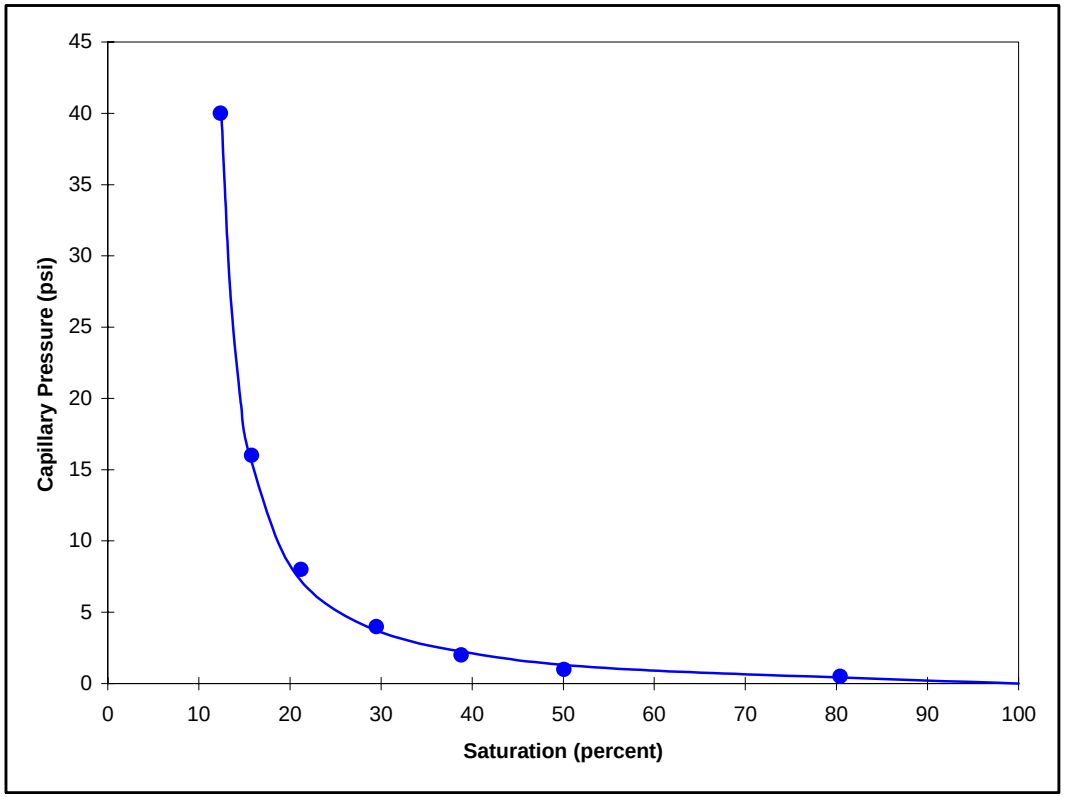

CAPILLARY PRESSURE
Overburden

Client	Origin Energy Resources Limited	**Air Permeability**	149 milliDarcy's
Well	Yolla-4	**Porosity**	18.4 percent
Sample	98		
Depth	2967.87 metres		
Test Method	Air/Brine Porous Plate @ Overburden		
Overburden	5000 psi		

Capillary Pressure (psi)	Brine Saturation (percent)
1.0	97.2
2.0	68.7
4.0	53.2
8.0	34.3
16	22.4
25	16.3
40	12.1

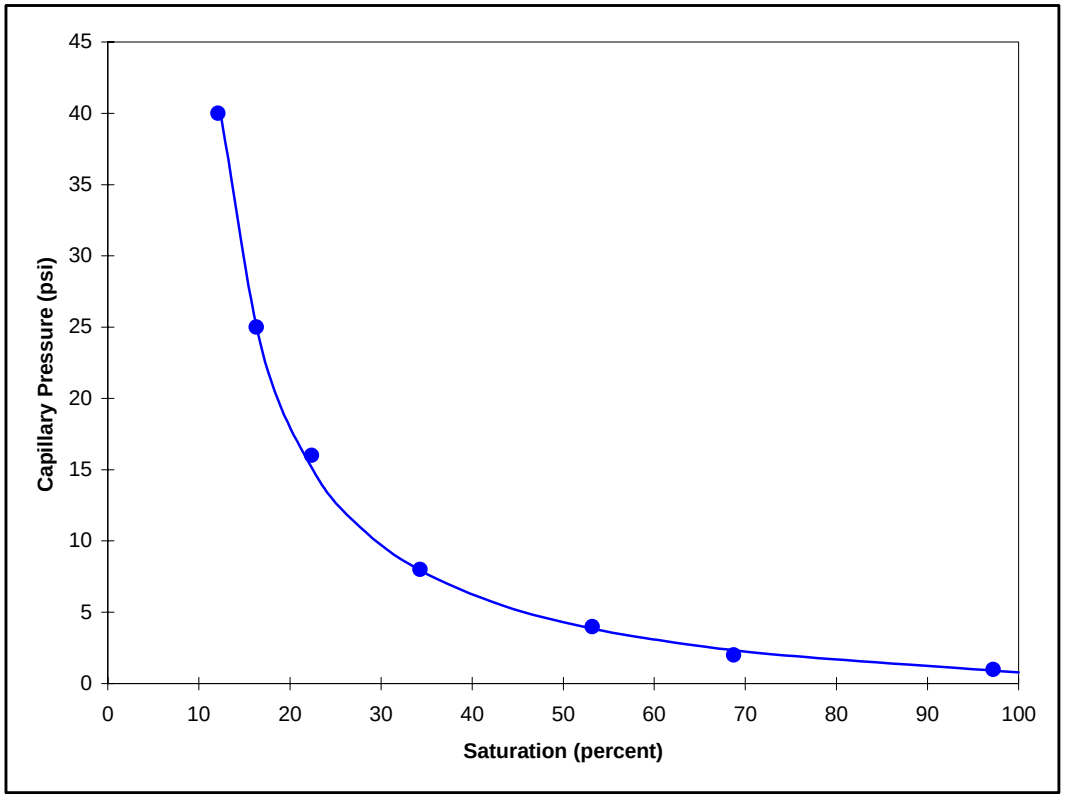

CAPILLARY PRESSURE
Overburden

Client	Origin Energy Resources Limited	**Air Permeability**	534 milliDarcy's
Well	Yolla-4	**Porosity**	17.5 percent
Sample	115		
Depth	2972.75 metres		
Test Method	Air/Brine Porous Plate @ Overburden		
Overburden	5000 psi		

Capillary Pressure (psi)	Brine Saturation (percent)
0.50	96.2
1.0	71.7
2.0	57.0
4.0	40.5
8.0	26.7
16	15.3
40	8.3

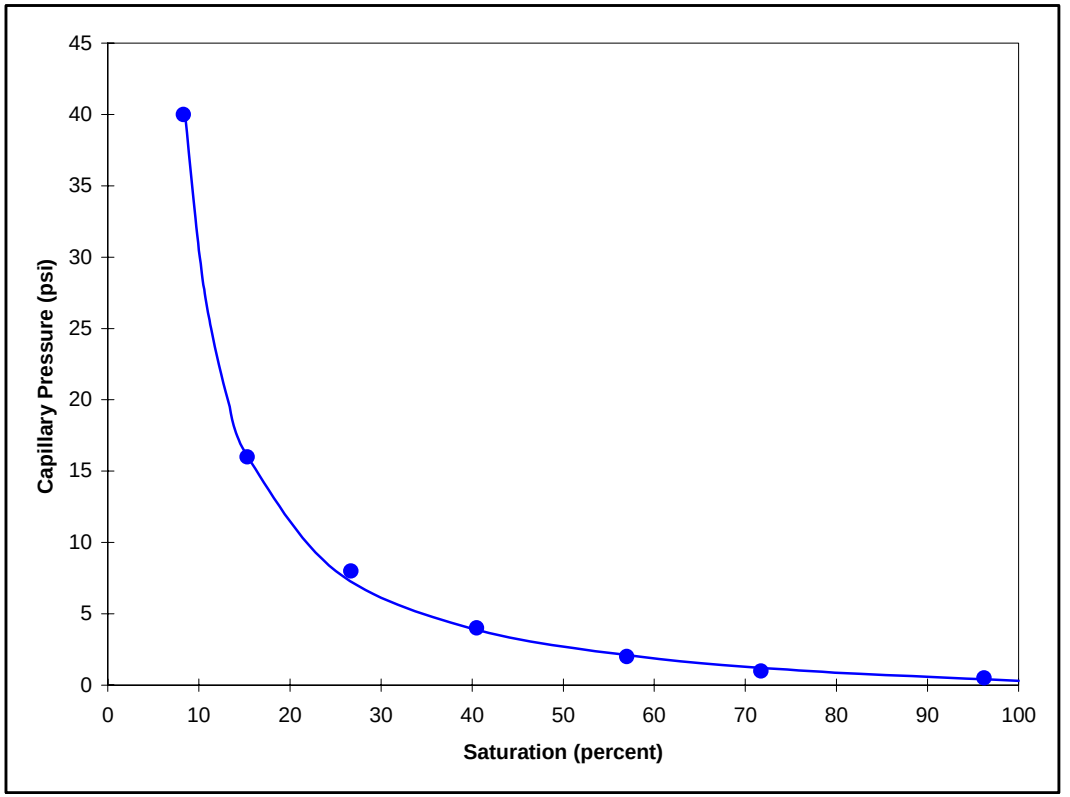

CAPILLARY PRESSURE
Overburden

Client	Origin Energy Resources Limited	**Air Permeability**	258 milliDarcy's
Well	Yolla-4	**Porosity**	18.1 percent
Sample	117		
Depth	2973.35 metres		
Test Method	Air/Brine Porous Plate @ Overburden		
Overburden	5000 psi		

Capillary Pressure (psi)	Brine Saturation (percent)
0.25	97.1
0.50	88.6
1.0	65.8
2.0	43.4
4.0	34.4
8.0	22.0
40	12.5

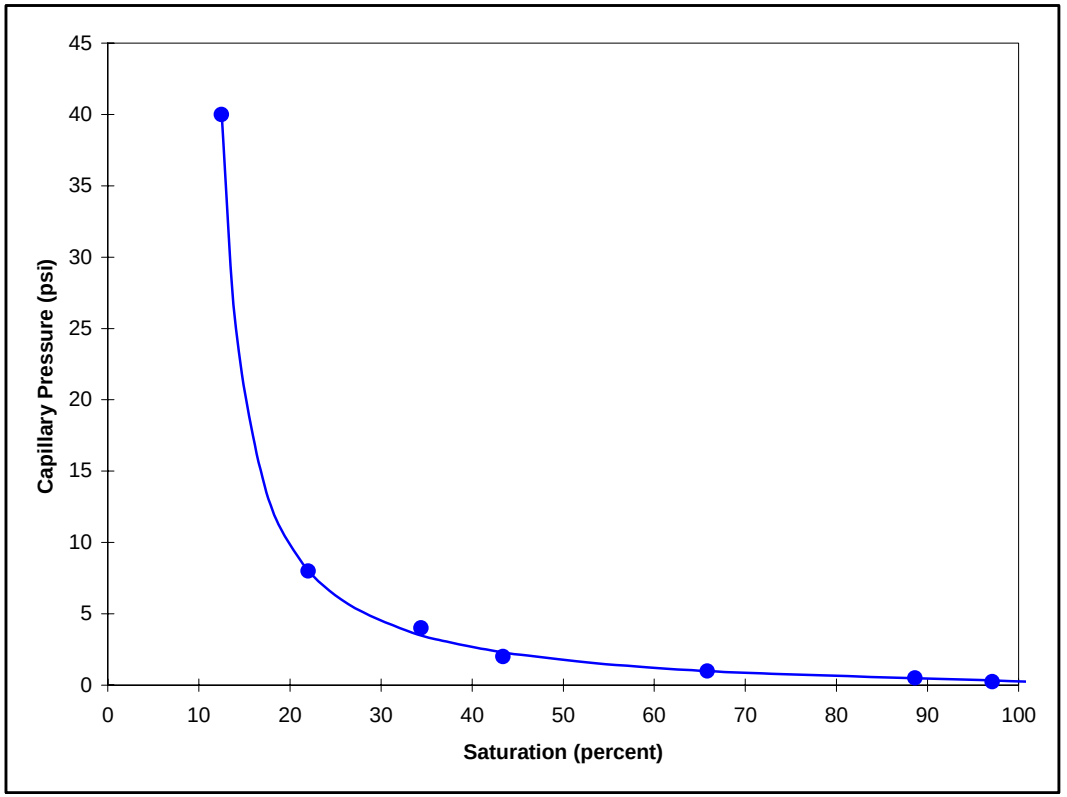

CAPILLARY PRESSURE
Overburden

Client	Origin Energy Resources Limited	**Air Permeability**	763 milliDarcy's
Well	Yolla-4	**Porosity**	20.8 percent
Sample	120		
Depth	2974.25 metres		
Test Method	Air/Brine Porous Plate @ Overburden		
Overburden	5000 psi		

Capillary Pressure (psi)	Brine Saturation (percent)
0.50	92.5
1.0	58.6
2.0	35.4
4.0	28.8
8.0	18.8
16	12.6
40	8.9

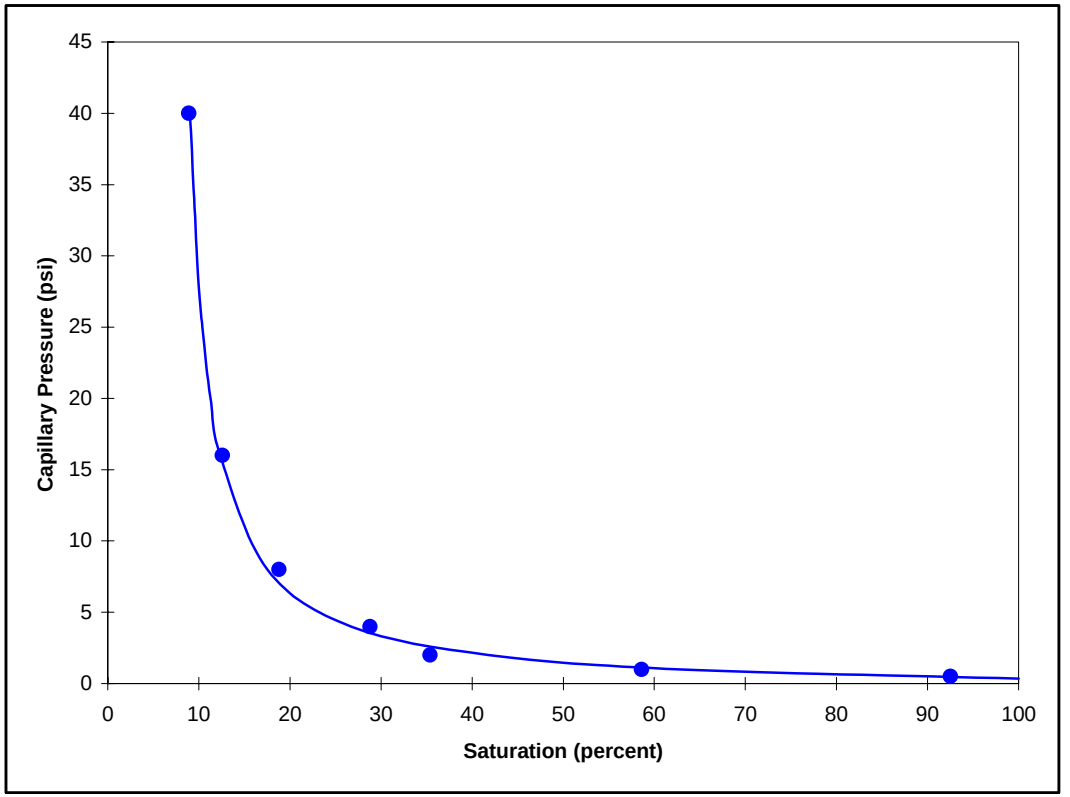

CAPILLARY PRESSURE
Overburden

Client	Origin Energy Resources Limited	**Air Permeability**	177 milliDarcy's
Well	Yolla-4	**Porosity**	18.6 percent
Sample	121		
Depth	2974.57 metres		
Test Method	Air/Brine Porous Plate @ Overburden		
Overburden	5000 psi		

Capillary Pressure (psi)	Brine Saturation (percent)
1.0	96.3
2.0	64.8
4.0	49.1
8.0	34.3
16	20.9
40	12.1

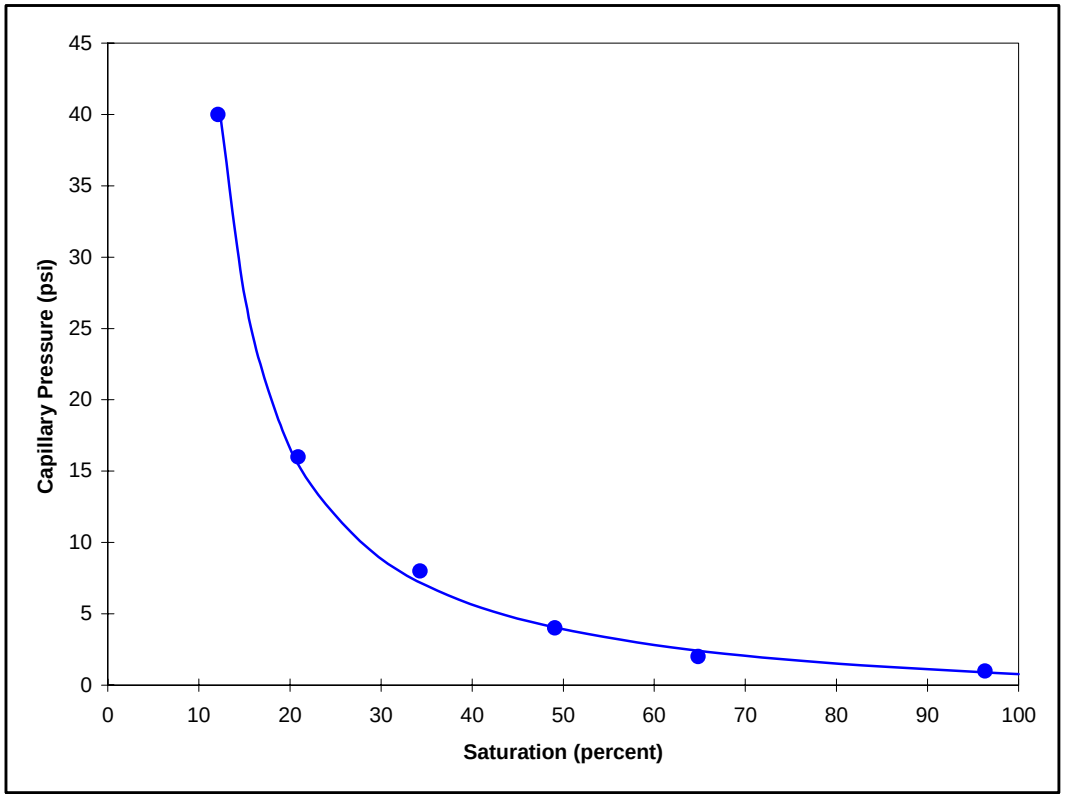

CAPILLARY PRESSURE
Overburden

Client	Origin Energy Resources Limited	**Air Permeability**	41.8 milliDarcy's
Well	Yolla-4	**Porosity**	16.1 percent
Sample	132		
Depth	2978.26 metres		
Test Method	Air/Brine Porous Plate @ Overburden		
Overburden	5000 psi		

Capillary Pressure (psi)	Brine Saturation (percent)
2.0	98.4
4.0	66.4
8.0	48.3
16	31.8
25	23.8
40	17.9

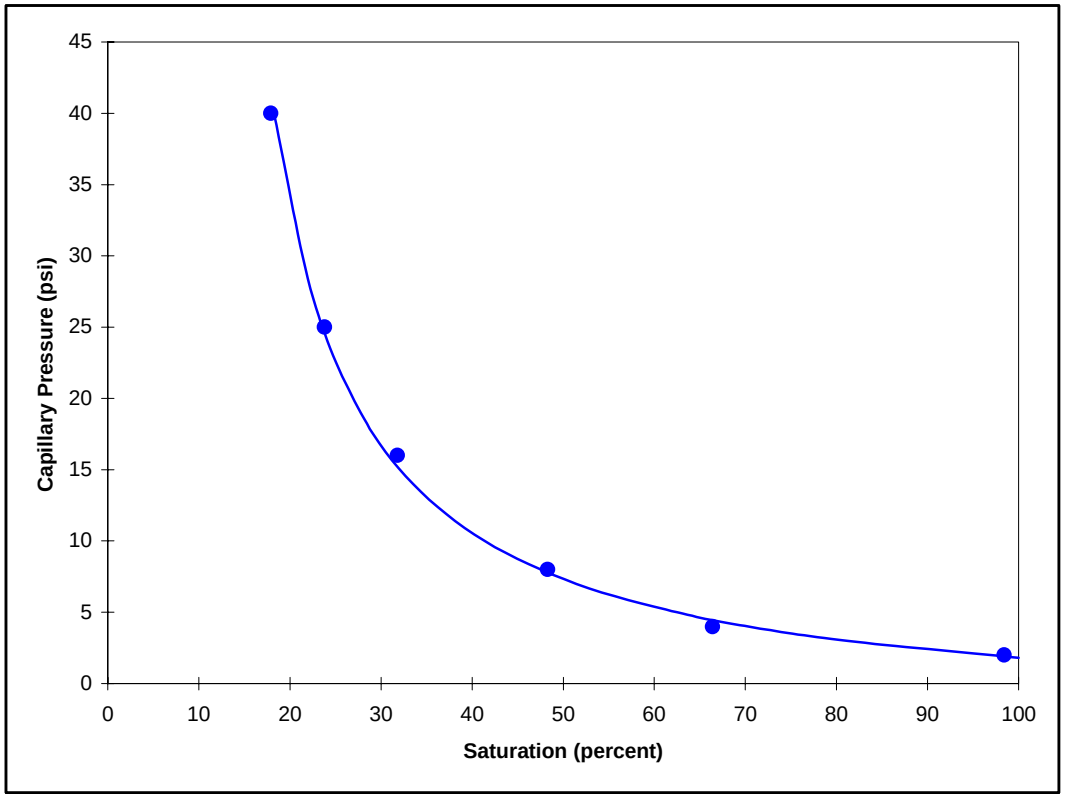

CAPILLARY PRESSURE
Overburden

Client	Origin Energy Resources Limited	**Air Permeability**	65.9 milliDarcy's
Well	Yolla-4	**Porosity**	16.7 percent
Sample	135		
Depth	2979.15 metres		
Test Method	Air/Brine Porous Plate @ Overburden		
Overburden	5000 psi		

Capillary Pressure (psi)	Brine Saturation (percent)
1.0	96.4
2.0	91.3
4.0	54.8
8.0	35.3
16	24.0
25	18.9
40	16.3

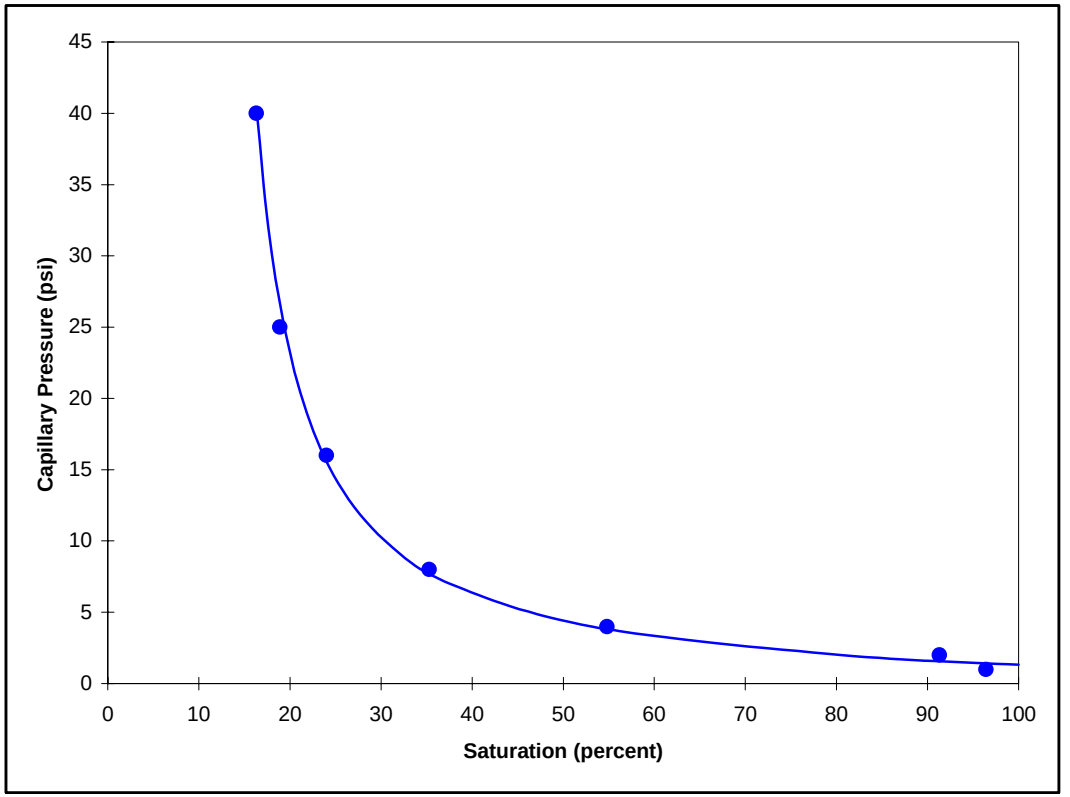

CAPILLARY PRESSURE

Client Origin Energy Resources Limited
Well Yolla-4

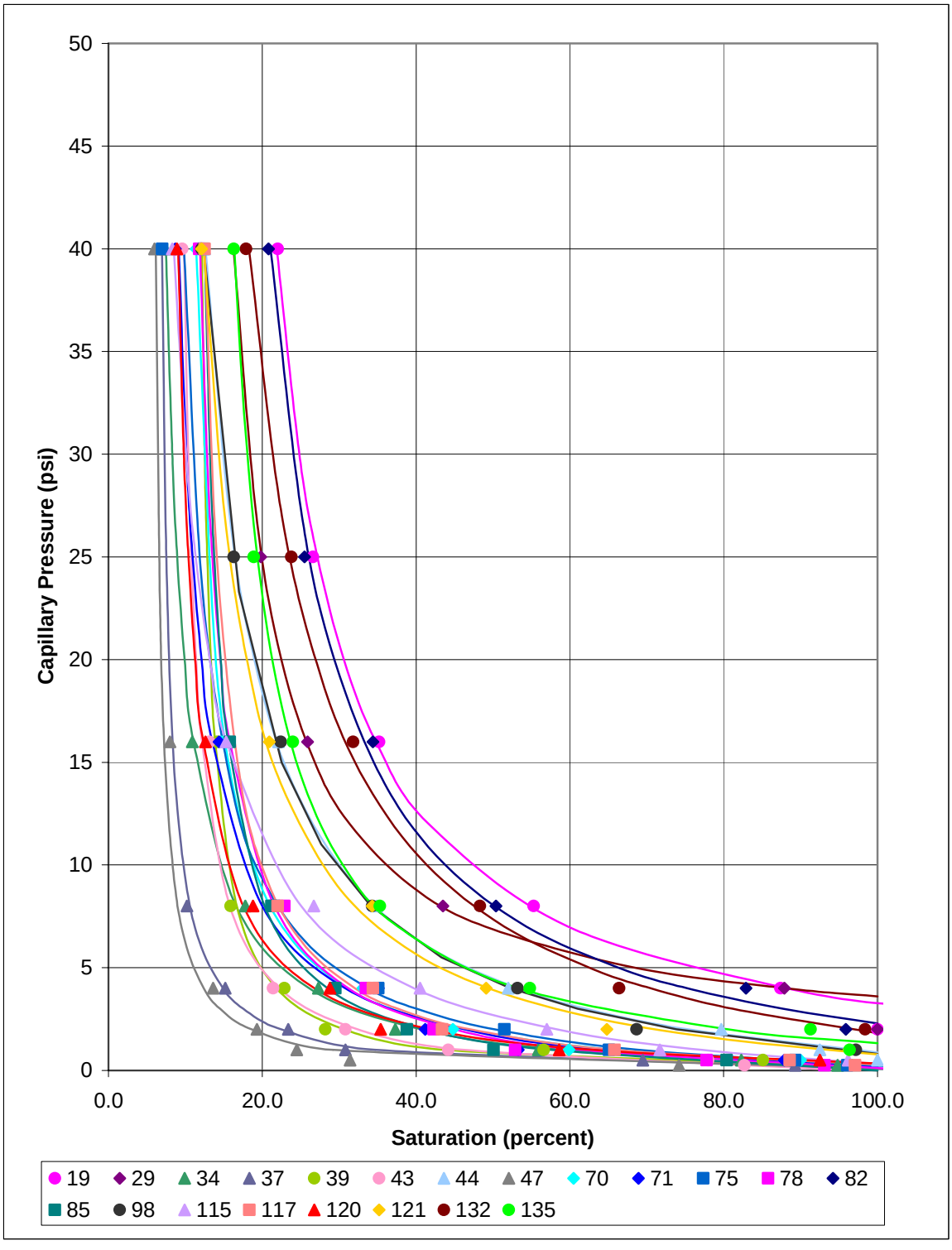

J FUNCTION

Client Origin Energy Resources Limited
Well Yolla-4

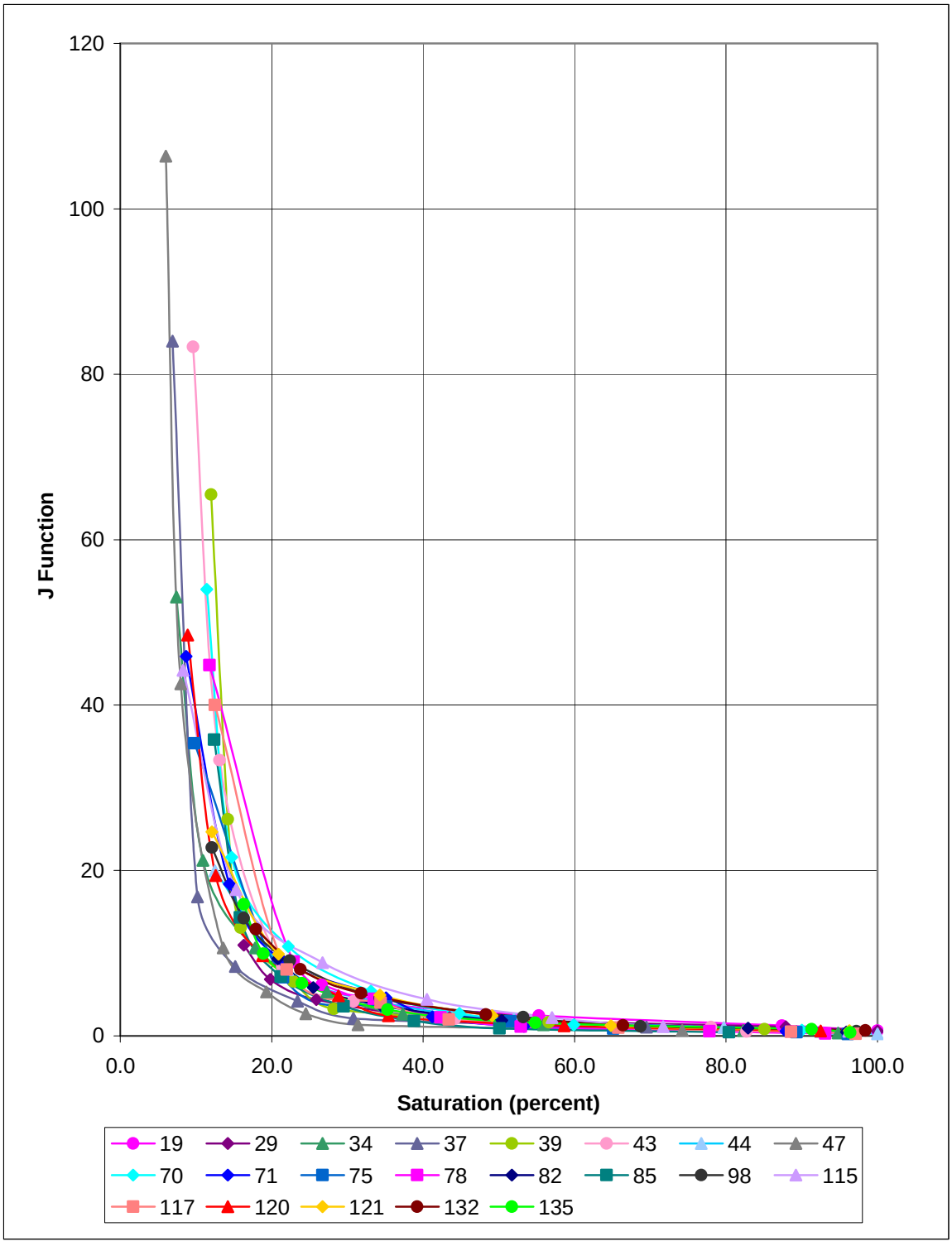

CHAPTER 4

ELECTRICAL PROPERTIES AND CAPILLARY PRESSURE

4.2 Test Results

4.2.4 Cation Exchange Capacity

CATION EXCHANGE CAPACITY

Client Origin Energy Resources Limited
Well Yolla-4

Sample Number	Depth (metres)	Porosity (percent)	Grain Density (g/cm^3)	Cation Exchange Capacity (meq/100g)		Quantity of Cation Exchangeable Clay Qv (meq/cm^3)	
				Uncrushed	Crushed	Uncrushed	Crushed
19	2898.45	16.0	2.67	0.05	0.29	0.01	0.04
37	2903.41	22.4	2.69	0.14	0.25	0.01	0.02
39	2903.92	21.0	2.70	0.09	0.16	0.01	0.02
43	2904.98	23.0	2.65	0.19	0.22	0.02	0.02
47	2906.08	22.6	2.66	0.05	0.20	0.01	0.02
71	2959.81	21.0	2.65	0.14	0.19	0.01	0.02
82	2963.06	15.5	2.66	0.33	0.37	0.05	0.05
85	2963.93	19.8	2.63	0.23	0.23	0.02	0.02
120	2974.25	21.7	2.64	0.16	0.16	0.02	0.02
135	2979.15	17.6	2.64	0.05	0.28	0.01	0.03

CHAPTER 4

ELECTRICAL PROPERTIES AND CAPILLARY PRESSURE

4.2 Test Results

4.2.5 Summary

FORMATION RESISTIVITY FACTOR

Client	Origin Energy Resources Limited	**Rw of Saturant**	0.241 at 25ºC
Well	Yolla-4	**Overburden**	5000 psi

Sample Number	Depth (metres)	Permeability to Air (milliDarcy's)	Porosity (percent)	Formation Factor FF	Cementation Exponent m	Saturation Exponent n	Shaley Sand Equivalent † Formation Factor FF*	Shaley Sand Equivalent † Cementation Exponent m*	Shaley Sand Equivalent † Saturation Exponent n*
19	2898.45	8.8	14.9	30.3	1.79	2.18	30.5	1.80	2.19
37	2903.41	2326	21.1	14.7	1.73	1.78	14.9	1.74	1.83
39	2903.92	1325	19.8	19.0	1.82	1.64	19.1	1.82	1.66
43	2904.98	2386	22.0	15.1	1.79	1.58	15.3	1.80	1.63
47	2906.08	3800	21.5	14.0	1.72	1.56	14.0	1.72	1.58
71	2959.81	658	20.0	17.2	1.77	1.76	17.4	1.77	1.80
82	2963.06	19.7	14.5	33.2	1.81	1.66	34.5	1.83	1.74
85	2963.93	357	17.8	21.6	1.78	1.77	22.1	1.79	1.83
120	2974.25	763	20.8	16.6	1.79	1.82	16.8	1.80	1.87
135	2979.15	65.9	16.7	23.9	1.77	1.73	24.1	1.78	1.74

† Calculated from Cation Exchange Capacity

RESIDUAL SATURATION

Client Origin Energy Resources Limited
Well Yolla-4

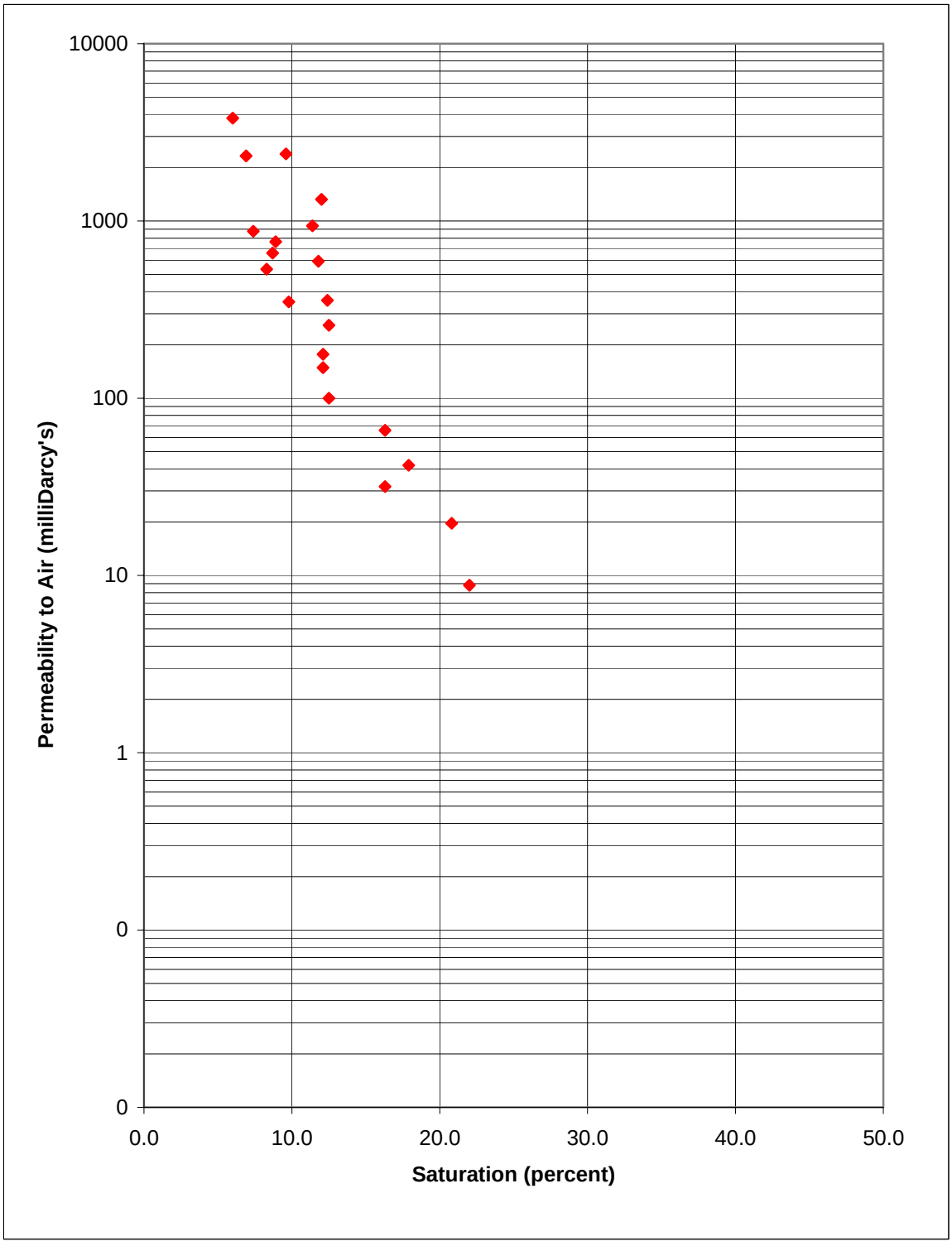

CHAPTER 5

RESIDUAL GAS

5.1 Test and Calculation Procedures

5. RESIDUAL GAS

5.1 Test and Calculation Procedures

5.1.1 Permeability to Air at Residual Water Saturation

On completion of capillary pressure desaturation the samples at residual water saturation (Swr) underwent effective permeability to air. Each sample was individually placed into a hydrostatic cell with an overburden pressure of 5000 psi applied. A known pressure of humidified air was applied to the upstream face of each sample, creating a flow of air through the core plug. Effective permeability to air was calculated using Darcy's Law through knowledge of the upstream pressure, flow rate, viscosity of air and sample dimensions.

$$Keg = \frac{2000.BP.\mu.q.L}{(P_1^2 - P_2^2).A}$$

where	Keg	=	*effective permeability to air @ Swr (milliDarcy's)*
	BP	=	*barometric pressure (atmospheres)*
	μ	=	*gas viscosity (cP)*
	q	=	*flow rate (cm^3/s)*
	L	=	*sample length (cm)*
	P_1	=	*upstream pressure (atmospheres)*
	P_2	=	*downstream pressure (atmospheres)*
	A	=	*sample cross sectional area (cm^2)*

5.1.2 Waterflood

The selected samples at residual water saturation were placed into a thick walled rubber sleeve and the assembly loaded into a hydrostatic cell. An overburden pressure of 5000 psi was applied.

Brine was pumped through the samples at a low rate (4 cc/hour). Flow continued until gas production ceased and a brine permeability at residual gas saturation was determined through knowledge of the differential flooding pressure, flow rate, viscosity of brine and the sample dimensions.

$$Kw\ @\ Sgr = \frac{14696.q.L.\mu T}{\Delta P.A}$$

where	*14696*	=	*units conversion*
	$Kw\ @\ Sgr$	=	*permeability to brine at residual gas saturation (mD)*
	q	=	*flow rate (cm^3/s)*
	ΔP	=	*differential flooding pressure (psig)*
	L	=	*sample length (cm)*
	A	=	*sample cross sectional area (cm^2)*
	μT	=	*brine viscosity (cP) at T (° C)*

The flow rate was then increased (to 4cc/min) and further gas production measured. Once stable gas saturation was reached permeability was measured as per above.

COMMENTS:

It was noted that the absolute permeability to air is very close to the permeability @ irreducible/initial water saturation.

In theory the Kg @ Swi should be lower than the absolute Ka. However it was noted at the time that these results did not always follow expected trends:

Samples 37, 39 and 78 the Kg is effectively equal to the Ka
Samples 80 and 117 follow the expected trend Ka>Kg
Sample 135 is atypical Kg>Ka.

This was noted at the time, and checks were made to confirm the data was correct. In fact additional samples (ex-Pc/RI samples that weren't scheduled for waterfloods) were run and the same erratic trends were noted. Whilst it is unusual it is not unique – we have seen this phenomenon before.

For samples 37, 39 and 78 as noted above Kg effectively is the same as the Ka. This is acceptable in the higher permeable samples. The residual brine saturation is in the smaller pores that are not effectively or significantly contributing to the overall permeability. Sample 135 is indeed atypical though.

As an aside to this issue at the recent Society of Core Analysts Symposium in October last year a paper was presented that highlighted a similar effect. The paper is "Mobilisation of Trapped Gas from below the Gas-Water Contact" ref SCA2004-29 by Andrew Cable et al, quote as follows:

"*The effective gas permeability at Swi was higher than the absolute gas permeability which maybe a result of a 'lubrication effect'. Additional (independent) laboratory analysis undertaken on this core also reported similar permeability 'anomalies'. Published papers describing similar effects have also been identified for reference.*

ACS makes no warranty as to the "lubrication effect" – however the concept of Swi in smaller pore throats that basically do not effectively contribute to the overall permeability, is much more readily acceptable.

Sample 135 is currently drying after being cleaned post all analyses. We will repeat the "original" Ka to see if the actual permeability of this sample has changed since the Ka was first determined.

The absolute Ka for Sample 135 was repeated post analysis. The value was the analysis was repeated by two different technicians with consistent results. This is in effect the same as the Kg at Swi, consistent with the other samples.

CHAPTER 5

RESIDUAL GAS

5.2 Test Results

WATERFLOOD

Client Origin Energy Resources Limited
Well Yolla-4

Saturant 26000 ppm
Overburden 5000 psi

Sample Number	Permeability to Air (milliDarcy's)	Porosity (percent)	Initial Brine Saturation (percent)	Permeability to Air @ Swir (milliDarcy's)	Low Rate		Bump Flood		Gas Recovery	
					Residual Gas Saturation (percent)	Effective Brine Permeability (milliDarcy's)	Residual Gas Saturation (percent)	Effective Brine Permeability (milliDarcy's)	Percent of Pore Volume (percent)	Percent of Gas in Place (percent)
37	2326	21.1	6.9	2385	35.7	301	31.6	378	61.5	66.1
39	1325	19.8	12.0	1340	33.4	162	29.0	168	59.0	67.0
78	593	18.9	11.8	588	33.7	21.8	28.7	54.3	59.5	67.5
82	29.8	14.5	20.8	19.9	27.4	1.55	12.8	8.1	66.4	83.8
117	258	18.1	12.5	245	33.7	6.2	27.0	53.7	60.5	69.1
135	65.9	16.7	16.3	70.9	25.5	2.58	15.1	20.6	68.6	82.0

APPENDIX I

FLUID PROPERTIES

FLUID PROPERTIES

Brine

26000 ppm NaCl equivalent

Density	=	1.023	g/cm^3 @ 25°C
Resistivity	=	0.241	ohm.m @ 25°C
Viscosity	=	1.011	cP @ 25°C

APPENDIX II

EQUIPMENT SCHEMATICS

POROSIMETER SCHEMATIC

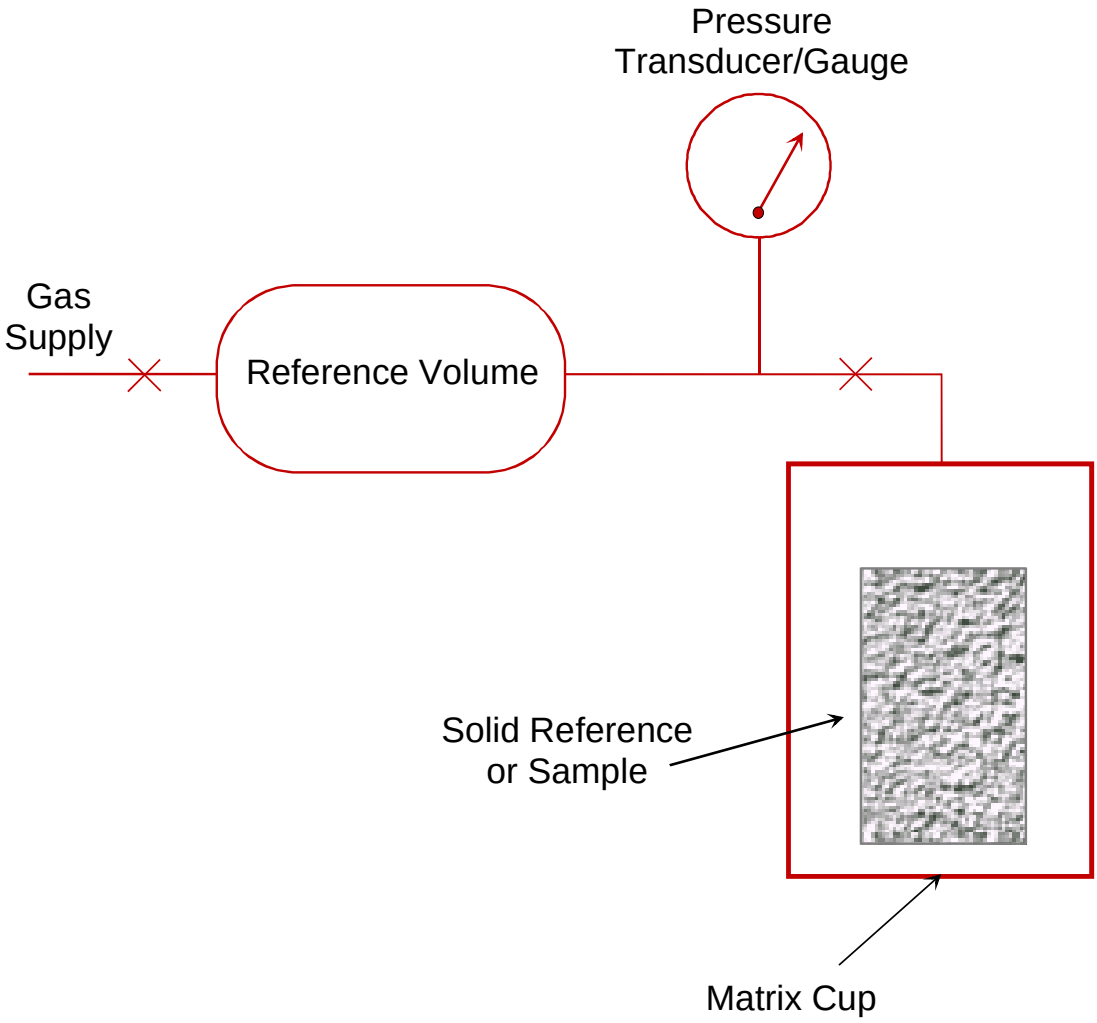

P1.V1 (reference) = P2.V2 (sample)

GAS PERMEAMETER SCHEMATIC (Hydrostatic)

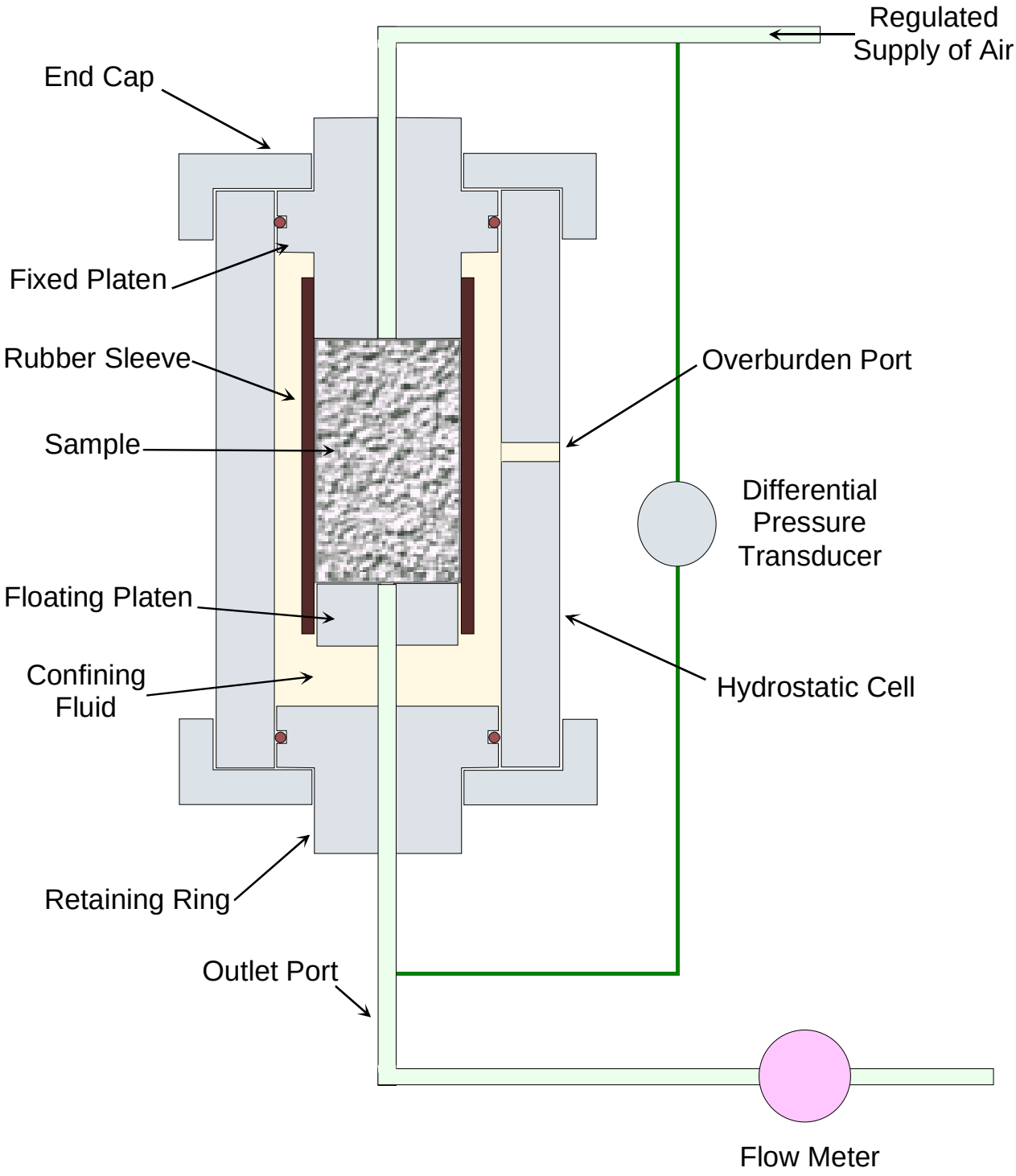

ACS Laboratories Pty Ltd
ABN: 81 008 273 005

HYDROSTATIC CAPILLARY PRESSURE CELL

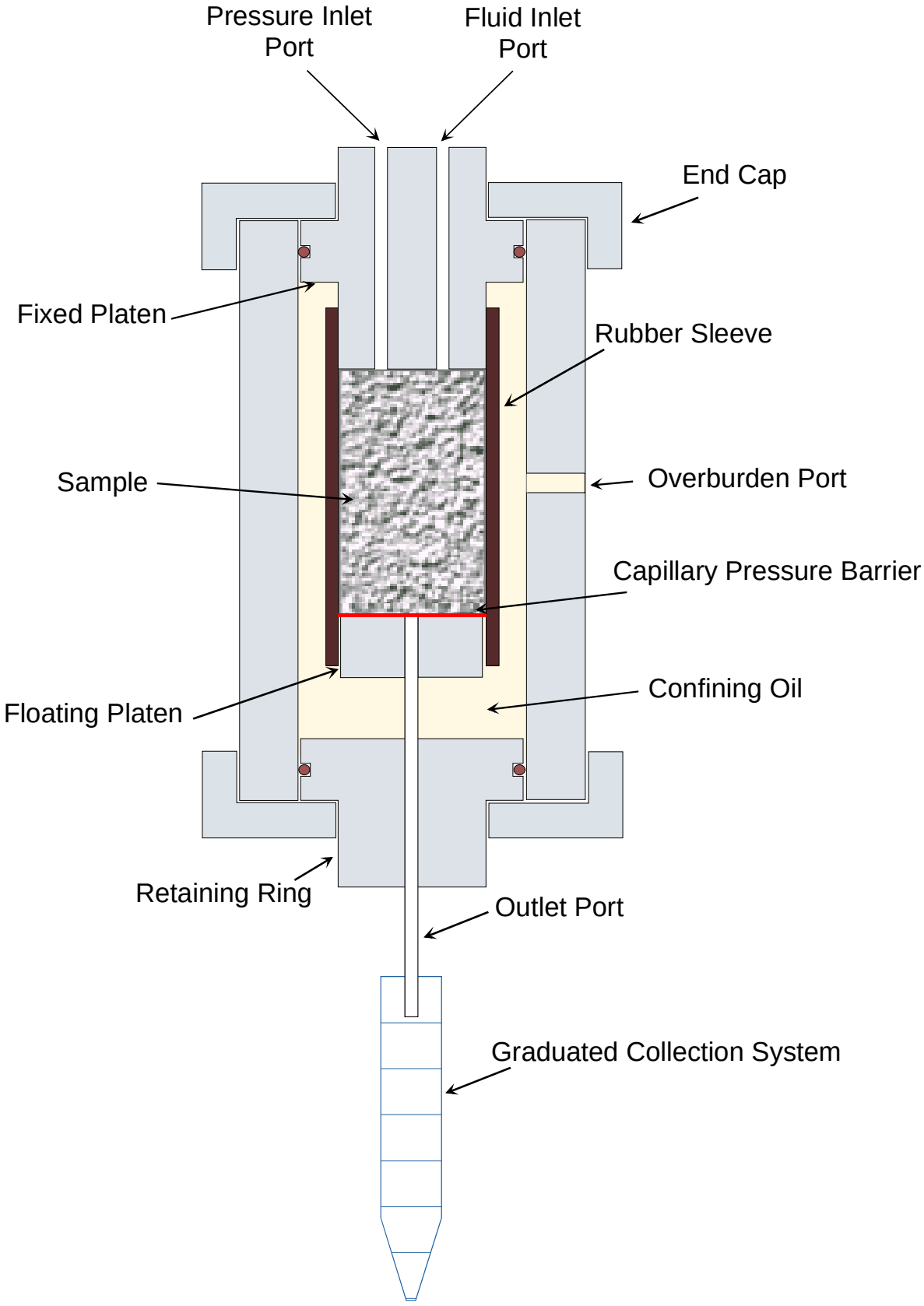

ACS Laboratories Pty Ltd
ABN: 81 008 273 005

CT SCANNER SCHEMATIC

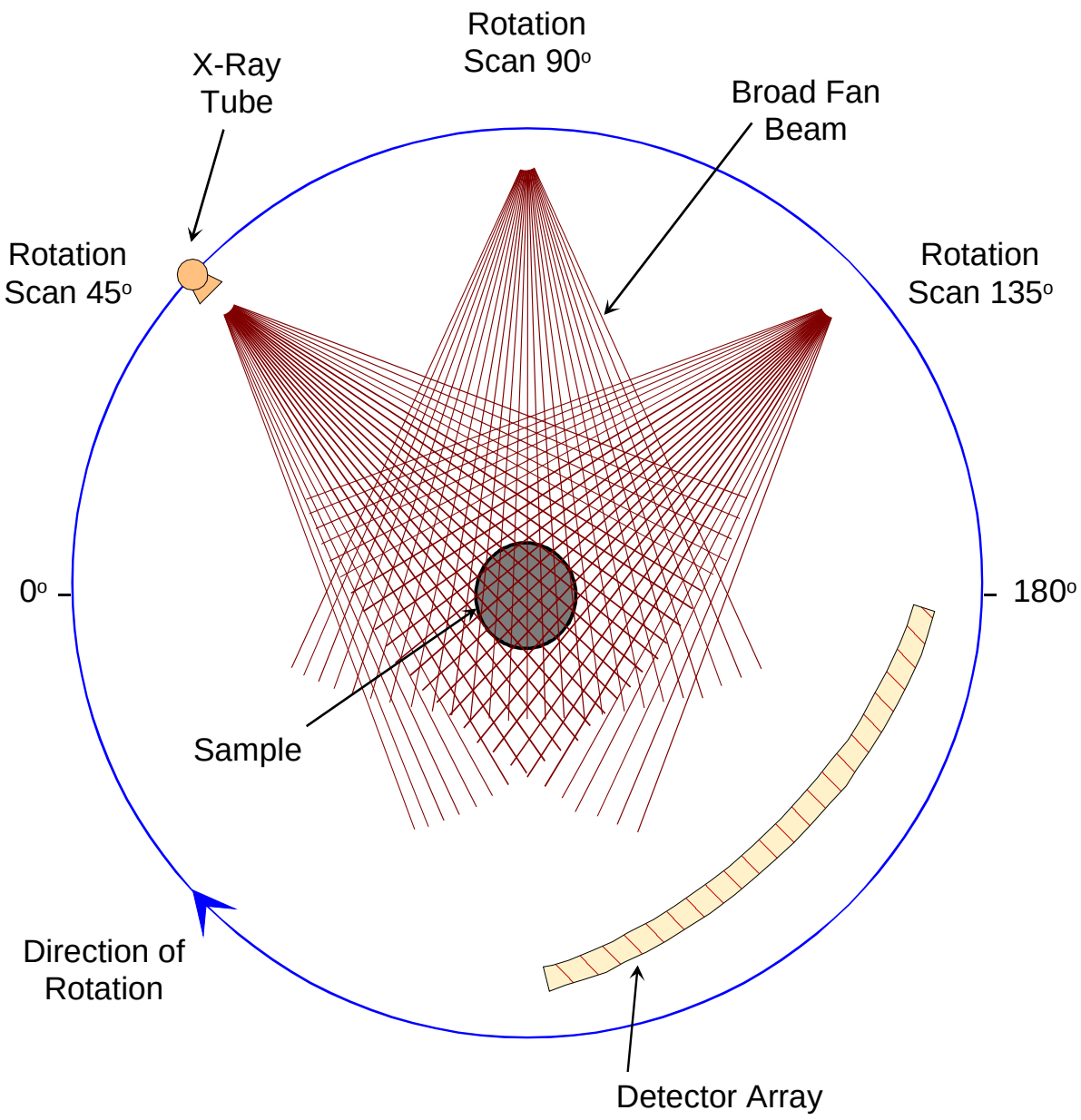

LIQUID PERMEABILITY SCHEMATIC

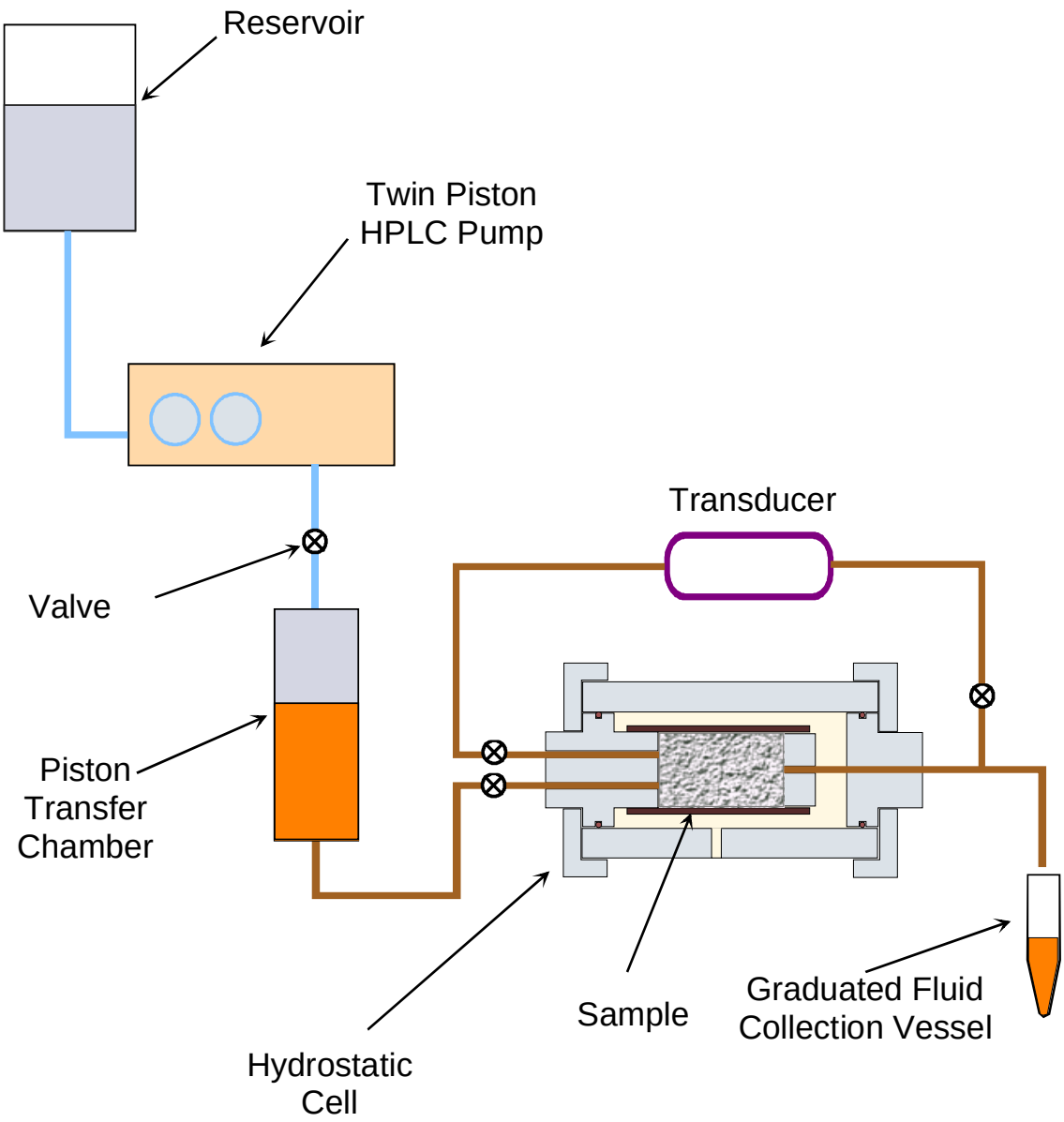

DEAN-STARK APPARATUS

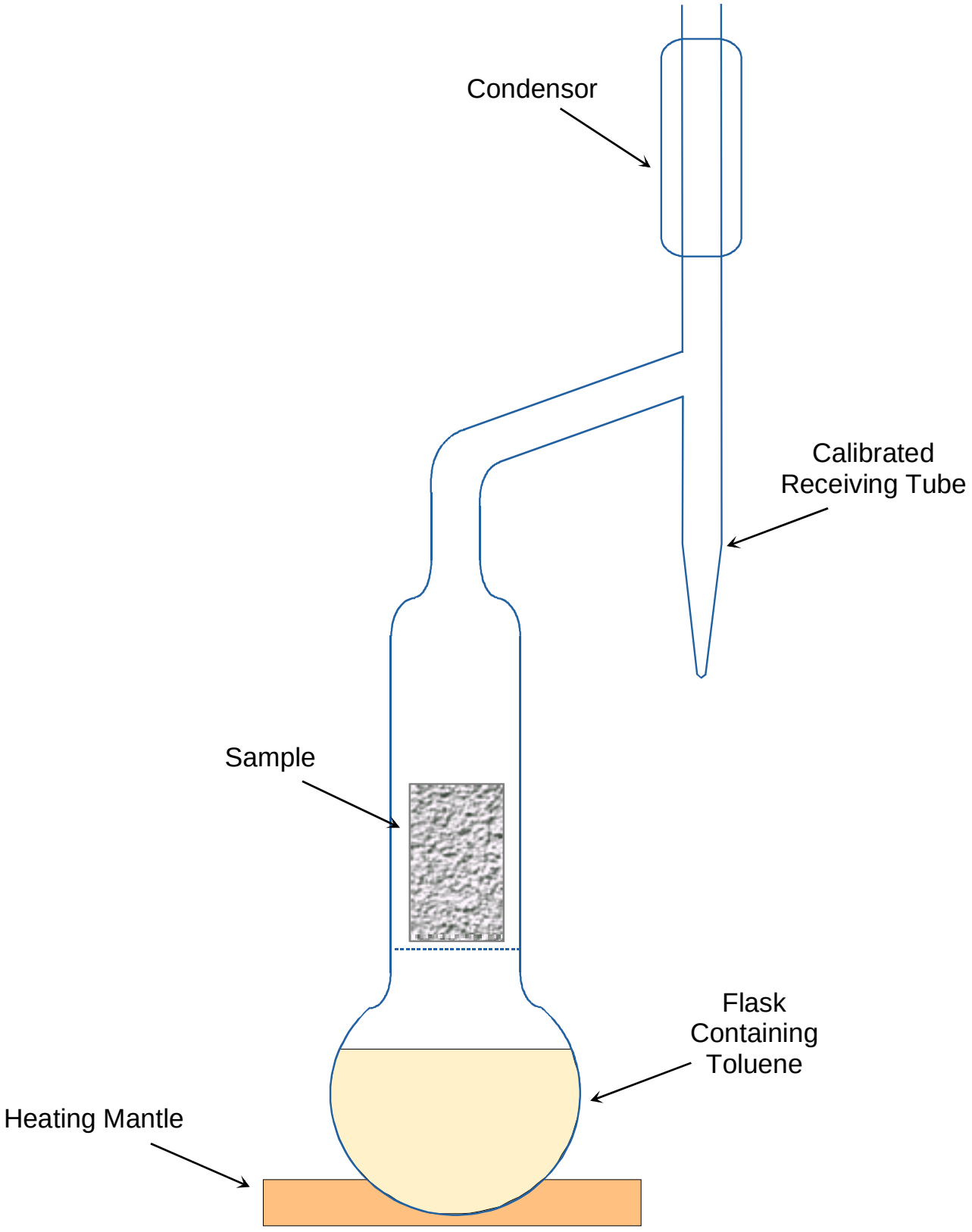

ACS Laboratories Pty Ltd
ABN: 81 008 273 005

APPENDIX III

ABBREVIATIONS

ABBREVIATIONS for CORE PROPERTIES

a	Intercept (assumed = 1)
A	Sample Cross Sectional Area (cm^2)
ABPc	Air-Brine Capillary Pressure
Amb	Ambient Conditions (No Overburden Pressure)
B	Equivalent Conductance of Clay Exchange Cations ($mho/m.cm^2.meq^{-1}$)
β	Beta Factor (ft^{-1})
BF	Basic Flood
BHN	Brinell Hardness Number (kg/mm^2)
BP	Barometric Pressure (atm)
CEC	Cation Exchange Capacity (meq/100g dry sample)
Cent	Centrifuge
Co	Conductivity of Fully Brine Saturated Sample (mho/m)
cP	Centipoise
Cw	Conductivity of Brine (mho/m)
Dr	Drainage (i.e. draining of the wetting fluid - usually brine)
Φ	Porosity
FF	Formation Factor
*FF**	Shaly Sand Equivalent Formation Factor
g	grams
HeInj	Helium Injection
HgInj	Mercury Injection Capillary Pressure
Imb	Imbibition (i.e. imbibition of the wetting fluid - usually brine)
K	Permeability (mD)
Ka	Air Permeability (mD)
Keg	Effective Permeability to Gas (mD)
Keo	Effective Permeability to Oil (mD)
Kew	Effective Permeability to Water (mD)
Kg	Gas Permeability (mD)
KgKo	Gas-Oil Relative Permeability

ACS Laboratories Pty Ltd
ABN: 81 008 273 005

ABBREVIATIONS for CORE PROPERTIES

KgKw	Gas-Water Relative Permeability
Klink or Kl	Klinkenberg Permeability (mD)
Ko	Oil Permeability (mD)
Krg	Relative Gas Permeability
Kro	Relative Oil Permeability
Krw	Relative Water Permeability
Kw	Brine Permeability (mD)
KwKo	Oil-Water Relative Permeability
L	Sample Length (cm)
m	Cementation Factor
*m**	Shaly Sand Equivalent Cementation Factor
mD	milliDarcy's
n	Saturation Exponent
*n**	Shaly Sand Equivalent Saturation Exponent
OB	Overburden Pressure (psig)
OBPc	Oil-Brine Capillary Pressure
P	Pressure (psi)
Pc	Capillary Pressure (psig)
PP	Porous Plate
PvComp	Pore Volume Compressibility
PVR	Pore Volume Reduction (cm^3)
ρ	Density (g/cm^3)
q	Flow Rate (cm^3/s)
θ	Contact Angle (degrees)
Qv	Volume Concentration of Clay Exchange Cations (meq/cm^3)
r	Radius (cm)
Rc	Sample Resistance (ohm)
RCA	Routine Core Analysis

ABBREVIATIONS for CORE PROPERTIES

ResCon	Reservoir Conditions
RI	Resistivity Index
RICP	Resistivity Index & Capillary Pressure
Ro	Resistivity of Fully Brine Saturated Sample (ohm.m)
Rt	Resistivity of Partially Saturated Sample (ohm.m)
Rw	Resistivity of Brine (ohm.m)
S	Saturation
s	Seconds
SCA	Special Core Analysis
Sg	Gas Saturation
Sgr	Residual Gas Saturation
SngPt	Single Point
So	Oil Saturation
Sor	Irreducible Oil Saturation (or Residual Oil Saturation)
SS	Steady State
Sw	Brine Saturation
Swi	Initial Water Saturation
Swir	Irreducible Water Saturation
Swr	Residual Water Saturation
T	Temperature (^{o}C)
USS	Unsteady State
μ	Viscosity (cP)
Vb	Bulk Volume (cm^3)
Vg	Grain Volume (cm^3)
Vp	Pore Volume (cm^3)
ω	Angular Velocity (rad/s)
Wett	Wettability
Wt	Weight (g)

CT SCAN REPORT

of

YOLLA-4

for

ORIGIN ENERGY RESOURCES LIMITED

by

ACS LABORATORIES PTY LTD

30 August, 2004

Origin Energy Resources Limited
Level 6
1 King William Street
ADELAIDE SA 5000

Attention: Joe Parver

Origin Energy Resources Limited
GPO Box 148
BRISBANE QLD 4001

Attention: Andy Hall

CT SCAN REPORT: 0475-08

MATERIAL: Core Plugs

LOCALITY: Yolla-4

WORK REQUIRED: CT Scanning

Please direct technical enquiries regarding this work to the signatories below under whose supervision the work was carried out.

KEVIN H FLYNN
General Manager

CONTENTS

CHAPTERS **PAGE**

APPENDICES

CHAPTER 1

INTRODUCTION

1. INTRODUCTION

This report presents images of plugs selected for analyses as part of Origin Energy Resources Limited Yolla-4 special core analysis study. CT scanning images have been digitally superimposed onto single pages (for easier comparison) in Chapter 3 of this report.

CHAPTER 2

CT SCANNING PROCEDURE

2. CT SCANNING PROCEDURE

CT Scanning was undertaken in order that internal inhomogeneities and/or drilling fluid invasion zones may be noted. Typical inhomogeneities may be clasts, bedding sedimentary structures, cementation, fractures and any other discontinuities that may not be readily visible to the naked eye.

The principle of CT Scanning and its applications is presented by Hove et al, 1987 and Wellington and Vinegar, 1987.

CT Scanners generate cross-sectional image slices through the sample by revolving an X-ray tube around the sample and obtaining projections at many different angles (Appendix I). From these image slices, a cross-sectional image was reconstructed by a back projection algorithm in the scanner's computer.

As the samples were frozen at time of scanning we were unable to place orientation lines on the plugs. The sample was placed vertically within the scanner and a longitudinal section image obtained. The sample was then rotated through exactly 90^{o} and another section image recorded. These two images are labelled '0' and '90' on the prints.

CHAPTER 3

CT SCANNING IMAGES

Yolla-4
C.T. Scans

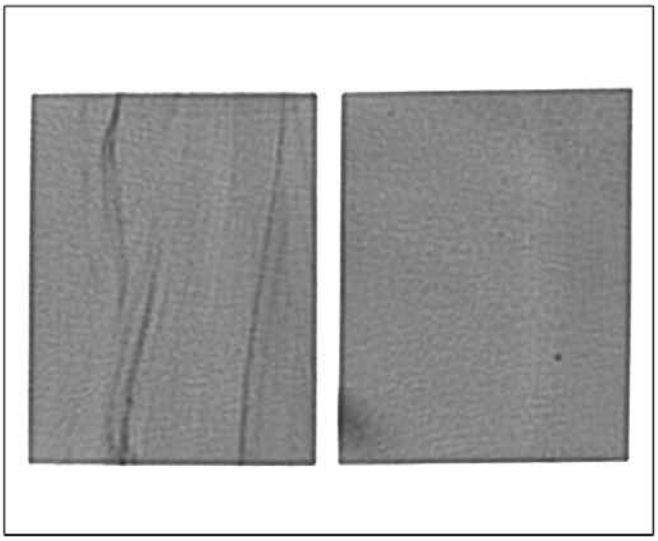

Sample No:	19
Depth:	2898.45 m
Permeability:	11.7 mD
Porosity:	16.0 %

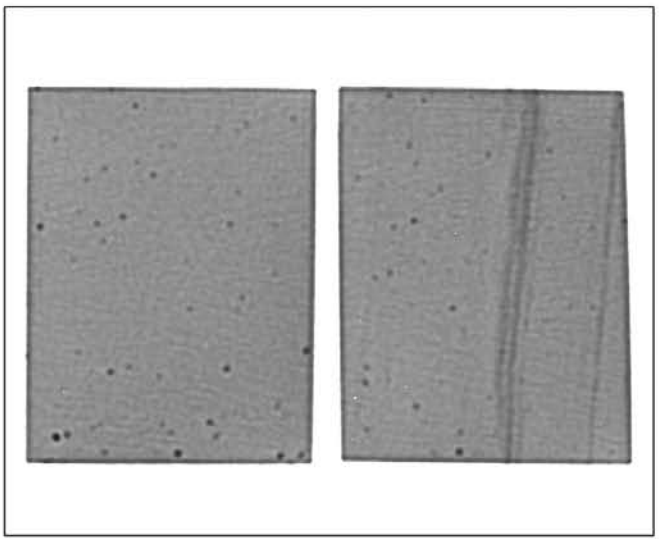

Sample No:	29
Depth:	2901.32 m
Permeability:	35.9 mD
Porosity:	17.7 %

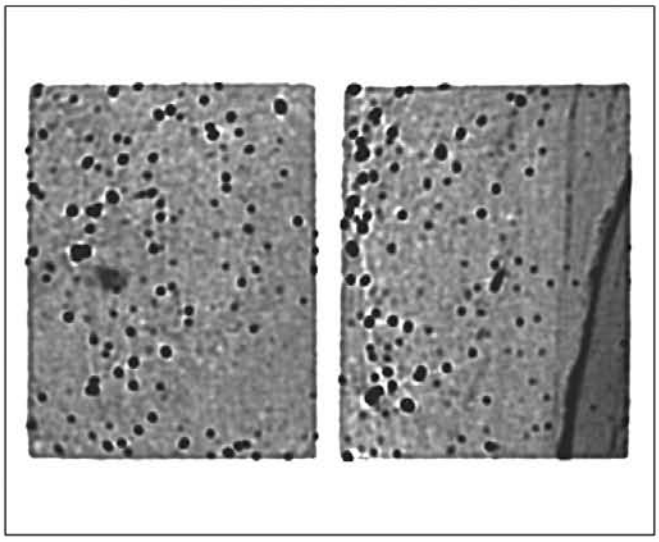

Sample No:	34
Depth:	2902.49 m
Permeability:	1105 mD
Porosity:	20.9 %

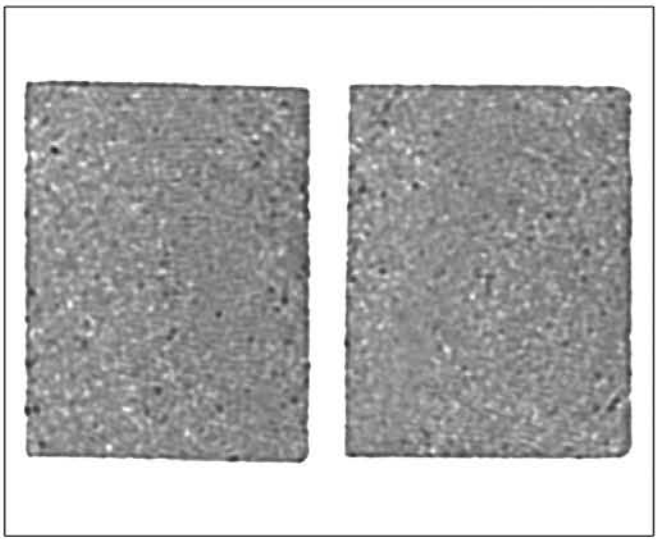

Sample No.:	37
Depth:	2903.41 m
Permeability:	2723 mD
Porosity:	22.4 %

Yolla-4
C.T. Scans

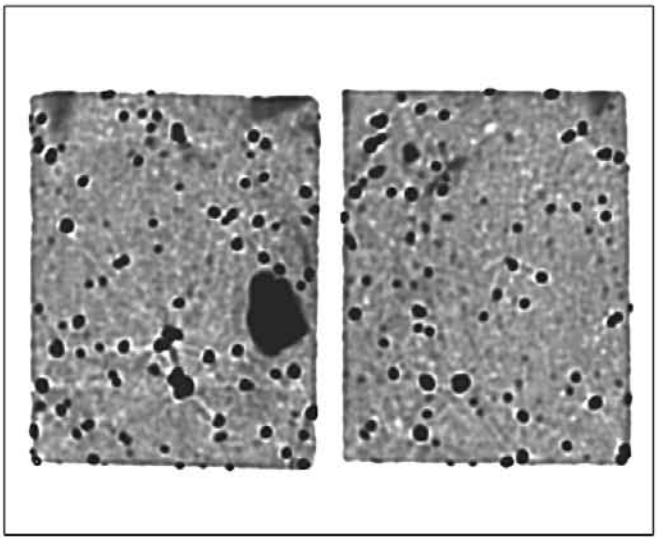

Sample No:	39
Depth:	2903.92 m
Permeability:	1676 mD
Porosity:	21.0 %

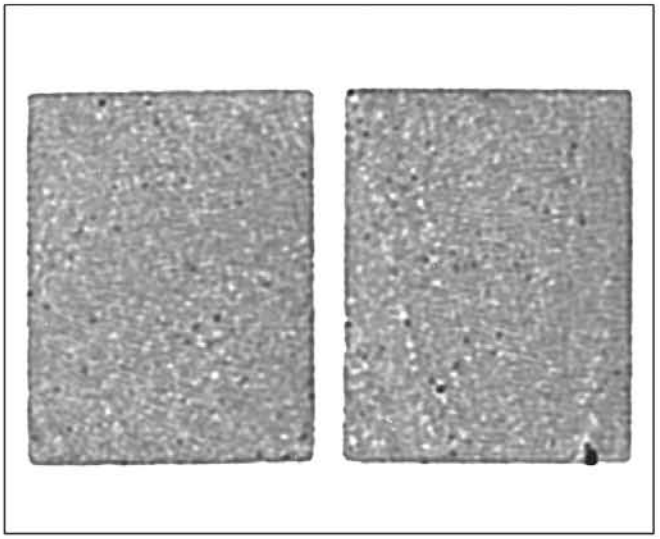

Sample No:	43
Depth:	2904.98 m
Permeability:	3110 mD
Porosity:	23.0 %

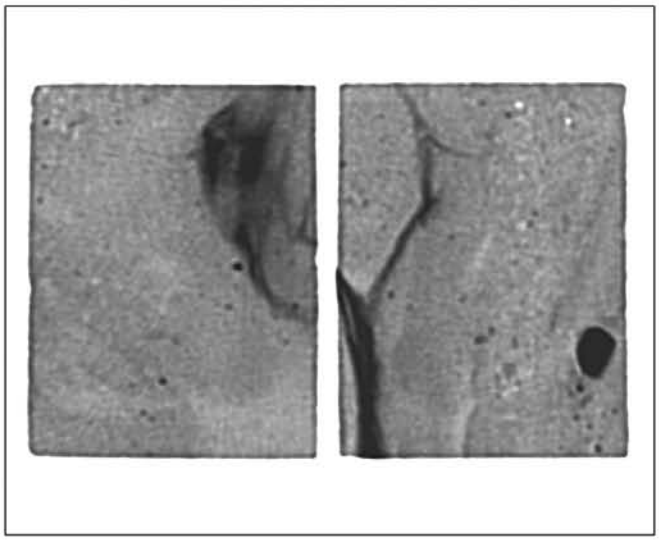

Sample No:	44
Depth:	2905.17 m
Permeability:	123 mD
Porosity:	17.0 %

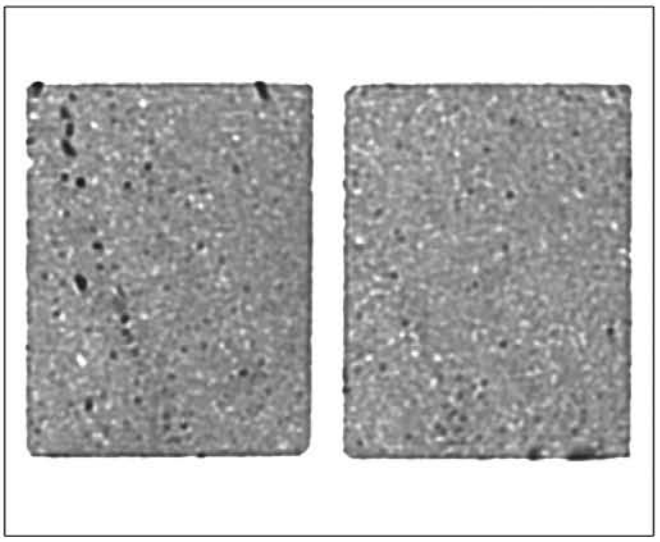

Sample No.:	47
Depth:	2906.08 m
Permeability:	4616 mD
Porosity:	22.6 %

Yolla-4
C.T. Scans

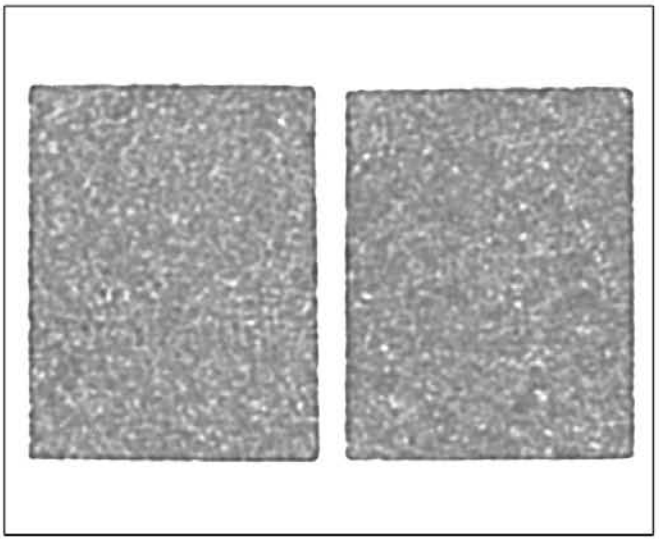

Sample No:	70
Depth:	2959.50 m
Permeability:	1169 mD
Porosity:	21.6 %

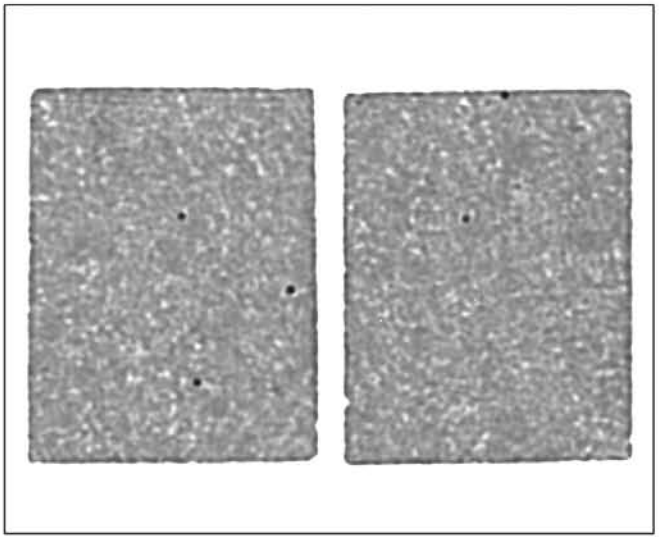

Sample No:	71
Depth:	2959.81 m
Permeability:	790 mD
Porosity:	21.0 %

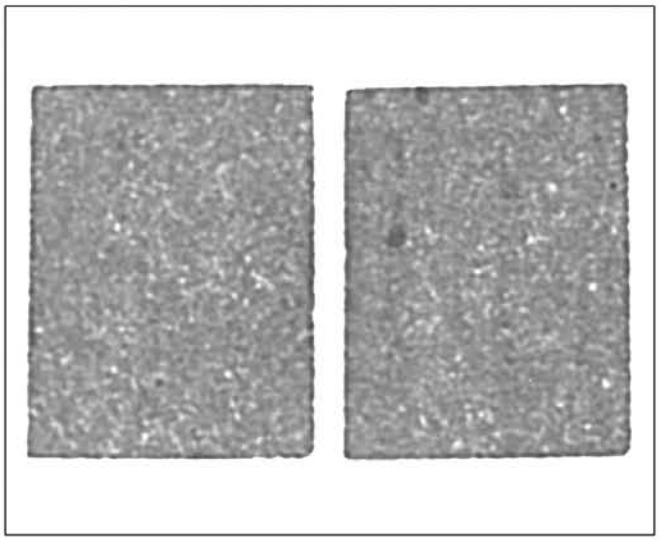

Sample No:	75
Depth:	2960.95 m
Permeability:	440 mD
Porosity:	19.2 %

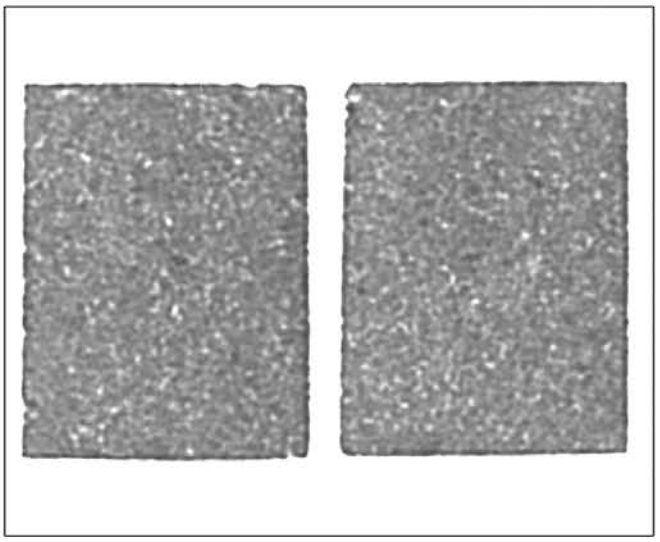

Sample No.:	78
Depth:	2961.87 m
Permeability:	743 mD
Porosity:	20.6 %

Yolla-4
C.T. Scans

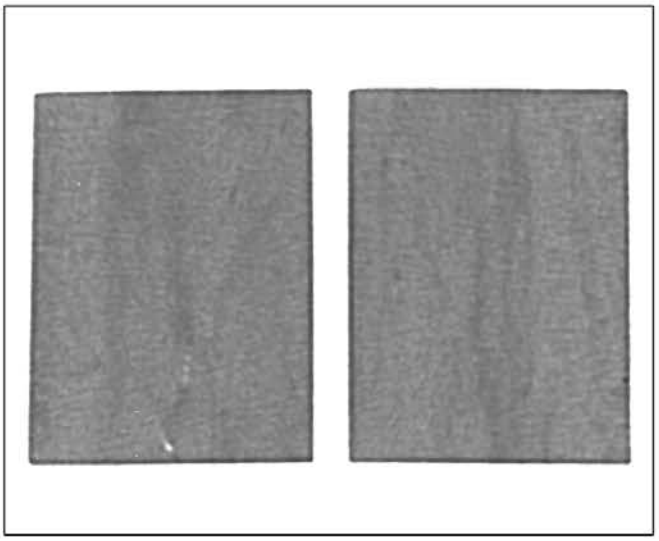

Sample No:	82
Depth:	2963.06 m
Permeability:	24.7 mD
Porosity:	15.5 %

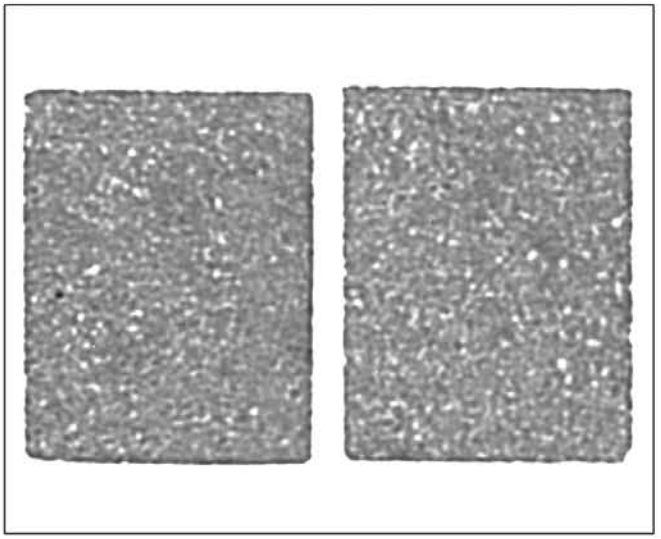

Sample No:	85
Depth:	2963.93 m
Permeability:	499 mD
Porosity:	19.8 %

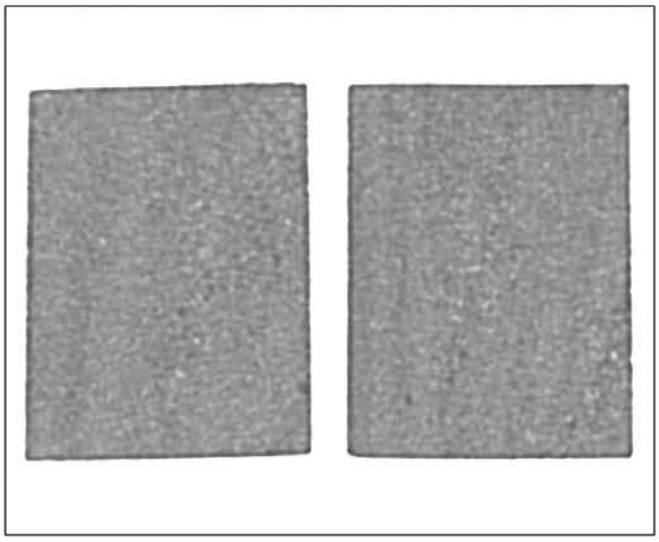

Sample No:	98
Depth:	2967.87 m
Permeability:	183 mD
Porosity:	19.4 %

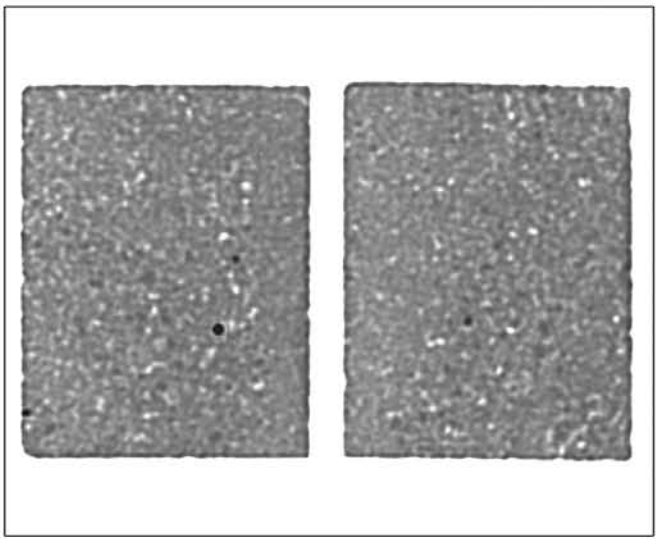

Sample No.:	115
Depth:	2972.75 m
Permeability:	649 mD
Porosity:	18.7 %

Yolla-4
C.T. Scans

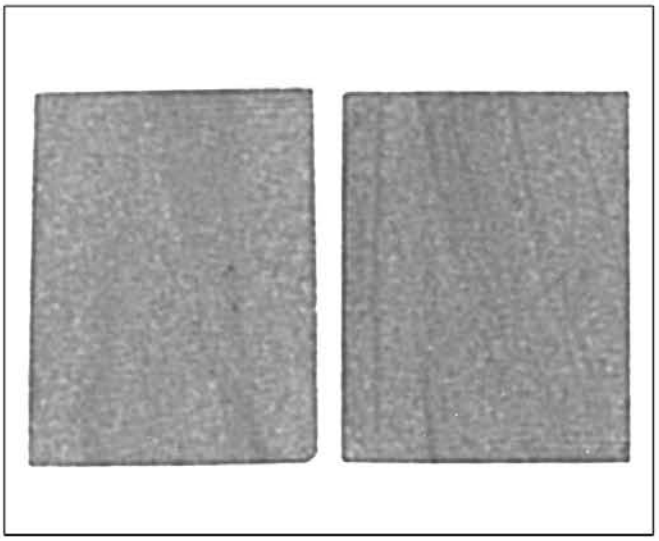

Sample No:	117
Depth:	2973.35 m
Permeability:	299 mD
Porosity:	19.2 %

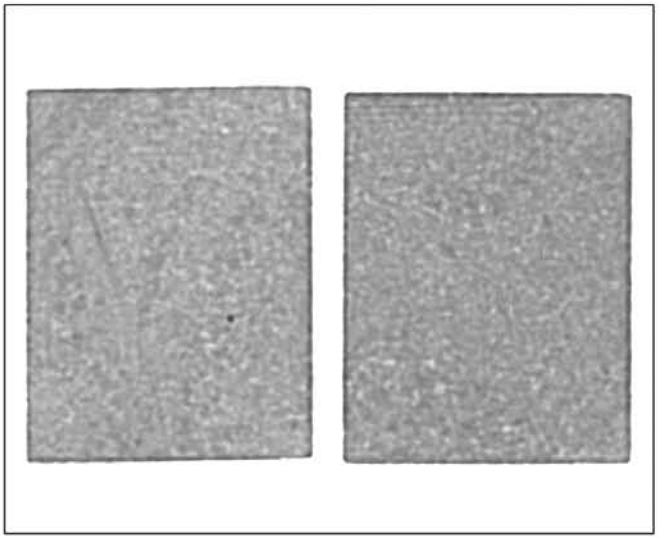

Sample No:	120
Depth:	2974.25 m
Permeability:	904 mD
Porosity:	21.7 %

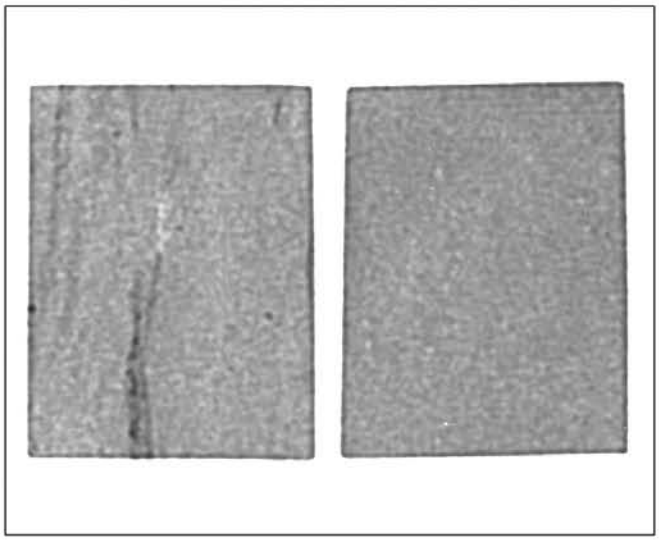

Sample No:	121
Depth:	2974.57 m
Permeability:	209 mD
Porosity:	19.7 %

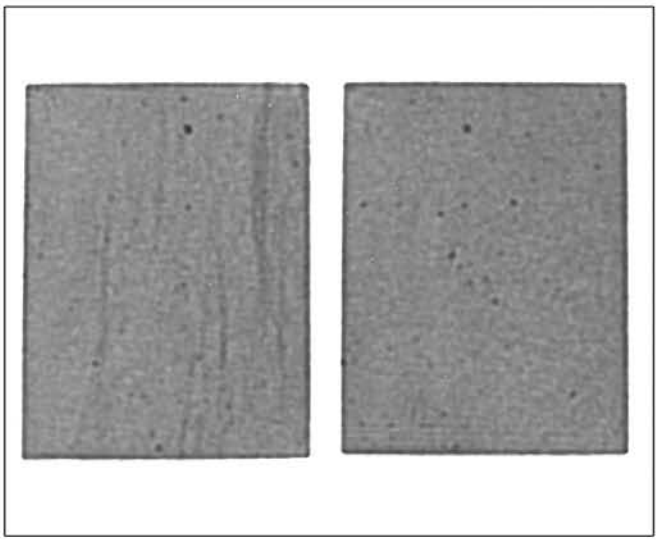

Sample No.:	132
Depth:	2978.26 m
Permeability:	49.5 mD
Porosity:	17.1 %

Yolla-4
C.T. Scans

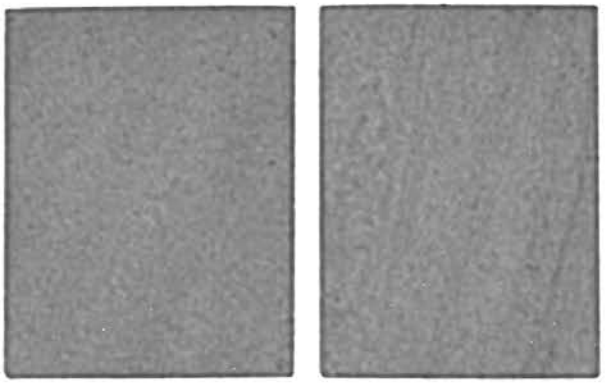

Sample No:	135
Depth:	2979.15 m
Permeability:	75.3 mD
Porosity:	17.6 %

APPENDIX 1

CT SCANNER SCHEMATIC

CT SCANNER SCHEMATIC

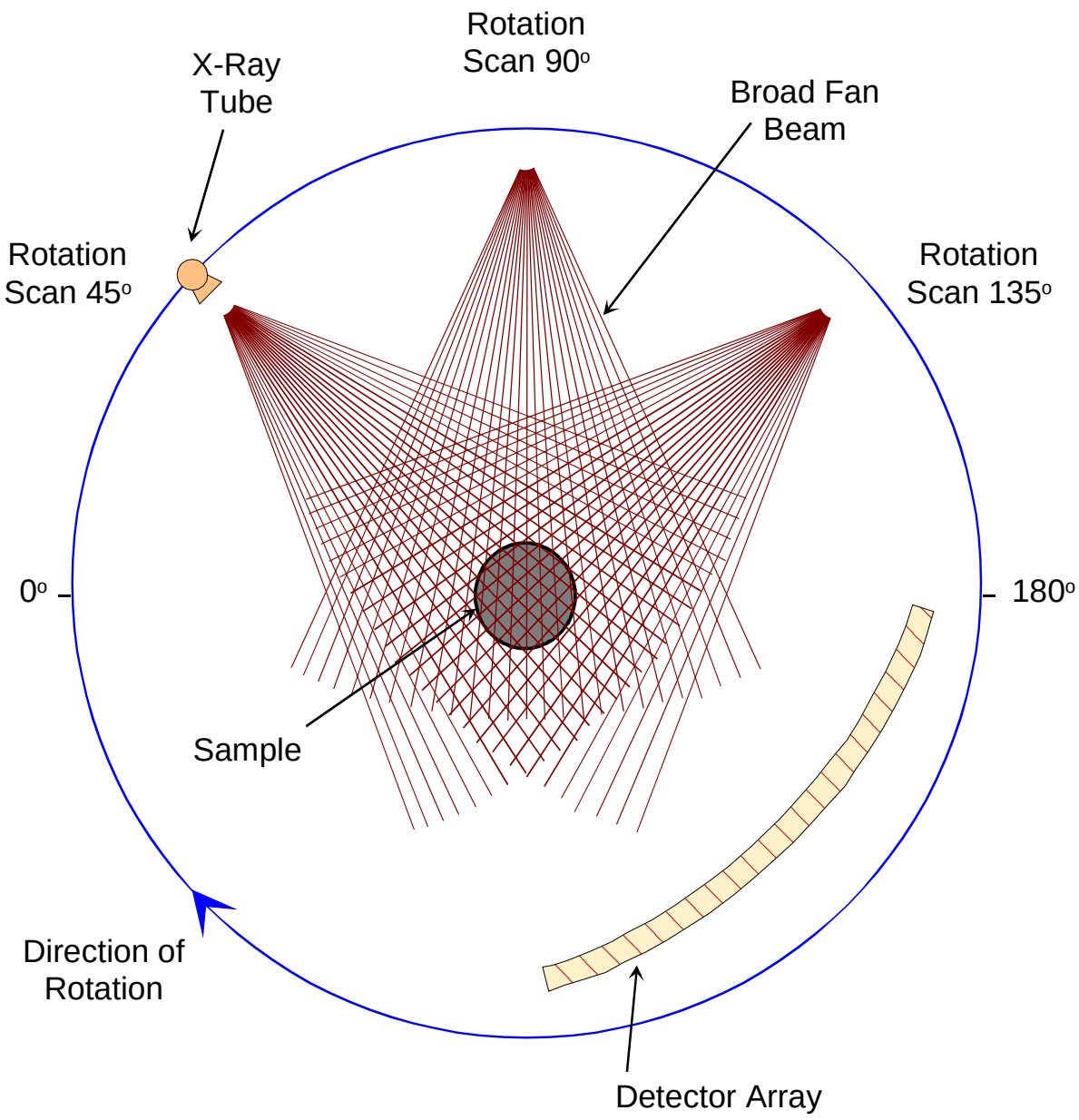

APPENDIX 10: FMI INTERPRETATION REPORT

Origin energy

delivering the goods

Yolla 4

Formation Micro-Imager (FMI) Interpretation Report

T/L1
BASS BASIN

December 2004

SUMMARY

This report presents processed and interpreted FMI images from the intervals, 2550 – 2600 m, 2890 - 3030 m and 3110 – 3180 m within Yolla 4. The studied succession within Yolla 4 is of Palaeocene-Eocene age, and is characterised by low structural dips, typically in the range 3º-5º, as is listed below.

Structural Zone	Depth Interval	Tectonic Tilt	Comments
2550 – 2600 m			
Zone I	2550 – 2557	8.4°/235°	Fracture or fault bound at 2557 m
Zone II	2557 – 2560	9.8°/316°	Fracture or fault bound at 2560 m
Zone III	2560 – 2566	6.5°/205°	Fracture or fault bound at 2566 m
Zone IV	2566 - 2570	11.7°/318°	Fracture or fault bound at 2570 m
Zone V	2570 – 2600	5.8°/239°	
2890 – 3030 m			
Zone I	2890 - 2955	5.3°/081°	Fracture or fault bound at 2955 m
Zone II	2955 - 3030	5.0°/318°	
3110 - 3180			
Zone I	3110 - 3139	2.5°/321°	Change in mudstone dip overlying sandstone 3139 m
Zone II	3139 – 3171	3.8°/256°	Change in mudstone dip 3171 m
Zone III	3171 - 3180	3.2°/305°	

Lithofacies identified from FMI images have been calibrated with cuttings descriptions, and with cored intervals in Yolla 4. Cuttings descriptions match well with lithofacies interpretations derived using wireline log response and FMI image fabrics, and indicate a succession comprising sandstone and mudstone with minor coal. The FMI lithofacies interpretations compare closely with core observations for sampled lithologies, and identify sandstones, mudstones, heterolithic intervals (comprising dm scale intercalations of sandstone, siltstone and mudstone) and thin coals. Six lithofacies associations have been identified within the studied section. These are interpreted as having been deposited in a marginal marine / lacustrine (shelf-shoreface?) or fan deltaic setting (prodelta and sub-aqueous shoal water type delta front), and alluvial fans; this setting comprises transverse drainage produced by active faulting within a half-graben. The lithofacies associations identified are summarised as follows:

I. Mudstones that occur at the base of upward coarsening facies successions. (interpreted as either prodeltaic muds, or shelf-shoreface deposits)
II. Heterolithic intercalations of sandstone siltstone and mudstone, typically occurring within the lower-mid parts of upward coarsening facies successions (interpreted as either distal fan delta, or shelf-shoreface deposits).
III. Stratified sandstones with mottled image fabric and low angle (typically <5º) internal bedding surfaces, typically occurring towards the top of upward coarsening facies successions (shoreface deposits).
IV. Successions (often erosively based) of stratified sandstones and pebbly sandstones with dominant internal bedding fabrics inclined at angles <10°, rare intervals of up to 25° (distal sheetflood deposits with shallow incised channels).
V. Thin mudstone- heterolithic successions interbedded with lithofacies association IV (possible interdistributary bay / lagoon fill, coastal plain deposits).
VI. Coals (deposits of swampy coastal plain environments).

Sandstones of Lithofacies Association IV are likely to form the main reservoir intervals. Lithofacies Association III may form a secondary reservoir interval and typically have over an order of magnitude less permeability than the sheetflood deposits.

Palaeotransport analyses of sandstones from Lithofacies Association III reveals them to be characterised by internal stratification fabrics with very wide ranging sedimentary dip azimuth, suggesting they were originally deposited as "flat lying' strata. Few palaeotransport interpretations can be made for these sandstones. However, in some examples, a dominant sedimentary dip is present, and may represent onshore migration of fair weather wave formed structures whereas the minor flow direction may represent offshore flow during storm events. In most cases, this can broadly be interpreted to have had NE – SE onshore direction and a NW – SW offshore direction.

Palaeotransport analyses of sandstones from Lithofacies Association IV reveals them to be characterised by low angle internal stratification fabrics with variable azimuth. The relationship between intra-set flat lamination, intra-set lamination and coset boundaries suggest that sediment transport occurred normal to the depositional dip i.e. bedforms migrated down fan. Interpreted fan slope drainage directions are variable and no consistent drainage direction can be inferred.

TABLE OF CONTENTS

LIST OF TABLES

LIST OF FIGURES

LIST OF ENCLOSURES

		Scale
Enclosure 1	Quality control plot of FMI log, 2550 – 2600 m	1:250
Enclosure 2	Quality control plot of FMI log, 2885 – 3190 m	1:500
Enclosure 3	Overview structural summary log, 2550 – 2600 m	1:250
Enclosure 4	Overview structural summary log, 2890 – 3190 m	1:500
Enclosure 5	Data overview plot, 2550 – 2600 m	1:200
Enclosure 6	Data overview plot, 2890 – 3180 m	1:200
Enclosure 7	Sedimentological summary plot, 2890 – 2920 m	1:100
Enclosure 8	Sedimentological summary plot, 2960 – 3030 m	1:100
Enclosure 9	Sedimentological summary plot, 3115 – 3170 m	1:100
Enclosure 10	Core composite plot, 2895 – 2930 m	1:20
Enclosure 11	Core composite plot, 2960 – 3000 m	1:20

INTRODUCTION

The processing and interpretation of the Formation Micro-Imager (FMI) images from Yolla 4 are documented in this report. The detailed sedimentological report is based on FMI images for the intervals 2550 – 2600 m, 2890 – 3030 m and 3110 – 3180 m.

Objectives

The well details and project objectives for Yolla 4 are summarised in Table 1 with the data that was incorporated into this study.

Table 1. Summary of well details, study objectives and the data set used for this analysis.

Well Details	
Well: Surface Latitude: Surface Longitude: Intervals of interest:	Yolla 4 39° 50' 40.592" S 145° 49' 06.0569" E Palaeocene – Eocene succession interpreted as marginal marine/lacustrine – alluvial environment.
Summary of study objectives	
Log Depth Intervals	Objectives
2550 – 2600 m 2890 – 3030 m 3110 – 3180 m	Processing of FMI images to provide speed corrected false colour images. QC of images to determine the quantity of information that is interpretable.
2550 – 2600 m 2890 – 3030 m 3110 – 3180 m	Summary structural overview using automatic dip calculations, supplemented by manual dip-picking.
2550 – 2600 m 2890 – 3030 m 3110 – 3180 m	Overview sedimentological interpretation of features evident within FMI images with the aim of focusing upon variations in palaeocurrent transport directions. This required the manual characterisation of dip features and their interpretation over these intervals.
2550 – 2600 m 2890 – 3030 m 3110 – 3180 m	Detailed sedimentological interpretation and lithofacies characterisation.
Data incorporated in study	
2550 – 2600 m 2890 – 3030 m 3110 – 3180 m	Open hole logs from Platform Express suite. Raw FMI data in DLIS format.
2898.1 – 2925.6 m	Core 1 (2892.05 – 2919.6 m Drillers depth)
2962.3 – 2989.7 m	Core 2 (2962.3 – 2989.7 m Drillers depth)
2550 – 2600 m 2890 – 3030 m 3110 – 3180 m	Cuttings description

Depth and directional references

Unless otherwise mentioned, all depths in this report reference log depths. Orientation data is referenced using the standard convention of dip/dip azimuth. For example, 3°/313° indicates a dip of 3° (measured from the horizontal) towards 313° (referenced clockwise from north). Borehole orientation data follows a convention of deviation/azimuth of deviation. For example, 2°/300° indicates an 2° deviation from the vertical towards 300° (SW).

PROCESSING AND QUALITY CONTROL

The Formation Micro-Imager (FMI) tool was run by Schlumberger on 14th July 2004 in the 8½ inch section of Yolla 4 over the interval 2333 – 3250 m.

The Schlumberger Formation Micro-Imager tool is a pad based micro-resistivity imaging device, with an array of 24 measuring electrodes (buttons) on each of pad and flap, with 192 buttons in total. Flaps are offset vertically from the pads by approximately 6 inches. The electrodes are 0.2 inch in diameter and data is sampled at 0.1 inch vertically and horizontally with a bedding resolution of approximately 1 cm. The data is processed to provide 75% coverage of the borehole wall in an 8.5 inch hole. This data also provides 12 Stratigraphical High Resolution Dipmeter (SHDT) tool curves for standard dipmeter processing.

Processing was carried out over the logged interval using Terrasciences TerraStation Formation Viewer module.

The mud system was sea water/Drispac/Soltex with a resistivity range of 0.181 – 0.197 Ωm, a viscosity of 70 S and a density of 9.35 lbm/gal. The fluid losses encountered during drilling were minimal. The borehole reached a maximum temperature of 133°C.

An FMI log quality control plots are shown in Enclosures 1 and 2. These plots provide detailed information concerning hole orientation, tool orientation, hole condition and FMI operating parameters.

Borehole conditions

FMI image quality is related to borehole condition, which is good throughout the section in Yolla 4 with clear geological detail visible and only minor image artefacts. Borehole deviation is 23.6°/201.5° at 2547 m and 24.7/202.2 at 2611.5 m, 23.2/199.3 at 2842.9 m, 12.3/197.2 at 3077 m, 9.8/198.9 at 3105.9 m and 7.2/194.7 at 3193 m.

A summary of hole conditions is included in Table 2.

Within the uppermost study interval (2550 – 2600 m) the HCAL shows that the hole is consistently in gauge until approximately 2590 m where there is breakout in both the C1 and C2 calipers of up to 15 inches associated with a coal seam. Within the 2890 – 3030 m interval there is consistent but minor ovalisation (up to 1 inch) in the direction of the C2 calliper. This breakout is more severe in the mudstone intervals whereas the hole is in gauge in porous sandstones. In the lower interval (3110 – 3180 m) there is consistent minor ovalisation of the hole toward the C2 calliper. In all cases the breakout is aligned in an approximate east – west orientation, which may reflect the orientation of the minimum horizontal stress.

Table 2. Summary of hole conditions through the study intervals in Yolla 4

Normal Hole Size	Interval Depth	Comments
2550 – 2600 m		
8.5	2550 - 2591	In gauge
	2591 – 2600	Up to 15" overgauge in C1 & C2
2890 – 3030 m		
8.5	2890 – 2896	1" overgauge
	2896 – 2903	0.5" overgauge
	2903 – 2912	In gauge
	2912 – 2925	0.5" overgauge
	2925 – 2942	1" overgauge
	2942 – 2950	0.5" overgauge
	2950 – 2960	1" overgauge
	2960 – 3030	0.5" overgauge
3110 – 3180 m		
8.5	3110 – 3180	0.5" overgauge

Data processing

Speed correction

The accelerometer speed correction utility corrects FMI micro-resistivity data for minor variations in recording velocity induced by tool or cable friction. Extremes in velocity variation may occur when the tool is either stationary or rapidly accelerating as a result of being stuck or the logging being stopped for pipe removal. The most important parameter for the speed correction procedure is the zero-sum window, which prevents cumulative build-up of erroneous shifts within a window. Thus all shifts applied by the speed correction should add up to zero within a certain window length. The length of this window is decided by experimenting and the general roughness of the logging run. In the case of Yolla-2, a window of 4 ft was chosen. The speed correction shift curve is calculated by double integration of the Z-accelerometer curve with the cable speed representing the window constant. The resulting shift curve is then applied to synchronously to all curves in the log.

Image processing

Before generating the false-colour images from the speed corrected data, the individual curves are transferred back to their physical depth referenced positions. The images are produced with two types of resistivity scaling:

- *Static normalised* images have the same relative resistivity scaling over larger intervals and therefore illustrate large-scale resistivity variations related to lithology and phase changes. Dependent on Emex current variability.

- *Dynamic normalised* images were scaled within a 0.5 m sliding window, thereby maximising the expression of more detailed rock fabrics (and noise).

In this study, the dynamic normalised images were used primarily for bedding, lithofacies and structure identification. Image polarity was correctly matched to openhole resistivity logs.

Block depth shifts

No block depth shifts were applied to the Yolla 4 data.

Dip processing

Two types of dip computation were conducted on the Yolla 4 dataset.

Computed dip correlations were carried out on the SHDT curve sub-set from the loaded interval (Enclosures 1 - 2). These correlations use refined least-squares algorithms with regression coefficients cut-offs for each correlation pair. The interval computation parameters were aimed at correlating bedding features using pad-to-pad (PTP) algorithms with the following parameters:

- 60 cm correlation interval, 50 cm step distance and a 70° search angle (referenced to borehole axis) and the cut-off set at 0.2 for individual curve pairs.

This computation also included stacking of three consecutive correlation surfaces. The stacking of dips in this way tends to smooth dip patterns and trends and is a viable method of "quick-look" identification of structural dip. These parameters are referenced as "4X2X70ST3" in Enclosure 1 and 2. Detailed interpretation of dip patterns should not be carried out on results from this processing.

Manual dips were computed directly from the images using the TerraStation Formation Viewer (e.g. Enclosures 3-4). The major advantage of the manual dip technique is that each feature may then be classified into a geological category and that only the results in which the interpreter has confidence are used for further interpretation. A further advantage of manual dip picking is the ability to measure and orientate discordant surfaces such as fractures and faults, which are unlikely to be correlated by standard interval correlation techniques

SEDIMENTOLOGICAL ANALYSIS

Tectonic tilt determination

Prior to detailed sedimentary analyses, it is first required to evaluate structural dip, so that the sedimentary surfaces identified in FMI images can be restored to their original orientation or "sedimentary dip". Structural dip (or tectonic tilt) is the attitude of formations resulting solely from tectonic movements. Structural dip is best determined from beds that were originally deposited as horizontally stratified deposits. These beds can include mudstones, or parallel stratified laminations within heterolithic successions comprising interbedded sandstone-mudstone laminae. The structural dip interpretation within well Yolla-4 was an iterative process involving:

- Initial evaluation of automatic computed dips to identify general data trends.
- Manual picking of shale bed dips to confirm tectonic tilt throughout the studied succession.

Tectonic tilt evaluated on the basis of dip data through shale intervals is summarised in Table 3. Before undertaking a sedimentological interpretation structural dip was removed from the "manual" data set. The structural dip was removed following identification of intervals of strata (structural zones) of consistent structural dip. The structural dips are summarised in Enclosures 3 and 4.

Table 3. Tectonic tilt summary of Yolla 4.

Structural Zone	Depth Interval	Tectonic Tilt	Comments
2550 – 2600 m			
Zone I	2550 – 2558	8.3°/239°	Fracture or fault bound at 2558 m
Zone II	2558 – 2561	10.2°/310°	Fracture or fault bound at 2561 m
Zone III	2561 – 2567	6.3°/207°	Fracture or fault bound at 2567 m
Zone IV	2567 - 2571	16.3°/309°	Fracture or fault bound at 2571 m
Zone V	2571 – 2600	5.2°/237°	
2890 – 3030 m			
Zone I	2890 - 2955	5.3°/081°	Fracture or fault bound at 2955 m
Zone II	2955 - 3030	5.0°/318°	
3110 - 3180			
Zone I	3110 - 3139	2.5°/321°	Change in mudstone dip overlying sandstone 3139 m
Zone II	3139 – 3171	3.8°/256°	Change in mudstone dip 3171 m
Zone III	3171 - 3180	3.2°/305°	

Cumulative dip azimuth plots for mudstone bedding surfaces within the studied intervals (2550 – 2600 m, 2890 – 3030 m and 3110 – 3180 m) from Yolla 4 are presented in Figures 1 and 2 respectively. These plots clearly illustrate the structural subdivisions proposed for this well.

Classification of sedimentary features

Classification of sedimentary surfaces recognised from borehole image logs is a 3 stage iterative process involving:

- First pass dip picking. This phase of feature identification is carried out in conjunction with examination of wireline logs, and results in a simple 2-fold sub-division of dip features into mudstone and "others".
- Structural dip is removed from the data set using a workstation based stereographic technique to provide sedimentary dips.
- Sedimentary dips are re-classified in the workstation environment. Wireline logs are used to drive lithofacies interpretation. Sedimentary dips within sandstone lithologies are characterised using a hierarchical scheme depending upon their dip and orientation.

The hierarchical scheme applied to Yolla 4 is illustrated in Figure 3 and Table 4 below, and sedimentary dips for the studied intervals 2890 - 3030 m and 3110 - 3180 m are indicated in Enclosures 7 – 9.

Table 4. Classification of surfaces identified from FMI images.

Dip type	Interpreted dip category	Colour	Description
LB	Lithological boundary	Blue green	Low true dip angle surfaces which define a marked resistivity between overlying and underlying beds. Wireline logs indicate a lithological contrast.
LBe	Erosional lithological boundary	Dark green	Erosive surfaces which define a marked resistivity between overlying and underlying beds. Truncation of bedding fabrics beneath the surface may be evident. Wireline logs indicate a lithological contrast.
LBc	Cemented lithological boundary	Pale blue green	Sharply defined highly resistive or conductive bed. Bounding surfaces may define planar or "nodular" features. Normally associated with change in wireline log response.
ISS	Intra set surface	Yellow	Inclined surfaces typically dipping at a true dip angle greater than 5°. Surfaces may be inclined at angles up to 25°-30° (i.e. close to angle of repose), and occur within distinct groups of similar orientation. Surfaces typically show cm-dm scale spacing in borehole image logs. They are discordant to set (or bed) and coset boundaries.
SB	Set (bed) boundary	Brown	Surfaces within sandstone lithologies which are typically (though not exclusively) inclined at sedimentary dip of < 15°. Set boundaries define a group or "set" of intraset surfaces of similar orientation. The set boundary is distinguished from the intraset surfaces by its different orientation. Set boundaries typically occur at dm - m scale spacing in borehole image logs.
CSB	Coset boundary	Cyan	A surface separating a group of sets of similar orientation. Note: Coset boundaries may also define a single bed or set displaying a significantly different internal fabric to those sets surrounding it. Set boundaries are typically identified at m scale spacing in borehole image logs. Note: Coset boundaries may also define a single bed or set at dm scale which displays a significantly different internal fabric to those sets surrounding it.
ISSf	Flat/horizontal	Purple	Near horizontal intraset surfaces with true dip angle (<5°), characterised by resistivity contrast several cm thick. Sedimentary dip azimuth may be variable due to flat lying nature of these beds, and errors associated with fitting dips to such surfaces. Surfaces typically show cm scale spacing in borehole image logs.
PDf	Poorly defined feature	Dark purple	These surfaces may be any of the above but are very poorly defined in terms of continuity around the borehole.
XSB	Small scale cross beds	Red	Cm-dm scale cross stratification fabric, too small to be characterised in detail.
MUDS	Shale bedding	Green	Confident bedding features with consistent magnitudes.
HETS	Heterolithic bedding	Orange	Confident bedding features with approximately consistent magnitudes.

Lithofacies characterisation

Lithofacies identification was first carried out using FMI images in conjunction with openhole log suites. The FMI interpretations were then calibrated against data from the cored intervals (Core 1 2898.1 – 2925.6 and Core 2 2962.3 – 2989.7 m). In this way, the initial FMI interpretations were not influenced by preconceptions gained from having seen the core, and an understanding of likely interpretation confidence was obtained.

Lithofacies identified from FMI logs.

The sedimentological interpretation of FMI images and dipmeter data were carried out with the aid of gamma ray, density, neutron porosity and sonic logs. Lithofacies were interpreted on the basis of variations in wireline log response in conjunction with fabrics observed in FMI images (Table 5). During interpretation, cuttings descriptions were also used to help provide a guide to lithology, but were found to have only moderate depth resolution (i.e. matching of cuttings description to log /response) due to dispersion of cuttings during circulation of drilling muds. Four broad lithofacies were interpreted as being present, i.e. sandstones, mudstones, finely inter-bedded heterolithic successions and coals. Heterolithic successions comprise centimetre-decimetre scale interbedded sandstone, siltstone and mudstone beds. Coals formed a minor lithofacies within the study intervals, and are clearly recognisable by their low density, high porosity and high resistivity log response (Figure 4).

Lithofacies types were classified according to a simple scheme using mnemonics based upon interpreted lithology and contained fabric, the latter being determined from borehole image log and associated dip data. Examples of identified lithofacies are summarised below in Table 5.

Table 5. Lithofacies identified from FMI images within the study intervals.

Inferred Lithology/Grain Size	Typical Log Response	Image Log Fabrics	Lithofacies Mnemonic
Sandstone	GR <30 API RHO8 2.2 – 2.4 g/cc HTNP 0.12 – 0.20	Laminated	Sl
		Cemented	Sc
		Fine scale mottled or "speckled" texture with poorly defined or disrupted lamination fabric	Sm
		Coarse scale mottled texture with poorly defined or disrupted lamination fabric. Mottling comprises resistivity elements several cm in diameter	Scm
Heterolithics	GR 30 – 55 API RHO8 2.4 – 2.65 g/cc HTNP 0.2 – 0.25	Laminated	Hl
		Mottled with disrupted lamination fabric	Hm
Mudstone	GR 55 – 110 API RHO8 2.65 – 2.75 g/cc HTNP 0.25 – 0.35	Laminated	Ml
		Mottled with disrupted lamination fabric	Mm
Coal	GR variable typically <30 API RHO8 <2.2 g/cc HNTP >0.35	Laminated	Cl
		Mottled	Cm

The hierarchical combinations of different lithofacies mnemonics were used to provide detailed descriptions of lithofacies types. In these descriptions, the enclosure of lithofacies mnemonics in parenthesis was used to denote the minor presence of a lithofacies type, or poor development or preservation of a sedimentary structure, e.g.

Mm (Ml) mottled mudstones with relict lamination or minor laminated intervals.

Sm (Sl) mottled sandstone with poorly defined relict lamination.

Sl (Sm) laminated sandstone with minor fabric loss due to mottling / disruption of lamination etc.

Figures 5 - 9 illustrate examples of different lithofacies types for the lithologies identified, together with their fabric index.

Calibration of image log fabrics using core and cuttings descriptions

Calibration of image log fabrics was carried out using:

- Cuttings descriptions through the logged intervals. Cuttings descriptions are summarised on Enclosures 5 and 6.

- Core from the intervals 2898.1 – 2925.6 m and 2962.3 – 2989.7 m was available to calibrate fabrics observed in borehole image logs. A comparison of core and image logs is illustrated in Enclosures 10 and 11.

Image log calibration using cuttings

Generally, cuttings descriptions match well with lithofacies interpretations derived using wireline log response and FMI image fabrics. Cuttings descriptions reveal a succession comprising sandstone, siltstone and claystone with rare intervals of coal.

Characterisation of heterolithic successions comprising individual beds beneath the resolution of wireline logs is difficult. However, image logs revealing extreme resistivity variation within strata containing cm-dm scale bedding fabrics provide some insight as to the presence of these heterogeneous lithologies. Cuttings descriptions through successions interpreted from wireline log and FMI as comprising heterolithic deposits, invariably yield documentation of cuttings of claystone, siltstone and sandstone in varying proportions.

There is approximately 6 m difference in depth between the drillers depth and the loggers depth.

Image log calibration using core

A good overall match exists between image log interpretations and core observations through Core 1 (2898.1 – 2925.6 m) and Core 2 (2962.3 – 2989.7 m) (Enclosures 10 and 11). These cored intervals are considered to be representative of the lower two study intervals because the cores are not limited to the reservoir intervals, but contain non-reservoir as well, and this can be used to extrapolate to un-cored intervals.

Mottled fabrics predominantly occur outside of the cored intervals and there is uncertainty in the interpretation of this lithofacies as this fabric in borehole image logs may arise from a number of different mechanisms. These could include:

- Differential cementation or the presence of nodular cements.
- Artefacts such as scattered drilling debris on the borehole wall.
- Textural variations due to biogenic disruption of sediments (bioturbation or rootlets).
- Textural variations associated with dewatering fabrics in sediments.
- The presence of coarse detritus such as pebbles or clay flakes.

Core observations within the cored intervals have revealed two different types of sedimentary fabric that have produced mottled image log fabrics. These are:

The presence of granular and pebbly lithologies (gravels, and coarse granular-pebbly sandstones) with clasts up to 2 cm diameter.

The presence of sandstone/heterolithic/mudstone lithologies with overall mottled character and often poorly defined stratification. The lithologies within this interval contain rootlets and often occur in association with coal.

Close examination of FMI images reveals that mottled textures are present at 2 distinct scales:

Speckled image texture, in which scattered mottles and speckles occur at *circa* 1 cm scale, and are associated with diffuse bedding fabric. Comparison with the cored intervals indicates that this “fine” scale mottling occurs within a range of lithologies displaying poorly defined lamination, vague and vague mottled texture. These intervals are not characterised by the presence of coarse detritus (pebble clasts etc.).

Strongly mottled image texture, in which mottles are defined by resistivity features of several cm diameter, so that often, only 2 or three "mottles" may be seen across an individual FMI pad. Core calibration reveals that this "coarse" mottling corresponds to intervals containing granular and pebbly sandstones.

Heterolithic lithologies sampled by the cores do contain evidence of bioturbation, and mottled / disrupted lamination fabrics observed within image logs through mudstone lithologies may reflect bioturbation within sediments. However, in the absence of sufficient core calibration, this interpretation should be treated with caution. Similar fabrics could be generated by a variety of phenomena including nodular cementation patchy sand distribution etc.

FMI derived lithological fabric index

The hierarchical lithofacies nomenclature scheme applied to description of lithofacies from borehole image logs was also be used to provide a simple 4 fold fabric index as illustrated for sandstones in Table 6 below. This type of fabric index may be useful for comparison of reservoir properties with image log derived lithological properties. Note, if mottled fabrics identified within sandstones are due to bioturbation, this fabric index may also approximate to a 4 fold bioturbation index, which may be useful in construction of sedimentary models using data derived from image logs.

Table 6. Simple fabric index (applied to sandstone lithofacies) based upon mnemonics scheme used for FMI interpretation of lithofacies. Note the fabric index may approximate to a bioturbation index within sandstone lithologies free of granular-pebbly detritus.

Lithofacies	Approximate degree of fabric development within sediments.	Fabric Index
Sl	Minimal <10%	1
Sl (Sm)	approximately 25 %	2
Sm (Sl)	approximately 75 %	3
Sm	near total 100 %	4

The implication of the fabric index is that low indices will result in strongly anisotropic reservoir properties (e.g. Kv > Kh). If due to phenomenon such as bioturbation creating mottled image fabric and loss of stratification, higher fabric indices may reflect more homogeneous reservoir properties (e.g. decrease in Kv:Kh ratio due to loss of stratification).

Lithofacies associations

The sedimentary deposits in the intervals 2550 – 2600 m, 2890 – 3030 m and 3110 – 3180 m within Yolla 4 comprise a heterolithic succession of sandstones and mudstones with minor intervals of coal. The successions can be sub-divided into a number of discrete sub-units based upon log trends and stacking patterns of interpreted lithofacies.

In particular, upward decreasing gamma ray log trends, and NPHI and RHOB log response which trends towards sandstones indicate stacked successions of upward coarsening / upward cleaning deposits that represent parasequences. Sedimentary dips within these

upward cleaning successions are typically low (< 12°). However, upward cleaning (and coarsening) trends are in some cases punctuated by development of sandstones with blocky log character, and elevated sedimentary dips in excess of 12°.

The upward coarsening parasequences described are consistent with a model of deposition in a marginal lacustrine/marine environment, with upward coarsening profiles forming as a result of shoreface or delta front progradation. Blocky sandstones characterised by sedimentary surfaces with elevated dips may represent the deposits of distributary channels or upper shoreface/foreshore environments. The lithofacies identified are described in detail in the following sections. In the absence of core calibration for some intervals, the following discussions are should be considered speculative.

Observed vertical transitions in lithofacies types identified in borehole images have enabled lithofacies to be grouped into genetically related successions of strata or *lithofacies associations*, which have some environmental significance (Walker 1992). Six lithofacies associations were identified within the studied data set, and their distribution within the studied intervals is illustrated in Enclosures 7 – 9. The lithofacies associations identified are summarised below.

Lithofacies Association I

Lithofacies Association I is argillaceous, mainly comprising mudstone lithologies (Ml and Mm), with minor interbedded heterolithic lithologies. The mudstones occur at the base of successions displaying overall upward cleaning (and coarsening) gamma ray log trend (e.g. 2995 –3000 m Enclosure 8) and commonly display a mottled fabric, which decreases in intensity upward through the succession. This may reflect decreasing intensity of cementation mottling upward through the succession. Bioturbation of this lithofacies association within the cored intervals is absent or very minimal and limited to trophic generalists e.g. *Skolithos* (Pemberton and Wrightman, 1992).

Generally, Lithofacies Association I forms relatively thick deposits up to several metres thick, and is characterised by blocky to serrate, overall high gamma-ray log response (>55 API), reflecting the presence of a predominantly argillaceous succession of lithofacies types. Gamma ray log response within mudstones typically decreases slightly upward, forming part of an overall upward decreasing trend. Lithofacies Association I typically pass upward into heterolithic lithofacies of Lithofacies Association II.

The mudstones of Lithofacies Association I display low sedimentary dip (typically <10°), with wide ranging dip azimuths (covering 360^{o} spread) indicative of their original deposition as parallel stratified sediments upon a flat lying substrate.

Sedimentation within Lithofacies Association I was probably dominated by suspension fallout of argillaceous material, resulting in the accumulation of laminated mudstone lithofacies (Ml, etc.). The mottled and disrupted bedding fabrics identified are most likely due to cementation, as the Core 1 contains siderite concretions indicating anoxic or reducing conditions during deposition. The low diversity and low density of bioturbation is a result of poorly oxygenated water (Beynon and Pemberton, 1992). In most examples this appears to have been most intense towards the base of upward coarsening successions suggesting that anoxic conditions prevailed in deeper water.

As mudstones grade upward into sandier deposits, the proportion of mottling decreases, reflecting increased oxygenation conditions and the presence of low diversity bioturbation.

Lithofacies Association II

Lithofacies Association II comprises heterolithic lithologies. Heterolithic sediments consist of centimetre to decimetre scale interbedded sandstones and mudstones, and often display a highly mottled image fabric. Within the studied intervals, heterolithic deposits may form successions in excess of 5 m thick. Heterolithic deposits predominantly occur towards the base of facies successions which display overall upward cleaning (and coarsening) gamma ray log trend.

Sedimentary dips within heterolithic deposits are typically characterised by low angle fabrics (inclined typically <10° sedimentary dip). Removal of structural dip reveals these bedding fabrics to be characterised wide ranging (up to 360° spread) dip azimuths, indicative of their original deposition as approximately horizontally stratified sediments.

Bioturbation is more prevalent in this lithofacies and reflects increased oxygenation of waters but the low diversity and small size of the structures reflects control by environmental conditions e.g. salinity, oxygenation, nutrient availability etc. (Beynon and Pemberton, 1992).

Heterolithic nature of these deposits suggests deposition via both tractional and suspension processes. In a shallow marine/lacustrine setting, this style of deposition may have occurred at or around fair weather wave base in lower-shoreface setting, or perhaps in the sub-aqueous portion of a shoal water type delta front.

Lithofacies Association III

Lithofacies Association III mainly comprises sandstone lithologies, with a variety of different internal fabrics (fine scale mottled, well laminated, mottled with relict lamination etc.). Well preserved lamination fabrics are not generally common within images through sandstone lithologies. Lithofacies Association III is characterised by low angle sedimentary dips (typically approximately 10°), and forms successions up to 5 m thick within the studied sections. The sandstones typically rest gradationally upon heterolithic deposits of Lithofacies Association II, in the upper parts of upward coarsening successions. The sandstones of Lithofacies Association III are distinguished from those of Lithofacies Association (IV) discussed below by lower sedimentary dips. The low angle sedimentary dips (typically <10° rarely up to 15°), characteristic of this lithofacies association, often displaying dm to m scale cosets, which may display a relatively tight cluster of unimodal dip azimuths. Flat lying intraset surfaces are also common within this lithofacies association. Few interpretations can be made as to the relative spatial distribution of laminated versus mottled image fabrics within sandstones from this lithofacies association.

The low angle stratification within these sediments is indicative of deposition by tractional processes. The occurrence of these sediments within the upper parts interpreted upward coarsening lithofacies successions, and the often variable orientations of cosets comprising low angle internal stratification that is common within some successions may be consistent with deposition in a shallow marine/lacustrine environment. In these settings, both unidirectional and oscillatory currents (together forming combined flows) during storms produce variety of 2- and 3-dimensional bedforms as evident in the core data. Sedimentary fabrics characterised by sets of low angle stratification of variable orientation may indicate deposition as low amplitude, perhaps strongly 3-dimensional mounded bedforms. In a shallow marine/lacustrine setting, this style of deposition may have

occurred above fair weather wave base in shoreface setting. Successions where low angle surfaces display more unimodal distribution of azimuths may indicate the presence of a more significant palaeoslope or sediment transport and deposition under the influence of more unidirectional current systems. Alternately, the low angle parallel lamination fabrics could be consistent with deposition as sands within the upper parts of a shoal water type delta front.

Lithofacies Association IV

This FMI derived lithofacies is sand dominated, mainly comprising Scm, Sm, Sl, Sm(Sl) and Sl(Sm), with minor heterolithic and mudstone lithofacies. Association IV occurs in successions up to 20 m thick within the studied intervals. Three intervals within the studied succession have been assigned to Lithofacies Association IV, and few conclusions can be drawn concerning the spatial distribution of different lithologies within these deposits.

Interpretation of manually picked dips from FMI images indicates the presence of intraset surfaces inclined at angles up to 20°, these steeply inclined surfaces distinguishing this lithofacies association from Lithofacies Association III above. However, both Lithofacies Associations are dominated by Sl, and are differentiated on the basis of position in the succession. Lithofacies Association III occurs at the top of the upward cleaning/upward coarsening successions, whereas, Lithofacies Association IV occurs in thick, amalgamated sandstone units.

The coset boundaries occur at dm to m scale and dip data sets, in places, for Lithofacies Association IV indicate an essentially unimodal overall distribution of azimuths for flat intraset surfaces, with low azimuthal dispersion within cosets. These distributions are SE for deposits of Lithofacies Association IV in the interval 2962 - 2979 m, the coset boundaries in this interval have a similar orientation to the ISSf indicating downfan progradation of sheetflood deposits. Other intervals have variable orientations implying deposition as flat lying sediments.

The cross stratified sediments of Lithofacies Association IV may represent the deposits of channels (fluvial or distributary) within an alluvial setting, however, the dominance of Sl and the thin cross stratified sets indicates unconfined sheetfloods. Evidence of primary stratification within these deposits testifies to the development and migration of bedforms, with the locally cross-bedding indicating dunes and sand waves. Mottled FMI lithofacies Scm reflects the presence of coarse grained pebbly sandstones and mudstone rip up clasts. Finer scale mottling and disrupted lamination / relict internal stratification fabrics within lithofacies Sm may indicate de-stratification a result of sediment de-watering. De-watering may have arisen as a result of pore-pressure adjustments during rapid deposition and burial of sediments, or as a result of a rapid rise / fall in fluvial stage. Alternatively, the mottling could result from biogenic activity (rootlets).

The cosets of strata are typically thin, which indicates shallow water depth and the dominance of Sl imply upper flow regime conditions. Palaeotransport implications for this lithofacies association are discussed in detail in the following sections.

Lithofacies Association V

Lithofacies Association V comprises mudstones and heterolithic lithologies with varying degrees of lamination. They are indistinguishable from the lithologies of Lithofacies I and II. However, they occur as typically thin (1-3 m) successions interbedded with lithologies

interpreted as sub-aerial sheetflood deposits, suggesting an alluvial origin. Mudstone lithologies may occur interbedded with sheetflood sandstones as a result of deposition of suspension fines during waning flow stage (Benvenuti, 2003). Thicker mudstone deposits may represent abandonment of sheetflood lobes or lagoonal settings.

Core observation has revealed that argillaceous lithologies in the interval 2898 – 2903 m log depth (2892 m – 2897 m core depth) contain a variety of sedimentary fabrics. These include flat lamination, rootlets and rare bioturbation comprising *Planolites* and *fugichnia*. These suggest that mudstones in this interval were deposited in a lagoonal or marginal marine / lacustrine environment, and that the sheetflood deposits passed rapidly into the marine / lacustrine environment, implying an alluvial fan / fan delta setting.

In FMI images, these lithologies are indistinguishable from those argillaceous lithologies which occur in the lower parts of large scale upward cleaning cycles (i.e. *Lithofacies Association I*). Mudstone lithologies are assigned to Lithofacies Association V purely on the basis of their close association with stacked sheetflood sandstones of Lithofacies Association IV.

Lithofacies Association VI

Coals form a minor lithology within the studied section, with the thickest development in the upper interval (2596.5 – 2599 m). Elsewhere, coals are typically less than 1 m thick e.g. 2899.5 – 2900.6 m in Core 1. They are characterised by high resistivity, low density and high porosity. In images they either display little internal structure, other than rare flat lying internal "bedding" surfaces or have a mottled texture reflecting a lack of internal structure.

Coals occur towards the top of small scale upward coarsening mudstone-heterolithic sandstone successions and in association with thick sandstone intervals.

Summary

The integrated analyses of wireline log signature and FMI fabric allows identification of a variety of different lithofacies types. Calibration with cuttings descriptions and the core has permitted lithofacies interpretation from FMI logs over intervals where there is no core data. However, the thick intervals of mudstone were not sampled and therefore, the environmental interpretations for these intervals is only speculative.

Summary of environmental interpretations

A brief summary of the sedimentary successions analysed in detail and their environmental interpretation is provided in the following sections. Detailed discussions of palaeotransport observations are included in the Bedform Orientation and Sediment Dispersal section of this report.

Interval 3139 – 3167 m

Wireline logs and FMI interpretations through this interval suggest that it comprises an overall coarsening then fining upward succession. The succession is overall heterolithic with mudstone / heterolithics interbedded with sandstone at the base that passes upwards into sandstone. The sandstone is overlain by the fining upward succession of heterolithics and mudstone. Details are summarised below in Table 7.

Table 7. Summary of deposits in the interval 3139 – 3167 m

Interval 3139 - 3167 m			
Depth (m)	**Lithofacies Association**	**Brief Description**	**Interpretation**
3167 - 3165	V	Laminated mudstone overlain by heterolithics	Occurs at top fining upward succession without coals suggesting shallow marine / lacustrine. Mottling is rare to absent, inferring anoxic conditions. Alternatively, succession could represent coastal plain environments
3165 – 3163	IV	Blocky log response, comprising laminated sandstone. Mottling present as small elongate, high resistivity patches	Blocky sandstone with harp base and top, low sedimentary dips and mudstone rip up clasts indicates upper flow regime deposition, possibly as unconfined, low density distal sub-aerial sheetfloods (Benvenuti, 2003).
3163 – 3160	V	Interbedded mudstone and heterolithics in coarsening upward succession. Heterolithic strata thicken upwards	Small scale coarsening upward succession is consistent with progradation of shoreface / fan delta deposits
3160 - 3149	IV, rare II	Interval comprises dominantly Sl with minor Sm(Sl). Sedimentary dips are typically <10°. Thin interbedded heterolithics separate the interval into three sandstone packages	Sandstones are interpreted as sheetflood deposits. Sandstones consistently have shallow dips.
3149 - 3145	II	Heterolithic strata, rare sedimentary dips up to 20°. Small scale coarsening upward succession	Upward coarsening profile overlying sheetflood deposits suggests possible subaqueous fan delta deposition by high density turbidity currents (Benvenuti, 2003)
3145 – 3139	I	Massive and laminated mudstones in a fining upward succession	Fining upward succession dominated by mudstone and overlying subaqueous fan delta implies deepening, e.g. lower shoreface to offshore transition

Interval 3118 – 3131 m

This interval comprises two staked upward cleaning (coarsening) successions as identified on wireline logs and FMI interpretations. The succession is heterolithic with the coarsening upward successions typically comprising mudstone at the base overlain by heterolithics and sandstone. The upper boundary of these successions is sharp. Details are summarised in Table 8.

Table 8. Summary of deposits in the interval 3118 – 3131 m

Interval 3118 - 3131 m			
Depth (m)	**Lithofacies Association**	**Brief Description**	**Interpretation**
3131 - 3118	I -> II -> III	Two stacked cleaning (coarsening) upward successions comprising laminated mudstones, heterolithics and laminated sandstones. The succession is mudstone dominated. Low angle sedimentary dips (<5°) and wide ranging azimuths indicate flat lying deposition	The upward coarsening profile is consistent with deposition in a prograding shoreface / deltaic environment. Mudstone indicates deposition within deeper water, lack of bioturbation implies anoxic bottom conditions.

Interval 2960 – 2997 m

Wireline logs and FMI interpretations in this interval suggest this it comprises a lower heterolithic succession of strata and an upper sandstone dominated interval. Two large scale upward cleaning (coarsening) successions are present. The uppermost of these was intersected in Core 2 and is overlain by a thick package of amalgamated sandstone. Details are summarised in Table 9.

Table 9. Summary of deposits in the interval 2960 – 2997 m

Interval 2960 – 2997 m			
Depth (m)	**Lithofacies Association**	**Brief Description**	**Interpretation**
2997 - 2985	I -> II -> III	Upward cleaning (coarsening) succession comprising massive to laminated mudstones, heterolithics and laminated sandstones. Upper 5 m of succession has been cored	Upward coarsening profile suggests a progradational shoreface environment. Core shows a dominance of low angle lamination and wave formed structures.
2985 - 2982	IV	Laminated sandstone with rare intervals of sedimentary dips over 10° record predominantly SE – S dip azimuths.	Distal sub-aerial low concentration sheetflood deposits with S – SE drainage.
2982 - 2979	IV and VI	Mottled and weakly laminated coal interbedded with mottled sandstone	Core indicates that the mottled sandstone is produced by rootlets at the base of the coal, forming a seat earth. The coal is autochthonous.
2979 – 2962	IV	Sandstones are typically laminated with sedimentary dips rarely exceeding 10°. Mottled sandstones occur toward the middle of the succession	Core over this interval shows a dominance of low angle lamination that is interpreted as distal sub-aerial, low concentration unconfined flows. The mottled sandstones correlate with pebbly sandstone and pebble conglomerate that is interpreted as medial, sub-aerial spreading of hyperconcentrated flows on an alluvial fan environment (Benvenuti, 2003)
2962 - 2960	I	Massive to laminated mudstone	The lack of coarse clastics indicates quiet water deposition. The stratigraphic position overlying sheetflood deposits possibly implies a back barrier lagoon environment deposited during the initial phase of transgression.

Interval 2899 – 2920 m

Wireline logs and FMI interpretations through this interval suggest that it comprises a heterolithic succession of strata arranged in an upward cleaning (coarsening) succession, overlain by a fining upward package. Sandstones dominate the middle of the interval. Details are summarised in Table 10.

Table 10. Summary of deposits in the interval 2899 – 2920 m

Interval 2899 – 2920 m			
Depth (m)	**Lithofacies Association**	**Brief Description**	**Interpretation**
2920 - 2912	I -> II -> III/IV	Stacked small scale upward coarsening cycles. Massive and laminated mudstones pass upwards into heterolithic and laminated sandstones. The coarsening upward cycles toward the top of the interval contain lithofacies association IV that rarely have sedimentary dips <10°.	The small scale coarsening upward cycles are arranged in an overall progradational succession. Core from this interval indicates a sub-aqueous (LA I – III) to sub-aerial (LA IV) deposition in a fan delta environment. Cross bedding in LA IV indicates a SE drainage. Bioturbation is rare and limited to heterolithic strata.
2912 - 2908	IV	Laminated to massive sandstone, sedimentary dips rarely exceed 10°	Distal sub-aerial sheetflood deposits with SE drainage
2908 – 2903	III	Laminated to massive sandstone with rare sedimentary dips >10°.thin mudstone drapes.	The presence of massive and laminated sandstones implies shallow sub-aerial deposition. The reduced grainsize and mudstone drapes may indicate progressive abandonment of the active lobe.
2903 – 2899	V, rare VI	Heterolithic interval of mottled, laminated sandstone, heterolithic strata and massive to laminated mudstone with thin coal beds.	Mottled sandstones result from rootlets that are present below the coal beds. The abundance of rootlets indicates abandonment of the fan delta lobe and development of coastal mires.

Interval 2550 – 2600 m

Wireline logs and FMI interpretations through this interval suggest that it comprises a heterolithic succession of strata, with lithologies comprising mudstones, heterolithics, sandstones and minor coal. A series of upward cleaning (coarsening) and upward fining trends are evident from log suites. The succession is dominated by heterolithic intervals. Details of interpretations are summarised in Table 11.

Table 11. Summary of deposits in the interval 2550 – 2600 m

Interval 2550 - 2600 m			
Depth (m)	**Lithofacies Associations**	**Brief Description**	**Interpretation**
2600 – 2599	I	Mottled to weakly laminated mudstone	Short interval studied forms part of upward fining trend
2599 – 2596.5	VI	Laminated coal	Overlies mottled mudstone and implies in situ accumulation on floodplain environment
2596.5 – 2592	I	Massive to laminated mudstones	Interval forms top of upward fining trend interpreted as floodplain environment.
2592 - 2576	I -> II, rare III	Massive to laminated mudstones pass upward into a succession of heterolithic strata	Upward coarsening profile suggests possible low energy shoreface
2576 – 2564	I, II, rare VI and III	Aggradational stacking of mudstone and heterolithic strata, with rare coal beds and thin sandstones with sedimentary dips up to 25°	Aggradational stacking and presence of thin coals implies coastal plain setting
2564 - 2550	I -> II	Massive to laminated mudstones pass upward into a succession of heterolithic strata	Upward coarsening profile suggests possible low energy shoreface

BEDFORM ORIENTATION AND SEDIMENT DISPERSAL

Following sub-division of the succession into the six lithofacies associations described above, detailed analysis of the orientation of different bedforms within these successions was undertaken in order to evaluate sediment dispersal, and orientation of the depositional system. Sedimentary dips for the different bedding categories identified are summarised in Enclosures 7 – 9. Cumulative dip azimuth plots for the intervals 2890 – 2920 m, 2960 – 2997 m and 3139 – 3167 m are shown in Figures 10 – 12.

Lithofacies Associations I, II & III

Sedimentary dips within mudstone and heterolithic lithologies (interpreted as comprising cm-dm scale interbedded sandstone and mudstone laminae) from lithofacies associations I and II typically display 360º azimuthal spread, indicative of the original deposition of these lithologies as "flat lying" effectively parallel stratified sediments. These sediments are mainly interpreted to have been deposited in shallow marine / lacustrine settings, in shelf-shoreface or prodelta-fan delta environments. However, in some intervals, e.g. where they occur as part of a well developed overall upward cleaning succession comprising Lithofacies Associations I to III, heterolithic lithologies display a preferred orientation, possibly reflecting palaeoslope.

Sedimentary dips within sandstones of lithofacies association III are also typically highly variable, and indicative of original deposition as "flat lying" sediments. This may have occurred within shallow shoreface settings or as sub-aqueous fan deltas. However, intraset surfaces (XBS) and flat lying intraset surfaces (ISSF) do show bimodal orientations with a dominance of surfaces in one direction (NE to SE) with only a minor component oriented at 180° to the main direction. Core data indicates that this Lithofacies Association represents a shoreface environment dominated by wave formed structures. The main flow direction (NE – SE) may represent onshore migration of fair weather wave formed structures whereas the minor flow direction may represent offshore flow during storm events.

Lithofacies Association IV

The low gamma ray log response typical of Lithofacies Association IV, indicates that these successions contain a significant proportion of clean, potentially high reservoir quality sandstones. This Lithofacies Association within Yolla 4 is interpreted as distal sub-aerial sheetflood deposits on the basis of the dominance of low angle lamination and core intersections.

The quartzose composition of the cored intervals indicates that fan delta / alluvial fan was sheetflood dominated as deposits containing a high percentage of mud typically comprise debris flows. Sheetfloods result from flashy concentration of runoff over drainage basin colluvial slopes, leading to sediment laden and catastrophic water discharge downslope. Debris flows do not form due to the low concentration of clay in the colluvium, insufficient sediment concentration, or slow rate of sediment entrainment in the flow. Sheetfloods are unconfined flows that expand as they move down fan. They develop when sediment charged flash floods reach a fan and attenuate because of the lack of channel walls, and the multi-directional slope of the fan surface caused by its semi-conical form. The most prevalent sheetflood facies consists of vertically alternating planar bedded couplets pebbly lags (in distal fan environments, termed the distal sand skirt) interstratified with

laminated sandstone. The planar bedded sets have distally decreasing slopes of 2 - 8° parallel to the fan surface, that produce a concave profile (Blair and McPherson, 1994).

Debris flows are initiated by two mechanisms, the most common involves transformation of a disintegration of a colluvial slide into a debris flow by entrainment of air and water through the jostling, deformation and loss of particle individuality as it moves downslope. This transformation requires the presence of water in the colluvium, and is therefore most apt to occur during or immediately after excessive precipitation. The second initiation mechanism occurs where fast moving water intersects a drainage basin slope mantled by abundant sediment. The ensuing reaction, in which the water dissipates its energy by dispersing clasts through mixing, can result in rapid entrainment of sediment, air and water to produce a debris flow. Debris flow dominated alluvial fans have constant slopes with values between 5 and 15° (Blair and McPherson, 1994). See Table 12 for the characteristics of debris flow (Type I) and sheetflood dominated (Type II) alluvial fans.

The high porosity, permeability; as evident from the core data; and connectivity of permeable units have major implications for volumetrics and production strategies.

The main intervals of sheetflood deposits assigned to lithofacies association IV have been identified within the intervals studied in detail.

The main intervals of sheetflood deposits occur:
3160 – 3149 m
2985 – 2962 m
2912 – 2903 m

The orientation of bedding surfaces within these intervals are summarised in Tables 13 – 15 below.

Table 12. Characteristics of Type I verses Type II alluvial fans (Blair and McPherson, 1994)

Feature	Type I Alluvial Fan	Type II Alluvial Fan
Dominant primary process and facies	Debris flows, especially lobe facies	Sheetfloods, especially couplet facies
Minor primary process	Rockfall, rock slide, rock avalanche, colluvial slide, incised channel	Rockfall, rock slide, rock avalanche, colluvial slide, incised channel, non-cohesive debris flow
Dominant secondary process	Winnowing by overland flows and wind to produce deflation pavements, boulder mantles, gullies and shallow channels	Winnowing by overland flows and wind to produce deflation pavements, gullies and shallow distributary channels
Typical grainsize and sorting	Very poorly sorted clayey boulder, pebble and cobble gravel	Poorly sorted sandy and bouldery, cobble to pebble gravel
Downfan trend in maximum clast size	Relatively constant	Typically decreases from boulders to pebbles or sand
Typical grain shape	Angular	Angular to sub-angular
Typical stratification style	Poorly or subtly stratified except for secondary winnowed surfaces	Well stratified coarse gravel and sandy fine gravel couplets
Presence of granular or sandy interbeds	Rare	Common
Presence of a distal sand skirt facies	Rare	Common
Presence of depositional matrix clay	Common	Rare
Drainage basin size	Small to moderate	Small to large
Feeder channel length	Short to moderate	Moderate to long
Typical bedrock lithology underlying the drainage basin	Pelitic metamorphic rocks, mudstone, aphanitic volcanic rocks, or mafic plutonic rocks; also weathering of granitic or gneissic rocks in humid climate	Quartzite, quartz rich conglomerate or sandstone; also granitic or gneissic rocks weathering in an arid climate
Clay abundance in the drainage basin colluvial slopes	Moderate to abundant	Rare
Common average slope values	5 - 15°	2 - 8°
Downfan slope style	Constant to straight	Distally decreasing or plano-concave
Permeability	Low	High
Porosity	Low	High
Connectivity of permeable units	Low	High

Table 13. Bedding orientations, sheetflood deposits within the interval 3160 – 3149 m

Interval 3160 – 3149 m (Log depth)				
Depth (m)	Orientation of ISSf's	Orientation of XBS's	Orientation of CSB's	Comments
3149 – 3152	WNW NNE E Variable	Not present	ENE	Variable orientation may reflect original flat lying deposition in distal sand skirt facies
3152 – 3156	S	SSW	S	Low angle bedforms oriented in same orientation as CSB indicating down slope progradation
3156 - 3160	S E Variable	Not present	SSW	Intervals of thin cosets of ISSf with variable orientation. May reflect original flat lying deposition in distal sand skirt facies

Table 14. Bedding orientations, sheetflood deposits within the interval 2985 – 2962 m.

Interval 2985 – 2962 m (Log depth)				
Depth (m)	Orientation of ISSf's	Orientation of XBS's	Orientation of CSB's	Comments
2962 - 2978	SE Variable	SSE	SE	Low angle bedforms oriented in same orientation as CSB indicating down slope progradation. The presence of XBS may indicate shallow incised channels with lower flow regime deposits. SBs oriented within 30° of ISSf and XBS indicating downstream progradation.
2978 - 2981				No bedding fabric measured
2981 - 2985	S Variable	SSE	SSE	Variable orientation may reflect original flat lying deposition in distal sand skirt facies. SBs oriented in same direction (SSE) as XBS indicating downstream progradation.

Table 15. Bedding orientation, sheetflood deposits within the interval 2912 – 2903 m.

Interval 2912 – 2903 m (Log depth)				
Depth (m)	Orientation of ISSf's	Orientation of XBS's	Orientation of CSB's	Comments
2903 - 2912	NE Variable	SE	NE	Variable orientation may reflect original flat lying deposition in distal sand skirt facies. Core data indicates dominance of distal facies with flat lying dips. XBS may indicate shallow incised channels with SE drainage.

Lithofacies Associations V – VI

These data sets are too small and biased for orientation analyses.

CONCLUSIONS

1. The studied successions dip at low angles in variable orientations. A number of structural zones have been defined, these are summarised as follows:

Interval 2550 – 2600 m

Zone I	2550 – 2558	8.3°/239°	Fracture or fault bound at 2558 m
Zone II	2558 – 2561	10.2°/310°	Fracture or fault bound at 2561 m
Zone III	2561 – 2567	6.3°/207°	Fracture or fault bound at 2567 m
Zone IV	2567 - 2571	16.3°/309°	Fracture or fault bound at 2571 m
Zone V	2571 – 2600	5.2°/237°	

Interval 2890 – 3030 m

Zone I	2890 - 2955	5.3°/081°	Fracture or fault bound at 2955 m
Zone II	2955 - 3030	5.0°/318°	

Interval 3110 – 3180 m

Zone I	3110 - 3139	2.5°/321°	Change in mudstone dip overlying sandstone 3139 m
Zone II	3139 – 3171	3.8°/256°	Change in mudstone dip 3171 m
Zone III	3171 - 3180	3.2°/305°	

2. Detailed structural evaluation over the 2550 – 2600 m interval was conducted to determine the location of faulting. No discrete fault planes were evident; however there were pronounced, sharp changes in structural dip at 2558, 2561, 2567 and 2571 m. Several small fault and fracture zones were identified in other intervals but there is minimal disruption to reservoir sections.

3. The sedimentary succession is highly heterolithic, comprising sandstones, mudstones and heterolithic intervals composed of dm scissile intercalations of sandstone, siltstone and mudstone.

4. Six lithofacies associations have been identified, these comprise:

   VII. Mudstones that occur at the base of upward coarsening facies successions. (interpreted as either prodeltaic muds, or shelf-shoreface deposits)
   VIII. Heterolithic intercalations of sandstone siltstone and mudstone, typically occurring within the lower-mid parts of upward coarsening facies successions (interpreted as either distal fan delta, or shelf-shoreface deposits).
   IX. Stratified sandstones with mottled image fabric and low angle (typically <5º) internal bedding surfaces, typically occurring towards the top of upward coarsening facies successions (shoreface deposits).
   X. Successions (often erosively based) of stratified sandstones and pebbly sandstones with dominant internal bedding fabrics inclined at angles <10°, rare intervals of up to 25° (distal sheetflood deposits with shallow incised channels).
   XI. Thin mudstone- heterolithic successions interbedded with lithofacies association IV (possible interdistributary bay / lagoon fill, coastal plain deposits).
   XII. Coals (deposits of swampy coastal plain environments).

5. Sandstones of Lithofacies Association IV are likely to form the main reservoir intervals. Lithofacies Association III may form a secondary reservoir interval and typically have over an order of magnitude less permeability than the sheetflood deposits.

6. Palaeotransport analyses of sandstones from Lithofacies Association III reveals them to be characterised by internal stratification fabrics with very wide ranging sedimentary dip azimuth, suggesting they were originally deposited as "flat lying' strata. Few palaeotransport interpretations can be made for these sandstones. However, in some examples, a dominant sedimentary dip is present, and may represent onshore migration of fair weather wave formed structures whereas the minor flow direction may represent offshore flow during storm events. In most cases, this can broadly be interpreted to have had NE – SE onshore direction and a NW – SW offshore direction.

7. Palaeotransport analyses of sandstones from Lithofacies Association IV reveals them to be characterised by low angle internal stratification fabrics with variable azimuth. The relationship between intra-set flat lamination, intra-set lamination and coset boundaries suggest that sediment transport occurred normal to the depositional dip i.e. bedforms migrated down fan. Interpreted fan slope drainage directions are variable and no consistent drainage direction can be inferred.

8. In the absence of a detailed core calibration over the 3167 – 3139 m interval, environmental interpretations are highly subjective. However, observed lithofacies stacking patterns do appear to be consistent with an interpretation of deposition of strata within a marginal marine / lacustrine fan deltaic setting.

REFERENCES

Benvenuti, M., 2003. Facies analysis and tectonic significance of lacustrine fan-deltaic successions in the Pliocene-Pleistocene Mugello Basin, Central Italy. *Sedimentary Geology*, 157, 197-234.

Beynon, B.M. and Pemberton, S.G. 1992. Ichnological signature of a brackish water deposit: an example from the Lower Cretaceous Grand Rapids Formation, Cold Lake Oil Sands area, Alberta. *In:* Pemberton, S.G. ed: *Applications of Ichnology to Petroleum Exploration: A Core Workshop.* Society for Sedimentary Geology, Tulsa, 199-221.

Blair, T.C. and McPherson, J.G., 1994. Alluvial fans and their natural distinction from rivers based on morphology, hydraulic processes, sedimentary processes and facies assemblages. *Journal of Sedimentary Research*, 64, 450-489.

Pemberton S.G. and Wightman, D.M. 1992. Ichnological characteristics of brackish water deposits. *In:* Pemberton, S.G. ed: *Applications of Ichnology to Petroleum Exploration: A Core Workshop.* Society for Sedimentary Geology, Tulsa, 141-167.

Walker, R.G. 1992. Facies models. *In:* Walker, R.G. and James, N.P. eds. *Facies Models: Response to Sea Level Change*, Geological Association of Canada, Newfoundland, 1-14.

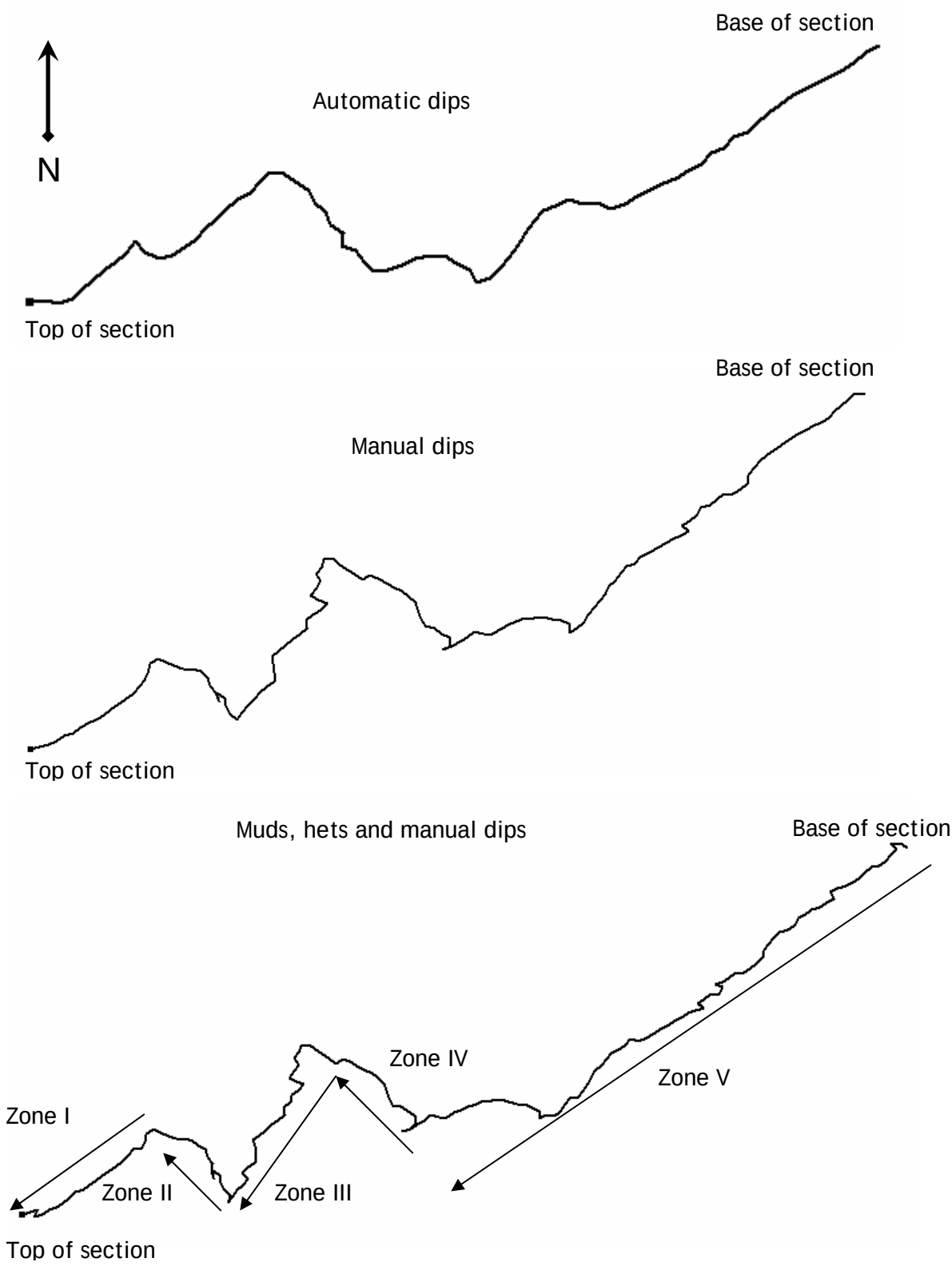

Figure 1. Cumulative automatic, manual and muds and hets, dip azimuth plots for studied section (2550 – 2600 m).

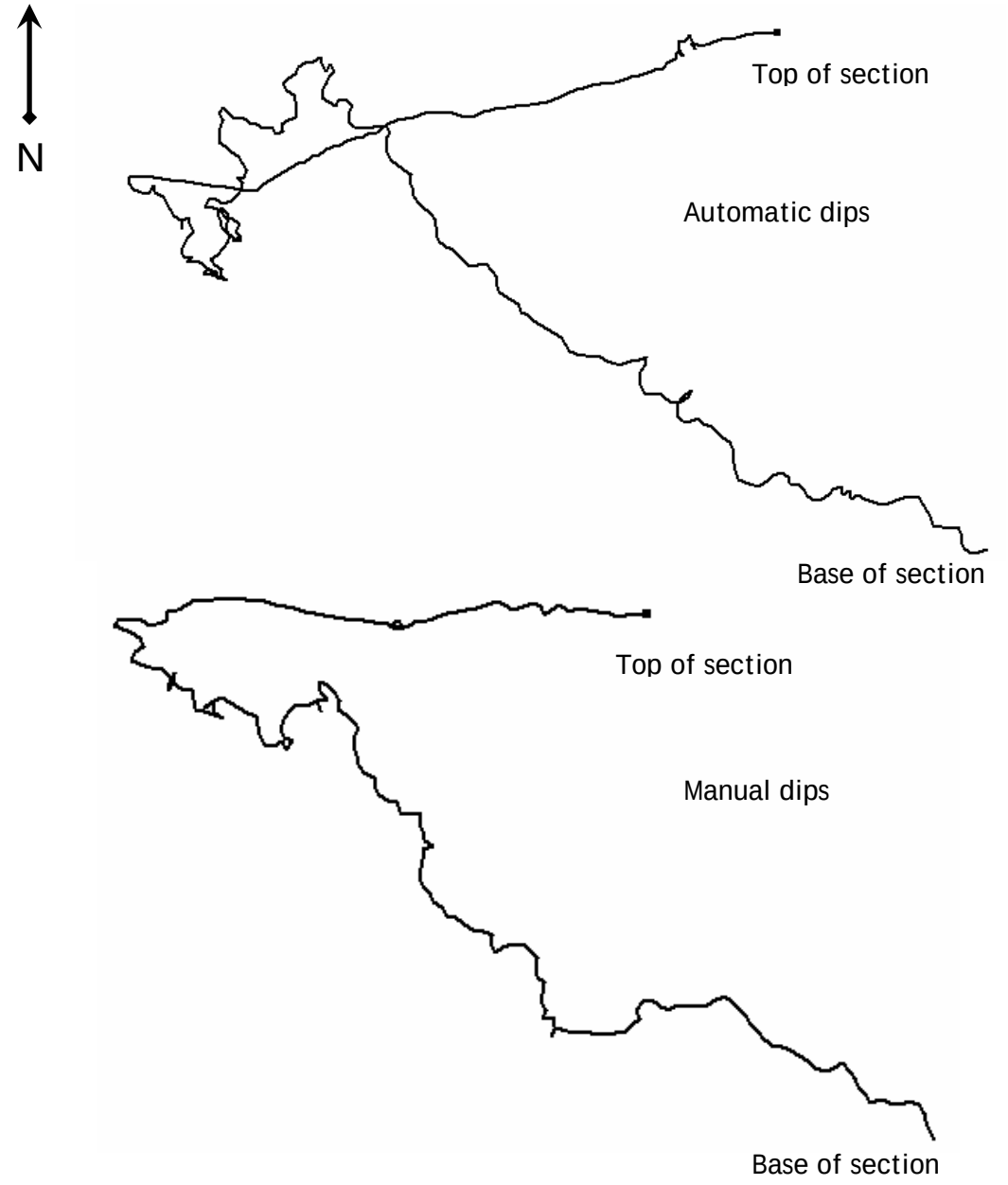

Figure 2. Cumulative automatic, manual and mud hets dip azimuth plots for the studied section (2890 – 3180 m)

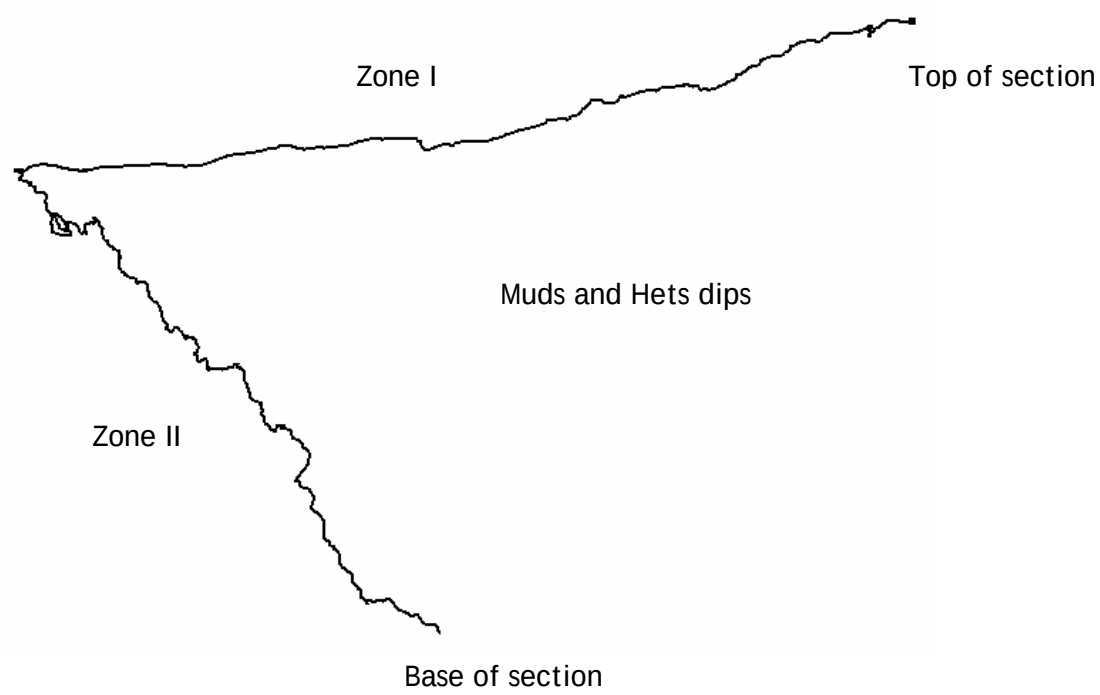

Figure 2. Cont.

Code	Description	Interpreted category
MUD	Confident bedding features, with consistent magnitudes.	Shale Bedding
HETS	Confident bedding surfaces characterised by high resistivity contrasts.	Inter-bedded dm-scale sand and mud. (Heterolithics)
LB	Low true dip angle (typically less than 5°), marked resistivity contrast with overlying/underlying beds	Lithological boundary
LBe	Low true dip angle (typically less than 5°), marked resistivity contrast with overlying/underlying beds and truncation of underlying beds.	Erosional lithological boundary
LBc	Separates a highly resistive zone from overlying and underlying beds. May be a planar layer or non-planar nodular feature.	Cemented lithological boundary
SB	Surface (typically less than 15°) enclosing a bed that may have internal stratification with consistent dip and azimuth.	Set (bed) boundary
CSB	Surface separating groups of beds or a single bed displaying a significantly different character.	Coset boundary
ISS	Steeply dipping true dip angle (15-40°), highly discordant to set (bed) boundaries, and are characterised by resistivity contrast of cm scale with constant dip azimuth trends.	Intra set, cross-bedding surface
ISSF	Near horizontal surfaces with true dip angle (<5°), characterised by resistivity contrast several cm thick. Azimuth trends may be variable due to the low precision associated with determining the azimuth of flat lying beds.	Flat/horizontal intra set surface
FRAC	Generally discordant plane with moderate to steep dip (resistive or conductive).	Fracture
FAULTR	Generally discordant plane with moderate to steep dip, with identifiable displacement (resistive or conductive).	Fault

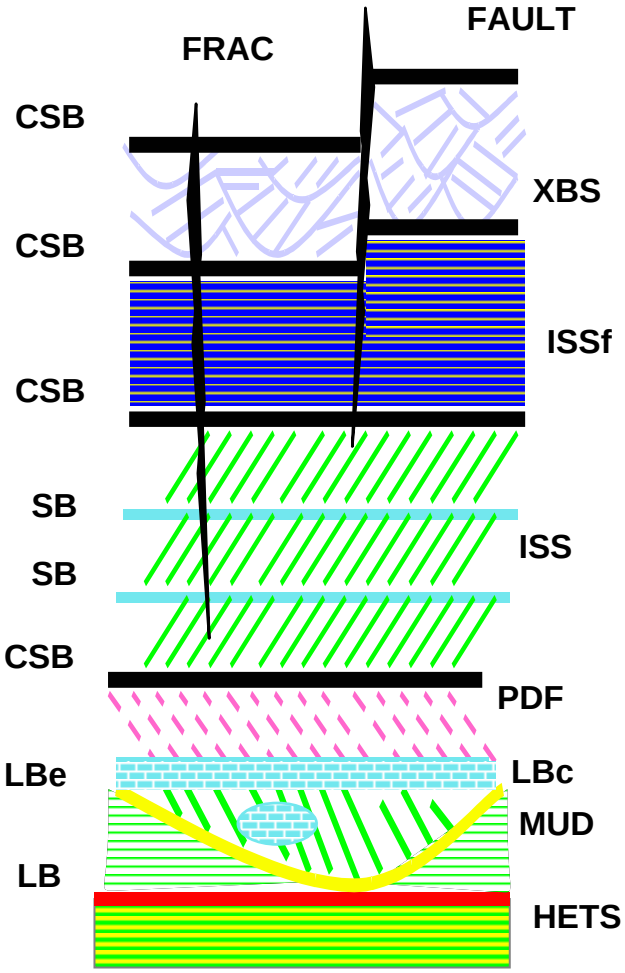

Figure 3. Dip categories used in this study.

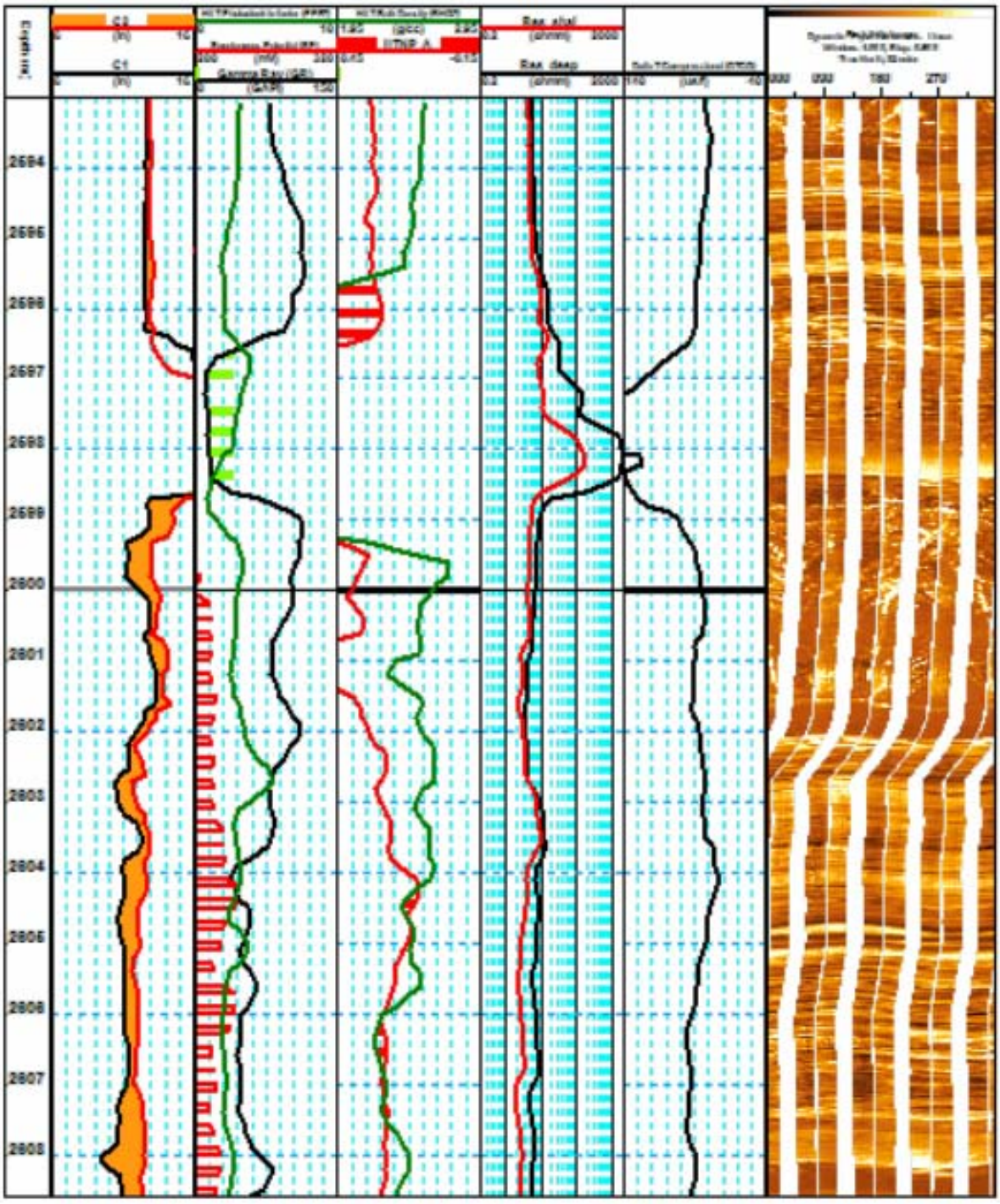

Figure 4. Example of coal (lithofacies VI) in interval 2596 – 2599 m.

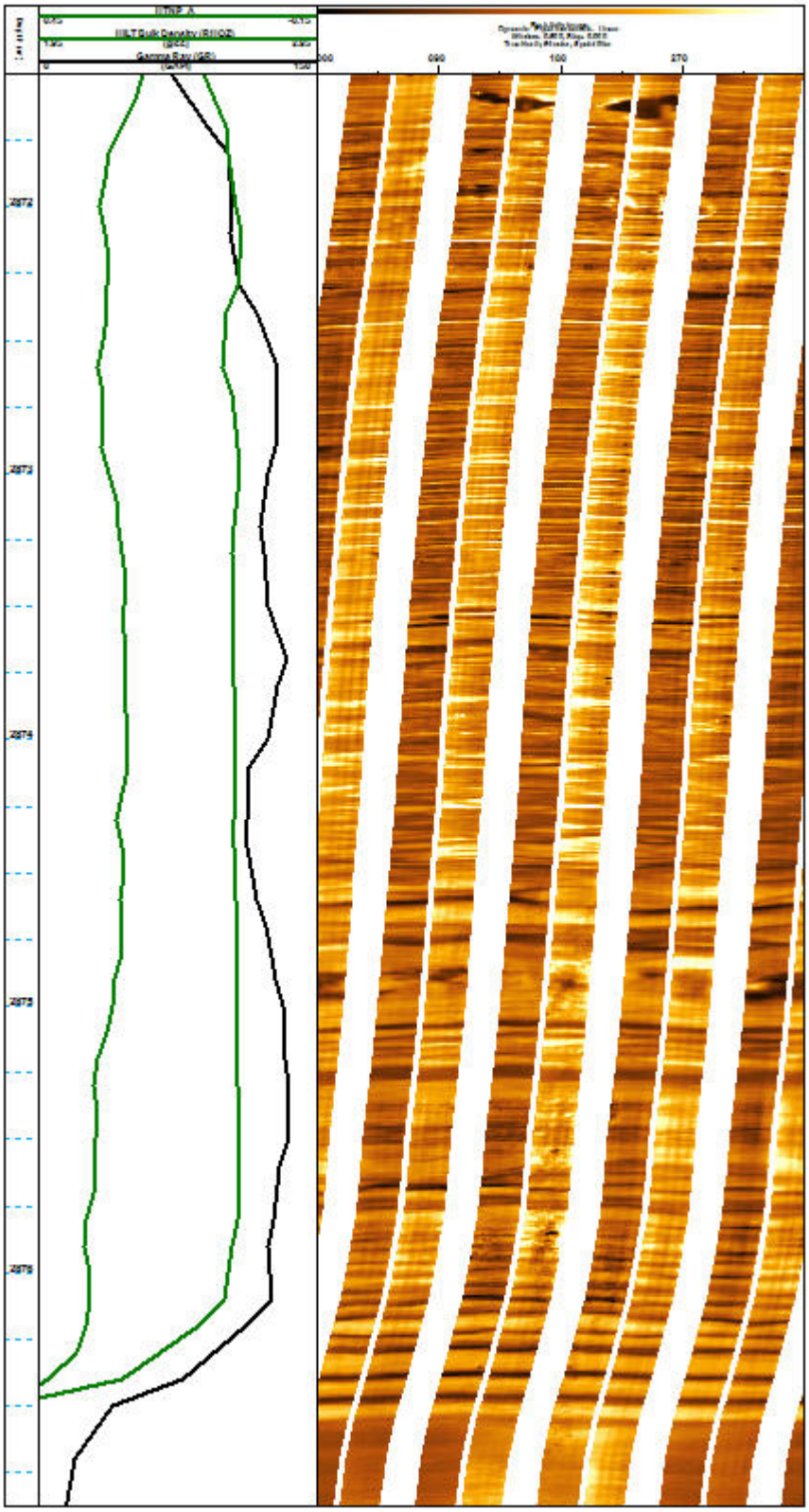

Figure 5 FMI Image through well laminated mudstone (lithofacies MI)

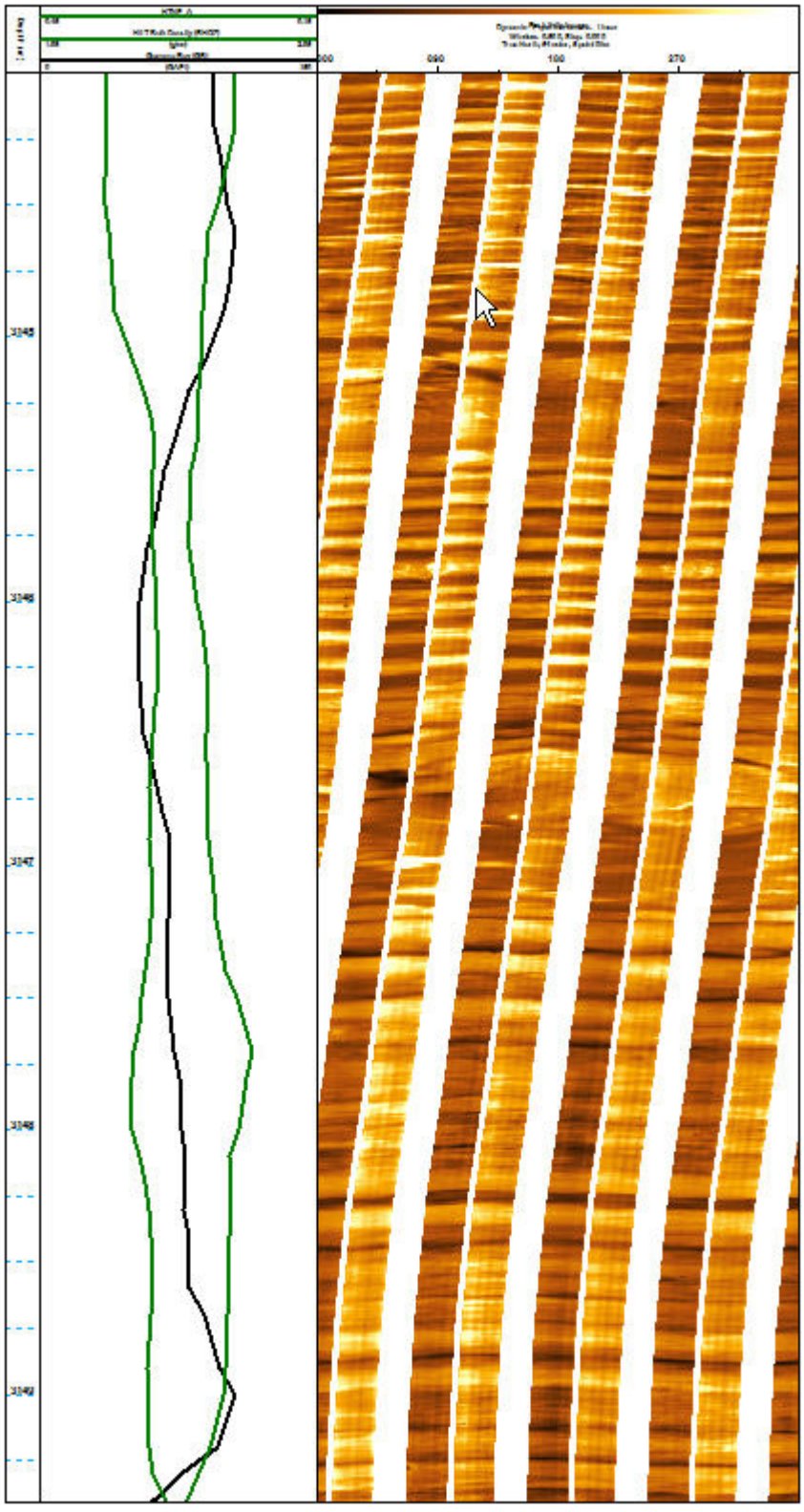

Figure 6. FMI image through dm-scale heterolithic sst-mudstone lithofacies with well developed lamination fabric (Hl) 3144 – 3145 m, 3145.5 – 3146.5 m and 3147 – 3149 m; and less well developed fabric (Hm) 3145 – 3145.5 and 3146.5 – 3147 m.

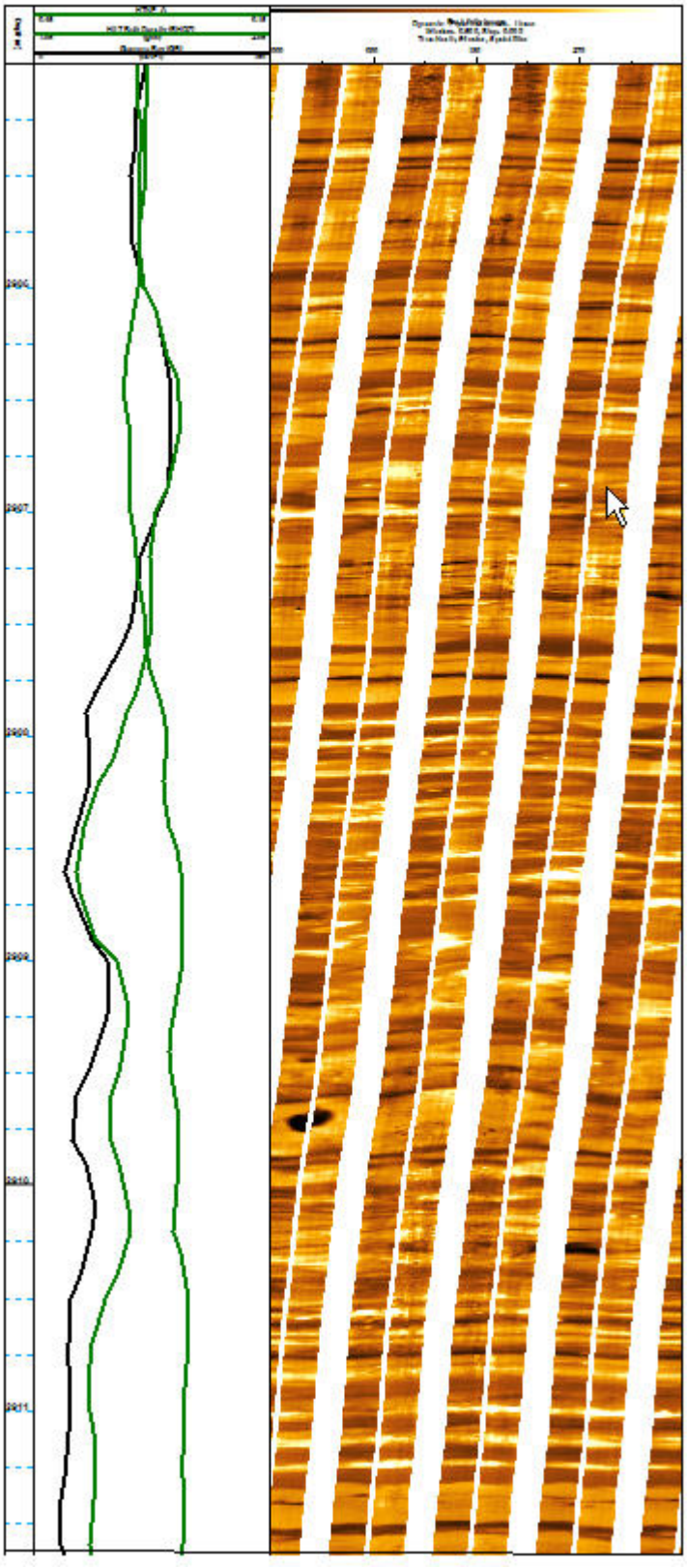

Figure 7. FMI image illustrating well laminated sandstone Sl with thin mottled sandstone with vague lamination Sm(Sl) 2908.5 – 2909 m.

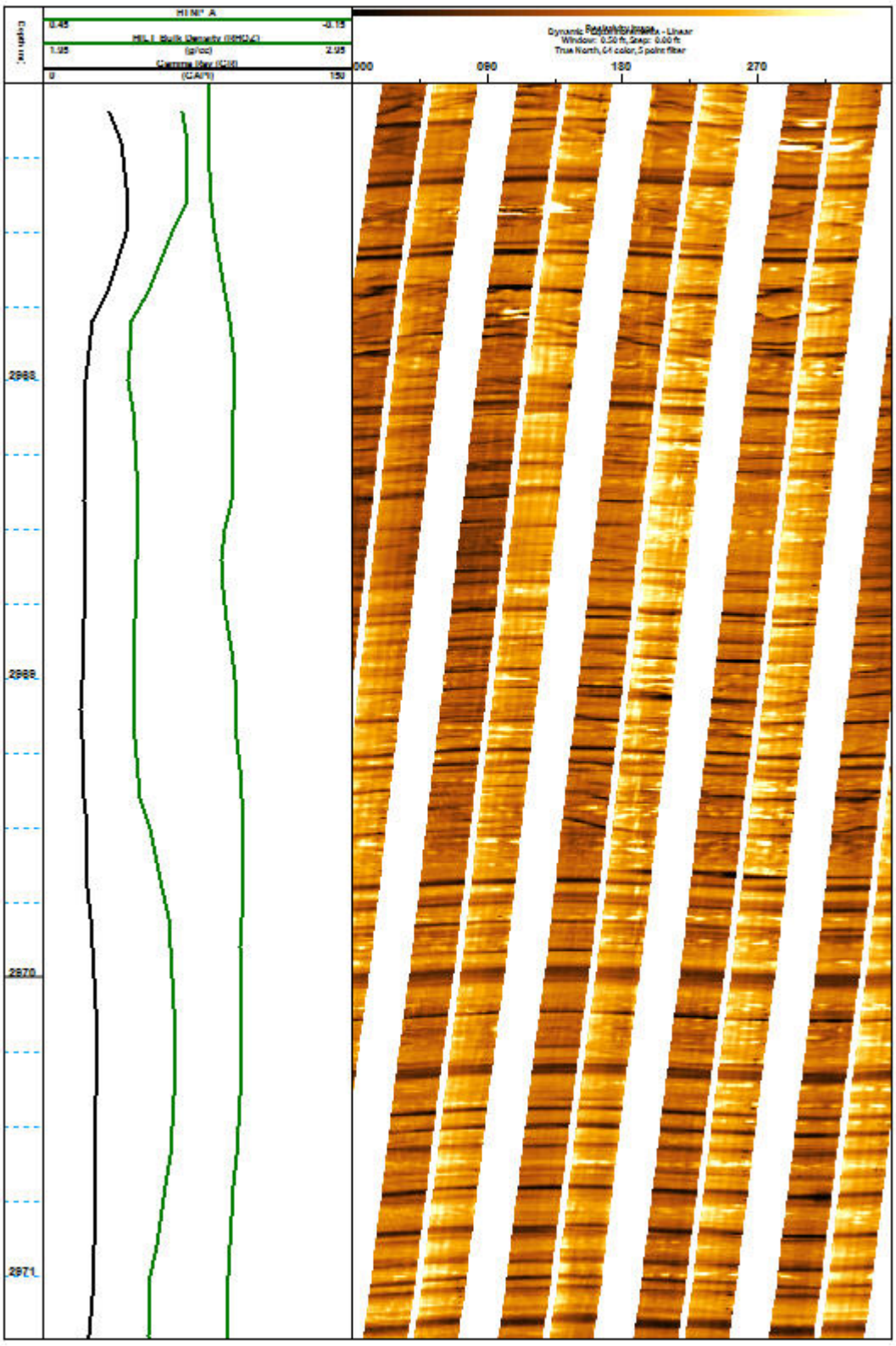

Figure 8. FMI image illustrating sandstone with coarse scale mottled fabric, Scm. Core calibration reveals that this lithofacies comprise pebble conglomerate and pebbly sandstone.

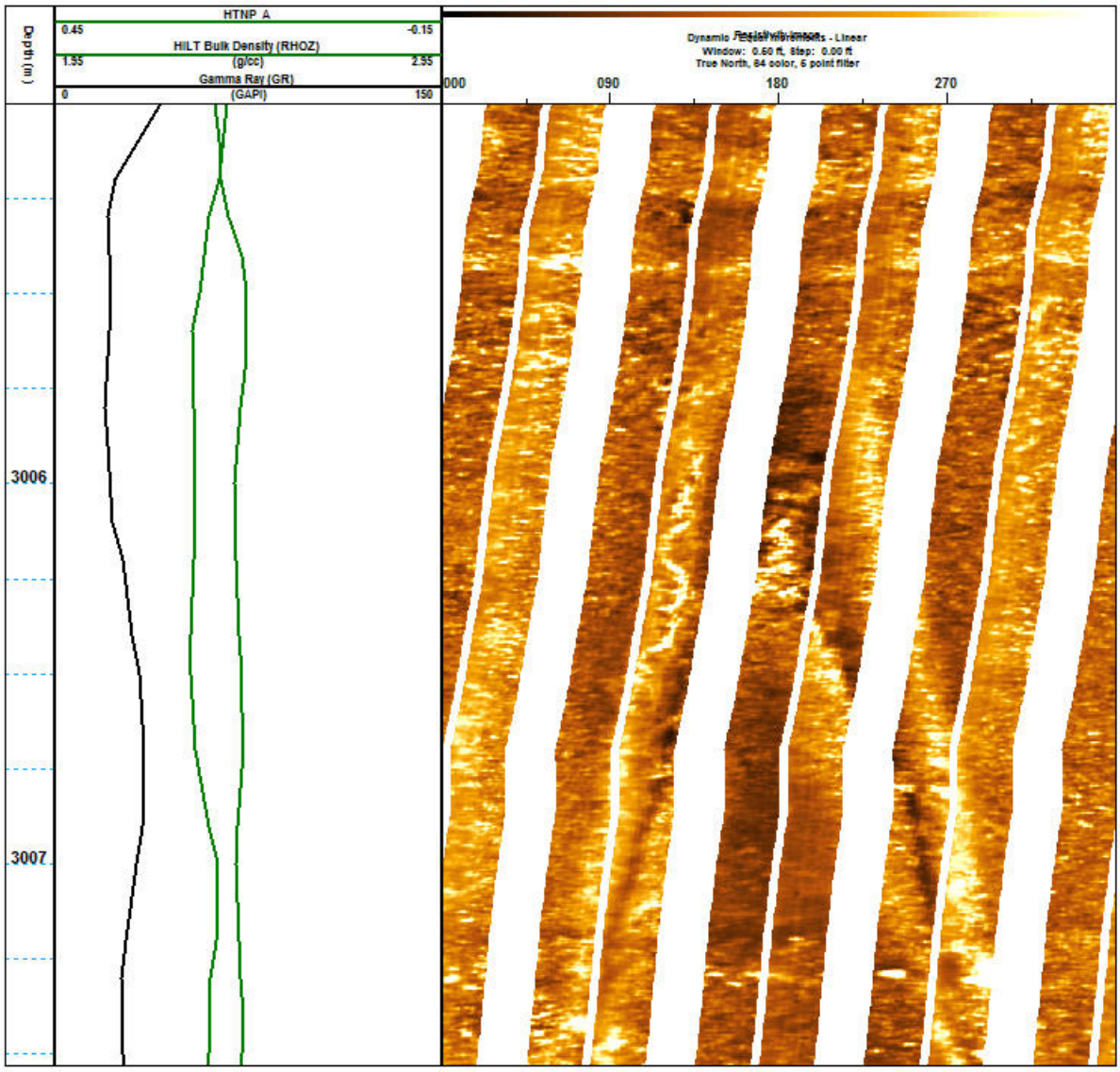

Figure 9. FMI image illustrating sandstone with fine scale mottled fabric with weak lamination, Sm(Sl). Note conductive high angle fracture.

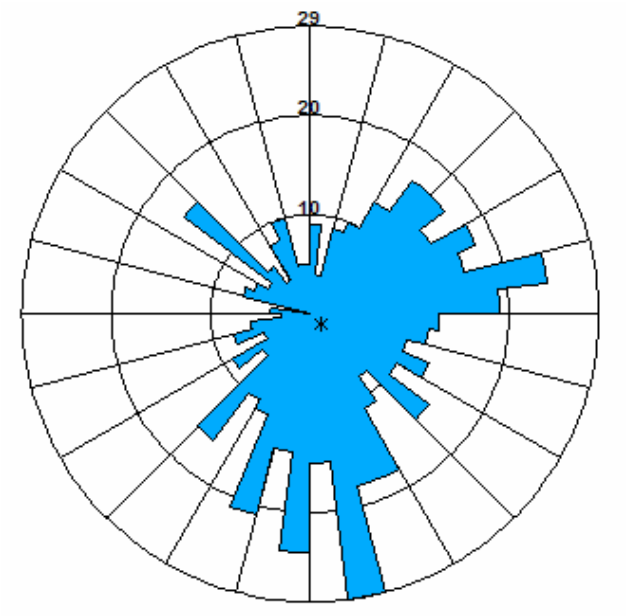

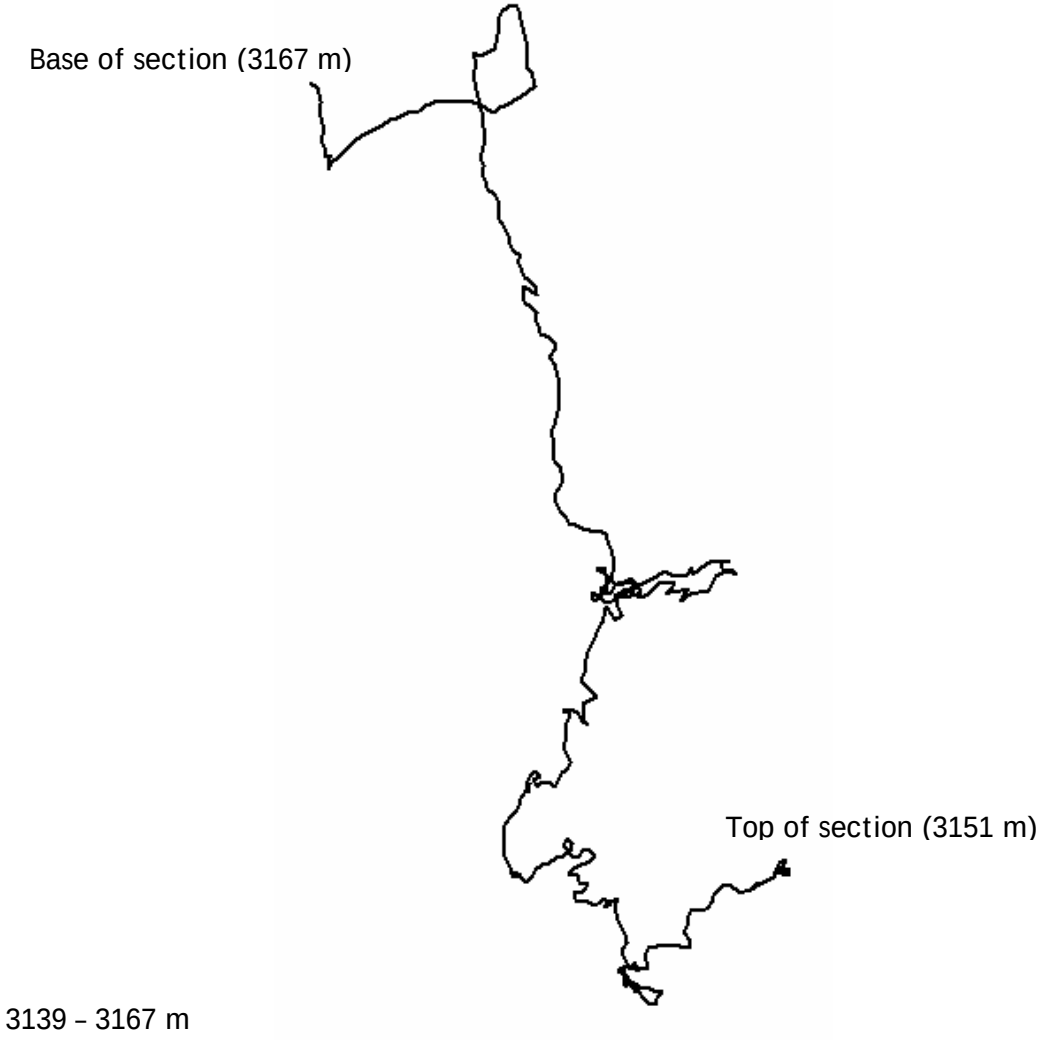

Figure 10. Cumulative dip azimuth plot for the interval 3167 – 3151 m. ISSf and ISS intraset surfaces (flat) are shown with structural dip removed. ISSf surfaces are dominant and large changes in azimuth are associated with these nearly flat lying structures. HETS and MUD surfaces only, occur above 3151 m.

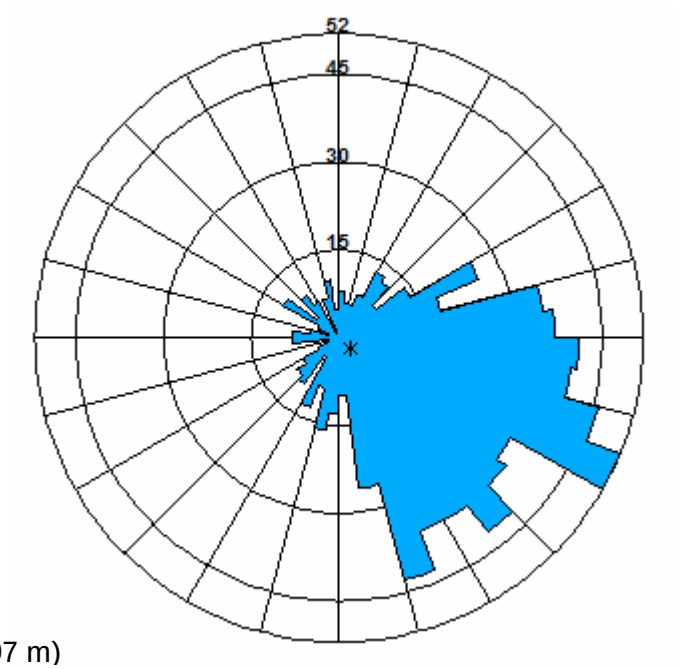

Base of section (2997 m)

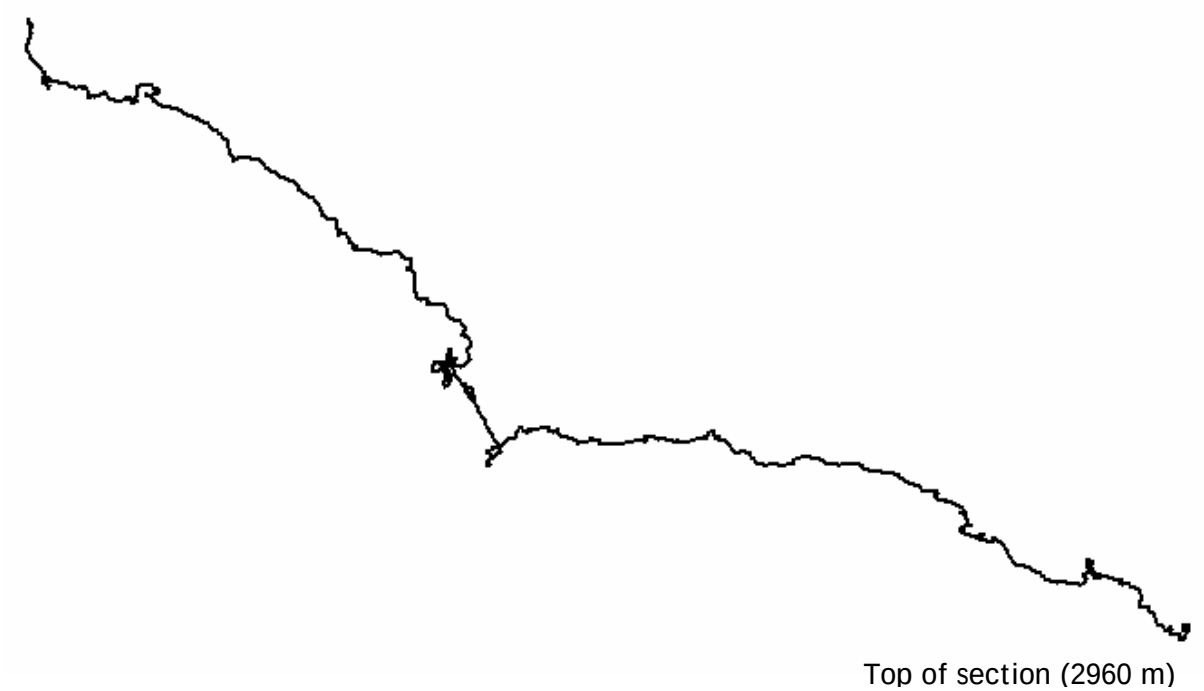

Top of section (2960 m)

2960 – 2997 m

Figure 11. Cumulative dip azimuth plot for the interval 2997 – 2960 m. ISSf and ISS intraset surfaces (flat) are shown with structural dip removed. ISSf surfaces are dominant and large changes in azimuth are associated with these nearly flat lying structures.

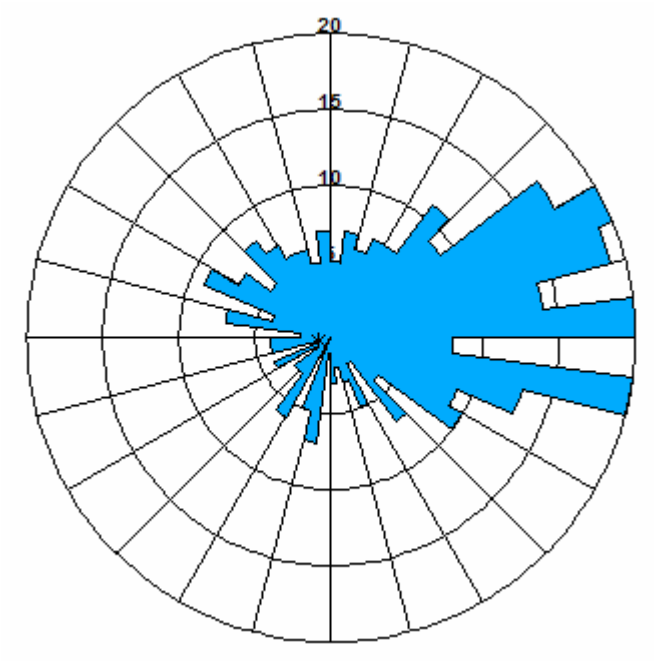

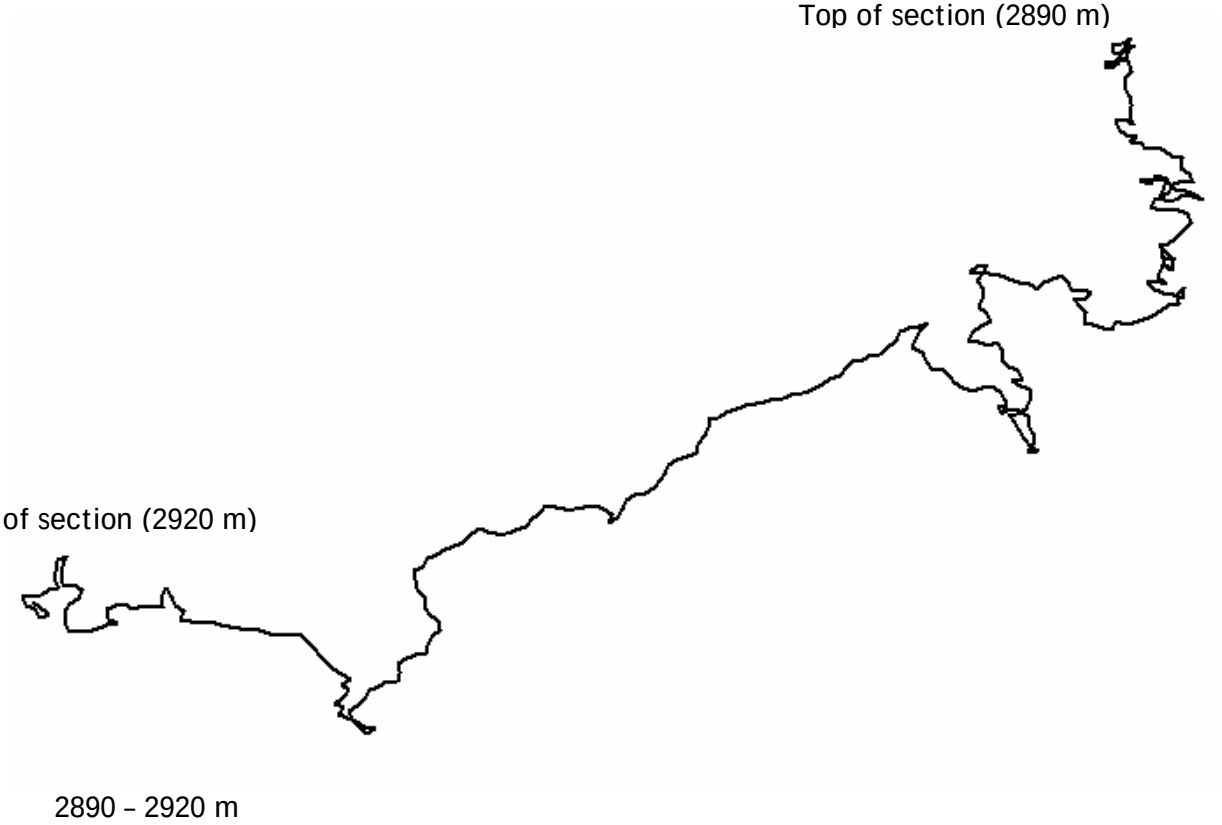

2890 – 2920 m

Figure 12. Cumulative dip azimuth plot for the interval 2890 – 2920 m. ISSf and ISS intraset surfaces (flat) are shown with structural dip removed. ISSf surfaces are dominant and large changes in azimuth are associated with these nearly flat lying structures.

ENCLOSURE 1: YOLLA 4 1:250 2550 - 2600 M QUALITY CONTROL PLOT

BIT SIZE: 8.5 IN
BH TEMP: 125 DegC
BOREHOLE SALINTY: 27000 PPM
FLUID LOSS: 3.8 cm3
MUD DENSITY: 9.45 lb/g
MUD pH: 8.9
MUD TYPE: Sea water / Dripsac/Soltex
MUD VISCOSITY: 70 S
SURFACE LATITUDE: 39 50' 40.592" S
SURFACE LONGITUDE: 145 49' 06.0569" E
RUN DATE:14-Jul-2004
2336.00 - 3242.46 METRES

Origin energy
delivering the goods

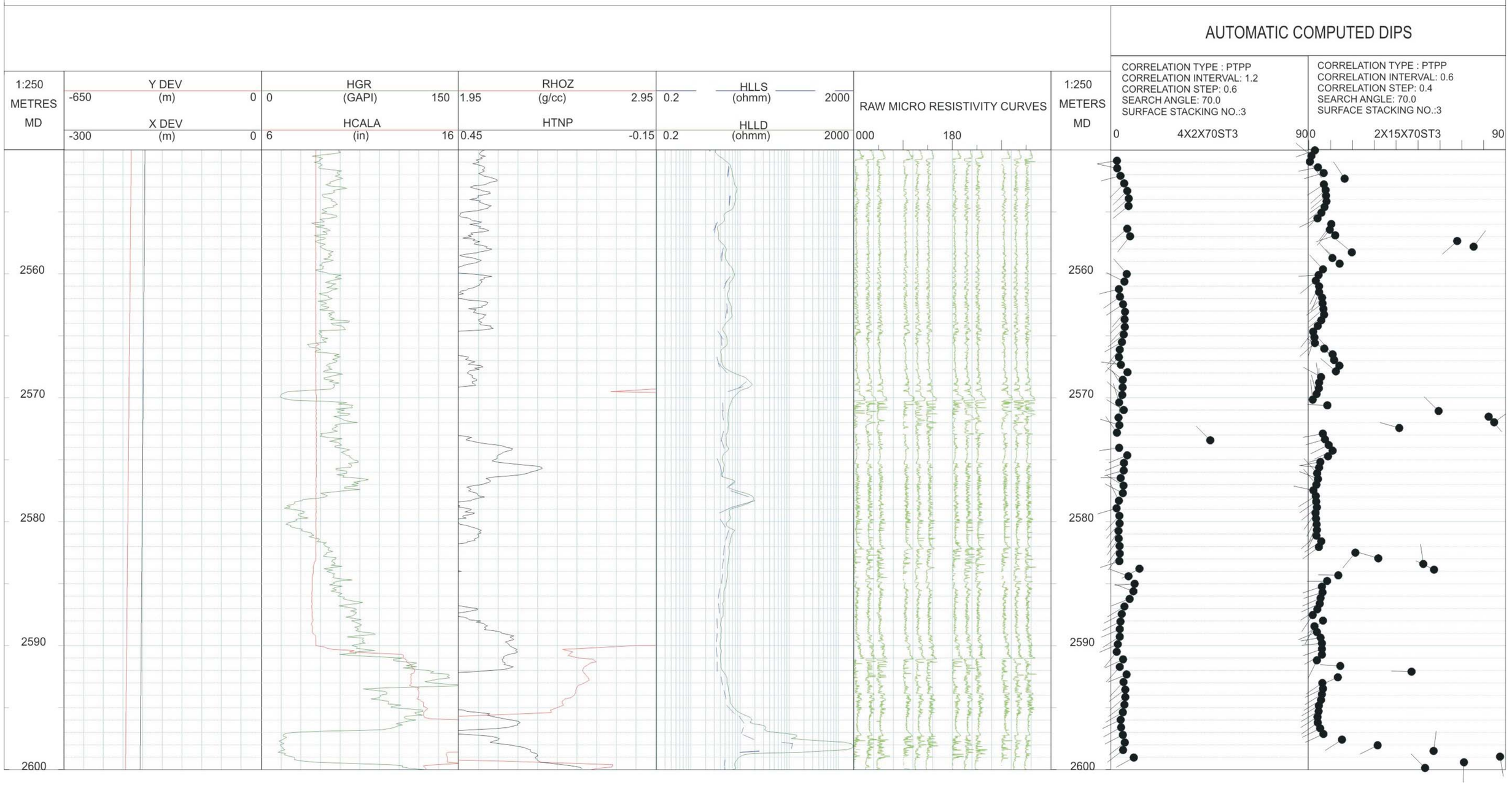

ENCLOSURE 2: YOLLA 4 1:500 2885 - 3190 M QUALITY CONTROL PLOT

BIT SIZE: 8.5 IN
BH TEMP: 125 DegC
BOREHOLE SALINTY: 27000 PPM
FLUID LOSS: 3.8 cm3
MUD DENSITY: 9.45 lb/g
MUD pH: 8.9
MUD TYPE: Sea water / Dripsac/Soltex
MUD VISCOSITY: 70 S
SURFACE LATITUDE: 39 50' 40.592" S
SURFACE LONGITUDE: 145 49' 06.0569" E
RUN DATE:14-Jul-2004
2336.00 - 3242.46 METRES

Origin energy
delivering the goods

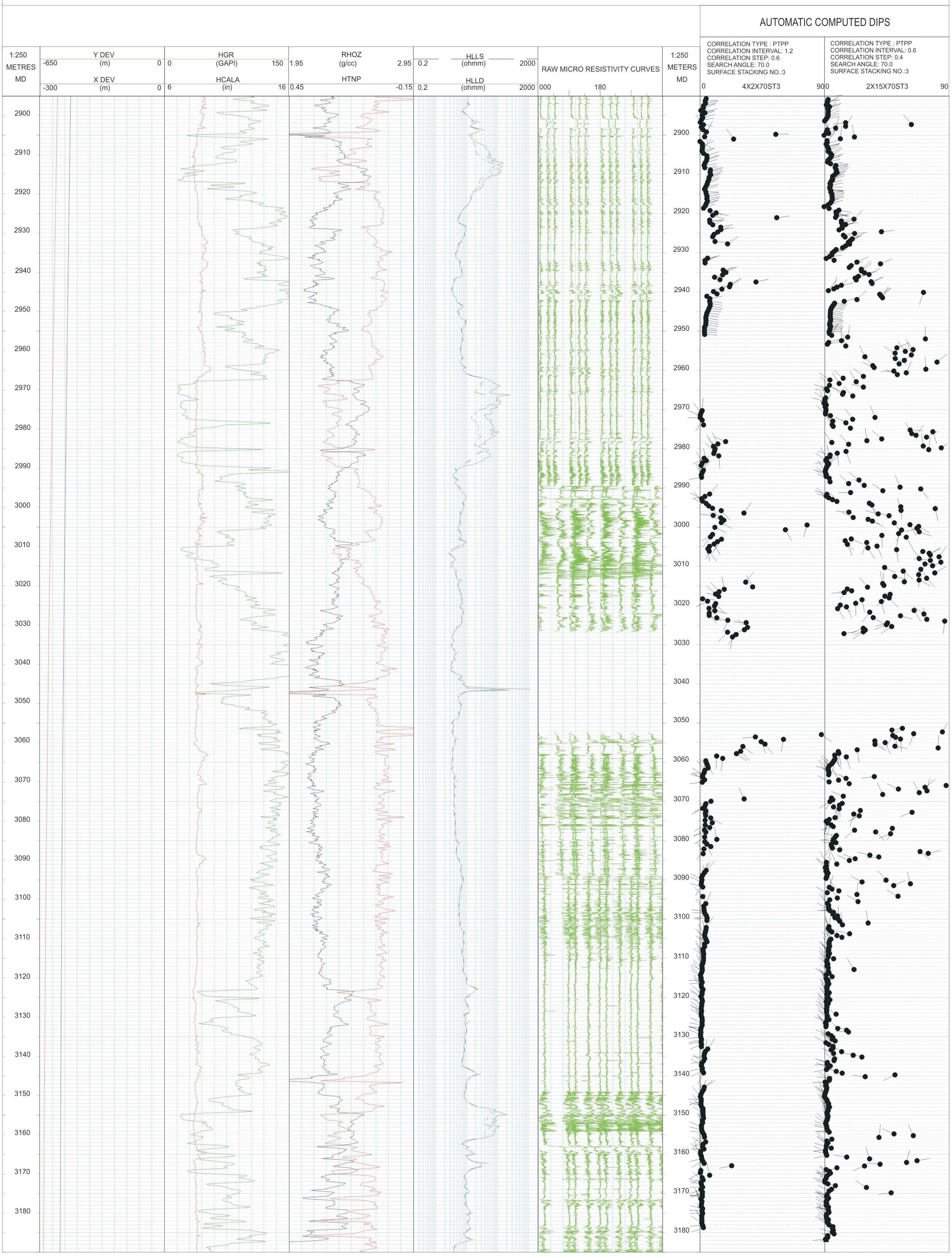

ENCLOSURE 3:

YOLLA 4 1:250 2550 - 2600 M STRUCTURAL SUMMARY PLOT

FRACTURE / FAULT STRIKE

ST FRAC
ST FAULT

MANUAL DIPS

LB
LBc
LBe
SB
CSB
ISS
ISSf
XSB
PDf
HETS
MUD
FAULT
FRAC

Origin energy

delivering the goods

1:250 METRES MD

HCAL (in) 6 16

HGR (GAPI) 0 150

RHOZ (g/cc) 1.95 2.95

HTNP 0.45 -0.15

HLLS (ohmm) 0.2 2000

HLLD (ohmm) 0.2 2000

Y_FMI_0.pck 0 90

STRUCTURAL ZONES

MUDS
HETS

Y_FMI_0.pck

ZONE I 8.4/235 DEG

ZONE II 9.8/316 DEG

ZONE III 6.5/205 DEG

ZONE IV 11.7/318 DEG

ZONE V 5.8/239 DEG

AUTOMATIC COMPUTED DIPS

4X2X70ST3 0 90

2560

2570

2580

2590

2600

ENCLOSURE 4:

YOLLA 4 1:500 2890 - 3190 M STRUCTURAL SUMMARY PLOT

FRACTURE / FAULT STRIKE

ST FRAC
ST FAULT

MANUAL DIPS

LB
LBc
LBe
SB
CSB
ISS
ISSf
XSB
PDf
HETS
MUD
FAULT
FRAC

Origin energy

delivering the goods

1:500
METRES
MD

BS (in) 6 16
C2 (in) 6 16
C1 (in) 6 16

HGR (GAPI) 0 150

RHOZ (g/cc) 1.95 2.95
HTNP 0.45 -0.15

HLLS (ohmm) 0.2 2000
HLLD (ohmm) 0.2 2000

Y_FMI_0.pck 0 90

STRUCTURAL ZONES
MUDS
HETS
Y_FMI_0.pck

AUTOMATIC COMPUTED DIPS
4X2X70ST3 0 90

ZONE I 5.3/081 DEG

ZONE II 5.0/318 DEG

ZONE I 2.5/321 DEG

ZONE II 3.8/256 DEG

ZONE III 3.2/305 DEG

ENCLOSURE 5:

YOLLA 4 1:200 2550 - 2600 M DATA OVERVIEW PLOT

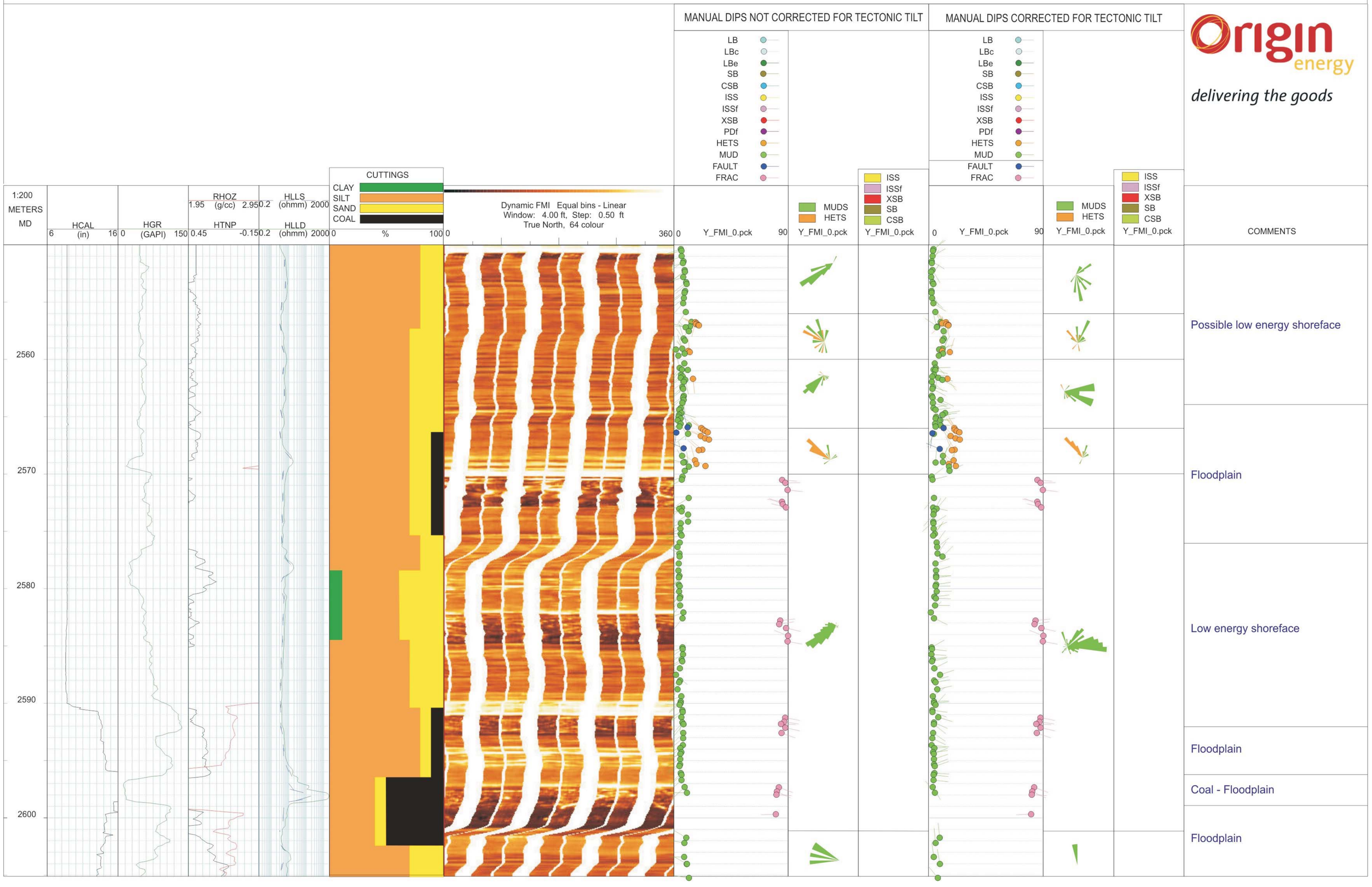

ENCLOSURE 6:

YOLLA 4 1:200 2890 - 3180 M DATA OVERVIEW PLOT

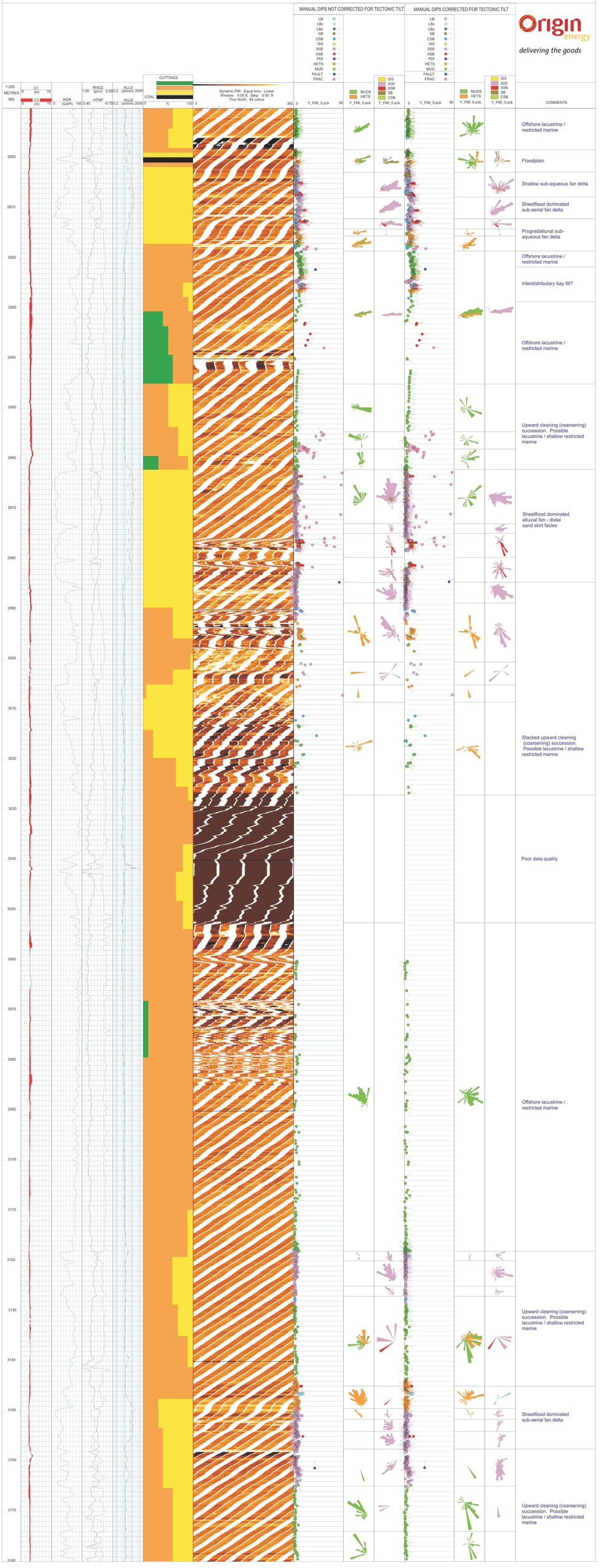

ENCLOSURE 7:

YOLLA 4 1:100 2890 - 2920 M SEDIMENTOLOGICAL COMPOSITE PLOT

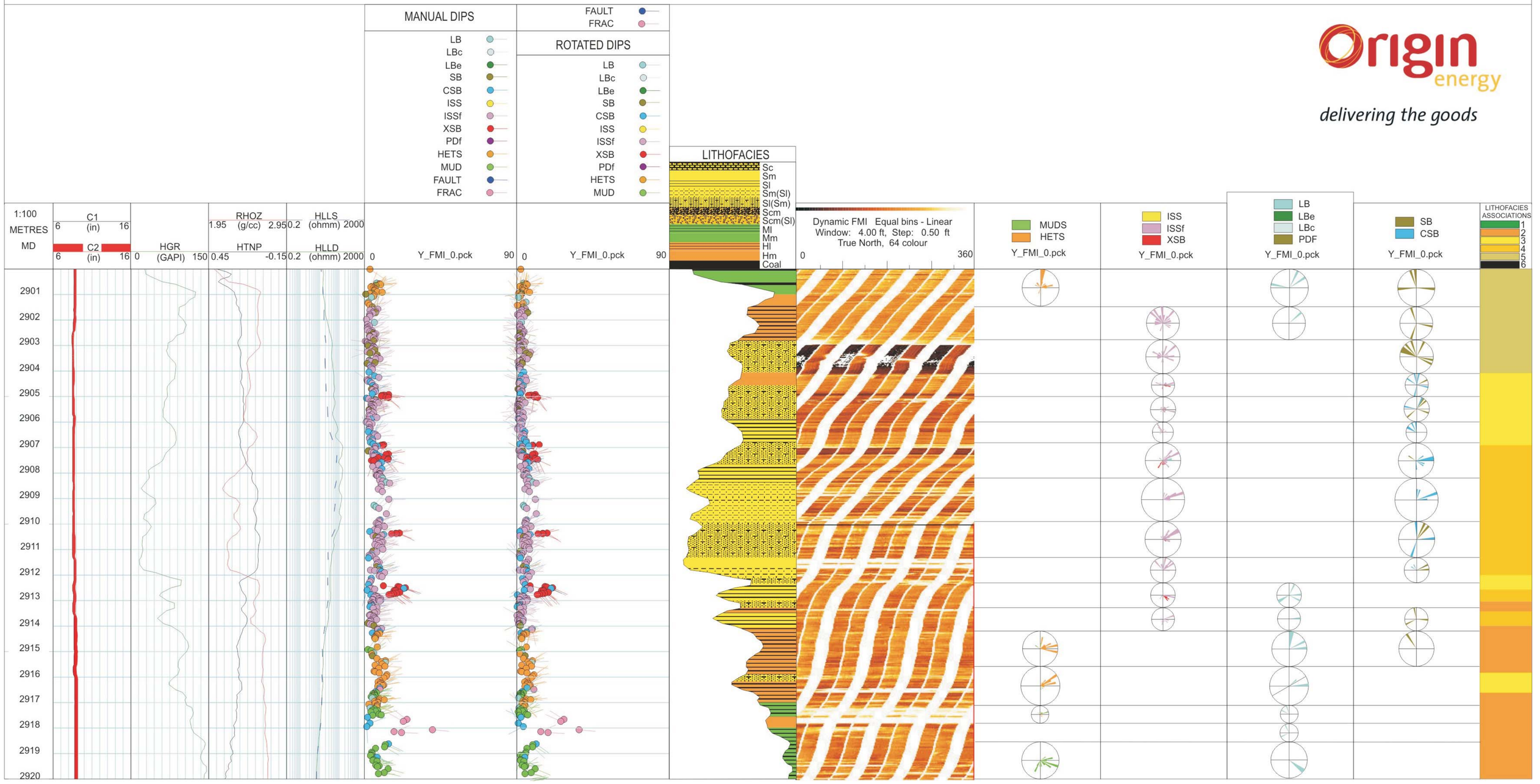

Origin energy

delivering the goods

ENCLOSURE 8:

YOLLA 4 1:100 2960 -3030 M SEDIMENTOLOGICAL COMPOSITE PLOT

Origin energy

delivering the goods

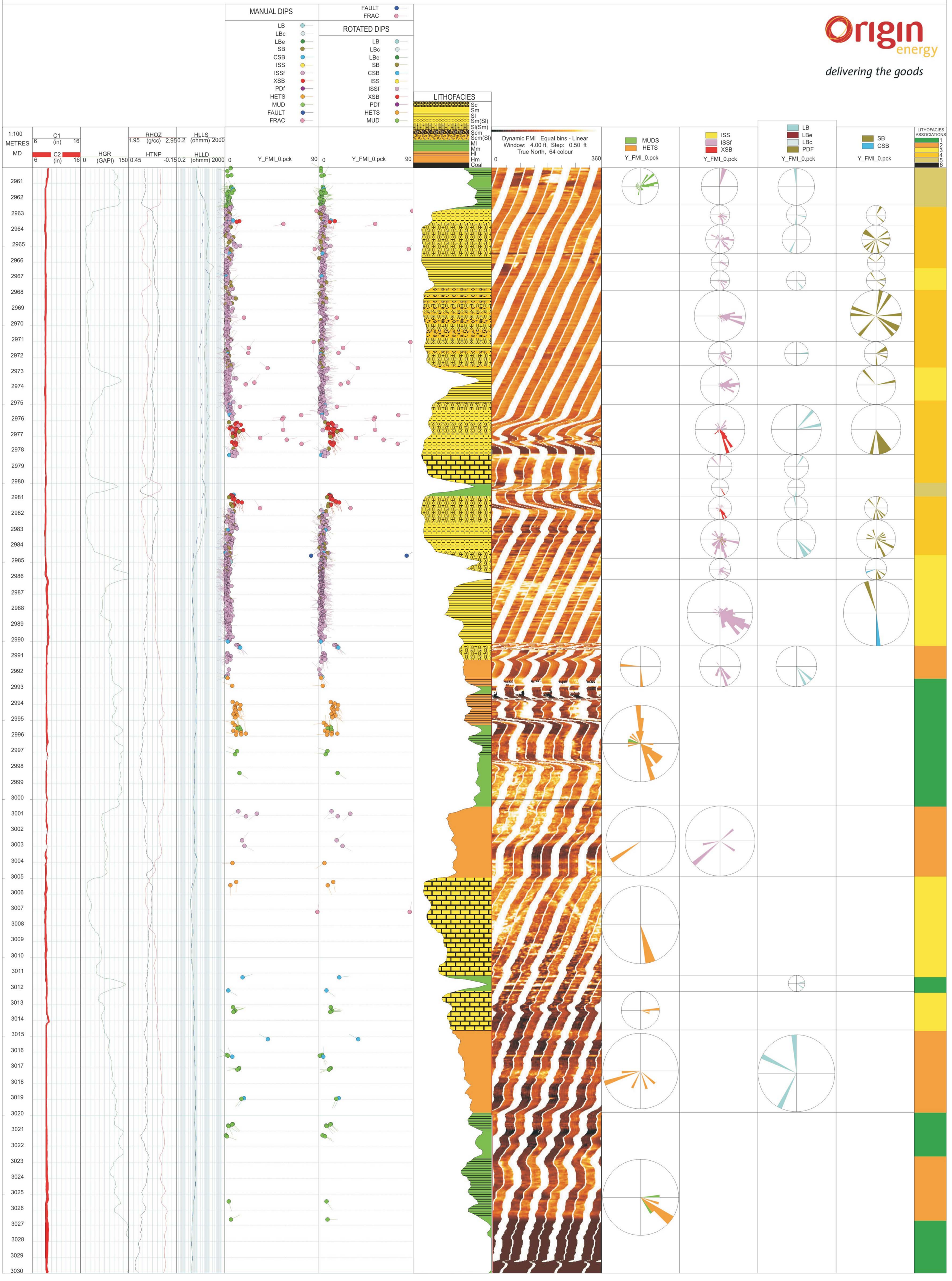

ENCLOSURE 9:

YOLLA 4 1:100 3115 -3170 M SEDIMENTOLOGICAL COMPOSITE PLOT

Origin energy

delivering the goods

MANUAL DIPS: LB, LBc, LBe, SB, CSB, ISS, ISSf, XSB, PDf, HETS, MUD, FAULT, FRAC

ROTATED DIPS: LB, LBc, LBe, SB, CSB, ISS, ISSf, XSB, PDf, HETS, MUD

FAULT, FRAC

LITHOFACIES: Sc, Sm, Sl, Sm(Sl), Sl(Sm), Scm, Scm(Sl), Ml, Mm, Hl, Hm, Coal

1:100 METRES MD

C1 6 (in) 16; C2 6 (in) 16

HGR 0 (GAPI) 150

RHOZ 1.95 (g/cc) 2.95; HTNP 0.45 -0.15

HLLS 0.2 (ohmm) 2000; HLLD 0.2 (ohmm) 2000

0 Y_FMI_0.pck 90

0 Y_FMI_0.pck 90

Dynamic FMI Equal bins - Linear
Window: 4.00 ft, Step: 0.50 ft
True North, 64 colour
0 360

MUDS, HETS — Y_FMI_0.pck

ISS, ISSf, XSB — Y_FMI_0.pck

LB, LBe, LBc, PDF — Y_FMI_0.pck

SB, CSB — Y_FMI_0.pck

LITHOFACIES ASSOCIATIONS 1 2 3 4 5 6

3116 3117 3118 3119 3120 3121 3122 3123 3124 3125 3126 3127 3128 3129 3130 3131 3132 3133 3134 3135 3136 3137 3138 3139 3140 3141 3142 3143 3144 3145 3146 3147 3148 3149 3150 3151 3152 3153 3154 3155 3156 3157 3158 3159 3160 3161 3162 3163 3164 3165 3166 3167 3168 3169 3170

ENCLOSURE 10: YOLLA 4 1:20 2895 -2930 M CORE COMPOSITE PLOT

ENCLOSURE 11:

YOLLA 4 1:20 2960 -3000 M CORE COMPOSITE PLOT

Origin energy
delivering the goods

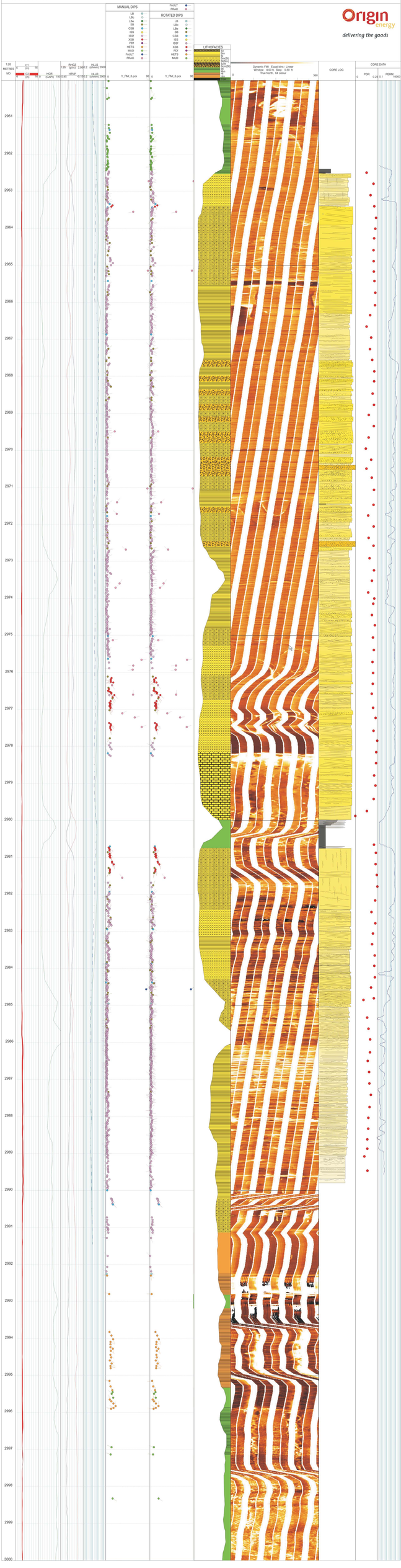

ENCLOSURE 1: COMPOSITE LOG

Yolla-4
Composite Well Log

Origin energy

Well Location

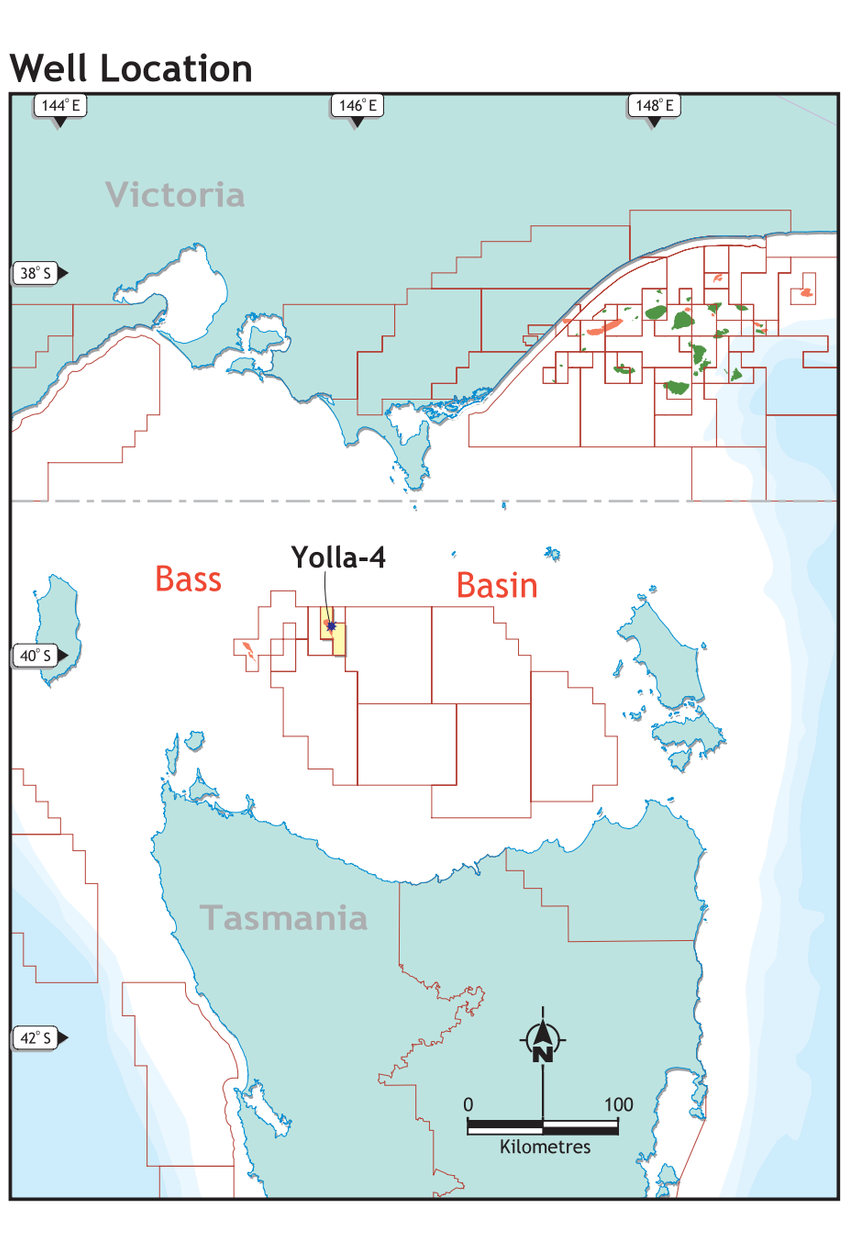

Well Data Card

Well: Yolla-4
Well Type: Deviated Well
Well Status: Cased Gas Producer
Tenement: T/L1
State: Tasmania
Basin: Offshore Bass
Location: Latitude: 39°50' 40.592" South
Easting: 398 905.07 mE
Longitude: 145°49' 06.0569" East
Northing: 5 588 821.47 mN
(GDA 94; AMG Zone 55, Central Meridian 147°East).

Seismic Ref.
(Platform): Yolla 3D Seismic Survey, Inline 480, Xline 1000
(2755 Sst): Yolla 3D Seismic Survey, Inline 475, Xline 951
Elevation: 43m (RT-AMSL)
Water Depth: 80.8m (LAT to seabed)
Total Depth (Drillers): 3235 mMDRT
Rig on Location: 20:00hrs 06/06/2004
Spud: 21:45hrs 18/06/2004
TD Reached: 22:00hrs 11/07/2004
Rig Released: 12:30hrs 08/08/2004
Permit Interests: Origin Energy Resources Limited (Operator) 32.5%
Origin Energy Northwest Pty Ltd 5%
AWE Petroleum Pty Ltd 30%
CalEnergy Gas (Australia) Ltd 20%
Wandoo Petroleum Pty Ltd 12.5%
Rig Name: ENSCO 102
Rig Type: Jack-up
Drilling Contractor: ENSCO Australia Pty Ltd
Well Cost: A$ 24,603,034
Service Company: Schlumberger (Wireline); Sperry-Sun (LWD)

Casing Schematic

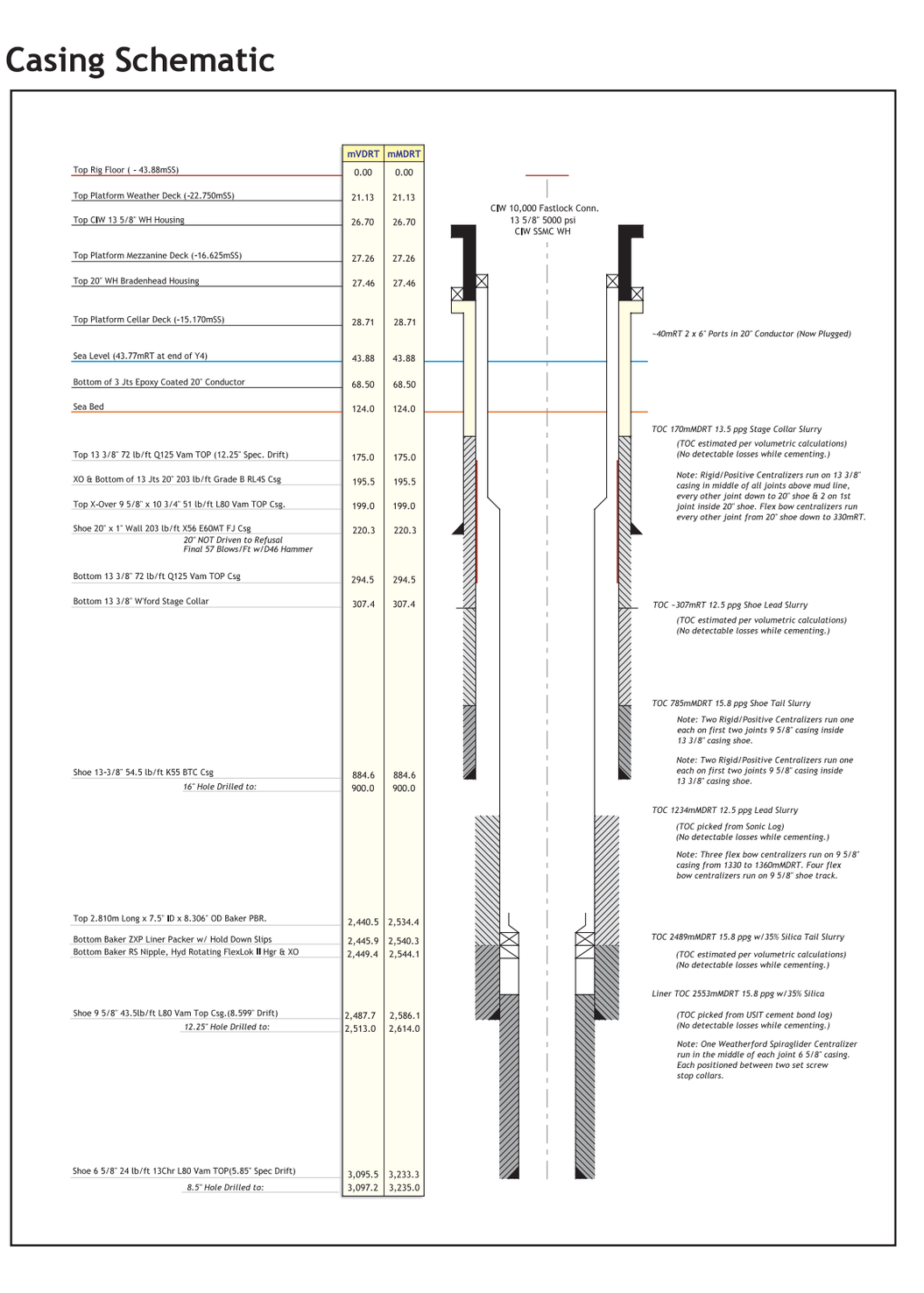

Time vs Depth

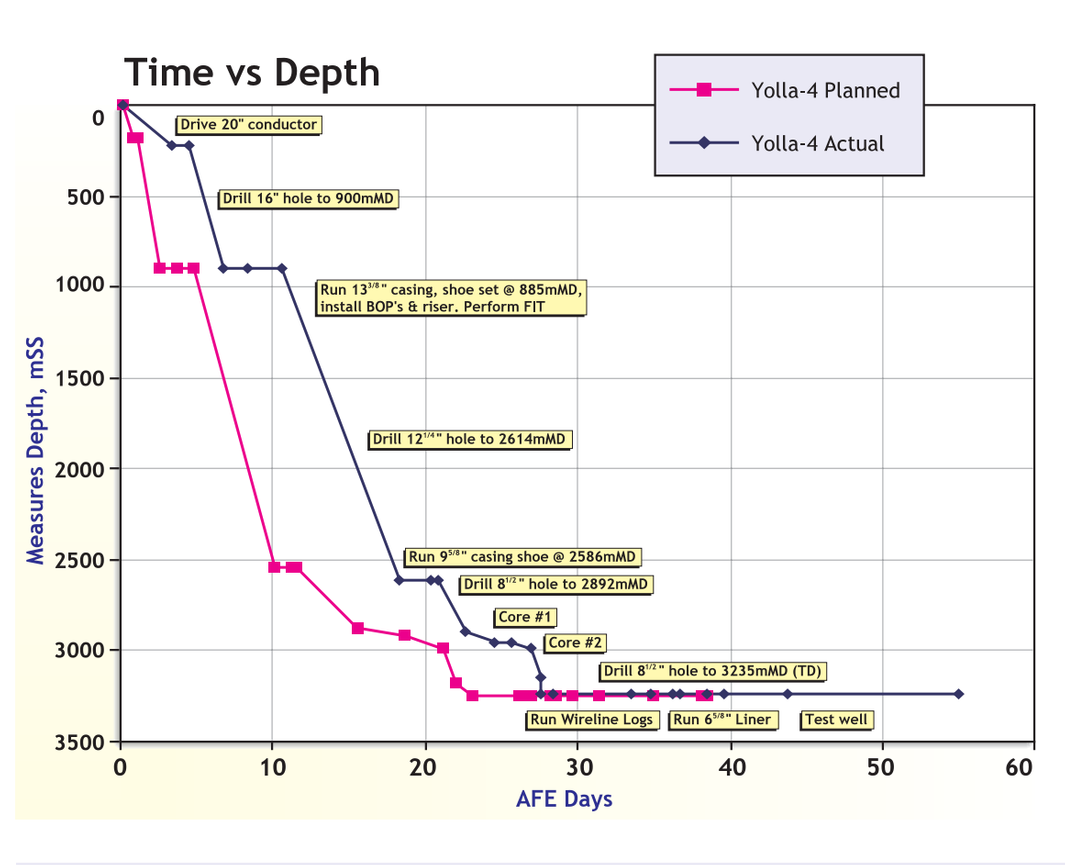

Formation Tops

Formation / Seismic Marker	Tops (m) m MDRT	m TVDSS	THICK (rel to TVD)	TWT (ms)	Remarks/Shows
Torquay Group	123.8	80.8	971.2	108	No Returns 123.8 - 900.0 mMDRT. Claystone, calcareous.
Upper Angahook Formation	1095	1052	188.0	942	Claystone, calcareous in part
Angahook Volcanics	1283	1240	134.0	1134	Volcanic Tuff interbedded with claystone and sandstone and minor siltstone
Lower Angahook (Oligocene)	1418	1374	288.2	1232	Interbedded sandstone, siltstone and claystone, grain size decreasing with depth
Demons Bluff Formation	1726	1662.2	142	1419	Siltstone with minor interbedded sandstone and occasional dolomite
Eastern View Coal Measures	1883	1804.2	1198	1517	Interbedded Sandstone, coal, siltstone and minor claystone
TEV4	*1912*	*1830.6*	*(17.4)*	*1534*	*Sandstone*
Fault	*2582.5*	*2441.4*	*NA*	*1915*	
2458 sand	*2603.7*	*2460.7*	*(14.5)*	*1933*	*Oil-bearing sandstone*
Top Igneous Intrusive	*2723.4*	*2569.7*	*(40.1)*	*1998*	*Gabbro*
2718 sand	*2864.8*	*2698.3*	*(6.1)*	*2064*	*Tight sandstone*
2755 sand	*2902.7*	*2733.3*	*(8.7)*	*2081*	*Gas-bearing sandstone*
2809 sand	*2962.6*	*2789.0*	*(20.8)*	*2108*	*Gas-bearing sandstone*
2844 sand	*3005.0*	*2828.8*	*(9.4)*	*2126*	*Gas-bearing sandstone*
2952 sand	*3118.2*	*2938.5*	*(11.7)*	*2183*	*Tight sandstone*
2973 sand	*3149.4*	*2969.3*	*(15.9)*	*2198*	*Gas-bearing sandstone*
Basal Volcanics	3182.6	3002.2	52.1+	2215	Volcanics: basalt and weathered basalt
Total Depth	3235	3054.3			

Wireline Log Runs

Suite #	Run #	Logs Acquired	Interval (mMDRT)
1	1	PEX-HRLA-CMR-SP-GR-LEHQT	2776 - 2542
1	2	PEX-HRLA-CMR-SP-GR-LEHQT	3235.5 - 2590
1	3	FMI-DSI-HNGS-ECS-LEHQT	3220 - 2590 (HNGS-DSI to 120)
1	4	VSI-GR-LEHQT (offset VSP survey)	765 - 3225
1	5	MDT-GR-CMR-LEHQT	3206 - 2594
1	6	MSCT-GR-LEHQT	3159 - 2604
1	7	USIT-CBL-VDL-GR-CCL	3185 - 2546

Logging Parameters

Suite	Run	Bit Size	Fluid Type	Density (lbm/gal)	Viscosity (s)	Fluid Loss (cm3)	pH	RM @ measured Temp (ohm.m@oC)	RMF @ measured Temp (ohm.m@oC)	RMC @ measured Temp (ohm.m@oC)
1	1-6	8 ½"	Sea Water Drispac Soltex	9.35	70	3.8	8.9	0.197 @22°C	0.181 @21°C	0.215 @19°C

Temperature Data Recorded During Wireline Logging

Suite #	Run #	Maximum Recorded Temperature (°C)	Bottom Hole Depth (mRT)	Time Circulation Stopped	Time Logger on bottom
1	1	111	2776	12/07/04 05:00	12/07/04 17:30
1	2	126	3235.5	13/07/04 18:00	14/07/04 04:30
1	3	133	3220	13/07/04 18:00	14/07/04 12:55
1	4	136	3225	13/07/04 18:00	15/07/04 01:45
1	5	146	3206	13/07/04 18:00	15/07/04 11:15
1	6	146	3159	13/07/04 18:00	17/07/04 04:00

Yolla-4-CWL.dgn 02-05

Lithologies

Shale | Siltstone | Sandstone | Coal | Volcanics | Dolomitic Sandstone

Legend

Cement plug | Casing shoe | Core recovered | MDT Data: Invalid point, Valid point | Side wall cores: Attempted, Recovered | Perforation


SILTSTONE 1870 - 1880 mRT:
SILTSTONE: dark grey/brown, medium, soft - firm, sub blocky, clastic grains: 30% clay, 50% silt, 20% very fine sand, accessories: arenaceous 20 %, micro mica tr %, carbonaceous grains tr %
Top EVCM (1883.00)
SANDSTONE AND SILTSTONE 1880 - 1914 mRT:
SANDSTONE: medium brown, very soft, sub blocky, clastic grains: 30% clay, 30% silt, 40% very fine sand, well sorted, sub rounded, sub spherical, cements/strengths: argillaceous/weak, accessories: carbonaceous grains tr % porosity: inter granular trace.
SILTSTONE: brownish/grey, black/grey, very soft, sub blocky, calcareous grains trace% clay, clastic grains: 20% clay, 40% silt, 30% very fine sand, accessories: arenaceous, pyrite tr %, carbonaceous grains and micro laminae tr %.
1908m - 1914m Fluorescence: trace, very dull, pinpoint, dark yellow, no direct cut, no crush cut and no residue ring.
Top TEV4 (1912.00)
VERY FINE GRAINED SANDSTONE AND SILTSTONE 1914 - 1938 mRT:
SANDSTONE: off white light green, very soft, sub blocky, clastic grains: 30% clay, 70% very fine sand, well sorted, sub rounded, sub elongate, cements/strengths: argillaceous/weak, siliceous/weak, accessories: glauconite 3 % porosity: inter granular, trace.
SILTSTONE: brownish/grey, black/grey, very soft, sub blocky, clastic grains: 20% clay, 40% silt, 30% very fine sand, accessories: arenaceous 10 %, pyrite tr %, carbonaceous specks tr %
FINE TO MEDIUM GRAINED SANDSTONE AND SILTSTONE 1938 - 1968 mRT:
SANDSTONE: off white light brown grey/brown, soft - friable, sub blocky clastic grains: 30% clay, 30% fine sand, 40% medium sand, moderately sorted, sub rounded, sub elongate, cements/strengths: argillaceous/weak, siliceous/weak, pyrite/strong, accessories: pyrite tr % porosity: inter granular 3%.
SILTSTONE: brown grey, soft - friable, sub fissile, clastic grains: 10% clay, 70% silt, tr% very fine sand, accessories: mc tr %, carbonaceous grains tr %
SANDSTONE (FINE AND VERY COARSE), SILTSTONE OCCASIONAL COAL 1968 - 2022 mRT:
SANDSTONE: off white, clear translucent, loose - soft, sub blocky, clastic grains: 30% clay, 10% medium sand, 40% coarse sand, 20% very coarse sand, poorly sorted, sub angular, sub spherical, siliceous/weak, accessories: kaolinite 25 % porosity: inter granular 20%.
SANDSTONE: white, off white, soft, sub blocky, clastic grains: 30% clay, 70% fine sand, well sorted, rounded, sub spherical, argillaceous/weak, accessories: kaolinite 25 % porosity: inter granular 5%.
SILTSTONE: medium brown, black/brown, soft-friable, sub fissile, clastic grains: tr% clay, 70% silt, 30% very fine sand, accessories: mica tr %, carbonaceous grains and laminae tr %.
COAL: black coloured, firm, brittle, blocky, vitreous to sub vitreous.
Y4 fault (2582.50)
Top 2458 Sand (2603.70)
Base 2458 Sand (2619.59)
COAL: black, firm brittle, blocky, rare sub conchoidal to common hackly fracture, tr% clay, tr% silty.
MASSIVE SILTSTONE AND COAL NEAR BASE 2670 - 2712 mRT:
SILTSTONE: dark grey greyish/black, firm, sub blocky to sub fissile, clastic grains: trace% clay, 95% silt, 5% very fine sand, accessories: argillaceous tr %, micro mica tr %
COAL: black, dull to sub vitreous, firm, blocky and brittle, sub conchoidal to hackly fracture, tr% silt.
SLIGHTLY METAMORPHOSED SILTSTONE ABOVE IGNEOUS INTRUSIVE 2712 - 2719 mRT:
SILTSTONE: (1) grey/black, sub vitreous, firm moderately hard, blocky, clastic grains: 100% silt, cements/strengths: pyrite/strong, accessories: vitreous carbonaceous 20 %, pyrite tr %
SILTSTONE: (2) dark grey greyish/black, firm, sub fissile, clastic grains: tr% clay, 95% silt, 5% very fine sand, accessories: argillaceous tr %, micro mica tr %
top sill (2723.40)
IGNEOUS INTRUSIVE 2719 - 2767 mRT:
IGNEOUS INTRUSIVE: (granodiorite) mottled white green, speckled black, soft to firm occasionally hard, medium to coarse crystal size, common quartz, biotite, plagioclase, black to green pyroxene, calcareous, commonly altered to clay with a chlorotic ground mass.
MASSIVE SILTSTONE TRACE DOLOMITE 2767 - 2860 mRT:
SILTSTONE: medium - dark grey, brownish grey, friable - firm, sub fissile, clastic grains: 25% clay, 70% silt, 5% very fine sand, accessories: dolomite in part tr %, micro mica tr %, pyrite tr %,
DOLOMITE: (trace) light brown/tan coloured, firm moderately hard, blocky, 5% clay.
INTERBEDDED SANDSTONE AND SILTSTONE 2860 - 2866 mRT:
SANDSTONE: (30%), light greyish yellow, soft - firm, sub blocky, clastic grains: 10% clay, 10% silt, 50% very fine sand, 30% fine sand, moderately sorted, sub angular, sub elongate to sub spherical, cements/strengths: siliceous/weak, argillaceous weak, accessories: argillaceous matrix 10 - 20%, porosity: inter granular 3%. Fluorescence see below.
SILTSTONE: (70%) medium - dark grey brownish grey, friable - firm, sub fissile clastic grains: 20% clay, 75% silt, 5% very fine sand, accessories: micro mica tr %, fine pyrite tr %
Top 2718 Sand (2864.80)
Base 2718 Sand (2871.40)
Top 2755 Sand (2902.70)
Base 2755 Sand (2912.10)
Top 2809 Sand (2962.60)
Base 2809 Sand (2984.80)
Top 2844 Sand (3005.00)
Base 2844 Sand (3014.90)
Top 2952 Sand (3118.20)
Base 2952 Sand (3130.10)
Top 2973 Sand (3149.40)
Base 2973 Sand (3165.40)
Top basal volcanics (3182.60)